Neural Plasticity

Post-Stroke Neural Plasticity: Functional and Structural Reorganization during Stroke Recovery

Lead Guest Editor: Xiaozheng Liu
Guest Editors: Yating Lv, Yu Zheng, Xize Jia, and Jan D. Reinhardt

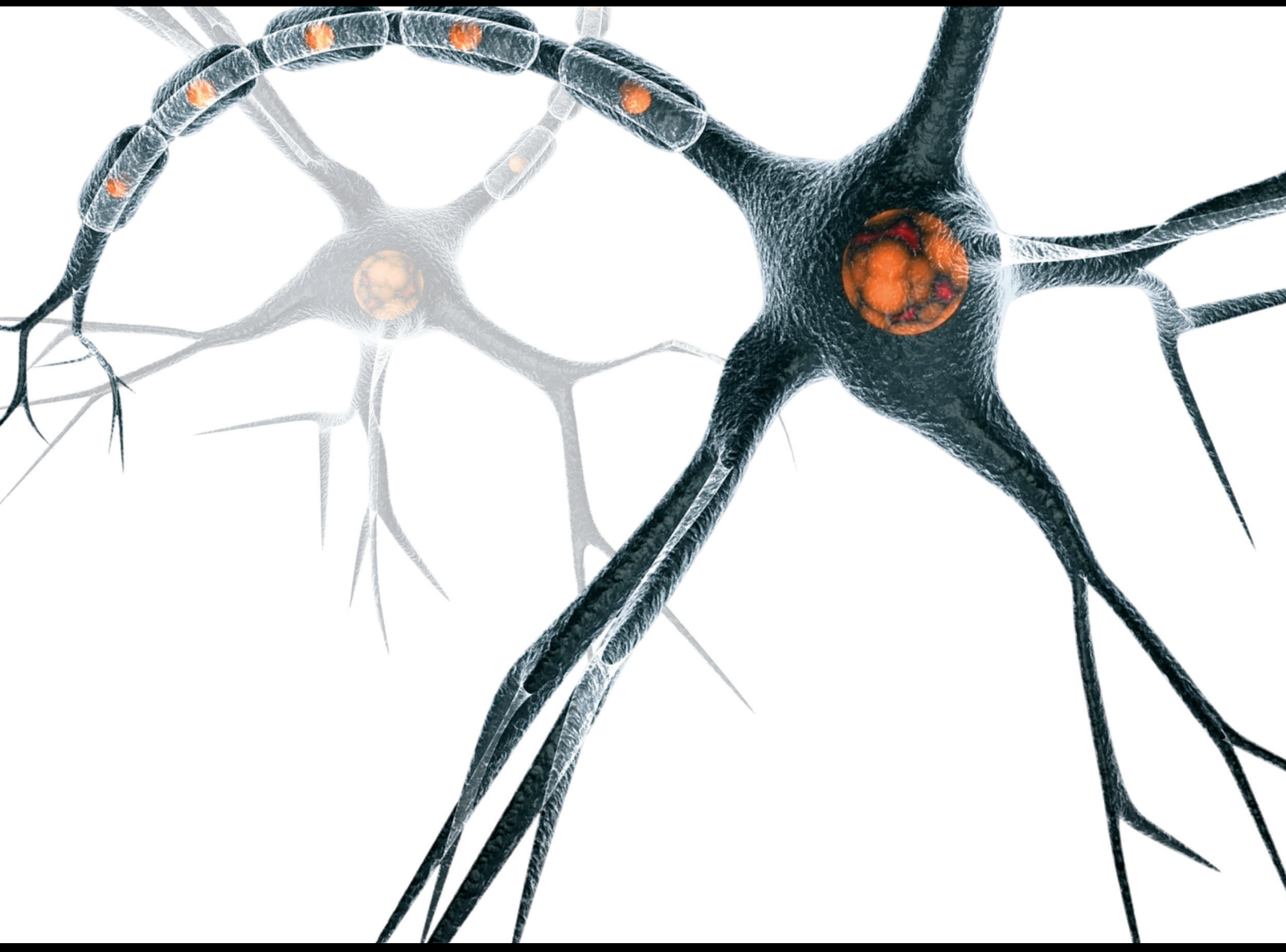

Post-Stroke Neural Plasticity: Functional and Structural Reorganization during Stroke Recovery

Neural Plasticity

Post-Stroke Neural Plasticity: Functional and Structural Reorganization during Stroke Recovery

Lead Guest Editor: Xiaozheng Liu
Guest Editors: Yating Lv, Yu Zheng, Xize Jia, and Jan D. Reinhardt

Contents

The Effect of Virtual Reality on Motor Anticipation and Hand Function in Patients with Subacute Stroke: A Randomized Trial on Movement-Related Potential
Ling Chen, Yi Chen, Wen Bin Fu, Dong Feng Huang, and Wai Leung Ambrose Lo
Research Article (14 pages), Article ID 7399995, Volume 2022 (2022)

Frequency-Specific Changes of Amplitude of Low-Frequency Fluctuations in Patients with Acute Basal Ganglia Ischemic Stroke
Xuemei Quan, Su Hu, Chaoguo Meng, Lulu Cheng, Yujie Lu, Yumei Xia, Wenmei Li, Huo Liang, Mengting Li, and Zhijian Liang
Research Article (10 pages), Article ID 4106131, Volume 2022 (2022)

Effectiveness of a Novel Contralaterally Controlled Neuromuscular Electrical Stimulation for Restoring Lower Limb Motor Performance and Activities of Daily Living in Stroke Survivors: A Randomized Controlled Trial
Ying Shen, Lan Chen, Li Zhang, Shugang Hu, Bin Su, Huaide Qiu, Xingjun Xu, Guilan Huang, Zhifei Yin, Jinyu Yang, Chuan Guo, and Tong Wang
Research Article (9 pages), Article ID 5771634, Volume 2022 (2022)

Distinctive Gut Microbiota Alteration Is Associated with Poststroke Functional Recovery: Results from a Prospective Cohort Study
Yini Dang, Xintong Zhang, Yu Zheng, Binbin Yu, Dijia Pan, Xiaomin Jiang, Chengjie Yan, Qiuyu Yu, and Xiao Lu
Research Article (16 pages), Article ID 1469339, Volume 2021 (2021)

A New Classification System for Postinterventional Cerebral Hyperdensity: The Influence on Hemorrhagic Transformation and Clinical Prognosis in Acute Stroke
Yuan Shao, Yuyun Xu, Yumei Li, Xuehua Wen, and Xiaodong He
Research Article (12 pages), Article ID 6144304, Volume 2021 (2021)

Structural and Functional Deficits in Patients with Poststroke Dementia: A Multimodal MRI Study
Huaying Cai, Zhiyong Zhao, Linhui Ni, Guocan Han, Xingyue Hu, Dan Wu, Xianjun Ding, and Jin Wang
Research Article (11 pages), Article ID 3536234, Volume 2021 (2021)

Longitudinal Changes of Sensorimotor Resting-State Functional Connectivity Differentiate between Patients with Thalamic Infarction and Pontine Infarction
Peipei Wang, Zhenxiang Zang, Miao Zhang, Yanxiang Cao, Zhilian Zhao, Yi Shan, Qingfeng Ma, and Jie Lu
Research Article (9 pages), Article ID 7031178, Volume 2021 (2021)

Electroacupuncture Promotes the Survival of the Grafted Human MGE Neural Progenitors in Rats with Cerebral Ischemia by Promoting Angiogenesis and Inhibiting Inflammation
Juan Li, Luting Chen, Danping Li, Min Lu, Xiaolin Huang, Xiaohua Han, and Hong Chen
Research Article (11 pages), Article ID 4894881, Volume 2021 (2021)

Contents

Hindawi
Neural Plasticity
Volume 2022, Article ID 6259693, 9 pages
https://doi.org/10.1155/2022/6259693

Research Article

High-Frequency Cerebellar rTMS Improves the Swallowing Function of Patients with Dysphagia after Brainstem Stroke

Ling-hui Dong, Xiaona Pan, Yuyang Wang, Guangtao Bai, Chao Han, Qiang Wang, and Pingping Meng

Department of Physical Medicine and Rehabilitation, The Affiliated Hospital of Qingdao University, No. 16, Jiangsu Road, Shinan District, Qingdao, Shandong Province, China

Correspondence should be addressed to Pingping Meng; mengpp@qduhospital.cn

Received 8 February 2022; Revised 5 May 2022; Accepted 12 May 2022; Published 11 August 2022

Academic Editor: Xi-Ze Jia

Objective. To explore the efficacy of high-frequency repetitive transcranial magnetic stimulation (rTMS) of the swallowing motor area of the cerebellum in patients with dysphagia after brainstem stroke. *Methods*. A total of 36 patients with dysphagia after brainstem stroke were recruited and divided into 3 groups. Before stimulation, single-pulse transcranial magnetic stimulation (TMS) was used to determine the swallowing dominant cerebellar hemisphere and the representation of the mylohyoid muscle. The three groups of patients received bilateral cerebellar sham stimulation, dominant cerebellar rTMS + contralateral sham stimulation, or bilateral cerebellar rTMS. The stimulus plan for each side was 10 Hz, 80% resting movement threshold (rMT), 250 pulses, 1 s per stimulus, and 9 s intervals. Sham rTMS was performed with the coil held at 90° to the scalp. The changes in the motor evoked potential (MEP) amplitude and the clinical swallowing function scales of the patients after stimulation were compared among the three groups. *Results*. 34 patients were finally included for statistical analysis. The scores of penetration aspiration scale (PAS) and functional dysphagia scale (FDS) of the patients after 2 weeks of rTMS in the unilateral stimulation group and bilateral stimulation group were better than that in the sham stimulation group, and there was no significant difference between the two groups. The increase in the MEP amplitude of the cerebral hemisphere in the bilateral stimulation group was higher than that in the other two groups, and the increase in the MEP amplitude in the unilateral stimulation group was higher than that in sham stimulation group. There was no correlation between the improvement in patients' clinical swallowing function (PAS scores and FDS scores) and the increase in MEP amplitude in either the unilateral stimulation group or the bilateral stimulation group. *Conclusion*. High-frequency rTMS in the cerebellum can improve swallowing function in PSD patients and increase the excitability of the representation of swallowing in the bilateral cerebral hemispheres. Compared with unilateral cerebellar rTMS, bilateral stimulation increased the excitability of the cerebral swallowing cortex more significantly, but there was no significant difference in clinical swallowing function.

1. Introduction

Dysphagia is one of the most common sequelae of stroke. The incidence of poststroke dysphagia (PSD) is more than 50% [1], which usually leads to complications such as malnutrition, pneumonia, and dehydration [2, 3]. Some stroke patients recover from dysphagia within 2 weeks of its onset. However, many patients still have long-term dysphagia and rely on enteral or parenteral nutrition for survival [4, 5]. Thus, searching for an effective therapeutic method becomes an important task to speed up the recovery of swallowing function and reduce these risks.

Currently, the available treatment methods for PSD are mainly based on compensation technology and physical therapy [6, 7]. Physiotherapy aims to strengthen the muscle groups (facial muscles, suprahyoid muscles) to restore tension, strength, range of motion, speed, and coordination [8]. Although some progress has been made in these treatments, the clinical evidence for PSD treatment is limited [9].

Due to the lack of effective treatments, researchers have begun to explore ways to promote the recovery of swallowing function by enhancing neuroplasticity. Previous neuroimaging studies found that the regional cerebral blood flow of the bilateral cerebellum was significantly increased when healthy subjects swallowed saliva spontaneously, suggesting that the cerebellum may be involved in spontaneous swallowing [10, 11]. In addition, a task-state functional magnetic resonance study found that the cerebellum showed functional connections with the primary motor cortex, inferior frontal gyrus, basal ganglia, and thalamus during swallowing. Its role may be related to the coordination of oral and pharyngeal muscle tissues [12].

Based on the above findings in the field of neuroimaging, Jayasekeran et al. tried to use external force to interfere with the cerebellum to explore its impact on swallowing. Studies have found that stimulating a healthy human cerebellum with a single pulse of TMS can generate pharyngeal contractor motor evoked potentials (MEPs) similar to those found when stimulating the cerebral cortex. It has also been found that the use of repetitive transcranial magnetic stimulation (rTMS) at the target can induce stronger MEPs, which means that cerebellar rTMS may promote swallowing movement [13]. Since the effect of rTMS depends on various stimulation parameters (mode, frequency, intensity, pulse number, etc.) [14], Vasant et al. used different pulse numbers and different stimulation frequencies (5, 10, and 20 Hz) of unilateral cerebellar hemisphere rTMS and found that only 10 Hz stimulation could obviously improve the MEP amplitude of the swallowing cortex in both cerebral hemispheres. The effect was the highest at 250 pulses and could last for at least 30 minutes. Regardless of which side of the cerebellar hemisphere was stimulated, there was no difference in the improvement of excitability of the bilateral cerebral cortex hemispheres [15].

In addition, the study used inhibitory rTMS in the swallowing cortex of healthy volunteers to simulate dysphagia after unilateral cortical stroke. It was found that unilateral and bilateral cerebellar rTMS (10 Hz, 250 pulses) can inhibit the negative behavioural effects caused by cortex suppression and improve cortical excitability. The excitability of the cerebral cortex after bilateral cerebellar rTMS is improved more significantly [16]. Vasant et al. used a case to report the positive effect of cerebellar rTMS on the swallowing function of a patient whose stroke centre was following a right posterior inferior cerebellar artery territory infarction [17]. The reason for this result is unclear, and it may be related to the increased signal afferent to the brainstem by cerebellar rTMS.

However, the credibility of individual case analyses is limited. Thus, we investigated the effect and safety of rTMS on dysphagia patients with brainstem stroke by comparing unilateral, bilateral, or sham cerebellar rTMS stimulation.

2. Methods

2.1. Participants. This study included 36 patients who were hospitalized in the West Coast Ward of the Rehabilitation Medicine Department of the Affiliated Hospital of Qingdao University from May 2020 to May 2021. The inclusion criteria were as follows: patients diagnosed with a brainstem stroke; patients with a duration of the disease less than 6 months; patients with PSD lasting for more than 2 weeks; swallowing disorders confirmed by the videofluoroscopic swallowing study (VFSS). The exclusion criteria were as follows: patients suffering from other diseases that may cause swallowing disorders; patients with combined stroke sites other than the brainstem; patients with an unstable condition; patients with severe cognitive impairment; and patients with contraindications to transcranial magnetic stimulation. This study was approved by the Ethics Committee of the Affiliated Hospital of Qingdao University (QYFY WZLL 26615). All subjects were aware of the study protocol and signed an informed consent form. The enrolled patients were divided into 3 groups using stratified blocked randomization: a sham stimulation group ($n = 12$), a unilateral stimulation group ($n = 12$), and a bilateral stimulation group ($n = 12$). Neither the patients nor the physicians responsible for the evaluation were aware of the distribution of the treatment options in each group. The study design and flow chart are illustrated in Figure 1.

2.2. rTMS Protocols. rTMS was delivered by a magnetic stimulator (Yiruide CCY-IA, Wuhan, China) with a 70 mm circular coil, with a maximum stimulator output of 3.0 Tesla. Before rTMS, the MEP amplitude of the mylohyoid muscle of the bilateral cerebral cortex was recorded. The patients sat in a relaxed position and used alcohol to clean the neck skin, which could remove oil and increase the electrical conductivity between the skin and the electrode. Using a single-pulse TMS system, the coil was tangent to the skull at 45°, and the electromyogram of the mylohyoid muscle was recorded through the surface electrode. The recording electrode was placed 2 cm on the left and right sides of the midpoint of the connection between the mandible and the middle of the hyoid bone. The reference electrode was attached to the mandibular angle. Moving within the area of 2-4 cm in front of the apex of the patient's skull and 4-6 cm from the side, an 80% output was used to obtain the largest motor evoked potential, which is the representation of the mylohyoid muscle of the cerebral cortex. Single-pulse TMS acts on the representation of the mylohyoid muscle motor cortex and gradually reduces the output intensity to determine the rMT. rMT is defined as the lowest TMS intensity of 5 out of 10 trials that can excite the MEP amplitude greater than 50 μv and expressed as a percentage of the maximum output intensity of the stimulator. The average of 5 effective MEP amplitudes was recorded as an index to quantify the excitability of the brain swallowing cortex. The same method was used to find the representation of bilateral cerebellar mylohyoid muscles movement 1 cm below the patient's extraoccipital carina and 3 cm laterally and to determine the rMT and MEP amplitudes (Figure 2), the dominant side with the lower rMT or the higher motor evoked potential amplitude when the rMT was equal. In the unilateral stimulation group, the dominant cerebellum was selected for rTMS, and then, the contralateral side was sham stimulated. In the bilateral group, the dominant side

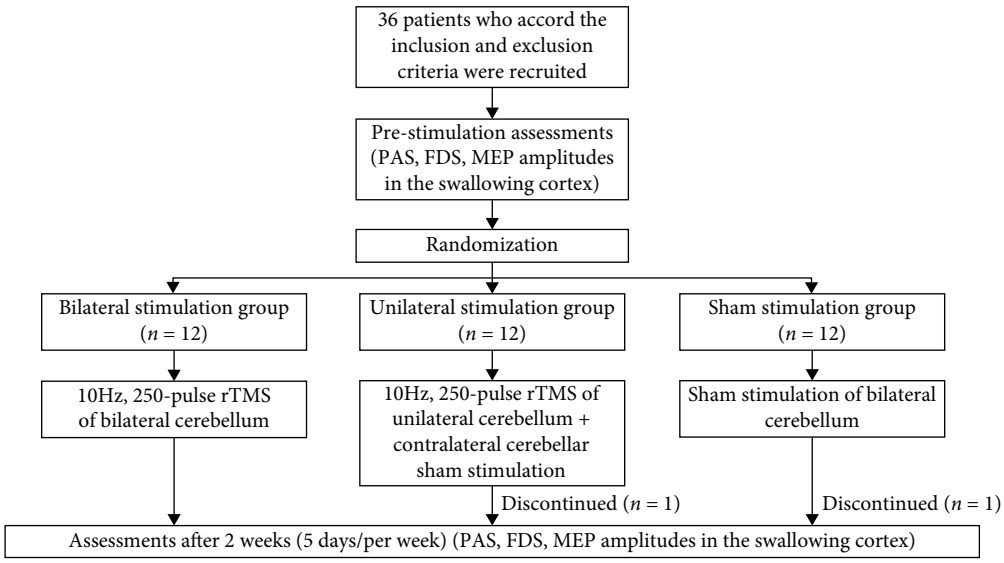

Figure 1: The study design and flow chart.

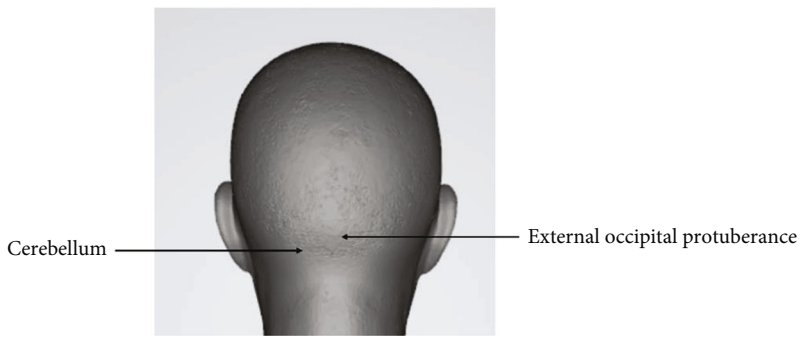

Figure 2: Schematic diagram of the cerebellum.

rTMS was performed first, followed by the contralateral side rTMS. In the sham stimulation group, the dominant side sham stimulus was performed first, followed by the contralateral side sham stimulus. The stimulus plan for each side was 10 Hz, 80% rMT, 250 pulses, 1 s per stimulus, and 9 s intervals. Sham rTMS was performed with the coil held at 90° to the scalp. Treatment was provided for a total of 2 weeks, 5 days a week, once a day. The 3 groups of patients received conventional dysphagia rehabilitation performed by a well-trained physical therapist after each rTMS treatment. Traditional swallowing function training included temperature stimulation, air pulse stimulation, taste stimulation, tongue resistance training, and throat lift training, and the training is about 20 minutes after the daily rTMS treatment.

2.3. Swallowing Function Assessments. According to the standard manual guidelines, a speech therapist performed the VFSS to assess the patients' swallowing function [18]. The VFSS is the gold standard for evaluating swallowing physiology and is commonly used in clinical settings [19]. In this study, the same protocol for the VFSS in the fluoroscopy laboratory was used for all subjects. Both lateral and posteroanterior images were obtained following oral administration of 5 ml of a thick liquid (fruit pudding) mixed with diluted barium. All materials were standardized. The FDS is a scale used to quantify the severity of dysphagia [20], and the PAS is used to evaluate airway invasion [21]. The FDS and PAS scores were determined by a speech therapist who was not informed about the study and patient grouping according to the VFSS.

2.4. Statistical Analysis. IBM SPSS Statistics 22.0 (IBM SPSS, Armonk, NY, USA) was used for the data analysis. Enumeration data were expressed as rates (%), and the chi-square test was adopted. Measurement data were expressed as the mean ± standard deviation (±sd), and the Kolmogorov–Smirnov test was used to determine whether the metrological data followed a normal distribution. Within-group comparisons before and after treatment were performed using paired t tests. The independent samples t test was utilized for comparisons between two groups. Comparisons among multiple groups were made using one-way analysis of variance with the LSD-t (homogeneity of variance) or Dunnett's T3 (heterogeneity of variance) post hoc test. The correlation analyses were performed using Pearson correlation. The difference

Table 1: Demographic and clinical characteristics of patients in the three study groups.

	Bilateral stimulation group	Unilateral stimulation group	Sham stimulation group	*P* value
No. of subjects	12	11	11	
Age (years)	49.67 ± 11.28	54.18 ± 10.54	57.55 ± 8.57	0.219
Sex (males : females)	6 : 6	7 : 4	6 : 5	0.815
Type of stroke (ischemia : hemorrhage)	11 : 1	10 : 1	9 : 2	0.821
Site of lesion (pons : medulla oblongata : multiple brainstem stroke)	9 : 2 : 1	8 : 1 : 2	9 : 1 : 1	0.830
Disease course (days)	25.5 ± 9.28	21 ± 5.7	24.91 ± 6.89	0.318
PAS (baseline scores)	6.5 ± 1.17	6.73 ± 1.19	6.55 ± 0.93	0.876
FDS (baseline scores)	24.33 ± 5.85	22.55 ± 4.89	23.36 ± 4.48	0.707

Values are presented as the number or mean ± standard deviation. PAS: penetration aspiration scale; FDS: functional dysphagia scale.

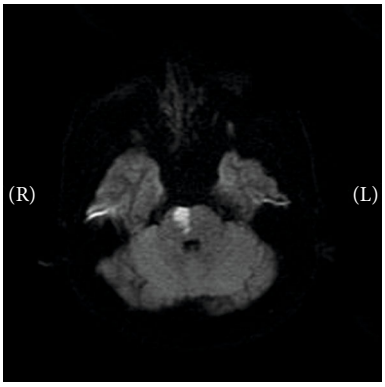

Figure 3: Pontine stroke.

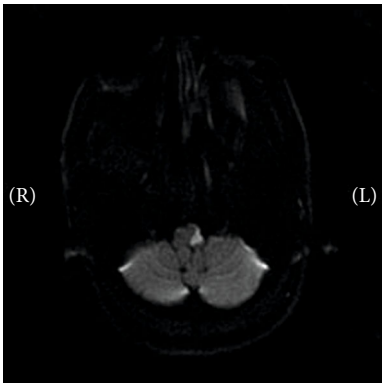

Figure 4: Medullary stroke.

was considered statistically significant when the *P* value was less than 0.05 ($P < 0.05$).

3. Results

A total of 36 eligible PSD patients were included in this study. At baseline, the three groups of patients had no significant differences in demographic and clinical characteristics, such as age, sex distribution, disease course, and PAS and FDS scores. During the study period, 1 person in the unilateral stimulation group dropped out due to personal reasons, and 1 person in the sham stimulation group fell off due to personal reasons. Thirty-four patients finally completed the experiment, and details are shown in Table 1. Several representative MRI images showed the lesions in Figures 3–5. Three patients (2 in the bilateral stimulation group and 1 in the unilateral stimulation group) experienced a short-term headache during the treatment, and all recovered within 5 minutes after the stimulation. No patients had seizures during or after the treatment.

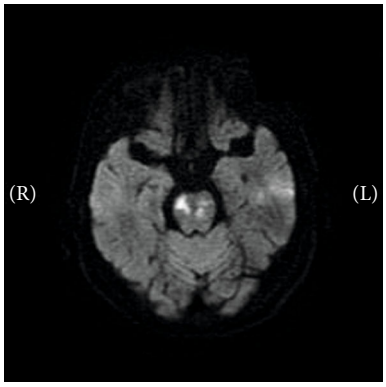

Figure 5: Multiple brainstem stroke.

3.1. Clinical Assessment. The paired *t* test results showed that the PAS and FDS scores of the patients in the unilateral stimulation group and bilateral stimulation group after 2 weeks of rTMS were better than those before treatment, but there was no significant change in the sham stimulation group. The results of one-way analysis of variance showed that after 2 weeks of treatment, the PAS and FDS scores of the unilateral stimulation group and bilateral stimulation group were better than those of the sham stimulation group, and there was no significant difference between the two groups (Figure 6). This finding indicates that cerebellar rTMS can promote the recovery of swallowing function in patients with brainstem stroke, and there is

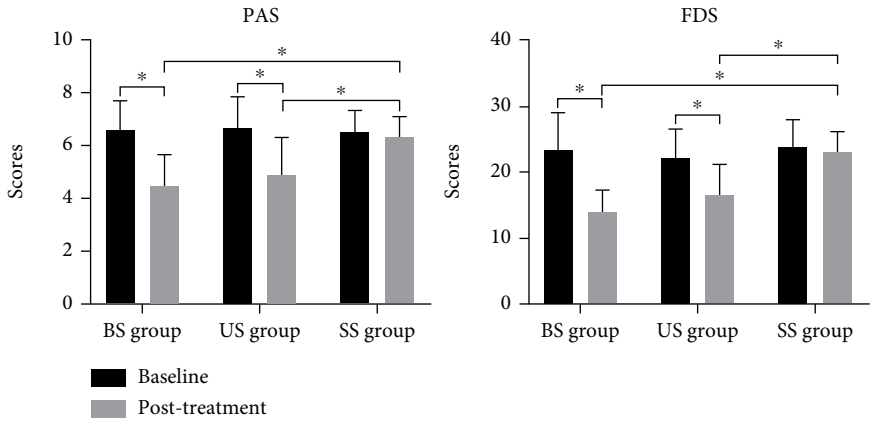

Figure 6: Changes in clinical swallowing function in patients after repeated transcranial magnetic stimulation. BS group: bilateral stimulation group; US group: unilateral stimulation group; SS group: sham stimulation group; PAS: penetration aspiration scale; FDS: functional dysphagia scale. $^{*}P < 0.05$.

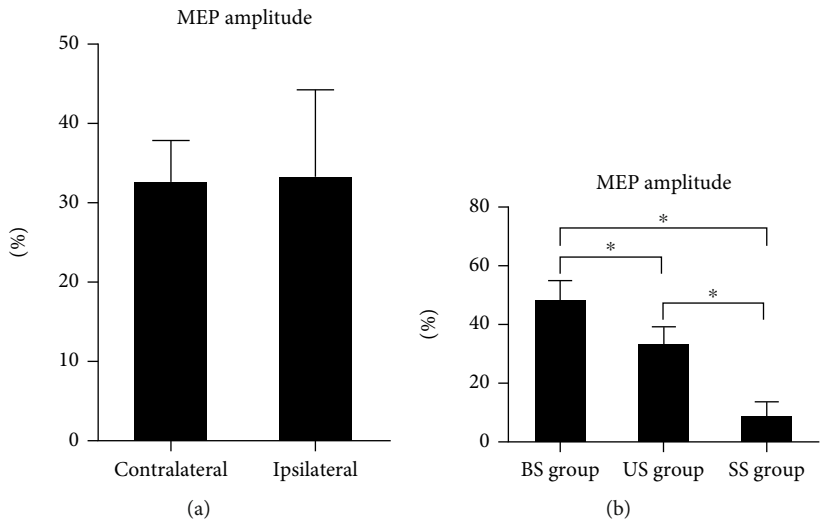

Figure 7: Changes in MEP amplitude in the motor area of the suprahyoid muscle group in the cerebral cortex after treatment. BS group: bilateral stimulation group; US group: unilateral stimulation group; SS group: sham stimulation group; MEP: motor evoked potential. (a) In the US group, the increase in MEP amplitude in the contralateral cerebral cortex (relative to the dominant cerebellum) was not different from that in the ipsilateral cerebral cortex (relative to the dominant cerebellum). (b) The increase in the MEP amplitude of the cerebral hemisphere in the BS group was higher than that in the other two groups, and the increase in MEP amplitude in the US group was higher than that in the SS group. $^{*}P < 0.05$.

no significant difference between unilateral stimulation and bilateral stimulation.

3.2. Neurophysiological Measurements. The independent sample t test results showed that after 2 weeks of treatment, the increase in MEP amplitude in the contralateral cerebral cortex (relative to the dominant cerebellum) in the unilateral stimulation group was not different from that in the ipsilateral cerebral cortex (relative to the dominant cerebellum) (Figure 7(a)). Since unilateral cerebellar rTMS has no difference in the influence of the MEP amplitude of the cerebral cortex on both sides, the bilateral average elevation amplitude was used for one-way analysis of variance. The results showed that the increase in the MEP amplitude of the cerebral hemisphere in the bilateral stimulation group was higher than that in the other two groups, and the increase in MEP amplitude of the unilateral stimulation group was higher than that of the sham stimulation group (Figure 7(b)). This finding indicates that cerebellar rTMS can improve the excitability of the representative regions of the mylohyoid muscle of a patient's bilateral brain. Unilateral cerebellar stimulation had no significant difference in the effects of the cerebral cortex on both sides, and the effect of bilateral stimulation was higher than that of unilateral stimulation.

3.3. Correlation Analyses. The results of the Pearson correlation analysis showed that there was no correlation between

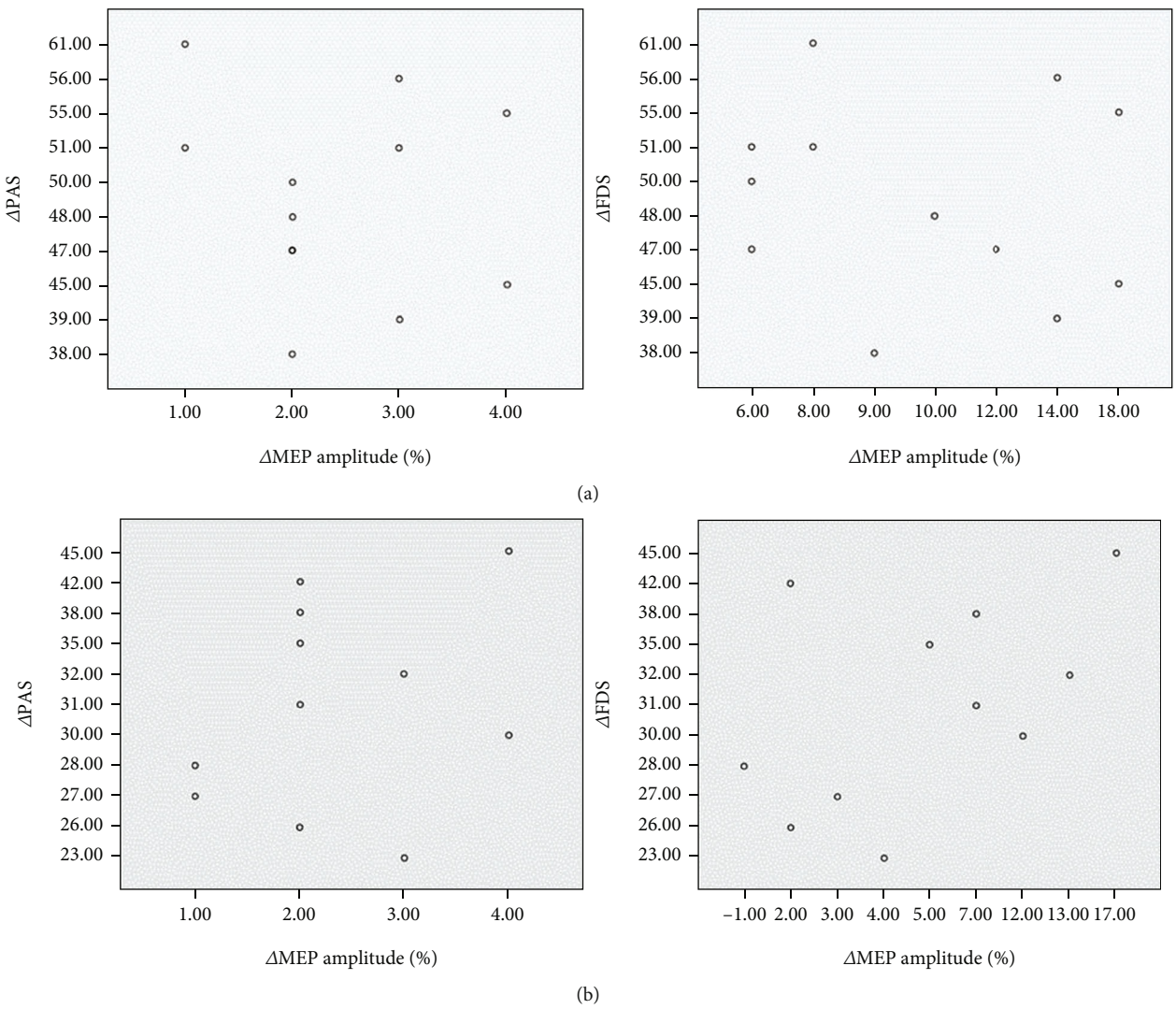

Figure 8: The results of the Pearson correlation analysis showed that there was no correlation between the improvement in patients' clinical swallowing function (ΔPAS: the improvement of PAS after treatment; ΔFDS: the improvement of FDS after treatment) and the increase in MEP amplitude (ΔMEP amplitude: the improvement of MEP amplitude after treatment) in either the unilateral stimulation group or the bilateral stimulation group. PAS: penetration aspiration scale; FDS: functional dysphagia scale; MEP: motor evoked potential. (a) The scatter plot of bilateral stimulation group; (b) the scatter plot of unilateral stimulation group.

the improvement of patients' clinical swallowing function (PAS scores and FDS scores) and the increase in MEP amplitude in either the unilateral stimulation group or the bilateral stimulation group (Figure 8). This finding indicates that the improvement in clinical swallowing function after cerebellar rTMS stimulation may not be directly related to the improvement in MEP amplitude in the representation of the mylohyoid muscle of the brain.

4. Discussion

The results of the study showed that, compared with sham stimulation, performing 10 Hz of excitatory rTMS on the mylohyoid muscle motor cortex of the cerebellum for 2 weeks can improve the clinical swallowing function of patients with dysphagia after brainstem stroke. There was no significant difference between unilateral stimulation and bilateral stimulation. Furthermore, regardless of unilateral stimulation or bilateral stimulation, an increase in the excitability of the motor cortex of the mylohyoid muscle was observed, and the increase in the bilateral group was higher than that in the unilateral group. There was no correlation between the improvement in clinical swallowing function and the increase in cerebral cortex excitability. rTMS is a noninvasive stimulation method to promote neurological recovery after stroke. The conclusion means that cerebellar high-frequency rTMS can improve swallowing function in patients with dysphagia after brainstem stroke and increase the excitability of bilateral cerebral swallowing cortex.

Compared to the known cortical swallowing pathways, the cerebellum and its connections to the brainstem and intracortical swallowing centres are poorly understood. Previous electrophysiological studies have shown that there may be simultaneous connections between unilateral cerebellar

hemisphere and bilateral cerebral cortical motor areas [15, 16, 22]. Vasant et al. conducted a study of cerebellar rTMS based on different parameters and found that 250 pulses of cerebellar rTMS (10 Hz) resulted in increased excitability of the bilateral swallowing cortex [15]. In addition, Sasegbon et al.'s study found that cerebellar rTMS was able to reverse the MEP effects and behavioural effects of cortical virtual damage inhibition. Consistent with the findings of previous studies, an improvement in the inhibitory effect was observed regardless of whether rTMS was applied to the ipsilateral or contralateral side of the virtual lesion [22]. Sasegbon et al. then further researched this topic and found that compared with unilateral cerebellar rTMS, bilateral cerebellar rTMS led to stronger changes in cerebral cortex excitability [16].

The cerebellum is connected to the brainstem through three pairs of cerebellar peduncles and communicates with various motor nuclei of the brainstem and motor areas of the cortex through these cerebellar peduncles [23]. On the contralateral side, the role of the cerebellum in the upwards transmission of information may be via the dentate nucleus of the cerebellar hemisphere. Efferent axons from the dentate nucleus enter the contralateral motor cortex after passing through the thalamus [24]. On the ipsilateral side, the pathway through which cerebellar rTMS functions may originate from the cerebellar parietal nucleus, which is in contact with components of the central pattern generator (CPG) in the brainstem [23]. CPGs are responsible for controlling swallowing and are closely associated with the bilateral motor cortex [25].

As early as 1998, Hamdy et al. showed that the recovery of swallowing function after unilateral cerebral cortical stroke may be related to the improvement of the function of the uninjured side of the cerebral swallowing cortex [26]. However, the exact mechanisms underlying the recovery of swallowing function after stroke remain unclear. In previous studies of rTMS in the treatment of PSD, the stimulation targets were mostly located in the cerebral cortex. One study focused on the unaffected cerebral cortex and attempted to apply high-frequency rTMS to improve unaffected cortical function to compensate for the affected hemisphere. The results showed that the application of high-frequency rTMS in the unaffected cerebral hemisphere can improve the PAS score of PSD patients, and the treatment effect can be sustained for at least two weeks after the end of treatment [27]. In addition, one study showed that combined stimulation of bilateral cerebral cortex appeared to be more effective than unilateral stimulation. This study demonstrates that 10 Hz bilateral high-frequency rTMS can improve swallowing function in patients with PSD. After 2 weeks of treatment, the patients' swallowing function and risk of aspiration were improved compared with those before treatment, and the effect was better than unilateral stimulation group [28]. Unfortunately, both studies mainly included patients with hemispheric stroke. Few studies have studied brainstem stroke. One study has shown that high-frequency rTMS in the cerebral pharyngeal motor cortex can improve clinical function in patients with dysphagia after brainstem stroke [29]. High-frequency rTMS in the bilateral pharyngeal motor cortex may increase the excitability of corticobulbar projections to the brainstem swallowing nucleus, leading to improved swallowing function. High-frequency rTMS in the cerebellum can also improve cerebral swallowing cortex excitability in healthy volunteers and PSD patients simulated by virtual damage [15, 16, 22]. In addition, the cerebellum is connected to the brainstem through three cerebellar peduncles, which communicate directly with various motor nuclei of the brainstem [23]. Since our correlation analysis found that the recovery of swallowing function in PSD patients was not correlated to the improvement of the excitability of the swallowing motor area of the cerebral cortex, it suggested that the recovery of swallowing function in these patients may be the result of the joint actions of multiple brain regions. We hypothesize that cerebellar high-frequency rTMS can directly and positively affect the brainstem via the cerebellar angle and indirectly excite the brainstem via excitatory effects on the swallowing cortex of the brain, resulting in improved swallowing.

In the present study, we found that both the unilateral cerebellar stimulation group and the bilateral stimulation group had increased excitability of the representation of swallowing in the bilateral cerebral cortex, while the sham stimulation group had no change. The increase in the bilateral group was higher than that in the unilateral group, and this greater excitatory effect may be due to greater stimulus input. Unfortunately, this change was not reflected in the clinical effect. Although the clinical swallowing function scores of the unilateral and bilateral groups were better than those of the sham stimulation group, there was no significant difference between the two groups. This may imply that changes in cortical excitability caused by bilateral stimulation are not sufficient to make a difference in the clinical effect.

Unlike previous studies [28, 30–34], the patients' clinical swallowing function in the sham stimulation group (traditional rehabilitation training) in our study did not improve. In previous studies, few patients with brainstem stroke were included because there was no restriction on the stroke site of the patients. We believe that differences in injury site may lead to different treatment effects. This suggests that dysphagia caused by damage to the swallowing center in the brainstem may be more difficult to recover. This means that rTMS may play a more important role in patients with brainstem injury than in patients with cerebral cortical stroke.

Overall, an earlier study by Vasant et al. identified the optimal parameters for cerebellar rTMS to improve cortical excitability [15]. Sasegbon simulated stroke patients through virtual damage and found that cerebellar rTMS could affect the inhibitory MEP effects and behavioural effects caused by the virtual damage, and the effect of bilateral cerebellar stimulation was higher than that of unilateral stimulation [16, 22]. Our study confirmed that cerebellar rTMS is beneficial for the recovery of swallowing function in patients with PSD; by treating patients with brainstem stroke with rTMS, the excitability of the swallowing cortex in the bilateral cerebral hemispheres can be improved.

5. Conclusion

High-frequency rTMS in the cerebellum can improve swallowing function in PSD patients and increase the excitability of the representation of swallowing in the bilateral cerebral hemispheres. Compared with unilateral cerebellar rTMS, bilateral stimulation increased the excitability of the cerebral swallowing cortex more significantly, but there was no significant difference in the improvement of clinical swallowing function. The improvement in the clinical swallowing function of the patients was not correlated with the increased excitability of the swallowing motor area of the cerebral cortex.

6. Limitation

Because electrophysiological assessments can only be applied to the swallowing cortex, changes in brainstem function in patients were not assessed in this study. The correlation analysis results showed that there was no significant correlation between the excitability changes of bilateral cerebral cortex and the improvement of swallowing function. This suggests that the effects of cerebellar rTMS on swallowing do not only work by improving the swallowing excitatory cortex of the brain. In future studies, the exact mechanism by which cerebellar rTMS affects swallowing function should be further explored.

Data Availability

The data that support the findings of this study are available from the corresponding author upon reasonable request.

Conflicts of Interest

The authors declare that they have no conflicts of interest.

Authors' Contributions

Linghui Dong, Pingping Meng, and Xiaona Pan contributed to conception and design of the study. Linghui Dong and Chao Han conducted data collection. Linghui Dong and Yuyang Wang performed the statistical analysis. Linghui Dong wrote the first draft of the manuscript. Pingping Meng, Qiang Wang, Chao Han, and Guangtao Bai wrote sections of the manuscript. All authors contributed to manuscript revision and read and approved the submitted version.

Acknowledgments

This work was supported by the Key Research & Development Projects of Shandong Province (grant no. 2019GSF108262).

References

[1] L. Rofes, N. Vilardell, and P. Clavé, "Post-stroke dysphagia: progress at last," *Neurogastroenterology and Motility*, vol. 25, no. 4, pp. 278–282, 2013.

[2] M. Arnold, K. Liesirova, A. Broeg-Morvay et al., "Dysphagia in acute stroke: incidence, burden and impact on clinical outcome," *PLoS One*, vol. 11, no. 2, article e0148424, 2016.

[3] A. Timmerman, R. Speyer, B. Heijnen, and I. Klijn-Zwijnenberg, "Psychometric characteristics of health-related quality-of-life questionnaires in oropharyngeal dysphagia," *Dysphagia*, vol. 29, no. 2, pp. 183–198, 2014.

[4] D. Smithard, P. O'Neill, C. Parks, and J. Morris, "Complications and outcome after acute stroke. Does dysphagia matter?," *Stroke*, vol. 29, no. 7, 1998.

[5] D. Smithard, P. O'Neill, R. England et al., "The natural history of dysphagia following a stroke," *Dysphagia*, vol. 12, no. 4, pp. 188–193, 1997.

[6] O. Jones, J. Cartwright, A. Whitworth, and N. Cocks, "Dysphagia therapy post stroke: an exploration of the practices and clinical decision-making of speech-language pathologists in Australia," *International Journal of Speech-Language Pathology*, vol. 20, no. 2, pp. 226–237, 2018.

[7] D. L. Cohen, C. Roffe, J. Beavan et al., "Post-stroke dysphagia: a review and design considerations for future trials," *International Journal of Stroke*, vol. 11, no. 4, pp. 399–411, 2016.

[8] D. G. Smithard, "Dysphagia management and stroke units," *Current Physical Medicine and Rehabilitation Reports*, vol. 4, no. 4, pp. 287–294, 2016.

[9] C. Geeganage, J. Beavan, S. Ellender, and P. Bath, "Interventions for dysphagia and nutritional support in acute and subacute stroke," *Cochrane Database of Systematic Reviews*, vol. 10, article CD000323, 2000.

[10] M. Suzuki, Y. Asada, J. Ito, K. Hayashi, H. Inoue, and H. Kitano, "Activation of cerebellum and basal ganglia on volitional swallowing detected by functional magnetic resonance imaging," *Dysphagia*, vol. 18, no. 2, pp. 71–77, 2003.

[11] I. Humbert and J. Robbins, "Normal swallowing and functional magnetic resonance imaging: a systematic review," *Dysphagia*, vol. 22, no. 3, pp. 266–275, 2007.

[12] K. Mosier and I. Bereznaya, "Parallel cortical networks for volitional control of swallowing in humans," *Experimental Brain Research*, vol. 140, no. 3, pp. 280–289, 2001.

[13] V. Jayasekeran, J. Rothwell, and S. Hamdy, "Non-invasive magnetic stimulation of the human cerebellum facilitates cortico-bulbar projections in the swallowing motor system," *Neurogastroenterology and Motility*, vol. 23, no. 9, 2011.

[14] J. Lefaucheur, A. Aleman, C. Baeken et al., "Evidence-based guidelines on the therapeutic use of repetitive transcranial magnetic stimulation (rTMS): an update (2014-2018)," *Clinical Neurophysiology*, vol. 131, no. 2, pp. 474–528, 2020.

[15] D. H. Vasant, E. Michou, S. Mistry, J. Rothwell, and S. Hamdy, "High-frequency focal repetitive cerebellar stimulation induces prolonged increases in human pharyngeal motor cortex excitability," *The Journal of Physiology*, vol. 593, no. 22, pp. 4963–4977, 2015.

[16] A. Sasegbon, C. J. Smith, P. Bath, J. Rothwell, and S. Hamdy, "The effects of unilateral and bilateral cerebellar rTMS on human pharyngeal motor cortical activity and swallowing behavior," *Experimental Brain Research*, vol. 238, no. 7-8, pp. 1719–1733, 2020.

[17] D. Vasant, A. Sasegbon, E. Michou, C. Smith, and S. Hamdy, "Rapid improvement in brain and swallowing behavior induced by cerebellar repetitive transcranial magnetic stimulation in poststroke dysphagia: a single patient case-controlled

study," *Neurogastroenterology and Motility*, vol. 31, no. 7, article e13609, 2019.

[18] M. Alvarez, M. Turbino, C. Barros, V. Pagnano, and O. Bezzon, "Comparative study of intermaxillary relationships of manual and swallowing methods," *Brazilian Dental Journal*, vol. 20, no. 1, pp. 78–83, 2009.

[19] M. Rugiu, "Role of videofluoroscopy in evaluation of neurologic dysphagia," *Acta Otorhinolaryngolica Italica*, vol. 27, no. 6, pp. 306–316, 2007.

[20] T. Han, N. Paik, and J. Park, "Quantifying swallowing function after stroke: a functional dysphagia scale based on videofluoroscopic studies," *Archives of Physical Medicine and Rehabilitation*, vol. 82, no. 5, pp. 677–682, 2001.

[21] N. Pizzorni, E. Crosetti, E. Santambrogio et al., "The penetration-aspiration scale: adaptation to open partial laryngectomy and reliability analysis," *Dysphagia*, vol. 35, no. 2, pp. 261–271, 2020.

[22] A. Sasegbon, M. Watanabe, A. Simons et al., "Cerebellar repetitive transcranial magnetic stimulation restores pharyngeal brain activity and swallowing behaviour after disruption by a cortical virtual lesion," *The Journal of Physiology*, vol. 597, no. 9, pp. 2533–2546, 2019.

[23] T. Roostaei, A. Nazeri, M. Sahraian, and A. Minagar, "The human cerebellum," *Neurologic Clinics*, vol. 32, no. 4, pp. 859–869, 2014.

[24] A. Errante, S. Ziccarelli, G. Mingolla, and L. Fogassi, "Grasping and manipulation: neural bases and anatomical circuitry in humans," *Neuroscience*, vol. 458, no. 458, pp. 203–212, 2021.

[25] I. Steuer and P. Guertin, "Central pattern generators in the brainstem and spinal cord: an overview of basic principles, similarities and differences," *Reviews in the Neurosciences*, vol. 30, no. 2, pp. 107–164, 2019.

[26] S. Hamdy, Q. Aziz, J. Rothwell et al., "Recovery of swallowing after dysphagic stroke relates to functional reorganization in the intact motor cortex," *Gastroenterology*, vol. 115, no. 5, pp. 1104–1112, 1998.

[27] J. Park, J. Oh, J. Lee, J. Yeo, and K. Ryu, "The effect of 5Hz high-frequency rTMS over contralesional pharyngeal motor cortex in post-stroke oropharyngeal dysphagia: a randomized controlled study," *Neurogastroenterology and Motility*, vol. 25, no. 4, 2013.

[28] E. Park, M. Kim, W. Chang et al., "Effects of bilateral repetitive transcranial magnetic stimulation on post-stroke dysphagia," *Brain Stimulation*, vol. 10, no. 1, pp. 75–82, 2017.

[29] E. Khedr and N. Abo-Elfetoh, "Therapeutic role of rTMS on recovery of dysphagia in patients with lateral medullary syndrome and brainstem infarction," *Journal of Neurology, Neurosurgery, and Psychiatry*, vol. 81, no. 5, pp. 495–499, 2010.

[30] L. Kim, M. Chun, B. Kim, and S. Lee, "Effect of repetitive transcranial magnetic stimulation on patients with brain injury and dysphagia," *Annals of Rehabilitation Medicine*, vol. 35, no. 6, pp. 765–771, 2011.

[31] K. Lim, H. Lee, J. Yoo, and Y. Kwon, "Effect of low-frequency rTMS and NMES on subacute unilateral hemispheric stroke with dysphagia," *Annals of Rehabilitation Medicine*, vol. 38, no. 5, pp. 592–602, 2014.

[32] J. Du, F. Yang, L. Liu et al., "Repetitive transcranial magnetic stimulation for rehabilitation of poststroke dysphagia: a randomized, double-blind clinical trial," *Clinical Neurophysiology*, vol. 127, no. 3, pp. 1907–1913, 2016.

[33] M. Tarameshlu, N. Ansari, L. Ghelichi, and S. Jalaei, "The effect of repetitive transcranial magnetic stimulation combined with traditional dysphagia therapy on poststroke dysphagia: a pilot double-blinded randomized-controlled trial," *International Journal of Rehabilitation Research*, vol. 42, no. 2, pp. 133–138, 2019.

[34] N. Ünlüer, Ç. Temuçin, N. Demir, S. Serel Arslan, and A. Karaduman, "Effects of low-frequency repetitive transcranial magnetic stimulation on swallowing function and quality of life of post-stroke patients," *Dysphagia*, vol. 34, no. 3, pp. 360–371, 2019.

Hindawi
Neural Plasticity
Volume 2022, Article ID 4203698, 10 pages
https://doi.org/10.1155/2022/4203698

Research Article

Performance Comparison of Different Neuroimaging Methods for Predicting Upper Limb Motor Outcomes in Patients after Stroke

Jingyan Tao,[1] **Zhaoqing Li**,[2,3] **Yang Liu**,[1] **Jianhua Li**,[1] **and Ruiliang Bai**[2,3,4]

[1]*Department of Physical and Rehabilitation Medicine, Sir Run Run Shaw Hospital, School of Medicine, Zhejiang University, Hangzhou 310029, China*
[2]*Department of Physical and Rehabilitation Medicine of Sir Run Run Shaw Hospital and Interdisciplinary Institute of Neuroscience and Technology, School of Medicine, Zhejiang University, Hangzhou 310029, China*
[3]*Key Laboratory of Biomedical Engineering of Ministry of Education, College of Biomedical Engineering and Instrument Science, Zhejiang University, Hangzhou 310029, China*
[4]*MOE Frontier Science Center for Brain Science and Brain-Machine Integration, School of Brain Science and Brain Medicine, Zhejiang University, Hangzhou 310029, China*

Correspondence should be addressed to Zhaoqing Li; lizhaoqing@zju.edu.cn, Jianhua Li; zjdxsyfkfk@126.com, and Ruiliang Bai; ruiliangbai@zju.edu.cn

Received 3 November 2021; Revised 17 March 2022; Accepted 17 May 2022; Published 6 June 2022

Academic Editor: Yating Lv

Several neuroimaging methods have been proposed to assess the integrity of the corticospinal tract (CST) for predicting recovery of motor function after stroke, including conventional structural magnetic resonance imaging (sMRI) and diffusion tensor imaging (DTI). In this study, we aimed to compare the predicative performance of these methods using different neuroimaging modalities and optimize the prediction protocol for upper limb motor function after stroke in a clinical environment. We assessed 28 first-ever stroke patients with upper limb motor impairment. We used the upper extremity module of the Fugl-Meyer assessment (UE-FM) within 1 month of onset (baseline) and again 3 months poststroke. sMRI (T1- and T2-based) was used to measure CST-weighted lesion load (CST-wLL), and DTI was used to measure the fractional anisotropy asymmetry index (FAAI) and the ratio of fractional anisotropy (rFA). The CST-wLL within 1 month poststroke was closely correlated with upper limb motor outcomes and recovery potential. CST-wLL ≥ 2.068 cc indicated serious CST damage and a poor outcome (100%). CST-wLL < 1.799 cc was correlated with a considerable rate (>70%) of upper limb motor function recovery. CST-wLL showed a comparable area under the curve (AUC) to that of the CST-FAAI ($p = 0.71$). Inclusion of extra-CST-FAAI did not significantly increase the AUC ($p = 0.58$). Our findings suggest that sMRI-derived CST-wLL is a precise predictor of upper limb motor outcomes 3 months poststroke. We recommend this parameter as a predictive imaging biomarker for classifying patients' recovery prognosis in clinical practice. Conversely, including DTI appeared to induce no significant benefits.

1. Introduction

Stroke is a major disease that can lead to disability. Upper limb motor impairment is common after a stroke and may compromise patients' quality of life and severely affect their daily living [1, 2]. Predicting relevant upper limb motor outcomes and recovery potential is challenging for rehabilitation therapists and clinicians. Previous studies have explored several clinical scales and imaging techniques to identify the relevant predictors for motor recovery after stroke. Early studies predicted motor outcome by clinically assessing initial motor dysfunction [3]. Wegen et al. [4] proposed that two simple movements, shoulder abduction and finger extension, within 72 hours after stroke could predict recovery of hemiplegic upper limb function at 6 months. Increasing studies have tried to predict motor outcomes by neuroimaging markers measuring the structural integrity of the CST or the excitability of the motor cortex. For example, task-related brain activation in functional magnetic resonance imaging (fMRI) was correlated with hand function

recovery [5]. fMRI activation in the supplementary motor area obtained early after stroke provided independent prediction of long-term motor outcome [6]. Several studies have predicted recovery based on brain structural MRI (sMRI) or diffusion tensor imaging (DTI) [7–11].

Early conventional sMRI (e.g., T1- or T2-based MRI) showed that lesion size was correlated with motor dysfunction [7, 8, 12]. DTI-based studies further indicated that the lesion location, especially those involving critical structures such as motion-related cortical areas (primary and non-primary motor areas), the corona radiata, the posterior limb of the internal capsule (PLIC) [13], and the CST, could predict upper limb function recovery potential [9–11]. DTI-derived metrics of the CST, specifically the fractional anisotropy asymmetry index (FAAI) and the ratio of fractional anisotropy (rFA) between ipsi- and contralesional CST, are the most frequently used predictor variables in prognostic studies [14, 15]. Some studies quantified lesion size and location as the concept of lesion load—a combined measure of the stroke lesion overlapped with a canonical CST [16, 17]. Feng et al. [16] reported that CST-wLL in the acute phase was a strong predictor of upper limb motor recovery at 3 months.

Structural imaging analysis is usually based on DTI. However, owing to its costs and hardware requirements, DTI is not routinely performed in stroke and rehabilitation units, especially in developing countries. T1- and T2-weighted images are involved in early MRI scans after strokes. Few studies have compared the performance of sMRI-derived CST-wLL and DTI-derived metrics for predicting recovery of upper limb motor function. In this study, we aimed to optimize the clinical prediction model protocol in the clinical environment by comparing the performances of different neuroimaging modalities. We focused on whether including DTI would significantly benefit patients. Thus, we quantitatively analyzed the CST-wLL, which is calculated from the lesion volume in the T2 image overlaid on the CST map from the standard template. Further, we explored the relationship between the CST-wLL and upper limb motor function after stroke and compared them with other DTI-derived predictor variables. We hypothesized that compared with DTI-derived metrics, CST-wLL can more precisely predict upper limb motor recovery after stroke.

2. Methods

2.1. Study Participants. This prospective study included patients with first-onset stroke exhibiting varying degrees of unilateral limb motor impairment. Clinical and neuroimaging assessments were performed within 1 month after the stroke (baseline), and motor function recovery was followed up at least 3 months after the stroke. All participants were inpatients at the Department of Physical and Rehabilitation Medicine, Sir Run Run Shaw Hospital, School of Medicine, Zhejiang University, between 2017 and 2021, who underwent 1-month inpatient rehabilitation treatment including standard physical therapy and occupational therapy (Figure 1). The clinical trial was conducted in accordance with the Helsinki Declaration after approval by the Ethics Committee of the Sir Run Run Shaw Hospital and Zhejiang University School of Medicine. All relevant procedures were conducted with patients' full understanding and receipt of their written consent. Inclusion criteria were (1) cerebral hemisphere infarction (ischemic) confirmed via routine MRI scanning, (2) first-onset stroke, (3) hemiplegia of one limb within 1 month after onset, (4) stroke subtype based on TOAST criteria: large vessel atherosclerotic disease, and (5) age > 18 years. Exclusion criteria were (1) infarcts in both cerebral hemispheres, (2) cerebral hemorrhage or hemorrhage after stroke, (3) disturbance of consciousness, (4) unstable vital signs or failure of vital organs, (5) inability to remain in a supine position for 20 minutes, (6) MRI contraindications, (7) previous history of other neurological or orthopedic diseases that may have affected upper limb function, and (8) history of severe dementia or depression not controlled by medication. Patients were reassessed 3 months after their stroke.

2.2. Clinical Measures. The upper extremity (UE) module of the Fugl-Meyer assessment (UE-FM) was conducted within the baseline period (within 1 month of onset) and 3 months after the stroke. The UE-FM scale contains 33 items to comprehensively quantify upper limb motor impairment. The therapist, who was blinded to the imaging results, observed 30 voluntary UE motions and 3 tendon tap responses and provided an ordinal rating (2 = approximate to normal ability/response, 1 = partial ability, and 0 = unable to perform/no response). The scores were added to obtain a total score and recorded (66 maximum). Higher scores indicated less limb impairment; lower scores indicated more limb impairment. The scale has excellent intrarun and interrun reliability, test-retest reliability, and internal consistency [18].

2.3. Image Processing and Data Analysis. The GE Discovery 750 W 3.0 THD dual-gradient 16-channel MRI system with an 8-channel head and neck combined coil was used for the MRI. T1-weighted high-resolution imaging, T2 fluid-attenuated inversion recovery (FLAIR) imaging, and DTI were performed. Structural T1-weighted images were obtained using fast gradient echo sequencing prepared via three-dimensional (3D) magnetization (repetition time: 8.5 ms; echo time: 3.9 ms; 150 slices; voxel size: $1 \times 1 \times 1$ m m^3). Additional neuroimaging sequencing parameters were T2 FLAIR (repetition time: 11000 ms; echo time: 125 ms; 31 slices; voxel size: $0.49 \times 0.49 \times 6.50\ mm^3$) and DTI (32 directions; *b*-value: 1000 seconds/mm^2; 60 slices; voxel size: $1.75 \times 1.75 \times 1.75\ mm^3$, TR = 8000 ms, TE = 80.7 ms). Neuroimaging data were analyzed by radiologists who were blinded to all clinical data.

2.4. Calculation of CST-wLL. Images were preprocessed with FSL 5.0.9 (https://fsl.fmrib.ox.ac.uk/fsl/) [19]. Lesion areas were manually drawn on the T2 image, which was linearly matched with the respective T1-weighted image and then transformed to the lesion mask. The CST-wLL was calculated using MATLAB with homemade script as previously described [17]. In contrast to Lin et al. [17], the canonical

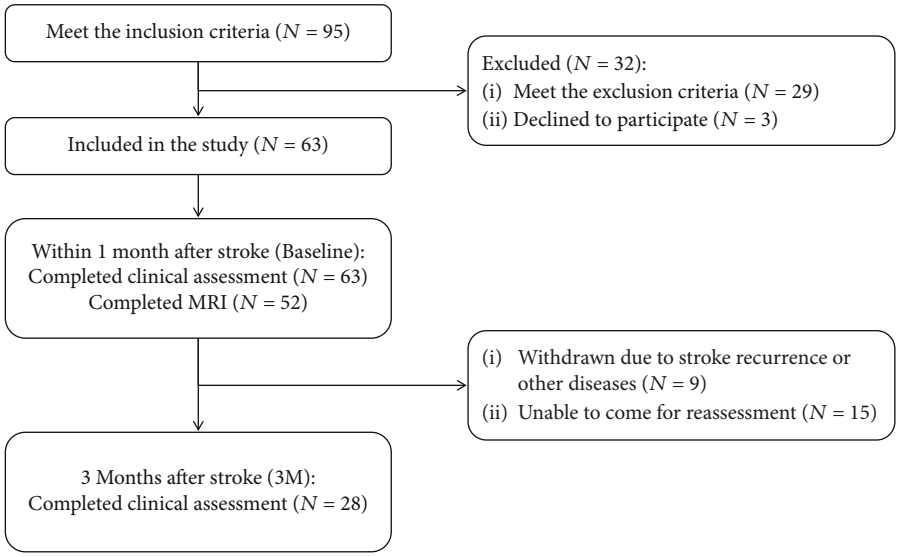

Figure 1: Flowchart of the recruitment process.

Table 1: Patient characteristics. N (%) for categorical variables; mean ± SD for continuous variables. UE-FM outcome groups: severe: 3M UE-FM score, ≤25; mild-moderate: 3M UE-FM score, 26–66. p value: the statistical difference between two groups of patients.

Variable	All (n = 28)	UE-FM outcome groups		p value
		Severe (n = 9)	Mild-moderate (n = 19)	
Sex				
Male	19 (67.9%)	8 (88.9%)	11 (57.9%)	0.20
Female	9 (32.1%)	1 (11.1%)	8 (42.1%)	
Age (years)	62.8 ± 9.7	60.3 ± 10.2	63.9 ± 9.5	0.39
Education (years)	8 ± 2.9	9 ± 3.7	7.6 ± 2.5	0.32
Days of baseline MRI	19.8 ± 6.1	21 ± 6.3	19.2 ± 6.1	0.49
Days of baseline UE-FM	16.6 ± 6.8	17.7 ± 7.1	16.2 ± 6.8	0.60
Days of 3M UE-FM	112 ± 16.4	114.9 ± 20.5	110.7 ± 14.5	0.59
Baseline UE-FM score	19.6 ± 16.4	6.3 ± 3.0	25.9 ± 16.4	<0.001
3M UE-FM score	39.4 ± 19.9	13.6 ± 5	51.6 ± 9.5	<0.001
FM Pct (%)	47.5 ± 30.5	12 ± 8.7	64.3 ± 20.8	<0.001

Table 2: MRI statistics. Mean ± SD and median (P25, P75) for continuous variables. UE-FM outcome groups: severe: 3M UE-FM score, ≤25; mild-moderate, 3M UE-FM score, 26–66. p value: the statistical difference between two groups of patients. Log-lesion size: log-transformed lesion size.

Variable	All (n = 28)	UE-FM outcome groups		p value
		Severe (n = 9)	Mild-moderate (n = 19)	
Lesion size (cc)	4.906 (3.539, 11.732)	24.080 (10.052, 34.955)	3.964 (2.853, 6.213)	0.002
Log-lesion size	0.803 ± 0.521	1.286 ± 0.503	0.575 ± 0.351	0.002
LL (cc)	1.372 ± 0.947	2.128 ± 0.996	1.013 ± 0.695	0.011
CST-wLL (cc)	1.431 ± 1.464	2.714 ± 1.789	0.823 ± 0.760	0.013
PLIC-rFA	0.747 ± 0.158	0.592 ± 0.139	0.820 ± 0.106	0.001
PLIC-FAAI	0.155 ± 0.111	0.265 ± 0.108	0.103 ± 0.065	0.002
CST-rFA	0.795 ± 0.126	0.666 ± 0.119	0.856 ± 0.072	0.001
CST-FAAI	0.119 ± 0.081	0.205 ± 0.078	0.079 ± 0.042	0.001

Table 3: Correlation analysis. $^{**}p < 0.001$, $^{*}p < 0.05$.

	3M UE-FM	UE-FM Pct
Log-lesion size	−0.67**	−0.645**
LL	−0.623**	−0.614*
CST-wLL	−0.688**	−0.615**
PLIC-rFA	0.739**	0.62**
PLIC-FAAI	−0.739**	−0.628**
CST-rFA	0.774**	0.677**
CST-FAAI	−0.788**	−0.691**

Table 4: Univariate regression analysis.

	3M UE-FM		UE-FM Pct	
	R^2	p value	R^2	p value
Lesion size	0.271	0.005	0.224	0.011
LL	0.388	<0.001	0.377	<0.001
CST-wLL	0.473	<0.001	0.378	<0.001
PLIC-rFA	0.546	<0.001	0.384	<0.001
PLIC-FAAI	0.546	<0.001	0.394	<0.001
CST-rFA	0.599	<0.001	0.458	<0.001
CST-FAAI	0.62	<0.001	0.477	<0.001

CST used in this study was determined by nonlinearly registering the CST template from the Natbrainlab (http://www.natbrainlab.co.uk/atlas-maps) [20] into the T1-weighted images. Images were visually checked at each step for quality control of the image registration. The weighted overlap was introduced with consideration of the narrowing of the CST as it descends from the motor cortex to the PLIC. The weighted factor in each slice was calculated by multiplying the lesion-tract overlap on each slice by the ratio of the maximum cross-sectional area of the tract to the cross-sectional area of the tract on that particular slice. For a particular slice, z, containing $n(z, I)$ voxels with intensity $\geq I$, the weighted factor $f(z, I)$ was calculated as

$$f(z, I) = \frac{n(z^*, I)}{n(z, I)}, \tag{1}$$

where $n(z^*, I)$ indicates the number of voxels on slice z^* containing the most voxels of intensity $\geq$ I. For each patient, the wLL volume was calculated using

$$V_{\text{weighted}} = \sum_{m=1}^{m_{\max}} (V_{\text{raw}} \bullet f(z(m), I(m)), \tag{2}$$

where $m_{\max}$ is the total number of intersecting voxels between the lesion map and CST map, $I(m)$ is the intensity of the mth voxel located on slice $z(m)$, and $f(z(m), I(m)$ is the weighting factor for the voxel.

2.5. FAA Estimation of CST and PLIC. The CST (or PLIC) fractional anisotropy asymmetry (FAA) is defined as the mean rFA between the affected (FAaff) and the unaffected (FAunaff) CST (or PLIC): rFA = FAunaff/FAaff. The FAAI was computed as a ratio: FAAI = (FAunaff − FAaff)/(FAunaff + FAaff) [21]. Before calculating the FAA of each patient's CST and PLIC, the diffusion MRI data were preprocessed in TORTOISE to correct for motion, eddy current, and geometric distortion [22, 23], and the diffusion data (the B0 image) were registered into respective T1-weighted images. We then estimated the diffusion tensor using a nonlinear least squares method in TORTOISE and generated a map of FA values.

The CST determined by calculating the weighted lesion-CST overlap was also used here. The MNI152 T1 template with 2 mm resolution was nonlinearly registered into patients' T1-weighted images, and the generated 3D deformation field was used on the PLIC template from JHU (http://neurovault.org/) to transform it to each patient's T1-weighted image space. Finally, the FAA estimations of CST and PLIC were calculated in MATLAB using a homemade script.

2.6. Statistical Analysis. The primary outcome was the UE-FM score 3 months after the stroke (3M UE-FM), and the secondary outcome was the UE-FM recovery percentage (UE-FM Pct). The mean and standard deviation (SD) were used to express normally distributed data; the median (P25–P75) and interquartile range were used to express nonnormally distributed data. Student's t-test and analysis of variance were used for normally distributed variables; the Mann-Whitney U test was used for asymmetrically distributed variables. Normally distributed variables were analyzed via Pearson correlation, and all others were analyzed via Spearman's rank correlation. Univariate and multivariate regression analyses were conducted to assess the factors influencing 3M UE-FM or UE-FM Pct. Feng et al. [16] defined UE-FM scores ≤ 25 at 3 months as poor motor outcomes. The UE-FM recovery percentage was defined as UE − FM Pct = [(3M UE-FM) − (baseline UE-FM)]/[66 − (baseline UE-FM)] [24]. Receiver operating characteristic (ROC) curve analysis was used to evaluate the cut-off point for CST-wLL on the baseline with the greatest sensitivity and specificity for predicting UE-FM 3 months poststroke and the UE-FM recovery percentage. The DeLong test was used to estimate the difference between ROC models. Statistical analyses were conducted in SPSS for Windows version 25.0 (SPSS Inc., Chicago, IL, USA) and software R (version 4.0.5). Statistical significance was defined as $p < 0.05$.

3. Results

3.1. Patient Characteristics. Twenty-eight patients completed the imaging and clinical assessments at both the baseline and 3-month follow-up (Figure 1). Table 1 summarizes the clinical characteristics and baseline assessments. Patients' ages ranged from 46 to 83 years. Patients were assessed at 7–29 days after stroke onset and reassessed at 90–191 days. MRIs were scanned 10–31 days after onset. From a possible high

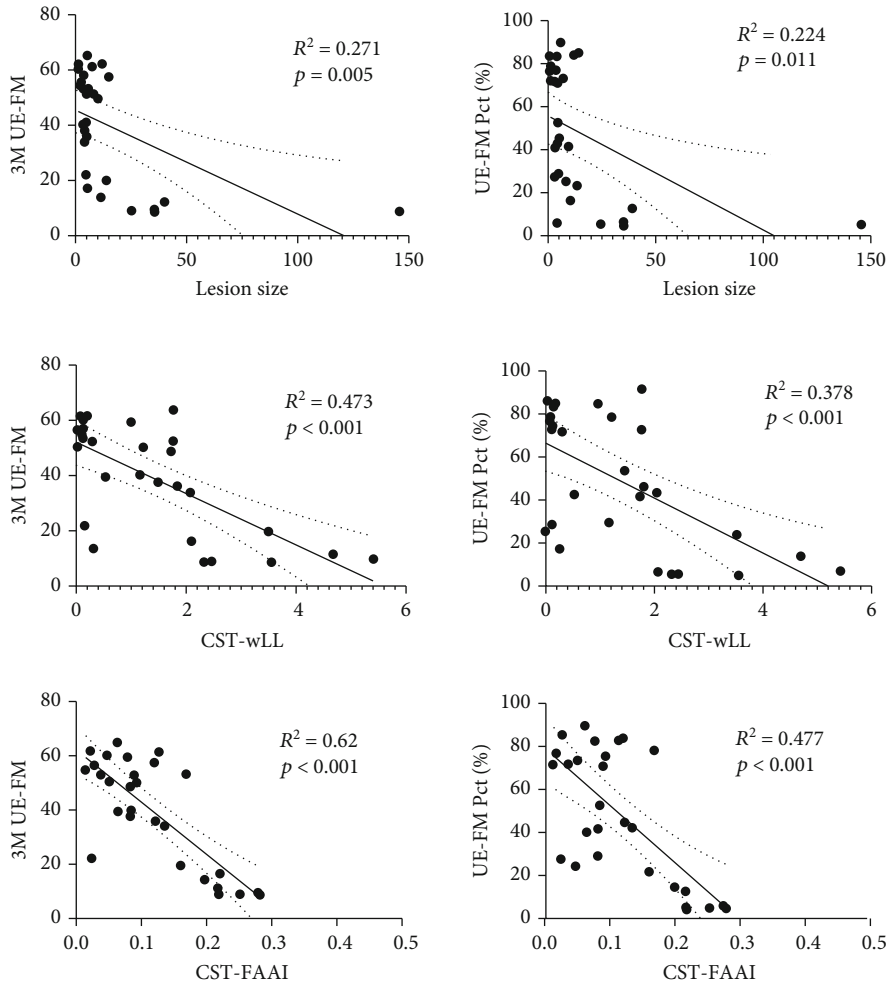

Figure 2: Univariate regression analysis for lesion size, CST-wLL, and CST-FAAI.

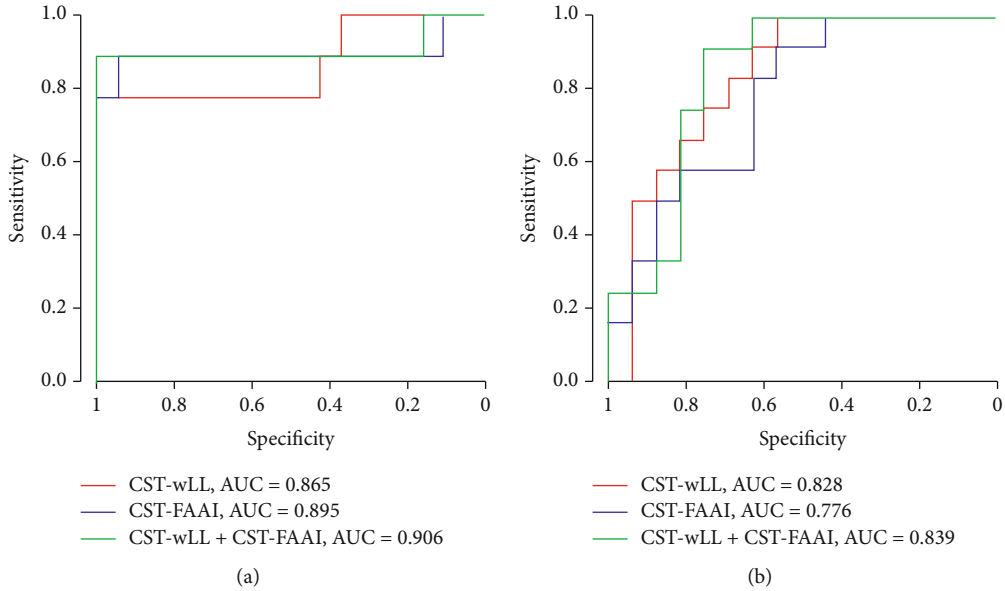

Figure 3: ROC for (a) poor motor outcomes (defined as 3M UE-FM ≤ 25) and (b) considerable proportional recovery (defined as UE-FM Pct ≥ 70%).

Table 5: ROC analyses for predicting 3M UE-FM.

Predictor variables	Accuracy	Sensitivity	Specificity	PPV	NPV	AUC
Lesion size	0.857	0.778	0.895	0.778	0.895	0.871
LL	0.786	0.889	0.737	0.615	0.933	0.836
wLL	0.929	0.778	1	1	0.905	0.865
PLIC-rFA	0.786	1	0.684	0.6	1	0.912
PLIC-FAAI	0.786	1	0.684	0.6	1	0.912
CST-rFA	0.929	0.889	0.947	0.889	0.947	0.895
CST-FAAI	0.929	0.889	0.947	0.889	0.947	0.895
CST-wLL & CST-FAAI	0.964	0.889	1	1	0.95	0.906

Table 6: ROC analyses for predicting UE-FM Pct.

Predictor variables	Accuracy	Sensitivity	Specificity	PPV	NPV	AUC
Lesion size	0.786	0.5	1	1	0.727	0.766
LL	0.821	0.917	0.75	0.733	0.923	0.818
wLL	0.75	1	0.562	0.632	1	0.828
PLIC-rFA	0.821	0.833	0.812	0.769	0.867	0.818
PLIC-FAAI	0.821	0.833	0.812	0.769	0.867	0.818
CST-rFA	0.714	0.917	0.562	0.611	0.9	0.776
CST-FAAI	0.714	0.917	0.562	0.611	0.9	0.776

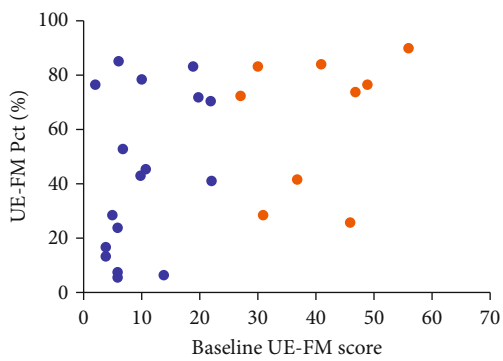

Figure 4: For patients with serious initial dysfunction (blue points), the recovery percentage varied from limited to considerable. This was the same for patients with mild initial dysfunction (orange points).

score of 66, the baseline UE-FM scores ranged from 2 to 56, and the UE-FM scores 3 months poststroke ranged from 8 to 65.

3.2. MRI Statistics. We analyzed the sMRI-based lesion size (lesion volume), LL, and CST-wLL (cc) and the DTI-based PLIC-rFA, CST-rFA, PLIC-FAAI, and CST-FAAI. The normality test results showed that the LL, CST -wLL, PLIC-rFA, CST-rFA, PLIC-FAAI, and CST-FAAI were normally distributed, while lesion size was not. The log-transformed lesion size (log-lesion size) was normally distributed (Table 2, Supplementary Figure 1).

3.3. Correlation and Regression Analyses. Pearson correlation analysis was conducted for LL, CST-wLL, PLIC-rFA, PLIC-FAAI, CST-rFA, CST-FAAI, 3M UE-FM, and UE-FM Pct. Lesion size was log-transformed for the analysis. Log-lesion size, LL, CST-wLL, PLIC-rFA, PLIC-FAAI, CST-rFA, and CST-FAAI were all well correlated with 3M UE-FM and UE-FM Pct (Table 3). When age, gender, and education years were controlled, the partial correlation analysis showed a similar result (Supplementary Table 1).

Univariate regression analysis was performed to evaluate whether the variance (R^2) of the 3M UE-FM or UE-FM Pct could be explained by lesion size, LL, CST-wLL, PLIC-rFA, PLIC-FAAI, CST-rFA, or CST-FAAI (Table 4, Supplementary Figure 2). CST-wLL was more strongly correlated with 3M UE-FM than was lesion size. The CST-FAAI from the template mask also correlated significantly with 3M UE-FM (Figure 2). CST-wLL was more highly correlated with UE-FM Pct than was lesion size. The CST-FAAI from the template mask was also significantly correlated with UE-FM Pct (Figure 2). When multivariate regression analysis was performed with 3M UE-FM as the dependent variable and lesion size, LL, CST-wLL, PLIC-rFA, CST-rFA, PLIC-FAAI, and CST-FAAI as the independent variables, the model selection results based on stepwise showed that CST-FAAI was the most significant predictor for 3M UE-FM (adjusted $R^2 = 0.606$, $F = 42.484$, beta $= -0.788$, $p < 0.001$). When multivariate regression analysis was performed with UE-FM Pct as the dependent variable and lesion size, LL, CST-wLL, PLIC-rFA, CST-rFA, PLIC-FAAI, and CST-FAAI as the independent variables, the model selection results based on stepwise showed that CST-FAAI was the most significant predictor for UE-FM Pct (adjusted $R^2 = 0.457$, $F = 23.734$, beta $= -0.691$, $p < 0.001$).

3.4. CST-wLL Threshold Analysis. Consistent with Lin et al. [17], we defined the upper limb motor function outcome as poor if the UE-FM score was ≤25 at 3 months poststroke. Analysis of the ROC curve showed that when CST-wLL was used to predict motor outcome 3 months poststroke, the cut-off point was 2.068, with 77.8% sensitivity, 100% specificity, 100% PPV, 90.5% NPV, and 0.865 AUC (Figure 3). Hence, a CST-wLL ≥ 2.068 cc on an MRI within 1 month indicated a poor function outcome. The CST-FAAI also showed a high predictive value, with an AUC of 0.895 (Table 5). The CST-wLL showed a comparable AUC from other classification models with CST-FAAI ($p = 0.71$, by DeLong test), and other metrics, including sensitivity, specificity PPV, and NPV, changed only slightly. Including extra-CST-FAAI did not significantly increase the AUC ($p = 0.58$, CST-wLL vs. CST-wLL and CST-FAAI, by DeLong test).

Prabhakaran et al. [24] discovered that some patients with stroke had a 70% near-fixed proportional upper limb motor recovery within 3 months. Analysis of the ROC curve showed that when CST-wLL was used to predict the motor recovery percentage, the cut-off point was 1.799, with 100% sensitivity, 56.2% specificity, 63.2% PPV, 100% NPV, and 0.828 AUC (Figure 3). In other words, a CST-wLL < 1.799 cc within 1 month indicated a considerable proportional recovery (≥70%) of the patient's upper limb motor function within 3 months after onset. The CST-FAAI showed lower accuracy, sensitivity, specificity, PPV, NPV, and AUC (Table 6).

4. Discussion

We found that CST-wLL obtained from routine sMRI examinations within 1 month of stroke onset was closely correlated with upper limb motor function outcomes 3 months poststroke. CST-wLL was more relevant than lesion size as a predictor of upper limb motor recovery. CST-wLL ≥ 2.068 cc indicated serious CST damage and a poor outcome (100%). CST-wLL < 1.799 cc within 1 month poststroke indicated that patients would recover a considerable proportion (≥70%) of their upper limb motor functions within 3 months after stroke onset. CST-FAAI may be the optimal predictor for upper limb motor outcomes in patients after stroke. However, CST-wLL showed a comparable AUC to that of DTI-derived metrics, such as CST-FAAI, for predicting recovery of upper limb motor function and proportional recovery.

As a predictor of upper limb motor function prognosis 3 months poststroke, CST-wLL can be used as a predictive imaging biomarker to classify patients for rehabilitation. This would help practitioners set more realistic rehabilitation goals, integrate resources, and improve efficiency. A CST-wLL ≥ 2.068 cc indicated a poor outcome (100%), and these patients could receive specific initial rehabilitation based on predictive stratification [17, 25]. A recent study suggested that a 3-week CST-wLL was the strongest predictor of the ability to grasp and control finger forces 6 months poststroke [26]. A CST-wLL > 5.5 cc strongly predicted low-to-minimal recovery in unimanual motor impairment and bimanual activity performance (specificity: 0.91) [27].

In our study, CST-FAAI may be the optimal predictor for upper limb motor outcomes. However, CST-wLL showed a comparable precise prediction with DTI-derived metrics such as CST-FAAI. The rFA and FAAI between ipsilateral and contralateral CST are the most commonly used DTI-derived metrics for predicting motor recovery [28]. Higher baseline FA and rFA values have been correlated with better motor recovery and can predict motor function outcomes in patients after ischemic stroke [14]. A meta-analysis including fifteen studies with 414 patients revealed that FA in the subacute phase after ischemic stroke is a good predictor of functional motor recovery and showed moderate quality based on the GRADE system [29]. However, these DTI-derived metrics represent diffusion directions of the water molecules and their patterns along the axon, i.e., "CST structural characteristics." Calculating the CST-wLL enables quantifying how much "CST structural integrity" has been damaged due to stroke; this allows more accurately predicting the recovery of upper limb motor function [26]. Few studies have compared the performance of different neuroimaging modalities. Doughty et al. [30] suggested that CST lesion load in the acute phase predicts 3-month outcomes better than the FAA of regions of interests (ROIs) distal to the lesion. A recent study estimating CST injury by the proposed method with diffusion metrics extracted from the diffusional kurtosis imaging (DKI) sequence and with the first principal component (PC1) of the metrics found that DKI_AK, AFD_total, and PC1 showed similar predictive values to those of wLL for functional outcomes [31]. Although previous studies have confirmed that FA is a good predictor of 3-month functional outcomes, our results suggested that the AUCs for CST-wLL in the subacute phase were similar to those of the FAAI. Another microstructural study suggested that the baseline asymmetry measures in the PLIC for the orientation dispersion index of the neurite orientation dispersion and density imaging (NODDI) model explained 83% of the variance of the upper extremity FM outcomes whereas FA values explained only 49% [10]. However, the NODDI model is not routinely available in stroke units. The method proposed in our study for estimating CST injury is more easily implemented in clinical settings.

As a potential imaging biomarker for poststroke motor outcomes, wLL has some advantages over functional MR and DTI, including high patient compliance and examination convenience [25, 32]. T2-WI sequences are routinely available for patient care, whereas fMRI or DTI is not a routine examination in stroke units and rehabilitation units considering its costs and hardware requirements, especially in developing countries. We used the CST model from the standard template [15] instead of the tractography results from locally acquired DTI data of age-matched healthy controls. As the major purpose of this study is to compare between the prediction performance with structural MRI only and with DTI, it is important to not acquire any new DTI data for the calculations within the structural MRI group. In this study, PLIC-rFA, PLIC-FAAI, CST-rFA, and CST-FAAI from the CST template were highly correlated with the outcomes of upper limb motor function, which is consistent with the results of previous studies [15]. Prior

studies that calculated CST-wLL used heterogeneous methods, and the templates used and methods of overlap varied substantially [16, 26, 33]. However, these studies showed significant agreement between methods for estimating CST injury, suggesting that these methods are relatively precise [34].

CST-wLL was also highly correlated with the proportion of recovery of upper limb motor function. Previous studies [24, 35] found that approximately 70% of the maximum recovery potential of most stroke patients, apart from those with serious initial motor impairment, may be realized. Our results showed that the initial severity of the motor impairment did not predict the proportion of recovery. Some patients with serious initial dysfunction still achieved a substantial proportion (≥70%) of functional recovery, while some patients with mild initial dysfunction showed limited recovery potential (Figure 4). CST-wLL showed considerable predictive values for proportional recovery. Our results suggested that CST-wLL showed considerable predictive values for proportional recovery. CST-wLL < 1.799 cc within 1 month indicated recovery of a large proportion (≥70%) of upper limb motor function within 3 months after onset. This was consistent with the results of a previous study [16], which showed that the CST-wLL could be used to predict the recovery proportion. Stinear et al. [21] indicated that an FAAI of 0.25 is a "point of no return," beyond which functional potential is severely limited. In this study, CST-wLL showed higher accuracy, sensitivity, specificity, PPV, NPV, and AUC than did FAAI. Consequently, CST-wLL can be used as a classification variable to predict recovery potential for individual stroke patients [36], thus directing clinical motor function rehabilitation and increasing rehabilitation efficiency.

Our study and methodology have some limitations. First, although we improved spatial standardization, individual differences must be considered when taking the CST localization from the standardized mask, especially in brains with large lesions, where the results may be less accurate than those in brains with small lesions. Second, the study only included patients with first-onset acute ischemic stroke and excluded patients with second- or third-onset stroke, which may affect the generalizability of the results. Additionally, the sample size was too small to incorporate rehabilitation treatment factors, drug treatment factors, depression, and perfusion therapy for multiple regression analysis to further clarify the weight of CST-wLL as a neuroimaging biomarker in predicting upper limb motor recovery. More pioneering approaches, such as machine learning algorithms and deep learning for classification and prediction, have been proposed as they can capture complex and nonlinear relationships [37] and show great potential in integration of voluminous clinical data and imaging data for predicting motor function prognosis at much quicker speeds and at higher accuracy without bias [38–41]. However, machine learning algorithms generally require a large sample size and diverse sample distribution to train the algorithm and improve the generalization, and it remains challenging to implement these algorithms in clinical routines [42]. The current study provides a practical way to predict the motor outcomes in the clinical environment, and the prediction model can be further improved by combining with advanced machine learning algorithms as we have a larger sample size from different hospitals in the future. Finally, as a threshold for classification of upper limb motor outcomes and recovery potential, CST-wLL must be further defined and verified with larger sample sizes in future studies.

CST-wLL obtained from routine sMRI within 1 month after stroke onset may serve as a potential imaging biomarker for predicting upper limb motor function prognosis and recovery potential 3 months poststroke. This study optimized the prediction model (protocol) in the clinical environment by comparing the performance of sMRI-derived CST-wLL and DTI-derived metrics for predicting upper limb motor recovery. Including extra-DTI will not induce significant benefits. However, as a clinical predictive imaging biomarker of motor function recovery and a classification variable to guide future stroke rehabilitation, CST-wLL still requires verification in studies with larger samples. Accurate metrics and predictive models are critical for defining an optimal neurorehabilitation protocol that will promote motor recovery and maximize functional outcomes for stroke survivors.

Glossary

CST:	Corticospinal tract
MRI:	Magnetic resonance imaging
sMRI:	Structural magnetic resonance imaging
DTI:	Diffusion tensor imaging
UE:	Upper extremity
UE-FM:	Upper extremity module of the Fugl-Meyer assessment
3M UE-FM:	The UE-FM score 3 months after the stroke
UE-FM Pct:	UE-FM recovery percentage
LL:	Lesion load
CST-wLL:	CST-weighted lesion load
PLIC:	Posterior limb of the internal capsule
FAA:	Fractional anisotropy asymmetry
FAAI:	Fractional anisotropy asymmetry index
rFA:	Ratio of fractional anisotropy
AUC:	Area under the curve
PPV:	Positive predictive value
NPV:	Negative predictive value
fMRI:	Functional magnetic resonance imaging
TOAST:	Trial of ORG 10172 in Acute Stroke Treatment
FLAIR:	Fluid-attenuated inversion recovery
ROC:	Receiver operating characteristic
ROIs:	Regions of interests
GRADE:	Grading of Recommendations Assessment, Development and Evaluation
DKI:	Diffusional kurtosis imaging
NODDI:	Neurite orientation dispersion and density imaging.

Data Availability

All data included in this study are available upon request by contact with the corresponding author.

Conflicts of Interest

The authors declare that they have no conflicts of interest.

Acknowledgments

This work was supported by the Young Talent Support Plan of Zhejiang Medical Science and Technology Project (Grant No. 2019RC196); the Hangzhou Medical Health Science and Technology Project (Grant No. A20200014); the Natural Science Foundation of Zhejiang Province, China (Grant No. LR20H180001); and the MOE Frontier Science Center for Brain Science & Brain-Machine Integration, Zhejiang University.

Supplementary Materials

Supplementary Figure 1. Statistical differences in MRI between severe and mild-moderate patients. $^{*}p < 0.05$. Supplementary 2. Univariate regression analysis. *Removed outlier point (lesion size = 145.48).Supplementary Table 1.Partial correlation analysis. Note: $^{**}p < 0.001$ and $^{*}p < 0.05$. Supplementary Table 2. Differences in brain images between severe and mild-moderate patients. Red ROI: lesion mask; blue ROI: CST mask; red circle: PLIC mask; yellow circle: CST mask. *(Supplementary Materials)*

References

[1] C. V. Granger, A. L. Holland, M. Kellyhayes et al., "Post-stroke rehabilitation," *Journal of the American Association of Nurse Practitioners*, vol. 7, pp. 607–623, 2010.

[2] G. J. Hankey, "Stroke," *Lancet*, vol. 389, no. 10069, pp. 641–654, 2017.

[3] P. Langhorne, F. Coupar, and A. Pollock, "Motor recovery after stroke: a systematic review," *Lancet Neurology*, vol. 8, no. 8, pp. 741–754, 2009.

[4] E. V. Wegen, R. Nijland, J. Veerbeek, and G. Kwakkel, "Presence of finger extension and shoulder abduction within 72 hours poststroke predicts functional recovery," *Stroke*, vol. 91, no. 10, pp. e24–e24, 2010.

[5] I. Loubinoux, S. Dechaumont-Palacin, E. Castel-Lacanal et al., "Prognostic value of fMRI in recovery of hand function in subcortical stroke patients," *Cerebral Cortex*, vol. 17, no. 12, pp. 2980–2987, 2007.

[6] J. Du, F. Yang, Z. Zhang et al., "Early functional MRI activation predicts motor outcome after ischemic stroke: a longitudinal, multimodal study," *Brain Imaging and Behavior*, vol. 12, no. 6, pp. 1804–1813, 2018.

[7] J. P. Mohr, M. A. Foulkes, A. T. Polis et al., "Infarct topography and hemiparesis profiles with cerebral convexity infarction: the Stroke Data Bank," *Journal of Neurology Neurosurgery & Psychiatry*, vol. 56, no. 4, pp. 344–351, 1993.

[8] J. L. Saver, K. C. Johnston, D. Homer, R. Wityk, and E. C. Haley, "Infarct volume as a surrogate or auxiliary outcome measure in ischemic stroke clinical trials," *Stroke; a Journal of Cerebral Circulation*, vol. 30, no. 2, pp. 293–298, 1999.

[9] E. Moulton, S. Magno, R. Valabregue, M. Amor-Sahli, and C. Rosso, "Acute diffusivity biomarkers for prediction of motor and language outcome in mild-to-severe stroke patients," *Stroke*, vol. 50, no. 8, pp. 2050–2056, 2019.

[10] K. Hodgson, G. Adluru, L. G. Richards et al., "Predicting motor outcomes in stroke patients using diffusion spectrum MRI microstructural measures," *Frontiers in Neurology*, vol. 10, 2019.

[11] J. Puig, G. Blasco, J. Daunis-I-Estadella et al., "Decreased corticospinal tract fractional anisotropy predicts long-term motor outcome after stroke," *Stroke*, vol. 44, pp. 2016–2018, 2013.

[12] C. L. Chen, F. T. Tang, H. C. Chen, C. Y. Chung, and M. K. Wong, "Brain lesion size and location: effects on motor recovery and functional outcome in stroke patients," *Archives of Physical Medicine & Rehabilitation*, vol. 81, no. 4, pp. 447–452, 2000.

[13] J. Puig, S. Pedraza, G. Blasco et al., "Acute damage to the posterior limb of the internal capsule on diffusion tensor tractography as an early imaging predictor of motor outcome after stroke," *Ajnr American Journal of Neuroradiology*, vol. 32, no. 5, pp. 857–863, 2011.

[14] H. A. Shaheen, S. S. Sayed, M. M. Magdy, M. A. Saad, A. M. Magdy, and L. I. Daker, "Prediction of motor recovery after ischemic stroke: clinical and diffusion tensor imaging study," *Journal of Clinical Neuroscience*, vol. 96, pp. 68–73, 2022.

[15] B. Kim, B. E. Fisher, N. Schweighofer et al., "A comparison of seven different DTI-derived estimates of corticospinal tract structural characteristics in chronic stroke survivors," *Journal of Neuroscience Methods*, vol. 304, pp. 66–75, 2018.

[16] W. Feng, J. Wang, P. Y. Chhatbar et al., "Corticospinal tract lesion load: an imaging biomarker for stroke motor outcomes," *Annals of Neurology*, vol. 78, pp. 860–870, 2015.

[17] L. L. Zhu, R. Lindenberg, M. P. Alexander, and G. Schlaug, "Lesion load of the corticospinal tract predicts motor impairment in chronic stroke," *Stroke*, vol. 41, no. 5, pp. 910–915, 2010.

[18] D. J. Gladstone, C. J. Danells, and S. E. Black, "The Fugl-Meyer assessment of motor recovery after stroke: a critical review of its measurement properties," *Neurorehabilitation and Neural Repair*, vol. 16, no. 3, pp. 232–240, 2002.

[19] M. Jenkinson, C. F. Beckmann, T. E. Behrens, M. W. Woolrich, and S. M. Smith, "FSL," *Neuroimage*, vol. 62, no. 2, pp. 782–790, 2012.

[20] M. Thiebaut de Schotten, D. H. Ffytche, A. Bizzi et al., "Atlasing location, asymmetry and inter-subject variability of white matter tracts in the human brain with MR diffusion tractography," *NeuroImage*, vol. 54, no. 1, pp. 49–59, 2011.

[21] C. M. Stinear, P. A. Barber, P. R. Smale, J. P. Coxon, M. K. Fleming, and W. D. Byblow, "Functional potential in chronic stroke patients depends on corticospinal tract integrity," *Brain*, vol. 130, pp. 170–180, 2007.

[22] C. Pierpaoli, L. Walker, M. O. Irfanoglu, A. Barnett, and M. Wu, "TORTOISE: An Integrated Software Package for Processing of Diffusion MRI Data," in *In ISMRM 18th annual meeting*, NIH, Bethesda, MD, United States, 2010.

[23] M. O. Irfanoglu, P. Modi, A. Nayak, E. Hutchinson, J. Sarlls, and C. Pierpaoli, "DR-BUDDI (Diffeomorphic Registration for Blip-Up blip-Down Diffusion Imaging) method for correcting echo planar imaging distortions," *NeuroImage*, vol. 106, pp. 284–299, 2015.

[24] S. Prabhakaran, E. Zarahn, C. Riley et al., "Inter-individual variability in the capacity for motor recovery after ischemic stroke," *Neurorehabilitation and Neural Repair*, vol. 22, no. 1, pp. 64–71, 2008.

[25] C. M. Stinear, W. D. Byblow, S. J. Ackerley, M. C. Smith, and P. A. Barber, "PREP2: a biomarker-based algorithm for predicting upper limb function after stroke," *Annals of Clinical and Translational Neurology*, vol. 4, no. 11, pp. 811–820, 2017.

[26] G. V. Pennati, J. Plantin, L. Carment et al., "Recovery and prediction of dynamic precision grip force control after stroke," *Stroke*, vol. 51, pp. 944–951, 2020.

[27] J. Plantin, M. Verneau, A. K. Godbolt et al., "Recovery and prediction of bimanual hand use after stroke," *Neurology*, vol. 97, no. 7, pp. e706–e719, 2021.

[28] M. K. I. Zolkefley, Y. M. S. Firwana, H. Z. M. Hatta et al., "An overview of fractional anisotropy as a reliable quantitative measurement for the corticospinal tract (CST) integrity in correlation with a Fugl-Meyer assessment in stroke rehabilitation," *Journal of Physical Therapy Science*, vol. 33, no. 1, pp. 75–83, 2021.

[29] J. F. Jin, Z. T. Guo, Y. P. Zhang, and Y. Y. Chen, "Prediction of motor recovery after ischemic stroke using diffusion tensor imaging: a meta-analysis," *World Journal of Emergency Medicine*, vol. 8, no. 2, p. 99, 2017.

[30] C. Doughty, J. Wang, W. Feng, D. Hackney, E. Pani, and G. Schlaug, "Detection and predictive value of FA changes of the CST in the acute phase of a stroke," *Stroke*, vol. 47, no. 6, pp. 1520–1526, 2016.

[31] Y. Li, S. Yan, G. Zhang et al., "Tractometry-based estimation of corticospinal tract injury to assess initial impairment and predict functional outcomes in ischemic stroke patients," *Journal of Magnetic Resonance Imaging*, vol. 55, no. 4, pp. 1171–1180, 2022.

[32] E. B. Quinlan, L. Dodakian, J. See, A. McKenzie, J. C. Stewart, and S. C. Cramer, "Biomarkers of rehabilitation therapy vary according to stroke severity," *Neural Plasticity*, vol. 2018, 9867198 pages, 2018.

[33] C. H. Park and S. H. Ohn, "The predictive value of lesion and disconnectome loads for upper limb motor impairment after stroke," *Neurological Sciences*, vol. 43, no. 5, pp. 3097–3104, 2022.

[34] D. J. Lin, A. M. Cloutier, K. S. Erler et al., "Corticospinal tract injury estimated from acute stroke imaging predicts upper extremity motor recovery after stroke," *Stroke*, vol. 50, pp. 3569–3577, 2019.

[35] C. Winters, E. E. H. Van Wegen, A. Daffertshofer, and G. Kwakkel, "Generalizability of the proportional recovery model for the upper extremity after an ischemic stroke," *Neurorehabilitation & Neural Repair*, vol. 29, pp. 614–622, 2015.

[36] C. M. Stinear, W. D. Byblow, S. J. Ackerley, P. A. Barber, and M. C. Smith, "Predicting recovery potential for individual stroke patients increases rehabilitation efficiency," *Stroke*, vol. 48, no. 4, pp. 1011–1019, 2017.

[37] A. S. Lundervold and A. Lundervold, "An overview of deep learning in medical imaging focusing on MRI," *Zeitschrift für Medizinische Physik*, vol. 29, no. 2, pp. 102–127, 2019.

[38] J. K. Kim, Z. Lv, D. Park, and M. C. Chang, "Practical machine learning model to predict the recovery of motor function in patients with stroke," *European Neurology*, pp. 1–7, 2022.

[39] G. Liu, J. Wu, C. Dang et al., "Machine learning for predicting motor improvement after acute subcortical infarction using baseline whole brain volumes," *Neurorehabilitation and Neural Repair*, vol. 36, no. 1, pp. 38–48, 2022.

[40] J. K. Kim, M. C. Chang, and D. Park, "Deep learning algorithm trained on brain magnetic resonance images and clinical data to predict motor outcomes of patients with corona radiata infarct," *Frontiers in Neuroscience*, vol. 15, p. 795553, 2022.

[41] D. Hassabis, D. Kumaran, C. Summerfield, and M. Botvinick, "Neuroscience-inspired artificial intelligence," *Neuron*, vol. 95, no. 2, pp. 245–258, 2017.

[42] U. K. Patel, A. Anwar, S. Saleem et al., "Artificial intelligence as an emerging technology in the current care of neurological disorders," *Journal of neurology*, vol. 268, pp. 1623–1642, 2021.

Hindawi
Neural Plasticity
Volume 2022, Article ID 5635596, 23 pages
https://doi.org/10.1155/2022/5635596

Review Article

Revealing the Neuroimaging Mechanism of Acupuncture for Poststroke Aphasia: A Systematic Review

Boxuan Li,[1,2,3] **Shizhe Deng**,[1,2] **Bomo Sang**,[1,2,3] **Weiming Zhu**,[1,2,3] **Bifang Zhuo**,[1,2,3] **Menglong Zhang**,[1,2,3] **Chenyang Qin**,[1,2,3] **Yuanhao Lyu**,[1,2,3] **Yuzheng Du**,[1,2] **and Zhihong Meng**[1,2]

[1]*First Teaching Hospital of Tianjin University of Traditional Chinese Medicine, Tianjin, China*
[2]*National Clinical Research Center for Chinese Medicine Acupuncture and Moxibustion, Tianjin, China*
[3]*Tianjin University of Traditional Chinese Medicine, Tianjin, China*

Correspondence should be addressed to Yuzheng Du; drduyuzheng@163.com and Zhihong Meng; profmengzhihong@163.com

Received 18 December 2021; Revised 21 February 2022; Accepted 29 March 2022; Published 21 April 2022

Academic Editor: Xi-Ze Jia

Background. Aphasia is a common symptom in stroke patients, presenting with the impairment of spontaneous speech, repetition, naming, auditory comprehension, reading, and writing function. Multiple rehabilitation methods have been suggested for the recovery of poststroke aphasia, including medication treatment, behavioral therapy, and stimulation approach. Acupuncture has been proven to have a beneficial effect on improving speech functions in repetition, oral speech, reading, comprehension, and writing ability. Neuroimaging technology provides a visualized way to explore cerebral neural activity, which helps reveal the therapeutic effect of acupuncture therapy. In this systematic review, we aim to reveal and summarize the neuroimaging mechanism of acupuncture therapy on poststroke aphasia to provide the foundation for further study. *Methods*. Seven electronic databases were searched including PubMed, Web of Science, Embase, Cochrane Central Register of Controlled Trials, China National Knowledge Infrastructure, the Wanfang databases, and the Chinese Scientific Journal Database. After screening the studies according to the inclusion and exclusion criteria, we summarized the neuroimaging mechanism of acupuncture on poststroke aphasia, as well as the utilization of acupuncture therapy and the methodological characteristics. *Result*. After searching, 885 articles were retrieved. After removing the literature studies, animal studies, and case reports, 16 studies were included in the final analysis. For the acupuncture type, 10 studies used manual acupuncture and 5 studies used electroacupuncture, while body acupuncture (10 studies), scalp acupuncture (7 studies), and tongue acupuncture (8 studies) were applied for poststroke aphasia patients. Based on blood oxygen level-dependent (BOLD) and diffusion tensor imaging (DTI) technologies, 4 neuroimaging analysis methods were used including amplitude of low-frequency fluctuation (ALFF), regional homogeneity (ReHo), seed-based analysis, and independent component analysis (ICA). Two studies reported the instant acupuncture effect, and 14 studies reported the constant acupuncture's effect on poststroke aphasia patients. 5 studies analyzed the correlation between the neuroimaging outcomes and the clinical language scales. *Conclusion*. In this systematic review, we found that the mechanism of acupuncture's effect might be associated with the activation and functional connectivity of language-related brain areas, such as brain areas around Broca's area and Wernicke's area in the left inferior temporal gyrus, supramarginal gyrus, middle frontal gyrus, and inferior frontal gyrus. However, these studies were still in the preliminary stage. Multicenter randomized controlled trials (RCT) with large sample sizes were needed to verify current evidence, as well as to explore deeply the neuroimaging mechanisms of acupuncture's effects.

1. Introduction

Aphasia is an acquired language malfunction caused by the disorder of the speech center [1]. Stroke is the top leading cause of disability in China and is the major cause of mortality [2]. Each year, approximately 2 million Chinese people get attacked by the new-onset stroke [3]. Aphasia is a grave symptom of stroke, presenting with language malfunctions including spontaneous speech, repetition, naming, auditory comprehension, reading, and writing [4]. According to epidemiology research, the incidence of aphasia after the first stroke onset ranges from 23% to 38% [5–7]. Compared with the nonaphasia poststroke patients, the patient's mortality rate in the hospital is nearly 2 times higher and the hospital stay is 1.6 times longer [8, 9]. Chronic aphasia devastates patients' social participation and life quality. Moreover, the costs of aphasia rehabilitation are considerable, which aggravates the health economic burden [10]. It is estimated that the expense of rehabilitation varies from $89 to $864 according to the severity of aphasia [11], and prolonged hospital stay (0.66 days) contributes to high hospitalization costs ($971.35) in poststroke aphasia patients [12].

Multiple approaches have been used for aphasia treatment such as medication treatment, behavioral therapy, and stimulation approach [4, 13, 14]. Acupuncture originates from Traditional Chinese Medicine, and it has been practiced to treat aphasia for more than 3000 years. Plenty of studies have proven the therapeutic effect of acupuncture on aphasia, and a lot of evidence has indicated the beneficial effect of acupuncture on improving speech functions, including repetition, oral speech, reading, comprehension, and writing [15, 16]. Alone with speech and language therapies, acupuncture has become a pervasive treatment for poststroke aphasia [17]. Among the various acupuncture therapies, scalp acupuncture and tongue acupuncture are indispensable for poststroke aphasia. Both of their theories were developed based on the combination of the traditional Chinese meridian theory and the holographic theory [18, 19]. It has been demonstrated that scalp acupuncture has a beneficial effect on improving the daily activity ability of stroke patients [20]. Meanwhile, neural imaging technology provides a visualized way to reveal the brain activity mechanism of scalp acupuncture [21, 22]. Recent studies reported the effectiveness pathways of acupuncture on language function [23–25]. However, the mechanism of the recovery process is not fully illustrated. Clinical researches showed multiform language function impairments and the aphasia recovery process [26]. Apart from the relationship based on the structure-function hypothesis, evidence has been found in the variation of cerebral blood perfusion, brain functional connection, and neural activity, which enriched the mechanism of aphasia recovery [27–29]. Taking advantage of multidisciplinary combinations such as neuroimaging technology, researchers can explore the aphasia recovery mechanism in detail.

The functional magnetic resonance imaging (fMRI) provides a noninvasive way to explore the brain neural activity, which is a helpful tool to reveal the therapeutic effect of both instant acupuncture and constant acupuncture therapies [30]. The resting-state fMRI (rsfMRI) is proposed to be a practical approach to investigate spontaneous brain activity, which helps uncover the pathological mechanism. Accordingly, task-based fMRI is viewed as a tool to reflect the task-response properties evoked by specific stimulates [31]. Multiple analysis approaches have been applied to display the characteristics of the rsfMRI signals. ALFF is suggested to measuring the amplitude of fluctuation in the low-frequency range of neural activity in the resting state directly [32, 33]. It offers evidence of spontaneous brain activity at a single voxel level. In previous researches, ALFF is applied to study the effect of acupuncture therapy [34, 35]. ReHo is considered a useful tool to detect the regional functional homogeneity of neural synchronization, which provides features of brain connection within a specified voxel and the neighboring voxels [36]. Degree centrality is viewed to characterize the functional connectivity in the information communication of the brain network. It presents the single voxel value according to the functional connectivity strength within the brain network [37]. Functional connectivity (FC) is utilized to reveal the functional information communication between brain regions that are separated at the anatomic level, and ICA is proposed to explore the independent spatial sources of neural activity based on the whole brain function [38, 39].

With the use of neuroimaging technology, researchers make efforts to illustrate the central pathway of acupuncture's effect on poststroke aphasia. Acupuncture was taken as stimulation, and its instant effect was detected in the task-based fMRI [40]. Previously, researchers found the brain activation evoked by electroacupuncture was remarkably consistent with the activation induced by the image naming task, which included the left inferior frontal gyrus that accounts for the speech function [41]. Accordingly, rsfMRI was used to evaluate the cerebral functional state before and after acupuncture treatment. Based on the classical language function theory, studies focused on the anatomic structural regions proved that the decreased ALFF value in the left temporal pole was correlated with the naming function [42]. Recent studies revealed the connectivity in the surviving brain regions, which played a role in brain network studies [43, 44]. It has been verified that acupuncture could strengthen the language-related brain network in the left hemisphere [45].

The classic hypothesis of aphasia focused on the cortical lesions such as Broca's area and Wernicke's area. Using the MRI technology, researchers uncovered the damage of subcortical grey matter by scanning the two brains of Paul Broca's patients [46], while recent studies reported the new findings that neither the long-term aphasia condition nor the damage of anterior arcuate fasciculus can be fully explained by the infarction of Broca's area [47]. Other studies devoted to the brain network mechanism found disparate pathways in the aphasia recovery process [48]. Yet, the relationship between clinical effects and neuroimaging changes remains unclear. Hence, the objective of this review is to analyze the possible relationship between acupuncture stimulation, clinical effects, and cerebral response. Meanwhile, using the systematic review method, we aim to summarize

the current acupuncture method, neuroimaging techniques, and potential cerebral mechanism of poststroke aphasia recovery.

2. Method

2.1. Included Criteria

(i) *Types of studies*: published randomized and nonrandomized controlled clinical studies of acupuncture on poststroke aphasia in English and Chinese

(ii) *Participants*: patients that were diagnosed with aphasia following a stroke in WHO criteria; the type of aphasia was not limited.

(iii) *Interventions*: acupuncture therapy included manual acupuncture (MA), electroacupuncture (EA), scalp acupuncture, and tongue acupuncture or combined with the control group treatment

2.2. Searching Strategies. We searched 7 electronic databases including PubMed, Web of Science, Embase, Cochrane Central Register of Controlled Trials, China National Knowledge Infrastructure, the Wanfang databases, and the Chinese Scientific Journal Database from January 2009 to September 2021 for relevant studies. References lists of identified publications, conference literature, and bibliographies of reviews were also inspected for further literature. The searching strategy and searching terms are listed in Table 1. The Preferred Reporting Items for Systematic Reviews and Meta-Analyses (PRISMA) statement was followed, and the PRISMA 2020 Checklist was attached in the supplemental material (available here) [49].

2.3. Study Selection. After searching, 885 articles were put into NoteExpress software (version 3.2.0). After removing the duplicated studies, the remaining 870 articles were screened by two reviewers through browsing titles and abstracts. Then, 68 remaining articles were selected by reading the full texts according to the inclusion criteria and exclusion criteria. Eventually, 16 articles got included in the final analysis. Disagreements were solved by consulting the third reviewer.

2.4. Data Extraction. The data extraction table was preset by BXL using Excel software, following the PRISMA statement and the STandards2 for Reporting Interventions in Controlled Trails of Acupuncture (STRICTA) guideline. The following information from the eligible studies was recorded by BMS and WMZ: publishing year, author, funding organization, study type, sample size, participants' information (stroke type, aphasia duration, and handedness), intervention details (needle session, needle duration, needle frequency, needle type, acupoint, needle response, control interventions, and treatment duration), and outcome details (outcome index, neuroimaging technologies, scanning design, image acquisition time, and neuroimaging results).

2.5. Data Analysis. In this systematic review, the characteristics of the included studies were analyzed using the bibliometric method. Then, the risk of bias assessment was conducted using the *Cochrane risk-of-bias tool for randomized trials* (*RoB 2*) [50, 51]. Finally, the neuroimaging outcomes were summarized to provide neural mechanism evidence of acupuncture for constant effect and instant effect on poststroke aphasia patients.

Table 1: Searching strategy and searching terms.

1	Aphasia
2	Acupuncture
3	Electroacupuncture
4	Needle
5	Stroke
6	Apoplexy
7	Cerebral vascular accident
8	Cerebral infarction
9	Magnetic resonance imaging
10	fMRI
11	Diffusion tensor imaging
12	DTI
13	Blood oxygen level dependent
14	BOLD
15	Amplitude of low-frequency fluctuation
16	ALFF
17	Region of interest
18	ROI
19	Regional homogeneity
20	ReHo
21	Independent component analysis
22	ICA
23	Functional connectivity
24	FC
25	Neuroimaging
26	Arterial spin labeling
27	ASL
28	Acupuncture-related terms: 2 OR 3 OR 4
29	Stroke-related terms: 5 OR 6 OR 7 OR 8
30	Neuroimaging-related terms: 9 OR 10 OR 11 OR 12 OR 13 OR 14 OR 15 OR 16 OR 17 OR 18 OR 19 OR 20 OR 21 OR 22 OR 23 OR 24 OR 25 OR 26 OR 27
31	Final searching terms: 1 AND 28 AND 29 AND 30

3. Result

3.1. Study Overview. A total of 885 studies were searched. After removing the duplicated studies, reviews, animal studies, and other ineligible clinical studies according to the screening protocol, 16 studies remained for the final analysis (Figure 1). The publishing date of the included studies was from March 2010 to August 2021. All of the 16 studies were conducted in China. The included 16 studies listed the funding organizations or the ethical committee. For the study type, there were 8 RCTs with 390 patients, 8 observational studies with 156 patients, and 96 healthy volunteers. The sample size ranges from 7 to 100. One study performed the

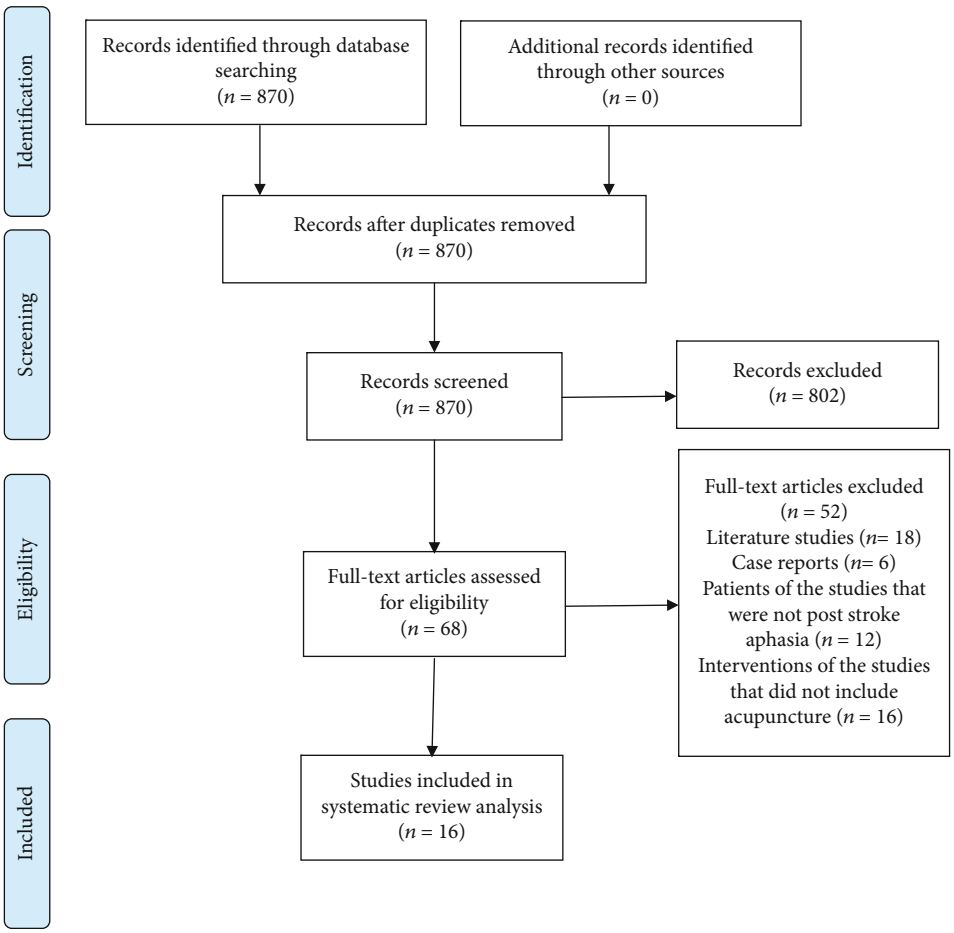

Figure 1: The flow diagram of literature screening.

blinding procedure on patients and used the sealed envelope to conduct the allocation concealment. The risk of bias assessment of included randomized controlled trials is summarized in Figure 2. When evaluating the randomization process, we took matched factors including gender, age, level of education, and disease duration (poststroke aphasia) into account. 4 studies that did not completely match these factors were graded as having some concerns. As for the deviation from intended intervention, the 8 included RCTs did not perform a blinding procedure for acupuncturists, and only one study reported conducting blinding procedures for participants. As a result, the included 8 RCTs were graded as having some concerns. All the 8 included RCTs reported the data in detail, while one study which did not describe the assessment procedure was graded as having some concerns; another study did not report the blinding of outcome assessor and was graded as high risk. For the part on the selection of the reported results, two studies did not illustrate the multiple eligible outcome measurements and were graded as having some concerns. Overall, 7 RCTs were graded as having some concerns, and one RCT was graded as high risk.

3.2. Patients' Information. A total of 546 poststroke aphasia patients and 96 healthy volunteers were included. The patients' basic information are listed in Table 2. 10 studies focused on the patients for the stroke onset within 6 months, another 4 studies [52–55] reported patients' stroke duration of more than 6 months, and 2 studies did not report the duration of stroke [56, 57]. The duration of aphasia was from 0 days to 2 years. For the type of stroke, 9 studies focused on patients with ischemic stroke, 2 studies reported both ischemic stroke and hemorrhage stroke, and 4 studies did not describe or limit the stroke type. 14 studies reported patients who were right-handed, and 2 studies did not report the handedness [58, 59]. For the type of aphasia, 6 studies reported Broca aphasia, and another 9 studies did not limit the type of aphasia.

3.3. Intervention. According to the STRICTA guideline [66], the needle stimulation included manual acupuncture (10 studies) and electroacupuncture (5 studies). The type of acupuncture therapy included body acupuncture (10 studies), scalp acupuncture (7 studies), and tongue acupuncture (8 studies). For the acupoint selection, all of the 16 studies selected acupoints based on the Traditional Chinese Medicine theory and meridian system. 22 acupoints were mentioned for a total of 64 times in the 16 studies, with RN23 (Lianquan, 8/16) and EX-HN12 (Jinjin and Yuye, 8/16) being the most frequently used acupoints. Other top 4 used

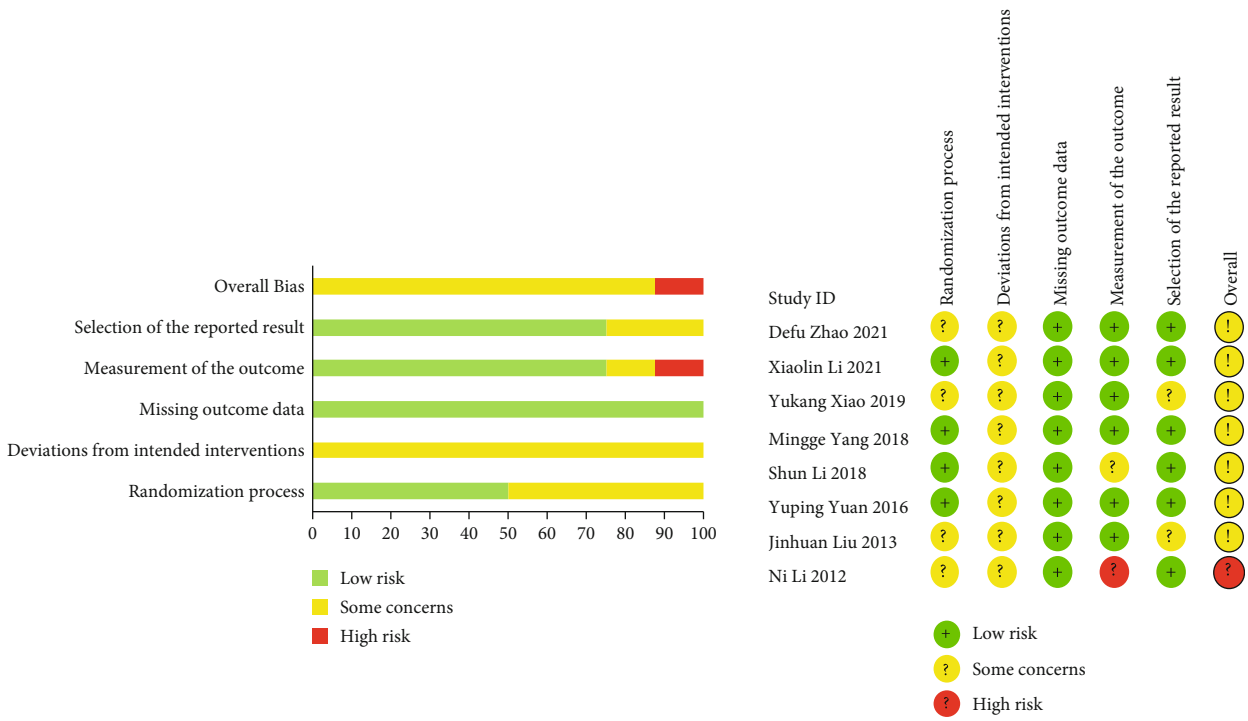

Figure 2: Risk of bias assessment of included randomized controlled trials.

acupoints included HT5 (Tongli, 7/16), DU20 (Baihui, 7/16), GB39 (Xuanzhong, 6/16), and EX-HN1 (Sishencong, 5/16). 4 scalp acupuncture areas were involved in 4 studies for 10 times involving MS6 (anterior oblique line of vertex-temporal, the line joining anterior EX-HN1 and GB6 Xuanli), MS7 (posterior oblique line of vertex-temporal, the line joining DU20 and GB7 Qubin), MS10 (anterior temporal line, the line joining GB4 Hanyan and GB6), and the scalp projection areas of cerebral infarction regions [67]. The responses that acupuncture elicited were described as "de qi" in 9 studies. The acupuncture type, needling type, scalp acupuncture areas, and acupoint selection are demonstrated in Figure 3 and Table 3.

3.4. Comparison. The included 16 studies contain the following 7 comparison types: acupuncture plus language rehabilitation vs. language rehabilitation [42, 57–59, 64, 65], acupuncture plus language rehabilitation vs. nonpoint needle plus language rehabilitation [45], acupuncture plus language rehabilitation vs. healthy volunteer [56, 62, 63], acupuncture plus conventional treatment vs. conventional treatment [61], acupuncture vs. nonpoint needle [53], acupuncture vs. acupuncture [54, 55], and acupuncture vs. healthy volunteer [60] (Table 3).

3.5. Outcome

3.5.1. Aphasia Assessment. For the poststroke aphasia evaluation, 5 aphasia assessment scales were used including Western Aphasia Battery (WAB; 7 studies; 24.00%), Boston Diagnostic Aphasia Exam (BDAE; 7 studies; 28.00%), Chinese Rehabilitation Research Center Standard Aphasia Examination (CRRCAE; 6 studies; 28.00%), Aphasia Battery of Chinese (ABC; 3 studies; 12.00%), and Chinese Functional Communication Profile (CFCP; 2 studies; 8.00%). The National Institutes of Health Stroke Scale (NIHSS) was used in 2 studies to evaluate neurological function. Meanwhile, activities of daily living (ADL), Stroke-Aphasia Quality of Life-39 (SAQOL-39), and Medical Outcome Study Short Form-36 (SF-36) were applied to assess the activity capability. Figure 4 shows the proportion of aphasia assessment scales.

3.5.2. fMRI Scanning Method. 7 studies conducted task-based fMRI using BOLD to observe the brain activation, with linguistic tasks such as word generation; the other 9 studies conducted rsfMRI to detect the spontaneous brain activity (6 with BOLD technology [52, 53, 56, 59, 60, 62], 2 with DTI technology [45, 63], and 1 with both BOLD and DTI technologies [42]). For the observing time point, 2 studies compared the instant effects of acupuncture [53, 54]; the other 14 studies compared the acupuncture effects after the constant treatments (12 to 30 sessions). The outcome details are listed in Table 4.

3.5.3. Cerebral Response of Constant Acupuncture

(1) Activation in Broca's Area. For the studies focused on the effect of constant acupuncture therapy, by observing the signal power of neural activities, studies that used tongue acupuncture and scalp acupuncture reported enhanced activation in Broca's area on poststroke Broca's aphasia patients, compared with participants who received language rehabilitation or conventional treatment [61, 65]; another

Table 2: The overview of the 16 included studies.

Publication year	First author	Funding organization	fMRI examination time	Study type	Stroke type	Aphasia duration	Type of AG patient	Number of acupuncture group	Type of CG patient	Number of control group	Treatment duration	Handedness	Outcome index
2021	Binlong Zhang [42]	Dongzhimen Hospital Affiliated to Beijing University of Chinese Medicine	Before and after treatment	Observational	Ischemic	1-6 months	Poststroke Broca aphasia	36	Healthy volunteer	24	Not depicted	Right handed	WAB, BDAE
2021	Defu Zhao [58]	Natural Science of Guizhou Province	Before and after treatment	RCT	Not depicted	16 days-5 months	Poststroke aphasia	48	Poststroke aphasia	48	1 month	Not depicted	CRRCAE, MoCA, clinic efficacy
2021	Xiaolin Li [45]	National Research Projects for Public Welfare Industries	Before and after treatment	RCT	Ischemic	14 days-6 months	Poststroke Broca aphasia	21	Poststroke Broca aphasia	20	8 weeks	Right handed	CRRCAE
2019	Binlong Zhang [60]	Dongzhimen Hospital Affiliated to Beijing University of Chinese Medicine	Before and after treatment	Observational	Ischemic	1-6 months	Poststroke aphasia	31	Healthy volunteer	26	1 month	Right handed	WAB, BDAE
2019	Yukang Xiao [59]	Affiliated Hospital of Hubei University of Medicine	Before and after treatment	RCT	Not depicted	0-6 weeks	Poststroke aphasia	50	Poststroke aphasia	50	30 days	Not depicted	CRRCAE, CFCP, SAQOL-39
2018	Mingge Yang [52]	Rehabilitation Hospital Affiliated to Fujian University of Traditional Chinese Medicine	Before and after treatment	RCT	Not limited	Within 2 years	Poststroke Broca aphasia	15	Poststroke Broca aphasia	15	4 weeks	Right handed	CRRCAE, BDAE, SF-36
2018	Shun Li [61]	Guangdong Provincial Science and technology Project	Before and after treatment	RCT	Ischemic	14 days-3 months	Poststroke Broca aphasia	11	Poststroke Broca aphasia	12	1 month	Right handed	CRRCAE, CFCP, ADL
2017	Jingling Chang [53]	Doctoral Fund of the Ministry of Education of China	Instant	Observational	Ischemic or HE	14 days-2 years	Poststroke Broca aphasia	22	Poststroke Broca aphasia	21	Instant acupuncture	Right handed	CRRCAE, BDAE
2016	Aiqin Wang [62]	Dongzhimen Hospital Affiliated to Beijing University of Chinese Medicine	Before and after treatment	Observational	Ischemic in cortical	1-6 months	Poststroke Broca aphasia	10	Healthy volunteer	10	30 days	Right handed	WAB, BDAE
2016	Binlong Zhang [56]	Dongzhimen Hospital Affiliated to Beijing University of Chinese Medicine	Before and after treatment	Observational	11 ischemic and 1 hemorrhage in basal ganglia	—	Poststroke aphasia	12	Healthy volunteer	12	30 days	Right handed	WAB, BDAE
2016	Jinying Liu [63]	Dongzhimen Hospital Affiliated to Beijing University of Chinese Medicine	Before and after treatment	Observational	IS	32-90 days	Poststroke Broca aphasia	10	Healthy volunteer	10	30 days	Right handed	BDAE, WAB
2016				RCT		—		20		20	4 weeks		

Table 2: Continued.

Publication year	First author	Funding organization	fMRI examination time	Study type	Stroke type	Aphasia duration	Type of AG patient	Number of acupuncture group	Type of CG patient	Number of control group	Treatment duration	Handedness	Outcome index
	Yuping Yuan [57]	Xinjiang Medical University	Before and after treatment		Ischemic in the left hemisphere		Poststroke aphasia		Poststroke aphasia			Right handed	ABU, NIHSS
2013	Jinhuan Liu [64]	Research Project of Hubei Provincial Department of Education	Before and after treatment	RCT	Not limited	7-10 days	Poststroke aphasia	10	Poststroke aphasia	10	30 days	Right handed	ABC, clinic efficacy
2012	Ni Li [65]	Affiliated Hospital of Hubei University of Traditional Chinese Medicine	Before and after treatment	RCT	Ischemic	0-6 months	Poststroke Broca aphasia	20	Poststroke Broca aphasia	20	4 weeks	Right handed	ABC, NIHSS, ADL
2011	Geng Li [54]	Hong Kong Jockey Club Charities Trust	Instant	Observational	6 ischemic and 1 hemorrhage in the left hemisphere	More than 6 months	Poststroke aphasia	7	Healthy volunteer	14	Instant acupuncture	Right handed	WAB
2010	Anson C.M. Chau [55]	The study was approved by the institutional review board of the University of Hong Kong/Hospital Authority Hong Kong West Cluster	Before and after treatment	Observational	Ischemic in the left hemisphere	17 ± 8 months	Poststroke aphasia	5	Poststroke aphasia	2	24 days	Right handed	CAB

ABC: Aphasia Battery of Chinese; ABU: Aphasia Battery of Uighur; ADL: activities of daily living; AG: acupuncture group; BDAE: Boston Diagnostic Aphasia Exam; CAB: Cantonese Aphasia Battery; CFCP: Chinese Functional Communication Profile; CG: control group; CRRCAE: China Rehabilitation Research Center Aphasia Examination; MoCA: Montreal Cognitive Assessment; NIHSS: National Institutes of Health Stroke Scale; RCT: randomized controlled trial; SAQOL-39: Stroke-Aphasia Quality of Life-39; SF-36: Medical Outcome Study Short Form-36; WAB: Western Aphasia Battery.

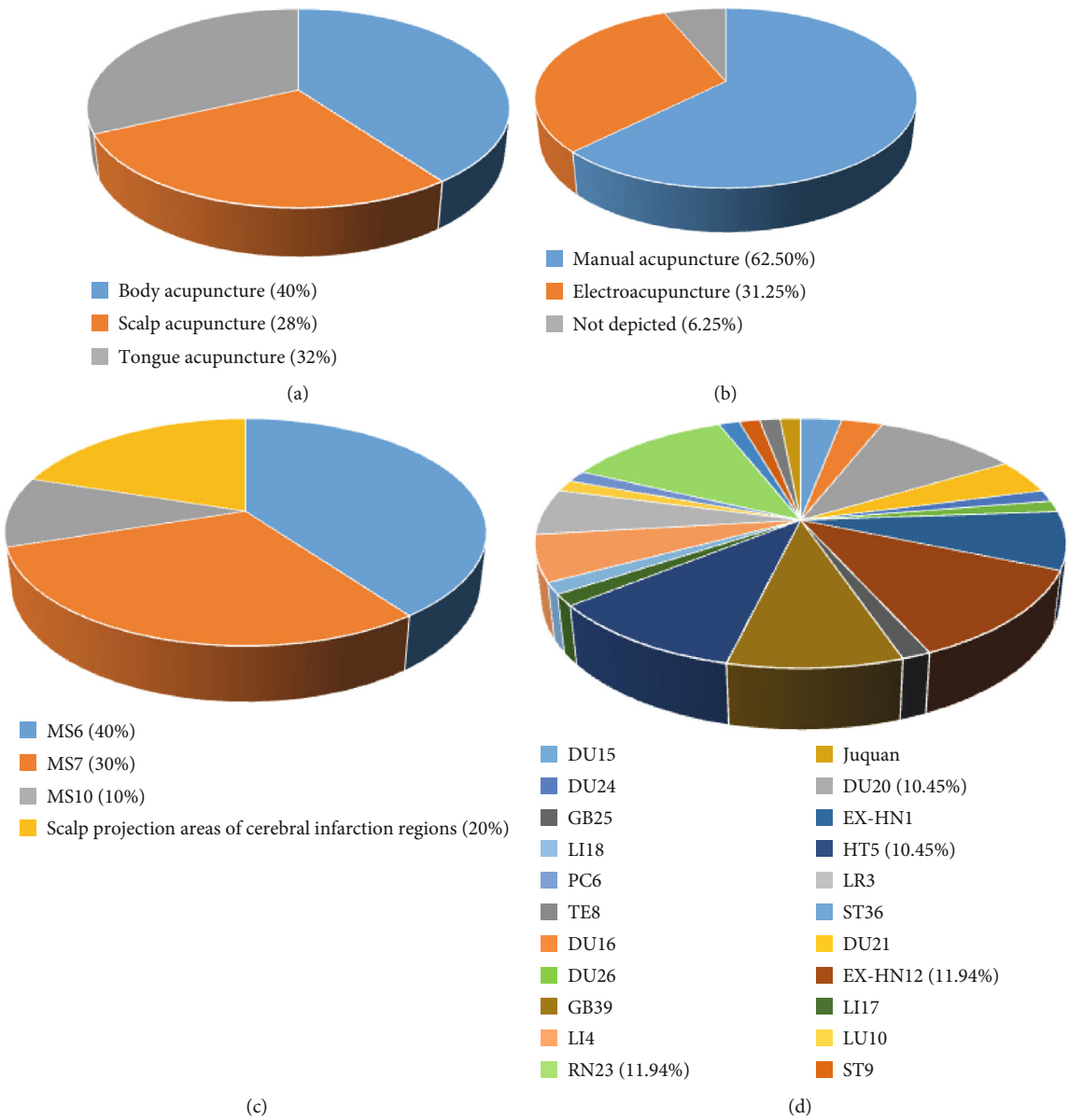

Figure 3: Acupuncture details. Note: (a) acupuncture therapy type: with 40% body acupuncture, 28% scalp acupuncture, and 32% tongue acupuncture. (b) Needling type: with 62.50% manual acupuncture, 31.25% electroacupuncture, and 6.25% not depicted. (c) Scalp acupuncture type: with 40% MS6, 30% MS7, 10% MS10, and 20% scalp projection areas of cerebral infarction regions. (d) Acupoint selection: the acupoints that are used above 10% included RN23 (11.94%), EX-HN12 (11.94%), HT5 (10.45%), and DU20 (10.45%).

study with the intervention of scalp acupuncture (MS6 and MS7) found more activated voxels in the projection area of scalp acupuncture, which was located in Broca's area as well as was associated with language function [57]. Additionally, compared with the task of word generation stimulation, a more powerful activation was found in Broca's area after conducting electroacupuncture stimulation on poststroke Broca aphasia patients [54].

(2) Activation in Mirror-Image Areas of Broca's Area. For the activation in mirror-image areas, one study reported significant increases of activation areas in the right hemisphere compared to the left hemisphere in the right-hand patients [64]. Another study reported a negative activation in the mirror-image areas on poststroke Broca aphasia patients after receiving tongue acupuncture for one month [61].

As for studies based on ALFF technology, one study reported the decreased ALFF (left temporal pole) and increased ALFF around mirror-image areas of Broca's area (right supramarginal gyrus, right inferior frontal gyrus, and left angular gyrus) in poststroke aphasia patients compared with the healthy volunteers before treatment [60]. After treatment, increased ALFF was found (left temporal pole) on poststroke aphasia patients.

(3) Brain Functional Connectivity Based on Dual-Stream Model. For the functional connectivity within the brain

Table 3: Intervention details.

Publication year	First author	AG interventions	Needle session	Needle duration	Needle frequency	Needle type	Acupoint	Needle response	CG interventions
2021	Binlong Zhang	Acupuncture and language rehabilitation	Not depicted	Not depicted	Not depicted	Not depicted	Not depicted	Not depicted	Language rehabilitation
2021	Defu Zhao	MA and language rehabilitation	24	30 days	6 times per week	Body acupuncture	DU26 (Shuigou), DU20 (Baihui), DU15 (Yamen), DU16 (Fengfu), DU24 (Shenting)	De qi	Language rehabilitation
2021	Xiaolin Li	MA and language rehabilitation	24	8 weeks	3 times per week	Body acupuncture, scalp acupuncture, tongue acupuncture	HT5 (Tongli), GB39 (Xuanzhong), EX-HN12 (Jinjin, Yuye), RN23 (Lianquan), DU20 (Baihui), EX-HN1 (Sishencong), scalp projection areas of cerebral infarction regions	De qi	Nonpoint needle and language rehabilitation
2019	Binlong Zhang	MA	12	30 days	3 times per week	Body acupuncture, scalp acupuncture, tongue acupuncture	HT5 (Tongli), GB39 (Xuanzhong), EX-HN12 (Jinjin, Yuye), RN23 (Lianquan), DU20 (Baihui), EX-HN1 (Sishencong), scalp projection areas of cerebral infarction regions	De qi	Healthy volunteer
2019	Yukang Xiao	MA and language rehabilitation	30	30 days	Once per day	Scalp acupuncture, tongue acupuncture	MS6, GB25 (Fengchi), DU16 (Fengfu), DU15 (Yamen), RN23 (Lianquan), EX-HN12 (Jinjin, Yuye), ST9 (Renying), LI17 (Tianding), LI18 (Futu), LU10 (Yuji)	Not depicted	Language rehabilitation
2018	Mingge Yang	MA and language rehabilitation	20	4 weeks	5 times per week	Scalp acupuncture	MS6, MS10	De qi	Language rehabilitation
2018	Shun Li	MA and conventional treatment	24	30 days	6 times per week	Body acupuncture	RN23 (Lianquan)	De qi	Conventional treatment
2017	Jingling Chang	EA (2 Hz, 2 mA)	Instant	—	—	Body acupuncture	HT5 (Tongli), GB39 (Xuanzhong)	Not depicted	Nonpoint needle
2016	Aiqin Wang	MA and language rehabilitation	12	30 days	3 times per week	Body acupuncture, tongue acupuncture	HT5 (Tongli), GB39 (Xuanzhong), EX-HN12 (Jinjin, Yuye), RN23 (Lianquan), DU20 (Baihui), EX-HN1 (Sishencong), LI4 (Hegu), LR3 (Taichong)	De qi	Healthy volunteer
2016	Binlong Zhang	MA and language rehabilitation	12	30 days	3 times per week	Body acupuncture, tongue acupuncture	HT5 (Tongli), GB39 (Xuanzhong), EX-HN12 (Jinjin, Yuye), RN23 (Lianquan), DU20 (Baihui), EX-HN1 (Sishencong), LI4 (Hegu), LR3 (Taichong)	Not depicted	Healthy volunteer

Table 3: Continued.

Publication year	First author	AG interventions	Needle session	Needle duration	Needle frequency	Needle type	Acupoint	Needle response	CG interventions
2016	Jinying Liu	MA and language rehabilitation	12	30 days	3 times per week	Body acupuncture, tongue acupuncture	EX-HN12 (Jinjin, Yuye), RN23 (Lianquan), DU20 (Baihui), EX-HN1 (Sishencong), LI4 (Hegu), LR3 (Taichong), HT5 (Tongli), GB39 (Xuanzhong)	Not depicted	Healthy volunteer
2016	Yuping Yuan	EA and language rehabilitation	24	4 weeks	6 times per week	Scalp acupuncture	MS6, MS7, DU20 (Baihui)	De qi	Language rehabilitation
2013	Jinhuan Liu	EA and language rehabilitation	12	30 days	3 times per week	Scalp acupuncture, tongue acupuncture	MS7, HT5 (Tongli), DU21 (Qianding), RN23 (Lianquan), EX-HN12 (Jinjin, Yuye)	Not depicted	Language rehabilitation
2012	Ni li	MA and language rehabilitation	20	4 weeks	5 times per week	Scalp acupuncture, tongue acupuncture	MS7, DU21 (Qianding), EX-HN12 (Jinjin, Yuye), Juquan	Not depicted	Language rehabilitation
2011	Geng Li	EA (2 Hz, mild stimulation)	Instant	—	—	Body acupuncture	TE 8 (Sanyangluo)	De qi	EA (2 Hz, mild stimulation)
2010	Anson C.M. Chau	EA	24	8 weeks	3 times per week	Body acupuncture	LI4 (Hegu), PC6 (Neiguan), LR3 (Taichong), ST36 (Zusanli)	De qi	EA

AG: acupuncture group; CG: control group; EA: electroacupuncture; MA: manual acupuncture.

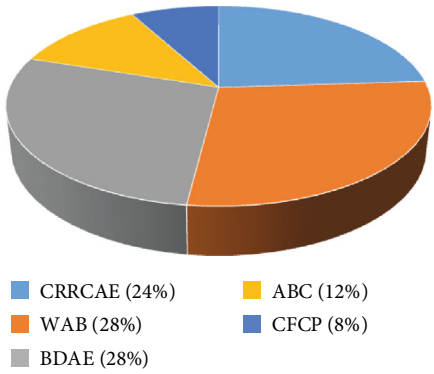

Figure 4: The proportion of aphasia assessment scales. Note: 24% Chinese Rehabilitation Research Center Standard Aphasia Examination (CRRCAE), 28% Western Aphasia Battery (WAB), 28% Boston Diagnostic Aphasia Exam (BDAE), 12% Aphasia Battery of Chinese (ABC), and 8% Chinese Functional Communication Profile (CFCP).

neural activity, the dual-stream model was proposed by Hickok and Poeppel [68, 69] and was used to illustrate the speech and language function in terms of brain cortical anatomy. As a complement of the classical Wernicke-Lichtheim model, it enriched the relationship of speech and language impairment and provided a practical way to help to understand the brain network [70, 71]. Based on the dual-stream model, one trial conducted the region of interest (ROI) analysis to detect brain functional connectivity [60]. After acupuncture, a reduction of the functional connectivity inside the dual-stream network was shown. Meanwhile, the intensified functional connectivity between the left inferior temporal gyrus and the middle frontal gyrus can be seen. For the studies based on the analysis of ReHo, the outcomes were partly consistent [52, 58]. Both of the two reported increased ReHo in the brain areas including the right fusiform gyrus, right inferior frontal gyrus, and left superior frontal gyrus and the decreased ReHo in the left inferior temporal gyrus and the right lingual gyrus. Besides that, compared with the control groups after treatment, an increased ReHo in the left anterior cuneiform lobe was detected in patients that received body acupuncture and Schuell language rehabilitation training; also, a decreased ReHo was found in the right anterior central gyrus [58], while patients that received scalp acupuncture and Schuell language rehabilitation training showed an increased ReHo in the right medial temporal lobe and cerebellum and decreased ReHo in the left caudate nucleus and right precentral gyrus [52].

(4) Brain Functional Connectivity Based on Interactive Model. The brain function was in an interactive model with complex integrity; thus, the brain network theory was proposed to explore the brain functional activity in detail [72, 73]. Using ICA and other techniques, the functional changes of different brain network models were uncovered [74]; for example, the default-model network was considered to reflect the spontaneous brain activity on the resting state, playing a key role in revealing the self-generated cognitive function [75], and the frontoparietal network was suggested to be associated with the creation of verbal language [76]; the attention network is defined as modulating the orienting, alerting, and executive work, and so on [77]. The damage of the cerebral anatomy structure integrity resulted in the impairment of language function [78, 79]. Compared with healthy participants, impairment was found in the integrity of white matter in poststroke aphasia patients [63]. After a 12-session acupuncture, improvements were shown in the left superior corona radiata, right posterior corona radiata, left external capsule, left superior longitudinal fasciculus, and left superior fronto-occipital fasciculus. In terms of ICA analysis, one study reported that after a 10-session acupuncture, there were reinforced functional connectivity (left superior frontal gyrus, right postcentral gyrus) and decreased functional connectivity (right supramarginal gyrus) within the right frontoparietal network of poststroke aphasia patients [62]. Additionally, decreased functional connectivity (left anterior central gyrus, left middle frontal gyrus) was found within the anterior default-model network. Another study reported that after receiving a 24-session acupuncture therapy, the intensified functional connectivity was shown in the left hemisphere within the frontoparietal network, default-model network, dorsal attention network, ventral attention network, and sensorimotor network of the poststroke aphasia patients, while no significant changes were found in the right hemisphere [45].

(5) Correlation between fMRI and Clinical Evaluation. The aphasia quotient (AQ) of WAB was correlated with the fraction anisotropy (FA) value of the left uncinate fasciculus in the poststroke aphasia patients. After treatment, the improvement of AQ was correlated with the ALFF value change in the left TP [42]. Using the functional connectivity analysis method, one trial revealed the AQ changes had a positive correlation with the intensified connectivity between the left inferior temporal gyrus and the middle frontal gyrus [60]. Another study found that the axial diffusivity value of the left superior longitudinal fasciculus had a negative correlation with AQ [63]. For the naming scores of WAB, a positive correlation was observed with the FA value of the right supramarginal gyrus [42] and the left uncinate fasciculus [62], while negative correlations were found in the mean diffusivity (MD) value and radial diffusivity (RD) value of the left superior longitudinal fasciculus [63]. Additionally, the repetition score was proven to have a positive correlation with the FA value of the right supramarginal gyrus [42]. Moreover, spontaneous speech and auditory comprehension were associated with the FA value of the left uncinate fasciculus [62]. Considering the characteristic of Cantonese, Chau's study used the Cantonese Aphasia Battery (CAB), which is the Cantonese version of WAB to assess the language function impairment. The study found a correlation between AQ of CAB and BOLD signal activation in the lesion of Wernicke's speech area on chronic poststroke aphasia patients.

For the CRRCAE score, one study investigated its relation with fractional anisotropy [45]. After treatment, the

Table 4: Neuroimaging outcomes.

Publication year	First author	Sample size	Neuroimaging technologies	Scanning design	Image acquisition time	Comparison	Neuroimaging results
2021	Binlong Zhang	60 (36 poststroke aphasia, 24 healthy volunteers)	rsfMRI, BOLD (ALFF), and DTI (FA)	—	Before and after acupuncture treatment	AG after treatment vs. healthy volunteer in ALFF	Decreased ALFF: the left temporal pole and increased ALFF in the right supramarginal gyrus, right inferior frontal gyrus, and left angular gyrus Correlation: the repetition scores have a positive correlation with the FA value of the right supramarginal gyrus
						AG after treatment vs. healthy volunteer in DTI	Decreased FA value: bilateral uncinate fasciculus. No significant difference was found in FA between poststroke aphasia patients before and after treatment. Correlation: the amount of damage in the left uncinate fasciculus was associated with WAB-AQ.
2021	Defu Zhao	96 (poststroke aphasia)	rsfMRI, BOLD (ReHo); task-state fMRI, BOLD (task-induced brain activation)	Task state: 20 s; resting state: 20 s; word generation task	Before and after acupuncture treatment	AG after treatment vs. CG after treatment	Increased ReHo: the right fusiform gyrus, right inferior frontal gyrus, left anterior cuneiform lobe, and left superior frontal gyrus. Decreased ReHo: the left inferior temporal gyrus, right lingual gyrus, and right anterior central gyrus.
						AG after treatment vs. AG before treatment	Increases intensified functional connectivity: the left hemisphere within the frontoparietal network, default-model network, dorsal attention network, ventral attention network, and sensorimotor network; no significant changes were found in the right hemisphere.
2021	Xiaolin Li	50 (poststroke aphasia)	rsfMRI, DTI (FA)	—	Before and after acupuncture treatment	AG after treatment vs. CG after treatment	Increased value: brain network connectivity, brain network node efficiency, and local brain network node efficiency in dorsal attention network 2 and frontoparietal network 1; brain network node degree centrality in sensorimotor network 2, ventral attention network 1, and ventral attention network 2. Correlation between FA and CRRCAE: FA value in the right inferior longitudinal fasciculus with the reading score and calculation score, FA value in the left cingulate gyrus with the speech score, right inferior longitudinal fasciculus with the reading score, and left superior longitudinal fasciculus with the writing score.
2019	Binlong Zhang	57 (31 poststroke aphasia, 26 healthy volunteers)	rsfMRI, BOLD (ROI)	—	Before and after acupuncture treatment	AG before treatment vs. healthy volunteer	Increased: the connectivity inside the dual-stream network, the connectivity between the dual-stream network and other brain areas except for the opposite dual-stream network. Decreased: the global efficiency of the dual-stream network, the average path length of the left middle

Table 4: Continued.

Publication year	First author	Sample size	Neuroimaging technologies	Scanning design	Image acquisition time	Comparison	Neuroimaging results
							gyrus, and correlated with the score of spontaneous speech and BDAE.
						AG after treatment vs. AG before treatment	Increased: the connectivity with other regions (left inferior temporal gyrus to the right middle frontal gyrus). Decreased: the connectivity inside the dual-stream network (the left posterior middle temporal gyrus to the left middle temporal gyrus; left upper middle temporal gyrus to the left middle temporal gyrus). Correlation: the ALFF change of the left temporal pole was positively correlated with WAB-AQ change.
						AG before treatment vs. CG before treatment	Activated brain areas: primary sensorimotor cortex ($n = 6^*/8^\#$), temporal lobe ($n = 12^*/11^\#$), occipital lobe ($n = 10^*/10^\#$), and basal ganglia ($n = 3^*/4^\#$), but no significant change was found ($P > 0.05$).
2019	Yukang Xiao	100 (poststroke aphasia)	rsfMRI, BOLD (ReHo)	—	Before and after acupuncture treatment	AG after treatment vs. AG before treatment	Activated brain areas: primary sensorimotor cortex ($n = 35/8$), temporal lobe ($n = 32/11$), occipital lobe ($n = 34/10$), and basal ganglia ($n = 15/4$); significant changes were found in the activated areas ($P < 0.05$).
						AG after treatment vs. CG after treatment	Activated brain areas: primary sensorimotor cortex ($n = 17^*/35^\#$), temporal lobe ($n = 15^*/32^\#$), occipital lobe ($n = 16^*/34^\#$), and basal ganglia ($n = 5^*/15^\#$); activated areas in AG significantly increased compared with CG ($P < 0.05$).
2018	Mingge Yang	30 (poststroke aphasia)	rsfMRI, BOLD (ROI)	—	Before and after acupuncture treatment	AG after treatment vs. CG after treatment	Increased ReHo: left dorsolateral superior frontal gyrus, insula, precuneus, and calcarine. Right triangle inferior frontal gyrus, fusiform gyrus, medial temporal lobe, and cerebellum. Decreased ReHo: left inferior temporal gyrus, caudate nucleus, right lingual gyrus, and precentral gyrus. Correlation: the auditory comprehension function impairment correlated with the lower ReHo value of the temporal gyrus.
2018	Shun Li	23 (poststroke aphasia)	Task-based fMRI, BOLD (task-induced brain activation)	Task state: 30 s; resting state: 30 s; word generation task	Before and after acupuncture treatment	AG after treatment vs. AG before treatment	Increased activated areas: left hemisphere Broca's area. Negative activated areas: mirror area of Broca's area in the right hemisphere.
						CG after treatment vs. CG before treatment	No significant changes were found in the activated areas; the Broca's area in the left hemisphere and

Table 4: Continued.

Publication year	First author	Sample size	Neuroimaging technologies	Scanning design	Image acquisition time	Comparison	Neuroimaging results
							the mirror area of Broca's area in the right hemisphere were symmetrically activated.
2017	Jingling Chang	22 poststroke aphasia	rsfMRI, BOLD (ROI)	Needling state: 30 s; resting state: 30 s	Instant acupuncture	AG after treatment vs. AG before treatment	Increased activated areas: the left hemisphere.
						AG before treatment vs. healthy volunteer	Decreased FC: left frontal parietal network (left inferior frontal gyrus, left inferior parietal lobule); right frontal parietal network (inferior parietal lobule); salience network (the right middle frontal gyrus, right anterior cingulate); anterior default mode network (left angular gyrus); posterior default mode network (right superior frontal gyrus, left superior parietal lobule, right anterior cuneiform lobe, right inferior frontal gyrus).
2016	Aiqin Wang	20 (10 poststroke aphasia, 10 healthy volunteers)	rsfMRI, BOLD (ROI)	—	Before and after acupuncture treatment	AG after treatment vs. AG before treatment	Increased FC: right frontal parietal network (left superior frontal gyrus, right postcentral gyrus). Decreased FC: right frontal parietal network (right supramarginal gyrus); anterior default mode network (left anterior central gyrus, the left middle frontal gyrus). No significant changes of FC were found in the left frontal parietal network, posterior default mode network, and salience network.
							Correlation: the average FC value of decreased brain area in the anterior default mode network (left anterior central gyrus, the left middle frontal gyrus) had a negative correlation with the spontaneous score. The FC of the right frontal parietal network (right supramarginal gyrus) had a positive correlation with AQ, repetition, and naming scores.
2016	Binlong Zhang	24 (12 poststroke aphasia, 12 healthy volunteers)	rsfMRI, BOLD (ICA)	—	Before and after acupuncture treatment	AG before treatment vs. CG before treatment	Increased brain areas: auditory network (right anterior central gyrus). Decreased brain areas: right frontoparietal network, frontoparietal network 1, auditory network (left inferior frontal gyrus, the left middle frontal gyrus, the right middle frontal gyrus).
						AG after treatment vs. AG before treatment	Increased brain areas: executive control network, auditory network (left paracentral lobule, the right middle frontal gyrus, right superior frontal gyrus).

Table 4: Continued.

Publication year	First author	Sample size	Neuroimaging technologies	Scanning design	Image acquisition time	Comparison	Neuroimaging results
						AG before treatment vs. healthy volunteer	Impairment of white matter: bilateral external capsule, bilateral uncinate fasciculus, left cingulate gyrus, left anterior limb of the internal capsule, left superior fronto-occipital fasciculus, and left inferior fronto-occipital fasciculus.
2016	Jinying Liu	10 poststroke aphasia	rsfMRI, DTI (ROI)	—	Before and after acupuncture treatment	AG after treatment vs. AG before treatment	Increased values: left superior corona radiata (AD), right posterior corona radiata (AD, MD), left external capsule (MD, RD), left superior longitudinal fasciculus (AD, MD, RD), and left superior fronto-occipital fasciculus (AD, MD, RD).
							Correlation: for the left superior longitudinal fasciculus, both of the MD value and RD value had negative correlations with WAB naming scores; the AD value had a negative correlation with AQ.
2016	Yuping Yuan	40 (poststroke aphasia)	Task-based fMRI, BOLD (task-induced brain activation)	Task state: 32 s; resting state: 32 s; word generation task	Before and after acupuncture treatment	AG after treatment vs. AG before treatment	Significant differences were found in activated voxel numbers in brain areas related to language function ($P < 0.05$).
						AG after treatment vs.CG after treatment	No significant changes were found in the poststroke aphasia patients ($P > 0.05$).
						CG after treatment vs. CG before treatment	Significant changes were found in the following brain areas: bilateral medial frontal gyrus, bilateral middle frontal gyrus, bilateral inferior frontal gyrus, bilateral anterior central gyrus, left angular gyrus, and left posterior superior temporal gyrus.
2013	Jinhuan Liu	20 (poststroke aphasia)	Task-based fMRI, BOLD (task-induced brain activation)	Task state: 20 s; resting state: 20 s; word generation task	Before and after acupuncture treatment	AG after treatment vs. AG before treatment	Significant changes were found in the following brain areas: bilateral medial frontal gyrus, bilateral superior frontal gyrus, bilateral middle frontal gyrus, bilateral inferior frontal gyrus, bilateral anterior cuneiform lobe, posterior cingulate cortex, left angular gyrus, left posterior superior temporal gyrus, bilateral cuneus, bilateral lingual gyrus, bilateral inferior occipital gyrus, bilateral basal ganglia, splenium of corpus callosum, and right posterior cerebellar lobe.
						AG after treatment vs. CG after treatment	Significant changes were found in the following brain areas: left superior frontal gyrus, left middle frontal gyrus, bilateral inferior frontal gyrus, left anterior central gyrus, left postcentral gyrus, left paracentral lobule, left posterior superior temporal gyrus, posterior

Table 4: Continued.

Publication year	First author	Sample size	Neuroimaging technologies	Scanning design	Image acquisition time	Comparison	Neuroimaging results
							cingulate cortex, bilateral anterior cuneiform lobe, bilateral cuneus, left angular gyrus, bilateral lingual gyrus, right hippocampus, right parahippocampal gyrus, bilateral superior occipital gyrus, bilateral inferior occipital gyrus, right posterior cerebellar lobe, left superior cerebellar lobule, and splenium of corpus callosum.
2012	Ni li	40 (poststroke aphasia)	Task-based fMRI, BOLD (task-induced brain activation)	Task state: 20 s; resting state: 20 s	Before and after acupuncture treatment	AG after treatment vs. AG before treatment	Increased activated areas: Broca's area.
						AG after acupuncture vs. AG before acupuncture	Significant activation in the left inferior frontal gyrus (opercular part, triangular part or insula), right inferior frontal gyrus, or parietal lobe (Rolandic operculum or triangular part). Strong activation on the lesion side of superior and middle frontal gyrus.
2011	Geng Li	21 (7 poststroke aphasia, 14 healthy volunteers)	Task-based fMRI, BOLD (task-induced brain activation)	Needling state: 45 s; resting state: 45 s; word generation task	Instant acupuncture	Healthy volunteer after acupuncture vs. healthy volunteer before acupuncture	Activated brain areas: left superior and middle frontal gyrus, but relatively weaker compared with AG.
						AG after WG vs. AG before WG	Activated brain areas: left inferior frontal gyrus (1 poststroke aphasia) and right inferior frontal gyrus (2 poststroke aphasia).
						AG after acupuncture vs. AG after WG	Activated brain areas: the right insula, left precentral gyrus, right median cingulate, and paracingulate gyrus of the limbic lobe. Significantly smaller activation: both sides of superior and middle frontal gyrus induced by acupuncture compared with WG task.
2010	Anson C.M. Chau	7 (poststroke aphasia)	Task-based fMRI, BOLD (task-induced brain activation)	Linguistic task	Before and after acupuncture treatment	Well-recovered group vs. poor-recovered group, both received electroacupuncture	Activated brain areas: the left, middle, and superior temporal gyrus.

[#]AG: acupuncture group; [*]CG: control group; AD: axial diffusivity; ALFF: amplitude of low-frequency fluctuation; AQ: aphasia quotient; BOLD: blood oxygen level dependent; CRRCAE: Chinese Rehabilitation Research Center Standard Aphasia Examination; DTI: diffusion tensor imaging; FA: fraction anisotropy; FC: functional connectivity; ICA: independent component analysis; MD: mean diffusivity; RD: radial diffusivity; ReHo: regional homogeneity; ROI: region of interest; rsfMRI: resting-state functional magnetic resonance; WAB: Western Aphasia Battery; WG: word generation.

poststroke aphasia patients in the acupuncture group showed several positive correlations in the following aspects: the reading score and calculation score with the FA value in the right inferior longitudinal fasciculus, the speech score with the FA value in the left cingulum cingulate, the writing score with the left superior longitudinal fasciculus, and the reading score with the right inferior longitudinal fasciculus. Another trial reported that the auditory comprehension function impairment correlated with the lower ReHo value of the temporal gyrus [52].

3.5.4. Cerebral Response of Instant Acupuncture. For the instant effect of acupuncture therapy, Xiao et al.'s study showed that after instant acupuncture stimulation [59], compared with the control group, more activated brain areas emerged in the primary sensorimotor cortex, temporal lobe, occipital lobe, and basal ganglia area of patients in the acupuncture group. One study reported that compared with the activation on the left side of healthy subjects (right-handed), increased neuron activity signals emerged on the lesion side (4 in the left side and 2 in the right side) of poststroke aphasia patients (superior frontal gyrus and middle frontal gyrus) after needling TE 8 with electroacupuncture in a rest-activation model. Similar to the outcome of Liu et al.'s study [64], there were significant increases of activation areas in the right hemisphere compared to the left hemisphere in the right-hand patients [53]. In terms of the correlation among the instant effect, language function, and daily activity ability, improvements in the reading ability, oral speech, and listening comprehension and in the CFCP were shown, as well as in the SAQOL-39 score.

4. Discussion

4.1. Innovation of This Systematic Review. This systematic review analyzed the mechanism of acupuncture on poststroke aphasia patients through summarizing current clinical neuroimaging researches. Previously, the systematic review and meta-analyses focused on the clinical effects of acupuncture on poststroke aphasia. Both Tang et al.'s study in 2019 and Zhang et al.'s study in 2021 reported acupuncture's clinical effects on poststroke aphasia [15, 17]. To deeply reveal the mechanism of poststroke aphasia's recovery, neuroimaging research was conducted. The existing systematic reviews that intended to explore the neuroimaging mechanism usually concentrated on the specific language recovery hypothesis such as language-related brain region activation or brain functional connectivity. Using meta-analyses, Zhang et al. in 2021 reported the relationship between the damage of dual-pathway tracts and language function impairment, addressing the neural mechanism of the Dual-Pathway White Matter [43]. Du et al.'s study compared regional activation between poststroke aphasia patients and healthy volunteers, implying the significance of dominant and nondominant language networks [24]. Though these studies provided valuable findings, they did not focus on the specific treatment of poststroke aphasia. With the growing number of neuroimaging researches of acupuncture on poststroke aphasia, the multiple models of imaging technologies and various fMRI test indexes provide direct evidence on revealing the neural signals under different conditions. Compared with other systematic reviews, this study analyzed the neural mechanism of acupuncture on poststroke aphasia by summarizing the multiple models of neuroimaging research. Moreover, our study analyzed the correlation between clinical indexes and neuroimaging outcomes, hoping to provide practical methods for the clinic. The findings of neural mechanisms can be summarized as the activation of language-related brain regions and functional changes of brain connectivity.

4.2. Hypothesis of Poststroke Aphasia Recovery Mechanism. Based on the classical theories of poststroke aphasia that derived from the anatomical locations, the impairments of Broca's area (the left inferior frontal gyrus) and Wernicke's area (the left superior temporal gyrus) are the most studied hypotheses [80]. Through BOLD-fMRI, significant brain activation induced by acupuncture stimulation was discovered in 14 studies, indicating that acupuncture might be a powerful stimulation for poststroke aphasia patients. By observing the ALFF changes, Zhang et al.'s study showed a correlation between the left temporal pole and AQ after acupuncture therapy, stressing the importance of the left uncinate fasciculus and left temporal pole in the recovery of poststroke aphasia [42]. To evaluate the effect in detail, Li and Yang's study compared acupuncture stimulation with word generation task, and the outcome showed a more powerful efficacy in the acupuncture group [54]. While word generation was a basic process during speech and comprehension rehabilitation, their findings indicated that acupuncture intensified the recovery process and played a role as a complementary therapy. Zhang et al.'s study and Li and Yang's study were consistent with current evidence, for both language-related brain areas and the survived brain structures around language regions, playing roles in the recovery of poststroke aphasia [81]. In accordance, clinical studies applied acupuncture in the projection of the language-related brain areas, proven to have effects in improving repetition and naming functions. Previously, meta-analysis based on clinical trials suggested that the stimulation therapy over language-related brain regions was beneficial for the naming performance [82].

As for findings related to functional changes of brain connectivity, through efforts of language researchers, studies have revealed that the ventral stream accounts for the language comprehension function [83] and the dorsal stream accounts for speech generation and speech perception [68]. Among the included 16 trials, only one study reported the recovery of language function emphasized on the hypothesis of the dual-stream model. According to Zhang's study in 2019 [60], there was a stronger connection within the dual-stream model and a weaker connection between the left inferior temporal gyrus and the right middle frontal gyrus in poststroke aphasia patients compared to the healthy subjects. After treatment, the abnormal connections in poststroke aphasia patients showed a fallback tendency, and the connection intensity between the left inferior temporal gyrus and the right middle frontal gyrus correlated with AQ value

and spontaneous speech. The outcomes were consistent with the hypotheses of Fridriksson's study [71], implying that the intensified connection between the dual-stream model in the bilateral hemisphere might be a potential target in poststroke aphasia's recovery. According to recent studies, evidence has been shown that enhanced cerebral blood flow and increased activation of the right hemisphere emerged after stroke, which highlighted the indispensable role of the right hemisphere in the recovery process of aphasia [84, 85].

Beneath the brain function changes, adequate cerebral blood flow perfusion provides the metabolism supports for the neural activities [27]. Researches focused on the cerebral blood of poststroke aphasia patients found worse perfusion in regions around the core lesions [86]. Hypoperfusion in the perilesional tissue correlates with the severity of language impairment. Thus, cerebral perfusion was considered as a prognosis factor that influences the language function recovery process [87, 88]. Substantial evidence was reported of acupuncture's effect on the cerebral perfusion and angiogenesis promotion in the cerebral ischemic condition [89–91], indicating that the boom of collateral circulation which plays as a compensatory part might be a potent pathophysiologic basis. Nevertheless, sparse studies provide limited evidence for acupuncture's effect on the cerebral perfusion in poststroke aphasia patients. Hence, further study could take this area into account.

4.3. Current Methodology of Included Studies

4.3.1. Sample Size. According to a literature review of 1461 fMRI studies, the medium sample size of the highly cited studies was 14.5 [92]. The small sample size (Mumford's study, $n = 30$) decreased the reliability of expected effect sizes [93]. Meanwhile, the statistical significance and true effects vary greatly as the sample size changes. Desmond and Glover's study showed that 12 subjects can meet the requirement of the typical activation on a voxel-based level (80% power, $\alpha = 0.05$) [94]. In this study, the medium sample size of the included studies was 27. 8 studies had a sample size below 30 participants, and 8 studies had a sample size between 30 and 100 participants. Considering that the calculation of fMRI is different from other trials, setting a standardized protocol is a practicable way to improve the statistical power, especially in multicenter studies [95].

4.3.2. Blinding and Concealment. Among the 16 included trials, only one study conducted the blinding procedure [45]. Though the therapeutic effects of acupuncture have been widely demonstrated by plenty of studies, the placebo effect was considered in some objective-evaluated studies [96, 97]. To reveal the real effect of acupuncture, the blinding procedure is strongly recommended. Currently, blinding interventions such as blunt needles without penetration, superficial needling, and nonaffected meridian needling are applied in researches [98, 99]. Apart from the acupuncture method, efforts are made to minimize the placebo effect, including limiting interactions between therapists and participants, adding to objective outcome measurements [100]. In this review, fMRI as an objective outcome is less affected by the placebo effect. However, the fMRI is easily affected by even a subtle stimulation, which might cause mixed bias to the specific effect of acupoint-based acupuncture therapy. Thus, the nonmeridian point needling or the nontherapeutic acupoint needling can be applied as a blinding control [101].

4.3.3. Intervention. Among the included 16 studies, one study did not mention the detail of acupuncture, 10 studies performed manual acupuncture, and 5 studies performed electroacupuncture. 9 studies described the acupuncture response as "de qi," which was induced by manipulation of the practitioner. But none of the "de qi" responses was quantitatively evaluated. In Traditional Chinese Medicine theory, "de qi" response is the core role to ensure the therapeutic effect of acupuncture, making it the ultimate goal in the manipulation of acupuncture practitioners. However, the "de qi" response is perceived mostly by patients and partly felt by the practitioner. Moreover, fMRI recorded the BOLD signal changes according to different "de qi" responses, and the signal activation in the right anterior insula correlated with the "de qi" degree. Thus, the assessment scales help with the visualization of the "de qi" response, providing an objective standard for clinical practice. Currently, there are several assessment scales for acupuncture senses, such as Visual Analog Scales (VAS) that quantified the five acupuncture senses and the anxiety degree and the Massachusetts General Hospital Acupuncture Sensation Scale (MASS) that contains VAS and two subscales which are used to evaluate the acupuncture sensation spreading and patients' mood. Apart from these scales, the Southampton Needling Sensation Questionnaire (SNSQ), Park Questionnaire, and Subjective Acupuncture Sensation Scale (SASS) are frequently used among studies.

4.3.4. Outcome Index. Among the 16 included studies, the most frequently used language assessments were CRRCAE, WAB, BDAE, ABC, and CFCP. WAB and BDAE were the most commonly used assessment tools for aphasia, and both of them were utilized for the clinical diagnosis of neurological disorders. Compared with BDAE, WAB was more popular for the brief design, which provides a quicker and more convenient assessment for clinicians and patients [102]. The WAB was recommended by the Research Outcome Measurement in Aphasia consensus statement to evaluate the poststroke aphasia recovery and is prevalently practiced in western countries [103]. It can be used to diagnose the aphasia type and to measure the aphasia impairment by calculating AQ. The Chinese version of WAB was practicable for the poststroke aphasia assessment for its comprehensive characteristic. However, it remains to be explored whether the accuracy of WAB is influenced by the language diversity and culture gap. Hence, the aphasia assessment tools based on Mandarin were explored. ABC was formulated based on WAB with unified guidelines, scoring standards, pictures and text cards, and aphasia classification according to standardized requirements [104–106]. It can be applied in aphasia patients with different handedness and education level. Moreover, it was sensitive to mild language impairment, and the quantitative result was a practical tool for the

clinician. Another tool was CRRCAE, which was designed by the China Rehabilitation Research Center according to the Mandarin characteristic and Chinese culture [107]. It contains the evaluation of general conditions and language function [108]. It was estimated that 91% of aphasia patients could complete the evaluation in items of oral comprehension and listening comprehension, making it prevalent among Chinese aphasia patients [109]. The result of CRRCAE was classified into 6 grades and could be presented as a curve at different phases of aphasia, which provided a visualized way for the aphasia recovery process [110]. Nevertheless, CRRCAE was only applied for adult patients, and the 30 items cost too much time for evaluation. Hence, it requires clinicians to choose the preferred tools to evaluate the aphasia condition correctly.

4.4. Limitation. There are still some limitations in this review. Firstly, multiple imaging technologies and fMRI test indexes (ReHo\ALFF\ICA) were conducted in the current included studies. On the one hand, the abundant findings helped to reveal the neural signals under different conditions; on the other hand, the inconsistent study protocols made it hard to carry out the quantitative meta-analyses. Since rigorous meta-analysis is an indispensable tool for providing evidence for healthcare policy and clinical practice [111, 112], future researches should be more cautious about the study design. Secondly, the included studies were all conducted in China, and the included participants were Chinese speakers. Considering the language diversity between Chinese characteristics and English letters, language and publication bias might exist. Thirdly, though most of the studies contained more than 20 participants (14/16), some studies contained less than 10 participants. Given the instability raised from small sample sizes, this might be a potential origin of heterogeneity. Despite 12 subjects being proven to meet the requirement of neuroimaging studies [96], trials with large sample sizes are required to minimize the risks of bias such as inadequate randomization or unstable outcomes. Thus, future studies were needed to deeply explore neuroimaging mechanisms of acupuncture's effects, as well as to provide more evidence to validate current findings.

5. Conclusion

In this study, we summarized current evidence of neuroimaging in the effects of acupuncture on poststroke aphasia. Through the systematic review method, we found that the mechanism of acupuncture's effect might be associated with the activation and functional connectivity of language-related brain areas. Moreover, the relationship between specific language function and clinical language function scales was revealed. However, these studies were still in the preliminary stage. Thus, multicenter RCT is needed to verify current evidence. Meanwhile, further neuroimaging mechanisms of acupuncture's effects should be explored to help predict the recovery process of post-stroke aphasia.

Data Availability

The data used to support the findings of this study are from the published literature.

Conflicts of Interest

The authors declare that the research was conducted in the absence of any commercial or financial relationships that could be construed as a potential conflict of interest.

Authors' Contributions

BXL was responsible for the conceptualization, methodology, and writing of the manuscript. SZD was responsible for the supervision and project administration. BMS and WMZ were responsible for data collection and data curation. BFZ and BLZ were responsible for the tables, figures, and checklists. CYQ and YHL were responsible for coordinating the study. YZD and ZHM were responsible for funding acquisition. All authors contributed to the article and approved the submitted version. Boxuan Li, Shizhe Deng and Bomo Sang contributed equally to this manuscript.

Acknowledgments

This research was funded by the Ministry of Science and Technology of the People's Republic of China, National Key Research and Development Program of China (2018YFC1706001, 2019YFC0840709); Tianjin Municipal Science and Technology Bureau, Tianjin Science and Technology Project (18PTLCSY00050, 18PTLCSY00060); and the First Teaching Hospital of Tianjin University of Traditional Chinese Medicine, Exploration and Innovation Project (YB202112).

Supplementary Materials

PRISMA 2020 Checklist. It contains the 27 checklist items that pertain to the content of a systematic review, including the title, abstract, introduction, methods, results, discussion, and other information. *(Supplementary Materials)*

References

[1] A. R. Damasio, "Aphasia," *The New England Journal of Medicine*, vol. 326, no. 8, pp. 531–539, 1992.

[2] M. Zhou, H. Wang, X. Zeng et al., "Mortality, morbidity, and risk factors in China and its provinces, 1990-2017: a systematic analysis for the Global Burden of Disease Study 2017," *Lancet*, vol. 394, no. 10204, pp. 1145–1158, 2019.

[3] C M Association, *China guideline for cerebrovascular disease prevention and treatment*, Ministry of Health of the People's Republic of China, 2007.

[4] M. F. F. B. Anna Basso, "Handbook of Clinical Neurology, Chapter 27 Rehabilitation of Aphasia," *Handbook of Clinical Neurology*, vol. 110, p. 145, 2013.

[5] M. Zhang, L. Geng, Y. Yang, and H. Ding, "Cohesion in the discourse of people with post-stroke aphasia," *Clinical Linguistics & Phonetics*, vol. 35, no. 1, pp. 2–18, 2021.

[6] E. De Cock, K. Batens, D. Hemelsoet, P. Boon, K. Oostra, and V. De Herdt, "Dysphagia, dysarthria and aphasia following a first acute ischaemic stroke: incidence and associated factors," *European Journal of Neurology*, vol. 27, no. 10, pp. 2014–2021, 2020.

[7] A. Bersano, F. Burgio, M. Gattinoni, L. Candelise, and PROSIT Study Group, "Aphasia burden to hospitalised acute stroke patients: need for an early rehabilitation programme," *International Journal of Stroke*, vol. 4, no. 6, pp. 443–447, 2009.

[8] A. C. Laska, A. Hellblom, V. Murray, T. Kahan, and M. Von Arbin, "Aphasia in acute stroke and relation to outcome," *Journal of Internal Medicine*, vol. 249, no. 5, pp. 413–422, 2001.

[9] H. L. Flowers, S. A. Skoretz, F. L. Silver et al., "Poststroke aphasia frequency, recovery, and outcomes: a systematic review and meta-analysis," *Archives of Physical Medicine and Rehabilitation*, vol. 97, no. 12, pp. 2188–2201.e8, 2016.

[10] S. Lee, Y. Na, W. S. Tae, and S. B. Pyun, "Clinical and neuroimaging factors associated with aphasia severity in stroke patients: diffusion tensor imaging study," *Scientific Reports*, vol. 10, no. 1, p. 12874, 2020.

[11] M. Jacobs, P. M. Briley, H. H. Wright, and C. Ellis, "Marginal assessment of the cost and benefits of aphasia treatment: evidence from community-based telerehabilitation treatment for aphasia," *Journal of Telemedicine and Telecare*, pp. 1357633X–2098277X, 2021.

[12] C. Wu, Y. Qin, Z. Lin et al., "Prevalence and impact of aphasia among patients admitted with acute ischemic stroke," *Journal of Stroke and Cerebrovascular Diseases*, vol. 29, no. 5, p. 104764, 2020.

[13] J. Fridriksson and A. E. Hillis, "Current approaches to the treatment of post-stroke aphasia," *Journal of Stroke*, vol. 23, no. 2, pp. 183–201, 2021.

[14] C. Picano, A. Quadrini, F. Pisano, and P. Marangolo, "Adjunctive approaches to aphasia rehabilitation: a review on efficacy and safety," *Brain Sciences*, vol. 11, no. 1, p. 41, 2021.

[15] H. Tang, W. Tang, F. Yang, W. Wu, and G. Shen, "Efficacy of acupuncture in the management of post-apoplectic aphasia: a systematic review and meta-analysis of randomized controlled trials," *BMC Complementary and Alternative Medicine*, vol. 19, no. 1, 2019.

[16] B. Zhang, Y. Han, X. Huang et al., "Acupuncture is effective in improving functional communication in post-stroke aphasia: a systematic review and meta-analysis of randomized controlled trials," *Wiener Klinische Wochenschrift*, vol. 131, no. 9-10, pp. 221–232, 2019.

[17] Y. Zhang, Z. Wang, X. Jiang, Z. Lv, L. Wang, and L. Lu, "Effectiveness of acupuncture for poststroke aphasia: a systematic review and meta-analysis of randomized controlled trials," *Complementary Medicine Research*, vol. 28, no. 6, pp. 545–556, 2021.

[18] J. Wu, H. Yin, D. Wang, Z. Zhu, and Z. Sun, "Origin and development situation of scalp acupuncture therapy," *Journal of Guangzhou University of Traditional Chinese Medicine*, vol. 36, no. 11, pp. 1783–1787, 2019.

[19] J. G. Sun and X. R. Sun, "Tongue acupuncture," *Zhongguo Zhen Jiu*, vol. 30, no. 4, pp. 347-348, 2010.

[20] X. Hu, B. Li, and X. Wang, "Scalp acupuncture therapy combined with exercise can improve the ability of stroke patients to participate in daily activities," *Complementary Therapies in Clinical Practice*, vol. 43, p. 101343, 2021.

[21] W. Y. Chung, S. Y. Liu, J. C. Gao et al., "Modulatory effect of international standard scalp acupuncture on brain activation in the elderly as revealed by resting-state fMRI," *Neural Regeneration Research*, vol. 14, no. 12, pp. 2126–2131, 2019.

[22] H. Liu, L. Chen, G. Zhang et al., "Scalp acupuncture enhances the functional connectivity of visual and cognitive-motor function network of patients with acute ischemic stroke," *Evidence-based Complementary and Alternative Medicine*, vol. 2020, Article ID 8836794, 11 pages, 2020.

[23] D. Yuan, H. Tian, Y. Zhou et al., "Acupoint-brain (acubrain) mapping: common and distinct cortical language regions activated by focused ultrasound stimulation on two language-relevant acupoints," *Brain and Language*, vol. 215, p. 104920, 2021.

[24] Y. Du, Y. Lee, C. He et al., "The changed functional status of the brain was involved in patients with poststroke aphasia: coordinate-based (activation likelihood estimation) meta-analysis," *Brain and Behavior: A Cognitive Neuroscience Perspective*, vol. 10, no. 12, article e1867, 2020.

[25] J. Xiao, H. Zhang, J. Chang et al., "Effects of electro-acupuncture at Tongli (HT 5) and Xuanzhong (GB 39) acupoints from functional magnetic resonance imaging evidence," *Chinese Journal of Integrative Medicine*, vol. 22, no. 11, pp. 846–854, 2016.

[26] R. M. Lazar, A. E. Speizer, J. R. Festa, J. W. Krakauer, and R. S. Marshall, "Variability in language recovery after first-time stroke," *Journal of Neurology, Neurosurgery & Psychiatry*, vol. 79, no. 5, pp. 530–534, 2008.

[27] N. T. Abbott, C. J. Baker, C. Chen, T. T. Liu, and T. E. Love, "Defining hypoperfusion in chronic aphasia: an individualized thresholding approach," *Brain Sciences*, vol. 11, no. 4, p. 491, 2021.

[28] M. Martzoukou, A. Nousia, G. Nasios, and S. Tsiouris, "Adaptation of melodic intonation therapy to Greek: a clinical study in Broca's aphasia with brain perfusion SPECT validation," *Frontiers in Aging Neuroscience*, vol. 13, p. 433, 2021.

[29] J. D. Stefaniak, R. S. W. Alyahya, and M. A. Lambon Ralph, "Language networks in aphasia and health: a 1000 participant activation likelihood estimation meta-analysis," *NeuroImage*, vol. 233, p. 117960, 2021.

[30] Y. Lv, L. Li, Y. Song et al., "The local brain abnormalities in patients with transient ischemic attack: a resting-state fMRI study," *Frontiers in Neuroscience*, vol. 13, p. 24, 2019.

[31] M. D. Fox and M. E. Raichle, "Spontaneous fluctuations in brain activity observed with functional magnetic resonance imaging," *Nature Reviews Neuroscience*, vol. 8, no. 9, pp. 700–711, 2007.

[32] Z. Y. Feng, H. Yong, Z. C. Zhe et al., "Altered baseline brain activity in children with ADHD revealed by resting- state functional MRI," *Brain and Development*, vol. 29, no. 2, pp. 83–91, 2007.

[33] B. Biswal, F. Z. Yetkin, V. M. Haughton, and J. S. Hyde, "Functional connectivity in the motor cortex of resting human brain using echo-planar MRI," *Magnetic Resonance in Medicine*, vol. 34, no. 4, pp. 537–541, 1995.

[34] Y. Zhang, Z. Wang, J. Du et al., "Regulatory effects of acupuncture on emotional disorders in patients with menstrual migraine without aura: a resting-state fMRI study," *Frontiers in Neuroscience*, vol. 15, p. 726505, 2021.

[35] A. Xiang, Y. Yu, X. Jia et al., "The low-frequency BOLD signal oscillation response in the insular associated to immediate analgesia of ankle acupuncture in patients with chronic low back pain," *Journal of Pain Research*, vol. 12, pp. 841–850, 2019.

[36] X. Zuo, T. Xu, L. Jiang et al., "Toward reliable characterization of functional homogeneity in the human brain: preprocessing, scan duration, imaging resolution and computational space," *NeuroImage*, vol. 65, pp. 374–386, 2013.

[37] X. Zuo, R. Ehmke, M. Mennes et al., "Network centrality in the human functional connectome," *Cerebral Cortex*, vol. 22, no. 8, pp. 1862–1875, 2012.

[38] R. L. Buckner, J. Sepulcre, T. Talukdar et al., "Cortical hubs revealed by intrinsic functional connectivity: mapping, assessment of stability, and relation to Alzheimer's disease," *Journal of Neuroscience*, vol. 29, no. 6, pp. 1860–1873, 2009.

[39] M. P. van den Heuvel and H. E. Hulshoff Pol, "Exploring the brain network: a review on resting-state fMRI functional connectivity," *European Neuropsychopharmacology*, vol. 20, no. 8, pp. 519–534, 2010.

[40] S. Liu, M. Li, W. Tang, G. Wang, and Y. Lv, "An fMRI study of the effects on normal language areas when acupuncturing the Tongli (HT5) and Xuanzhong (GB39) acupoints," *Journal of International Medical Research*, vol. 45, no. 6, pp. 1961–1975, 2017.

[41] L. Li, X. Liu, F. Wu et al., "Electroacupuncture stimulation of language-implicated acupoint Tongli (HT 5) in healthy subjects: an fMRI evaluation study," *Chinese Journal of Integrative Medicine*, vol. 24, no. 11, pp. 822–829, 2018.

[42] B. Zhang, J. Chang, J. Park et al., "Uncinate fasciculus and its cortical terminals in aphasia after subcortical stroke: a multimodal MRI study," *NeuroImage: Clinical*, vol. 30, p. 102597, 2021.

[43] J. Zhang, S. Zhong, L. Zhou et al., "Correlations between dual-pathway white matter alterations and language impairment in patients with aphasia: a systematic review and meta-analysis," *Neuropsychology Review*, vol. 31, no. 3, pp. 402–418, 2021.

[44] E. Gleichgerrcht, M. Kocher, T. Nesland, C. Rorden, J. Fridriksson, and L. Bonilha, "Preservation of structural brain network hubs is associated with less severe post-stroke aphasia," *Restorative Neurology and Neuroscience*, vol. 34, no. 1, pp. 19–28, 2015.

[45] X. Li, *An fMRI study of YiSuiXingShen acupuncture on the cerebral microstructure and functional network of post-stroke aphasia patients, [Ph.D. thesis]*, Beijing Uni, 2021.

[46] N. F. Dronkers, O. Plaisant, M. T. Iba-Zizen, and E. A. Cabanis, "Paul Broca's historic cases: high resolution MR imaging of the brains of Leborgne and Lelong," *Brain*, vol. 130, no. 5, pp. 1432–1441, 2007.

[47] A. Gajardo-Vidal, D. L. Lorca-Puls, P. Team et al., "Damage to Broca's area does not contribute to long-term speech production outcome after stroke," *Brain*, vol. 144, no. 3, pp. 817–832, 2021.

[48] X. Chen, L. Chen, S. Zheng et al., "Disrupted brain connectivity networks in aphasia revealed by resting-state fMRI," *Frontiers in Aging Neuroscience*, vol. 13, p. 666301, 2021.

[49] M. J. Page, J. E. McKenzie, P. M. Bossuyt et al., "The PRISMA 2020 statement: an updated guideline for reporting systematic reviews," *BMJ*, vol. 372, article n71, 2021.

[50] S J P M Higgins JPT, *Cochrane Handbook for Systematic Reviews of Interventions Version 6.2*, Cochrane, 2021.

[51] J. A. C. Sterne, J. Savović, M. J. Page et al., "RoB 2: a revised tool for assessing risk of bias in randomised trials," *BMJ*, vol. 366, p. l4898, 2019.

[52] M. Yang, *The resting state fMRI regional homogeneity study of the acupuncture in the treatment of post-stroke motor aphasia, [M.S. thesis]*, Fujian Uni, 2018.

[53] J. Chang, H. Zhang, Z. Tan, J. Xiao, S. Li, and Y. Gao, "Effect of electroacupuncture in patients with post-stroke motor aphasia," *Wiener Klinische Wochenschrift*, vol. 129, no. 3-4, pp. 102–109, 2017.

[54] G. Li and E. S. Yang, "An fMRI study of acupuncture-induced brain activation of aphasia stroke patients," *Complementary Therapies in Medicine*, vol. 19, pp. S49–S59, 2011.

[55] A. C. Chau, C. R. Fai, X. Jiang, P. K. Au-Yeung, and L. S. Li, "An fMRI study showing the effect of acupuncture in chronic stage stroke patients with aphasia," *Journal of Acupuncture and Meridian Studies*, vol. 3, no. 1, pp. 53–57, 2010.

[56] B. Zhang, *The resting state fMRI study and meta-analysis of acupuncture's effect on post-stroke aphasia, [M.S. thesis]*, Beijing Uni, 2016.

[57] Y. Yuan, *Effect of acupuncture combined with rehabilitation on post-stroke aphasia Uigur patients, [M.S. thesis]*, Xinjiang Medical Uni, 2016.

[58] D. Zhao, Y. Zhao, and X. Yang, "Effect of Du Meridian acupoint acupuncture combined with Schuell language rehabilitation training on the speech function, MoCA and the function of language center in aphasia patients after stroke," *Journal of Clinical and Experimental Medicine*, vol. 20, no. 8, pp. 886–890, 2021.

[59] Y. Xiao, D. Li, and H. Li, "Effect of scalp acupuncture combined with speech rehabilitation on post-stroke aphasia patients," *Neural Injury and Functional Reconstruction*, vol. 14, no. 11, pp. 581-582, 2019.

[60] B. Zhang, *The mechanism study of YiSuiXingShen acupuncture of aphasia based on dual-stream model, [Ph.D. thesis]*, Beijing Uni, 2019.

[61] S. Li, C. Song, S. Xue, Y. Wang, J. Lin, and R. Wang, "An fMRI study of acupuncture's effect on Broca aphasia," *Guangdong Medical Journal*, vol. 39, no. 10, pp. 1566–1569, 2018.

[62] A. Wang, *The resting state fMRI study based on brain function network of comprehensive Traditional Chinese Medicine therapy on post-stroke Broca aphasia, [M.S. thesis]*, Beijing Uni, 2016.

[63] J. Liu, *DTI study of XingShenHeYi acupuncture therapy combined with rehabilitation on post-stroke aphasia, [M.S. thesis]*, Beijing Uni, 2016.

[64] J. Liu, J. Chen, Z. Tan, N. Li, and Y. Zhao, "The effects of acupuncture combined with speech therapy on aphasia caused by stroke: clinical and fMRI study," *Chinese Journal of Physical Medicine and Rehabilitation*, vol. 35, no. 7, pp. 552–556, 2013.

[65] N. Li, *Clinical research of the acupuncture combined with Shuyuwan on post-stroke Broca aphasia, [M.S. thesis]*, Hubei Uni, 2012.

[66] H. MacPherson, D. G. Altman, R. Hammerschlag et al., "Revised STandards for Reporting Interventions in Clinical Trials of Acupuncture (STRICTA): extending the CONSORT statement," *Journal of Evidence-Based Medicine*, vol. 3, no. 3, pp. 140–155, 2010.

[67] World Health Organization, *Regional Office for the Western Pacific. Standard acupuncture nomenclature: a brief explanation of 361 classical acupuncture point names and their multilingual comparative list*, WHO Regional Office for the Western Pacific, 1993.

[68] G. Hickok and D. Poeppel, "The cortical organization of speech processing," *Nature Reviews Neuroscience*, vol. 8, no. 5, pp. 393–402, 2007.

[69] G. Hickok and D. Poeppel, "Dorsal and ventral streams: a framework for understanding aspects of the functional anatomy of language," *Cognition*, vol. 92, no. 1-2, pp. 67–99, 2004.

[70] J. Fridriksson, D. den Ouden, A. E. Hillis et al., "Anatomy of aphasia revisited," *Brain*, vol. 141, no. 3, pp. 848–862, 2018.

[71] J. Fridriksson, G. Yourganov, L. Bonilha, A. Basilakos, D. Den Ouden, and C. Rorden, "Revealing the dual streams of speech processing," *Proceedings of the National Academy of Sciences*, vol. 113, no. 52, pp. 15108–15113, 2016.

[72] A. J. Holmes, M. O. Hollinshead, T. M. O'Keefe et al., "Brain Genomics Superstruct Project initial data release with structural, functional, and behavioral measures," *Scientific Data*, vol. 2, no. 1, p. 150031, 2015.

[73] M. Oschmann, J. R. Gawryluk, and for the Alzheimer's Disease Neuroimaging Initiative, "A longitudinal study of changes in resting-state functional magnetic resonance imaging functional connectivity networks during healthy aging," *Brain Connectivity*, vol. 10, no. 7, pp. 377–384, 2020.

[74] A. J. Sihvonen, V. Leo, P. Ripollés et al., "Vocal music enhances memory and language recovery after stroke: pooled results from two RCTs," *Annals of Clinical Translational Neurology*, vol. 7, no. 11, pp. 2272–2287, 2020.

[75] G. M. Rossetti, G. D. Avossa, M. Rogan, J. H. Macdonald, S. J. Oliver, and P. G. Mullins, "Reversal of neurovascular coupling in the default mode network: evidence from hypoxia," *Journal of Cerebral Blood Flow & Metabolism*, vol. 41, no. 4, pp. 805–818, 2021.

[76] W. Zhu, Q. Chen, L. Xia et al., "Common and distinct brain networks underlying verbal and visual creativity," *Human Brain Mapping*, vol. 38, no. 4, pp. 2094–2111, 2017.

[77] D. Mannarelli, C. Pauletti, A. Currà et al., "The cerebellum modulates attention network functioning: evidence from a cerebellar transcranial direct current stimulation and attention network test study," *The Cerebellum*, vol. 18, no. 3, pp. 457–468, 2019.

[78] J. Zhang, W. Zheng, D. Shang et al., "Fixel-based evidence of microstructural damage in crossing pathways improves language mapping in post-stroke aphasia," *NeuroImage: Clinical*, vol. 31, p. 102774, 2021.

[79] M. Corbetta, L. Ramsey, A. Callejas et al., "Common behavioral clusters and subcortical anatomy in stroke," *Neuron*, vol. 85, no. 5, pp. 927–941, 2015.

[80] G. Hartwigsen and D. Saur, "Neuroimaging of stroke recovery from aphasia - insights into plasticity of the human language network," *NeuroImage*, vol. 190, pp. 14–31, 2019.

[81] R. Li, N. Mukadam, and S. Kiran, "Functional MRI evidence for reorganization of language networks after stroke," *Handbook of Clinical Neurology*, vol. 185, pp. 131–150, 2022.

[82] B. Elsner, J. Kugler, and J. Mehrholz, "Transcranial direct current stimulation (tDCS) for improving aphasia after stroke: a systematic review with network meta-analysis of randomized controlled trials," *Journal of Neuroengineering and Rehabilitation*, vol. 17, no. 1, p. 88, 2020.

[83] E. T. McKinnon, J. Fridriksson, G. R. Glenn et al., "Structural plasticity of the ventral stream and aphasia recovery," *Annals of Neurology*, vol. 82, no. 1, pp. 147–151, 2017.

[84] O. Elkana, R. Frost, U. Kramer, D. Ben-Bashat, and A. Schweiger, "Cerebral language reorganization in the chronic stage of recovery: a longitudinal fMRI study," *Cortex*, vol. 49, no. 1, pp. 71–81, 2013.

[85] J. Zhang, Z. Zhou, L. Li et al., "Cerebral perfusion mediated by thalamo-cortical functional connectivity in non-dominant thalamus affects naming ability in aphasia," *Human Brain Mapping*, vol. 43, no. 3, pp. 940–954, 2022.

[86] A. E. Hillis, P. B. Barker, N. J. Beauchamp, B. Gordon, and R. J. Wityk, "MR perfusion imaging reveals regions of hypoperfusion associated with aphasia and neglect," *Neurology*, vol. 55, no. 6, pp. 782–788, 2000.

[87] S. Rudilosso, A. Rodríguez, S. Amaro et al., "Value of vascular and non-vascular pattern on computed tomography perfusion in patients with acute isolated aphasia," *Stroke*, vol. 51, no. 8, pp. 2480–2487, 2020.

[88] C. K. Thompson, M. Walenski, Y. Chen et al., "Intrahemispheric perfusion in chronic stroke-induced aphasia," *Neural Plasticity*, vol. 2017, 15 pages, 2017.

[89] Y. Du, L. Shi, J. Li, J. Xiong, B. Li, and X. Fan, "Angiogenesis and improved cerebral blood flow in the ischemic boundary area were detected after electroacupuncture treatment to rats with ischemic stroke," *Neurological Research*, vol. 33, no. 1, pp. 101–107, 2011.

[90] Q. Y. Chang, Y. W. Lin, and C. L. Hsieh, "Acupuncture and neuroregeneration in ischemic stroke," *Neural Regeneration Research*, vol. 13, no. 4, pp. 573–583, 2018.

[91] D. Szucs and J. P. Ioannidis, "Sample size evolution in neuroimaging research: an evaluation of highly-cited studies (1990-2012) and of latest practices (2017-2018) in high-impact journals," *NeuroImage*, vol. 221, p. 117164, 2020.

[92] J. A. Mumford and T. E. Nichols, "Power calculation for group fMRI studies accounting for arbitrary design and temporal autocorrelation," *NeuroImage*, vol. 39, no. 1, pp. 261–268, 2008.

[93] J. E. Desmond and G. H. Glover, "Estimating sample size in functional MRI (fMRI) neuroimaging studies: statistical power analyses," *Journal of Neuroscience Methods*, vol. 118, no. 2, pp. 115–128, 2002.

[94] A. George, R. Kuzniecky, H. Rusinek, H. R. Pardoe, and for the Human Epilepsy Project Investigators, "Standardized brain MRI acquisition protocols improve statistical power in multicenter quantitative morphometry studies," *Journal of Neuroimaging*, vol. 30, no. 1, pp. 126–133, 2020.

[95] S. Xu, L. Yu, X. Luo et al., "Manual acupuncture versus sham acupuncture and usual care for prophylaxis of episodic migraine without aura: multicentre, randomised clinical trial," *BMJ*, vol. 368, article m697, 2020.

[96] H. C. Diener, K. Kronfeld, G. Boewing et al., "Efficacy of acupuncture for the prophylaxis of migraine: a multicentre randomised controlled clinical trial," *Lancet Neurology*, vol. 5, no. 4, pp. 310–316, 2006.

[97] J. F. Tu, J. W. Yang, G. X. Shi et al., "Efficacy of intensive acupuncture versus sham acupuncture in knee osteoarthritis: a randomized controlled trial," *Arthritis & Rheumatology*, vol. 73, no. 3, pp. 448–458, 2021.

[98] K. Streitberger and J. Kleinhenz, "Introducing a placebo needle into acupuncture research," *Lancet*, vol. 352, no. 9125, pp. 364-365, 1998.

[99] L. Zhao, D. Li, H. Zheng et al., "Acupuncture as adjunctive therapy for chronic stable angina: a randomized clinical trial," *JAMA Internal Medicine*, vol. 10, pp. 1388–1397, 2019.

[100] S. Deng, X. Zhao, R. Du et al., "Is acupuncture no more than a placebo? Extensive discussion required about possible bias," *Experimental and Therapeutic Medicine*, vol. 10, no. 4, pp. 1247–1252, 2015.

[101] A. Kertesz, "The Western Aphasia Battery: a systematic review of research and clinical applications," *Aphasiology*, vol. 36, no. 1, pp. 21–50, 2022.

[102] S. J. Wallace, L. Worrall, T. Rose et al., "A core outcome set for aphasia treatment research: the ROMA consensus statement," *International Journal of Stroke*, vol. 14, no. 2, pp. 180–185, 2019.

[103] C. Ellis, R. K. Peach, and K. Rothermich, "Relative weight analysis of the Western Aphasia Battery," *Aphasiology*, vol. 35, no. 10, pp. 1281–1292, 2021.

[104] A. Kertesz and E. Poole, "The aphasia quotient: the taxonomic approach to measurement of aphasic disability," *Canadian Journal of Neurological Sciences*, vol. 31, no. 2, pp. 175–184, 2004.

[105] D. Fromm, M. Forbes, A. Holland, S. G. Dalton, J. Richardson, and B. MacWhinney, "Discourse characteristics in aphasia beyond the Western Aphasia Battery cutoff," *American Journal of Speech-Language Pathology*, vol. 26, no. 3, pp. 762–768, 2017.

[106] S. Gao, *Aphasia*, Peaking University Medical Press, 2016.

[107] C. Bao and J. Zhang, "Discuss the advantages and disadvantages of Chinese Standard Aphasia Examination," *Chinese Manipulation & Rehabilitation Medicine*, vol. 8, no. 3, pp. 9-10, 2017.

[108] J. Cao, C. Zhao, M. Jin, and Y. Zhang, "Common methods for estimation of aphasia," *Chinese Journal of Clinical Rehabilitation*, vol. 10, no. 18, pp. 139–141, 2006.

[109] Q. Zhang, S. Ji, S. Li et al., "Reliability and validity of Chinese Rehabilitation Research Center Standard Aphasia Examination," *Chinese Journal of Rehabilitation Theory and Practice*, vol. 11, no. 9, pp. 703–705, 2005.

[110] T. Muka, M. Glisic, J. Milic et al., "A 24-step guide on how to design, conduct, and successfully publish a systematic review and meta-analysis in medical research," *European Journal of Epidemiology*, vol. 35, no. 1, pp. 49–60, 2020.

[111] A. P. Siddaway, A. M. Wood, and L. V. Hedges, "How to do a systematic review: a best practice guide for conducting and reporting narrative reviews, meta-analyses, and meta-syntheses," *Annual Review of Psychology*, vol. 70, no. 1, pp. 747–770, 2019.

[112] L. Shi, H. M. Cao, Y. Li et al., "Electroacupuncture improves neurovascular unit reconstruction by promoting collateral circulation and angiogenesis," *Neural Regeneration Research*, vol. 12, no. 12, pp. 2000–2006, 2017.

Hindawi
Neural Plasticity
Volume 2022, Article ID 3148739, 11 pages
https://doi.org/10.1155/2022/3148739

Review Article

Cognitive Dysfunction following Cerebellar Stroke: Insights Gained from Neuropsychological and Neuroimaging Research

Qi Liu,[1] **Chang Liu**,[1] **Yu Chen**,[2,3] **and Yumei Zhang**[4]

[1]*Department of Neurology, Beijing Tiantan Hospital, Capital Medical University, Beijing, China*
[2]*China National Clinical Research Center for Neurological Diseases, Beijing Tiantan Hospital, Capital Medical University, Beijing, China*
[3]*Department of Neurology, Memory and Aging Center, University of California, San Francisco, San Francisco, CA, USA*
[4]*Department of Rehabilitation, Beijing Tiantan Hospital, Capital Medical University, Beijing, China*

Correspondence should be addressed to Yu Chen; sherryyu.chen@ucsf.edu and Yumei Zhang; zhangyumei95@aliyun.com

Received 4 November 2021; Revised 10 March 2022; Accepted 31 March 2022; Published 15 April 2022

Academic Editor: Xiaozheng Liu

Although the cerebellum has been consistently noted in the process of cognition, the pathophysiology of this link is still under exploration. Cerebellar stroke, in which the lesions are focal and limited, provides an appropriate clinical model disease for studying the role of the cerebellum in the cognitive process. This review article targeting the cerebellar stroke population (1) describes a cognitive impairment profile, (2) identifies the cerebellar structural alterations linked to cognition, and (3) reveals possible mechanisms of cerebellar cognition using functional neuroimaging. The data indicates the disruption of the cerebro-cerebellar loop in cerebellar stroke and its contribution to cognitive dysfunctions. And the characteristic of cognitive deficits are mild, span a broad spectrum, dominated by executive impairment. The consideration of these findings could contribute to deeper and more sophisticated insights into the cognitive function of the cerebellum and might provide a novel approach to cognitive rehabilitation. The goal of this review is to spread awareness of cognitive impairments in cerebellar disorders.

1. Introduction

For many decades, the cerebellum has been considered a pure control machine for physical movement. However, several studies have shown the effect of the cerebellum on cognition and affect [1]. For the first time, Schmahmann et al. described a series of cognitive and behavioral dysfunctional symptoms in 20 patients with focal cerebellar lesions and summarized them with the term "cerebellar cognitive affective syndrome" (CCAS) [2]. The concept of CCAS is a milestone in the study of cerebellar cognition. In the past two decades, the role of the cerebellum in cognition has been widely verified in patients with different types of cerebellar disorders [3–5]. Cerebellar stroke, in which the lesion is confined to the cerebellum and not complicated by cerebral abnormities such as atrophy and hydrocephalus, provides an appropriate clinical model for studying the role of the cerebellum in the cognitive process. In addition, the distribution of cerebellar infarction lesions varied by different vascular territories, which was applicable to studying the cognitive topography of the cerebellum. Beyond physical disability, cognitive impairment has been recognized in cerebellar stroke patients, with approximately 64% of whom developed cognitive impairment and 24% of whom fulfilled diagnostic criteria for dementia [6].

In the current review, we aim to describe the cognitive profile following cerebellar damage, reveal the cognitive topography of the cerebellum, and explore the effect of the cerebral-cerebellar loop on cognition through the model of cerebellar stroke.

2. The Cognitive Deficit in Patients with Cerebellar Stroke

CCAS has been observed in patients with cerebellar infarction [7], which is characterized by executive function disturbances such as poor planning, perseveration of shifting set, abstract reasoning, and verbal fluency; visual-spatial

disorganization and impaired visual-spatial memory; dysprosodia such as language difficulties, mild anomia, and agrammatism; and personality change characterized by a flattening or blunting affect, disinhibited, and inappropriate behavior [2].

2.1. Visual-Spatial Cognition. Spatial ability refers to the capacity to understand, reason about, and remember the spatial relations among objects or space. Botez described that a patient with a left superior cerebellar artery infarct did worse in picture arrangement, Benton's judgment of line orientation, and Hooper's visual organization test [8]. This is the first time visual-spatial deficits have been reported in isolated cerebellar infarction patients. Since then, several studies have noted impaired performance on a range of visual-spatial measures in patients with cerebellar stroke, including the block design tasks from the Wechsler Intelligence Scale [9, 10], copying and recall of Rey-Osterrieth complex figure [11], letter cancellation test [12], "blank clock" test [6], character-line bisection task [13], and mental rotation tasks [14]. These observations are suggestive of abnormalities in the field of visuoconstruction, visual attention, visuospatial planning, and the actualization of visual concepts. Furthermore, consistent with the contralateral connections between the cerebellum and the cerebral cortex, studies have found that patients with left cerebellar lesions are more likely to have deficits in visual-spatial tasks [15, 16] implying a possible link between lateralization of damage and spatial information processing.

2.2. Language. Early in the twentieth century, Holmes (1922) described the effects on the speech of cerebellar damage, a condition later to become known as ataxic dysarthria [17], which is commonly explained by the uncoordinated muscle movement of the articulatory organs. With the development of neurolinguistics tests, such as the Boston Diagnostic Aphasia Examination (BDAE) and the Aachener Aphasia test (AAT), high-level and subtle language impairment secondary to cerebellar damage began to be discovered gradually. Marien described a patient with ischemic infarction in the vascular territory of the right cerebellar superior artery (SCA). The patient presented with normal performance on standard neuropsychological tests and intact conversational skills but performed significantly poorer than norms in tasks of verbal fluency (phonemic and semantic), word stem completion, and oral naming speed [18]. By summarizing his symptoms, Marien proposed the concept of cerebellar-induced aphasia, which is characterized by nonfluent aphasia, including reduced speech initiation, decreased dynamics of language, word-finding disturbances, marked agrammatism, and reading and writing difficulties [18].

The evidence of language dysfunctions in cerebellar disorders comes from several case-series analyses and case reports. The disability in verbal fluency and semantic access are considered as prominent language symptoms following cerebellar infarction [19]. In word generation and retrieval tasks, patients had slowed language production and problems detecting their own error. Another common language symptom is grammatical impairment. Silveri (1996) reported a male following right cerebellar infarction presented motor aphasia for the first time [20]. The patient manifested sentence production deficit but did not reveal cortical abnormality that could account for the behavior [20]. The underlying mechanism remains to be elucidated, and experts supposed that the disruption of the connection between the cerebellum and frontal cortex contributes to language impairments in cerebellar infarction. Other language deficits including transcortical sensory aphasia [19], impaired reading and writing [6], spatial dysgraphia [21], and lexical-semantic retrieval functions of nonnative languages [22] were also revealed in stroke patients whose lesions were confined to the cerebellum.

2.3. Working Memory. Working memory (WM) is the ability that allows information to be maintained temporarily and manipulated online during diverse cognitive demands and is the central executive function. Previous studies have revealed the impaired function of WM in patients following an isolated cerebellar infarction [9, 23, 24]. Ravizza et al. investigated that selective damage in verbal WM occurred secondary to cerebellar disorders, but articulatory rehearsal strategies were unaffected, supporting motor problems did not implicate the impaired WM system [23]. WM comprises an attentional control system, a central executive, and two subsidiary systems for the storage of visuospatial and verbal material [25, 26]. By means of comparisons between two traditional and presumably less demanding "short-term memory" tasks, digit and word span, and the more recent and demanding listening span task, patients with cerebellar infarction only perform significantly worse in respect of the listening span task, suggesting impairment of the central executive domains of WM [9]. The result was consistent with a previous functional magnetic imaging study, which provided evidence that the cerebellum participates in an amodal bilateral neuronal network representing the central executive during working memory n-back tasks [27].

2.4. Executive Function. Executive functions, which define the ability to orchestrate different cognitive tasks to achieve a specific goal, are not a separate concept. These cognitive abilities are required for adapting to changes in the environment, for example, the capacity to plan, anticipate results, and focus resources appropriately to objectives, as well as the ability to keep attention for lengthy periods of time while distracted by adverse surroundings [28]. Five processes were distinguished in previous studies: attention and inhibition, task management, planning, monitoring the contents of working memory, and encoding [29, 30]. Executive deficits have been reported in a variety of studies of patients following cerebellar infarction, including effects on attention [6, 31], sequencing [32, 33], inhibition of inappropriate responses [34], task planning [6, 28], integration, and organization [35], using standard neuropsychological tasks such as reversed digit span, category switching, Trails A and B, Go/No-Go test, and the Stroop color-word interference.

The term "executive function" has long been used synonymously with the term "frontal lobe function." [36] Executive disturbances are the most prominent symptom of

CCAS. The ascending cerebellar projections to the frontoparietal cortex and the feedback loops may be the neural substrates of cerebellar involvement in the processing of execution.

2.5. Neuropsychiatric Features. In addition to language, executive, and visuospatial impairments, other psychological deficits following cerebellar disorders have been reported [37]. The list of cognitive functions that are impaired as a result of cerebellar dysfunction is expansive, including source memory [38], which is the ability to remember original contextual (i.e., temporal and spatial) features of an event or information, metalinguistics ability to understand metaphorical expressions or construct sentences with pragmatic quality [39], social cognition such as face emotion recognition [40], procedural learning [41], spatial-temporal confusion [42], and loss of emotions [43].

Cognitive impairments after isolated cerebellar stroke span a broad spectrum and are mild and transient [44]. A few studies conducted on the subacute or chronic period have not detected any significant deficit in cerebellar cognition [6]. Furthermore, cognitive disorders in cerebellar infarctions may recover in time, which means that the prognosis is good [45, 46].Traditional neuropsychological tests, which may detect well-defined cognitive profiles caused by supratentorial cerebral damage, are sometimes inadequately sensitive to identify "subclinical" abnormalities that might occur as a result of cerebellar diseases [47].The use of specific tests to detect CCAS may be critical in understanding cognitive changes following cerebellar disorders. The CCAS scale, which was developed in 2018, is an easily applicable bedside test to detect CCAS in clinical practice [48].The scale is a 10-item battery including significantly abnormal cognitive tests between patients and healthy controls: semantic fluency, phonemic fluency, category switching, verbal memory, digit span forward and backward, cube drawing, similarities, and Go/No-Go test. A pass/fail judgment is established for each test based on a threshold score, and one, two, or three and more failed subtests were defined as possible, probable, or definite CCAS, respectively. The latter study showed the area under the receiver operating characteristic (ROC) curves was 0.84 in isolated cerebellar infarction, indicating the strong diagnostic value of CCAS scale [49].

3. Cerebellar Lesion Location Determines Functional Deficits

Lesion-deficit studies in patients with focal cerebellar infarction provide pivotal insights into structure-function correlations. Studies found that lesion size was not associated with cognitive outcomes. Even very large lesions did not produce significant impairment in cognitive performance if they did not extend into the specific site of the cerebellum [14, 50]. This evidence hypothesis shows a strict localization of functions in the cerebellum. And a motor-cognitive dichotomy has been well-recognized: tasks with a significant motor component are impacted by a lesion in the anterior lobe, whereas performance on cognitive tasks with limited motor demands is more affected by lesions in the cerebellar posterior lobe regions [14, 51], suggesting an explanation of dissociation between motor deficits with preserved cognition and cognitive deficits without ataxia in patients with cerebellar disorders [42, 52]. Previous studies indicated that patients with posterior inferior cerebellar artery (PICA) lesions damaged cognitive function than those with superior cerebellar artery (SCA) lesions, which were manifested as motor dysfunction [10, 32]. There are other publications, however, which come to a different conclusion: no obvious differences in cognitive functions were found between patients with infarction of the PICA and SCA [12, 34]. Because the common SCA territory includes the anterior lobe as well as a portion of the posterior lobe, cognitive dysfunctions in SCA patients with extended posterior lesions may not be unexpected.

For the vague identification of the different cerebellar regions divided by vascular territory, medial/lateral, anterior/posterior, or vermis/hemisphere, Larsell et al. (1972) constructed a detailed atlas of the human cerebellum [53]. The atlas divided the human cerebellum into ten regions marked with Roman numerals from the anterior (regions I-V) to the posterior (regions VI-X), which demonstrates the details of the cerebellar cortex within the three cardinal planes in Talairach proportional stereotaxic space and provides a more contemporary and accessible cerebellar nomenclature (Figure 1). Damage to regions VI and VII has been observed to be associated with impaired cognitive performance [51], matching the functional topography of the cerebellum in healthy controls using task-based and resting-state functional magnetic resonance imaging (fMRI) [54–57].

3.1. The Theory of Universal Cerebellar Transform. The theory of universal cerebellar transform (UCT) indicates that the cerebellum has a consistent internal structure and works as a modulator to optimize performance according to context [58]. The strict localization of functions in the cerebellum results from the heterogeneity of cerebellar connections with extracerebellar structures rather than variations in the cerebellar microstructure itself [59]. Functional neuroimaging studies confirmed that the cerebellum has extensive connectivity with different cerebral areas: the cerebellar posterior lobe connects with the prefrontal, posterior parietal, superior temporal, and limbic cortices, while the anterior lobe connects with the primary motor and premotor cortex [15, 60–62].Furthermore, resting-state functional connectivity analysis shows that the cerebellum can be divided into elaborate functional regions based on the patterns of anatomical connectivity between different regions of the cerebellum and association areas of the cerebral cortex [15, 56, 63] (Figure 2). Various psychological deficits following different cerebellar lesions are assumed to be a result of the interruption of different cerebro-cerebellar cognitive loops: prefrontal cortical associated cerebellar areas in relation to executive control, parietal cortical areas with respect to visuospatial function, and frontotemporal regions in relation to linguistic function.

3.2. Functional Topography of Cerebellum. Voxel-based lesion-symptom mapping (VLSM) is an imaging method that analyzes the relationship between brain lesions and

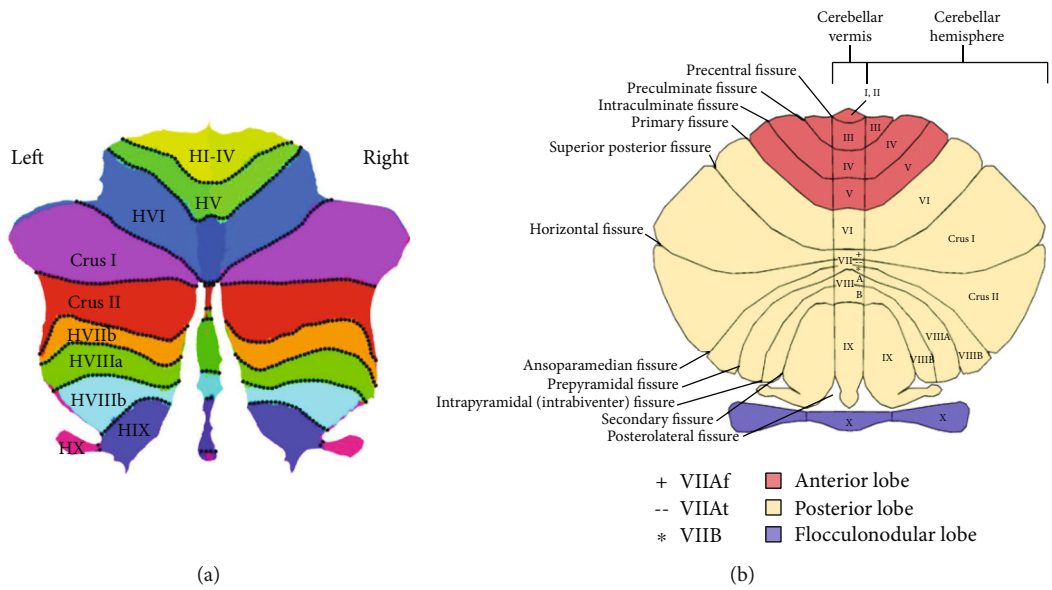

Figure 1: Flattened representation and illustration of the cerebellum and its major fissures, lobes, and lobules. Description: (a) Flattened representation of the human cerebellum developed by Diedrichsen et al. [105] In contrast to the vermis parts in the middle of the flat map, H stands for "hemispheric." (b) The anterior lobe is colored red; the posterior lobe is cream and the flocculonodular lobe is purple. In the lobule VII, the VIIAf at the vermis expands in the hemisphere to become the Crus I. The lobule VIIAt at the vermis merges with the Crus II in the hemisphere, whereas the lobule VIIB retains its structural integrity both at the vermis and in the hemispheres. Author's diagram adapted from Schmahmann et al. [106] and first published in D'Mello et al. [107].

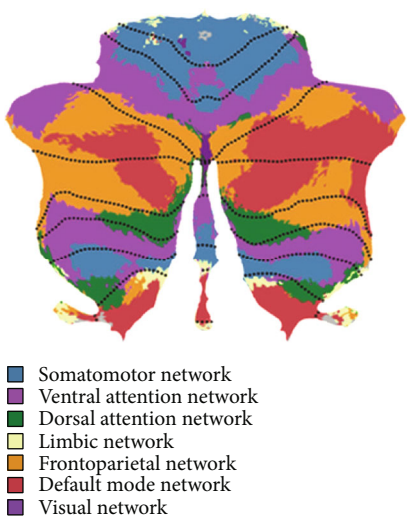

Figure 2: A map of the human cerebellum based on functional connectivity to seven major networks in the cerebrum. Description: Author's diagram adapted from Schmahmann et al. [108] and first published in Buckner et al. [61]

behavioral performance on a voxel-by-voxel basis [64]. This method offers better resolution than grouping stroke lesions by the affected artery or conducting region of interest analyses. With the use of VLSM, cerebellar functional topography can be described well in the disease model of cerebellar stroke for its confined lesions.

Consistent with traditional group analyses, the study of VLSM further confirmed damage in the posterior lobe, especially in the region of VI and VII that produced the cognitive impairment [12, 49, 51]. Richter et al. firstly used this technique in patients following isolated cerebellum infarction to reveal functional regions underpinning cognition in the cerebellum and demonstrated that impaired performance in a verbal fluency task was associated with the lesion of the right hemispheric region Crus II [12].Stoodly et al. (2016) found patients with damage to cerebellar lobules III–VI had worse ataxia symptoms, while posterior cerebellar damage involving lobules VII and VIII was a risk factor for cognitive deficits, which further validated the anterior-sensorimotor/posterior-cognitive dichotomy in the cerebellum (Figure 3). In addition, different locations of lesions were found to lead to significantly poorer scores on particular cognitive tasks, such as language (right Crus I and II extending through IX), spatial (bilateral Crus I, Crus II, and right lobule VIII), and executive function (lobules VII–VIII) [51].Chirino-Pérez et al. recently conducted a support vector regression-based multivariate VLSM study in 22 patients with chronic isolated cerebellar strokes and used the CCAS scale to detect cognition damage more sensitively. They found global cognition impairment was associated with damage to the right lateral posterior lobe of the cerebellum, particularly in region VI and Crus I [49]. The subanalyses of this study also revealed that semantic fluency, category switching, and cube drawing were impaired severely when damage was involved right VI, VIIb, Crus I, and Crus II [49].

In addition, some other studies of VLSM using specific cognitive tasks focused on exploring a link between specific cognitive impairment and lesion location in patients with cerebellar infarction. Those studies observed that impaired

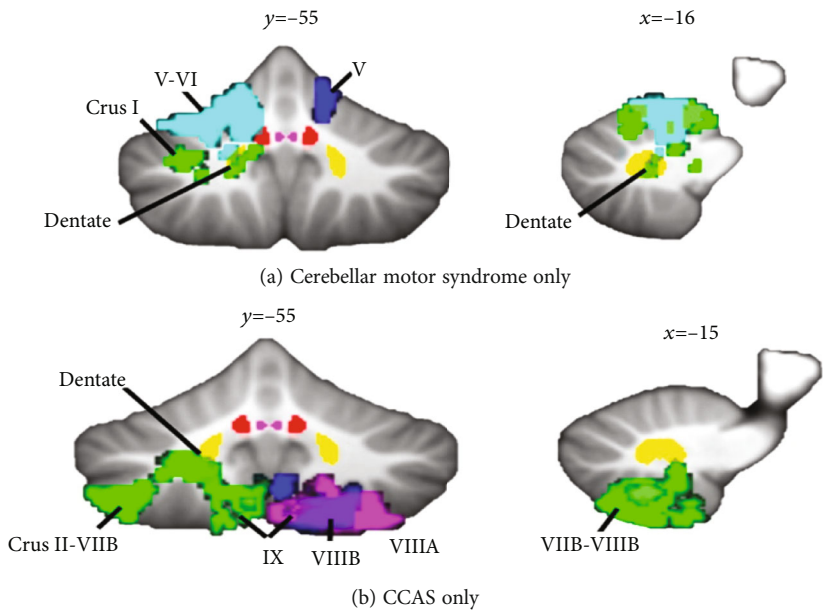

Figure 3: Lesion symptom mapping in patients with cerebellar infarction. Description: (a) Lesions of lobules IV–V of the anterior lobe extending into adjacent lobule VI produce the cerebellar motor syndrome of ataxia but not cerebellar cognitive affective syndrome (CCAS). (b) Lesions confined to posterior lobe lobules Crus II through lobule IX produce the cerebellar cognitive affective syndrome but no motor ataxia. Different colors represent the lesions of individual patients. Author' s diagram developed by Stoodley et al. [51].

phonemic fluency correlated with lesions in right Crus II, IX, and X and the deep nuclei; [65] visual attention deficit correlated with lesions of the pyramid of the vermis, the culmen, and partly the inferior semilunar lobule; [66] visuomotor rotation adaptation damage correlated with lesions in region VI; [67] impaired spatial and temporal visual attention correlated with the left posterior cerebellar region Crus II; [31]and difficulties in the recognition of emotion from voices (emotional prosody) correlated with lesions in the right region VIIb and VIII, and Crus I and II [68, 69]. More details are provided in Table 1. Studies of VLSM make an effort to identify cerebellar regions which are crucial to the presence of cognitive dysfunction and describe a precise cerebellum cognitive functional topography. The conclusion of those studies is consistent with studies on healthy subjects [54, 70].

4. Cerebro-Cerebellar Loop: Evidence from Neuroimaging

The cognitive deficits following cerebellar damage were held to result from the disrupted connectivity between the posterior cerebellum lobe and cerebral association areas [71]. Anatomic and imaging studies have indicated that the cerebro-cerebellar loop consists of afferent inputs through cortico-ponto-cerebellar projections and an efferent pathway through the cerebello-thalamic-cortical [72]. At the cellular level, there exists a direct excitatory loop from the cortex through the cerebellar nucleus dentatus and an inhibitory input through the Purkinje cells in the cerebellar cortex.

Studies employing fMRI in cerebellar stroke patients further provide evidence for a cortico-cerebellar connection as the functional substrate of cognition. Ziemus et al. explored the activation pattern changes during an n-back working memory task in patients with isolated cerebellar infarct: compared with healthy controls, bilateral increased BOLD activations in the ventrolateral prefrontal cortex, dorsolateral prefrontal cortex, parietal cortex, presupplementary motor area, and anterior cingulate were found in cerebellar patients during the task [35]. Wang et al. revealed that the abnormal alterations in the right posterior cingulate gyrus, bilateral median cingulate and paracingulate gyri, and right precuneus may play a core role in the cognitive impairment following cerebellar infarctions using diffusion tensor imaging [73]. Fan et al. found that the lower fractional amplitude of low-frequency fluctuation in the left hippocampus and right cingulate gyrus is related to poor cognitive performance in patients with acute posterior cerebellar infarction [74].

4.1. Crossed Cerebello-Cerebral Diaschisis and Lateralization. Crossed cerebello-cerebral diaschisis (CCD) has been described in patients with focal cerebellar lesions showing decreased cerebral perfusion and metabolism contralateral to cerebellar lesions [75].The cellular and molecular events of Wallerian degeneration that spread over the cerebello-cerebral tracts distant from the primary cerebellar lesions are speculated to be a possible mechanism for the phenomenon [76, 77]. Functional neuroimaging studies using single photon emission computed tomography (SPECT), positron emission tomography (PET), and near-infrared spectroscopy have demonstrated that cerebral hypometabolism and hypoperfusion may contribute to cognitive dysfunction in cerebellar infarction [8, 18, 78–81]. A quantified SPECT study showed that, in the absence of any structural damage in the supratentorial brain regions, contralateral hypoperfusion

Table 1: Voxel-based lesion-symptom mapping studies of cognitive function in patients following cerebellar infarction.

Number	Studies	Scanner	Subjects	Task/clinical performance	Result
1	Richter (2007)	3T	21 patients vs. 25 controls	Verb generation task, neglect tests (letter cancellation, line bisection), visual extinction test, verbal fluency task	Impaired performance in the verbal fluency task correlated with lesions in the right region Crus II
2	Baier (2010)	3T	26 patients vs. 15 controls	Covert visual attention task	Impaired covert visual attentional processes correlated with lesions in vermal structures such as the pyramid
3	Stoodley (2016)	3T	18 patients vs. norms	Wechsler Adult Intelligence Test-3, Trails A and B, Wisconsin Card Sorting Task, Wechsler Memory Scale, fluency task, Boston Naming Test, Benton Judgment of Line Orientation, mental rotation and Rey figure task	Cognitive impairment correlated with lesions in posterior lobe. More specifically, lesions of right Crus I and II extending through IX lead to poorer scores on language, lesions of bilateral Crus I, Crus II and right region VIII associate with spatial, and lesions of region VII–VIII associate with executive function
4	Kim (2017)	3T	24 patients vs. norms	Geriatric Depression Scale	Lesions in left VI, VIIb, VIII, Crus I, and Crus II are related with severity of depressive symptoms
5	Thomasson (2019)	3T	15 patients vs. 15 controls	Emotional prosody recognition task	Emotional misattributions correlated with lesions in right region VIIb, VIII and IX; and rhythm discrimination correlated with lesions in region VIIb
6	Pérez (2021)	3T	22 patients vs. 22 controls	Montreal Cognitive Assessment, cerebellar cognitive affective syndrome scale(CCAS-s)	Lesions in right region VI and Crus I are related with poor performance of CCAS-s, semantic fluency subtest, and cube drawing subtest; lesion in right region VIIb, Crus I, and Crus II are related with poor category switching score
7	Craig (2021)	1.5 T	14 patients vs. 24 controls	Reflexive and voluntary covert attention task, attentional blink task, sustained attention to response task	Deficits in spatial and temporal visual attention correlated with lesions of left Crus II
8	Thomasson (2021)	1.5T	24 patients vs. 24 controls	Emotional prosody recognition task	Emotional misattributions correlated with lesions in the right region VIIb, VIII, Crus I and II

in the left medial frontal lobe secondary to the cerebellar lesion may explain frontal lobe symptoms such as executive dysfunction, apathy, and disinhibition [79].

For the crossing of cerebello-cortico-cerebellar connections, the functional lateralization of cerebellar disorders is currently being considered. Clinical studies showed patients with cerebellar infarction lesions in the right posterior lobe manifested poorer cognitive performance than in left-lateralized regions [49, 50].In addition, studies also indicated the cognitive characteristics of different cerebellar hemispheric infarcts: language dysfunctions often follow damage to the right cerebellar hemisphere, whereas visual-spatial disability can result from left cerebellar hemisphere lesions [51, 82]. However, the side of the lesion showed no significant effect on cognitive performance in other studies [12, 32]. Two possible reasons may help explain this inconsistent conclusion. One hypothesis is that, as bilateral cortical activation was observed during linguistic and spatial tasks [83, 84], cerebral cortex functions are not always completely lateralized. An alternative interpretation is that cerebellar reserve, the capacity of the cerebellum to compensate for tissue damage or loss of function by the formation of new synaptic connections with cerebral cortical neurons [85], can prompt changes in connectivity between distinct networks and lead to reorganization of cerebellar functional topography [86].

5. Theory of Cerebellar Cognitive Function

Dysmetria of thought (DoT) is proposed as a fundamental framework attempting to explain the cognitive symptoms in patients with focal cerebellar lesions [87]. The intact cerebellar function facilitates actions harmonious with the goal, appropriate to the context, and judged accurately and reliably according to the strategies mapped out prior to and during the behavior. It is hypothesized that the prefrontal discharges are regulated and modulated rather than generated, by cerebellar structures. Cognitive dysfunctions following cerebellar disorders are associated not with the death of cortical neurons but with “discordance” in their operation, which explains why cognitive impairments after focal cerebellar disorders in adults are mild or transient.

Other theories which are compatible with the DoT theory on how the cerebellum modulates cognitive function

have been inspired by anatomical and physiological studies. These include the theories of biological clock [88], timing machine [89], error detection [90], sequence learning [91], automatization [92], dynamic state monitoring [93], neuronal machine [94], and implementing supervised learning using computational and engineering organizational principles [95].

6. Future Perspective

CCAS identifies the key characteristics of cerebellar patients' cognitive and emotional impairments. Aside from deficits of executive functions, visuospatial cognition, linguistic functions, and personality changes in cerebellar disorders, the involvement of the cerebellum in metalanguage and social cognition has also been discovered [39, 40]. Metalinguistic abilities include explicit awareness of abstract language representations. Patients with cerebellar lesions may have defects in perceiving ambiguities, formulating intelligible statements for a specific context, inferring logically, and comprehending figurative language, in contrast to the grammatical and semantic abilities that have been retained [39]. Social cognition is the process of observing and understanding the behavior and mental state of others, including oneself, in response to nonverbal or verbal stimuli [96]. Distortions in social cognition are usually regarded as the underlying dysfunction causing severe malfunctions in social and affective function. Mirroring, mentalizing, and abstract judgment are three sets of categories of social cognition. According to an activation likelihood estimation meta-analysis, the cerebellum is not responsible for any specific function but rather increases the efficiency with which other neocortical regions accomplish their own processes [97]. The role of the cerebellum in metalanguage and social cognition is consistent with the unifying framework of the UCT and the DoT and provides new insights into the nature of the cognitive impairments in patients with the CCAS.

Besides the cerebellar functional topography mentioned above, a recent resting-state imaging analysis revealed novel functional properties of cerebellar double motor representation (lobules I-VI and VIII) and triple nonmotor representation (lobules VI/Crus I, Crus II/VIIB, and IX/X) [63]. The first cerebellar motor representation that targets the primary motor cortex is engaged in motor control, whereas the second cerebellar motor representation that targets regions surrounding the precentral gyrus is more important for movement planning rather than movement execution [55]. The three cognitive representations are considered in the same way: the relationship between the first and second motor representations is similar to that of the first/second and third cognitive representations [57, 63]. And future studies are needed to explore what different functions are enabled by the different cognitive representations and what the differing consequences of lesions to the different representations are. Also, experts indicated that functional subdivisions did not align with lobular borders, which are often utilized to summarize functional data; they suggested that the novel parcellation serves as a functional atlas should be performed for future neuroimaging research [56]. Due to the localization and diversity of the lesions, cerebellar stroke could be a good disease model to demonstrate a more detailed and specific cerebellar functional topography by using fMRI techniques.

Due to the role in motor and nonmotor function, the cerebellum is attracting scientists interested in basic and clinical research of neuromodulation. Transcranial direct current stimulation (tDCS) and repetitive transcranial magnetic stimulation (rTMS) of the cerebellum can modify cognitive function, and targeted stimulation to narrow areas within the cerebellum produces differential effects on cognitive tasks such as language, memory and learning, and visuospatial orientation [98, 99]. Previous research has confirmed the validity of cerebellar noninvasive stimulation. A previous study reported that a patient with a left cerebellar stroke showed improvement on tasks modeling procedural learning after administration of rTMS to the unaffected right cerebellar hemispheres [41]. In addition, cerebellum-targeted rehabilitation exercises have provided a realistic opportunity for intervention in mental diseases such as autism spectrum disorders, affective disorders, and psychotic spectrum disorders, as well as Alzheimer's disease and aphasia [100, 101]. However, because of the highly convoluted nature of the cerebellar cortex, effects of noninvasive cerebellar brain stimulation are difficult to anticipate, and the robustness and replicability of previous findings will need to be evaluated before any recommendations on these forms of therapy can be made [102]. More research should be done to standardize the stimulation paradigms of cerebellum-targeted brain stimulation [103, 104].

7. Conclusion

Cerebellar involvement in cognition has long been a research topic but is gaining increasing clinical attention. This review provides new details about how cognitive dysfunctions manifest in cerebellar stroke. Evidence from neuroimaging and patient populations suggests that the posterolateral cerebellum contributes to cognitive processing and demonstrates a detailed functional topography using VLSM. In addition, the disruption of the cerebro-cerebellar loop has been considered as the mechanism of CCAS. The application of the tools of contemporary cognitive neuroscience may allow us to understand the cerebellum's role in cognition and emotion more in-depth. And new opportunities may also be possible for rehabilitation intervention in neuropsychiatry by targeting focal areas in the cerebellar node of the distributed cerebro-cerebellar networks subserving human cognition and emotion.

Conflicts of Interest

The authors declare that they have no conflicts of interest.

Authors' Contributions

Yu Chen and Yumei Zhang contributed equally to this work.

Acknowledgments

We are grateful to the patients and their families for their continued support of our research. Y. Z is supported by the National Natural Science Foundation of general project (81972144). Y.C. is supported by the National Natural Science Foundation of China Youth Program (82001124) and an early career research fellowship funded by Beijing Tiantan Hospital, Capital Medical University (2020MP06).

References

[1] L. F. Koziol, D. Budding, N. Andreasen et al., "Consensus paper: the cerebellum's role in movement and cognition," *The Cerebellum*, vol. 13, no. 1, pp. 151–177, 2014.

[2] J. D. Schmahmann and J. C. Sherman, "The cerebellar cognitive affective syndrome," *Brain*, vol. 121, no. 4, pp. 561–579, 1998.

[3] A. Stezin, S. Bhardwaj, S. Hegde et al., "Cognitive impairment and its neuroimaging correlates in spinocerebellar ataxia 2," *Parkinsonism & Related Disorders*, vol. 85, pp. 78–83, 2021.

[4] R. Maas, S. Killaars, B. van de Warrenburg, and D. J. L. G. Schutter, "The cerebellar cognitive affective syndrome scale reveals early neuropsychological deficits in SCA3 patients," *Journal of Neurology*, vol. 268, no. 9, pp. 3456–3466, 2021.

[5] N. Ahmadian, K. van Baarsen, M. van Zandvoort, and P. A. Robe, "The cerebellar cognitive affective syndrome-a meta-analysis," *The Cerebellum*, vol. 18, no. 5, pp. 941–950, 2019.

[6] L. A. Kalashnikova, Y. V. Zueva, O. V. Pugacheva, and N. K. Korsakova, "Cognitive impairments in cerebellar infarcts," *Neuroscience and Behavioral Physiology*, vol. 35, no. 8, pp. 773–779, 2005.

[7] E. Bolceková, M. Mojzeš, Q. Van Tran et al., "Cognitive impairment in cerebellar lesions: a logit model based on neuropsychological testing," *Cerebellum & Ataxias*, vol. 4, no. 1, p. 13, 2017.

[8] T. Botez-Marquard, J. Léveillé, and M. I. Botez, "Neuropsychological functioning in unilateral cerebellar damage," *Canadian Journal of Neurological Sciences*, vol. 21, no. 4, pp. 353–357, 1994.

[9] J. Malm, B. Kristensen, T. Karlsson, B. Carlberg, M. Fagerlund, and T. J. N. Olsson, "Cognitive impairment in young adults with infratentorial infarcts," *Neurology*, vol. 51, no. 2, pp. 433–440, 1998.

[10] C. Exner, G. Weniger, and E. Irle, "Cerebellar lesions in the PICA but not SCA territory impair cognition," *Neurology*, vol. 63, no. 11, pp. 2132–2135, 2004.

[11] M. Hoffmann and F. Schmitt, "Cognitive impairment in isolated subtentorial stroke," *Acta Neurologica Scandinavica*, vol. 109, no. 1, pp. 14–24, 2004.

[12] S. Richter, M. Gerwig, B. Aslan et al., "Cognitive functions in patients with MR-defined chronic focal cerebellar lesions," *Journal of Neurology*, vol. 254, no. 9, pp. 1193–1203, 2007.

[13] E. J. Kim, K. D. Choi, M. K. Han et al., "Hemispatial neglect in cerebellar stroke," *Journal of the Neurological Sciences*, vol. 275, no. 1-2, pp. 133–138, 2008.

[14] J. D. Schmahmann, J. Macmore, and M. Vangel, "Cerebellar stroke without motor deficit: clinical evidence for motor and non-motor domains within the human cerebellum," *Neuroscience*, vol. 162, no. 3, pp. 852–861, 2009.

[15] J. X. O'Reilly, C. F. Beckmann, V. Tomassini, N. Ramnani, and H. Johansen-Berg, "Distinct and overlapping functional zones in the cerebellum defined by resting state functional connectivity," *Cerebral Cortex*, vol. 20, no. 4, pp. 953–965, 2010.

[16] T. Kellermann, C. Regenbogen, M. De Vos, C. Mossnang, A. Finkelmeyer, and U. Habel, "Effective connectivity of the human cerebellum during visual attention," *The Journal of Neuroscience*, vol. 32, no. 33, pp. 11453–11460, 2012.

[17] J. R. Brown, F. L. Darley, and A. E. Aronson, "Ataxic dysarhria," *International Journal of Neurology*, vol. 7, no. 2, pp. 302–318, 1970.

[18] P. Mariën, J. Saerens, R. Nanhoe et al., "Cerebellar induced aphasia: case report of cerebellar induced prefrontal aphasic language phenomena supported by SPECT findings," *Journal of the Neurological Sciences*, vol. 144, no. 1-2, pp. 34–43, 1996.

[19] P. Mariën, H. Baillieux, H. J. De Smet et al., "Cognitive, linguistic and affective disturbances following a right superior cerebellar artery infarction: a case study," *Cortex*, vol. 45, no. 4, pp. 527–536, 2009.

[20] M. Silveri, M. Leggio, and M. J. N. Molinari, "The cerebellum contributes to linguistic production: a case of agrammatic speech following a right cerebellar lesion," *Neurology*, vol. 44, no. 11, pp. 2047–2050, 1994.

[21] M. C. Silveri, S. Misciagna, M. G. Leggio, and M. Molinari, "Spatial dysgraphia and cerebellar lesion: a case report," *Neurology*, vol. 48, no. 6, pp. 1529–1532, 1997.

[22] P. Mariën, K. van Dun, J. Van Dormael et al., "Cerebellar induced differential polyglot aphasia: a neurolinguistic and fMRI study," *Brain and Language*, vol. 175, pp. 18–28, 2017.

[23] S. M. Ravizza, C. A. McCormick, J. E. Schlerf, T. Justus, R. B. Ivry, and J. A. Fiez, "Cerebellar damage produces selective deficits in verbal working memory," *Brain*, vol. 129, no. 2, pp. 306–320, 2006.

[24] L. S. Hokkanen, V. Kauranen, R. O. Roine, O. Salonen, and M. Kotila, "Subtle cognitive deficits after cerebellar infarcts," *European Journal of Neurology*, vol. 13, no. 2, pp. 161–170, 2006.

[25] C. Jarrold and A. D. Baddeley, "Short-term memory for verbal and visuospatial information in down's syndrome," *Cognitive Neuropsychiatry*, vol. 2, no. 2, pp. 101–122, 1997.

[26] C. Constantinidis and T. Klingberg, "The neuroscience of working memory capacity and training," *Nature Reviews Neuroscience*, vol. 17, no. 7, pp. 438–449, 2016.

[27] M. Küper, P. Kaschani, M. Thürling et al., "Cerebellar fMRI activation increases with increasing working memory demands," *The Cerebellum*, vol. 15, no. 3, pp. 322–335, 2016.

[28] F. Manes, A. Villamil, S. Ameriso, M. Roca, and T. Torralva, ""Real life" executive deficits in patients with focal vascular lesions affecting the cerebellum," *Journal of the Neurological Sciences*, vol. 283, no. 1-2, pp. 95–98, 2009.

[29] E. E. Smith, R. A. Koeppe, E. Awh, S. Minoshima, and M. A. Mintun, "Spatial working memory in humans as revealed by PET," *Nature*, vol. 363, no. 6430, pp. 623–625, 1993.

[30] E. E. Smith and J. Jonides, "Storage and executive processes in the frontal lobes," *Science*, vol. 283, no. 5408, pp. 1657–1661, 1999.

[31] B. T. Craig, A. Morrill, B. Anderson, J. Danckert, and C. L. Striemer, "Cerebellar lesions disrupt spatial and temporal visual attention," *Cortex*, vol. 139, pp. 27–42, 2021.

[32] A. M. Tedesco, F. R. Chiricozzi, S. Clausi, M. Lupo, M. Molinari, and M. G. Leggio, "The cerebellar cognitive profile," *Brain*, vol. 134, no. 12, pp. 3672–3686, 2011.

[33] M. Silveri, A. Di Betta, V. Filippini, and M. Leggio, "Verbal short-term store-rehearsal system and the cerebellum. Evidence from a patient with a right cerebellar lesion," *Brain*, vol. 121, no. 11, pp. 2175–2187, 1998.

[34] J. P. Neau, E. Arroyo-Anllo, V. Bonnaud, P. Ingrand, and R. Gil, "Neuropsychological disturbances in cerebellar infarcts," *Acta Neurologica Scandinavica*, vol. 102, no. 6, pp. 363–370, 2000.

[35] B. Ziemus, O. Baumann, R. Luerding et al., "Impaired working-memory after cerebellar infarcts paralleled by changes in BOLD signal of a cortico-cerebellar circuit," *Neuropsychologia*, vol. 45, no. 9, pp. 2016–2024, 2007.

[36] A. R. Mayes and J. J. Downes, "What do theories of the functional deficit(s) underlying amnesia have to explain?," *Memory*, vol. 5, no. 1-2, pp. 3–36, 1997.

[37] J. Schmahmann, J. Weilburg, and J. Sherman, "The neuropsychiatry of the cerebellum - insights from the clinic," *Cerebellum*, vol. 6, no. 3, pp. 254–267, 2007.

[38] C. Tamagni, C. Mondadori, P. Valko, P. Brugger, B. Schuknecht, and M. Linnebank, "Cerebellum and source memory," vol. 63, no. 4, pp. 234–236, 2010.

[39] X. Guell, F. Hoche, and J. D. Schmahmann, "Metalinguistic deficits in patients with cerebellar dysfunction: empirical support for the dysmetria of thought theory," *Cerebellum*, vol. 14, no. 1, pp. 50–58, 2015.

[40] F. Hoche, X. Guell, J. Sherman, M. Vangel, and J. J. C. Schmahmann, "Cerebellar contribution to social cognition," *The Cerebellum*, vol. 15, no. 6, pp. 732–743, 2016.

[41] S. Torriero, M. Oliveri, G. Koch et al., "Cortical networks of procedural learning: evidence from cerebellar damage," *Neuropsychologia*, vol. 45, no. 6, pp. 1208–1214, 2007.

[42] K. Paulus, I. Magnano, M. Conti et al., "Pure post-stroke cerebellar cognitive affective syndrome: a case report," *Neurological Sciences*, vol. 25, no. 4, pp. 220–224, 2004.

[43] J. Annoni, R. Ptak, A. Caldara-Schnetzer, A. Khateb, and B. Z. Pollermann, "Decoupling of autonomic and cognitive emotional reactions after cerebellar stroke," *Annals of Neurology*, vol. 53, no. 5, pp. 654–658, 2003.

[44] M. P. Alexander, S. Gillingham, T. Schweizer, and D. T. Stuss, "Cognitive impairments due to focal cerebellar injuries in adults," *Cortex*, vol. 48, no. 8, pp. 980–990, 2012.

[45] A. Nickel, B. Cheng, H. Pinnschmidt et al., "Clinical outcome of isolated cerebellar stroke-a prospective observational study," *Frontiers in Neurology*, vol. 9, p. 580, 2018.

[46] Y. Erdal, S. Perk, C. Keskinkılıc, B. Bayramoglu, A. S. Mahmutoglu, and U. Emre, "The assessment of cognitive functions in patients with isolated cerebellar infarctions: a follow-up study," *Neuroscience Letters*, vol. 765, article 136252, 2021.

[47] M. Noroozian, "The role of the cerebellum in cognition: beyond coordination in the central nervous system," *Neurologic Clinics*, vol. 32, no. 4, pp. 1081–1104, 2014.

[48] F. Hoche, X. Guell, M. G. Vangel, J. C. Sherman, and J. D. Schmahmann, "The cerebellar cognitive affective/Schmahmann syndrome scale," *Brain*, vol. 141, no. 1, pp. 248–270, 2018.

[49] A. Chirino-Pérez, O. Marrufo-Meléndez, J. Muñoz-López et al., "Mapping the Cerebellar Cognitive Affective Syndrome in Patients with Chronic Cerebellar Strokes," *The Cerebellum*, vol. 2022, no. 21, pp. 208–218, 2021.

[50] M. A. Shin, O. T. Park, and J. H. Shin, "Anatomical correlates of neuropsychological deficits among patients with the cerebellar stroke," *Annals of Rehabilitation Medicine*, vol. 41, no. 6, pp. 924–934, 2017.

[51] C. J. Stoodley, J. P. MacMore, N. Makris, J. C. Sherman, and J. D. Schmahmann, "Location of lesion determines motor vs. cognitive consequences in patients with cerebellar stroke," *NeuroImage: Clinical*, vol. 12, pp. 765–775, 2016.

[52] S. Richter, B. Aslan, M. Gerwig et al., "Patients with chronic focal cerebellar lesions show no cognitive abnormalities in a bedside test," *Neurocase*, vol. 13, no. 1, pp. 25–36, 2007.

[53] J. D. Schmahmann, J. Doyon, D. McDonald et al., "Three-dimensional MRI atlas of the human cerebellum in proportional stereotaxic space," *NeuroImage*, vol. 10, no. 3, pp. 233–260, 1999.

[54] C. J. Stoodley and J. D. Schmahmann, "Functional topography in the human cerebellum: a meta-analysis of neuroimaging studies," *NeuroImage*, vol. 44, no. 2, pp. 489–501, 2009.

[55] C. Stoodley, E. Valera, and J. J. N. Schmahmann, "Functional topography of the cerebellum for motor and cognitive tasks: an fMRI study," *NeuroImage*, vol. 59, no. 2, pp. 1560–1570, 2012.

[56] M. King, C. Hernandez-Castillo, R. Poldrack, R. Ivry, and J. Diedrichsen, "Functional boundaries in the human cerebellum revealed by a multi-domain task battery," vol. 22, no. 8, pp. 1371–1378, 2019.

[57] X. Guell, J. D. E. Gabrieli, and J. D. Schmahmann, "Triple representation of language, working memory, social and emotion processing in the cerebellum: convergent evidence from task and seed-based resting-state fMRI analyses in a single large cohort," *NeuroImage*, vol. 172, pp. 437–449, 2018.

[58] J. D. Schmahmann, "Disorders of the cerebellum: ataxia, dysmetria of thought, and the cerebellar cognitive affective syndrome," *The Journal of Neuropsychiatry and Clinical Neurosciences*, vol. 16, no. 3, pp. 367–378, 2004.

[59] J. Diedrichsen, M. King, C. Hernandez-Castillo, M. Sereno, and R. J. N. Ivry, "Universal transform or multiple functionality? Understanding the contribution of the human cerebellum across task domains," *Neuron*, vol. 102, no. 5, pp. 918–928, 2019.

[60] J. A. Bernard, R. D. Seidler, K. M. Hassevoort et al., "Resting state cortico-cerebellar functional connectivity networks: a comparison of anatomical and self-organizing map approaches," *Frontiers in Neuroanatomy*, vol. 6, p. 31, 2012.

[61] R. Buckner, F. Krienen, A. Castellanos, J. Diaz, and B. T. T. Yeo, "The organization of the human cerebellum estimated by intrinsic functional connectivity," *Journal of Neurophysiology*, vol. 106, no. 5, pp. 2322–2345, 2011.

[62] F. Middleton and P. L. Strick, "Cerebellar projections to the prefrontal cortex of the primate," *Journal of Neuroscience*, vol. 21, no. 2, pp. 700–712, 2001.

[63] X. Guell, J. Schmahmann, J. Gabrieli, and S. S. Ghosh, "Functional gradients of the cerebellum," *eLife*, vol. 7, article e36652, 2018.

[64] E. Bates, S. M. Wilson, A. P. Saygin et al., "Voxel-based lesion-symptom mapping," *Nature Neuroscience*, vol. 6, no. 5, pp. 448–450, 2003.

[65] P. P. Urban, J. Marx, S. Hunsche et al., "Cerebellar speech representation: lesion topography in dysarthria as derived

from cerebellar ischemia and functional magnetic resonance imaging," *Archives of Neurology*, vol. 60, no. 7, pp. 965–972, 2003.

[66] B. Baier, M. Dieterich, P. Stoeter, F. Birklein, and N. G. Muller, "Anatomical correlate of impaired covert visual attentional processes in patients with cerebellar lesions," *The Journal of Neuroscience*, vol. 30, no. 10, pp. 3770–3776, 2010.

[67] R. Burciu, J. Reinold, K. Rabe et al., "Structural correlates of motor adaptation deficits in patients with acute focal lesions of the cerebellum," *Experimental Brain Research*, vol. 232, no. 9, pp. 2847–2857, 2014.

[68] M. Thomasson, D. Benis, A. Saj et al., "Sensory contribution to vocal emotion deficit in patients with cerebellar stroke," *NeuroImage: Clinical*, vol. 31, article 102690, 2021.

[69] M. Thomasson, A. Saj, D. Benis, D. Grandjean, F. Assal, and J. Peron, "Cerebellar contribution to vocal emotion decoding: insights from stroke and neuroimaging," *Neuropsychologia*, vol. 132, article 107141, 2019.

[70] S. H. Chen, M. H. Ho, and J. E. Desmond, "A meta-analysis of cerebellar contributions to higher cognition from PET and fMRI studies," *Human Brain Mapping*, vol. 35, no. 2, pp. 593–615, 2014.

[71] J. D. Schmahmann and D. N. Pandya, "The cerebrocerebellar system," *International Review of Neurobiology*, vol. 41, pp. 31–60, 1997.

[72] J. D. Schmahmann, "The cerebrocerebellar system: anatomic substrates of the cerebellar contribution to cognition and emotion," *International Review of Psychiatry*, vol. 13, no. 4, pp. 247–260, 2001.

[73] D. Wang, Q. Yao, M. Yu et al., "Topological disruption of structural brain networks in patients with cognitive impairment following cerebellar infarction," *Frontiers in Neurology*, vol. 10, p. 759, 2019.

[74] L. Fan, J. Hu, W. Ma, D. Wang, Q. Yao, and J. Shi, "Altered baseline activity and connectivity associated with cognitive impairment following acute cerebellar infarction: a resting-state fMRI study," *Neuroscience Letters*, vol. 692, pp. 199–203, 2019.

[75] K. Broich, A. Hartmann, H. Biersack, and R. Horn, "Crossed cerebello-cerebral diaschisis in a patient with cerebellar infarction," *Neuroscience Letters*, vol. 83, no. 1-2, pp. 7–12, 1987.

[76] M. Strother, C. Buckingham, C. Faraco et al., "Crossed cerebellar diaschisis after stroke identified noninvasively with cerebral blood flow-weighted arterial spin labeling MRI," *European Journal of Radiology*, vol. 85, no. 1, pp. 136–142, 2016.

[77] C. van Niftrik, M. Sebök, G. Muscas et al., "Investigating the association of wallerian degeneration and diaschisis after ischemic stroke with BOLD cerebrovascular reactivity," *Frontiers in Physiology*, vol. 12, article 645157, 2021.

[78] K. Saita, T. Ogata, J. Watanabe et al., "Contralateral cerebral hypometabolism after cerebellar stroke: a functional near-infrared spectroscopy study," *Journal of Stroke and Cerebrovascular Diseases*, vol. 26, no. 4, pp. e69–e71, 2017.

[79] H. Baillieux, H. J. De Smet, A. Dobbeleir, P. F. Paquier, P. P. De Deyn, and P. Marien, "Cognitive and affective disturbances following focal cerebellar damage in adults: a neuropsychological and SPECT study," *Cortex*, vol. 46, no. 7, pp. 869–879, 2010.

[80] M. Fujii, K. Tanigo, H. Yamamoto et al., "A case of dysgraphia after cerebellar infarction where functional NIRS guided the task aimed at activating the hypoperfused region," *Case Reports in Neurological Medicine*, vol. 2021, Article ID 6612541, 9 pages, 2021.

[81] M. I. Botez, J. Léveillé, R. Lambert, and T. Botez, "Single photon emission computed tomography (SPECT) in cerebellar disease: cerebello-cerebral diaschisis," *European Neurology*, vol. 31, no. 6, pp. 405–412, 2004.

[82] C. J. Stoodley and J. D. Schmahmann, "Evidence for topographic organization in the cerebellum of motor control versus cognitive and affective processing," *Cortex*, vol. 46, no. 7, pp. 831–844, 2010.

[83] S. Knecht, M. Deppe, B. Dräger et al., "Language lateralization in healthy right-handers," *Brain*, vol. 123, no. 1, pp. 74–81, 2000.

[84] K. Ferrara, A. Seydell-Greenwald, C. Chambers, E. Newport, and B. Landau, "Development of bilateral parietal activation for complex visual-spatial function: evidence from a visual-spatial construction task," *Developmental Science*, vol. 24, no. 4, article e13067, 2021.

[85] A. Keller, K. Arissian, and H. Asanuma, "Formation of new synapses in the cat motor cortex following lesions of the deep cerebellar nuclei," *Experimental Brain Research*, vol. 80, no. 1, pp. 23–33, 1990.

[86] J. Conrad, M. Habs, M. Ruehl et al., "Structural reorganization of the cerebral cortex after vestibulo-cerebellar stroke," *NeuroImage: Clinical*, vol. 30, article 102603, 2021.

[87] J. D. Schmahmann, "Dysmetria of thought: clinical consequences of cerebellar dysfunction on cognition and affect," *Trends in Cognitive Sciences*, vol. 2, no. 9, pp. 362–371, 1998.

[88] V. Braitenberg, D. Heck, and F. Sultan, "The detection and generation of sequences as a key to cerebellar function: experiments and theory," *Behavioral and Brain Sciences*, vol. 20, no. 2, pp. 229–245, 1997.

[89] R. Ivry and S. W. Keele, "Timing functions of the cerebellum," *Journal of Cognitive Neuroscience*, vol. 1, no. 2, pp. 136–152, 1989.

[90] J. Fiez, S. Petersen, and M. Cheney, "Impaired non-motor learning and error detection associated with cerebellar damage. A single case study," *Brain*, vol. 115, no. 1, pp. 155–178, 1992.

[91] M. Molinari, M. G. Leggio, A. Solida et al., "Cerebellum and procedural learning: evidence from focal cerebellar lesions," *Brain*, vol. 120, no. 10, pp. 1753–1762, 1997.

[92] J. Doyon, R. Laforce Jr., G. Bouchard et al., "Role of the striatum, cerebellum and frontal lobes in the automatization of a repeated visuomotor sequence of movements," *Neuropsychologia*, vol. 36, no. 7, pp. 625–641, 1998.

[93] M. J. B. Paulin, "The role of the cerebellum in motor control and perception," *Brain, Behavior and Evolution*, vol. 41, no. 1, pp. 39–50, 2004.

[94] M. Ito, "Cerebellar circuitry as a neuronal machine," *Progress in Neurobiology*, vol. 78, no. 3-5, pp. 272–303, 2006.

[95] J. Raymond and J. F. Medina, "Computational principles of supervised learning in the cerebellum," *Annual Review of Neuroscience*, vol. 41, no. 1, pp. 233–253, 2018.

[96] F. Van Overwalle, "Social cognition and the brain: a meta-analysis," *Human Brain Mapping*, vol. 30, no. 3, pp. 829–858, 2009.

[97] F. Van Overwalle, K. Baetens, P. Mariën, and M. Vandekerckhove, "Social cognition and the cerebellum:

a meta-analysis of over 350 fMRI studies," *NeuroImage*, vol. 86, pp. 554–572, 2014.

[98] G. Grimaldi, G. P. Argyropoulos, A. Boehringer et al., "Non-invasive cerebellar stimulation–a consensus paper," *Cerebellum*, vol. 13, no. 1, pp. 121–138, 2014.

[99] P. A. Pope and R. C. Miall, "Restoring cognitive functions using non-invasive brain stimulation techniques in patients with cerebellar disorders," *Frontiers in Psychiatry*, vol. 5, p. 33, 2014.

[100] R. O. Brady Jr., I. Gonsalvez, I. Lee et al., "Cerebellar-prefrontal network connectivity and negative symptoms in schizophrenia," *American Journal of Psychiatry*, vol. 176, no. 7, pp. 512–520, 2019.

[101] N. Woodward and C. J. Cascio, "Resting-state functional connectivity in psychiatric disorders," *JAMA Psychiatry*, vol. 72, no. 8, pp. 743-744, 2015.

[102] L. Miterko, K. Baker, J. Beckinghausen et al., "Consensus paper: experimental neurostimulation of the cerebellum," *Cerebellum*, vol. 18, no. 6, pp. 1064–1097, 2019.

[103] R. Cassani, G. Novak, T. Falk, and A. A. Oliveira, "Virtual reality and non-invasive brain stimulation for rehabilitation applications: a systematic review," *Journal of neuroengineering and rehabilitation*, vol. 17, no. 1, p. 147, 2020.

[104] N. Butti, E. Biffi, C. Genova et al., "Virtual Reality Social Prediction Improvement and Rehabilitation Intensive Training (VR-SPIRIT) for paediatric patients with congenital cerebellar diseases: study protocol of a randomised controlled trial," *Trials*, vol. 21, no. 1, p. 82, 2020.

[105] J. Diedrichsen and E. Zotow, "Surface-based display of volume-averaged cerebellar imaging data," *PLoS One*, vol. 10, no. 7, article e0133402, 2015.

[106] N. Gordon, "The cerebellum and cognition," *European Journal of Paediatric Neurology*, vol. 11, no. 4, pp. 232–234, 2007.

[107] A. D'Mello and C. J. Stoodley, "Cerebro-cerebellar circuits in autism spectrum disorder," *Frontiers in Neuroscience*, vol. 9, p. 408, 2015.

[108] J. Schmahmann, X. Guell, C. Stoodley, and M. Halko, "The theory and neuroscience of cerebellar cognition," *Annual Review of Neuroscience*, vol. 42, no. 1, pp. 337–364, 2019.

Hindawi
Neural Plasticity
Volume 2022, Article ID 5379876, 17 pages
https://doi.org/10.1155/2022/5379876

Research Article

Identifying Key Biomarkers and Immune Infiltration in Female Patients with Ischemic Stroke Based on Weighted Gene Co-Expression Network Analysis

Haipeng Xu,[1] Kelin He,[1,2] Rong Hu,[1] YanZhi Ge,[3] Xinyun Li,[1] Fengjia Ni,[1] Bei Que,[1] Yi Chen,[1] and Ruijie Ma[1,2]

[1]*The Third School of Clinical Medicine (School of Rehabilitation Medicine), Zhejiang Chinese Medical University, Key Laboratory of Acupuncture and Neurology of Zhejiang Province, Hangzhou, Zhejiang, China*
[2]*Department of Acupuncture and Moxibustion, Third Affiliated Hospital of Zhejiang Chinese Medical University, Hangzhou, Zhejiang, China*
[3]*The First Clinical Medical College, Zhejiang Chinese Medical University, Hangzhou, Zhejiang, China*

Correspondence should be addressed to Ruijie Ma; maria7878@sina.com

Received 24 December 2021; Revised 24 February 2022; Accepted 7 March 2022; Published 8 April 2022

Academic Editor: Xi-Ze Jia

Stroke is one of the leading causes of death and disability worldwide. Evidence shows that ischemic stroke (IS) accounts for nearly 80 percent of all strokes and that the etiology, risk factors, and prognosis of this disease differ by gender. Female patients may bear a greater burden than male patients. The immune system may play an important role in the pathophysiology of females with IS. Therefore, it is critical to investigate the key biomarkers and immune infiltration of female IS patients to develop effective treatment methods. Herein, we used weighted gene co-expression network analysis (WGCNA) to determine the key modules and core genes in female IS patients using the GSE22255, GSE37587, and GSE16561 datasets from the GEO database. Subsequently, we performed functional enrichment analysis and built a protein-protein interaction (PPI) network. Ten genes were selected as the true central genes for further investigation. After that, we explored the specific molecular and biological functions of these hub genes to gain a better understanding of the underlying pathogenesis of female IS patients. Moreover, the "Cell type Identification by Estimating Relative Subsets of RNA Transcripts (CIBERSORT)" was used to examine the distribution pattern of immune subtypes in female patients with IS and normal controls, revealing a new potential target for clinical treatment of the disease.

1. Introduction

Stroke is one of the leading causes of death and long-term disability in the world. Every year, it is estimated that 96 million new cases of ischemic stroke and 41 million new cases of hemorrhagic stroke are diagnosed worldwide [1]. Arterial occlusion-related ischemic stroke is a major cause of the majority of strokes, accounting for 87 percent of stroke cases and nearly half of all deaths [2]. Current evidence shows that [3] the focus of IS treatment is on timely blood clot removal and long-term secondary prevention. However, the molecular mechanism of IS remains unknown. In addition, gender differences in stroke patients may influence clinical manifestations, epidemiological features, pathophysiology, prognoses, and outcomes. Therefore, a study of stroke patients with no gender differences may result in biased results [4, 5]. Previous research indicates that [6] women had a higher risk of stroke-related death than men, with six out of ten women dying from stroke. This increased risk could be attributed to a variety of factors, one of which is that women live averagely longer, which increases their risk of stroke. Meanwhile, other risk factors such as high blood pressure

during pregnancy and certain types of birth control medication increase their overall risk of stroke [7]. As such, we only used data of female IS patients.

Researchers frequently use WGCNA to investigate the complex relationships between genes and phenotype; it converts gene expression data to co-express module, allowing a better understanding of the network signal responsible for phenotypic characteristics [8]. This approach has been widely used in a variety of biological processes whereby it plays a significant role in the comparison of differentially expressed genes and the discovery of co-expression module genes [9]. The WGCNA approach has provided functional interpretation tools in system biology, and it is widely used in stroke-related research [10–12]. In this study, we used genes in three GEO datasets from female patients with ischemic stroke and healthy controls to build a co-expression network by WGCNA. In addition, we looked at the relative proportions of 22 different types of immune cells in 72 blood samples from IS patients and 24 blood samples from healthy females. We built co-expression modules based on the expression data of female IS patients and perform integrated bioinformatics analysis of the modules of interest, whose gene expression was specifically co-related to female IS patients and could provide potential therapeutic targets for disease management.

2. Materials and Methods

2.1. Dataset Information. The gene expression data used in this study were obtained from the Gene Expression Omnibus (GEO) database (https://www.ncbi.nlm.nih.gov/geo/) [13]. Data processing was divided into three stages. First, the one probe expression matrix files downloaded from the GEO database were normalized and log2 transformed. The platform annotation file was then matched with each probe expression matrix, and only well-annotated probes were retained. In order to ensure the accuracy of included data, we analyzed the average expression values of multiple probes corresponding to a gene. Finally, R package sva, installed from Bioconductor (https://bioconductor.org/), was applied to eliminate the heterogeneity caused by different experimental batches and platforms.

2.2. Construction of Co-Expression Network. The WGCNA method assists in investigating gene set expression. Herein, the WGCNA R package was used at various stages for the construction and module division of different gene networks through the following major steps [14]. The samples were clustered to see if any obvious outliers were present. Next, automatic network construction was used to construct the co-expression network. Hierarchical clustering and a dynamic tree-cutting function detection module were employed. Gene salience (GS) and module membership (MM) were calculated to correlate modules with clinical characteristics. The module with the largest absolute value of Pearson's correlation of module membership (MM) and a p-value <0.05 was defined as the hub module. MM >0.8 and GS >0.2 represented high module connectivity and high clinical significance, respectively. The corresponding module gene information was extracted for further analysis.

2.3. Functional Enrichment Analysis. The intersection genes of target modules were extracted from the network, and the enrichment analysis was performed to further investigate the functions of each module. Gene Ontology (GO) terms and the Kyoto Encyclopedia of Genes and Genomes (KEGG) pathways were considered to be enriched with thresholds of p-value <0.05 and an enriched gene count >2.

2.4. Immune Infiltration through CIBERSORT Analysis. CIBERSORT is a deconvolution algorithm that can analyze any immune cell subtype and accurately quantify the various immune cell components. We looked at analyzed immune infiltration in 72 female patients with ischemic stroke and 24 healthy females. These immune cells include immature B cells, memory B cells, and the other 19 types of immune cells. The percentage of each immune cell in the sample was calculated, with $p < 0.05$. The R software packages "ggplot 2" and "GGPUBR" were used to compare the levels of immune cell infiltration in female stroke patients and normal female subjects.

2.5. Protein-Protein Interaction (PPI) Network Analysis. Genes were imported into the STRING website (version: 11.0) to explore the mutual relationship between proteins encoded by different genes [15]. We ensured that the lowest interaction score is greater than 0.4, and isolated nodes in the network were removed. The analysis results were output to a TSV format file, and Cytoscape software (version: 3.7.1) was used for details processing and module analysis. Cytohubba is a plug-in that can find closely connected nodes in a complex network based on topology. It can be downloaded from the Cytoscape App Store. We used this plug-in to find the most significant cluster of 10 nodes in a PPI network using the default parameters.

2.6. Animal Experiments. Female SD rats (3-4 months old); mean body weight = 220 g) were provided by Shanghai Xipu Bikai experimental animal company (animal license No: SCXK (Shanghai) 2018-0006). Animal experiments were performed following the China legislation on the use and care of laboratory animals and were approved by the Medical Norms and Ethics Committee of Zhejiang Chinese Medical University. Female SD rats were randomly assigned to the normal group and the IS group (n = 8 per group).

2.7. Model Preparation. The middle cerebral artery occlusion (MCAO) model was established in 4-month-old female SD rats. First, the rats were anesthetized with 3% pentobarbital and then fixed on an operating table. A midline neck incision was used to expose the common carotid artery (CCA), external carotid artery (ECA), and internal carotid artery (ICA). A 6-0 nylon suture was inserted into the internal carotid artery through the external carotid artery stump and gently advanced to occlude the middle cerebral artery. Sham-operated animals underwent the same surgical operation but with no nylon suture insertion. Following that, the wound was then sutured and disinfected.

Table 1: The primers used in qRT-PCR.

Primers	Forward	Reverse
β-actin	5′-TGTCACCAACTGGGACGATA-3′	5′-GGGGTGTTGAAGGTCTCAAA-3′
PRS28	5′-GCTGGCTAGGGTAACTAAAGTGCTG-3′	5′-TCGGATGATAGAGCGGCTGGTG-3′
RPS6	5′-AGCGGTGGGAATGACAAACAAGG-3′	5′-CGCTTCCTCTCTCCAGTTCTCCTAG-3′
RPS15A	5′-ACAGGAAGGTTGAACAAGTGTGGAG-3′	5′-ACAATGAAACCAAACTGCCGTGATG-3′
RPL7	5′-TTGCCCTGAAGACACTGCGAAAG-3′	5′-GCCATCCTAGCCATGCGAATCTC-3′
RPL9	5′-ACACTGGGCTTCCGTTACAAGATG-3′	5′-CAACACCTGTCCTCATCCGAACC-3′
RPL31	5′-TCCTCGGGCACTCAAAGAAATTCG-3′	5′-CTCGGATGCGGTACGGAACATTC-3′
RPL14	5′-TGGAAAGCTGGTCGCAATCGTAG-3′	5′-CGCACTGTGTGGGAACTTGAGG-3′
PABPC1	5′-TACCAGCCAGCACCTCCTTCAG-3′	5′-CAGCGAGGACTTGGTCTTAGTTGAG-3′
PFDN5	5′-GCTGAGGATGCCAAGGACTTCTTC-3′	5′-CATCATTTCCACGACGGCTTGTTTC-3′
TNF	5′-ATGGGCTCCCTCTCATCAGTTCC-3′	5′-ATGGGCTCCCTCTCATCAGTTCC-3′

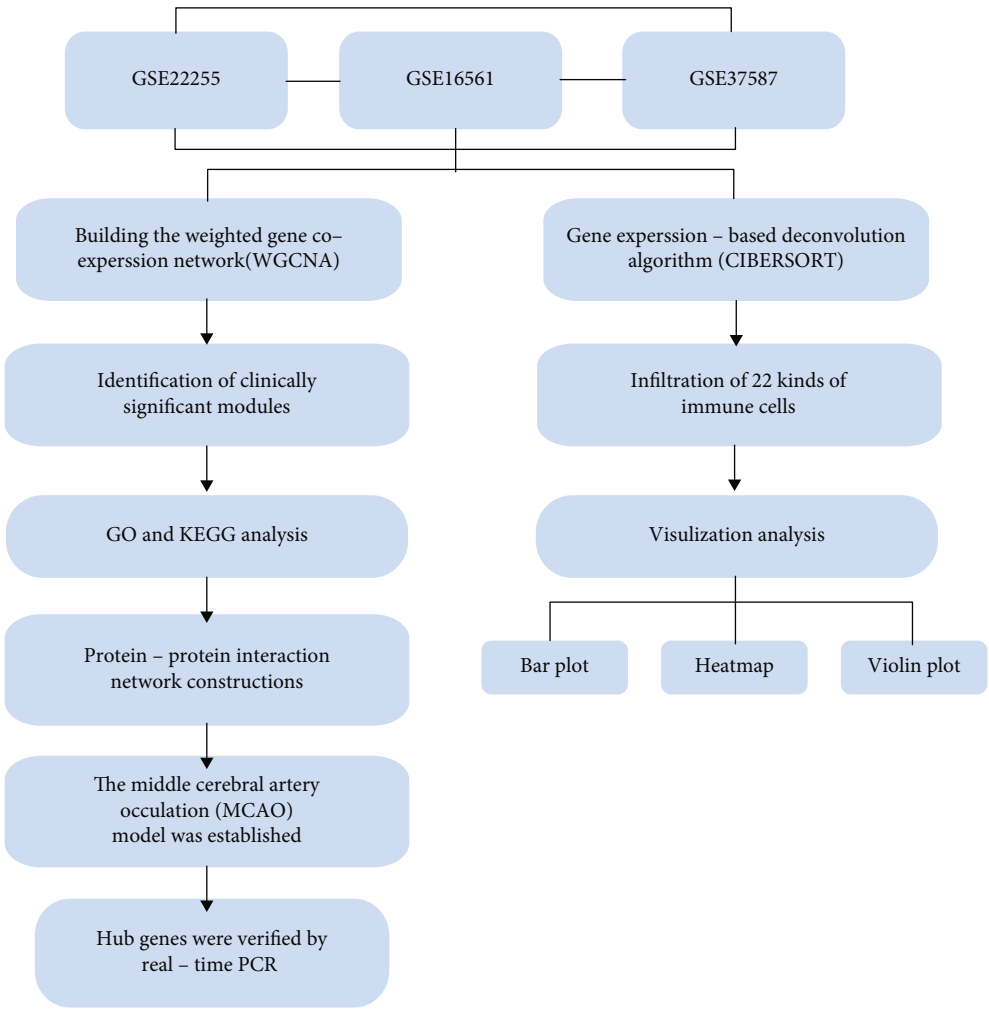

Figure 1: The workflow of the whole study.

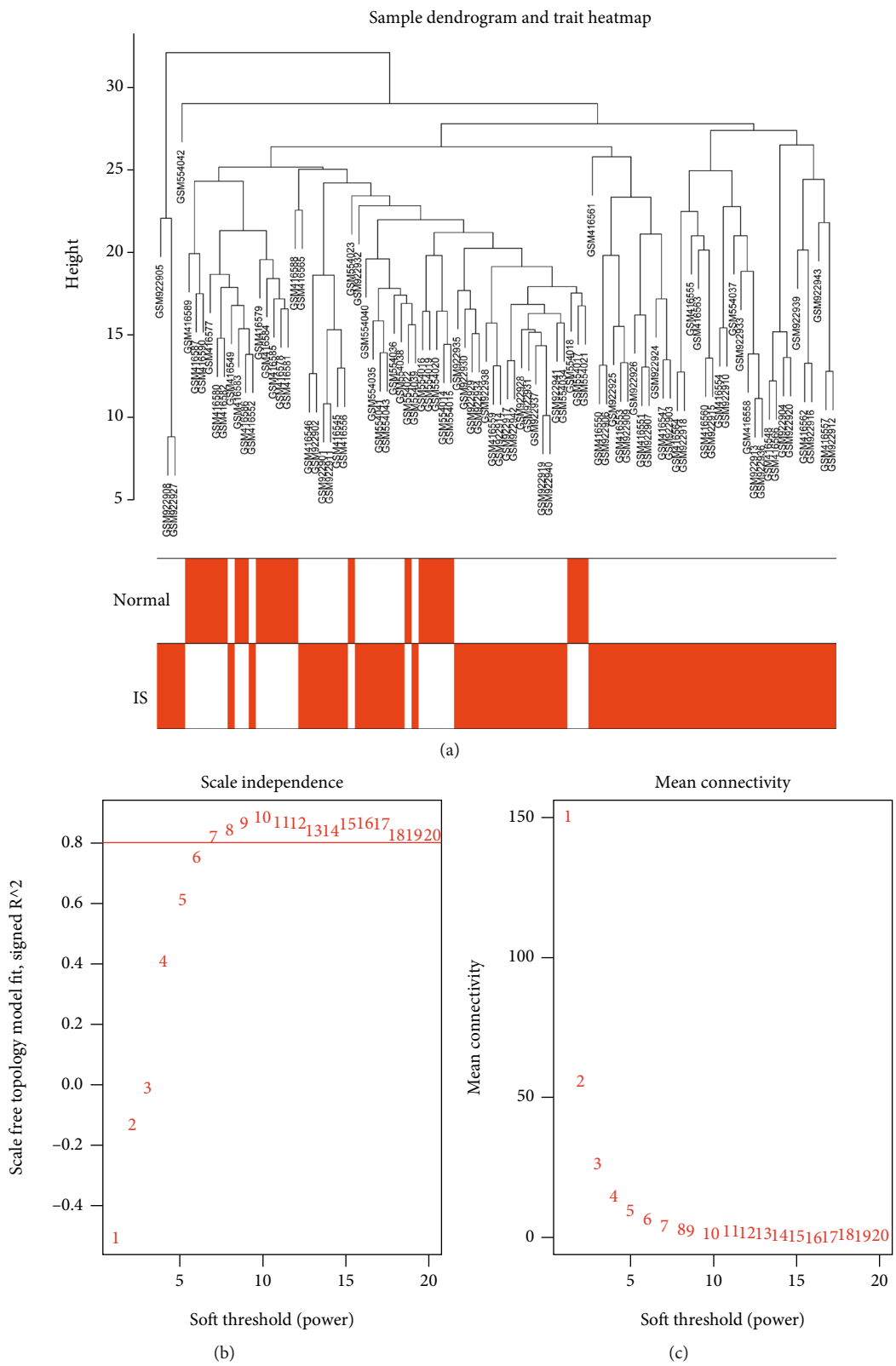

Figure 2: Construction and module division of the co-expression network. (a) Cluster tree diagram of the sample. The cluster tree reflects the distance between 96 samples. (b) Soft threshold (R^2) determination; the fitting degree R^2 increases with an increase in the soft threshold. When the fitting degree R^2 > 0.8 (red line), the corresponding network is more consistent with the scale-free network distribution. (c) Soft threshold selection (average connectivity).

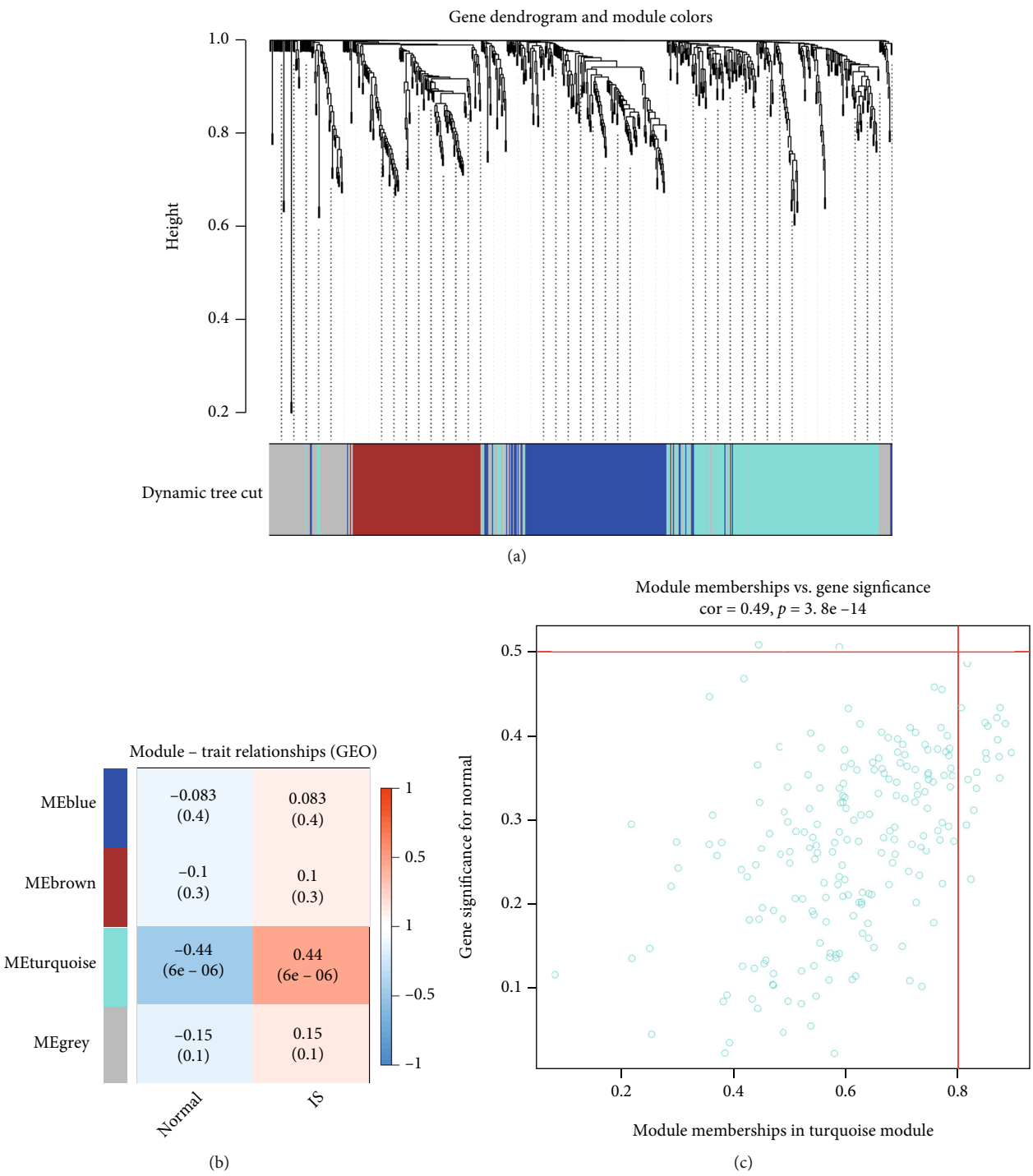

Figure 3: Continued.

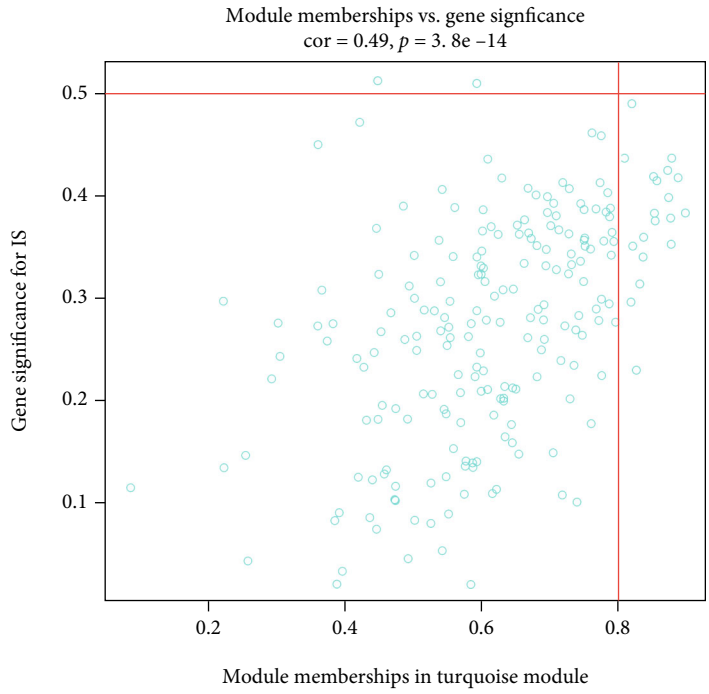

(d)

Figure 3: Identification of modules associated with clinical characteristics of IS females. (a) Cluster tree diagram and module feature relationship diagram for hierarchical cluster analysis to detect co-expression clustering with the corresponding color distribution. Each color represented a module in the gene co-expression network constructed by WGCNA. Heat map of the correlation between the module. (b) Characteristic gene in IS female samples and normal samples. ((c) and (d)) The relationship between the scatter plot of the members of the module and the genetic importance of morbid states.

All animals received intraperitoneal injection of penicillin (100 U/d) to prevent infection.

2.8. Quantitative Reverse Transcription PCR (qRT-PCR). qRT-PCR was used to confirm the expression of 10 hub genes in peripheral blood. qPCR was performed on the CFX96 Real-Time System (BioRad, USA) using the Fast Start Universal SYBR Green Master kit (TaKaRa Bio Inc., China) according to the manufacturer's protocol. The relative quantification was performed by the $\Delta\Delta$CT method. Primer sequences are listed in Table 1.

2.9. Statistical Analyses. All statistical analyses between control and experimental groups were completed using the GraphPad Prism8 and data were analyzed with a one-way ANOVA followed by Tukey Kramer tests. The results are presented as mean ± SEM; $p < 0.05$ denote statistical significance.

3. Results

3.1. Workflow. Figure 1 shows a schematic diagram of the workflow. A co-expression network was built in a sample of female IS patients and a sample of normal females, and several modules of clinical significance were identified. The function of the key modules was then examined to reveal the core differential genes in female stroke patients.

3.2. Constructing the Weighted Gene Co-Expression Network. The GSE22255, GSE37587, and GSE16561 datasets were obtained from the GEO database. A total of 24 normal samples and 72 IS samples were examined. The samples were first clustered, and the obvious outlier samples were eliminated by setting the threshold as illustrated in Figure 2(a). The sample cluster tree included 96 samples. After that, we selected the soft threshold. As illustrated in Figures 2(b) and 2(c), when R^2 > 0.8, the fitting degree was high enough and the mean connectivity was relatively high. Furthermore, we used the WGCNA R software package to construct the gene network and determined the module based on a certain soft threshold. A weighted gene co-expression network was built to split the cluster, and the co-expression modules were divided using dynamic cutting and module merging.

3.3. Identification of Clinically Significant Modules. The correlation analysis of gene expression and disease characteristics was performed by WGCNA, and four-gene expression modules were developed (Figure 3(a)). Next, we linked modules to clinical features and searched for the most important ones. As demonstrated in Figures 3(b) and 3(c), gene expression of the turquoise module was most closely related to the two groups of key factors (normal and IS) (r =0.44). Therefore, we selected the turquoise module for the subsequent analysis.

3.4. Functional Analysis of the Key Module. GO and KEGG analyses were performed on the turquoise module genes.

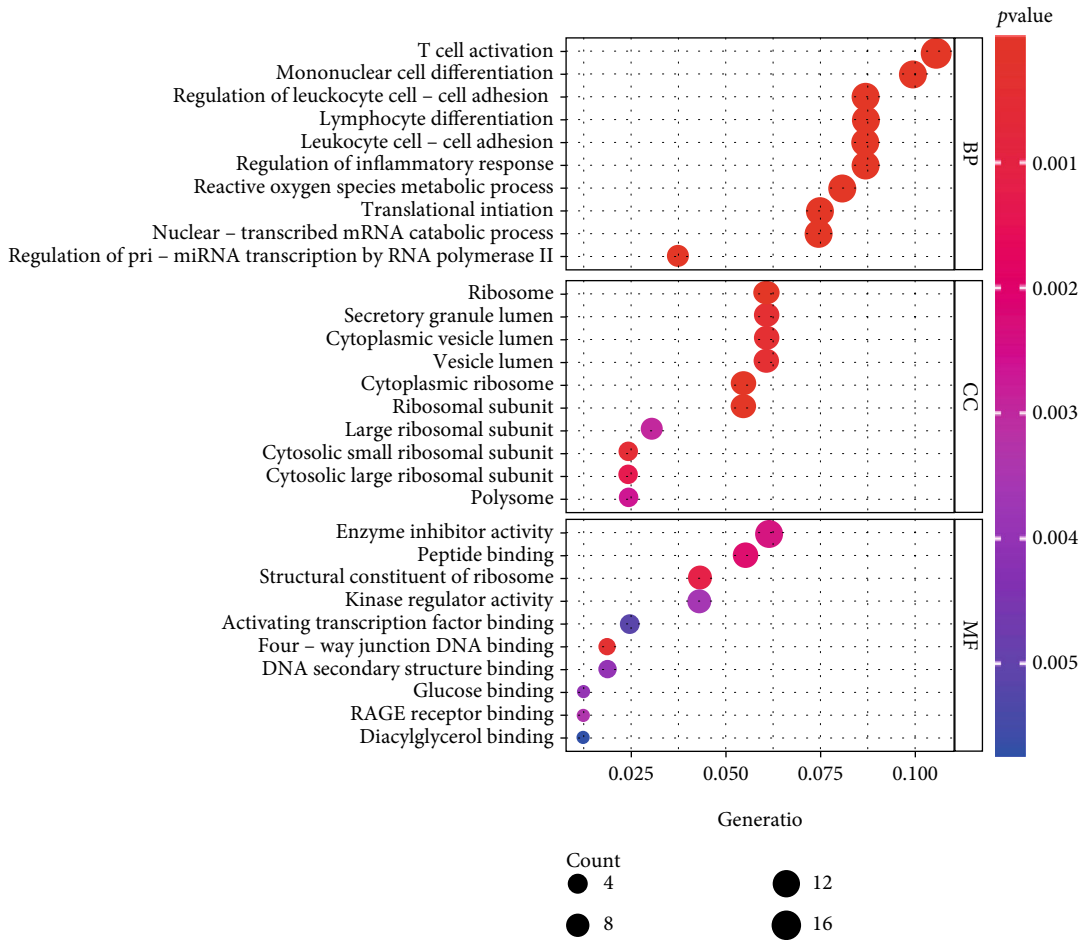

(a)

Figure 4: Continued.

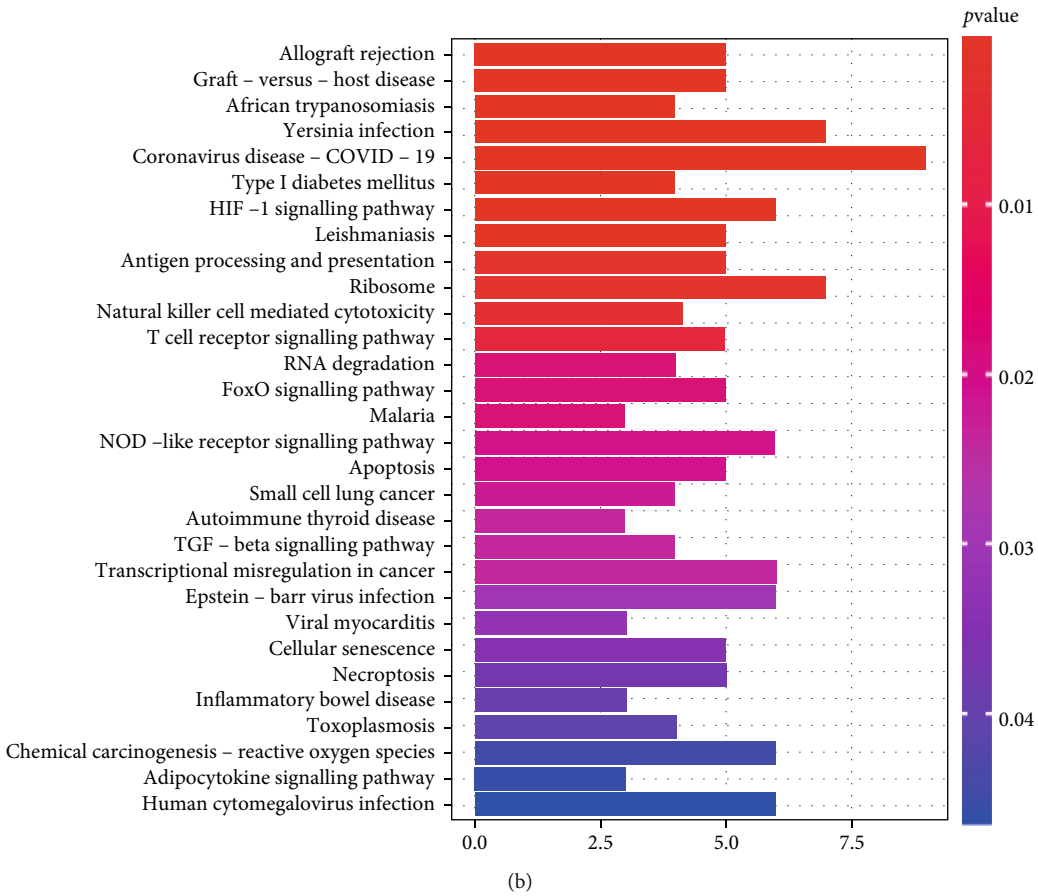

Figure 4: GO and KEGG pathway analysis. (a) GO analysis of genes involved in turquoise module. (b) Enriched pathways of genes in turquoise module by the KEGG.

The GO analyses results demonstrated that the genes were primarily related to the regulation of T cell activation, mononuclear cell differentiation, and neutrophil-mediated immunity in biological processes (BP) (Figure 4(a) and Table 2). Furthermore, gene cell components were primarily enriched in the ribosome and secretory granule lumen. In terms of molecular function (MF), genes were primarily enriched in enzyme inhibitor activity and ribosome structural constituents. Next, we performed functional analysis (KEGG analysis) on the genes in the turquoise module (Figure 4(b) and Table 3). The findings revealed an association between the regulation pathway of the turquoise module with the ribosome, the HIF–1 signaling pathway, and natural killer cell-mediated cytotoxicity.

3.5. Immune Infiltration Analyses. We explored the difference in immune infiltration of 22 immune cell subsets between female IS patients and healthy females. The histogram illustrated in Figures 5(a) and 5(b) depicts the distribution of various immune cells in the sample. The various colors represent different types of immune cells. The main immune infiltration cells included neutrophils, NK cells resting, macrophages M0, T cells CD8, and monocytes. The proportions of various infiltrated immune cell subsets were weakly moderately correlated (Figure 5(c)). F Neutrophils and macrophages M0, for example, was 0.48, and T cells CD8 and neutrophils was -0.53, and so on. Moreover, IS females had more monocytes and neutrophils when compared to healthy females (Figure 6(d)).

3.6. Identification of Hub Genes in the Functional Modules and Protein-Protein Interaction Network Construction. A total of 211 genes were identified from the clinically significant module (turquoise module) of the co-expression network. A PPI network was then constructed using the STRING database (Figure 6). Finally, cytoHubba was used to screen for and visualize the hub genes (RPS15A, RPS6, RPS28, RPL7, PABPC1, RPL31, RPL14, RPL9, PFDN5, TNF) in the network (Figure 7).

3.7. Validation of the Hub Genes Using qRT-PCR. qRT-PCR was used to reverify the 10 hub genes to further demonstrate the reliability of the WGCNA results. First, the stroke model was constructed by performing MCAO as described in the methods. Next, the peripheral blood was used for qRT-PCR. The results showed that the expression of the RPS28, RPS6, RPS15A, RPL9, TNF, and RPL31 genes were significantly higher in the IS model, whereas the expression of RPL7, PABPC1, and PFDN5 genes was significantly lower in the IS model (p-value<0.01). However, no statistically significant differences in expression levels were found between the two groups (Figure 8(f)).

Table 2: The top 10 GO enrichment terms of genes in turquoise module.

ONTOLOGY	ID	Description	p.adjust	Count
BP	GO:0042110	T cell activation	0.000472374	17
BP	GO:1903131	Mononuclear cell differentiation	0.000472374	16
BP	GO:0001819	Positive regulation of cytokine production	0.00120906	15
BP	GO:0002446	Neutrophil mediated immunity	0.003207892	15
BP	GO:0042119	Neutrophil activation	0.003207892	15
BP	GO:1903037	Regulation of leukocyte cell-cell adhesion	0.000472374	14
BP	GO:0030098	Lymphocyte differentiation	0.001054285	14
BP	GO:0007159	Leukocyte cell-cell adhesion	0.001059699	14
BP	GO:0050727	Regulation of inflammatory response	0.001059699	14
BP	GO:0022407	Regulation of cell-cell adhesion	0.003207892	14
CC	GO:0005840	Ribosome	0.003853809	10
CC	GO:0034774	Secretory granule lumen	0.022036358	10
CC	GO:0060205	Cytoplasmic vesicle lumen	0.022036358	10
CC	GO:0031983	Vesicle lumen	0.022036358	10
CC	GO:0022626	Cytosolic ribosome	8.41E-05	9
CC	GO:0044391	Ribosomal subunit	0.003853809	9
CC	GO:0031252	Cell leading edge	0.118712942	9
CC	GO:0005925	Focal adhesion	0.121501769	9
CC	GO:0030055	Cell-substrate junction	0.128157705	9
CC	GO:0045121	Membrane raft	0.006295321	8
MF	GO:0004857	Enzyme inhibitor activity	0.212404345	10
MF	GO:0042277	Peptide binding	0.212404345	9
MF	GO:0033218	Amide binding	0.247781289	9
MF	GO:0003712	Transcription coregulator activity	0.385576533	9
MF	GO:0003735	Structural constituent of ribosome	0.212404345	7
MF	GO:0019207	Kinase regulator activity	0.212404345	7
MF	GO:0019887	Protein kinase regulator activity	0.247781289	6
MF	GO:0030246	Carbohydrate binding	0.389028377	6
MF	GO:0045182	Translation regulator activity	0.247781289	5
MF	GO:0003714	Transcription corepressor activity	0.364059812	5

Table 3: The KEGG pathway enrichment analysis of genes in turquoise module.

ID	Description	p.adjust	Count
hsa05171	Coronavirus disease - COVID-19	0.049485195	9
hsa05135	Yersinia infection	0.049485195	7
hsa03010	Ribosome	0.050642504	7
hsa04066	HIF-1 signaling pathway	0.049485195	6
hsa04650	Natural killer cell mediated cytotoxicity	0.08036003	6
hsa04621	NOD-like receptor signaling pathway	0.247330937	6
hsa05202	Transcriptional misregulation in cancer	0.247330937	6
hsa05169	Epstein-Barr virus infection	0.293398065	6
hsa05208	Chemical carcinogenesis - reactive oxygen species	0.327462276	6

4. Discussion

Ischemic stroke, a neurological disease with a high morbidity and mortality rate, is one of the leading causes of permanent disability in adults [16]. Previous evidence indicates that [17] the etiology, risk factors, and prognosis of this disease all differ by gender. Of note, the risk of IS increases with an increase in the life expectancy of women. Ischemic stroke is also a common female complication during pregnancy and puerperium. Nearly 30 cases per 100000 cases of gestation

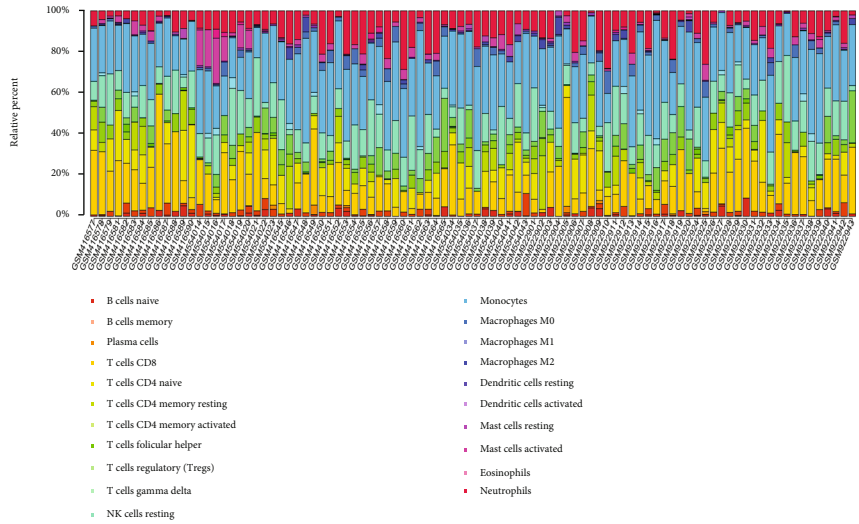

(a)

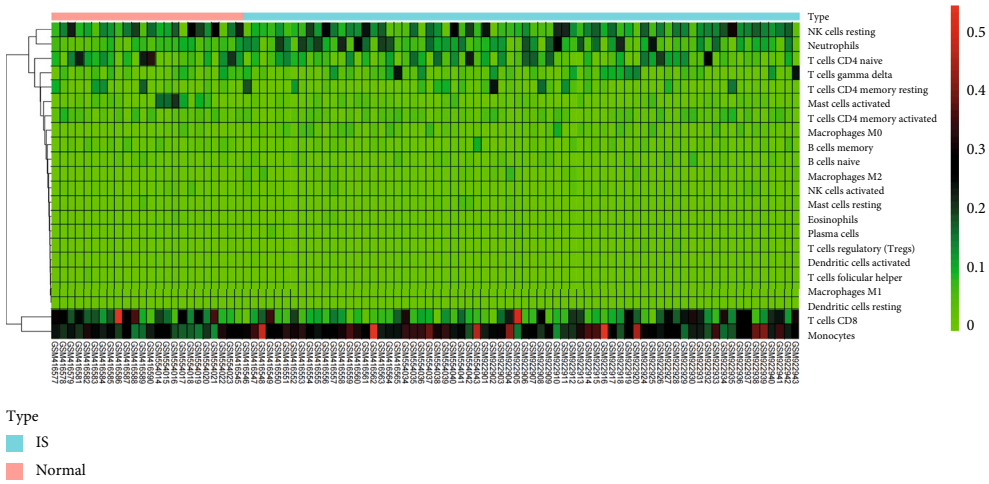

(b)

Figure 5: Continued.

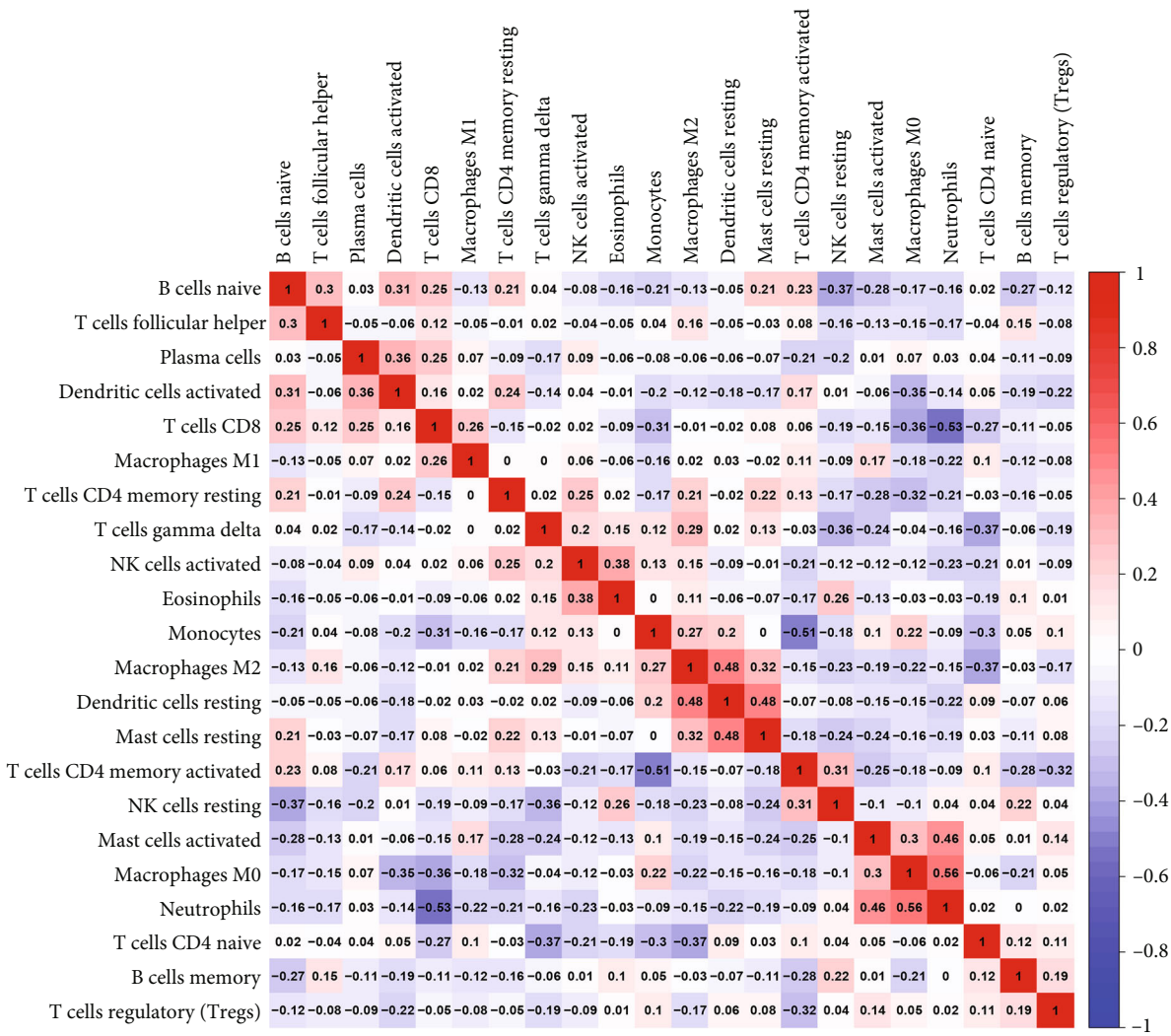

(c)

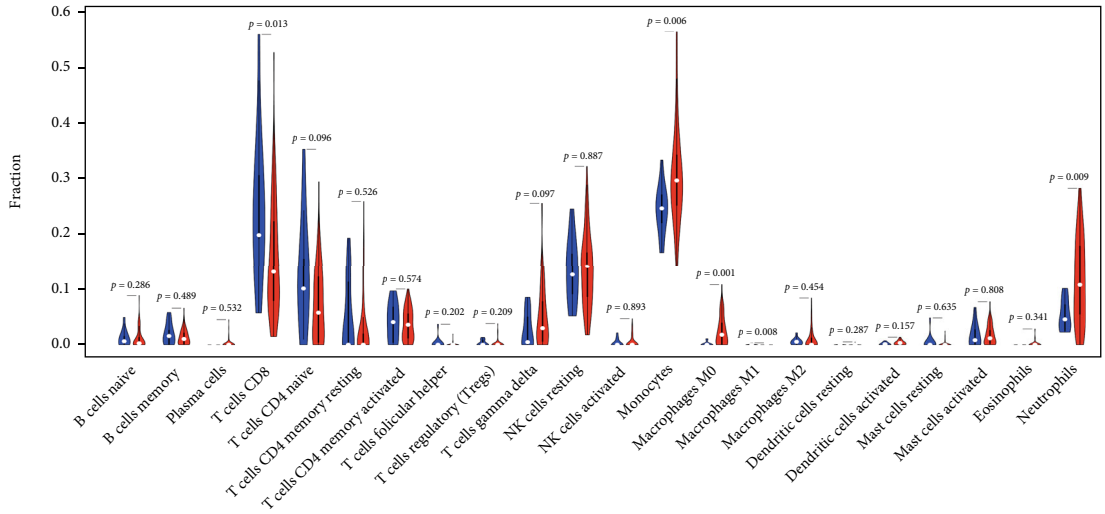

(d)

Figure 5: Immunoinfiltration of IS female and healthy female. (a) Percentage distribution of 22 immune cell subtypes in 96 samples from three datasets. (b) Heat map of the ratio of 22 immune cells in each sample. (c) Related heat maps of 22 immune cells. (d) Violin diagram of the difference in immune cell infiltration between female stroke patients and normal females.

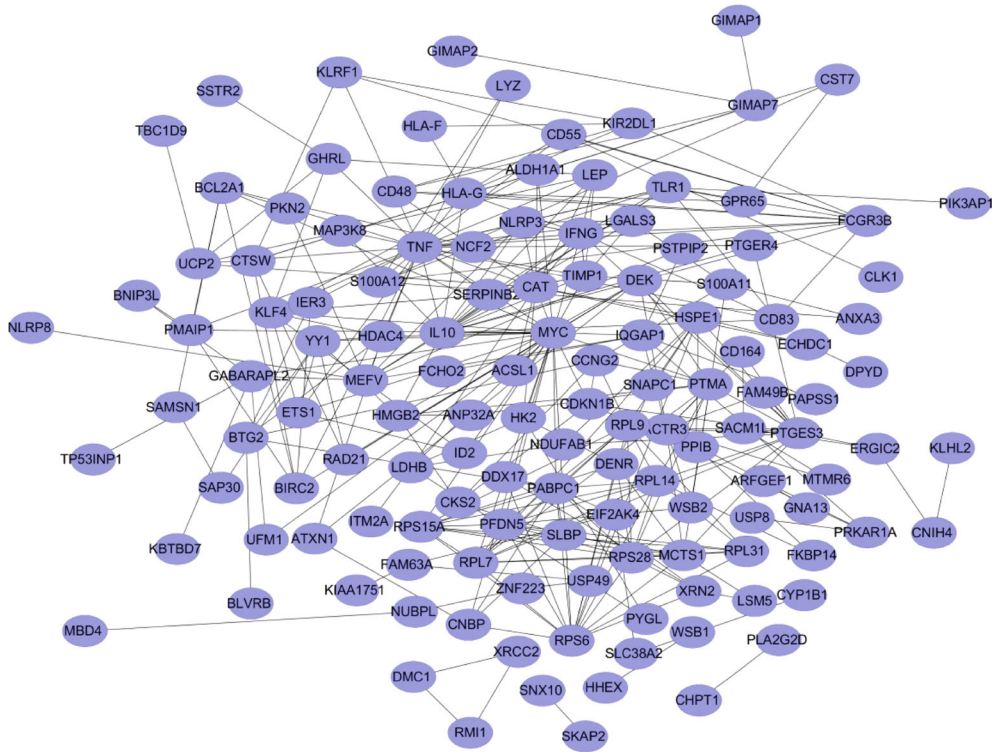

Figure 6: Protein-protein interaction (PPI) networks associated with differences in female patients with IS.

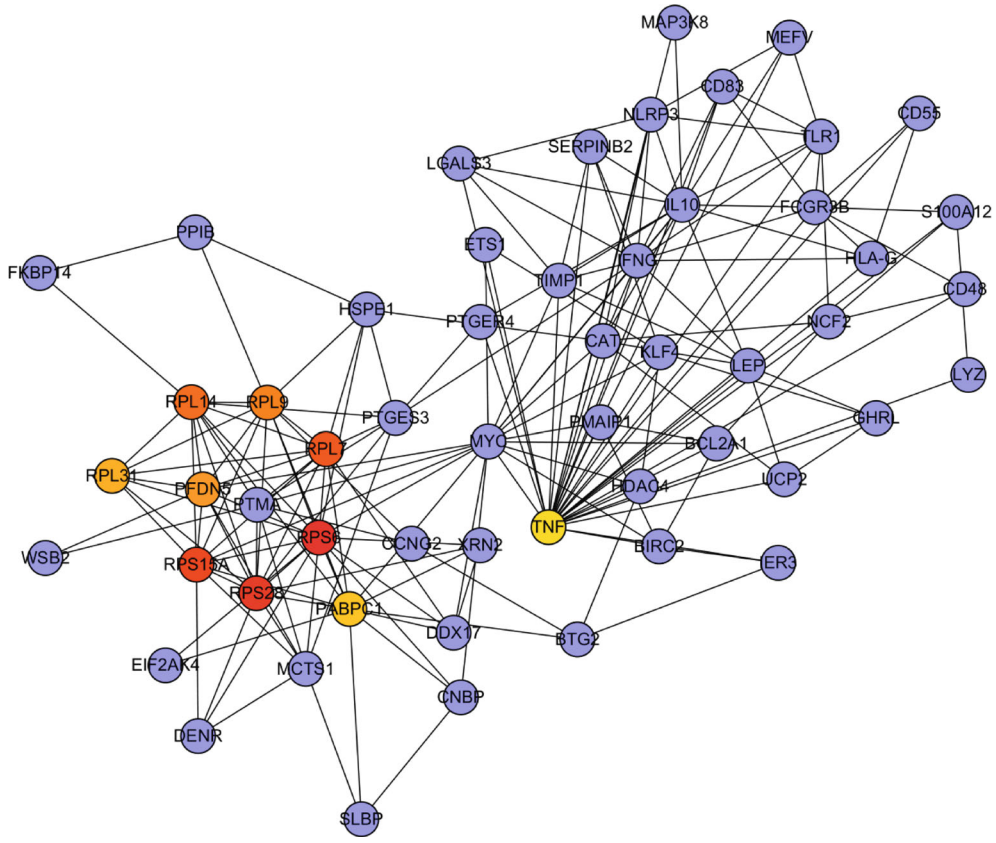

Figure 7: Core gene clusters in the co-expression network constructed from female IS patients. The depth of color indicated the levels of the central genes from low to high.

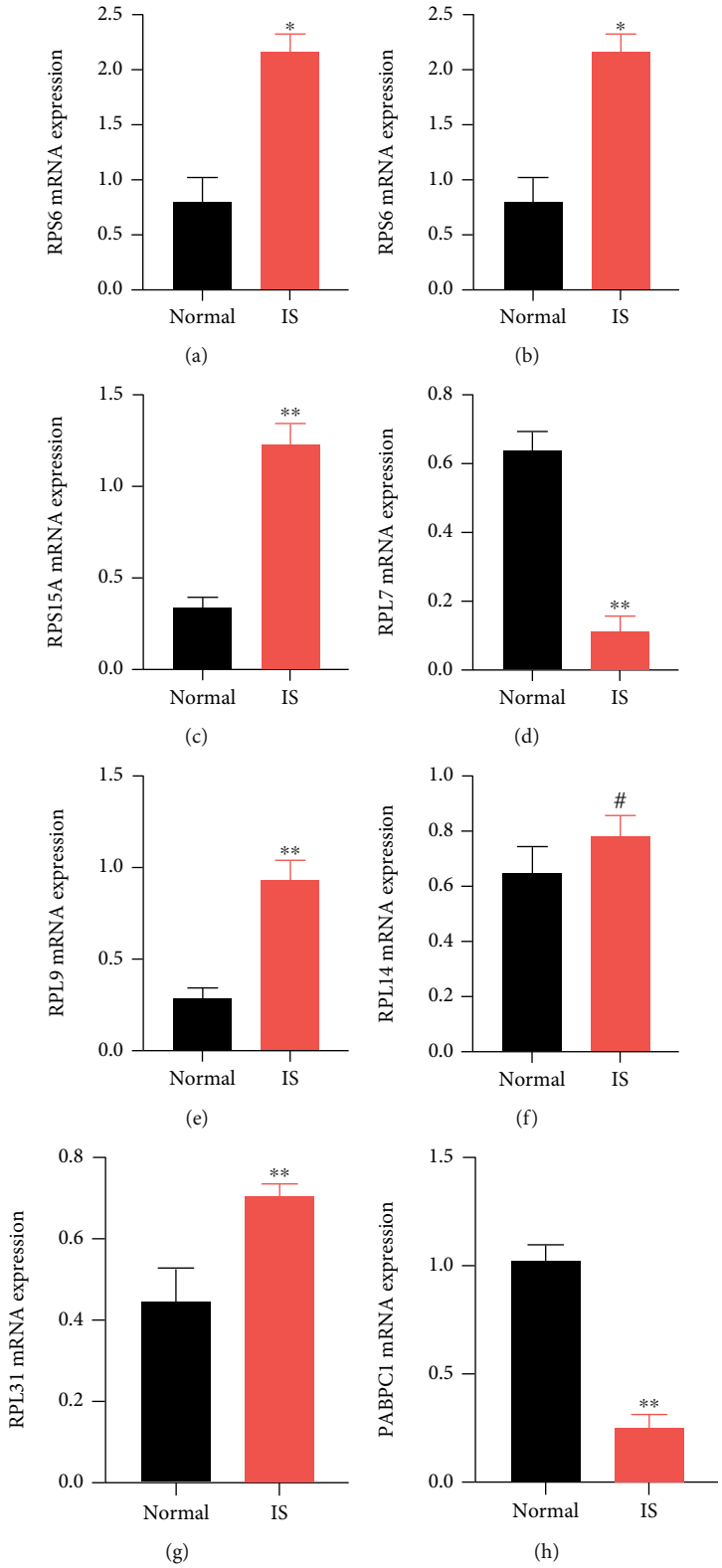

Figure 8: Continued.

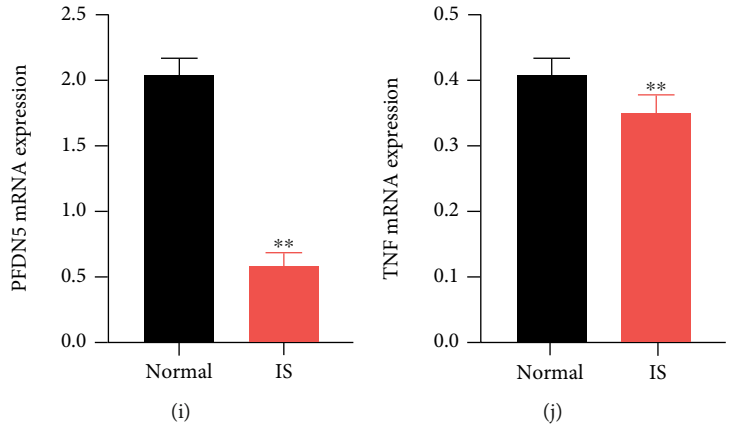

Figure 8: Validation of the hub genes by qRT-PCR. Black, normal samples; red, IS samples. ∗∗means p-value <0.01, and #means no difference. All data correspond to the average ± SEM. Statistical significance was assessed by the two-tailed Student's t-test.

(including all subtypes) show stroke symptoms in the two periods, with puerperae in high-risk groups having a higher incidence of IS [18]. In this view, females may bear a heavier burden than males.

Three dates were used in this study to collect 96 peripheral whole blood samples, 72 IS females and 24 normal females. We built a co-expression module using three datasets from WGCNA and confirmed that the turquoise module was crucial for females with IS (Figures 2 and 3). GO analysis demonstrated that immune response and ribosomes played critical roles in the pathogenesis of females with IS. Furthermore, KEGG analysis revealed that the main pathways of this disease in IS female patients were ribosome, HIF−1 signaling pathway, and natural killer cell-mediated cytotoxicity (Figure 4 and Tables 2 and 3). Ribosomal proteins (RPs) play an important role in the regulation of gene expression and protein synthesis [19]. Elsewhere, an experimental study found that cytoplasmic ribosomes play a role in functional recovery after ischemic stroke [20]. In the present study, the GO and KEGG results revealed that immune response and ribosomes are critical links in the mechanism of female patients with ischemic stroke.

Based on the above findings, we looked into the difference in immune infiltration of 22 immune cell subsets between IS females and healthy females. Mechanistically, the immune system is activated following ischemic stroke. A series of changes occur during immune cell migration to the ischemic area, resulting in either beneficial or detrimental effects on ischemic outcomes [21]. More importantly, certain key immune cells could become a new target for IS prevention or treatment. Our findings demonstrated that neutrophils, NK cells resting, macrophages, and T cells CD8 were the primary immune infiltrating cells.

Previous research has shown [22] that neutrophil infiltration is involved in recruitment of other immune cells. While some studies suggest that neutrophil infiltration may exacerbate ischemic stroke injury, other studies have discovered [23, 24] neutrophil involvement in tissue remodeling after stroke. NK cells are large granular lymphocytes of innate immunity that are required for IS immunosurveillance. NK cells regulate cellular immune response by blocking CD8 + T cell activation [25]. Infiltration of NK cells into the periinfarct area, on the other hand, can hasten neuronal death [26]. Improving NK cell infiltration into the periinfarct area is thus an important therapy for female patients with ischemic stroke that will eventually improve clinical responses. Macrophages are critical regulators of host defense in organisms, and they play critical roles in the repair of the central nervous system. In addition to providing neuroprotection, macrophages are a major source of proinflammatory cytokines [27]. These proinflammatory factors prevent the repair of brain tissue [28]. T cells regulate both innate and adaptive immunity, which may play a role in the pathogenesis of some neurological diseases [29]. Previous evidence shows that [30] activated and infiltrated microglia/macrophages after cerebral ischemia can stimulate activated CD4 + T cells to differentiate into Th1 or Th2 cells, which then produce proinflammatory or anti-inflammatory cytokines to damage or protect the brain. On the other hand, CD8+ cytotoxic T cells cause neuronal death and exacerbated brain injury via cell interaction. Findings from the present study demonstrate that T cells, macrophages, NK cells, and neutrophils may be important immune targets for the treatment of female ischemic stroke patients. The PPI network yielded 10 hub genes of female IS patients, which is consistent with the results of the GO and KEGG analyses.

Ribosomes have a wide range of complex functions. They are made up of several ribosomal proteins (RP), ribosomal RNA (rRNA), and small nucleolar RNA [31]. In terms of functions, ribosomal proteins are involved in a variety of critical biological processes in diseases. RPS15A (ribosomal protein S15A) is a component of the ribosomal 40s subunit that is involved in a series of biological processes, including proliferation, apoptosis, differentiation, and DNA repair [32]. Increasing evidence suggests that [33] RPS15A exerts critical functions in the development and progression of cancer. Ribosomal protein S6 (RPS6), a component of the cell translation system, has been shown to play a role in the progression of 40s ribosome biogenesis [34]. rpS6 phosphorylation is commonly used as a marker of neuronal activity in neuroscience [35]. Recent evidence shows that

[36] RPS28 regulates MHC Class I peptide generation for immunosurveillance. However, the dysfunction of RPS15A, RPS6, and RPS28 in females with ischemic stroke patients has never been reported. Similarly, the present study found upregulated levels of RPS15A, RPS6, and RPS28 in IS samples (Figures 8(a)–8(c)).

Ribosomal protein S7 (RPL7), ribosomal protein S31(RPL31), and ribosomal protein S9 (RPL9) are components of the large (60S) human ribosomal subunit. Overexpression of ribosome genes has been shown [37] to promote the translation and protein biosynthesis of Cardiac Allograft Rejection (AR) and cancer-related cytokines. Furthermore, ribosomes in stroke-induced peripheral immunosuppression may be a potential mechanism of sex disparities in outcome following IS [38]. Researchers implicate autoantigens, including RPL7, RPL31, RPL14, and RPL9, in the regulation of diseases such as systemic lupus erythematosus, rheumatoid arthritis, and systemic sclerosis [37]. Herein, we found higher levels of RPL31and RPL9 in IS samples compared to non-IS samples (Figures 8(e) and 8(g)). The IS model had significantly lower RPL7 genes, but there was no significant difference in RPL14 between the two groups (Figures 8(f) and 8(d)).

Our findings suggest a close association of PABPC1, PFDN5, and TNF with female ischemic stroke patients. PABPC1 (poly (A) binding protein cytoplasmic 1) is an important component of the RNA stabilization protein complex involved in germ cell development and mRNA translational regulation, and they have been linked to cancer [39]. Prefoldin (PFDN) is a co-chaperone protein widely accepted to play important roles in normal neuronal development and maintenance [40]. Mounting evidence had demonstrated that [41]inflammation is the principal cause of the pathology and physiology process of IS. Furthermore, the balance between proinflammatory cytokines and anti-inflammatory cytokines was linked to the progression and prognosis of IS patients [42]. Tumor necrosis factor (TNF) is a neuroinflammation cytokine and a potential target in future stroke therapy among the 10 core genes listed above. TNF regulates the size of ischemic injury. Following an ischemic stroke, TNF levels rise in cerebrospinal fluid (CSF) and blood [43]. This is consistent with our research. Additionally, furthermore, there is preliminary evidence that [44] targeting TNF may become a therapeutic approach in ischemic stroke. In addition, previous research has shown [45] a close association of ribosomes with immune cells. The 10 core genes identified in our present research were mostly ribosomal proteins. Therefore, we hypothesize that these genes are linked to T cells, macrophages, NK cells, and neutrophils in female ischemic stroke patients.

In conclusion, this study, for the first time, used microarray samples from IS females for WGCNA. We validated four immune-related gene expression modules and 10 central genes. The findings may be useful in further elucidating the pathogenesis of IS in female patients. Furthermore, we hypothesize that neutrophils and monocytes may play an important role in the disease progression of female IS patients. These findings could point to important biological targets for drug screening and drug design in IS females.

Data Availability

The data used to support the findings of this study are included within the article.

Conflicts of Interest

The authors declare that there is no conflict of interest regarding the publication of this paper.

Authors' Contributions

Haipeng Xu and Kelin He contributed equally to this work as co-first authors. Haipeng Xu and Ruijie Ma designed this study. Haipeng Xu and Kelin He analyzed the data. Haipeng Xu, YanZhi Ge, Rong Hu, and Kelin He wrote the manuscript. Xinyun Li, Fengjia Ni, Bei Que, and Yi Chen participated in the revision of the article. Ruijie Ma validated the manuscript. All authors had read and approved the final version of the paper. Kelin He contributed equally to this work. The manuscript is original, has not been submitted to or is not under consideration by another publication, has not been previously published in any language or any form, including electronic, and contains no disclosure of confidential information or authorship/patent application/funding source disputations.

Acknowledgments

We sincerely thank the third Clinical College of Zhejiang Chinese Medical University, Hangzhou, Zhejiang, China for offering the experimental areas. We also thank all teachers and students there for directing empirical methods. We thank Freescience (Contact Method: freescience@zju.edu.cn) for the help in language polishing. This work was supported by the Zhejiang Chinese Medical University Research Fund (No: 2018ZY17), the Chinese Medicine Research Program of Zhejiang Province (Nos: 2022ZQ047, 2020ZX011), and the Zhejiang Provincial Program for the Cultivation of High-level Innovative Health Talents.

Supplementary Materials

The detailed R code is summarized in the supplementary materials. *(Supplementary Materials)*

References

[1] B. C. V. Campbell, D. A. de Silva, M. R. Macleod et al., "Ischaemic stroke," *Nature Reviews. Disease Primers*, vol. 5, no. 1, p. 70, 2019.

[2] GBD 2016 Neurology Collaborators, "Global, regional, and national burden of neurological disorders, 1990-2016: a systematic analysis for the Global Burden of Disease Study 2016," *The Lancet Neurology*, vol. 18, no. 5, pp. 459–480, 2019.

[3] L. E. Ziganshina, T. Abakumova, and C. H. Hoyle, "Cerebrolysin for acute ischaemic stroke," *The Cochrane Database of Systematic Reviews*, vol. 2020, no. 9, article Cd007026, 2020.

[4] E. J. Benjamin, S. S. Virani, C. W. Callaway et al., "Correction to: Heart Disease and Stroke Statistics-2018 Update: A Report

from the American Heart Association," *Circulation*, vol. 137, no. 12, p. e493, 2018.

[5] H. Xu, Y. Ge, Y. Liu et al., "Identification of the key genes and immune infiltrating cells determined by sex differences in ischaemic stroke through co-expression network module," *IET Systems Biology*, vol. 16, no. 1, pp. 28–41, 2022.

[6] C. Zou, C. Wei, Z. Wang, and Y. Jin, "Sex differences in outcomes and risk factors among elderly patients with ischemic stroke," *Oncotarget*, vol. 8, no. 61, pp. 104582–104593, 2017.

[7] F. Z. Caprio and F. A. Sorond, "Cerebrovascular disease: primary and secondary stroke prevention," *The Medical Clinics of North America*, vol. 103, no. 2, pp. 295–308, 2019.

[8] X. Qiu, J. Lin, B. Liang, Y. Chen, G. Liu, and J. Zheng, "Identification of hub genes and microRNAs associated with idiopathic pulmonary arterial hypertension by integrated bioinformatics analyses," *Frontiers in Genetics*, vol. 12, p. 667406, 2021.

[9] L. B. Goldstein, R. Adams, K. Becker et al., "Primary prevention of ischemic stroke," *Stroke*, vol. 32, no. 1, pp. 280–299, 2001.

[10] Z. Li, Y. Cui, J. Feng, and Y. Guo, "Identifying the pattern of immune related cells and genes in the peripheral blood of ischemic stroke," *Journal of Translational Medicine*, vol. 18, no. 1, p. 296, 2020.

[11] G. Chen, L. Li, and H. Tao, "Bioinformatics identification of ferroptosis-related biomarkers and therapeutic compounds in ischemic stroke," *Frontiers in Neurology*, vol. 12, 2021.

[12] B. Feng, X. Meng, H. Zhou et al., "Identification of dysregulated mechanisms and potential biomarkers in ischemic stroke onset," *International Journal of General Medicine*, vol. 14, pp. 4731–4744, 2021.

[13] M. Chamankhah, E. Eftekharpour, S. Karimi-Abdolrezaee, P. C. Boutros, S. San-Marina, and M. G. Fehlings, "Genome-wide gene expression profiling of stress response in a spinal cord clip compression injury model," *BMC Genomics*, vol. 14, no. 1, 2013.

[14] P. Langfelder and S. Horvath, "WGCNA: an R package for weighted correlation network analysis," *BMC Bioinformatics*, vol. 9, no. 1, 2008.

[15] D. Szklarczyk, A. L. Gable, D. Lyon et al., "STRING v11: protein-protein association networks with increased coverage, supporting functional discovery in genome-wide experimental datasets," *Nucleic Acids Research*, vol. 47, no. D1, pp. D607–D613, 2019.

[16] Y. Wang, X. Wang, X. Zhang et al., "D1 receptor-mediated endogenous tPA upregulation contributes to blood-brain barrier injury after acute ischaemic stroke," *Journal of Cellular and Molecular Medicine*, vol. 24, no. 16, pp. 9255–9266, 2020.

[17] E. C. Miller and L. Leffert, "Stroke in pregnancy," *Anesthesia and Analgesia*, vol. 130, no. 4, pp. 1085–1096, 2020.

[18] I. Y. Elgendy, M. M. Gad, A. N. Mahmoud, E. C. Keeley, and C. J. Pepine, "Acute stroke during pregnancy and puerperium," *Journal of the American College of Cardiology*, vol. 75, no. 2, pp. 180–190, 2020.

[19] T. F. M. Carvalho, J. C. F. Silva, I. P. Calil, E. P. B. Fontes, and F. R. Cerqueira, "Rama: a machine learning approach for ribosomal protein prediction in plants," *Scientific Reports*, vol. 7, no. 1, p. 16273, 2017.

[20] A. Agarwal, S. Park, S. Ha et al., "Quantitative mass spectrometric analysis of the mouse cerebral cortex after ischemic stroke," *PLoS One*, vol. 15, no. 4, article e0231978, 2020.

[21] G. Yilmaz, T. V. Arumugam, K. Y. Stokes, and D. N. Granger, "Role of T lymphocytes and interferon-γ in ischemic stroke," *Circulation*, vol. 113, no. 17, pp. 2105–2112, 2006.

[22] G. J. Del Zoppo, G. W. Schmid-Schönbein, E. Mori, B. R. Copeland, and C. M. Chang, "Polymorphonuclear leukocytes occlude capillaries following middle cerebral artery occlusion and reperfusion in baboons," *Stroke*, vol. 22, no. 10, pp. 1276–1283, 1991.

[23] A. Rosell, E. Cuadrado, A. Ortega-Aznar, M. Hernández-Guillamon, E. H. Lo, and J. Montaner, "MMP-9-positive neutrophil infiltration is associated to blood-brain barrier breakdown and basal lamina type IV collagen degradation during hemorrhagic transformation after human ischemic stroke," *Stroke*, vol. 39, no. 4, pp. 1121–1126, 2008.

[24] J. Herz, P. Sabellek, T. E. Lane, M. Gunzer, D. M. Hermann, and T. R. Doeppner, "Role of neutrophils in exacerbation of brain injury after focal cerebral ischemia in hyperlipidemic mice," *Stroke*, vol. 46, no. 10, pp. 2916–2925, 2015.

[25] K. Soderquest, T. Walzer, B. Zafirova et al., "Cutting edge: CD8 + T cell priming in the absence of NK cells leads to enhanced memory responses," *Journal of Immunology (Baltimore, Md. : 1950)*, vol. 186, no. 6, pp. 3304–3308, 2011.

[26] Y. Gan, Q. Liu, W. Wu et al., "Ischemic neurons recruit natural killer cells that accelerate brain infarction," *Proceedings of the National Academy of Sciences of the United States of America*, vol. 111, no. 7, pp. 2704–2709, 2014.

[27] S. Wattananit, D. Tornero, N. Graubardt et al., "Monocyte-derived macrophages contribute to spontaneous long-term functional recovery after stroke in mice," *The Journal of neuroscience : the official journal of the Society for Neuroscience*, vol. 36, no. 15, pp. 4182–4195, 2016.

[28] D. Cihakova, J. G. Barin, M. Afanasyeva et al., "Interleukin-13 protects against experimental autoimmune myocarditis by regulating macrophage differentiation," *The American Journal of Pathology*, vol. 172, no. 5, pp. 1195–1208, 2008.

[29] P. L. McGeer and E. G. McGeer, "History of innate immunity in neurodegenerative disorders," *Frontiers in Pharmacology*, vol. 2, 2011.

[30] Y. Wang, J. H. Zhang, J. Sheng, and A. Shao, "Immunoreactive cells after cerebral ischemia," *Frontiers in Immunology*, vol. 10, 2019.

[31] X. Xie, P. Guo, H. Yu, Y. Wang, and G. Chen, "Ribosomal proteins: insight into molecular roles and functions in hepatocellular carcinoma," *Oncogene*, vol. 37, no. 3, pp. 277–285, 2018.

[32] W. Wang, S. Nag, X. Zhang et al., "Ribosomal proteins and human diseases: pathogenesis, molecular mechanisms, and therapeutic implications," *Medicinal Research Reviews*, vol. 35, no. 2, pp. 225–285, 2015.

[33] M. Y. Li, L. N. Fan, D. H. Han et al., "Ribosomal S6 protein kinase 4 promotes radioresistance in esophageal squamous cell carcinoma," *The Journal of Clinical Investigation*, vol. 130, no. 8, pp. 4301–4319, 2020.

[34] S. Kim, Y. H. Jang, G. C. Chau, S. Pyo, and S. H. Um, "Prognostic significance and function of phosphorylated ribosomal protein S6 in esophageal squamous cell carcinoma," *Modern Pathology*, vol. 26, no. 3, pp. 327–335, 2013.

[35] H. Xiao, H. Wang, E. A. Silva et al., "The Pallbearer E3 ligase promotes actin remodeling via RAC in efferocytosis by degrading the ribosomal protein S6," *Developmental Cell*, vol. 32, no. 1, pp. 19–30, 2015.

[36] J. Wei, R. J. Kishton, M. Angel et al., "Ribosomal proteins regulate MHC class I peptide generation for immunosurveillance," *Molecular Cell*, vol. 73, no. 6, pp. 1162–1173.e5, 2019.

[37] J. L. Woolford Jr. and S. J. Baserga, "Ribosome biogenesis in the yeast Saccharomyces cerevisiae," *Genetics*, vol. 195, no. 3, pp. 643–681, 2013.

[38] J. Q. Xie, Y. P. Lu, H. L. Sun et al., "Sex difference of ribosome in stroke-induced peripheral immunosuppression by integrated bioinformatics analysis," *BioMed Research International*, vol. 2020, Article ID 3650935, 15 pages, 2020.

[39] R. Su, J. Ma, J. Zheng et al., "PABPC1-induced stabilization of BDNF-AS inhibits malignant progression of glioblastoma cells through STAU1-mediated decay," *Cell Death & Disease*, vol. 11, no. 2, p. 81, 2020.

[40] Y. Lee, R. S. Smith, W. Jordan et al., "Prefoldin 5 Is Required for Normal Sensory and Neuronal Development in a Murine Model," *The Journal of Biological Chemistry*, vol. 286, no. 1, pp. 726–736, 2011.

[41] K. Duris, Z. Splichal, and M. Jurajda, "The role of inflammatory response in stroke associated programmed cell death," *Current Neuropharmacology*, vol. 16, no. 9, pp. 1365–1374, 2018.

[42] A. Dénes, S. Ferenczi, and K. J. Kovács, "Systemic inflammatory challenges compromise survival after experimental stroke via augmenting brain inflammation, blood- brain barrier damage and brain oedema independently of infarct size," *Journal of Neuroinflammation*, vol. 8, no. 1, p. 164, 2011.

[43] K. L. Lambertsen, B. Finsen, and B. H. Clausen, "Post-stroke inflammation-target or tool for therapy?," *Acta Neuropathologica*, vol. 137, no. 5, pp. 693–714, 2019.

[44] B. H. Clausen, M. Wirenfeldt, S. S. Høgedal et al., "Characterization of the TNF and IL-1 systems in human brain and blood after ischemic stroke," *Acta Neuropathologica Communications*, vol. 8, no. 1, p. 81, 2020.

[45] N. Dhanesha, R. B. Patel, P. Doddapattar et al., "PKM2 promotes neutrophil activation and cerebral thromboinflammation: therapeutic implications for ischemic stroke," *Blood*, vol. 139, no. 8, pp. 1234–1245, 2022.

Hindawi
Neural Plasticity
Volume 2022, Article ID 1560748, 10 pages
https://doi.org/10.1155/2022/1560748

Research Article

Functional Connectivity Changes in Multiple-Frequency Bands in Acute Basal Ganglia Ischemic Stroke Patients: A Machine Learning Approach

Jie Li,[1,2] **Lulu Cheng**,[3,4] **Shijian Chen**,[5] **Jian Zhang**,[5] **Dongqiang Liu**,[1,2] **Zhijian Liang**,[5] **and Huayun Li**[6,7]

[1]*Research Center of Brain and Cognitive Neuroscience, Liaoning Normal University, Dalian, China*
[2]*Key Laboratory of Brain and Cognitive Neuroscience, Liaoning Province, China*
[3]*School of Foreign Studies, China University of Petroleum (East China), Qingdao, China*
[4]*Shanghai Center for Research in English Language Education, Shanghai International Studies University, Shanghai, China*
[5]*Department of Neurology, The First Affiliated Hospital of Guangxi Medical University, Nanning, China*
[6]*College of Teacher Education, Zhejiang Normal University, Jinhua, China*
[7]*Key Laboratory of Intelligent Education Technology and Application, Zhejiang Normal University, Jinhua, China*

Correspondence should be addressed to Dongqiang Liu; 52213200021@stu.ecnu.edu.cn, Zhijian Liang; liangzhijian@gxmu.edu.cn, and Huayun Li; huayun@zjnu.edu.cn

Received 27 December 2021; Revised 7 February 2022; Accepted 21 February 2022; Published 20 March 2022

Academic Editor: Yu Zheng

Purpose. Several functional magnetic resonance imaging (fMRI) studies have investigated the resting-state functional connectivity (rs-FC) changes in the primary motor cortex (M1) in patients with acute basal ganglia ischemic stroke (BGIS). However, the frequency-specific FC changes of M1 in acute BGIS patients are still unclear. Our study was aimed at exploring the altered FC of M1 in three frequency bands and the potential features as biomarkers for the identification by using a support vector machine (SVM). *Methods*. We included 28 acute BGIS patients and 42 healthy controls (HCs). Seed-based FC of two regions of interest (ROI, bilateral M1s) were calculated in conventional, slow-5, and slow-4 frequency bands. The abnormal voxel-wise FC values were defined as the features for SVM in different frequency bands. *Results*. In the ipsilesional M1, the acute BGIS patients exhibited decreased FC with the right lingual gyrus in the conventional and slow-4 frequency band. Besides, the acute BGIS patients showed increased FC with the right medial superior frontal gyrus (SFGmed) in the conventional and slow-5 frequency band and decreased FC with the left lingual gyrus in the slow-5 frequency band. In the contralesional M1, the BGIS patients showed lower FC with the right SFGmed in the conventional frequency band. The higher FC values with the right lingual gyrus and left SFGmed were detected in the slow-4 frequency band. In the slow-5 frequency band, the BGIS patients showed decreased FC with the left calcarine sulcus. SVM results showed that the combined features (slow-4+slow-5) had the highest accuracy in classification prediction of acute BGIS patients, with an area under curve (AUC) of 0.86. *Conclusion*. Acute BGIS patients had frequency-specific alterations in FC; SVM is a promising method for exploring these frequency-dependent FC alterations. The abnormal brain regions might be potential targets for future researchers in the rehabilitation and treatment of stroke patients.

1. Introduction

Stroke can be divided into two categories: ischemic and hemorrhagic cerebrovascular disease [1–3], and about 80% of stroke pertains to ischemic [4, 5]. Ischemic stroke is one of the most common diseases which may cause adult death or disability, in which acute basal ganglia ischemic stroke (BGIS) is attributed to the lesion of basal ganglia, and it is

primarily associated with motor deficits in poststroke [6–8]. Motor function deficits are one of the main causes of disability in stroke patients and will seriously affect the patient's ability to live independently [9–11].

The primary motor cortex (M1) is one of the main brain regions involved in motor functions and the focus of many researchers exploring the neural mechanisms of motor function deficits. Resting-state functional magnetic resonance imaging (rs-fMRI) is a noninvasive neuroimaging tool with the advantage of no task demand or external stimulation and therefore demonstrated to be in the examination of brain functional deficits associated with a variety of neurological disorders [9, 10]. Functional connectivity (FC) is one of the most widely used methods in rs-fMRI [12–14], and it examined connectivity between two spatial regions of interest to quantify temporal coherence in rs-fMRI signal [15, 16]. Many studies have observed alterations of FC in stroke patients and showed that the abnormal connectivity related to behavioral deficits [17–21] and could provide crucial information on the neural mechanisms of motor recovery [22].

Up to now, FC was widely used for exploring the neurological mechanism of motor deficits in poststroke [23–25]. Studies showed that abnormal FC in stroke patients was correlated with their symptoms and deficits, and change in the strength of FC has also been found to be related to the change in the clinical assessment of motor function [26, 27]. For example, Zhang et al. found that patients with stroke had increased FC between the M1 and the inferior parietal cortex (IPL), frontal gyrus, supplementary motor area (SMA), and contralesional angular, while decreased FC was shown between the ipsilesional M1 and bilateral M1 [28]. Another study showed that poststroke subjects had an asymmetrical pattern of FC, which affected the hemisphere sensory cortex and was correlated with stroke severity [29]. However, previous FC studies mainly focused on the conventional band (0.01-0.08 Hz) [23–25, 30].

The human brain is a complex biological system that can generate a large number of oscillatory waves, and neural signals within different frequency bands exhibit different properties and physiological functions [31, 32]. Previous studies have subdivided the low-frequency range into four subfrequency bands [33, 34], among which gray matter activities mainly concentrated in the slow-4 (0.027-0.073 Hz) and slow-5 (0.01-0.027 Hz) frequency bands [34]. We examine the slow-5 and slow-4 bands because they have overlap with most of the conventional frequency bands and have minimal overlap with potential physiological noise frequency [34, 35]. Slow-4 has higher test-retest reliability and is more reliable for evaluating fMRI fluctuation amplitude signal than slow-5, and slow-5 and slow-4 showed higher power in different brain regions [34]. Moreover, recent studies have demonstrated that FC exhibited frequency-specific abnormalities in some neurological and psychiatric diseases and showed that fMRI signals in specific frequency bands might provide us with more sensitive information to understand the pathological mechanisms of disease [31, 32, 36]. Therefore, combining the importance of M1 brain regions for stroke patients, it is necessary to explore the frequency-specific alterations of FC in acute BGIS patients. In addition, to better understand disease detection sensitivity in frequency-specific FC, the machine learning approach is a powerful tool to classify patients from healthy controls. Support vector machine (SVM) was often used in MRI classification to detect biomarkers based on neuroimaging data, so that the contributing features in the classification model could help us have an in-depth understanding of the neurological mechanism of motor deficit in acute BGIS patients.

In this study, we used bilateral M1s as the regions of interest to determine whether stroke patients show abnormal FC between M1 and other voxels of the whole brain in three frequency bands (conventional, slow-5, and slow-4). Second, we explored the relationship between frequency-specific FC and clinical assessments. Third, we adopted SVM for classification with significantly different brain regions as imaging features. We hypothesized that FC changes in acute BGIS patients would exhibit frequency band specificity and that these abnormal FC could serve as effective biomarkers to identify patients and HCs, which might help us to better understand the neural mechanisms of motor deficit and provide support for future clinical rehabilitation treatment in acute BGIS patients.

2. Materials and Methods

2.1. Participants. We recruited 43 acute BGIS patients at the Department of Neurology, the First Affiliated Hospital of Guangxi Medical University. Patients were included using the following inclusion criteria: (1) patients were first onset acute BGIS (a consensus diagnosis was determined by a clinical neurologist and a radiologist); (2) age of patients was from 30 to 70 years; (3) the illness duration of BGIS patients ranged from 1 to 7 days (details shown in Table S1); (4) patients were right-handed before stroke; and (5) the National Institutes of Health Stroke Scale (NIHSS) scores of patients were no more than 8 (0 and 8 were included). Our study was approved by the Ethics Committee of the First Affiliated Hospital of Guangxi Medical University, and written informed consent was obtained from each participant. Besides, from the local community, we recruited 47 matched HCs who have no physical diseases or history of psychiatric or neurologic disorders.

To reduce the effect of confounding factors, we adopted a set of exclusion criteria: (1) inability to complete clinical scales, such as severe aphasia and auditory and/or visual disorder; (2) other neurological disorders which would affect the experiment, such as hemorrhage, multiple infarcts, leukoaraiosis, migraine, epilepsy, or psychiatric diseases; (3) any MRI contraindications; and (4) head motion exceeding 3 mm or 3°. Finally, our study included 28 acute BGIS patients and 42 HCs in the further analysis (2 BGIS patients and 1 HC had excessive head movement, the other 2 BGIS patients and 1 HC had incomplete data, and 11 BGIS patients and 3 HC were excluded for age and illness duration).

2.2. Clinical Scale Assessment. Patients were assessed by NIHSS to characterize the stroke severity and neurological

Table 1: Demographic and clinical information of participants.

	BGIS patients ($N = 28$)	HCs ($N = 42$)	p value
Age (years)	54.60 ± 8.90	54.85 ± 10.24	0.9
Gender (male/female)	23/5	19/23	0.0001
Education (years)	12.00 ± 3.23	12.28 ± 2.99	0.7
NIHSS score	3.60 ± 2.22	—	—
FMA score	77.03 ± 17.22	—	—

BGIS: basal ganglia ischemic stroke; HCs: healthy controls; NIHSS: National Institutes of Health Stroke Scale; FMA: Fugl-Meyer Assessment.

deficits [37] and assessed by the Fugl-Meyer Assessment scale (FMA) to characterize motor impairment [38]. Patients were assessed by NIHSS to characterize the stroke severity and neurological deficits [37] and assessed by the Fugl-Meyer Assessment scale (FMA) to characterize motor impairment [38].

2.3. Image Acquisition. Images were acquired using a 3.0 T Siemens Prisma MRI scanner with a 64-channel phased array head coil. The imaging parameters of resting-state fMRI data were as follows: repetition time (TR) = 2000 ms, echo time (TE) = 35 ms, voxel size = $2.6 \times 2.6 \times 3$ mm^3, matrix size = 64×64, field of view (FOV) = 240×240 mm^2, flip angle (FA) = 90°, slice number = 40, 6 minutes and 12 seconds, and 186 volumes. The acquisition parameters for anatomical T1-weighted images were as follows: TR = 2300 ms, TE = 2.98 ms, voxel size = $1 \times 1 \times 1$ mm^3, matrix size = 256×256, FOV = 256×256 mm^2, FA = 9°, slice number = 176, and 5 minutes and 21 seconds. All participants were required to remain awake, close their eyes, and keep relaxing during scanning.

2.4. Image Preprocessing. All images were preprocessed by using Statistical Parametric Mapping (SPM 12, http://www.fil.ion.ucl.ac.uk/spm) and Resting-State fMRI Data Analysis Toolkit plus (RESTplus V1.24, http://restfmri.net/forum/restplus) [39], implemented in the MATLAB R2017b platform (https://ww2.mathworks.cn/products/matlab.html). Briefly, the preprocessing steps included the following steps. (1) Remove the first ten volumes of each functional image and then keep 176 volumes. (2) Slice-time correction. (3) Realignment. (4) Normalization. The realigned images were spatially normalized to the Montreal Neurological Institute (MNI) space and resampled with a voxel size of $3 \times 3 \times 3$ m m^3. (5) Spatial smoothing with 6 mm full width at half maximum (FWHM). (6) Nuisance covariate regression. The nuisance regressors included the Friston-24 motion parameters [40], white matter signals [41], cerebrospinal fluid signals [41], and global mean signals [42]. We also removed the linear trends. (7) Filtering. The temporal band-pass filtering was, respectively, performed in the three frequency bands: conventional (0.01-0.08 Hz), slow-5 (0.01–0.027 Hz), and slow-4 (0.027–0.073 Hz).

2.5. Functional Connectivity Analyses. To calculate seed-based functional connectivity, we defined two regions of interest (ROIs) of the M1 with 6 mm diameter spheres. The ROIs are the left primary motor cortex (M1_L, MNI coordinates, -12, -30, 54) and the right primary motor cortex (M1_R, MNI coordinates, 12, -30, 54) in line with a previous study [43]. In three frequency bands, we then computed Pearson correlation coefficients between each ROI and the voxels of the whole brain to create correlation FC maps. Finally, we converted the correlation maps into Z values using Fisher's r-to-Z transformation to improve normality. Notably, the lesion side in the right basal ganglia of 15 cases was flipped to the left by the RESTplus V1.25 toolbox based on the MATLAB R2017b platform. Thus, we defined the M1_L as the ipsilesional M1 and defined the M1_R as the contralesional M1.

2.6. Statistical Analyses. All statistical analyses were conducted by the Statistical Product and Service Solutions version (SPSS 26.0, IBM, Armonk, NY, USA). The age and education of participants were compared using two-sample t-tests, and the gender of participants was compared using chi-squared tests (significance level: $p < 0.05$).

Two-sample t-tests were performed to identify the FC differences between acute BGIS patients and HCs in three frequency bands. We also applied the Gaussian random field (GRF) theory multiple comparison correction (voxel-level: $p < 0.005$, cluster-level: $p < 0.05$).

2.7. Correlation Analyses. To explore the relationship between the FC abnormalities and the function impairments, we then performed the Pearson correlation analysis between the aberrant FC and clinical scales (NIHSS and FMA). The statistical significance level was set at $p < 0.05$.

2.8. Feature Extraction and SVM Analyses. Abnormal brain regions were obtained from the group comparisons between patients and controls. The intergroup z values of FC difference were used as the classification features in this study. Specifically, we extracted voxel-wise z FC values from these brain clusters in each ROI in three frequency bands. Besides, z values of FC from abnormal brain regions in the conventional and subfrequency band (slow-4+slow-5) were also extracted and combined as features.

In this study, we employed the LIBSVM software package in MATLAB, in which a linear kernel support vector machine was conducted within each cluster in three frequency bands (http://www.csie.ntu.edu.tw/~cjlin/libsvm/) [44]. To reduce the risk of overfitting the training data, the SVM with linear kernel was used to extract the feature weights directly [45]. In the SVM model, the parameter C was set to 1, and the optimized linear kernel parameter γ

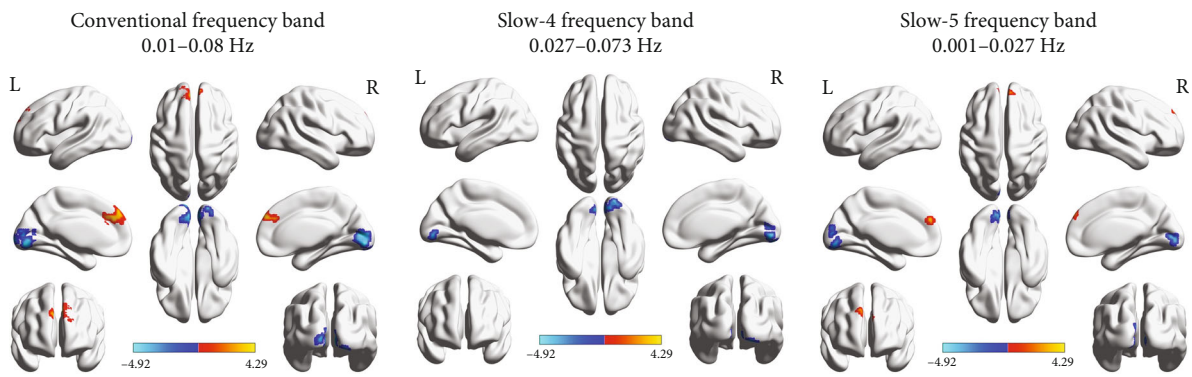

Figure 1: The functional connectivity alterations of the ipsilesional M1 in the three frequency bands.

Table 2: The functional connectivity alterations of the ipsilesional M1 in the three frequency bands.

Brain regions (BGIS patients > HCs)	Number of voxels	MNI coordinate			Peak t value
		x	y	z	
Conventional frequency band (0.01-0.08 Hz)					
Lingual_R	469	3	-84	-9	-4.9214
Frontal_Sup_Medial_R	171	15	57	42	4.2933
Slow-4 frequency band (0.027-0.073 Hz)					
Lingual_R	168	3	-84	-9	-4.6060
Slow-5 frequency band (0.01-0.027 Hz)					
Lingual_L	132	-3	-81	-3	-3.8903
Frontal_Sup_Medial_R	80	15	57	42	4.2933

Lingual_R: right lingual gyrus; Lingual_L: left lingual gyrus; Frontal_Sup_Medial_R: right medial superior frontal gyrus; MNI: Montreal Neurological Institute.

was set to 2^N (N ranges from −5 to 5). The performance of the SVM classifier was evaluated by a leave-one-out cross-validation method (LOOCV). The data of one participant is selected as the test sample, and data of other participants were used to train the SVM classifier. To evaluate the overall accuracy of the SVM, we repeated the classification test for each pair of participants. The performance of classification was evaluated by calculating the accuracy, sensitivity, specificity, precision, and area under the receiver operating characteristic (ROC) curve (AUC) [46].

3. Results

3.1. Demographic and Clinical Characteristics of the Participants. Our study included 70 subjects. Demographic and clinical data of all participants are summarized in Table 1. There was no significant difference between acute BGIS patients and HCs in age and education ($p > 0.05$). The significant difference between the two groups was found in gender ($p < 0.0001$).

3.2. Functional Connectivity Alterations of the Ipsilesional M1. In the conventional frequency band (0.01-0.08 Hz), the acute BGIS patients showed decreased FC values between the ipsilesional M1 and the right lingual gyrus and increased FC values between the ipsilesional M1 and the right medial superior frontal gyrus (SFGmed) compared with the HCs. In the slow-4 frequency band (0.027-0.073 Hz), acute BGIS patients exhibited decreased FC values between the ipsilesional M1 and the right lingual gyrus. In addition, we also found the decreased FC values between the ipsilesional M1 and the left lingual gyrus and the increased FC values between the ipsilesional M1 and the right SFGmed in the slow-5 frequency band (0.01-0.027 Hz) (details shown in Figure 1 and Table 2).

3.3. Functional Connectivity Alterations of the Contralesional M1. In the conventional frequency band, results showed that acute BGIS patients had increased FC values between the contralesional M1 and the right SFGmed. As for the slow-4 band, acute BGIS patients exhibited higher FC values in the left SFGmed and lower FC values in the right lingual gyrus. In the slow-5 frequency band, we found that acute BGIS patients had increased FC values between the contralesional M1 and the left calcarine sulcus (shown in Figure 2 and Table 3).

3.4. The Relationship between Abnormal FC Values and Clinical Scores. We performed the Pearson correlation analysis between FC values and clinical scores (including NIHSS and FMA scores) in all three frequency bands. No significant correlation was found between abnormal FC values and clinical scores ($p < 0.05$).

3.5. Classification Results. In the current study, Table 4 summarizes and shows the accuracies, sensitivities, specificities, and precisions of the classification for features in each ROI in three frequency bands and the combined features. The receiver operating characteristic (ROC) curve of the classifier for each feature is shown in Figure 3. Features in each of the three frequency bands and combined features demonstrated a significantly higher accuracy rate and AUC value than chance ($p < 0.05$). Specifically, both single features and the combined features had AUC values up to 0.73. In bilateral M1s, features in the conventional band had close AUC values ranging from 0.75 to 0.82. As for subbands (slow-4 and slow-5), the result also showed similar AUC values. The combined features in the conventional frequency band had the same classification performance AUC values of

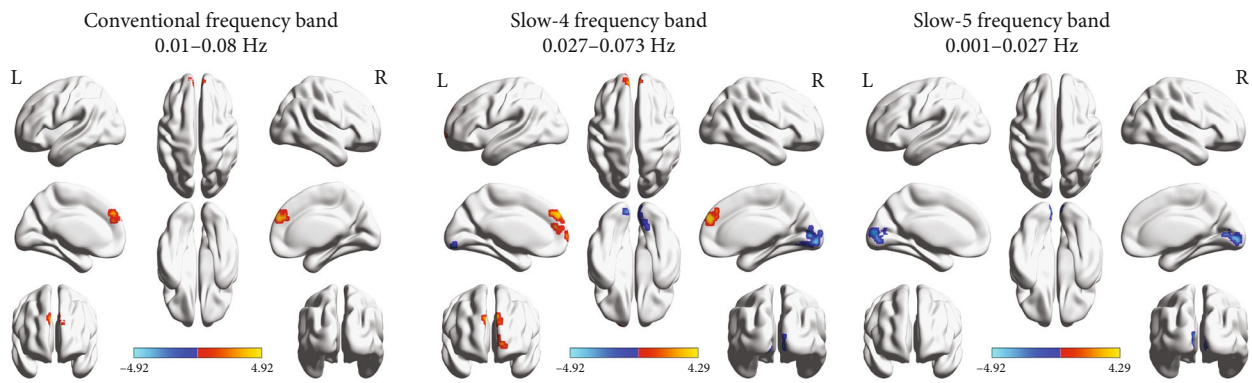

Figure 2: The functional connectivity alterations of the contralesional M1 in the three frequency bands.

Table 3: The functional connectivity alterations of the contralesional M1 in the three frequency bands.

Brain regions (BGIS patients > HCs)	Number of voxels	MNI coordinate			Peak t value
		x	y	z	
Conventional frequency band (0.01-0.08 Hz)					
Frontal_Sup_Medial_R	128	6	54	30	3.9253
Slow-4 frequency band (0.027-0.073 Hz)					
Lingual_R	179	12	-76	-12	-4.733
Frontal_Sup_Medial_L	216	0	48	24	4.6441
Slow-5 frequency band (0.01-0.027 Hz)					
Calcarine_L	137	-3	-96	6	-4.4748

Note: clusters located in the cerebellum are not reported. Lingual_R: right lingual gyrus; Frontal_Sup_Medial_R: right medial superior frontal gyrus; Frontal_Sup_Medial_L: left medial superior frontal gyrus; Calcarine_L: left calcarine sulcus; MNI: Montreal Neurological Institute.

Table 4: The results of a single or combined features in SVM Classification.

Feature	AUC	Accuracy (%)	Sensitivity (%)	Specificity (%)	Precision (%)
Ipsilesional M1					
Conventional	0.82	72.86	57.14	83.33	69.57
Slow-4	0.80	72.86	67.86	76.19	65.52
Slow-5	0.80	77.14	64.29	85.71	75.00
Contralesional M1					
Conventional	0.75	71.43	39.29	92.86	78.57
Slow-4	0.79	72.86	46.43	90.48	76.47
Slow-5	0.73	68.57	64.29	71.43	60.00
Combined					
Conventional	0.82	72.86	57.14	83.33	69.57
Slow-4 +Slow-5	0.86	80.00	60.71	92.86	85.00

0.82. Moreover, the combined features in subfrequency bands (slow-4 and slow-5) had the highest accuracy (80.00%) with an AUC value of 0.86.

4. Discussion

In our study, we explored the FC changes of the bilateral M1s in acute BGIS patients at three frequency bands, and we also adopted a machine learning approach based on SVM to identify the valuable neuroimaging biomarkers classifying the acute BGIS patients and HCs. The main findings of our study are the following. (1) In the conventional frequency band (0.01-0.08 Hz), acute BGIS patients showed significantly altered FC between the ipsilesional M1 and right media superior frontal gyrus (SFGmed) and right lingual gyrus, acute BGIS patients also showed increased FC values between contralesional M1 and the right SFGmed. (2) Changes of FC in patients with acute BGIS showed frequency bands specificity. (3) SVM results showed that features extracted based on the differences in subfrequency bands have the best performance in classification. Our results indicated that the altered FC in acute BGIS patients was frequency-dependent, and frequency-specific FC might provide us with new insights into the neural mechanisms in acute BGIS patients.

The M1 is not only involved in the motor performance and execution but also the planning, preparation, and learning process of the motor [47]. Besides, the M1 is also related to the recovery of motor function in stroke patients [48, 49]. We found significantly increased FC of bilateral M1s with right SFGmed in patients with acute BGIS, which further confirmed the previous conclusions that patients with stroke showed abnormal FC patterns in M1 with other brain regions [22, 50–52]. A previous study similarly found that stroke patients showed significantly increased FC between the ipsilesional M1 and the SFGmed and indicated that the FC changes were associated with motor function changes [28]. In addition, we also found decreased FC between ipsilesional M1 and right lingual gyrus in the acute BGIS patients. Similar to this, Stinear et al. showed that the excitability of ipsilesional M1 was reduced in acute stroke by using transcranial magnetic stimulation (TMS) [53]. Besides, previous evidence using task fMRI showed that efficient long-term motor recovery in stroke patients within the M1 area was related to reorganization within the surrounding motor cortex [54]. Our results further supported the findings

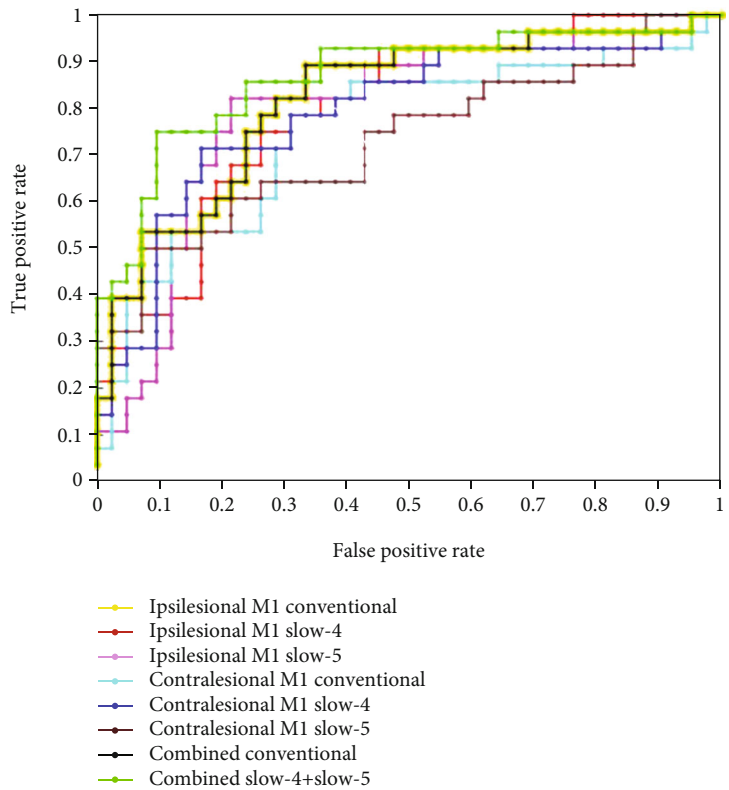

Figure 3: The receiver operating characteristic (ROC) curve in different features. The yellow line with a dot represents the ROC curve of the features in ipsilesional M1 in the conventional frequency band. The red line with a dot represents the ROC curve of the features in ipsilesional M1 in slow-4. The pink line with a dot represents the ROC curve of the features in ipsilesional M1 in slow-5. The cyan line with a dot represents the ROC curve of the features in contralesional M1 in the conventional frequency band. The blue line with a dot represents the ROC curve of the features in contralesional M1in slow-4. The brown line with a dot represents the ROC curve of the features in contralesional M1 in slow-5. The black line with a dot represents the ROC curve of the combined features in the conventional frequency band. The green line with a dot represents the ROC curve of the combined features in subfrequency bands (slow-4+slow-5).

that poststroke patients showed decreased local synchronization in the lingual gyrus and the right medial SFG, and the abnormal local synchronization had a positive correlation with aphasia severity [55]. In summary, the results indicated that the changes of FC between bilateral M1s and right SFGmed and the lingual gyrus might be related to the motor impairment of patients with BGIS.

In subfrequency bands, the FC of bilateral M1 showed frequency band specificity. As for ipsilesional M1, the FC of ipsilesional M1 with right lingual gyrus was more sensitive to the slow-4 than slow-5, whereas the FC of ipsilesional M1 with the right medial SFG and the left lingual gyrus were more sensitive to the slow-5 than slow-4. In terms of the contralesional M1, in the slow-5 band, the left calcarine sulcus showed decreased FC with contralesional M1 between acute BGIS patients and HCs. Hence, the FC of contralesional M1 with left media SFG and right lingual gyrus were more sensitive than the conventional band and the slow-5 band. Our findings were consistent with previous results, which showed that patients with stroke showed frequency-specific pathological characteristics. Zhu et al. demonstrated that abnormal changes in the regional properties of brain activity that occurred in the slow-5 band were more sensitive to the changes in the slow-4 [56]. Besides, the aberrant patterns of local synchronization were different in the slow-4 band and the slow-5 band in stroke patients [57]. These findings suggested that the FC patterns were sensitive to the specific frequency. Many studies have revealed frequency-dependent abnormalities in neurological and psychiatry diseases including autism spectrum disorder [58], schizophrenia [59, 60], and depression [36, 61]. Yu et al. demonstrated that schizophrenia patients showed larger local synchronization in the slow-4 band than in the slow-5 band in the fusiform gyrus, and superior frontal gyrus, whereas larger local synchronization in slow-5 was found in the culmen, parahippocampal gyrus, putamen, and dorsal middle prefrontal gyrus [60]. Besides, a recent study found that patients with bipolar disorder depression had increased functional interactions in the left pre-/postcentral gyrus, left fusiform gyrus (FG), and the left lingual gyrus (LG) in the slow-4 band, whereas patients showed decreased functional interactions in the left LG in the slow-5 band [36]. Previous studies demonstrated that the frequency specificities were widely presented in BOLD fMRI [62, 63]. Moreover, fMRI and electrophysiological studies have demonstrated that brain activities in independent frequency bands are related

to specific properties and physiological functions [64, 65]. Therefore, we highlighted the importance of FC within different frequency bands in patients with acute BGIS.

SVM has been widely used as a diagnostic and predictive aid in the field of clinical disease. SVM results showed that both single feature and combined features in the conventional band had the same classification performance. However, the combined features in subfrequency bands (slow-4 +slow-5) had the highest accuracy (80.00%) with an AUC value of 0.86. It indicated that FC changes in specific frequency bands could provide us with more sensitive information than the conventional frequency band. SVM results demonstrated abnormal FC values in bilateral M1s with the lingual gyrus and the media SFG in different frequency bands, which could be used to distinguish patients with acute BGIS from HCs with satisfactory accuracy, specificity, and sensitivity and precision, and facilitate the establishment of diagnostic indicators. Therefore, we inferred that abnormal FC values in subfrequency bands (slow-4+slow-5) could be used as a potential imaging biomarker to differentiate patients from controls. Previous findings have also revealed fMRI signal in the subfrequency band had a good diagnostic potential for Parkinson's disease and anxiety disorder [66, 67].

Moreover, many studies predefined the bilateral M1 as the target stimulus location of transcranial magnetic stimulation (TMS), which generates a descending volley in the corticospinal pathway, and elicits a motor evoked potential (MEP) in muscles of the contralateral limb [68]. Studies in acute stroke patients indicated that TMS on motor regions can lead to improvements in motor function [68]. One recent study explored frequency-dependent stimulation effects in a combined rTMS–fMRI approach and found that changes in FC strength because of low-frequency rTMS were even detectable 7 days after stimulation [69]. Combined with this result, future researchers might combine TMS technology and frequency-specific FC changes in M1 to help treat and recover for motor deficits in stroke patients. The exploration of the neural mechanisms of motor deficit in acute BGIS patients is necessary and might provide support for future clinical rehabilitation treatment in acute BGIS patients.

Taken together, the current results indicated that patients with acute BGIS showed frequency-specific FC abnormalities, which provided valuable information and neuroimaging biomarkers for exploring the pathological mechanisms of acute BGIS patients.

5. Limitations

Firstly, our study had a relatively small sample size. Therefore, future researchers can explore the changes in the specificity of different frequency bands in a larger sample of patients with acute BGIS. Second, our study focused on the cross-sectional changes between the acute BGIS patients and HCs; future investigators should consider longitudinal frequency-specific changes in the acute BGIS patients.

6. Conclusion

Alterations of FC in acute BGIS patients are frequency-specific, and the specific information can be well detected by the machine learning approach. Our study might provide new insights into the pathophysiology of acute BGIS patients. The frequency-specific FC abnormal brain areas might provide inspiration and assistance for clinical treatment and rehabilitation of stroke patients.

Data Availability

The raw data supporting the conclusions of this article will be made available by the authors, without undue reservation.

Conflicts of Interest

No conflict of interest is declared.

Authors' Contributions

Huayun Li, Zhijian Liang, and Dongqiang Liu conceived and designed the study. Shijian Chen and Jian Zhang performed the experiments and collected materials. Jie Li analyzed the data. Jie Li and Lulu Cheng wrote the first manuscript. All authors read and approved the final manuscript. Jie Li and Lulu Cheng have the same contribution to this work and should be considered co-first authors.

Acknowledgments

We thank all the participants in the study, and we also thank the Department of Neurology, the First Affiliated Hospital of Guangxi Medical University, for the materials and technical support. This study was supported by the Ministry of Education Humanities and Social Sciences Research Youth Fund Project (20YJC740008); the National Key R&D Program of China (No. 2018YFC1311305); the Nanning Qingxiu District Science and Technology Plan (No. 2020043); the Open Research Fund of College of Teacher Education, Zhejiang Normal University (No. jykf20003); and the Scientific Research Project of Department of Education of Liaoning Province (LQ2019031).

Supplementary Materials

Table S1: The time of functional magnetic resonance scanning after stroke. *(Supplementary Materials)*

References

[1] X. Xiang, M. Yu-rong, Z. Jiang-li, L. Le, X. Guang-qing, and H. Dong-feng, "Virtual reality-enhanced body weight-supported treadmill training improved lower limb motor function in patients with cerebral infarction," *Chinese Journal of Tissue Engineering Research*, vol. 18, no. 7, p. 1143, 2014.

[2] P. Wang, C. Zhang, X. Yang et al., "Whole body vibration training improves limb motor dysfunction in stroke patients: lack of evidence," *Chinese Journal of Tissue Engineering Research*, vol. 38, pp. 6205–6209, 2014.

[3] A. K. Boehme, C. Esenwa, and M. S. Elkind, "Stroke risk factors, genetics, and prevention," *Circulation Research*, vol. 120, no. 3, pp. 472–495, 2017.

[4] P. M. Rothwell, "Stroke: more trials, more answers," *The Lancet Neurology.*, vol. 11, no. 1, pp. 2-3, 2012.

[5] M. Traylor, M. Farrall, E. G. Holliday et al., "Genetic risk factors for ischaemic stroke and its subtypes (the METASTROKE Collaboration): a meta-analysis of genome-wide association studies," *The Lancet Neurology*, vol. 11, no. 11, pp. 951–962, 2012.

[6] A. Handley, P. Medcalf, K. Hellier, and D. Dutta, "Movement disorders after stroke," *Age and Ageing*, vol. 38, no. 3, pp. 260–266, 2009.

[7] R. Mehanna and J. Jankovic, "Movement disorders in cerebrovascular disease," *The Lancet Neurology*, vol. 12, no. 6, pp. 597–608, 2013.

[8] H. Liu, X. Peng, L. Dahmani et al., "Patterns of motor recovery and structural neuroplasticity after basal ganglia infarcts," *Neurology*, vol. 95, no. 9, pp. e1174–e1187, 2020.

[9] P. P. Langhorne, P. J. Bernhardt, and G. Kwakkel, "Stroke rehabilitation," *The Lancet*, vol. 377, no. 9778, pp. 1693–1702, 2011.

[10] S. M. Hatem, G. Saussez, M. Della Faille et al., "Rehabilitation of motor function after stroke: a multiple systematic review focused on techniques to stimulate upper extremity recovery," *Frontiers in Human Neuroscience*, vol. 10, p. 442, 2016.

[11] C. M. Stinear, C. E. Lang, S. Zeiler, and W. D. Byblow, "Advances and challenges in stroke rehabilitation," *The Lancet Neurology*, vol. 19, no. 4, pp. 348–360, 2020.

[12] M. D. Fox and M. E. Raichle, "Spontaneous fluctuations in brain activity observed with functional magnetic resonance imaging," *Nature reviews Neuroscience*, vol. 8, no. 9, pp. 700–711, 2007.

[13] M. H. Lee, C. D. Smyser, and J. S. Shimony, "Resting-state fMRI: a review of methods and clinical applications," *American Journal of Neuroradiology*, vol. 34, no. 10, pp. 1866–1872, 2013.

[14] S. Noble, D. Scheinost, and R. T. Constable, "A decade of test-retest reliability of functional connectivity: a systematic review and meta-analysis," *NeuroImage*, vol. 203, article 116157, 2019.

[15] K. J. Friston, C. D. Frith, P. F. Liddle, and R. Frackowiak, "Functional connectivity: the principal-component analysis of large (PET) data sets," *Journal of Cerebral Blood Flow & Metabolism*, vol. 13, no. 1, pp. 5–14, 1993.

[16] C. Grefkes and G. R. Fink, "Reorganization of cerebral networks after stroke: new insights from neuroimaging with connectivity approaches," *Brain*, vol. 134, Part 5, pp. 1264–1276, 2011.

[17] A. Baldassarre, L. Ramsey, C. L. Hacker et al., "Large-scale changes in network interactions as a physiological signature of spatial neglect," *Brain*, vol. 137, Part 12, pp. 3267–3283, 2014.

[18] A. R. Carter, K. R. Patel, S. V. Astafiev et al., "Upstream dysfunction of somatomotor functional connectivity after corticospinal damage in stroke," *Neurorehabilitation and Neural Repair*, vol. 26, no. 1, pp. 7–19, 2012.

[19] B. J. He, A. Z. Snyder, J. L. Vincent, A. Epstein, G. L. Shulman, and M. Corbetta, "Breakdown of functional connectivity in frontoparietal networks underlies behavioral deficits in spatial neglect," *Neuron*, vol. 53, no. 6, pp. 905–918, 2007.

[20] M. A. Urbin, X. Hong, C. E. Lang, and A. R. Carter, "Resting-state functional connectivity and its association with multiple domains of upper-extremity function in chronic stroke," *Neurorehabilitation and Neural Repair*, vol. 28, no. 8, pp. 761–769, 2014.

[21] A. R. Carter, S. V. Astafiev, C. E. Lang et al., "Resting interhemispheric functional magnetic resonance imaging connectivity predicts performance after stroke," *Annals of Neurology*, vol. 67, no. 3, pp. 365–375, 2010.

[22] C. H. Park, W. H. Chang, S. H. Ohn et al., "Longitudinal changes of resting-state functional connectivity during motor recovery after stroke," *Stroke*, vol. 42, no. 5, pp. 1357–1362, 2011.

[23] S. Larivière, N. S. Ward, and M. H. Boudrias, "Disrupted functional network integrity and flexibility after stroke: relation to motor impairments," *NeuroImage Clinical*, vol. 19, pp. 883–891, 2018.

[24] J. Lee, E. Park, A. Lee, W. H. Chang, D. S. Kim, and Y. H. Kim, "Alteration and role of interhemispheric and intrahemispheric connectivity in motor network after stroke," *Brain Topography*, vol. 31, no. 4, pp. 708–719, 2018.

[25] H. Wang, G. Xu, X. Wang et al., "The reorganization of resting-state brain networks associated with motor imagery training in chronic stroke patients," *IEEE Transactions on Neural Systems and Rehabilitation Engineering: A Publication of the IEEE Engineering in Medicine and Biology Society*, vol. 27, no. 10, pp. 2237–2245, 2019.

[26] A. M. Golestani, S. Tymchuk, A. Demchuk, B. G. Goodyear, and VISION-2 Study Group, "Longitudinal evaluation of resting-state FMRI after acute stroke with hemiparesis," *Neurorehabilitation and Neural Repair*, vol. 27, no. 2, pp. 153–163, 2013.

[27] G. Mirzaei and H. Adeli, "Resting state functional magnetic resonance imaging processing techniques in stroke studies," *Reviews in the Neurosciences*, vol. 27, no. 8, pp. 871–885, 2016.

[28] Y. Zhang, H. Liu, L. Wang et al., "Relationship between functional connectivity and motor function assessment in stroke patients with hemiplegia: a resting-state functional MRI study," *Neuroradiology*, vol. 58, no. 5, pp. 503–511, 2016.

[29] I. Frias, F. Starrs, T. Gisiger, J. Minuk, A. Thiel, and C. Paquette, "Interhemispheric connectivity of primary sensory cortex is associated with motor impairment after stroke," *Scientific Reports*, vol. 8, no. 1, article 12601, 2018.

[30] B. Biswal, F. Z. Yetkin, V. M. Haughton, and J. S. Hyde, "Functional connectivity in the motor cortex of resting human brain using echo-planar MRI," *Magnetic Resonance in Medicine*, vol. 34, no. 4, pp. 537–541, 1995.

[31] Z. He, Q. Cui, J. Zheng et al., "Frequency-specific alterations in functional connectivity in treatment- resistant and -sensitive major depressive disorder," *Journal of Psychiatric Research*, vol. 82, pp. 30–39, 2016.

[32] X. Wang, Y. Zhang, Z. Long et al., "Frequency-specific alteration of functional connectivity density in antipsychotic-naive adolescents with early-onset schizophrenia," *Journal of Psychiatric Research*, vol. 95, pp. 68–75, 2017.

[33] G. Buzsáki and A. Draguhn, "Neuronal oscillations in cortical networks," *Science*, vol. 304, no. 5679, pp. 1926–1929, 2004.

[34] X. N. Zuo, A. Di Martino, C. Kelly et al., "The oscillating brain: complex and reliable," *NeuroImage*, vol. 49, no. 2, pp. 1432–1445, 2010.

[35] A. T. Baria, M. N. Baliki, T. Parrish, and A. V. Apkarian, "Anatomical and functional assemblies of brain BOLD oscillations," *The Journal of Neuroscience: The Official Journal of the Society for Neuroscience*, vol. 31, no. 21, pp. 7910–7919, 2011.

[36] Y. Yang, Q. Cui, Y. Pang et al., "Frequency-specific alteration of functional connectivity density in bipolar disorder depression," *Progress in Neuro-Psychopharmacology & Biological Psychiatry*, vol. 104, article 110026, 2021.

[37] S. M. Goldstein, R. G. Curless, M. J. D. Post, and R. M. Quencer, "A new sign of neurofibromatosis on magnetic resonance imaging of children," *Archives of Neurology*, vol. 46, no. 11, pp. 1222–1224, 1989.

[38] A. R. Fugl-Meyer, L. Jääskö, I. Leyman, S. Olsson, and S. Steglind, "The post-stroke hemiplegic patient. 1. A method for evaluation of physical performance," *Scandinavian Journal of Rehabilitation Medicine*, vol. 7, no. 1, pp. 13–31, 1975.

[39] X.-Z. Jia, J. Wang, H.-Y. Sun et al., "RESTplus: an improved toolkit for resting-state functional magnetic resonance imaging data processing," *Science Bulletin*, vol. 64, no. 14, pp. 953-954, 2019.

[40] K. J. Friston, S. Williams, R. Howard, R. S. Frackowiak, and R. Turner, "Movement-related effects in fMRI time-series," *Magnetic Resonance in Medicine*, vol. 35, no. 3, pp. 346–355, 1996.

[41] X. Chen, B. Lu, and C. G. Yan, "Reproducibility of R-fMRI metrics on the impact of different strategies for multiple comparison correction and sample sizes," *Human Brain Mapping*, vol. 39, no. 1, pp. 300–318, 2018.

[42] M. D. Fox, D. Zhang, A. Z. Snyder, and M. E. Raichle, "The global signal and observed anticorrelated resting state brain networks," *Journal of Neurophysiology*, vol. 101, no. 6, pp. 3270–3283, 2009.

[43] J. Liu, W. Qin, J. Zhang, X. Zhang, and C. Yu, "Enhanced interhemispheric functional connectivity compensates for anatomical connection damages in subcortical stroke," *Stroke*, vol. 46, no. 4, pp. 1045–1051, 2015.

[44] C.-C. Chang and C.-J. Lin, "LIBSVM: a library for support vector machines," *ACM transactions on intelligent systems and technology (TIST)*, vol. 2, no. 3, pp. 1–27, 2011.

[45] F. Pereira, T. Mitchell, and M. Botvinick, "Machine learning classifiers and fMRI: a tutorial overview," *NeuroImage*, vol. 45, Supplement 1, pp. S199–S209, 2009.

[46] J. A. Hanley and B. J. J. R. McNeil, "The meaning and use of the area under a receiver operating characteristic (ROC) curve," *Radiology*, vol. 143, no. 1, pp. 29–36, 1982.

[47] K. Shindo, K. Kawashima, J. Ushiba et al., "Effects of neurofeedback training with an electroencephalogram-based brain-computer interface for hand paralysis in patients with chronic stroke: a preliminary case series study," *Journal of Rehabilitation Medicine*, vol. 43, no. 10, pp. 951–957, 2011.

[48] J. Liepert, C. Restemeyer, T. Kucinski, S. Zittel, and C. Weiller, "Motor strokes: the lesion location determines motor excitability changes," *Stroke*, vol. 36, no. 12, pp. 2648–2653, 2005.

[49] B. M. Young, Z. Nigogosyan, L. M. Walton et al., "Changes in functional brain organization and behavioral correlations after rehabilitative therapy using a brain-computer interface," *Frontiers in Neuroengineering*, vol. 7, p. 26, 2014.

[50] D. Yin, F. Song, D. Xu et al., "Patterns in cortical connectivity for determining outcomes in hand function after subcortical stroke," *PLoS One*, vol. 7, no. 12, article e52727, 2012.

[51] S. R. Almeida, J. Vicentini, L. Bonilha, B. M. De Campos, R. F. Casseb, and L. L. Min, "Brain connectivity and functional recovery in patients with ischemic stroke," *Journal of Neuroimaging*, vol. 27, no. 1, pp. 65–70, 2017.

[52] J. Chen, D. Sun, Y. Shi et al., "Alterations of static functional connectivity and dynamic functional connectivity in motor execution regions after stroke," *Neuroscience Letters*, vol. 686, pp. 112–121, 2018.

[53] C. Stinear, S. Ackerley, and W. Byblow, "Rehabilitation is initiated early after stroke, but most motor rehabilitation trials are not: a systematic review," *Stroke*, vol. 44, no. 7, pp. 2039–2045, 2013.

[54] A. Jaillard, C. D. Martin, K. Garambois, J. F. Lebas, and M. Hommel, "Vicarious function within the human primary motor cortex? A longitudinal fMRI stroke study," *Brain*, vol. 128, no. 5, pp. 1122–1138, 2005.

[55] M. Yang, J. Li, D. Yao, and H. Chen, "Disrupted intrinsic local synchronization in poststroke aphasia," *Medicine*, vol. 95, no. 11, article e3101, 2016.

[56] J. Zhu, Y. Jin, K. Wang et al., "Frequency-dependent changes in the regional amplitude and synchronization of resting-state functional MRI in stroke," *PLoS One*, vol. 10, no. 4, article e0123850, 2015.

[57] Z. Zhao, C. Tang, D. Yin et al., "Frequency-specific alterations of regional homogeneity in subcortical stroke patients with different outcomes in hand function," *Human Brain Mapping*, vol. 39, no. 11, pp. 4373–4384, 2018.

[58] H. Chen, X. Duan, F. Liu et al., "Multivariate classification of autism spectrum disorder using frequency-specific resting-state functional connectivity–a multi-center study," *Progress in Neuro-Psychopharmacology & Biological Psychiatry*, vol. 64, pp. 1–9, 2016.

[59] Y. Zhang, R. Yang, and X. Cai, "Frequency-specific alternations in the moment-to-moment BOLD signals variability in schizophrenia," *Brain Imaging and Behavior*, vol. 15, no. 1, pp. 68–75, 2021.

[60] R. Yu, M. H. Hsieh, H. L. Wang et al., "Frequency dependent alterations in regional homogeneity of baseline brain activity in schizophrenia," *PLoS One*, vol. 8, no. 3, article e57516, 2013.

[61] D. Russo, M. Martino, P. Magioncalda, M. Inglese, M. Amore, and G. Northoff, "Opposing changes in the functional architecture of large-scale networks in bipolar mania and depression," *Schizophrenia Bulletin*, vol. 46, no. 4, pp. 971–980, 2020.

[62] X. Song, Y. Zhang, and Y. Liu, "Frequency specificity of regional homogeneity in the resting-state human brain," *PLoS One*, vol. 9, no. 1, article e86818, 2014.

[63] L. Qian, Y. Zhang, L. Zheng, Y. Shang, J. H. Gao, and Y. Liu, "Frequency dependent topological patterns of resting-state brain networks," *PLoS One*, vol. 10, no. 4, article e0124681, 2015.

[64] R. K. Niazy, J. Xie, K. Miller, C. F. Beckmann, and S. M. Smith, "Spectral characteristics of resting state networks," *Progress in Brain Research*, vol. 193, pp. 259–276, 2011.

[65] M. Siegel, T. H. Donner, and A. K. Engel, "Spectral fingerprints of large-scale neuronal interactions," *Nature Reviews Neuroscience*, vol. 13, no. 2, pp. 121–134, 2012.

[66] Z. Zhang, M. Liao, Z. Yao et al., "Frequency-specific functional connectivity density as an effective biomarker for adolescent generalized anxiety disorder," *Frontiers in Human Neuroscience*, vol. 11, p. 549, 2017.

[67] Z. Y. Tian, L. Qian, L. Fang et al., "Frequency-specific changes of resting brain activity in Parkinson's disease: a machine learning approach," *Neuroscience*, vol. 436, pp. 170–183, 2020.

[68] E. H. Hoyer and P. A. Celnik, "Understanding and enhancing motor recovery after stroke using transcranial magnetic stimulation," *Restorative Neurology and Neuroscience*, vol. 29, no. 6, pp. 395–409, 2011.

[69] H. Zhang, N. Sollmann, G. Castrillon et al., "Intranetwork and internetwork effects of navigated transcranial magnetic stimulation using low- and high-frequency pulse application to the dorsolateral prefrontal cortex: a combined rTMS-fMRI approach," *Journal of Clinical Neurophysiology*, vol. 37, no. 2, pp. 131–139, 2020.

Hindawi
Neural Plasticity
Volume 2022, Article ID 1295908, 15 pages
https://doi.org/10.1155/2022/1295908

Research Article

The Effects of the Biceps Brachii and Brachioradialis on Elbow Flexor Muscle Strength and Spasticity in Stroke Patients

Binbin Yu, Xintong Zhang, Yihui Cheng, Lingling Liu, YanJiang, Jiayue Wang, and Xiao Lu

Department of Rehabilitation Medicine, The First Affiliated Hospital of Nanjing Medical University, Jiangsu, China

Correspondence should be addressed to Xiao Lu; luxiao1972@163.com

Received 4 November 2021; Revised 27 December 2021; Accepted 11 January 2022; Published 2 March 2022

Academic Editor: Xi-Ze Jia

Objective. Muscle weakness and spasticity are common consequences of stroke, leading to a decrease in physical activity. The effective implementation of precision rehabilitation requires detailed rehabilitation evaluation. We aimed to analyze the surface electromyography (sEMG) signal features of elbow flexor muscle (biceps brachii and brachioradialis) spasticity in maximum voluntary isometric contraction (MVIC) and fast passive extension (FPE) in stroke patients and to explore the main muscle groups that affect the active movement and spasticity of the elbow flexor muscles to provide an objective reference for optimizing stroke rehabilitation. *Methods*. Fifteen patients with elbow flexor spasticity after stroke were enrolled in this study. sEMG signals of the paretic and nonparetic elbow flexor muscles (biceps and brachioradialis) were detected during MVIC and FPE, and root mean square (RMS) values were calculated. The RMS values (mean and peak) of the biceps and brachioradialis were compared between the paretic and nonparetic sides. Additionally, the correlation between the manual muscle test (MMT) score and the RMS values (mean and peak) of the paretic elbow flexors during MVIC was analyzed, and the correlation between the modified Ashworth scale (MAS) score and the RMS values (mean and peak) of the paretic elbow flexors during FPE was analyzed. *Results*. During MVIC exercise, the RMS values (mean and peak) of the biceps and brachioradialis on the paretic side were significantly lower than those on the nonparetic side ($p < 0.01$), and the RMS values (mean and peak) of the bilateral biceps were significantly higher than those of the brachioradialis ($p < 0.01$). The MMT score was positively correlated with the mean and peak RMS values of the paretic biceps and brachioradialis ($r = 0.89$, $r = 0.91$, $r = 0.82$, $r = 0.85$; $p < 0.001$). During FPE exercise, the RMS values (mean and peak) of the biceps and brachioradialis on the paretic side were significantly higher than those on the nonparetic side ($p < 0.01$), and the RMS values (mean and peak) of the brachioradialis on the paretic side were significantly higher than those of the biceps ($p < 0.01$). TheMAS score was positively correlated with the mean RMS of the paretic biceps and brachioradialis ($r = 0.62$, $p = 0.021$; $r = 0.74$, $p = 0.004$), and the MAS score was positively correlated with the peak RMS of the paretic brachioradialis ($r = 0.59$, $p = 0.029$) but had no significant correlation with the peak RMS of the paretic biceps ($r = 0.49$, $p > 0.05$). *Conclusions*. The results confirm that the biceps is a vital muscle in active elbow flexion and that the brachioradialis plays an important role in elbow flexor spasticity, suggesting that the biceps should be the focus of muscle strength training of the elbow flexors and that the role of the brachioradialis should not be ignored in the treatment of elbow flexor spasticity. This study also confirmed the application value of sEMG in the objective assessment of individual muscle strength and spasticity in stroke patients.

1. Introduction

Stroke is a destructive neurological disease with high morbidity, disability, and mortality. It is the second leading cause of death and the leading cause of disability in the world [1, 2]. Approximately two-thirds of stroke survivors exhibit moderate to severe motor dysfunction, mainly manifesting as muscle weakness, spasticity, and coordination disorder, which greatly affects the quality of life of the patient [3]. Early effective rehabilitation training can greatly promote the functional recovery of patients, and the formulation of precise rehabilitation training programs depends on a

detailed rehabilitation assessment. The current clinical rehabilitation assessment of muscle strength mainly involves a manual muscle test (MMT). This method is simple and convenient but also subjective. More importantly, an MMT can evaluate only the overall strength of a group of muscles and is not accurate for a single muscle [4]. Commonly used assessment methods of spasticity are clinical scales, including the modified Ashworth scale (MAS), the clinical spasticity index (CSI), and the Tardieu scale (TS); of these scales, the MAS is the most widely used [5]. These methods are relatively mature in terms of testing procedures, but the results are subjective and difficult to accurately quantify due mainly to the tester's qualitative or semiquantitative evaluation of muscle tension [6, 7]. More importantly, these evaluation methods cannot be subdivided into specific muscles. Taking the elbow flexor muscles as an example, the MAS can only assess the overall muscle tension of the elbow flexor muscles and cannot assess the muscle tension of the biceps and brachioradialis individually. Thus, an important issue to be solved in the clinical rehabilitation of stroke is how to more objectively assess the strength and tension of individual muscles and more precisely analyze the dysfunction of stroke survivors.

Surface electromyography (sEMG) analyzes the bioelectric signals generated during various voluntary and involuntary movements of the neuromuscular system and is performed by guiding, amplifying, recording, and displaying the signals on the skin surface of the detected muscle through surface electrodes. In recent years, as an objective indicator of muscle strength and functional status assessment, sEMG has been widely used in clinical research in the field of neurorehabilitation. For example, Vinstrup et al. measured the sEMG activity of lower limb muscles and confirmed that bodyweight exercises can effectively activate most of the lower limb muscles of stroke patients [8]. Zanin et al. also used sEMG to evaluate the changes in the muscle strength of the wrist flexor muscles before and after acupuncture in stroke patients to verify the treatment effect [9]. In the case of effective control of the interference of measurement factors, the changes in sEMG signals can more objectively reflect the state of muscle function, muscle strength, and coordination of multiple muscle groups. The root mean square (RMS) is the most commonly used and reliable sEMG time-domain analysis index. The RMS value is determined by the change in the sEMG signal amplitude and reflects the change in the muscle contraction intensity. During voluntary exercise, the RMS value reflects changes in muscle strength, while during passive exercise, the RMS value may reflect the degree of muscle tension [10, 11]. Currently, sEMG is used mainly as an objective indicator of muscle strength in many clinical studies. Some studies have tried to adopt sEMG parameters for evaluating muscle spasms after stroke. The cocontraction index (CCI), which was calculated from raw sEMG data, was used to reflect the level of isolated movement across joints and the degree of muscle spasticity [12]. Therefore, one limitation of these previous studies is that they did not directly use sEMG parameters, such as the RMS, to measure spasms in individual muscles in stroke patients.

Previous studies have shown that sEMG can reflect the recruitment of motor units during muscle contraction by estimating the conduction velocity of muscle fibers, thereby objectively evaluating muscle strength [13, 14]. Muscle strength refers to the force of active muscle contraction, and muscle tension is essentially a kind of stretch reflex, which is the reflexive contraction of muscles in the process of passive stretching. Therefore, we reasonably infer that the changes in muscle contraction intensity during passive stretching detected by sEMG can also reflect muscle tension. Rudroff et al. simultaneously used intramuscular electromyography (EMG) and sEMG to record the EMG signal amplitude of the elbow flexor muscles during a submaximal isometric contraction and measured the muscle architecture through ultrasound [15]. It was found that the amplitude recorded by sEMG of the biceps and brachioradialis increased at a faster rate than that recorded by intramuscular EMG at different depths. This indicates that sEMG is more effective than intramuscular EMG in reflecting the overall function of the detected muscle group. Caufriez et al. analyzed the role of the brachioradialis in elbow flexion by sEMG and found that the electromyographic activity of the brachioradialis was much higher during maximum isometric contraction than during maximal voluntary contraction, especially under forearm supination [16]. The above studies have indicated that sEMG can objectively and quantitatively assess the muscle strength of stroke patients and demonstrate its potential for assessing muscle tone, revealing the important role of the brachioradialis in active elbow flexion. However, none of these studies combined muscle strength and muscle tension to comprehensively analyze the influence of the biceps and brachioradialis on elbow flexor activity.

Previous studies have demonstrated that the RMS value representing the amplitude of the EMG signal is correlated with the stretch reflex threshold, suggesting the application prospects of sEMG in the assessment of spasticity [17]. Pandyan et al. used sEMG and the MAS to quantify the clinical efficacy of botulinum toxin in treating elbow flexor spasticity [18]. The results showed that spasticity measured by elbow flexor (biceps) sEMG activity was significantly reduced compared with that before the injection, but the MAS failed to detect this improvement. This suggests that compared with the MAS assessment, sEMG may have higher sensitivity and accuracy in the assessment of spasticity. However, researchers detected the sEMG activity of only the biceps to evaluate elbow flexor spasticity, but the brachioradialis is also an important component of elbow flexion. The contribution of the brachioradialis in the active movement of elbow flexionsuggests that the brachioradialis may also play an important role in elbow flexor spasticity, which is worthy of further research for verification [16].

In this study, we aimed to compare the sEMG activity of the biceps and brachioradialis during maximum voluntary isometriccontraction (MVIC) and fast passive extension (FPE) in stroke patients, analyze the sEMG characteristics of the important muscles that cause elbow flexor weakness and spasticity, and provide a quantitative estimation method for muscle strength and spasticity in stroke patients. We also

analyzed the correlation between elbow flexor sEMG activity measured during MVIC exercises and the MMT evaluation results and the correlation between elbow flexor sEMG activity measured during FPE exercises and the MAS assessment results to explore the potential associations between them.

2. Materials and Methods

2.1. Study Design and Subjects. This study was conducted at the First Affiliated Hospital of Nanjing Medical University from 01 September 2021 to 20 October 2021. The protocol was approved by the Committee of Institutional Ethics (Institutional Review Board, 2021-SR-448) and registered at the Chinese Clinical Trial Registry (ChiCTR2100051880). Written informed consent was required from all subjects and could be provided by proxies for those unable to sign due to severe motor dysfunction.

The inclusion criteria were as follows: (1) age 18-80 years; (2) ischemic or hemorrhagic stroke confirmed with computed tomography (CT) or magnetic resonance imaging (MRI); (3) first-ever episode of hemispheric stroke and post-stroke duration > 2 months; (4) unilateral movement impairment; (5) impairment of upper limb (elbow flexors) function, namely, an MMT score of at least 2 and an MAS score of 2 or 3; (6) normal weight, 18.5 ≤ body mass index (BMI) < 24; (7) able to verbally respond to instructions; and (8) stable vital signs (systolic blood pressure of 90-140 mmHg, heart rate of 50-100/min, body temperature < 37.5°C, and blood oxygen saturation > 95%). Patients were excluded if (1) they had contracture of the elbow joint; (2) their condition was complicated with inflammation, pain, osteoarthrosis, or recent injury of an upper extremity; (3) they had other neurological, hematological system, cardiovascular, metabolic, or chronic hepatorenal diseases, a tumor or were pregnant; (4) they had severe cognitive or mental dysfunction; or (5) they were currently enrolled in another trial or participated in a clinical trial within 6 months.

2.2. Experimental Procedure. The sEMG signals were sampled using the FlexComp Infiniti system (Model SA7550, Thought Technology, Montreal, QC, Canada, 2048 Hz), which is a 10-channel multimodality encoder for real-time computerized physiological, biofeedback, and data acquisition. Disposable electrodes (Kendall, Medtronic, Minneapolis, MN, USA) were used for all sEMG recordings. Measurement was performed following the recommendations of the SENIAM project (Surface EMG for Non-Invasive Assessment of Muscles) [19]. All tests for all subjects were carried out at the same time of day in the same dedicated room at 22-28°C by a full-time inspector. Before sEMG recording, elbow flexor muscle tension was assessed with the MAS, and muscle strength was assessed with the MMT. Prior to the MMT assessment, subjects underwent 10 minutes of elbow flexor stretching on the paretic side to minimize the impact of elbow flexor spasm on the MMT assessment. BMI values were calculated to ensure that every subject met our inclusion criteria. The central skin surface of the biceps and brachioradialis belly was prepared and cleaned carefully with 75% alcohol. Then, an electrode plate (containing two detection electrodes 2 cm apart) was placed parallel to the muscle fiber orientation, and the electrodes were attached on the skin surface of the test muscle with bandages. The biceps surface electrode was placed on the line between the medial acromion and the fossa cubit 1/3 away from the fossa cubit, while the brachioradialis surface electrode was placed on the lateral side of the forearm 4 cm from the lateral epicondyle. The reference electrode was placed on the lateral epicondyle of the humerus (SENIAM recommendations, Figure 1) [19].

The following group of movements was completed by each subject: (1) MVIC of the nonparetic elbow flexors for 5 seconds, (2) MVIC of the paretic elbow flexors for 5 seconds, (3) FPE of the nonparetic elbow flexors conducted by assessors, and (4) FPE of the paretic elbow flexors conducted by assessors. The subjects rested for 10 minutes between each exercise session to ensure adequate relaxation before moving on to the next group of exercises. Before MVIC exercise, the inspector performed 10-minute stretch training on the paretic elbow flexor of the subject to reduce the influence of muscle spasm on isometric contraction in elbow flexion. During MVIC, each subject was required to sit with the shoulder slightly flexed, forearm supinated, wrist in a neutral position, and elbow placed at 45° of flexion. The inspector fixed the elbow with one hand and applied resistance to the wrist with the other hand. The subjects were instructed to flex their elbow with maximum strength against the resistance of the inspector and sustain the position for 5 seconds. This was repeated three times at an interval of 60 seconds. The maximal values from the three repetitions were taken as the MVIC. During FPE, each subject was instructed to maintain the sitting position with the shoulder and elbow both in a neutral position and forearm supinated, which made it easier to achieve a relaxed state. Our inspectors fixed the elbow with one hand and held the wrist with the other to assist the subject in completing fast passive elbow extension within 1 second. Since a spasm is characterized by a velocity-dependent hypertonic stretch reflex, we set the fast draft time to less than 1 second. This was repeated three times at an interval of 60 seconds. The maximal values from the three repetitions were taken as the FPE measurement. The subjects were allowed to practice in advance to ensure that all the participants could understand and cooperate with the MVIC and FPE measurements.

2.3. Data Preprocess. The EMG data were sampled at 2048 Hz. The sEMG signals during MVIC and FPE of the paretic and nonparetic elbow flexors were entered into a computer and analyzed using BioNeuro Infiniti Version 5.0 software (Thought Technology Ltd., Montreal West, QC, Canada). The raw EMG signals were rectified by calculating the RMS value using the following formula:

$$\mathrm{RMS} = \sqrt{\left(\overset{t}{\underset{t}{\int}}{}^{t+T} EMG^2(t)dt/T\right)}. \quad (1)$$

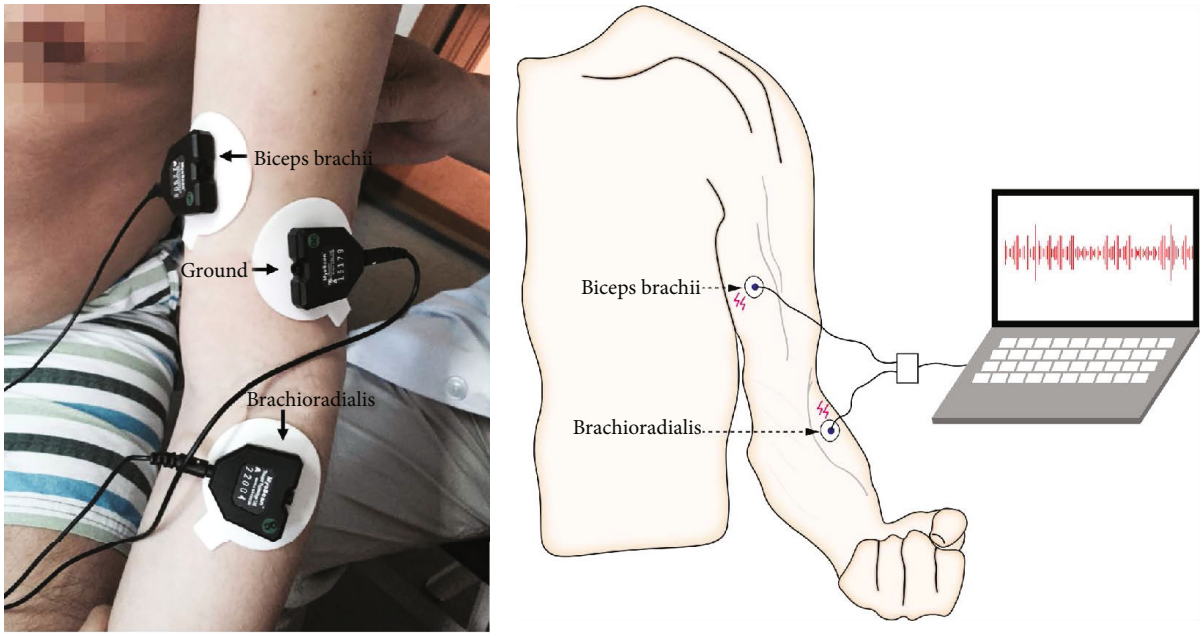

(a) (b)

Figure 1: Position of the electrodes on the left upper limb. (a) Electrode locations for the subjects in test. (b) Schematic drawing of electrode positions.

The mean and peak values of the RMS were selected for the analysis. The RMS value of the EMG signals was used to express the muscle activation intensity. During MVIC, a higher RMS value represented the recruitment of more motor units and better muscle strength [9]. We compared the recruitment of motor units between the paretic and nonparetic elbow flexors (biceps and brachioradialis) by analyzing the RMS values during MVIC. Additionally, we analyzed the main muscle groups on the paretic side related to the elbow flexor muscle strength by comparing the RMS values of the biceps and brachioradialis during MVIC. Finally, we analyzed the correlation between the RMS value of the elbow flexors collected during MVIC and the MMT score of the elbow flexor on the paretic side. During FPE, a larger RMS value represented more apparent muscle tension and higher spasticity of the muscle groups [6, 20]. We first compared spasms of the paretic and nonparetic elbow flexors by analyzing the RMS values during FPE. Additionally, we analyzed the contribution of the biceps and brachioradialis to elbow flexor spasticity by comparing the RMS values of the biceps and brachioradialis during FPE. Finally, we analyzed the correlation between the RMS value of the elbow flexors collected during FPE and the MAS score of the elbow flexor on the paretic side.

2.4. Statistical Analysis. An equivalence test of mean and standard deviation using one-sided tests on data from a parallel-group design achieved sample size of 14 per group upon 82% power at a 5% significance level when the true difference between the means was 15.00 (estimated based on our pilot results) and the standard deviation of 10.00 (equivalence limits of -25.00 and 25.00). Therefore, we set the final sample size of 15 per group in the current study.

All statistical analyses were performed with SPSS software 25.0 (Chicago, USA). EMG data were analyzed using BioNeuro Infiniti Version 5.0 software. The mean and peak RMS values during MVIC or FPE of the biceps and brachioradialis with the paretic and nonparetic sides were normally distributed and satisfied homogeneity of variance. Continuous variables are presented as the means and standard deviations. Categorical variables are presented as numbers and percentages. The differences in the RMS values of the elbow flexor muscles on the paretic and nonparetic sides and the RMS values of the homolateral biceps and brachioradialiswere compared using a two-tailed paired sample t test. The multiclassification MAS and MMT scores were assigned according to order. The MAS had possible scores of 0, 1, 1+, 2, 3, and 4, and a score of 0-5 was assigned. The MMT scores were divided into 6 grades (ranging from 0-5), and a score of 0-5 was assigned. Correlations between the RMS value and the MMT score of the paretic elbow flexor muscles during the MVIC exercise were estimated with the Spearman correlation analysis. Differences between groups were considered significant when p values were less than 0.05.

3. Results

In this study, we enrolled a total of 15 chronic poststroke hemiplegic patients (aged 50.93 ± 11.98, 10 males and 5 females) with different degrees of elbow flexor spasticity (MAS = 2, 3)from outpatient clinic (Table 1). Nine patients had experienced an ischemic stroke, and six had experienced an intraparenchymal hemorrhagic stroke. The poststroke duration ranged from 2 to 16 months, and the average disease duration was 7 months. There were more subjects with hemiparesis of the left side ($n = 11$, 73.3%). Because

Table 1: Subject demographic information.

Patient No.	Age (years)	Gender	Duration of stroke (months)	Side of hemiparesis (left/right)	Type of stroke	BMI	MMT	MAS
1	40	Female	6	Left	Ischemic	23.24	2	2
2	61	Male	3	Right	Hemorrhagic	23.67	3	3
3	43	Male	10	Left	Hemorrhagic	23.26	3	3
4	56	Female	15	Left	Ischemic	21.37	3	2
5	42	Female	6	Left	Hemorrhagic	22.64	2	3
6	65	Male	6	Left	Ischemic	23.18	3	3
7	39	Male	3	Left	Ischemic	23.81	4	2
8	29	Male	2	Left	Hemorrhagic	23.78	3	2
9	62	Female	8	Left	Ischemic	20.40	3	2
10	63	Male	11	Left	Ischemic	22.94	4	2
11	35	Female	3	Left	Ischemic	23.51	2	3
12	61	Male	8	Left	Ischemic	20.72	2	2
13	53	Male	16	Right	Hemorrhagic	20.98	4	3
14	64	Male	7	Right	Ischemic	23.38	3	2
15	51	Male	4	Right	Hemorrhagic	23.78	4	3

BMI: body mass index; MMT: manual muscle test; MAS: modified Ashworth scale.

subcutaneous fat layer thickening could indeed influence the sEMG signal, the BMI values of the 15 patients were estimated. The results showed that there were no abnormal BMI values and that the mean BMI of the patients was 22.71. All patients completed the study. After processing the raw EMG signals of the biceps and the brachioradialis during MVIC or FPE, the RMS value was computed. Figure 2 shows the raw EMG signals and RMS values of the paretic biceps and brachioradialis during MVIC and FPE from one subject selected randomly from the 15 subjects.

3.1. sEMG Comparative Analysis. To analyze the effects of the biceps and brachioradialis during MVIC, the sEMG signals of the elbow flexor muscles (the biceps and brachioradialis) on the paretic side were compared with those on the nonparetic side. To distinguish between the biceps and the brachioradialis, the sEMG signals of those muscles were also compared. The results showed that the RMS values during MVIC of the biceps (mean RMS: 84.70 ± 37.93; peak RMS: 141.65 ± 65.69) and brachioradialis (mean RMS: 48.82 ± 28.33; peak RMS: 77.92 ± 43.34) were significantly lower on the paretic side than on the nonparetic side ($p < 0.001$). Meanwhile, compared with those of the brachioradialis, the mean and peak RMS values of the biceps were significantly higher ($p = 0.007$) (Figure 3).

To gain insight into the role of the biceps and brachioradialis in elbow flexor spasticity, the sEMG signals of the elbow flexor muscles (the biceps and brachioradialis) on the paretic side during FPE were compared with those on the nonparetic side. To further characterize the effect of the biceps and brachioradialis, a comparison of the sEMG signals of those two muscles was performed. The results showed that the RMS values during FPE of the biceps (mean RMS: 27.01 ± 8.57; peak RMS: 48.79 ± 15.35) and brachioradialis (mean RMS: 42.96 ± 16.06; peak RMS: 86.82 ± 43.02) on the paretic side were significantly higher than those on the nonparetic side ($p < 0.001$). Moreover, compared with those of the biceps on the paretic side, the mean and peak RMS values of the brachioradialis were significantly higher ($p = 0.003$) (Figure 4).

3.2. Correlation between sEMG Values and Elbow Flexor Muscle Strength. The correlations between the mean and peak RMS values of the paretic biceps and brachioradialis during MVIC and the MMT score and the elbow flexor muscle strength are shown in Figures 5(a), 5(b), 5(e), and 5(f). Statistically significant correlations were detected between the mean RMS value of the paretic biceps during MVIC and elbow flexor muscle strength ($r = 0.89$, $p < 0.001$), the peak RMS value of the paretic biceps muscle during MVIC and elbow flexor muscle strength ($r = 0.91$, $p < 0.001$), the mean RMS value of the paretic brachioradialis during MVIC and elbow flexor muscle strength ($r = 0.82$, $p < 0.001$), and the peak RMS value of the paretic brachioradialis during MVIC and elbow flexor muscle strength ($r = 0.85$, $p < 0.001$).

Five prespecified subgroup analyses (sex, age, stroke type, poststroke duration, and hemiparetic side (left/right)) were carried out. The results showed that the mean RMS value of the paretic biceps muscle during MVIC was associated with elbow flexor muscle strength in males, those aged no more than 60 years, those with a poststroke duration of less than 6 months, and those with hemiparesis on the left side (Figure 5(c)). Meanwhile, the peak RMS value of the paretic biceps muscle during MVIC was associated with elbow flexor muscle strength in male patients, those aged no more than 60 years, those with ischemic stroke, and those with a poststroke duration of less than 6 months (Figure 5(d)). Moreover, the mean RMS value of the paretic brachioradialis during MVIC was associated with elbow flexor muscle strength in male patients, those with ischemic

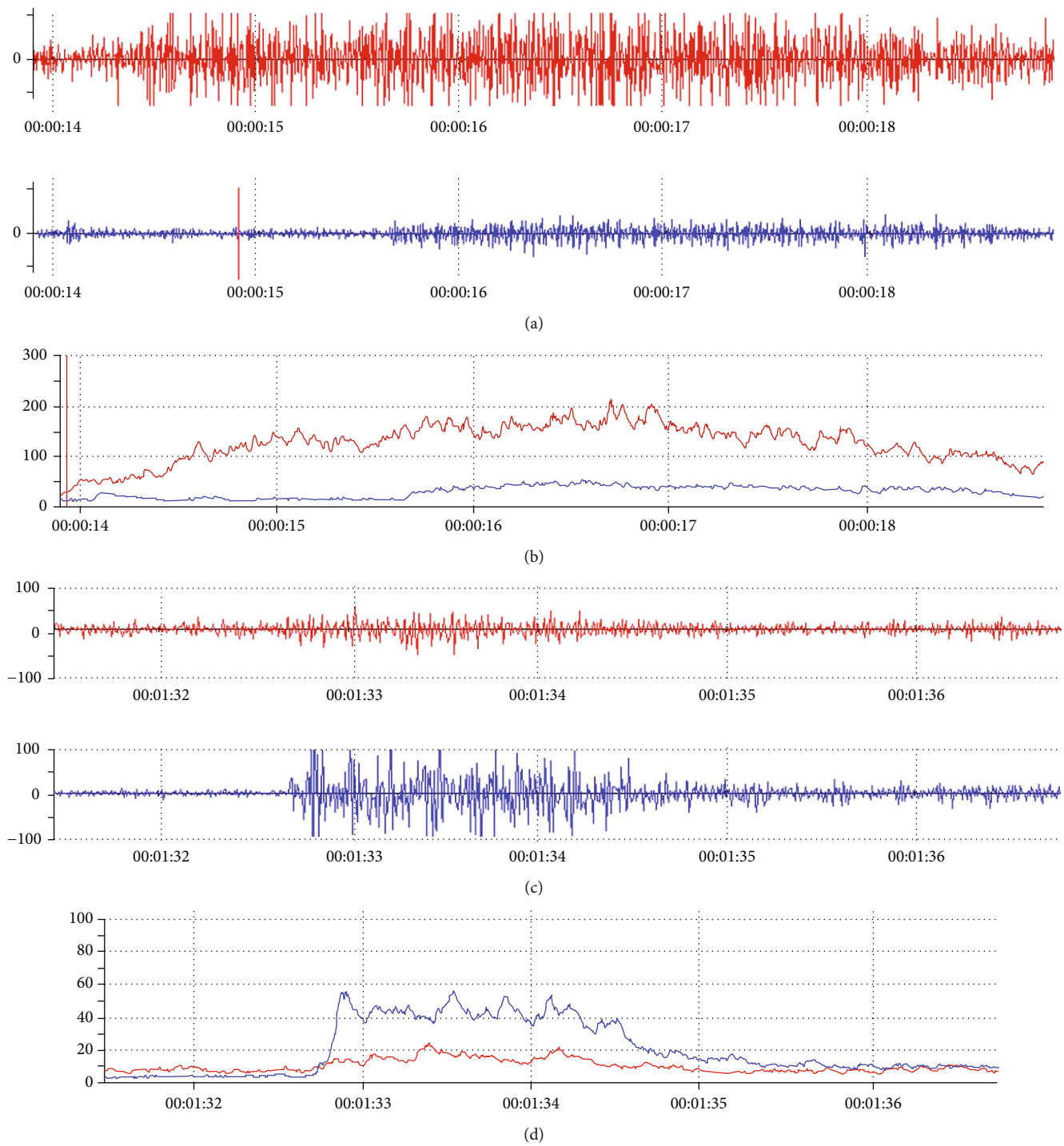

Figure 2: Raw sEMG signals and RMS values of the biceps and brachioradialis during MVIC and FPE on the paretic side. (a) Raw sEMG signals of the biceps brachii and brachioradialis during MVIC. (b) RMS values of the biceps brachii and brachioradialis during MVIC. (c) Raw sEMG signals of the biceps brachii and brachioradialis during FPE. (d) RMS values of the biceps brachii and brachioradialis during FPE. sEMG: surface electromyography. MVIC: maximum voluntary isometriccontraction; FPE: fast passive extension; RMS: root mean square. (red: biceps brachii; blue: brachioradialis).

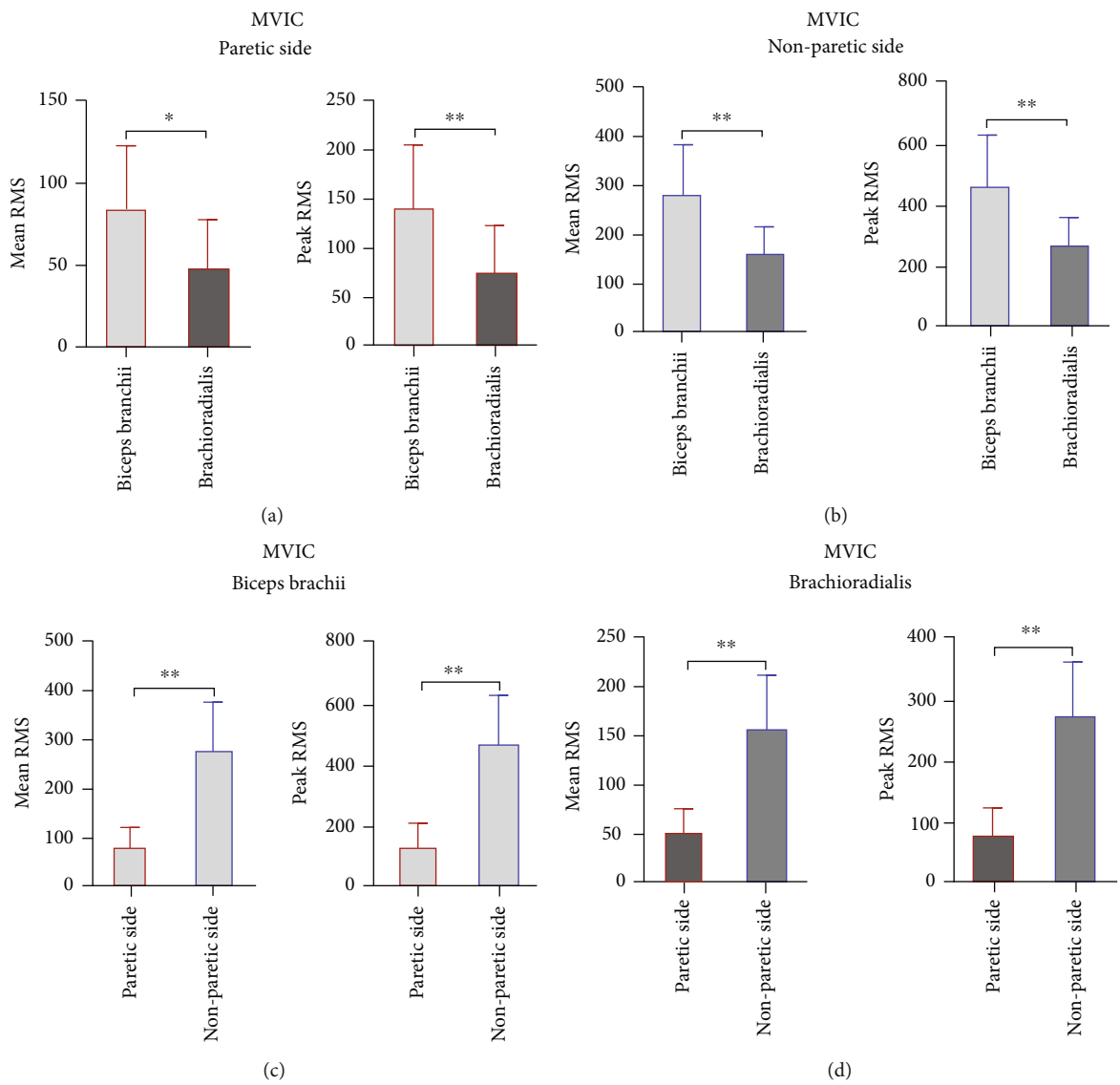

Figure 3: sEMG signals of the elbow flexor muscles (the biceps brachii and brachioradialis) during MVIC. (a) Mean RMS values of the biceps brachii and brachioradialis during MVIC on the paretic side. (b) Peak RMS values of the biceps brachii and brachioradialis during MVIC on the nonparetic side. (c) Mean RMS values of the biceps brachii during MVICon the paretic and nonparetic sides. (d) Mean RMS values of the biceps brachii during MVIC on the paretic and nonparetic sides. sEMG: surface electromyography; MVIC: maximum voluntary isometric contraction; RMS: root mean square; $^{*}p < 0.05$; $^{**}p < 0.005$.

stroke, those with a poststroke duration of more than 6 months, and those with hemiparesis on the left side (Figure 5(g)). Finally, the peak RMS value of the paretic brachioradialis during MVIC was associated with elbow flexor muscle strength in male patients, those aged less than 60 years, those with ischemic stroke, and those with hemiparesis on the left side (Figure 5(h)).

3.3. Correlation between sEMG Values and Elbow Flexor Muscle Tension. Correlation analysis of the mean and peak RMS values of the paretic biceps and brachioradialis during FPE and the MAS score for muscle tension in elbow flexion was also conducted. Statistically significant correlations were detected between the mean RMS values of the paretic biceps muscles during FPE and muscle tension in elbow flexion ($r = 0.62$, $p = 0.021$), the mean RMS values of the paretic brachioradialis during FPE and muscle tension in elbow flexion ($r = 0.74$, $p = 0.004$), and the peak RMS value of the paretic brachioradialis during FPE and muscle tension in elbow flexion ($r = 0.59$, $p = 0.029$) (Figures 6(a), 6(e), and 6(f)). However, there was no significant association between the peak RMS value of the paretic biceps muscles during FPE and muscle tension in elbow flexion ($r = 0.49$, $p = 0.072$) (Figure 6(b)).

Five prespecified subgroup analyses (sex, age, stroke type, poststroke duration, and hemiparetic side (left/right)) were also performed. The results showed one significant interaction in the prespecified subgroup analysis by sex, whereby the mean RMS value of the paretic brachioradialis during FPE was associated with muscle tension in elbow

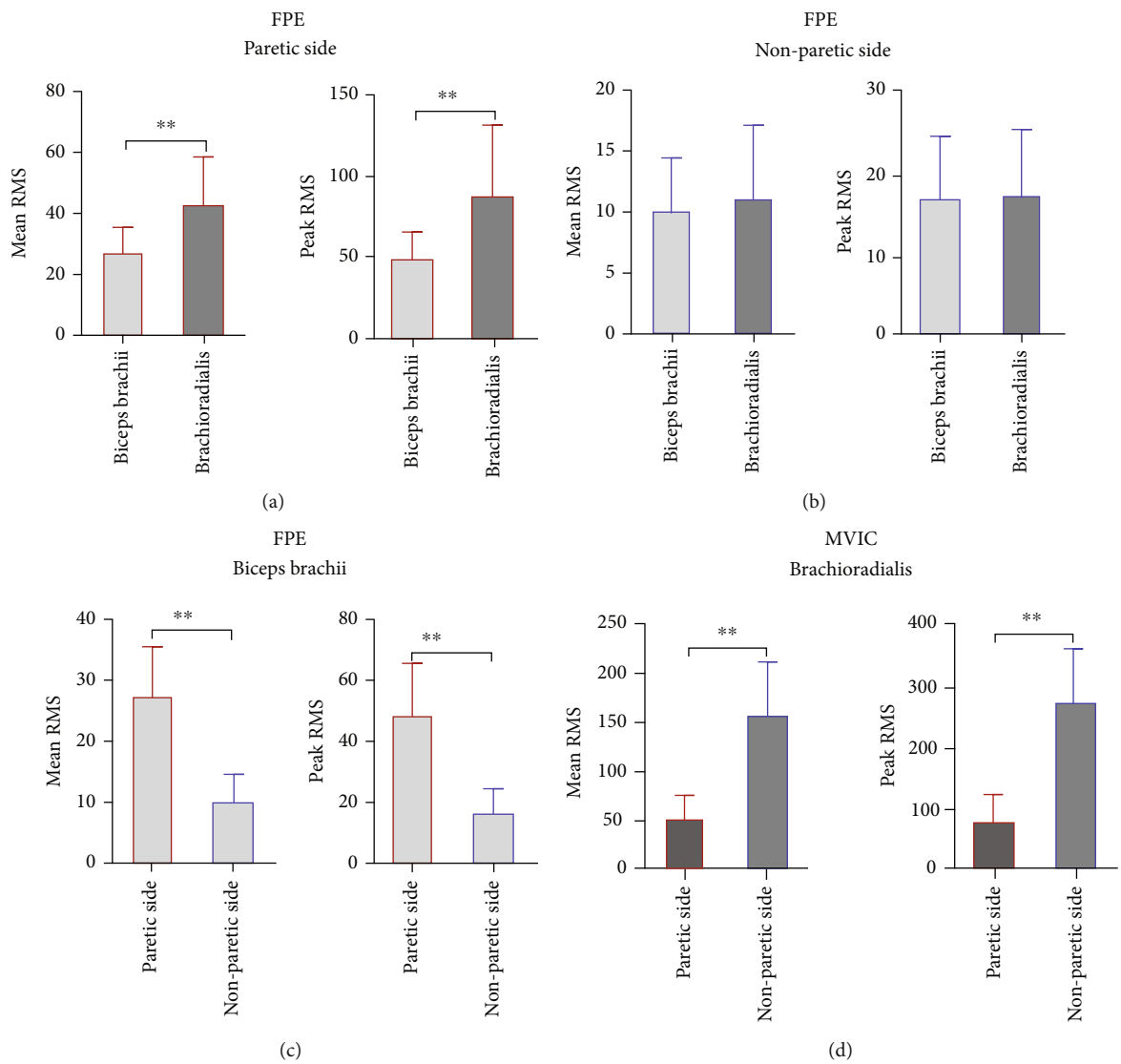

Figure 4: sEMG signals of the elbow flexor muscles (the biceps brachii and brachioradialis) during FPE. (a) Mean RMS values of the biceps brachii and brachioradialis during FPE on the paretic side. (b) Peak RMS values of the biceps brachii and brachioradialis during FPE on the nonparetic side. (c) Mean RMS values of the biceps brachii during FPE on the paretic and nonparetic sides. (d) Mean RMS values of the biceps brachii during FPEon the paretic and nonparetic sides. sEMG: surface electromyography; FPE: fast passive extension; RMS: root mean square; $^{*}p < 0.05$; $^{**}p < 0.005$.

flexion in men (Figure 6(g)). However, there were no statistically significant differences among the subgroups with respect to the mean or peak RMS value of the paretic biceps muscles during FPE, the MAS score for muscle tension in elbow flexion, the peak RMS value of the paretic brachioradialis during FPE, or the MAS score for muscle tension in elbow flexion (Figures 6(c), 6(d), and 6(h)).

4. Discussion

Stroke often leads to severe impairment of limb function and is associated with a decreased quality of life. Muscle weakness and spasm are the main factors affecting the functional recovery of stroke patients. To formulate an optimized rehabilitation program to maximize the functional recovery of patients, a reliable rehabilitation assessment is essential.

Currently, we often use the MMT for muscle strength assessment and the MAS for spasticity assessment in our clinical work. Both of these are semiquantitative assessment methods that are easy to perform but are susceptible to many unstable or uncontrollable factors. More importantly, these clinical scales are for the whole muscle group and cannot measure individual muscles. In addition, some detailed characteristics of the data are lost in the statistical processing of ordered multiclassification data, such as the MMT and MAS data, in clinical studies. In contrast, the continuous variable of sEMG can more comprehensively reflect the actual functional level of patients. Therefore, the objective and quantitative estimation method of sEMG was selected to compare the muscle strength and muscle tension levels of the biceps brachioradialis and brachioradialis in stroke patients, analyze the main muscle groups that affect the

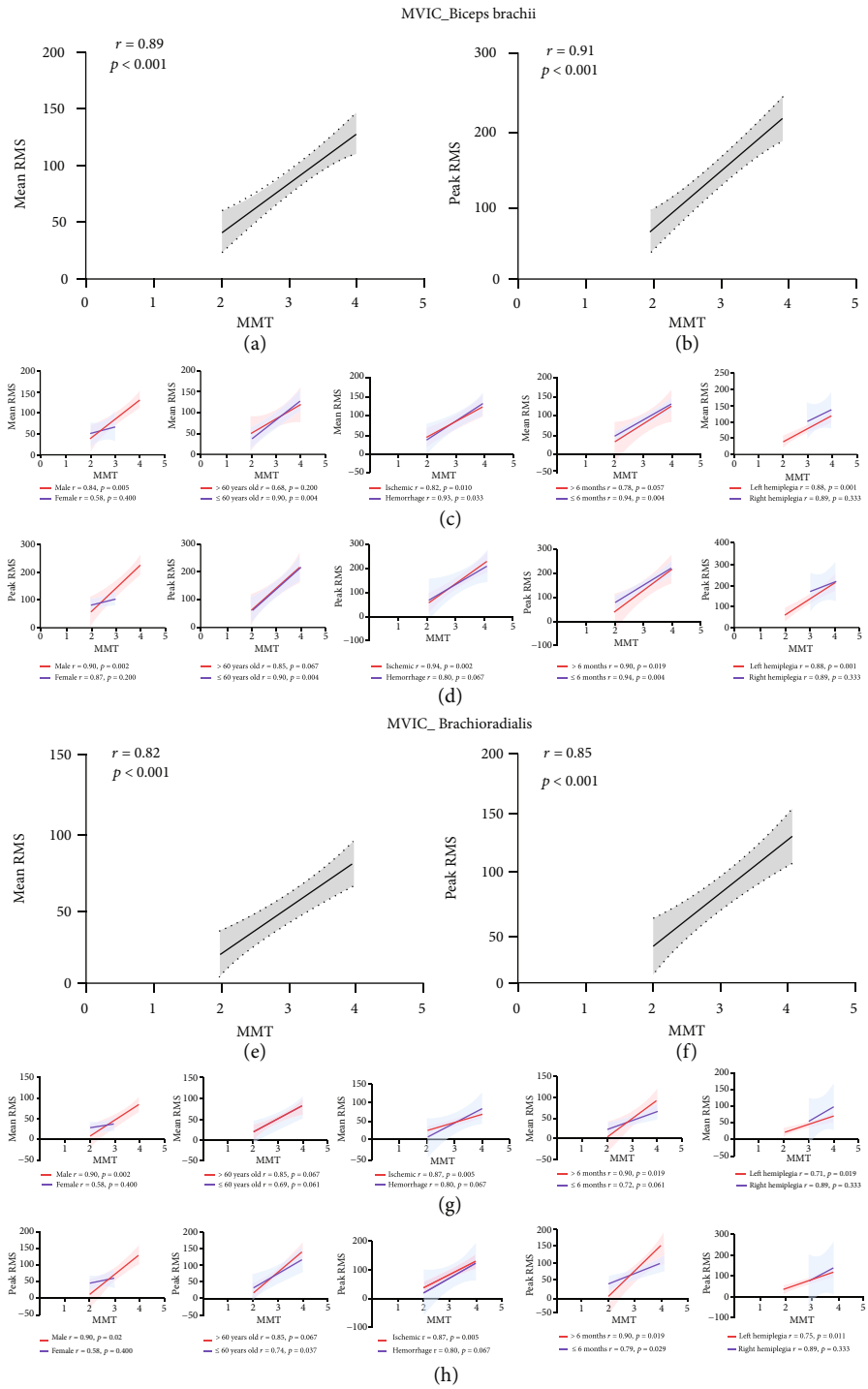

Figure 5: Correlation between sEMG values (mean and peak RMS values) and elbow flexion (biceps brachii and brachioradialis) muscle strength during MVIC on the paretic side. (a) Correlation between MMT score and mean RMS values of the biceps brachii during MVIC. (b) Correlation between MMT score and peak RMS values of the biceps brachii during MVIC. (c) Correlation between MMT score and mean RMS values of the biceps brachii during MVIC in subgroups (sex, age, stroke type, poststroke duration, and hemiparetic side (left/right)). (d) Correlation between MMT score and peak RMS values of the biceps brachii during MVIC in the subgroups (sex, age, stroke type, poststroke duration, and hemiparetic side (left/right)). (e) Correlation between MMT score and mean RMS values of the brachioradialis during MVIC. (f) Correlation between MMT score and peak RMS values of the brachioradialis during MVIC. (g) Correlation between MMT score and mean RMS values of the brachioradialis during MVIC in subgroups (sex, age, stroke type, poststroke duration, and hemiparetic side (left/right)). (h) Correlation between MMT score and peak RMS values of the brachioradialis during MVIC in the subgroups (sex, age, stroke type, poststroke duration, and hemiparetic side (left/right)). sEMG: surface electromyography; MVIC: maximum voluntary isometric contraction; MMT: manual muscle test; RMS: root mean square.

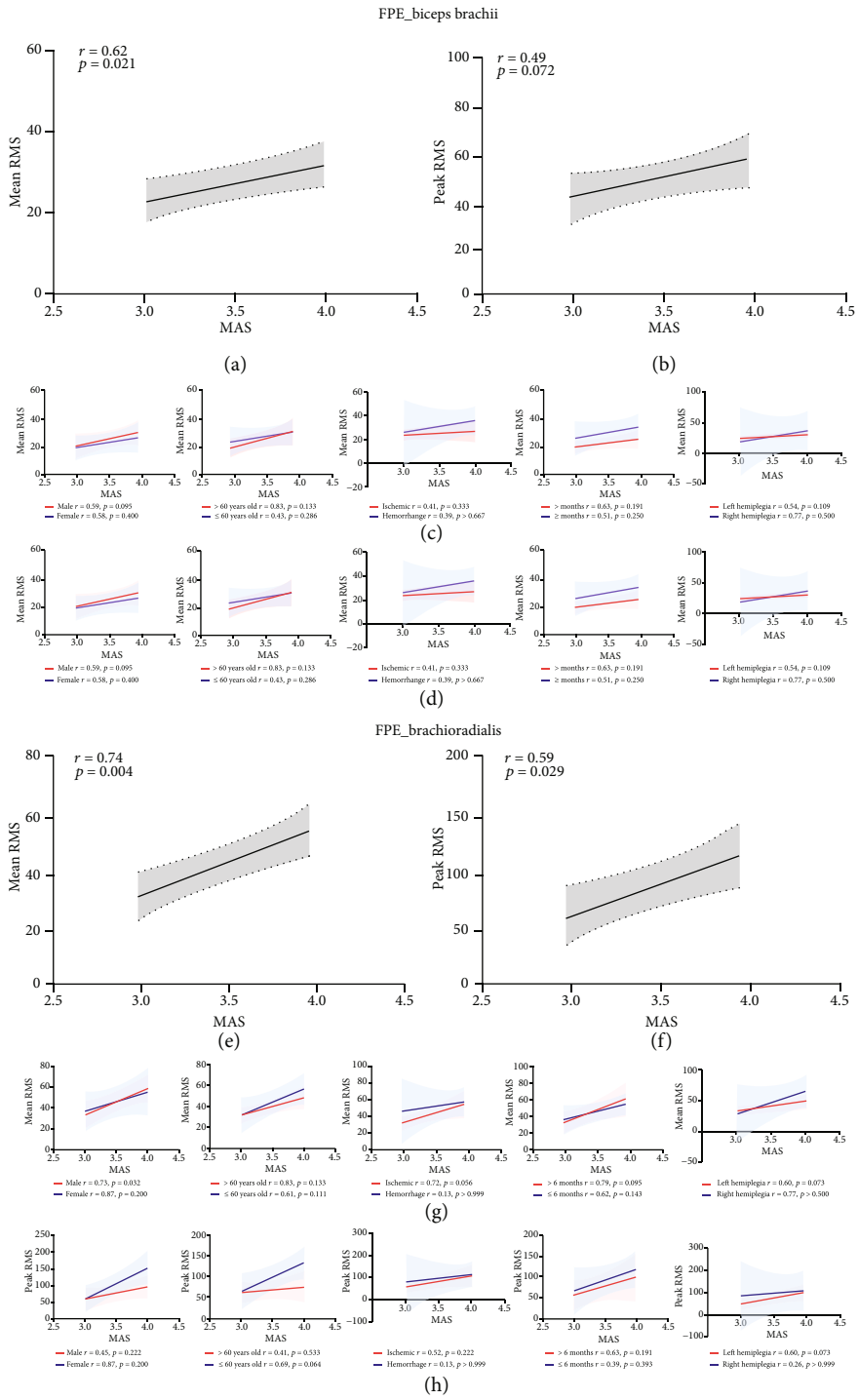

Figure 6: Correlation between sEMG values (mean and peak RMS values) and elbow flexion (biceps brachii and brachioradialis) muscle tension during FPE on the paretic side. (a) Correlation between MAS score and mean RMS values of the biceps brachii during FPE. (b) Correlation between MAS score and peak RMS values of the biceps brachii during FPE. (c) Correlation between MAS score and mean RMS values of the biceps brachii during FPE in the subgroups (sex, age, stroke type, poststroke duration, and hemiparetic side (left/right)). (d) Correlation between MAS score and peak RMS values of the affected biceps brachii during FPE in the subgroups (sex, age, stroke type, poststroke duration, and hemiparetic side (left/right)). (e) Correlation between MAS score and mean RMS values of the brachioradialis during FPE. (f) Correlation between MAS score and peak RMS values of the brachioradialis during FPE. (g) Correlation between MAS score and mean RMS values of the brachioradialis during FPE in the subgroups (sex, age, stroke type, poststroke duration, and hemiparetic side (left/right)). (h)Correlation between MAS score and peak RMS values of the brachioradialis during FPE in the subgroups (sex, age, stroke type, poststroke duration, and hemiparetic side (left/right)). sEMG: electromyography; FPE: fast passive extension; MAS: modified Ashworth scale; RMS: root mean square.

muscle strength and muscle tension of elbow flexor muscles, and explore a more objective evaluation to guide the optimization of clinical rehabilitation treatment programs.

sEMG is an objective, noninvasive method for neuromuscular function examination that has the advantages of real-time multitarget measurement and repeatability. It is used for quantitative and qualitative analyses of neuromuscular activity under various exercise states. Its reliability and validity in muscle strength assessment have been demonstrated in previous studies [21, 22]. sEMG mainly includes data in the time and frequency domains. The time-domain analysis is more mature and reliable and is widely used in clinical research [23]. The RMS value is the most important time-domain analysis index, which describes the effective value of discharge within a period of time, represents change in the myoelectric amplitude, and reflects the number of activated motor units and the degree of synchronization of the motor units involved in the activity. The mean and peak RMS values represent the mean and peak EMG activity during exercise, respectively. The combination of the two can objectively and reliably reflect the detected muscle contraction [24].

To analyze the effect of the biceps and brachioradialis on active contraction and to explore the application value of sEMG in the objective evaluation of muscle force, we first compared the sEMG value of the elbow muscle on the paretic side with that on the nonparetic side during MVIC exercise, and the results showed that the RMS values (mean and peak) of the paretic elbow flexors (biceps and brachioradialis) were significantly lower than those of the corresponding muscles on the nonparetic side ($p < 0.001$). sEMG values mainly reflect the recruitment properties of motor units during active contraction of the detected muscle, and orderly recruitment of motor units is crucial for effective muscle power generation [25, 26]. Hu et al. compared sEMG signals during isometric contraction of the first dorsal interosseous muscle in both paretic and nonparetic muscles of stroke patients and confirmed that stroke can lead to motor unit recruitment modifications in paretic muscles, which is the underlying cause of muscle weakness [27]. Our study also shows that the RMS value of the elbow flexor muscles on the paretic side decreased significantly during MVIC exercise compared with those on the nonparetic side, indicating that the recruitment ability of the paretic limb motor units decreased after stroke and that muscle strength decreased accordingly.

Then, we further compared the sEMG signals of the biceps and brachioradialis and found that the mean and peak RMS values of the paretic biceps were significantly higher than those of the brachioradialis ($p < 0.001$), and the same results were also found for the nonparetic side. The results indicate that the biceps is the muscle group with the higher sEMG signal expression than brachioradialis during active contraction of the elbow flexor muscles on both the paretic and nonparetic sides, suggesting its important role in the strength of the elbow flexor muscles. The biceps has been proven to be the main muscle group in elbow flexion and supination movements by intramuscular EMG [28]. Another study reported that biceps tendon injury can lead to severe impairment of elbow flexion and supination in patients [29]. However, the above studies focused only on the role of the biceps in elbow flexion and did not include the brachioradialis. In our study, multichannel sEMG was used to collect and compare the sEMG signals of the biceps and brachioradialis during the MVIC of the elbow flexor muscle, which further confirmed the vital role of the biceps in the active movement of the elbow flexor muscle through objective quantitative data.

Muscle weakness is a common finding after stroke, and approximately 65% of stroke survivors have obvious muscle paralysis [30]. Functional electrical stimulation is the most commonly used method for improving muscle strength in stroke patients with hemiplegia [31]. Eraifej et al. demonstrated that functional electrical stimulation of the upper extremity within two months after stroke can promote functional recovery and improve self-care in daily life [32]. Functional electrical stimulation with position selection is the key factor influencing the treatment effect. For example, the elbow flexor muscles include the biceps, brachioradialis, and brachialis muscles. There is no objective and detailed rehabilitation evaluation method to provide a reliable answer to the specific choice of muscle as the target of electrical stimulation. In clinical practice, the evaluation method is based mainly on the personal experience of therapists. Our results reveal the vital role of the biceps in the active movement of elbow flexion, indicating that the biceps should be given priority in the selection of electrical stimulation sites for elbow flexion. Whether electrical stimulation of the biceps is more conducive to the improvement of elbow flexor muscle strength than electrical stimulation of the brachioradialis needs further research for verification. Biofeedback and progressive resistance strength training have also proven to be effective treatments for improving the muscle strength of stroke patients [33, 34]. Similar to functional electrical stimulation, the selection of stimulation sites is also an important factor affecting the effect of electronic biofeedback therapy. Combined with the results of this study, we should consider the biceps as the main stimulation target. Our research confirms the important role of the biceps in the maximum isometric contraction of elbow flexion, suggesting that progressive resistance strength training with an emphasis on the biceps by adjusting the training position may be more beneficial to the recovery of muscle strength, and it is worthy of further exploration in clinical research. In addition, the important role of the biceps in the active movement of elbow flexor muscles should also be fully considered when botulinum toxin injection is used to treat elbow flexor spasticity, and the dose of injection should be properly controlled to avoid the potential risk of muscle strength decline caused by botulinum toxin injection, resulting in further aggravation of elbow flexor muscle weakness [35].

Finally, we analyzed the correlation between the RMS value of the elbow flexors collected during MVIC exercise and the MMT score of the elbow flexor muscle strength on the paretic side in stroke patients. The results show that the RMS value of the paretic elbow flexor muscles during MVIC exercise is positively correlated with the MMT score,

and this positive correlation was also present in most subgroup analyses. Onishi et al. revealed a quasilinear correlation between the EMG signal and the isometric force of the vastus lateralis [36]. However, the study only observed the vastus lateralis and did not assess other knee extension muscles. Our study explored the correlation between the sEMG signal of elbow flexor muscles (biceps and brachioradialis) and the MMT score, and the results indicated a positive correlation between the sEMG signal and muscle strength, suggesting that sEMG can well reflect the force of elbow flexor muscles.

To analyze the role of the biceps and brachioradialis in elbow flexor spasticity and to explore the application prospect of sEMG in the objective evaluation of spasticity, we first compared the sEMG signals of the elbow flexors on the paretic side with those on the nonparetic side during FPE exercise in stroke patients. The results showed that the RMS values of the biceps and brachioradialis on the paretic side were significantly higher than those of the corresponding muscle on the nonparetic side ($p < 0.001$). Spasticity is characterized by the high excitability of the stretch reflex induced by rapid drafting, which is the main feature of spastic muscle that distinguishes it from normal muscle. Thus, the most direct method for the quantitative assessment of spasticity is to identify the parameters related to the stretch reflex. The literature has confirmed that sEMG signals can effectively distinguish the occurrence of stretch reflexes, thus providing a method for evaluating spasticity [37]. Our study showed a significant difference in the expression of sEMG signals of the biceps and brachioradialis between the paretic and nonparetic sides during FPE exercise, suggesting that both the biceps and brachioradialis are important muscle groups causing elbow flexor spasticity.

Next, we further compared the sEMG signals of the paretic biceps and brachioradialis during FPE exercise. The results revealed that the brachioradialis showed significant reflex contraction during FPE and that both the peak and mean amplitudes of the sEMG signal exceeded those of the biceps. This suggests that the brachioradialis plays a significant role in elbow flexor spasticity in stroke patients, perhaps even exceeding the importance of the biceps, which is generally considered to be the dominant muscle group causing elbow flexor spasticity.

The main purpose of our comparison of the contributions of the biceps and brachioradialis in elbow flexor spasticity was to provide a reference for the treatment of elbow flexor spasticity after stroke. The elbow flexor is an important muscle group in the functional activities of the upper limb, and it is also the site with a high incidence of spasticity. Spasms limit the movement ability of the limb and inhibit the potential for recovery [38]. A total of 19-42.6% of stroke patients has spasticity that requires treatment; among them, up to 97% of patients with poststroke spasticity have moderate to severe motor dysfunction [39, 40]. The treatment of spasticity in the clinic mainly includes botulinum toxin injection, stretch training, posture placement, and range of motion training. Numerous reports have indicated that early local botulinum toxin injections combined with therapeutic training can reduce spasms and improve limb function [41–43]. Objective evaluations of spasms and injection plans (injection site and injection volume) are key factors affecting the efficacy of botulinum toxin injection [44]. In previous studies, botulinum toxin treatment strategies for elbow flexor spasticity all targeted the biceps muscle, and the role of the brachioradialis was often neglected [45, 46]. The literature also reveals that the biceps muscle is the main site of elbow flexor toxin injection, with an injection frequency 2-3 times higher than that of the brachioradialis [47]. However, our study indicates that the brachioradialis plays a noticeable role in elbow flexor spasticity, suggesting that rational allocation of brachioradialis doses should be considered in the formulation of a botulinum toxin injection regimen. Similarly, the effective implementation of therapeutic training depends on the objective evaluation of the spasm to determine the main muscles causing the spasm to more accurately lengthen the spastic muscle. Our study suggests that in rehabilitation training for elbow flexor spasticity, not only the biceps but also the brachioradialis should be considered. The local drafting position and movement should be used to strengthen the brachioradialis stretch to achieve more comprehensive effective control of elbow flexor spasticity.

Finally, we conducted a correlation analysis between the RMS value of the elbow flexors collected during rapid passive drafting of the paretic side and the MAS score. The results revealed that the mean RMS value of the elbow flexors during FPE exercise was positively correlated with the MAS scores. The peak RMS value of the brachioradialis was positively correlated with the MAS score, while the peak RMS value of the biceps was not significantly correlated with the MAS score. In the subgroup analysis, the mean RMS value of the paretic brachioradialis during FPE in the male subgroup was positively correlated with the MAS score, while no significant correlations were found in the other subgroups. Xie et al. demonstrated that there was a correlation between the sEMG amplitude in fast passive movement of the biceps and triceps and the MAS scores of flexor and extensor elbow muscles in stroke patients [48]. However, the study did not assess the brachioradialis, another important muscle of the elbow flexor. We included both the biceps and brachioradialis in our study and demonstrated that the RMS values of the two in FPE exercises are correlated with the elbow flexor MAS scores, demonstrating that both the biceps and the brachioradialis may be important muscle groups affecting elbow flexor spasticity. The results also indicate the application value of sEMG in the evaluation of elbow flexor spasticity. The reason why there is no significant correlation between the peak RMS value of the biceps and the MAS score may be related to the statistical deviation caused by the limited sample size in this study. The nonsignificant correlation in the other subgroups may also be related to the sample size. We will expand the sample size in future studies to further observe the correlation between them.

In this study, sEMG was used to quantitatively analyze the muscle strength and spasm of the biceps brachialis and brachioradialis. The results revealed that the biceps was the vital muscle in active elbow flexion and that the

brachioradialis plays a significant role in elbow flexor spasticity. However, there are many factors that affect sEMG detection, such as ambient temperature, body position, subcutaneous fat thickness, and active and passive exercise time. To minimize the interfering factors, this study was designed to adopt a unified approach in terms of the environment, inspector, position (forearm supination) and other factors, including a BMI of 18.5-24.0 according to the inclusion criteria. During the exercise of the MIVC or FPE, each subject rotated the forearm externally fixing the elbow joint on the iliac crest, which was useful to reduce the influence of movement on the detection results. More than those, electrodes were secured with adhesive tape and with a tensor bandage to prevent electrode movement during the experiment. The MVIC time was uniformly set to 5 seconds, and the fast passive extension time was set to be completed within 1 second. To ensure that the patients could achieve maximum muscle contraction, maintain the MVIC for 5 seconds, and fully relax their muscles without resistance in FPE exercise, we trained the patients ten times before the formal test. Each test action was repeated three times, and the maximum value was selected for analysis. Due to the strict limitations of the inclusion criteria, the sample size included in this study was limited. Therefore, the conclusions of this study should be interpreted with caution when applied in clinical practice since they were extracted from a limited sample. Future studies should comprehensively explore the underlying mechanisms using larger sample sizes. The brachialis was not included in this study, mainly because it is located in the deep layer of the lower half of the biceps, and its sEMG signal is covered by the biceps. In addition, only elbow flexor muscle groups were observed in this study, and other paralyzed muscles in stroke patients were not included. Future studies should be extended to other spastic muscles to better elucidate the specific muscles that affect spasticity and provide more comprehensive reference information for the optimization of rehabilitation training programs in clinical practice (the selection of electrical stimulation sites in hemiplegic limbs, the formulation of botulinum toxin injection programs, and the allocation of rehabilitation training priorities), achieve more accurate and efficient rehabilitation treatment, and promote the recovery of patients.

5. Conclusions

In this study, sEMG was used to confirm that the biceps plays a vital role in the MVIC of elbow flexion and that the brachioradialis plays a significant role in elbow flexor spasticity. The findings provide a quantitative and objective basis for the optimization of rehabilitation strategies for patients with stroke, such as the selection of electrical stimulation sites for elbow flexion, the focus of muscle strength training, and the administration of botulinum toxin injections. This research should be extended to the various spastic muscle groups of stroke patients, and sEMG should be used to analyze the main muscle groups that affect muscle strength and muscle tension to provide more objective evidence for the formulation of precise rehabilitation training programs.

Data Availability

The data used to support the findings of this study are available from the corresponding author upon request.

Conflicts of Interest

The authors declare that there is no conflict of interest regarding the publication of this article.

Authors' Contributions

Binbin Yu and Xintong Zhang contributed equally to this work.

Acknowledgments

This work was supported the National Key Research & Development Program of the Ministry of Science and Technology of the People's Republic of China (Grant numbers 2018YFC2002300 and 2018YFC2002301) and the Nanjing Municipal Science and Technology Bureau (Grant number 2019060002).

References

[1] P. B. Gorelick, "The global burden of stroke: persistent and disabling," *The Lancet Neurology*, vol. 18, no. 5, pp. 417-418, 2019.

[2] S. Mendis, "Stroke disability and rehabilitation of stroke: World Health Organization perspective," *International journal of stroke: official journal of the International Stroke Society*, vol. 8, no. 1, pp. 3-4, 2013.

[3] P. Langhorne, F. Coupar, and A. Pollock, "Motor recovery after stroke: a systematic review," *The Lancet Neurology*, vol. 8, no. 8, pp. 741–754, 2009.

[4] O. H. Kristensen, E. Stenager, and U. Dalgas, "Muscle strength and poststroke hemiplegia: a systematic review of muscle strength assessment and muscle strength Impairment," *Archives of Physical Medicine and Rehabilitation*, vol. 98, no. 2, pp. 368–380, 2017.

[5] R. W. Bohannon and M. B. Smith, "Interrater reliability of a modified Ashworth scale of muscle spasticity," *Physical Therapy*, vol. 67, no. 2, pp. 206-207, 1987.

[6] S. M. Aloraini, J. Gäverth, E. Yeung, and M. Mac Kay-Lyons, "Assessment of spasticity after stroke using clinical measures: a systematic review," *Disability and Rehabilitation*, vol. 37, no. 25, pp. 2313–2323, 2015.

[7] P. Ashby, A. Mailis, and J. Hunter, "The evaluation of spasticity," *Canadian Journal of Neurological Sciences*, vol. 14, no. S3, pp. 497–500, 1987.

[8] J. Vinstrup, J. Calatayud, M. D. Jakobsen et al., "Electromyographic comparison of conventional machine strength training versus bodyweight exercises in patients with chronic stroke," *Topics in Stroke Rehabilitation*, vol. 24, no. 4, pp. 242–249, 2017.

[9] M. S. Zanin, J. M. Ronchi, C. Silva Tde, A. C. Fuzaro, and J. E. Araujo, "Electromyographic and strength analyses of activation patterns of the wrist flexor muscles after acupuncture," *Journal of Acupuncture and Meridian Studies*, vol. 7, no. 5, pp. 231–237, 2014.

[10] D. Farina, R. Merletti, and R. M. Enoka, "The extraction of neural strategies from the surface EMG," *Journal of Applied Physiology*, vol. 96, no. 4, pp. 1486–1495, 2004.

[11] D. Farina, R. Merletti, and R. M. Enoka, "The extraction of neural strategies from the surface EMG," *Journal of Applied Physiology*, vol. 117, no. 11, pp. 1215–1230, 2014.

[12] M. Sin, W. S. Kim, D. Park et al., "Electromyographic analysis of upper limb muscles during standardized isotonic and isokinetic robotic exercise of spastic elbow in patients with stroke," *Journal of Electromyography and Kinesiology*, vol. 24, no. 1, pp. 11–17, 2014.

[13] J. Y. Hogrel, "Use of surface EMG for studying motor unit recruitment during isometric linear force ramp," *Journal of electromyography and kinesiology: official journal of the International Society of Electrophysiological Kinesiology*, vol. 13, no. 5, pp. 417–423, 2003.

[14] D. Farina and R. Merletti, "A novel approach for estimating muscle fiber conduction velocity by spatial and temporal filtering of surface EMG signals," *IEEE transactions on bio-medical engineering*, vol. 50, no. 12, pp. 1340–1351, 2003.

[15] T. Rudroff, D. Staudenmann, and R. M. Enoka, "Electromyographic measures of muscle activation and changes in muscle architecture of human elbow flexors during fatiguing contractions," *Journal of Applied Physiology*, vol. 104, no. 6, pp. 1720–1726, 2008.

[16] B. Caufriez, P. M. Dugailly, E. Brassinne, and F. Schuind, "The role of the muscle brachioradialis in elbow flexion: an electromyographic study," *The journal of hand surgery Asian-Pacific*, vol. 23, no. 1, pp. 102–110, 2018.

[17] K. S. Kim, J. H. Seo, and C. G. Song, "Portable measurement system for the objective evaluation of the spasticity of hemiplegic patients based on the tonic stretch reflex threshold," *Medical Engineering & Physics*, vol. 33, no. 1, pp. 62–69, 2011.

[18] A. D. Pandyan, P. Vuadens, F. M. van Wijck, S. Stark, G. R. Johnson, and M. P. Barnes, "Are we underestimating the clinical efficacy of botulinum toxin (type A)? Quantifying changes in spasticity, strength and upper limb function after injections of Botox to the elbow flexors in a unilateral stroke population," *Clinical Rehabilitation*, vol. 16, no. 6, pp. 654–660, 2002.

[19] R. Merletti and H. Hermens, "Introduction to the special issue on the SENIAM European Concerted Action," *Journal of electromyography and kinesiology: official journal of the International Society of Electrophysiological Kinesiology*, vol. 10, no. 5, pp. 283–286, 2000.

[20] G. Albani, V. Cimolin, M. Galli et al., "Use of surface EMG for evaluation of upper limb spasticity during botulinum toxin therapy in stroke patients," *Functional Neurology*, vol. 25, no. 2, pp. 103–107, 2010.

[21] J. P. van Dijk, D. F. Stegeman, M. J. Zwarts, and J. H. Blok, "Motor unit number estimation with high-density surface EMG: principles and implications," *Supplements to Clinical Neurophysiology*, vol. 60, pp. 105–118, 2009.

[22] R. Merletti, A. Botter, C. Cescon, M. A. Minetto, and T. M. Vieira, "Advances in surface EMG: recent progress in clinical research applications," *Critical Reviews in Biomedical Engineering*, vol. 38, no. 4, pp. 347–379, 2010.

[23] S. Guo, M. Pang, B. Gao, H. Hirata, and H. Ishihara, "Comparison of sEMG-based feature extraction and motion classification methods for upper-limb movement," *Sensors*, vol. 15, no. 4, pp. 9022–9038, 2015.

[24] V. S. Pereira-Baldon, A. B. de Oliveira, J. F. Padilha, A. M. Degani, M. A. Avila, and P. Driusso, "Reliability of different electromyographic normalization methods for pelvic floor muscles assessment," *Neurourology and Urodynamics*, vol. 39, no. 4, pp. 1145–1151, 2020.

[25] X. Hu, W. Z. Rymer, and N. L. Suresh, "Motor unit pool organization examined via spike-triggered averaging of the surface electromyogram," *Journal of Neurophysiology*, vol. 110, no. 5, pp. 1205–1220, 2013.

[26] C. J. De Luca and P. Contessa, "Hierarchical control of motor units in voluntary contractions," *Journal of Neurophysiology*, vol. 107, no. 1, pp. 178–195, 2012.

[27] X. Hu, A. K. Suresh, W. Z. Rymer, and N. L. Suresh, "Assessing altered motor unit recruitment patterns in paretic muscles of stroke survivors using surface electromyography," *Journal of Neural Engineering*, vol. 12, no. 6, article 066001, 2015.

[28] A. Naito, M. Yajima, H. Fukamachi et al., "Electrophysiological studies of the biceps brachii activities in supination and flexion of the elbow joint," *The Tohoku Journal of Experimental Medicine*, vol. 173, no. 2, pp. 259–267, 1994.

[29] S. Nesterenko, Z. J. Domire, B. F. Morrey, and J. Sanchez-Sotelo, "Elbow strength and endurance in patients with a ruptured distal biceps tendon," *Journal of Shoulder and Elbow Surgery*, vol. 19, no. 2, pp. 184–189, 2010.

[30] J. H. Cauraugh and S. B. Kim, "Chronic stroke motor recovery: duration of active neuromuscular stimulation," *Journal of the Neurological Sciences*, vol. 215, no. 1-2, pp. 13–19, 2003.

[31] G. You, H. Liang, and T. Yan, "Functional electrical stimulation early after stroke improves lower limb motor function and ability in activities of daily living," *NeuroRehabilitation*, vol. 35, no. 3, pp. 381–389, 2014.

[32] J. Eraifej, W. Clark, B. France, S. Desando, and D. Moore, "Effectiveness of upper limb functional electrical stimulation after stroke for the improvement of activities of daily living and motor function: a systematic review and meta-analysis," *Systematic Reviews*, vol. 6, no. 1, p. 40, 2017.

[33] S. L. Morris, K. J. Dodd, and M. E. Morris, "Outcomes of progressive resistance strength training following stroke: a systematic review," *Clinical Rehabilitation*, vol. 18, no. 1, pp. 27–39, 2004.

[34] L. A. Nelson, "The role of biofeedback in stroke rehabilitation: past and future directions," *Topics in Stroke Rehabilitation*, vol. 14, no. 4, pp. 59–66, 2007.

[35] I. R. Odderson, "Can botulinum toxin cause chronic muscle weakness," *Muscle & Nerve*, vol. 57, no. 3, pp. 350–352, 2018.

[36] H. Onishi, R. Yagi, K. Akasaka, K. Momose, K. Ihashi, and Y. Handa, "Relationship between EMG signals and force in human vastus lateralis muscle using multiple bipolar wire electrodes," *Journal of electromyography and kinesiology: official journal of the International Society of Electrophysiological Kinesiology*, vol. 10, no. 1, pp. 59–67, 2000.

[37] F. Pisano, G. Miscio, C. Del Conte, D. Pianca, E. Candeloro, and R. Colombo, "Quantitative measures of spasticity in post-stroke patients," *Clinical Neurophysiology: Official Journal of the International Federation of Clinical Neurophysiology*, vol. 111, no. 6, pp. 1015–1022, 2000.

[38] A. Picelli, S. Tamburin, F. Gajofatto et al., "Association between severe upper limb spasticity and brain lesion location in stroke patients," *BioMed Research International*, vol. 2014, Article ID 162754, 6 pages, 2014.

[39] R. D. Zorowitz, P. J. Gillard, and M. Brainin, "Poststroke spasticity: sequelae and burden on stroke survivors and caregivers," *Neurology*, vol. 80, no. 3, pp. S45–S52, 2013.

[40] S. Pundik, J. McCabe, M. Skelly, C. Tatsuoka, and J. J. Daly, "Association of spasticity and motor dysfunction in chronic stroke," *Annals of Physical and Rehabilitation Medicine*, vol. 62, no. 6, pp. 397–402, 2019.

[41] U. M. Fietzek, P. Kossmehl, L. Schelosky, G. Ebersbach, and J. Wissel, "Early botulinum toxin treatment for spastic pes equinovarus - a randomized double-blind placebo-controlled study," *European Journal of Neurology*, vol. 21, no. 8, pp. 1089–1095, 2014.

[42] S. Li and G. E. Francisco, "The use of botulinum toxin for treatment of spasticity," *Handbook of Experimental Pharmacology*, vol. 263, pp. 127–146, 2021.

[43] P. McCrory, L. Turner-Stokes, I. J. Baguley et al., "Botulinum toxin A for treatment of upper limb spasticity following stroke: a multi-centre randomized placebo-controlled study of the effects on quality of life and other person-centred outcomes," *Journal of Rehabilitation Medicine*, vol. 41, no. 7, pp. 536–544, 2009.

[44] I. Moeini-Naghani, T. Hashemi-Zonouz, and B. Jabbari, "Botulinum toxin treatment of spasticity in adults and children," *Seminars in Neurology*, vol. 36, no. 1, pp. 64–72, 2016.

[45] M. K. Childers, A. Brashear, P. Jozefczyk et al., "Dose-dependent response to intramuscular botulinum toxin type A for upper-limb spasticity in patients after a stroke [1]," *Archives of Physical Medicine and Rehabilitation*, vol. 85, no. 7, pp. 1063–1069, 2004.

[46] Y. T. Chen, C. Zhang, Y. Liu et al., "The effects of botulinum toxin injections on spasticity and motor performance in chronic stroke with spastic hemiplegia," *Toxins*, vol. 12, no. 8, p. 492, 2020.

[47] D. Intiso, V. Simone, F. Di Rienzo et al., "High doses of a new botulinum toxin type A (NT-201) in adult patients with severe spasticity following brain injury and cerebral palsy," *NeuroRehabilitation*, vol. 34, no. 3, pp. 515–522, 2014.

[48] P. Xie, Y. Song, C. Su, W. Xu, and Y. Du, "Analysis of correlation between surface electromyography and spasticity after stroke," *Journal of Biomedical Engineering*, vol. 32, no. 4, pp. 795–801, 2015.

Hindawi
Neural Plasticity
Volume 2022, Article ID 9662630, 8 pages
https://doi.org/10.1155/2022/9662630

Research Article

Application of Logistic Regression and Decision Tree Models in the Prediction of Activities of Daily Living in Patients with Stroke

Qile Zhang,[1] **Zheyu Zhang**,[2] **Xiuqing Huang**,[1] **Chun Zhou**,[1] **and Jian Xu**[1]

[1]*Department of Rehabilitation, The Quzhou Affiliated Hospital of Wenzhou Medical University, Quzhou People's Hospital, Quzhou, China*
[2]*The Second Clinical Medical College, Zhejiang Chinese Medical University, Hangzhou, China*

Correspondence should be addressed to Qile Zhang; zjzhangqile@163.com

Qile Zhang and Zheyu Zhang contributed equally to this work.

Received 29 August 2021; Revised 25 October 2021; Accepted 15 December 2021; Published 28 January 2022

Academic Editor: Yating Lv

An improvement in the activities of daily living (ADLs) is significantly related to the quality of life and prognoses of patients with stroke. However, the factors predicting significant improvement in ADL (SI-ADL) have not yet been clarified. Therefore, we sought to identify the key factors affecting SI-ADL in patients with stroke after rehabilitation therapy using both logistic regression modeling and decision tree modeling. We retrospectively collected and analyzed the clinical data of 190 patients with stroke who underwent rehabilitation therapy at our hospital between January 2020 and July 2020. General and rehabilitation therapy data were extracted, and the Barthel index (BI) score was used for outcome assessment. We defined SI-ADL as an improvement in the BI score by 15 points or more during hospitalization. Logistic regression and decision tree models were established to explore the SI-ADL predictors. We then used receiver operating characteristic (ROC) curves to compare the logistic regression and decision tree models. Univariate analysis revealed that compared with the non-SI-ADL group, the SI-ADL group showed a significantly shorter course of stroke, longer hospital stay, and higher rate of receiving occupational and speech therapies (all $P < 0.05$). Binary logistic regression analysis revealed the course of stroke at admission (odds ratio (OR) = 0.986, 95%confidence interval (CI) = 0.979–0.993; $P < 0.001$) and the length of hospital stay (OR = 1.030, 95 %CI = 1.013–1.047; P =0.001) as the independent predictors of SI-ADL. ROC comparisons revealed no significant differences in the areas under the curves for the logistic regression and decision tree models (0.808 *vs.* 0.831; $z = 0.977$, $P = 0.329$). Both models identified the course of disease at admission and the length of hospital stay as key factors affecting SI-ADL. Early initiation of rehabilitation therapy is of immense importance for improving the ADLs in patients with stroke.

1. Introduction

Stroke is a disease with focal neurological deficits caused by sudden cerebral blood circulation abnormalities [1]; it is associated with high mortality and disability rates. Although stroke-associated mortality has decreased with the improvement of medical technology, the number of patients with poststroke motor, sensory, speech, cognitive, psychological, and other dysfunctions has increased sharply [2]. In China, approximately 2 million patients are diagnosed with new-onset stroke every year [3]. Approximately 75% of these stroke survivors have varying degrees of disability; among these, more than 40% are severely disabled [4, 5]. This not only has a marked impact on the activities of daily living (ADLs) of patients but also places a heavy burden on their families.

Improvement in ADLs is significantly related to the quality of life and prognoses of patients with stroke. Previous studies have reported that rehabilitation therapy can improve limb function and ADLs, thereby helping patients return to normal life [6, 7]. In clinical practice, we found that some patients with stroke showed a significant improvement in ADL (SI-ADL) after rehabilitation therapy [8, 9], while other patients only showed a minimal improvement [10].

However, the factors affecting SI-ADL have not yet been clarified.

Therefore, we sought to identify the key factors predicting SI-ADL in patients with stroke after rehabilitation therapy, using both logistic regression modeling and decision tree modeling.

2. Materials and Methods

2.1. Patient Selection. Between January 2020 and July 2020, 190 patients with stroke underwent rehabilitation therapy at the Department of Rehabilitation of the Quzhou Affiliated Hospital of Wenzhou Medical University. We included patients with stroke, according to the diagnostic criteria adopted by the Fourth National Cerebrovascular Disease Academic Conference of the Chinese Society of Neurology in 1995 [11]. We included patients with stable vital signs or neurological deficit symptoms that no longer progressed after more than 48 hours, who had dysfunction, and who needed rehabilitation intervention. The exclusion criteria were as follows: (1) patients with severe cardiovascular, liver, kidney, digestive, and hematopoietic diseases that may endanger life; (2) patients with serious mental disorders; (3) patients with newly developed intracranial lesions or further aggravation of neurological deficits during hospitalization; (4) patients who refused continued rehabilitation; and (5) patients with incomplete clinical data acquired during hospitalization. We extracted data on demographics (age and sex), medical history, final diagnosis, course of stroke at admission, with or without rehabilitation therapy before admission, length of hospital stay, laboratory test results at admission, and medications used during hospitalization.

This study was approved by the human ethics committee of the Quzhou Affiliated Hospital of the Wenzhou Medical University (LS2018023). Written informed consent was obtained at the time of admission. The clinical investigation was conducted in accordance with the principles of the Declaration of Helsinki.

2.2. Rehabilitation Therapies. All patients received exercise therapy and physical factor treatment. In addition, patients received one or more treatments specific to their dysfunctions. Exercise therapy included proper limb positioning, joint range-of-motion training, muscle strength training, turnover, transfer training, bridge exercise, sitting and standing balance training, and walking and up-and-down stair training, among others. Each treatment session lasted for 40 min and was conducted once a day.

Physical factor treatment included neuromuscular electrical stimulation of the hemiplegic side. Different electrical stimulation sites were selected according to the patients' conditions. The commonly used stimulation sites included the deltoid, triceps brachii, extensor carpi longus radialis, quadriceps femoris, and tibialis anterior muscles. Each session lasted for 20 min and was conducted once a day.

Occupational therapy included training in shoulder antexion, abduction, elbow extension, forearm rotation, wrist extension, and finger flexion and extension movements. It also included upper limb virtual games and task-oriented training (such as washing and dressing). Each treatment session lasted for 40 min and was conducted once a day.

For speech therapy, the Schuell stimulation method was adopted to conduct progressive training in audiovisual understanding, retelling, oral expression, reading, and writing in a one-to-one manner. Each treatment session lasted for 40 min and was conducted once a day.

Cognitive therapy included computer-assisted targeted training in attention, orientation, visual space, executive ability, memory, and logical thinking. Each treatment session lasted for 40 min and was conducted once a day.

Swallowing therapy included guided lip exercises, ice stimulation of the oral and throat muscles, supraglottic swallowing, forced swallowing, empty swallowing, nodding swallowing, Mendelsohn swallowing and shaker manipulation, free drinking water training, and limiting the amount of one mouthful. Each treatment session lasted for 40 min and was conducted once a day.

Acupuncture treatment included stimulation of the acupoints in the Yangming meridian of the upper and lower limbs during the period of soft paralysis. For spasms, the principle of "taking acupoints by antagonistic muscles" was adopted. The acupoints that were often stimulated included the hand Sanli, Waiguan, Hegu, Jianyu, Bige, Yanglingquan, Zusanli, Jiexi, Weizhong, and knee Yangguan. Acupuncture was administered using 1.5–2.0-inch No. 30 acupuncture needles. The needles were inserted for 20 min, once a day.

Respiratory therapy included guided chest-expansion exercises, abdominal breathing training, and respiratory function improvement through the use of an incentive spirometer. For patients with foot drop and varus affecting the walking function, an orthosis was employed. We used a German Ottobock 50s1 ankle-foot orthosis for walking training.

For patients with unrelieved poststroke shoulder pain after manipulation and physical factor treatments, the lesion site on the shoulder was examined under the guidance of color Doppler ultrasound, and local injections were administered. These comprised a 3 mL lidocaine hydrochloride injection, 1 mL compound betamethasone injection, and 0.9% sodium chloride injection. These injections were administered only once in selected patients.

2.3. Outcome Evaluation. Data on the Barthel index (BI) scores at admission and discharge were extracted from the records. The BI scale assesses 10 ADLs, namely, feeding, bathing, grooming, dressing, bowels, bladder, toilet use, transfers, mobility, and stairs. Each item was scored 5, 10, or 15 points, and the total scores ranged from 0 to 100. A BI score of 60 points was chosen as the cut-off: a score ≥ 60 points indicated that the patient lived mostly or completely independently, while a score < 60 points indicated that the patient lived mostly or in complete dependence on the care of others [12]. In this study, SI-ADL was defined by an at least 15-point increase in the BI score at discharge. No significant improvement in the ADL (NSI-ADL) was defined by a less than 15-point increase in the BI score.

2.4. Development of the Logistic Regression Model and the Decision Tree Model. A binary logistic regression analysis model was established by taking variables with $P < 0.05$ in the univariate analysis as the independent variables and SI-ADL as the dependent variable.

Variables with $P < 0.05$ in the univariate analysis were further analyzed to develop the decision tree model. The model was established using the classification and regression tree method; the decision tree analysis was performed using the SPSS software (version 22.0). The decision tree grew "branches" by significance testing, with a split occurring at $\alpha = 0.05$. The time limit specified that the minimum sample size of the parent node was 20, and the minimum sample size of the offspring node was 5. If the sample size on the node failed to meet this requirement, the node was considered a terminal node and was not segmented.

2.5. Statistical Analysis. The SPSS 22.0 software (IBM) was used for data analysis. Continuous data are presented as frequencies and percentages. The two groups of measurement data are presented as means ± standard deviations or as medians (interquartile ranges, IQRs). The χ^2 test was used for the comparison of categorical variables, while the t-test or the Mann–Whitney nonparametric test was used for the comparison of continuous variables. Spearman correlation analysis was conducted to identify the correlations between the variables. Baseline variables with $P < 0.05$ in the univariate analysis were used to develop the binary logistic regression analysis model and the decision tree model, separately. Implementing the Delong method, receiver operating characteristic (ROC) curves obtained from the logistic regression and decision tree models were then compared using the MedCalc 15.0 software (MedCalc Software, Mariakerke, Belgium). Statistical significance was set at $P < 0.05$.

3. Results

3.1. Baseline Characteristics. Overall, 190 patients with stroke met the criteria for inclusion in our study (Figure 1); of these, 109 (57.4%) were diagnosed with cerebral infarction and 66 (34.7%) were women. The median age was 59 years (IQR: 48–70 years). The median course of stroke at admission was 49 days (IQR: 21–97 days), and the median length of hospital stay was 23 days (IQR: 13–39 days). A total of 110 patients (57.9%) had received rehabilitation therapy before admission. The median BI score of all patients was 45 (IQR: 20–66) at admission and 60 (IQR: 40–80) at discharge. Overall, 94 patients (49.5%) had a BI score ≥ 60 at discharge and 80 patients (42.1%) had SI-ADL at discharge.

3.2. Relationship between Rehabilitation Therapy and BI. Compared with patients who did not receive rehabilitation therapy before admission, those who had received rehabilitation therapy before admission had a higher BI score (45 *vs.* 35 points, $Z = -2.132$, $P = 0.033$) and a longer course of stroke (78 *vs.* 20 days, $t = 7.372$, $P < 0.001$); they also comprised a lower proportion of patients with cerebral infarction (50.9% *vs.* 66.3%, $\chi^2 = 4.457$, $P = 0.035$).

The BI scores at discharge of both patients with and without prior rehabilitation therapy had significant improvement when compared with the corresponding BI scores at admission (all $P < 0.001$); however, the BI scores at discharge themselves did not differ significantly between these two groups (with and without prior rehabilitation therapy: 60 *vs.* 65 points, $Z = -0.468$, $P = 0.639$). At discharge, there was no significant difference in the proportion of patients with SI-ADL between these two groups (with and without prior rehabilitation therapy: 38.2% *vs.* 47.5%, $\chi^2 = 1.650$, $P = 0.199$).

During hospitalization, all patients received exercise and physical therapies. Therefore, exercise therapy and physical therapy were not included in the calculation of the rehabilitation therapy types. Spearman's correlation analysis revealed that the number of rehabilitation therapies received by patients during hospitalization was positively correlated with the course of stroke at admission ($\rho = 0.197$, $P = 0.006$) and the length of hospital stay ($\rho = 0.277$, $P < 0.001$) and negatively correlated with a cerebral infarction diagnosis ($\rho = -0.248$, $P = 0.001$). There was no correlation between the number of rehabilitation therapies and SI-ADL ($\rho = 0.088$, $P = 0.288$).

There were no significant differences in the lengths of hospital stay between the group with a BI score < 60 at discharge and the group with a BI score ≥ 60 at discharge (median: 21 *vs.* 26, $Z = -0.799$, $P = 0.424$). In addition, the group with a BI score ≥ 60 at discharge received significantly fewer rehabilitation therapy types as compared with the group with a BI score < 60 at discharge (1 *vs.* 2, $Z = -4.727$, $P < 0.001$). The group with a BI score ≥ 60 at discharge received lesser speech, cognitive, swallowing, and respiratory therapies (all $P \leq 0.001$; Table 1). Additionally, patients who received speech, cognitive, swallowing, and respiratory therapies had significantly lower BI scores than those who did not receive these four rehabilitation therapies (all $P < 0.001$; see Supplementary table I). However, multivariate regression analysis revealed that none of these four therapies were risk factors for achieving a BI score ≥ 60 at discharge (see Supplementary Tables II and III).

3.3. Factors Associated with SI-ADL. Univariate analysis revealed that compared with patients with NSI-ADL, patients with SI-ADL had a shorter course of stroke at admission and a longer length of hospital stay and also comprised a higher proportion of those receiving occupational and speech therapies (all $P < 0.05$). There was no significant difference in the proportion of patients receiving cognitive, respiratory, and swallowing therapies between the NSI-ADL and SI-ADL groups (all $P > 0.05$; Table 2).

3.4. Characteristics of Patients with SI-ADL Based on the Decision Tree Model. The baseline variables with $P < 0.05$ in the univariate analysis were also used to develop the decision tree model to predict SI-ADL (Figure 2). The results showed that among the patients with a course of disease ≤ 100.5 days at admission, 52.8% had SI-ADL. Among the patients with a length of hospital stay > 15.5 days, 67.1% achieved SI-ADL. Only 32.2% of the patients with a length

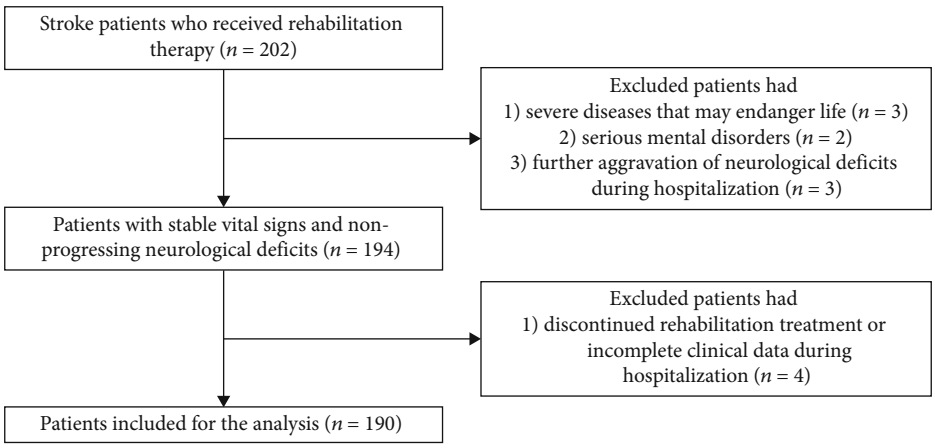

Figure 1: Study flowchart.

Table 1: Comparison of the rehabilitation therapies between patients with a BI score < 60 and ≥60 at discharge.

	BI score < 60 at discharge	BI score ≥ 60 at discharge	Test value	*P* value
Occupational therapy	87 (90.6)	87 (92.6)	$\chi^2 = 0.229$	0.632
Speech therapy	61 (63.5)	40 (42.6)	$\chi^2 = 8.402$	0.004
Cognitive therapy	49 (51)	21 (22.3)	$\chi^2 = 16.814$	<0.001
Swallowing therapy	40 (41.7)	15 (16)	$\chi^2 = 15.263$	<0.001
Acupuncture treatment	18 (18.8)	12 (12.8)	$\chi^2 = 1.279$	0.258
Respiratory therapy	34 (35.4)	6 (6.4)	$\chi^2 = 24.088$	<0.001
Configuration of orthosis	11 (11.5)	5 (5.3)	$\chi^2 = 2.321$	0.128
Steroid injection	6 (6.3)	4 (4.3)	$\chi^2 = 0.379$	0.538
Numbers of rehabilitation therapies, median (IQR)	2 (1–4)	1 (0–2)	$Z = -5.031$	<0.001

BI: Barthel index; IQR: interquartile range; WBC: white blood cell; LDL: low-density lipoprotein.

of hospital stay ≤ 15.5 days achieved SI-ADL. Among the patients with a course of disease > 100.5 days at admission, only 8.7% achieved SI-ADL after hospitalization. Among the patients whose length of hospital stay was >29.5 days, 30.0% achieved SI-ADL. Only 2.8% of the patients with a length of hospital stay < 29.5 days achieved SI-ADL.

3.5. Comparison of the Logistic Regression Model and the Decision Tree Model. For the logistic regression model, the area under the curve (AUC) was 0.808 (95%CI = 0.744–0.861, $P = 0.032$). For the decision tree model, the AUC was 0.831 (95%CI = 0.770–0.881, $P = 0.029$). Comparison of the ROC curves of the logistic regression and the decision tree models revealed no significant differences in the AUCs between the two ($z = 0.977$, $P = 0.329$; Figure 3).

4. Discussion

We investigated the factors that predict SI-ADL after rehabilitation therapy in patients with stroke. Both the logistic regression model and the decision tree model confirmed that the course of disease at admission and the length of hospital stay were the key factors affecting SI-ADL.

Previous studies have shown that the ADL level of patients with stroke at admission is positively correlated with the ADL level at discharge, suggesting that the higher the degree of functional independence at baseline, the better the effect of the rehabilitation therapy. However, in contrast to previous research, our study found that although the BI score (at admission) of patients who had received rehabilitation therapy before admission was higher than the score of those who had not, there were no significant differences in the BI scores at discharge between the two groups after receiving the rehabilitation therapy. This suggested that the plasticity of functional recovery in patients who had previously received rehabilitation therapy was relatively low. This may be because patients who have received rehabilitation therapy before admission usually have a longer course of the disease. Therefore, when they receive rehabilitation therapies for the second time, their sensitivities to these therapies are much lower than those of patients who have not received rehabilitation therapy previously. Li and Zhong [13] categorized 45 patients with stroke into three groups according to the disease course. Patients in whom the disease course was <1 month, 1–6 months, and >6 months were included in the first, second, and third groups, respectively. The

Table 2: Baseline characteristics between SI-ADL and NSI-ADL groups.

	Non-SI-ADL ($n = 110$)	SI-ADL ($n = 80$)	Test value	P value
Age (years), median (IQR)	60 (49–70)	58 (46–71)	$Z = -0.421$	0.674
Female, n (%)	38 (34.6)	28 (35.0)	$\chi^2 = 0.004$	0.948
Cerebral infarction, n (%)	66 (60.0)	43 (53.8)	$\chi^2 = 0.740$	0.390
Course of disease at admission (days) (IQR)	61 (29–142)	31 (10–65)	$Z = -4.048$	<0.001
Past medical history, n (%)				
Hypertension	86 (78.2)	59 (73.8)	$\chi^2 = 0.503$	0.478
Diabetes	38 (34.6)	18 (22.5)	$\chi^2 = 3.233$	0.072
Coronary heart disease	13 (11.8)	1 (1.3)	$\chi^2 = 7.579$	0.006
Atrial fibrillation	10 (9.1)	4 (5.0)	$\chi^2 = 1.136$	0.287
Stroke	14 (12.7)	5 (6.3)	$\chi^2 = 2.159$	0.142
Length of stay (days) (IQR)	14 (13–20)	30 (15–43)	$Z = -4.707$	<0.001
Systolic blood pressure at admission (mmHg) ($\bar{x} \pm s$)	130.68 ± 16.948	131.75 ± 19.255	$t = 0.400$	0.690
Diastolic blood pressure at admission (mmHg) ($\bar{x} \pm s$)	79.64 ± 12.336	79.65 ± 13.677	$t = 0.001$	1.000
WBC count at admission (10^9/L) ($\bar{x} \pm s$)	6.61 ± 2.418	6.70 ± 2.865	$t = 0.224$	0.823
LDL level at admission, (mmol/L) (IQR)	2.09 (1.60–2.54)	2.09 (1.68–2.97)	$Z = 1.790$	0.075
BI score at admission (IQR)	48 (28–75)	35 (20–55)	$Z = -2.609$	0.009
BI score at discharge (IQR)	50 (30–80)	65 (50–84)	$Z = -2.451$	0.014
Antihypertensive therapy, n (%)	70 (63.6)	46 (57.5)	$\chi^2 = 0.733$	0.392
Hypoglycemic therapy, n (%)	33 (30.0)	20 (25.0)	$\chi^2 = 0.576$	0.448
Occupational therapy, n (%)	97 (81.2)	77 (96.3)	$\chi^2 = 3.909$	0.048
Speech therapy, n (%)	49 (44.6)	52 (65.0)	$\chi^2 = 7.782$	0.005
Cognitive therapy, n (%)	37 (33.6)	33 (41.3)	$\chi^2 = 1.154$	0.283
Swallowing therapy, n (%)	34 (30.9)	21 (26.3)	$\chi^2 = 0.489$	0.484
Acupuncture treatment, n (%)	16 (14.6)	14 (17.5)	$\chi^2 = 0.304$	0.581
Respiratory therapy, n (%)	24 (21.8)	16 (20.0)	$\chi^2 = 0.092$	0.761
Configuration of orthosis, n (%)	6 (5.5)	1 (12.5)	$\chi^2 = 2.981$	0.084
Steroid injection, n (%)	7 (6.4)	3 (3.8)	$\chi^2 = 0.635$	0.426
Numbers of rehabilitation therapies, median (IQR)	1 (0–3)	2 (1–3)	$Z = -1.680$	0.093

IQR: interquartile range; WBC: white blood cell; LDL: low-density lipoprotein; BI: Barthel index. The baseline variables with $P < 0.05$ in the univariate analysis were included in the binary logistic regression analysis. The results showed that the stroke course at admission (odds ratio (OR) = 0.986, 95%confidence interval (CI) = 0.979–0.993, $P < 0.001$) and the length of hospital stay (OR = 1.030, 95%CI = 1.013–1.047, $P = 0.001$) were the significant predictors of SI-ADL, while occupational therapy (OR = 3.737, 95%CI = 0.930–15.017, $P = 0.063$) and speech therapy (OR = 1.625, 95%CI = 0.812–3.252, $P = 0.170$) were not.

ADL scores were evaluated before and after the comprehensive rehabilitation therapy. They found that the ADL scores of groups 1 and 2 were significantly improved after the rehabilitation therapy, but there was no significant increase in the ADLs in group 3 after rehabilitation. This study showed that the effect of rehabilitation therapy varies significantly at different stages after stroke onset. Moreover, patients who received rehabilitation therapy before admission were mostly patients with intracerebral hemorrhage; previous studies have shown that such patients are likely to have more serious sensory, motor, and cognitive impairments. Therefore, they require additional rehabilitation therapy, and the rehabilitation process is more difficult [14, 15]. Moreover, the degree of recovery of ADLs in patients with intracerebral hemorrhage is time-dependent; i.e., the later the rehabilitation intervention commences, the more difficult is the recovery [16]. Therefore, in patients who have already received rehabilitation therapy, the effect of the second rehabilitation therapy largely depends on the timing of the treatment. If the course of the disease is too long, even if they receive rehabilitation therapy again, the treatment effect may still be unsatisfactory.

In addition, a large number of previous studies have shown that the types of rehabilitation therapies are positively correlated with an increase in ADLs [17–20]. Zhang and Zhang [21] divided 160 patients with acute stroke into two groups: 80 patients in the control group were treated with conventional medical drugs, while 80 patients in the study

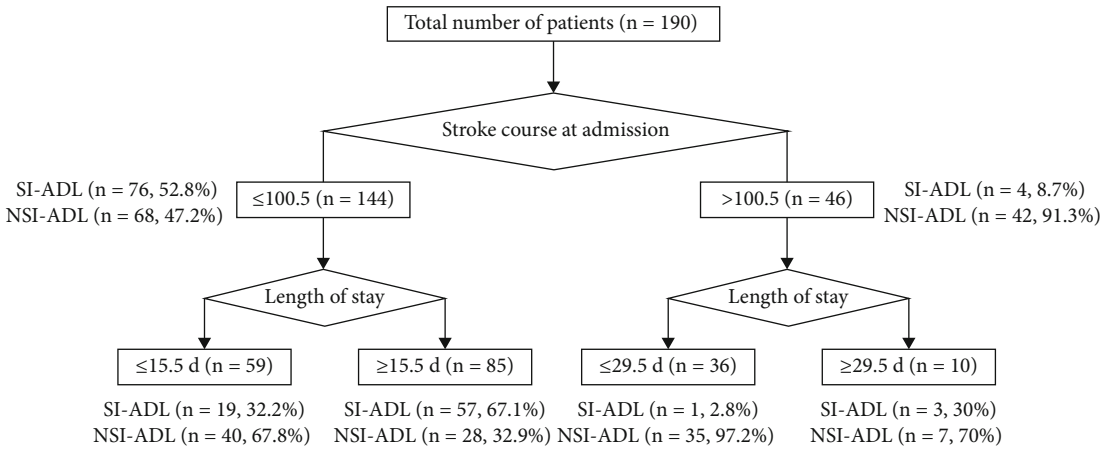

Figure 2: The SI-ADL decision tree model. The first decision node indicates the course of the stroke at admission, followed by the length of hospital stay.

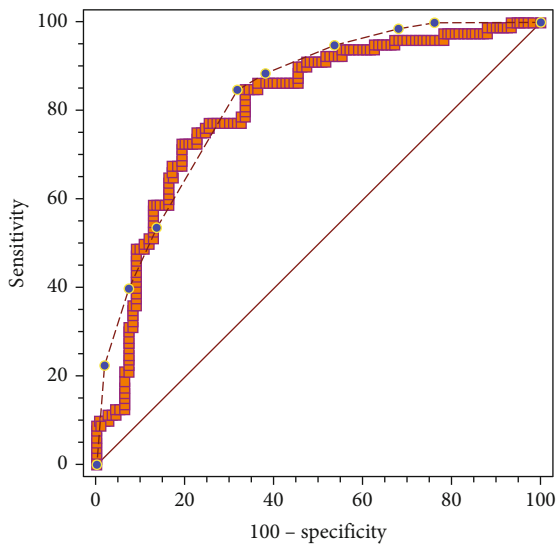

Figure 3: Comparison of the receiver operating characteristic curves between the two models. The red line with blue dots is the curve of the decision tree model, while the orange line is the curve of the logistic regression model. The area under the curve is 0.808 for the logistic regression model and 0.831 for the decision tree model. There are no significant differences between the two models.

group were treated with comprehensive rehabilitation therapy (such as exercise therapy, acupuncture, and traditional Chinese medicine). After 4 weeks, the limb motor ability and the BI scores of the patients in the study group were higher than those of the patients in the control group. Therefore, it is considered that comprehensive rehabilitation therapy can reduce the neurological deficit of patients, promote functional recovery of hemiplegic limbs, and improve ADLs. However, our study showed that patients who received more types of rehabilitation therapy did not have improved ADLs as compared with patients who received fewer types of rehabilitation therapies. This may be because the more the rehabilitation therapy administered to a patient, the more severe is the loss of basic neurological function, the longer is the course of the disease, and the longer is the hospital stay. It is worth noting that the condition of patients receiving comprehensive rehabilitation therapy still improved after treatment, and the two groups of patients had similar rehabilitation outcomes at discharge; this suggests that it is still valuable to provide comprehensive rehabilitation therapy and appropriately prolong the treatment time for patients with a serious condition and a long course of the disease. However, in the short term, it may not be possible to achieve a better recovery effect than in patients with milder symptoms.

Based on univariate analysis, it was clear that the course of the disease and a previous implementation of rehabilitation therapy at admission had an impact on the improvement of ADLs. In addition, through a binary logistic regression analysis, we showed that the course of the disease at admission and the length of hospital stay are the key factors for significant improvement in the ADLs; i.e., early rehabilitation intervention for patients with stroke and prolonged duration of rehabilitation treatment can improve the ADLs.

However, because logistic regression cannot quantify the variables that are meaningful for classification and the value of guiding the patients' treatment strategies in the clinic is limited, we further performed a decision tree analysis. The decision tree model is a reliable and effective analysis tool that can build an intuitive and understandable tree structure, quantifying the specific variables of certain prediction results and providing a basis for decision-making. Comparison of the ROC curves between the logistic regression model and the decision-tree model confirmed that the predictive value of the decision-tree model was not inferior to that of the logistic regression model; the decision tree could be used to formulate individualized rehabilitation strategies for patients with stroke.

The first consideration was the course of the disease at admission. For patients in whom the course of the disease at admission was less than 100.5 days, the probability of SI-ADL after hospitalization for rehabilitation therapy for more than 2 weeks was 67.1%. However, the probability of

SI-ADL was significantly lower in patients with a length of hospital stay of shorter than 2 weeks (only 32.2%). For patients in whom the course of the disease exceeded 100.5 days at admission, the probability of an SI-ADL was approximately 30.0% for those who were hospitalized for more than 1 month and only 2.8% for those who had been hospitalized for less than 1 month. This suggests that for patients with a long course of the disease (more than 3 months), the effect of short-term rehabilitation therapy is minimal. On the other hand, long-term inpatient rehabilitation therapy can significantly improve ADLs. Although the guidelines set the time of rehabilitation therapy for patients with stroke to within 48 hours to 2 weeks after the condition is stable, some studies have pointed out that the golden period of rehabilitation therapy is within 3 months after the stroke [22]. This is almost consistent with the 100.5 days of the course node automatically defined in the decision-tree analysis in this study. Ballester et al. [23] also found that with a longer course of the disease, the slow rehabilitation effect is due to the gradual decline in the patients' sensitivity to the treatment. For more than a year after the stroke, the patients' nerves still had some plasticity. By formulating accurate plans and adopting continuous individualized and progressive rehabilitation therapy schemes, the sensitivity to treatment can be increased and ADLs can still be improved.

The inability to implement and failure to implement rehabilitation early in many areas in China are some of the reasons for the nationwide high morality and mortality rates in patients with stroke; this has led to a huge socioeconomic burden [24]. Based on our study, although patients with late initiation of rehabilitation still benefited from adequate rehabilitation, those who had not received previous rehabilitation therapy had a lower BI score at admission. Those with lower BI scores required more types of rehabilitation during hospitalization, which resulted in an increased cost of rehabilitation. Furthermore, the shorter the stroke course, the shorter the time required for rehabilitation. Therefore, early initiation and adequate rehabilitation after stroke may be an important step for reducing the socioeconomic burdens on patients with stroke. However, early initiation of rehabilitation is limited by several barriers [25]. Tam et al. [26] used a rapid access outpatient stroke rehabilitation program for providing rehabilitation. This approach could alleviate problems such as rehabilitation ward unavailability and the inability to treat patients in the hospital for a long period. It could also improve patient compliance with rehabilitation and help both the doctors and patients choose the timing of rehabilitation initiation and treatment delivery in a flexible manner.

The limitations of this study were as follows. First, this was a retrospective single-center study with a small sample size, and selection bias may have occurred. In the future, we will perform prospective studies and expand the sample sizes to obtain more accurate results. Second, we did not conduct a long-term follow-up on the functional outcomes of the patients after discharge, because the description of the outcomes of patients with stroke generally includes the functional status, length of stay, and destination after discharge [27]. The length of stay is largely affected by the patient's economic status, medical insurance system, and other factors. In China, the postdischarge destination of patients with stroke is typically their homes, rather than nursing homes and care institutions for older patients. Thus, the length of hospital stay would be prolonged; this limits postdischarge destination as an outcome evaluation index. The functional status of the patients at discharge can avoid the influence of social factors; therefore, it is the most reliable predictor of patient outcomes after stroke [22].

5. Conclusions

Early initiation of rehabilitation and sustained rehabilitation therapy plays a key role in improving ADLs. Therefore, providing continuous and sustained rehabilitation therapy to patients with stroke, as early as possible, will help improve the efficiency of the rehabilitation therapy. This can significantly improve the quality of life of these patients.

Data Availability

The original data used to support the findings of this study are available from the corresponding author upon request.

Conflicts of Interest

The authors declare that there is no conflict of interest regarding the publication of this paper.

Authors' Contributions

QLZ and XQH were responsible for the study conceptualization and design. QLZ, ZYZ, XQH, and JX were responsible for literature review. QLZ and CZ were responsible for data analysis and interpretation of results. ZYZ, CZ, and JX were responsible for manuscript development. Qile Zhang and Zheyu Zhang contributed equally to this work and should be listed as co-first authors.

Acknowledgments

I would like to show my deepest gratitude to Dr. Sheng Zhang who has provided me with valuable guidance. This work was supported by a grant from the Quzhou Scientific and Technological Project (grant number 2018K22).

Supplementary Materials

Supplementary table I: comparison of the BI scores at admission between patients with and without rehabilitation therapy. Supplementary table II: univariate comparisons between BI scores < 60 and ≥60 at discharge. Supplementary table III: multivariate regression analysis for BI scores ≥ 60 at discharge. *(Supplementary Materials)*

References

[1] D. A. Cadilhac, J. Kim, N. A. Lannin et al., "Better outcomes for hospitalized patients with TIA when in stroke units: an

observational study," *Neurology*, vol. 86, no. 22, pp. 2042–2048, 2016.

[2] F. L. Liu, "Evaluation of the curative effect of early comprehensive rehabilitation of traditional Chinese medicine on acute stroke hemiplegia. Nei Mongol," *Journal of Traditional Chinese Medicine*, vol. 35, no. 15, 2016.

[3] Z. S. Wu, C. H. Yao, and D. Zhao, "Epidemiological study on the incidence and mortality of stroke in China," *Chinese Journal of Epidemiology*, vol. 24, no. 3, 2003.

[4] Y. Cui, S. H. Ma, and Q. W. Wu, "A study on the validity of the analysis and evaluation form of activities of daily living," *Chinese Journal of Rehabilitation Medicine*, vol. 28, no. 3, pp. 269-270, 2013.

[5] B.-H. Chao, F. Yan, Y. Hua et al., "Stroke prevention, and control system in China: CSPPC-Stroke Program," *International Journal of Stroke*, vol. 16, no. 3, pp. 265–272, 2021.

[6] J. Eraifej, W. Clark, B. France, S. Desando, and D. Moore, "Effectiveness of upper limb functional electrical stimulation after stroke for the improvement of activities of daily living and motor function: a systematic review and meta-analysis," *Systematic Reviews*, vol. 6, no. 1, p. 40, 2017.

[7] F. X. Guiu-Tula, R. Cabanas-Valdes, M. Sitja-Rabert, G. Urrutia, and N. Gomara-Toldra, "The efficacy of the proprioceptive neuromuscular facilitation (PNF) approach in stroke rehabilitation to improve basic activities of daily living and quality of life: a systematic review and meta-analysis protocol," *BMJ Open*, vol. 7, no. 12, article e016739, 2017.

[8] L. Peng, R. Xie, H. Cao, Y. Jiang, and Y. Liu, "Effect of early rehabilitation intervention on activities of daily living in stroke patients with hemiplegia," *Chinese Journal of Gerontology*, vol. 35, no. 8, pp. 2040-2041, 2015.

[9] H. Chen, Z. Yang, R. Pan et al., "Effect of integrated traditional Chinese and western medicine rehabilitation program on motor function, activities of daily living and quality of life in patients with hemiplegia after stroke," *Electronic Journal of Clinical Medical Literature*, vol. 36, no. 4, pp. 395–398, 2016.

[10] M. Yagi, H. Yasunaga, H. Matsui et al., "Impact of rehabilitation on outcomes in patients with ischemic stroke," *Stroke*, vol. 48, no. 3, pp. 740–746, 2017.

[11] Chinese Neuroscience Society, "Main points of diagnosis of major cerebrovascular diseases in China," *Chinese Journal of Neurology*, vol. 29, no. 6, pp. 379–381, 1996.

[12] B. Langhammer, K. S. Sunnerhagen, Å. Lundgren-Nilsson, S. Sällström, F. Becker, and J. K. Stanghelle, "Factors enhancing activities of daily living after stroke in specialized rehabilitation: an observational multicenter study within the Sunnaas International Network," *European Journal of Physical and Rehabilitation Medicine*, vol. 53, no. 5, pp. 725–734, 2017.

[13] Y. P. Li and L. Zhong, "Observation of the effect of comprehensive rehabilitation on patients with stroke in different periods," *Chinese Journal of Rehabilitation Theory and Practice*, vol. 8, no. 3, pp. 166–168, 2002.

[14] P. H. Katrak, D. Black, and V. Peeva, "Do stroke patients with intracerebral hemorrhage have a better functional outcome than patients with cerebral infarction?," *PM & R: The Journal of Injury, Function, and Rehabilitation*, vol. 1, no. 5, pp. 427–433, 2009.

[15] G. R. de Freitas, G. Devuyst, G. van Melle, and J. Bogousslavsky, "Motor strokes sparing the Leg," *Archives of Neurology*, vol. 57, no. 4, pp. 513–518, 2000.

[16] Y. Wang, X. F. Wang, and L. Yan, "Effect of early rehabilitation intervention on functional recovery of patients with cerebral hemorrhage," *Heilongjiang Medical Journal*, vol. 32, no. 6, pp. 441-442, 2008.

[17] C. S. Fu, "Effect of early comprehensive rehabilitation therapy on the functional reconstruction of patients with acute stroke," *China Modern Medicine*, vol. 26, no. 22, pp. 65–68, 2019.

[18] R. Gillen, H. Tennen, and T. McKee, "The impact of the inpatient rehabilitation facility prospective payment system on stroke program outcomes," *American Journal of Physical Medicine & Rehabilitation*, vol. 86, no. 5, pp. 356–363, 2007.

[19] L. de Wit, K. Putman, B. Schuback et al., "Motor and functional recovery after stroke," *Stroke*, vol. 38, no. 7, pp. 2101–2107, 2007.

[20] G. Kwakkel, R. C. Wagenaar, J. W. Twisk, G. J. Lankhorst, and J. C. Koetsier, "Intensity of leg and arm training after primary middle-cerebral-artery stroke: a randomised trial," *The Lancet*, vol. 354, no. 9174, pp. 191–196, 1999.

[21] X. N. Zhang and J. Zhang, "Effect observation of early comprehensive rehabilitation on acute cerebral apoplexy," *Clinical Research and Practice*, vol. 10, pp. 186-187, 2017.

[22] Z. Liang, C. N. Zhao, and Y. Y. Dong, "Clinical study on prediction of results of stroke rehabilitation," *Chinese Journal of Rehabilitation Theory & Practice*, vol. 8, no. 10, pp. 577-578, 2002.

[23] B. R. Ballester, M. Maier, A. Duff et al., "A critical time window for recovery extends beyond one-year post-stroke," *Journal of Neurophysiology*, vol. 122, no. 1, pp. 350–357, 2019.

[24] JianJun Yu, YongShan Hu, Y. Wu et al., "The effects of community-based rehabilitation on stroke patients in China: a single-blind, randomized controlled multicentre trial," *Clinical Rehabilitation*, vol. 23, no. 5, pp. 408–417, 2009.

[25] J. Bernhardt, G. Urimubenshi, D. B. C. Gandhi, and J. J. Eng, "Stroke rehabilitation in low-income and middle-income countries: a call to action," *The Lancet*, vol. 396, no. 10260, pp. 1452–1462, 2020.

[26] A. Tam, S. Mac, W. Isaranuwatchai, and M. Bayley, "Cost-effectiveness of a high-intensity rapid access outpatient stroke rehabilitation program," *International Journal of Rehabilitation Research*, vol. 42, no. 1, pp. 56–62, 2019.

[27] H. S. Levin, A. L. Benton, and R. G. Grossman, *Neurobehavioral Consequences of Closed Head Injury*, Oxford University Press, New York, 1982.

Hindawi
Neural Plasticity
Volume 2022, Article ID 7399995, 14 pages
https://doi.org/10.1155/2022/7399995

Research Article

The Effect of Virtual Reality on Motor Anticipation and Hand Function in Patients with Subacute Stroke: A Randomized Trial on Movement-Related Potential

Ling Chen,[1,2] **Yi Chen**,[2] **Wen Bin Fu**,[1,2] **Dong Feng Huang**,[3,4,5] **and Wai Leung Ambrose Lo**[3,4]

[1]*Department of Acupuncture and Moxibustion, The Second Clinical College of Guangzhou University of Chinese Medicine, Guangzhou, China*
[2]*Guangzhou University of Chinese Medicine, Guangzhou, China*
[3]*Department of Rehabilitation, The First Affiliated Hospital, Sun Yat-sen University, China*
[4]*Guangdong Engineering and Technology Research Center for Rehabilitation Medicine and Translation, Sun Yat-sen University, Guangzhou 510080, China*
[5]*Department of Rehabilitation Medicine, The Seventh Affiliated Hospital, Sun Yat-sen University, Shenzhen 518107, China*

Correspondence should be addressed to Dong Feng Huang; huangdf@mail.sysu.edu.cn
and Wai Leung Ambrose Lo; ambroselo0726@outlook.com

Received 24 September 2021; Accepted 9 December 2021; Published 24 January 2022

Academic Editor: Yating Lv

Background. Impaired cognitive ability to anticipate the required control for an upcoming task in patients with stroke may affect rehabilitation outcome. The cortical excitability of task-related motor anticipation for upper limb movement induced by virtual reality (VR) training remains unclear. *Aims*. To investigate the effect of VR training on the cortical excitability of motor anticipation when executing upper limb movement in patients with subacute stroke. *Methods*. A total of thirty-six stroke survivors with upper limb hemiparesis resulting from the first occurrence of stroke within 1 to 3 months were recruited. Participants were randomly allocated to the VR intervention group or conventional therapy group. Event-related potentials (ERPs) and electromyography (EMG) were used to simultaneously record the cortical excitability and muscle activities during palmar grasp motion. Outcome measures of the contingent negative variation (CNV) latency and amplitude, EMG reaction time, Upper Limb Fugl-Meyer Assessment (UL-FMA), Action Research Arm Test (ARAT), and National Institutes of Health Stroke Scale (NIHSS) were recorded pre- and postintervention. The between-group difference was analysed by mixed model ANOVA. *Results*. The EMG onset time of the paretic hand in the VR group was earlier than that observed in the control group ($t = 2.174$, $p = 0.039$) postintervention. CNV latency reduction postintervention was larger in the VR group than in the control group ($t = 2.411$, $p = 0.021$) during paretic hand movement. The reduction in CNV amplitude in the VR group was larger in the VR group than in the control group ($p < 0.001$ for all electrodes except for C3) when executing paretic hand movement. ARAT and UL-FMA scores were significantly higher in the VR group than in the control group ($p = 0.019$ and $p = 0.037$, respectively) postintervention. No significant difference in the reduction in NIHSS was found between the VR and control groups ($p = 0.072$). *Conclusions*. VR intervention is superior to conventional therapy to improve the cognitive neural process of motor anticipation and reduce the excessive compensatory activation of the contralesional hemisphere. The improvements observed in the cognitive neural process corroborated with the improvements in hand function.

1. Introduction

Stroke is one of the most severe issues encountered by the ageing population [1] as it is among the leading causes of long-term disability worldwide [2]. Published epidemiological study reported that approximately 60% of stroke survivors have motor dysfunction and 40% continue to have severe disability of the upper extremity [3]. Statistically, only 5% to 20% of stroke survivors recovered their upper limb function completely, 25% of them recover part of upper limb function, and 60% of them lost upper limb function completely [4]. Motor dysfunction of upper extremity contribute to reducing the ability to perform motor tasks such as reaching and grasping [5], which in turn affects the ability to perform activity of daily living such as eating, dressing, and washing [6, 7].

The clinical outcomes of upper extremity rehabilitation are influenced by cognitive function which directly affects the ability to acquire and execute functional skills [8, 9]. Motor anticipation is a key component of cognitive function which requires high level of the brain cognitive process [10]. It is one of the essential elements for successful motor execution since volitional movements are preceded by a period of planning, during which parameters are set for specific upcoming movement to achieve a specific goal [11]. Early literature on nonhuman primate reported increase in neural spike rate prior to movement initiation [12] which is considered a key signature of cognitive preparatory activity [11]. Study in human indicated that the brain activates 1.5 seconds before the execution of movements, while motor intention is perceived at 500 to 800 ms after the activation of the motor cortex [13]. On the other side, motor preparation requires the prediction of the physical properties of static objects and the dynamic loads generated by the objects in space [5, 14–16]. Studies in stroke survivors indicated that the ability to anticipate the required control to execute motor task is lacking [17] which contribute to motor intentionality and power accuracy out of control. Literature indicated that impaired anticipatory ability in stroke patients may present clinically as a marked increased grip force during object manipulation of the upper extremity [18–21].

The electrophysiological process that is associated with motor anticipation and whether changes in motor anticipation are associated with functional improvement are unclear in patients with stroke [22]. Existing studies indicated that a loss of frequency alpha band on the ipsilesional hemisphere was related to poor motor recovery outcome [23]. Improvement in coherence in the beta frequency band was reported to have linear relation with motor function improvement [24]. However, the frequency of alpha rhythm oscillations is associated with motor execution [25], and beta frequency is modulated during motor execution [26]. These electroencephalogram (EEG) components are suitable to assess neural activities during motor execution state but not the cognitive neural process of motor anticipation which takes place prior to the motor execution. Contingent negative variation (CNV) is a slow negative event-related potential (ERP) that can reflect the cognitive process of event-related motor preparation [27–29]. It is considered a reliable index for observing cortical excitability of motor anticipatory [22] and can be used to assess the cortical excitability during motor anticipation in stroke patients [30]. Study on source analysis indicated that CNV is generated from multiple sources, including cortical and subcortical generators of the anterior cingulate cortex, supplementary motor area, and primary motor area [27, 31, 32]. Stroke survivors with chronic hemiparesis demonstrated significantly enhanced latency and increased amplitude of late CNV at the midline during paretic and nonparetic hand preparation [27] which indicated greater anticipatory effort in response to task execution. This is given further support by a previous study which observed early CNV onset time with increased peak amplitudes of bilateral hemispheres in people with subacute stroke [31]. The study observed similar amount of computational demand from the contralesional and ipsilesional hemisphere during the motor planning phase, as reflected in the lack of significant difference in CNV latency and peak amplitude.

Virtual reality (VR) plays a prominent role in promoting functional recovery poststroke. It provides goal-orientated tasks and enriched motivational training to improve patients' ability to implement a planned motor task [32–34]. In addition, it has the potential to implement effective intervention at low cost [35]. A previously published meta-analysis identified 6 key principles of VR that are relevant to the neuroplasticity process. These principles include goal-oriented task, high number of repetition or training dosage, altering task difficulty, real-time feedback, increased users' motivation and engagement, and increased enjoyment of intensive task-relevant training [36]. Some of these principles are related to the motor planning process which may contribute to the improvement of upper limb motor function. The combination of exoskeletal support and VR was supposedly able to further promote the function recovery in patients with stroke [36]. A previous study utilised a combination of exoskeletal support and VR training to assess the impact on the motor planning process and gait function [37]. The study observed strong mu rhythm and event-related spectral perturbations post-VR intervention which were associated with clinical improvement in gait. This study offered some insight into the potential benefit of VR intervention on motor planning and subsequent functional recovery. To date, there is limited evidence on whether the cognitive neural process of motor planning may be improved by VR intervention and whether changes in the cognitive neural process may contribute to upper limb functional improvement. The aims of the present study were to investigate the impact of VR intervention on motor anticipation and upper limb function in people with subacute stroke. This study hypothesised that patients with stroke who underwent VR training had significant reduction in CNV latency and amplitude when executing palmar grasp movement with the paretic hand. Upper limb function would also improve significantly post-VR intervention. Improvements observed in the VR intervention group were significantly larger than the improvements observed in the conventional therapy group. A preprint of the article has previously been published [38].

2. Methods

2.1. Study Setting. This trial was a parallel randomized, single-blinded, controlled trial. Data collection took place in the Department of Rehabilitation, First Affiliated Hospital, Sun Yat-sen University.

2.2. Ethics. This study was approved by the Ethical Committee of the First Affiliated Hospital of Sun Yat-sen University (ethics approval number [2020]073). All participants were provided with a comprehensive explanation of the experimental procedure and a participant information sheet. Informed consent was obtained from all participants prior to study enrolment.

2.3. Recruitment and Sample Size. Recruitment took place between July 2016 and June 2018 in the inpatient ward of the Department of Rehabilitation Medicine, the First Affiliated Hospital of Sun Yat-sen University. The inclusion criteria were as follows: (1) first ever occurrence of stroke within 1 to 3 months, (2) stroke occurrence confirmed by magnetic resonance imaging (MRI) or computed tomography (CT), (3) age between 40 and 80 years, (4) having at least 20° of wrist flexion/extension and at least 10° of finger flexion and extension of the paretic limb, (5) able to sit for at least 30 minutes without assistance, and (6) no severe cognitive impairment (Mini-Mental State Examination > 21) [39]. The exclusion criteria were as follows: (1) brainstem injury, (2) hand deformity, and (3) visual field deficits. Suitable participants were identified by the clinical team during the routine medical admission procedure. Patients were then approached by a member of the research team who was not involved in providing medical care to explain about the study. All approached patients were asked to contact a member of the research team to express their interest.

Sample size was based on a pilot trial where 16 subacute stroke participants were allocated into VR and control groups. CNV latency during paretic hand movement postintervention was used as the primary outcome measure for sample size calculation. The calculation of sample size was conducted in the software GPower ver 3.1.2, using "A priori: Compute required sample size –given α, power, and effect size" as the type of power analysis. Preliminary results indicated a mean CNV latency of 1740.22 ms (SD 120.78) for the control group and 1614 ms (SD 122.61) for VR group postintervention, which gave an effect size of 0.50. With α error probability of 0.05 and a power of 0.95, a sample size of 36 was sufficient for the present study. Figure 1 shows the number of participants at each stage of the study.

2.4. Randomization, Concealment, and Blinding. Participants were randomly allocated to either VR group or control group in a 1 : 1 ratio by simple randomization. The randomization schedule was calculated in the statistical software SPSS (IBM SPSS Statistics version 20, USA) by a statistical expert from the Faculty of Medical Statistics and Epidemiology, Sun Yat-sen University. The sequence of allocation was kept in sealed envelopes and revealed by a member of the research team after the participant was enrolled. Participants were blinded from their group allocation but were informed that they had an equal chance of allocation to the VR or control group before study participation. The outcome assessor was blinded to group allocation, but the treating therapists were not blinded.

2.5. Procedure. Interventions were delivered for 2 weeks with 5 training sessions per week. Each session lasted for 60 minutes. Designated therapists provided either VR training or occupational therapy for upper limb function in addition to routine medical care and other rehabilitation deemed necessary by treating physicians.

2.6. Outcome Measures. Outcome measures of behavioural data included EMG onset time and CNV latency. CNV peak amplitude was adopted to assess the cortical excitability during the motor planning phase. Clinical assessment scales of the Action Research Arm Test (ARAT) [40], Upper Limb Fugl-Meyer Assessment (UL-FMA) [41], and National Institutes of Health Stroke Scale (NIHSS) were adopted to assess clinical functions.

2.7. Intervention. The nonimmersive VR intervention was delivered through an interactive training system (A2, YiKang Ltd., China) which comprised of a computer screen to display the virtual environment and a passive weight support exoskeleton arm. In a nonimmersive VR system, users interact with the virtual environment on a computer screen [42] with the exoskeleton arm as an interface. During VR intervention, participants were seated in front of a table facing the monitor, with the arms placed on the exoskeletal weight support. Figure 2(a) illustrates the setting of the VR system. The exoskeleton arm support provided passive weight support at the elbow and wrist joints. A grip sensor was embedded in the handle bar to detect the application of grip force. The VR training tasks were provided to train the motion of reaching and reach to grasp. These tasks were as follows: (1) fried egg, (2) apple picking, and (3) archery. The tasks of fried egg and apple picking involved the users to first reach out to a virtual object, grasp the virtual object, and then transfer it to a designated area. Both of these tasks were designed for grasping and finger movement training. For the archery task, participants were asked to grip and maneuverer the virtual arrow to aim the target, followed by the release of the virtual arrow. This training item was designed for the training of pinching motion. The training for each task lasted for 15 minutes, giving a total intervention time of 45 minutes. Participants in the control group received conventional occupational therapy that consisted of task-orientated motor training, including grip strength, selective finger movement, and activities of daily living. Training frequency was matched to that in the VR group.

2.8. ERP Paradigm. The ERP experimental procedure and paradigms adopted in the present study were in accordance with a published study [31]. Participants were seated in front of a table in an electrically shielded laboratory with shoulders positioned between 0 and 10° flexion, elbows at 130° flexion, and wrists orientated in a neutral position. The motion of palm opening and closing of the hand occurred in the horizontal plane. Figure 2(b) illustrates the starting

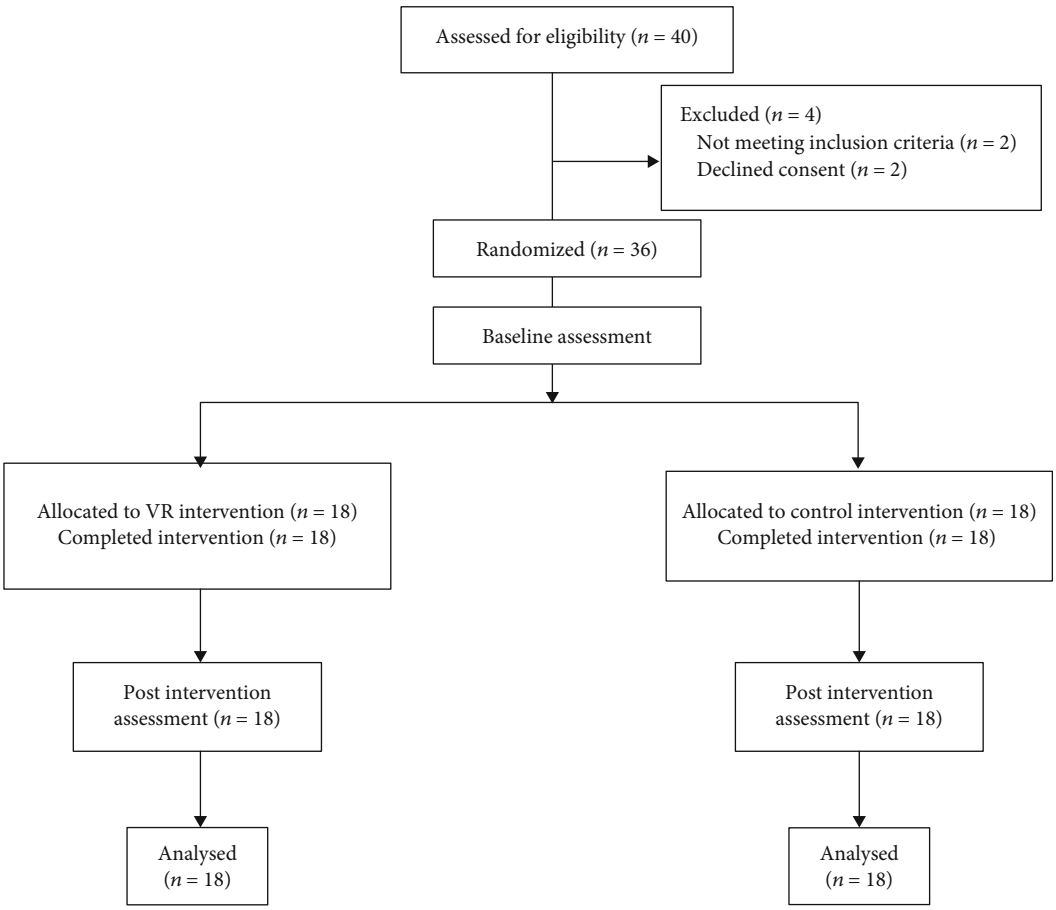

Figure 1: Flow diagram of the study.

position of the experiment. The procedure of the experiment was first explained to all participants verbally and was followed by 5 to 10 minutes of practice to familiarise with the protocol. Signal recording then began.

Figure 2(c) illustrates the locations of the EEG electrodes that record the regions of interest during simultaneous recording of EEG and EMG. The ERP paradigm was as follows: a white fixation point "+" first appeared in the centre of the screen for 500 ms. Then, visual and auditory cues (S1) were given simultaneously for 2000 ms. A picture cueing grasp motion with either the left or right hand was displayed on the screen, accompanied by an auditory cue to indicate right or left side palmar grasp. During S1, the participants were required to judge the palmar grasp task. Then, a grey reaction window (S2) of 3000 ms appeared; the participants performed left or right palmar grasp and avoid making compensatory movements. Then, a dark screen of 2000 ms appeared; the participants restored their fingers and then entered the next trial. The experiment consisted of 40 trials for each hand, totalling 80 trials. The order of the trials was randomized. Figure 3 illustrates the diagram of the ERP paradigm.

2.9. EEG. EEG activities were recorded by a 32-channel QuickAmp amplifier and Ag/AgCl scalp electrodes (Brain Products, Germany). The electrodes were positioned in accordance with the international 10-20 system. Electrodes were filled with conductive gel to maintain the impedance below 5 kΩ EEG. EMG signals were recorded in DC mode and sampled at 1000 Hz synchronized with event markers.

2.9.1. Regions of Interest. Six electrodes of interest related to motor function were extracted for EEG analysis (left hemisphere: F3 and C3, right hemisphere: F4 and C4, and midline region: Fz and Cz). The F3, F4, and Fz lie over the premotor cortex, and the C3, C4, and Cz lie over the primary motor cortex. For the purpose of statistical comparison, the left and right side hemispheres were flipped right to left in the participant with a right hemispheric lesion so that the "left" hemisphere was always the lesioned hemisphere [22].

2.10. EMG. The EMG activities were simultaneously recorded with EEG. Two surface electrodes were placed along the extensor digitorum using 2 surface electrodes with a 2 cm interelectrode distance. The EMG reaction time was measured with the time from S1 to the EMG onset as shown in Figure 4(a).

2.11. Signal Processing. EEG signals were referenced to the bilateral mastoid. Eye movement artefacts were removed through the Ocular Correction Independent Component Analysis (ICA) as part of the standard operating procedure [14]. EEG and EMG signals were filtered using a 50 Hz notch

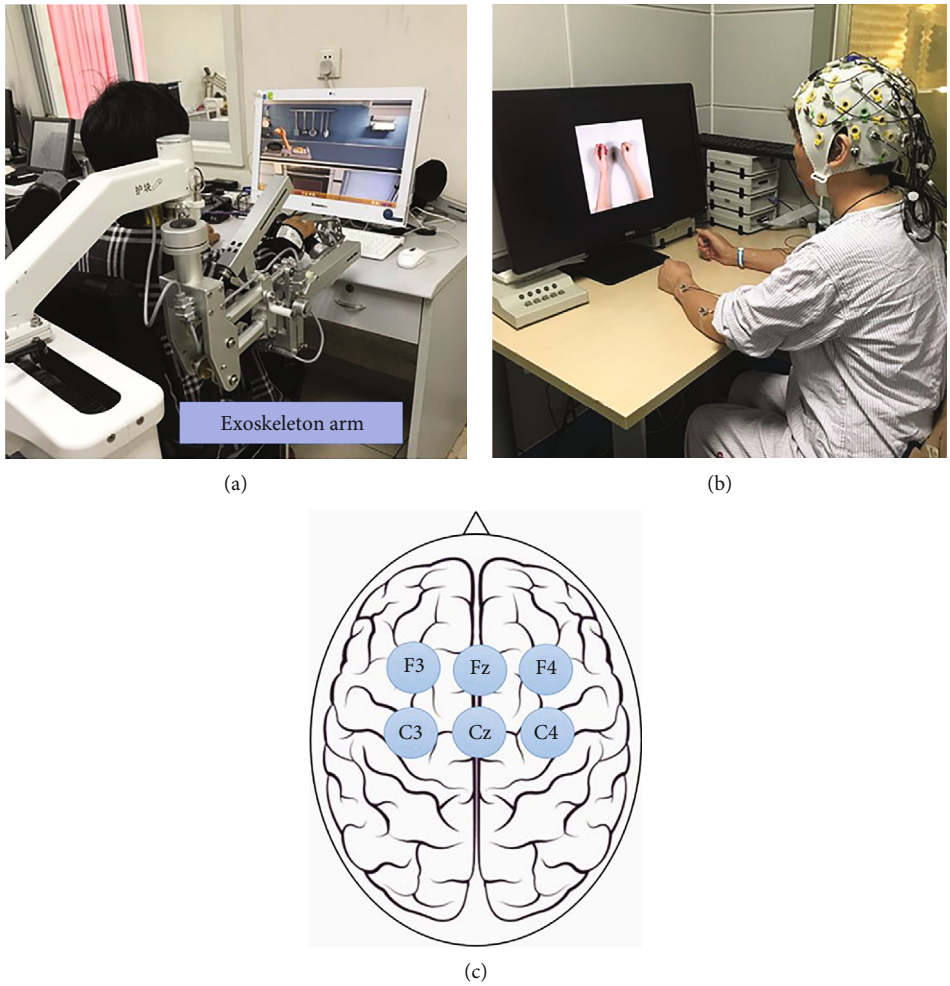

Figure 2: Diagrams of the experimental setup.

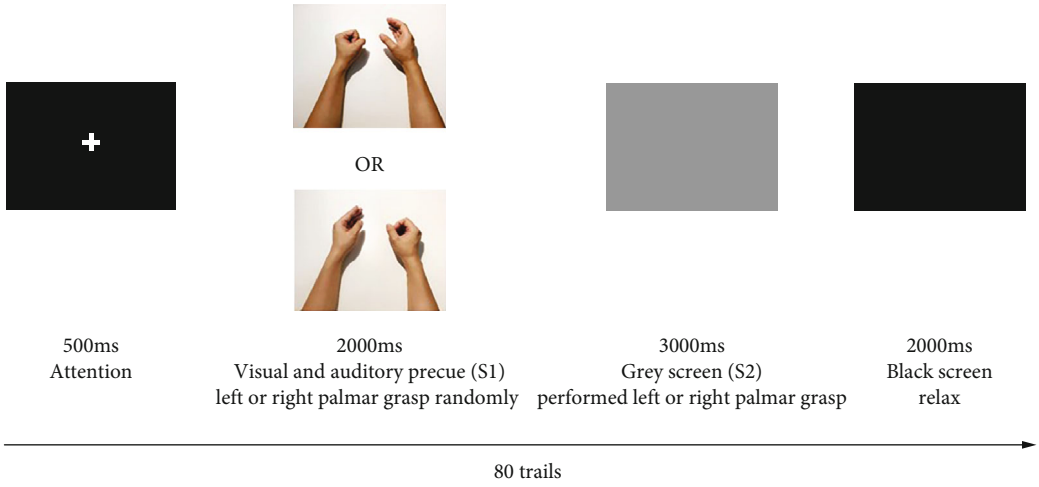

Figure 3: The ERP experiment paradigm.

filter and a bandpass filter from 0.1 to 30 Hz. In order to acquire stimulus-locked ERPs, the EEG and EMG signals were segmented into epochs of 500 ms pre- to 3000 ms post aligned to S1. The baseline was corrected according to the first 200 ms of the epochs, which was the 200 ms time window before the S1 onset.

The EMG reaction time was measured with the time from S1 to the EMG onset. As the maximum CNV amplitude was

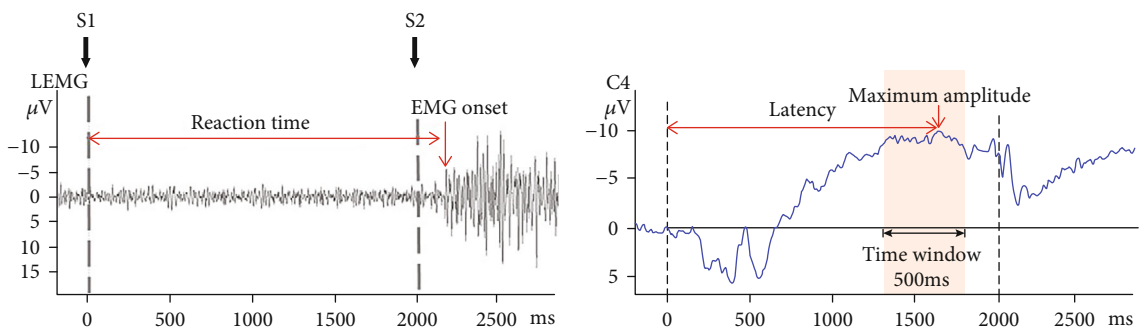

(a) EMG reaction time from S1 to the EMG onset

(b) Time window for CNV latency and mean amplitude

Figure 4: Timing window for signal processing data.

detected between 1300 ms and 1800 ms after S1, peak detection was used to detect the maximum CNV amplitude in this time window. The maximum amplitude must be higher than the amplitude of 2-3 points on the front and back sides [43]. The CNV latency was calculated as the time from S1 to the maximum amplitude. The mean CNV amplitude was calculated from 1300 to 1800 ms to acquire the average amplitude of the CNV potential (Figure 4(b)).

2.12. Statistical Analysis. Statistical analyses were performed using SPSS version 22 (IBM SPSS Statistics version 20, USA). The Wilcoxon signed-rank test was applied to verify the statistical significance of the changes in the ARAT, UL-FMA, and NIHSS within groups, and the Mann-Whitney U test was conducted to compare between the two groups. For EMG reaction time and CNV latency analyses, mixed model analysis of variance (ANOVA) was calculated, with TASK (paretic hand movement vs. nonparetic hand movement) and TIME (baseline vs. posttraining) as within-subject factors and GROUP (VR group vs. control group) as the between-subject factor. Mixed ANOVA with TASK (paretic hand movement vs. nonparetic hand movement), ELECTRODE (F3, C3, F4, C4, Fz, and Cz), and TIME (baseline vs. posttraining) as the within-subject factor and GROUP (VR group vs. control group) as the between-subject factor was performed to assess the training effects. The Greenhouse-Geisser adjustment was applied to adjust the degrees of freedom if the assumption of Mauchly's test of sphericity was not significant. Separate mixed model ANOVAs were tested for each level of electrodes. If there was a significant interaction in the within-subject factor and between-subject factor, then subsequent independent sample t-tests were performed to further investigate the differences between the two groups. The significance level for all statistical analyses was set at 0.05. Bonferroni-adjusted significance tests were performed to correct the p values of electrodes for multiple comparisons. Thus, the corrected significance level for the electrode was $\alpha = 0.05 \div 6 = 0.008$ [44].

3. Results

3.1. Demographics. A total of 40 patients were screened, and 4 patients were excluded. The final sample population included 36 participants with upper limb hemiplegia resulting from the first occurrence of stroke. All enrolled participants completed the study, and the number of participants included in the analysis was as planned. Eighteen participants were allocated to the VR group, and 18 participants were allocated to the control group. Table 1 gives a summary of the demographic data and clinical characteristics of the sample cohorts. The independent sample t-test showed no significant difference in the number of cases, sex, and age between the VR group and the control group ($p > 0.05$). The Mann-Whitney U tests showed no significant difference in the UL-FMA, ARAT, and NIHSS scores between the two groups before treatment ($p > 0.05$).

3.2. Behavioural Data

3.2.1. EMG Reaction Time. The mixed model ANOVA indicated a significant main effect of TIME ($F(1, 34) = 483.326$, $p \leq 0.001$) and a significant interaction between TIME and GROUP ($F(1, 34) = 5.680$, $p = 0.023$), as well as TIME and TASK ($F(1, 34) = 14.943$, $p \leq 0.001$). Subsidiary analysis showed that the EMG onset time of the nonparetic hand task was significantly earlier than that of the paretic hand task in both groups before treatment ($F(1, 34) = 21.099$, $p \leq 0.001$), whereas the two groups did not differ significantly of the nonparetic or the paretic hand task ($F(1, 34) = 0.339$, $p = 0.564$). After treatment, there was a significant main effect of TASK ($F(1, 34) = 5.286$, $p = 0.028$); the EMG onset time of the nonparetic and the paretic hand task in both groups was earlier than baseline (all $p \leq 0.001$). In addition, the EMG onset time of the paretic hand in the VR group was earlier than that observed in the control group ($t = 2.174$, $p = 0.04$). There is no significant difference in the EMG onset time of the nonparetic hand between the two groups ($t = 1.547$, $p = 0.13$). Table 2 presents the comparison of the EMG onset time before and after intervention for both groups.

3.2.2. CNV Latency. The mixed model ANOVA conducted on the CNV latency revealed a significant main effect of TIME ($F(1, 34) = 339.54$, $p < 0.001$) and a significant interaction between TIME and GROUP ($F(1, 34) = 4.855$, $p = 0.034$). Subsidiary analysis showed that at baseline, the main effect of GROUP ($F(1, 34) = 2.014$, $p = 0.165$) and the interaction between GROUP and TASK ($F(1, 34) = 0.013$, $p = 0.911$) did not reach significance, which indicated that there

Table 1: Demographics and clinical characteristics of the sample cohorts. UL-FMA: Upper Limb Fugl-Meyer Assessment; ARAT: Action Research Arm Test; NIHSS: National Institutes of Health Stroke Scale; MMSE: Mini-Mental State Examination.

	VR group ($n = 18$)	Control group ($n = 18$)
Age (SD), y	57.8 (8.4)	58.4 (9.3)
Sex		
Male	10	10
Female	8	8
UL-FMA	26.33 (6.04)	26.00 (7.09)
ARAT	18.55 (5.97)	18.33 (5.17)
NIHSS	5.44 (2.91)	5.39 (2.85)
MMSE	26.05 (2.64)	25.61 (2.87)

was no significant intergroup difference in the CNV latency at baseline. After treatment, a significant main effect of TASK ($F(1, 34) = 5.286$, $p = 0.028$) was observed. Subsequent analysis revealed that the CNV latency of the paretic and nonparetic hand in both groups were earlier than baseline (VR group: paretic hand: $t = 8.040$, $p \leq 0.001$, nonparetic hand: $t = 11.775$, $p \leq 0.001$; control group: paretic hand: $t = 11.886$, $p < 0.001$, nonparetic hand: $t = 11.106$, $p \leq 0.001$). In addition, the change in the CNV latency of the paretic hand after treatment was better in the VR group than in the control group ($t = 2.411$, $p = 0.021$), whereas the change of the nonparetic hand between the two groups did not differ ($t = 1.151$, $p = 0.258$). Table 3 presents the comparison of CNV latency before and after intervention for both groups during nonparetic and paretic hand movements.

3.3. CNV Amplitude. The mixed model ANOVA on the CNV amplitude between the VR group and control group of nonparetic and paretic hand tasks revealed a significant interaction between TASK, TIME, GROUP, and ELECTRODE ($F(5, 170) = 6.915$, $p \leq 0.001$), significant interaction between GROUP and TIME ($F(1, 34) = 156.167$, $p \leq 0.001$), and significant interaction between TIME and ELECTRODE ($F(5, 170) = 4.383$, $p = 0.01$). The CNV amplitude was modulated by TIME condition ($F(1, 34) = 501.293$, $p \leq 0.001$) and ELECTRODE condition ($F(5, 170) = 6.063$, $p \leq 0.001$). Therefore, TIME, GROUP, ELECTRODE, and TASK were tested for individual effects. At baseline, the interaction between TASK, GROUP, and ELECTRODE was not significant ($F(1, 34) = 0.267$, $p = 0.609$), which indicated that there was no significant difference in CNV amplitude of the nonparetic and paretic hand between the VR group and control group before treatment. After treatment, significant main effects of GROUP ($F(1, 34) = 3.393$, $p = 0.02$) on CNV amplitude were observed, which indicated significant improvement in CNV amplitude during nonparetic hand and paretic hand movement in both groups after treatment ($p \leq 0.001$). Further investigation revealed that there was a significant main effect of TIME on the paretic ($F(1, 34) = 2.744$, $p = 0.033$) and nonparetic hand ($F(1, 34) = 5.341$, $p \leq 0.001$) in the VR group and on the paretic ($F(1, 34) = 7.803$, $p \leq 0.001$) and nonparetic hand ($F(1, 34) = 7.944$, $p \leq 0.001$) in the control group. Then, the reduction in CNV amplitude between the VR group and control group after treatment was analysed. There was a significant interaction between TASK, GROUP, and ELECTRODE ($F(5, 170) = 3.560$, $p = 0.03$). The reduction in CNV amplitude in the VR group was better than that in the control group ($p \leq 0.001$) when executing paretic hand movement, while the reduction in CNV amplitude was better in the VR group than in the control group ($p \leq 0.001$) when executing nonparetic hand movement. Table 4 presents the changes in CNV amplitude in the VR and control groups during nonparetic hand and paretic hand movements. Figure 5 shows the topographic maps of participants in two groups when executing paretic and nonparetic hand movement tasks. Figures 6–9 give the graphical representations of CNV amplitudes for the VR and control groups during paretic and nonparetic hand movement.

3.4. Clinical Functions. The scores of UL-FMA, ARAT, and NIHSS improved in both groups after intervention. The improvements in ARAT and UL-FMA in the VR group were significantly higher than those in the control group (UL-FMA: $Z = -2.338$, $p = 0.02$; ARAT: $Z = -2.088$, $p = 0.04$). No significant difference in the reduction in NIHSS was observed between the VR and control groups ($Z = -1.801$, $p = 0.07$). Table 5 presents a summary of the changes in NIHSS, UL-FMA, and ARAT in the VR group and control group.

4. Discussion

The present study investigated the impact of VR intervention on motor anticipation and upper limb function in patients with subacute stroke. One of the main findings was that EMG response time was significantly shorter in the VR group than in the control group during paretic hand movement postintervention. The reduction of CNV latency and peak amplitude in the VR group was significantly more than that in the control group. The improvements of upper limb motor function were significantly higher in the VR group than in the control group after treatment.

4.1. EMG Onset and CNV Latency. The reaction time of EMG is attributed to the effect of muscle onset, whereas CNV latency is related to the brain's computational demand and cognitive processing speed when executing a movement [45–47]. Impairments in motor anticipation among subacute stroke patients could be manifested as a delay in EMG reaction time and increased preparation time of cerebral hemispheres. This is supported by neural electrophysiological study which indicated a significant increase in cortical preparatory activation correlated with a behavioural enhancement [48]. In this study, the EMG response time and CNV latency decreased after intervention in both groups, which indicated that the EMG onset was earlier and the motor anticipation time of bilateral cerebral hemispheres was shortened in both groups. Previous studies reported that subacute stroke patients demonstrated a typical response-priming effect, with extended reaction time and CNV latency [22, 31]. The shorter reaction time might

Table 2: Comparison of EMG onset time before and after intervention during nonparetic and paretic hand movements.

Group	Pre (ms)	Post (ms)	t	p
Nonparetic hand				
VR group	2419.71 ± 95.14	2378.93 ± 98.73	10.27	≤0.001
Control group	2449.56 ± 122.27	2418.75 ± 114.92	6.08	≤0.001
Paretic hand				
VR group	2526.3 ± 121.78	2472.06 ± 117.28	15.77	≤0.001
Control group	2532.19 ± 122.40	2486.56 ± 121.75	23.05	≤0.001

Table 3: Comparison of CNV latency before and after intervention during nonparetic and paretic hand movements.

Group	Pre (ms)	Post (ms)	In change (ms)	t	p
Nonparetic hand					
VR group	1661.33 ± 134.48	1553.00 ± 117.88	106.06 ± 54.39	11.78	≤0.001
Control group	1654.56 ± 197.50	1565.94 ± 197.77	88.61 ± 30.74	11.11	≤0.001
p			0.26	1.15	
Paretic hand					
VR group	1712.33 ± 143.99	1593.39 ± 134.39	111.89 ± 39.18	8.04	≤0.001
Control group	1714.33 ± 191.95	1631.56 ± 193.41	82.78 ± 30.73	11.89	≤0.001
p			0.02	2.41	

Table 4: Changes in CNV amplitude in the VR and control groups during nonparetic hand and paretic hand movements.

Nonparetic hand movement (mV)				Paretic hand movement (mV)		
Electrode	VR group	Control group	p	VR group	Control group	p
C3	2.06 ± 0.49	1.16 ± 0.26	≤0.001	1.84 ± 0.52	1.21 ± 0.37	≤0.001
Cz	2.11 ± 0.40	1.35 ± 0.27	≤0.001	2.18 ± 1.18	1.29 ± 0.24	0.01
C4	1.96 ± 0.34	1.31 ± 0.21	≤0.001	1.91 ± 0.58	1.08 ± 0.24	≤0.001
F3	1.37 ± 0.62	1.19 ± 0.19	0.26	1.92 ± 0.52	1.24 ± 0.19	≤0.001
Fz	2.27 ± 0.87	1.23 ± 0.31	≤0.001	2.09 ± 0.50	1.37 ± 0.30	≤0.001
F4	2.06 ± 0.94	1.20 ± 0.24	≤0.001	2.04 ± 0.71	1.05 ± 0.30	≤0.001

be related to the improvement in the neurocognitive process to plan an upcoming task. The larger reduction in reaction time in the VR group than that observed in the control group during paretic hand movement posttraining suggested that VR intervention may be more effective than conventional therapy training to improve the cognitive neural process. Task-oriented VR training requires the user to have an understanding of the upcoming task to be able to complete the task which in theory is able to improve cognitive function. The reduction in EMG reaction time and CNV latency tended to approach normal level postintervention, indicating an improvement in neural activation efficiency of motor anticipation and the improvement of motor dynamics of upper limb function [49]. Therefore, VR training may improve hemiplegic upper limb motor anticipation by promoting neuronal activation in stroke patients. This finding is consistent with a published study that investigated the cortical latency and central motor conduction time in stroke patients who underwent VR intervention [50] when assessed by transcranial magnetic stimulation. As with the finding of the present study, the improvement in cortical latency and central motor conduction time was significantly higher in the intervention group than in the control group. The potential mechanism underpins that the improvement in cognitive neural function is the reaction of brain neurotransmitters pathways, including cholinergic and dopaminergic pathways [51]. These provide further support that VR intervention may be superior to the control therapy in improving cognitive neural function.

4.2. CNV Amplitude. CNV amplitude is an index of anticipation and reflects the amount of cognitive neural resource [52] required to plan an upcoming task [29, 53]. Early literature reported cerebral activity of the contralesional hemisphere in the early stage of stroke during movement of the paretic side [54, 55]. A published study reported that

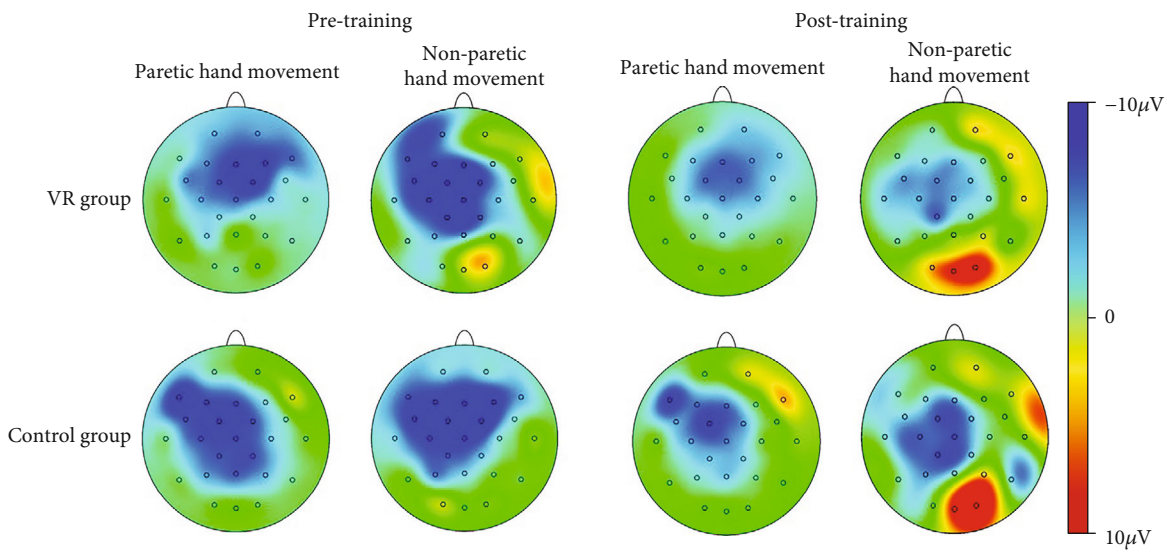

Figure 5: Topographic maps of participants in the two groups when executing paretic and nonparetic hand movement tasks.

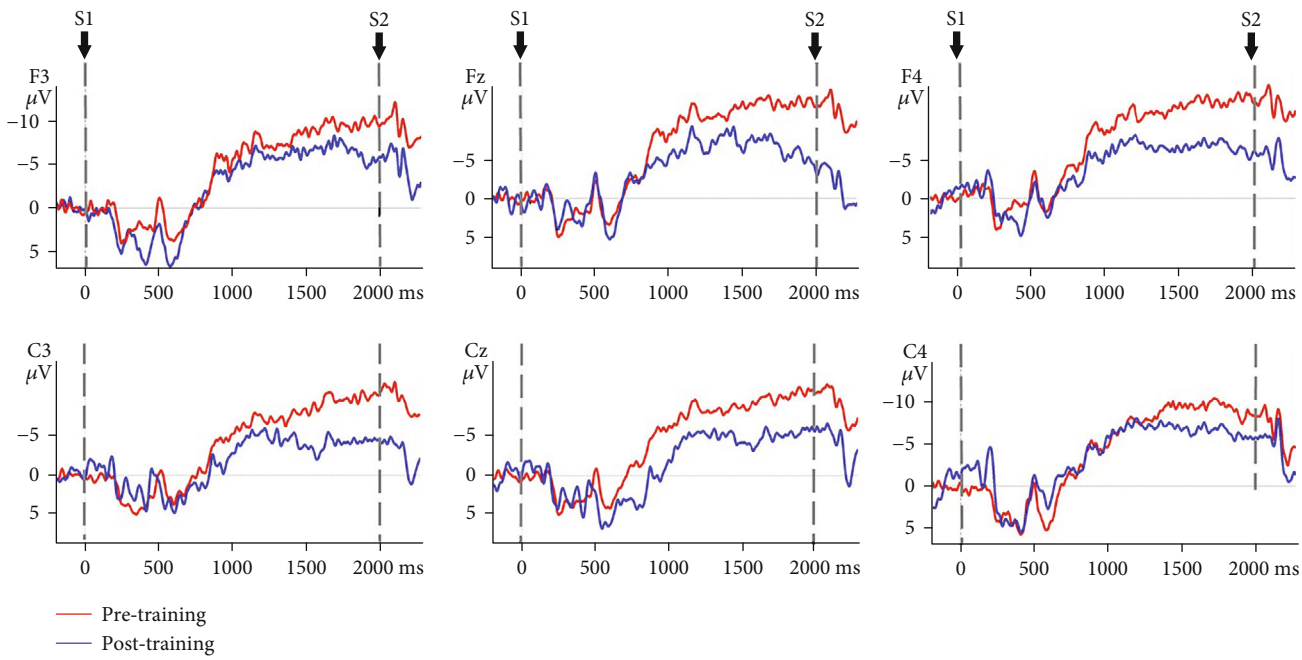

Figure 6: CNV amplitudes of the VR group during paretic hand movement. Negative is plotted upwards. Note: the 200 ms epoch prior to the S1 onset was the baseline CNV amplitude. The onset is at 0 ms point and is the S1 trigger time.

subacute stroke patients recruit additional neural resources from the contralesional hemisphere during the motor planning phase of grasp motion [27, 31], as indicated by an increase in CNV amplitude in the lesional and contralesional hemispheres during paretic hand movement. Our previous EEG study indicated significant increase in cortical activity at contralesional C4 and ipsilesional C3 electrodes during nonparetic hand movement in patients with stroke [31]. The increase in bilateral cortical activity is related to the compensatory overactivation of the contralesional hemisphere and the lack of cross hemispheric inhibition from the lesional to nonlesional hemisphere. The present study observed significantly larger reduction in CNV amplitude in the midline and contralesional and ipsilateral area during nonparetic hand movement and paretic hand movement in the VR group than in control group. The reduction in CNV amplitude corresponds to the improvement in upper limb function which provides further support that VR intervention may be effective in reducing interhemispheric misbalance compared to conventional training. The reduction in CNV amplitude postintervention is also consistent with MRI studies suggesting that neuroplasticity recovery

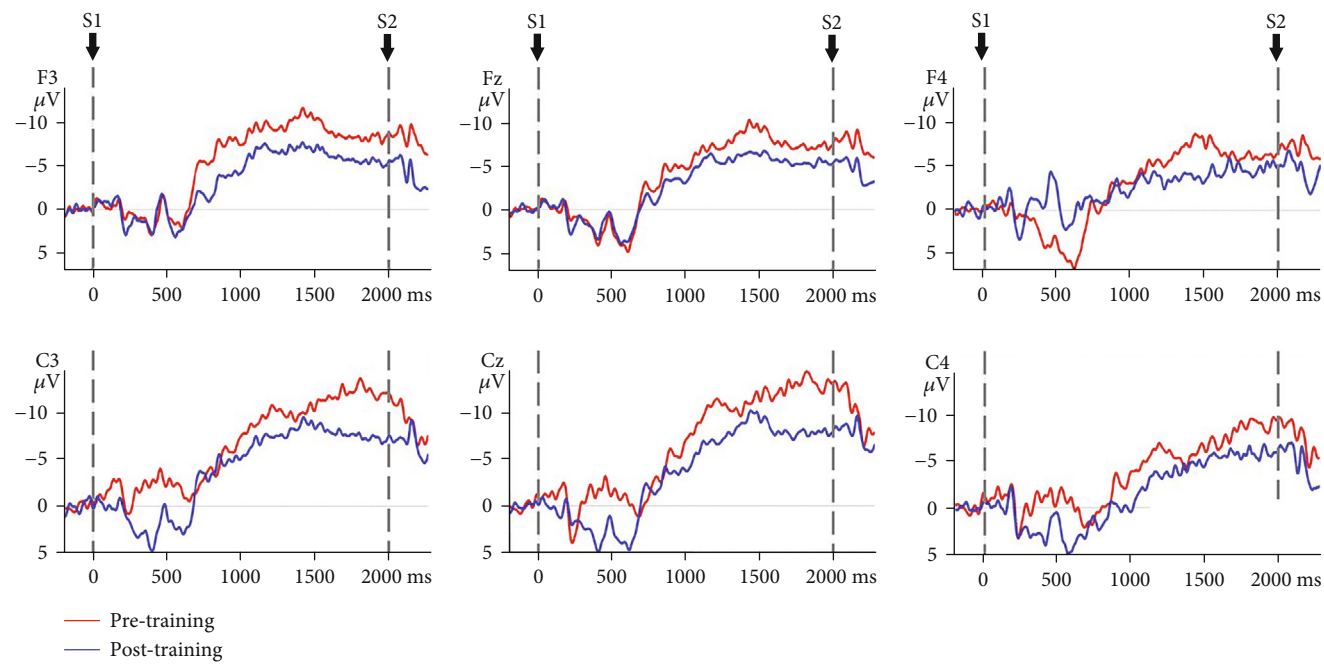

Figure 7: CNV amplitudes of the VR group during nonparetic hand movement. Note: negative is plotted upwards. The 200 ms epoch prior to the S1 onset was the baseline CNV amplitude. The onset is at 0 ms point and is the S1 trigger time.

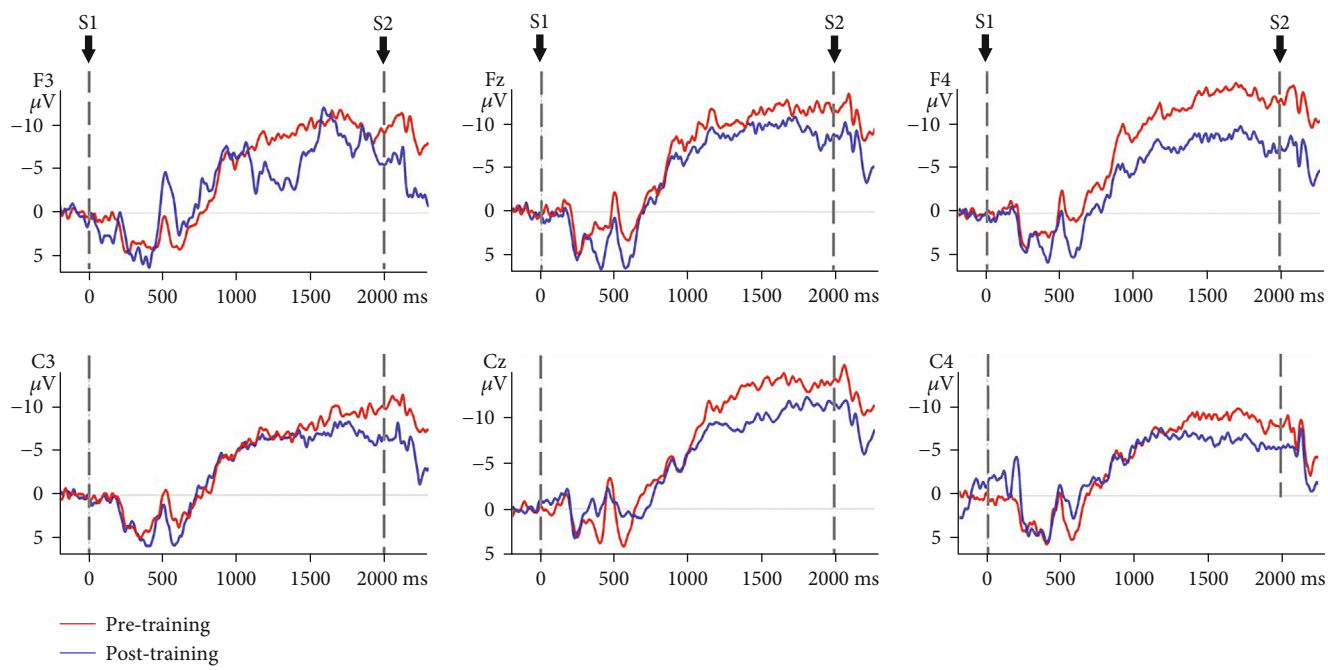

Figure 8: CNV amplitudes of the control group during paretic hand movement. Note: negative is plotted upwards. The 200 ms epoch prior to the S1 onset was the baseline CNV amplitude. The onset is at 0 ms point and is the S1 trigger time.

manifested as a decrease in sensorimotor cortex activation on the contralesional hemisphere [54], which can be interpreted as an increase in the efficiency of neural activation. Correlation between the recovery of motor function and relateralization of activation in the contralateral hemisphere was also reported [56]. Thus, the reorganization of motor control occurs after stroke and may involve the ipsilateral or contralateral cortex, depending on the location and size of the brain lesion and theoretically on the somatotopic organization of the residual pyramidal tracts [57]. The observed significantly larger reduction of CNV amplitude in the VR group during paretic hand movement provides further support that VR intervention may be effective in reducing hyperactivity of the contralesional hemisphere.

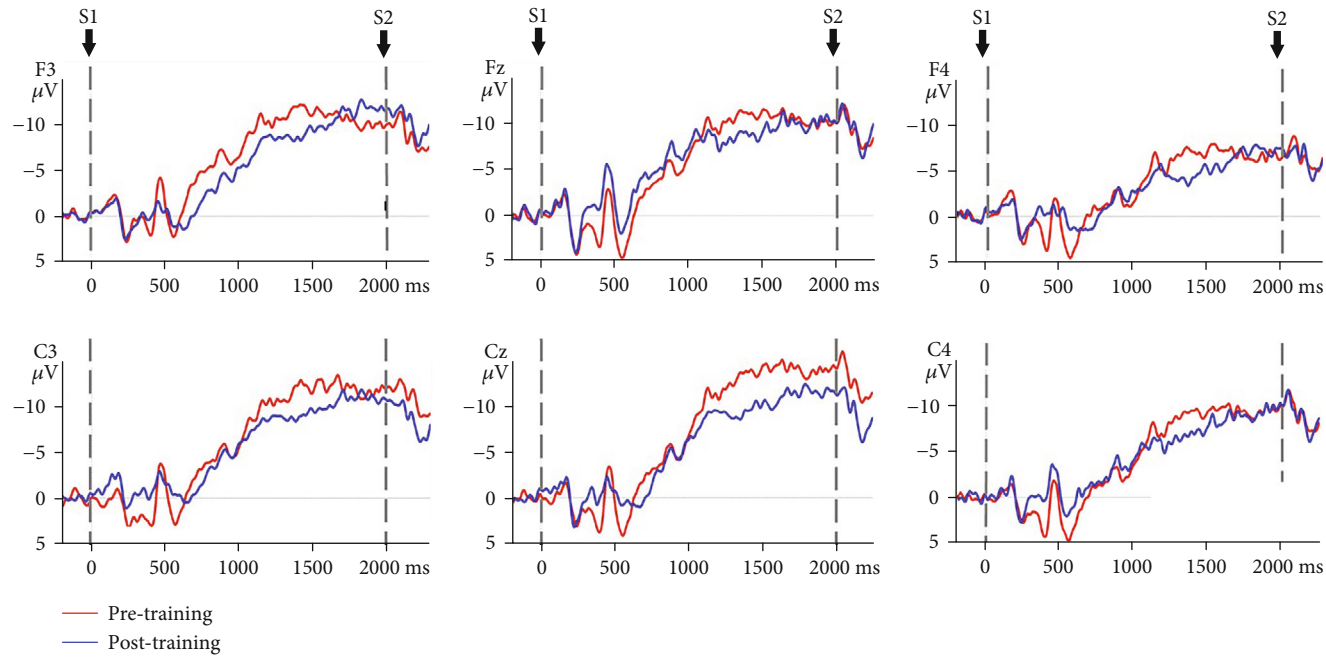

Figure 9: CNV amplitudes of the control group during nonparetic hand movement. Note: negative is plotted upwards. The 200 ms epoch prior to the S1 onset was the baseline CNV amplitude. The onset is at 0 ms point and is the S1 trigger time.

Table 5: A summary of the changes in NIHSS, UL-FMA, and ARAT in the VR group and control group.

Group	UL-FMA	ARAT	NIHSS
VR group	4.72 ± 0.87	5.06 ± 0.91	2.17 ± 0.83
Control group	3.89 ± 1.15	4.11 ± 1.20	1.83 ± 0.50
Z	-2.338	-2.09	-1.80
p	0.02	0.04	0.07

The finding is given further support by another study that reported a reduction in the lateral index and the decrease in excessive dominance of the contralateral hemisphere post-VR intervention. Therefore, this study further supports that VR intervention may be more effective in reducing hemispheric lateralization compared to conventional occupational therapy [49].

4.3. Upper Limb Function. Both of the ARAT and UL-FMA demonstrated significant improvements in both VR and conventional therapy groups. The improvements in both ARAT and FMA-UA were significantly higher in the VR group than in the control group. These findings indicated that VR training may be superior to the conventional therapy in promoting motor function of the upper limb. The improvement in upper limb function induced by VR intervention is consistent with the results reported in a systematic review of a small to medium effect in favor of VR intervention when compared with conventional therapy [8]. Despite the statistical significant difference observed between the VR and conventional therapy groups, the actual between-group differences in UL-FMA and ARAT were small and less than the minimal clinically important difference [58, 59]. A Cochrane review stated that studies that reported superior outcome of VR tended to adopt VR as an augmentation to usual dosage of therapy where participants received more treatment time than the control group [33]. This study adopted matched intervention time in both groups which may be a potential reason for the observed small difference.

4.4. Limitations. The data in the present study should be interpreted with caution due to its limitations. The study included participants at the subacute stage of stroke which limits the external validity of the finding. Future research should include participants at the acute and chronic stage of stroke to enhance the external validity of the findings. This study recruited participants who were between 40 and 80 years old. The wide age range limits the generalizability of the study findings. Further study that includes smaller age range of the sample population is recommended to substantiate the findings of the present study. The right to left flipping of the scalp site in participants with the right hemisphere lesion site may be considered a limitation. However, it is not uncommon in published literature that involves either EEG or fMRI study to perform the flipping as a means to increase statistical power [60]. The present study did not involve a follow-up period, and it remains unclear if the observed benefit may carry on in the longer term.

5. Conclusions

VR intervention is superior to conventional therapy in improving the cognitive neural process of motor anticipation and reducing the excessive compensatory activation of the contralesional hemisphere. The improvements observed

in the cognitive neural process corroborated with the improvements in hand function. No firm conclusion could be drawn if VR intervention is superior to conventional therapy in promoting hand function recovery due to the nonclinical significant difference observed between the two groups.

Data Availability

The data that support the findings of this study are available from the First Affiliated Hospital, Sun Yat-sen University, but restrictions apply to the availability of these data, which were used under license for the current study and are not publicly available. Data are however available from the authors upon reasonable request and with permission of the First Affiliated Hospital, Sun Yat-sen University.

Ethical Approval

This study was approved by the Ethical Committee of the First Affiliated Hospital of Sun Yat-sen University (Ethics no. [2014] 88). All participants were provided with a comprehensive explanation of the experimental procedure and a participant information sheet.

Consent

Participants were asked to provide written consent prior to study enrolment.

Disclosure

This manuscript was submitted as a preprint in the link https://www.researchsquare.com/article/rs-12504/v2. All funding bodies did not influence the design of the study and collection, analysis, and interpretation of the data and the writing of the manuscript.

Conflicts of Interest

The authors declare that they have no competing interests.

Authors' Contributions

All authors have read and approved the final manuscript. All authors meet the four primary ICMJE criteria for authorship. In addition, all authors have been actively involved in the study in different capacities: LC and WLAL designed the study and conducted all stages of the study including data collection, analysis, interpretation, and drafting of the manuscript. YC participated in the design of the research protocol, data analysis, and drafting of the manuscript. WLAL, WF, and LC revised the manuscript, interpreted the data, and managed the trial.

Acknowledgments

We would like to express our gratitude to everyone who participated in the described study. This study was supported by the National Natural Science Foundation of China (Grant Nos. 81971224 and 82004466), Foundation for Basic and Applied Basic Research of Guangdong Province (Grant No. 2019M652867), Scientific Research Project of Traditional Chinese Medicine Bureau of Guangdong Province (Grant No. 20201118), and Guangdong Medical Research Fund (Grant No. B2018268). The publication of the manuscript was supported by the Sun Yat-sen University Clinical Research 5010 Funding Programme (Grant No. 2014001).

References

[1] P. A. Vorkas, J. Shalhoub, M. R. Lewis et al., "Metabolic phenotypes of carotid atherosclerotic plaques relate to stroke risk: an exploratory study," *European Journal of Vascular and Endovascular Surgery*, vol. 52, no. 1, pp. 5–10, 2016.

[2] N. J. Kassebaum, M. Arora, R. M. Barber et al., "Global, regional, and national disability-adjusted life-years (DALYs) for 315 diseases and injuries and healthy life expectancy (HALE), 1990-2015: a systematic analysis for the Global Burden of Disease Study 2015," *Lancet*, vol. 388, no. 10053, pp. 1603–1658, 2016.

[3] H. S. Jorgensen, H. Nakayama, H. O. Raaschou, and T. S. Olsen, "Stroke: neurologic and functional recovery the Copenhagen Stroke Study," *Physical medicine and rehabilitation clinics of North America.*, vol. 10, no. 4, pp. 887–906, 1999.

[4] V. L. Feigin, C. M. Lawes, D. A. Bennett, and C. S. Anderson, "Stroke epidemiology: a review of population-based studies of incidence, prevalence, and case-fatality in the late 20th century," *Lancet Neurology*, vol. 2, no. 1, pp. 43–53, 2003.

[5] S. Hakkennes and J. L. Keating, "Constraint-induced movement therapy following stroke: a systematic review of randomised controlled trials," *The Australian Journal of Physiotherapy*, vol. 51, no. 4, pp. 221–231, 2005.

[6] G. Kwakkel, B. J. Kollen, J. van der Grond, and A. J. Prevo, "Probability of regaining dexterity in the flaccid upper limb," *Stroke*, vol. 34, no. 9, pp. 2181–2186, 2003.

[7] W. Rosamond, K. Flegal, G. Friday et al., "Heart disease and stroke statistics–2007 update: a report from the American Heart Association Statistics Committee and Stroke Statistics Subcommittee," *Circulation*, vol. 115, no. 5, pp. e69–171, 2007.

[8] A. Aminov, J. M. Rogers, S. Middleton, K. Caeyenberghs, and P. H. Wilson, "What do randomized controlled trials say about virtual rehabilitation in stroke? A systematic literature review and meta-analysis of upper-limb and cognitive outcomes," *Journal of Neuroengineering & Rehabilitation.*, vol. 15, no. 1, p. 29, 2018.

[9] A. A. Mullick, S. K. Subramanian, and M. F. Levin, "Emerging evidence of the association between cognitive deficits and arm motor recovery after stroke: a meta-analysis," *Restorative neurology and neuroscience.*, vol. 33, no. 3, pp. 389–403, 2015.

[10] J. P. Varghese, D. M. Merino, K. B. Beyer, and W. E. McIlroy, "Cortical control of anticipatory postural adjustments prior to stepping," *Neuroscience*, vol. 313, pp. 99–109, 2016.

[11] K. Svoboda and N. Li, "Neural mechanisms of movement planning: motor cortex and beyond," *Current Opinion in Neurobiology*, vol. 49, pp. 33–41, 2018.

[12] J. Tanji and E. V. Evarts, "Anticipatory activity of motor cortex neurons in relation to direction of an intended movement," *Journal of Neurophysiology*, vol. 39, no. 5, pp. 1062–1068, 1976.

[13] O. Bai, V. Rathi, P. Lin et al., "Prediction of human voluntary movement before it occurs," *Clinical Neurophysiology*, vol. 122, no. 2, pp. 364–372, 2011.

[14] J. F. Kalaska, "From intention to action: motor cortex and the control of reaching movements," *Advances in Experimental Medicine and Biology*, vol. 629, pp. 139–178, 2009.

[15] S. Y. Schaefer, K. Y. Haaland, and R. L. Sainburg, "Hemispheric specialization and functional impact of ipsilesional deficits in movement coordination and accuracy," *Neuropsychologia*, vol. 47, no. 13, pp. 2953–2966, 2009.

[16] S. Wetter, J. L. Poole, and K. Y. Haaland, "Functional implications of ipsilesional motor deficits after unilateral stroke," *Archives of physical medicine and rehabilitation.*, vol. 86, no. 4, pp. 776–781, 2005.

[17] S. Vahdat, M. Darainy, and D. J. Ostry, "Structure of plasticity in human sensory and motor networks due to perceptual learning," *The Journal of neuroscience: the official journal of the Society for Neuroscience.*, vol. 34, no. 7, pp. 2451–2463, 2014.

[18] J. Hermsdorfer, E. Hagl, and D. A. Nowak, "Deficits of anticipatory grip force control after damage to peripheral and central sensorimotor systems," *Human Movement Science*, vol. 23, no. 5, pp. 643–662, 2004.

[19] D. A. Nowak, J. Hermsd Rfer, and H. Topka, "Deficits of predictive grip force control during object manipulation in acute stroke," *Journal of Neurology*, vol. 250, no. 7, pp. 850–860, 2003.

[20] C. D. Takahashi and D. J. Reinkensmeyer, "Hemiparetic stroke impairs anticipatory control of arm movement," *Experimental Brain Research*, vol. 149, no. 2, pp. 131–140, 2003.

[21] C. Tan, J. Tretriluxana, E. Pitsch, N. Runnarong, and C. J. Winstein, "Anticipatory planning of functional reach-to-grasp: a pilot study," *Neurorehabilitation and Neural Repair*, vol. 26, no. 8, pp. 957–967, 2012.

[22] O. Yilmaz, N. Birbaumer, and A. Ramos-Murguialday, "Movement related slow cortical potentials in severely paralyzed chronic stroke patients," *Frontiers in Human Neuroscience.*, vol. 8, 2015.

[23] S. Finnigan and M. J. van Putten, "EEG in ischaemic stroke: quantitative EEG can uniquely inform (sub-)acute prognoses and clinical management," *Clinical Neurophysiology*, vol. 124, no. 1, pp. 10–19, 2013.

[24] P. Nicolo, S. Rizk, C. Magnin, M. D. Pietro, A. Schnider, and A. G. Guggisberg, "Coherent neural oscillations predict future motor and language improvement after stroke," *Brain: a journal of neurology.*, vol. 138, no. 10, pp. 3048–3060, 2015.

[25] M. Sabate, C. Llanos, E. Enriquez, B. Gonzalez, and M. Rodriguez, "Fast modulation of alpha activity during visual processing and motor control," *Neuroscience*, vol. 189, pp. 236–249, 2011.

[26] R. B. Willemse, J. C. de Munck, J. P. Verbunt et al., "Topographical organization of mu and Beta band activity associated with hand and foot movements in patients with perirolandic lesions," *The open neuroimaging journal.*, vol. 4, pp. 93–99, 2010.

[27] P. J. Dean, E. Seiss, and A. Sterr, "Motor planning in chronic upper-limb hemiparesis: evidence from movement-related potentials," *PLoS One*, vol. 7, no. 10, article e44558, 2012.

[28] O. F. do Nascimento, K. D. Nielsen, and M. Voigt, "Movement-related parameters modulate cortical activity during imaginary isometric plantar-flexions," *Experimental Brain Research*, vol. 171, no. 1, pp. 78–90, 2006.

[29] H. Leuthold, W. Sommer, and R. Ulrich, "Preparing for action: inferences from CNV and LRP," *Journal Of Psychophysiology.*, vol. 18, no. 2/3, pp. 77–88, 2004.

[30] F. Fattapposta, V. C. D'Agostino, F. My et al., "Psychophysiological aspects of voluntary skilled movement after stroke: a follow-up study," *Archives italiennes de biologie.*, vol. 146, no. 3-4, pp. 147–163, 2008.

[31] L. Chen, Y. Mao, M. Ding et al., "Assessing the relationship between motor anticipation and cortical excitability in subacute stroke patients with movement-related potentials," *Frontiers in Neurology*, vol. 9, p. 881, 2018.

[32] M. F. Levin, P. L. Weiss, and E. A. Keshner, "Emergence of virtual reality as a tool for upper limb rehabilitation: incorporation of motor control and motor learning principles," *Physical therapy.*, vol. 95, no. 3, pp. 415–425, 2015.

[33] K. E. Laver, B. Lange, S. George, J. E. Deutsch, G. Saposnik, and M. Crotty, "Virtual reality for stroke rehabilitation," *The Cochrane Database of Systematic Reviews*, vol. 2018, no. 1, article Cd008349, 2018.

[34] A. M. Tinga, J. M. Visser-Meily, M. J. van der Smagt, S. Van der Stigchel, R. van Ee, and T. C. Nijboer, "Multisensory stimulation to improve low- and higher-level sensory deficits after stroke: a systematic review," *Neuropsychology Review*, vol. 26, no. 1, pp. 73–91, 2016.

[35] R. Llorens, E. Noe, C. Colomer, and M. Alcaniz, "Effectiveness, usability, and cost-benefit of a virtual reality-based telerehabilitation program for balance recovery after stroke: a randomized controlled trial," *Archives of physical medicine and rehabilitation.*, vol. 96, no. 3, pp. 418–425.e2, 2015.

[36] M. Maier, B. Rubio Ballester, A. Duff, E. Duarte Oller, and P. Verschure, "Effect of specific over nonspecific VR-based rehabilitation on poststroke motor recovery: a systematic meta-analysis," *Neurorehabilitation and Neural Repair*, vol. 33, no. 2, pp. 112–129, 2019.

[37] R. S. Calabrò, A. Naro, M. Russo et al., "The role of virtual reality in improving motor performance as revealed by EEG: a randomized clinical trial," *Journal of Neuroengineering and Rehabilitation*, vol. 14, no. 1, p. 53, 2017.

[38] C. Ling, C. Yi, and L. Wai Leung Ambrose, *The effect of virtual reality on motor anticipation and hand function in patients with subacute stroke: a randomised trial on movement-related potential*, Wiley, Chichester, West Sussex, England, 2020.

[39] M. F. Folstein, S. E. Folstein, and P. R. McHugh, ""Mini-mental state": a practical method for grading the cognitive state of patients for the clinician," *Journal of Psychiatric Research*, vol. 12, no. 3, pp. 189–198, 1975.

[40] D. Carroll, "A quantitative test of upper extremity function," *Journal of Chronic Diseases*, vol. 18, no. 5, pp. 479–491, 1965.

[41] P. W. Duncan, M. Propst, and S. G. Nelson, "Reliability of the Fugl-Meyer assessment of sensorimotor recovery following cerebrovascular accident," *Physical therapy.*, vol. 63, no. 10, pp. 1606–1610, 1983.

[42] A. Henderson, N. Korner-Bitensky, and M. Levin, "Virtual reality in stroke rehabilitation: a systematic review of its effectiveness for upper limb motor recovery," *Topics in stroke rehabilitation.*, vol. 14, no. 2, pp. 52–61, 2007.

[43] S. J. Luck, *An Introduction to the Event-Related Potential Technique*, MIT Press, Cambridge, 2005.

[44] C. Krishef, *Fundamental Statistics for Human Services and Social Work*, PWS Pubslihers, Boxton, 1987.

[45] H. Arito and M. Oguri, "Contingent negative variation and reaction time of physically-trained subjects in simple and discriminative tasks," *Industrial Health*, vol. 28, no. 2, pp. 97–106, 1990.

[46] J. Cirillo, J. B. Finch, and J. G. Anson, "The impact of physical activity on motor preparation in young adults," *Neuroscience Letters*, vol. 638, pp. 196–203, 2017.

[47] W. Lang, H. Obrig, G. Lindinger, D. Cheyne, and L. Deecke, "Supplementary motor area activation while tapping bimanually different rhythms in musicians," *Experimental Brain Research*, vol. 79, no. 3, pp. 504–514, 1990.

[48] A. L. Smith and W. R. Staines, "Cortical and behavioral adaptations in response to short-term inphase versus antiphase bimanual movement training," *Experimental Brain Research*, vol. 205, no. 4, pp. 465–477, 2010.

[49] S. Saleh, H. Bagce, Q. Qiu, G. Fluet, and E. Tunik, "Mechanisms of neural reorganization in chronic stroke subjects after virtual reality training," *Conference proceedings: … Annual International Conference of the IEEE Engineering in Medicine and Biology Society. IEEE Engineering in Medicine and Biology Society. Conference.*, vol. 2011, pp. 8118–8121, 2011.

[50] H. Xie, H. Zhang, H. Liang et al., "A novel glasses-free virtual reality rehabilitation system on improving upper limb motor function among patients with stroke: a feasibility pilot study," *Medicine in Novel Technology and Devices*, vol. 11, article 100069, 2021.

[51] M. G. Maggio, D. Latella, G. Maresca et al., "Virtual reality and cognitive rehabilitation in people with stroke: an overview," *The Journal of neuroscience nursing: journal of the American Association of Neuroscience Nurses.*, vol. 51, no. 2, pp. 101–105, 2019.

[52] S. K. Jankelowitz and J. G. Colebatch, "Movement related potentials in acutely induced weakness and stroke," *Experimental Brain Research*, vol. 161, no. 1, pp. 104–113, 2005.

[53] C. H. Brunia and G. J. van Boxtel, "Wait and see," *International Journal of Psychophysiology*, vol. 43, no. 1, pp. 59–75, 2001.

[54] C. M. Butefisch, R. Kleiser, B. Korber et al., "Recruitment of contralesional motor cortex in stroke patients with recovery of hand function," *Neurology*, vol. 64, no. 6, pp. 1067–1069, 2005.

[55] N. S. Ward, M. M. Brown, A. J. Thompson, and R. S. Frackowiak, "Neural correlates of motor recovery after stroke: a longitudinal fMRI study," *Brain*, vol. 126, no. 11, pp. 2476–2496, 2003.

[56] A. Feydy, R. Carlier, A. Roby-Brami et al., "Longitudinal study of motor recovery after stroke," *Stroke*, vol. 33, no. 6, pp. 1610–1617, 2002.

[57] J. B. Green, Y. Bialy, E. Sora, and A. Ricamato, "High-resolution EEG in poststroke hemiparesis can identify ipsilateral generators during motor tasks," *Stroke*, vol. 30, no. 12, pp. 2659–2665, 1999.

[58] M. A. Cervera, S. R. Soekadar, J. Ushiba et al., "Brain-computer interfaces for post-stroke motor rehabilitation: a meta-analysis," *Annals of Clinical Translational Neurology*, vol. 5, no. 5, pp. 651–663, 2018.

[59] C. E. Lang, D. F. Edwards, R. L. Birkenmeier, and A. W. Dromerick, "Estimating minimal clinically important differences of upper-extremity measures early after stroke," *Archives of Physical Medicine and Rehabilitation*, vol. 89, no. 9, pp. 1693–1700, 2008.

[60] Q. Lin, H. Li, Y. R. Mao et al., "The difference of neural networks between bimanual antiphase and in-phase upper limb movements: a preliminary functional magnetic resonance imaging study," *Behavioural Neurology*, vol. 2017, 9 pages, 2017.

Hindawi
Neural Plasticity
Volume 2022, Article ID 4106131, 10 pages
https://doi.org/10.1155/2022/4106131

Research Article

Frequency-Specific Changes of Amplitude of Low-Frequency Fluctuations in Patients with Acute Basal Ganglia Ischemic Stroke

Xuemei Quan,[1,2] **Su Hu**,[3,4] **Chaoguo Meng**,[1] **Lulu Cheng**,[5,6] **Yujie Lu**,[7,8] **Yumei Xia**,[1] **Wenmei Li**,[5] **Huo Liang**,[9] **Mengting Li**,[3,4] **and Zhijian Liang**[1]

[1]*Department of Neurology, The First Affiliated Hospital of Guangxi Medical University, Nanning, China*
[2]*Department of Neurology, The People's Hospital of Guangxi Zhuang Autonomous Region, Nanning, China*
[3]*School of Teacher Education, Zhejiang Normal University, Jinhua, China*
[4]*Key Laboratory of intelligent Education Technology and Application of Zhejiang Province, Zhejiang Normal University, Jinhua, China*
[5]*School of Foreign Studies, China University of Petroleum, Qingdao, China*
[6]*Shanghai Center for Research in English Language Education, Shanghai International Studies University, Shanghai, China*
[7]*Department of Radiology, The First Affiliated Hospital of Guangxi Medical University, Nanning, China*
[8]*Department of Radiology, Sichuan Cancer Hospital and Institute, Sichuan Cancer Center, School of Medicine, University of Electronic Science and Technology of China, Chengdu, China*
[9]*Department of Rehabilitation, Guangxi International Zhuang Medicine Hospital, No. 8 Qiuyue Road, Nanning, China*

Correspondence should be addressed to Mengting Li; 201920200210@zjnu.edu.cn and Zhijian Liang; liangzhijian@gxmu.edu.cn

Received 4 November 2021; Revised 18 December 2021; Accepted 10 January 2022; Published 24 January 2022

Academic Editor: Yu Zheng

Objective. The purpose of this study was to investigate the characteristics of different frequency bands in the spontaneous brain activity among patients with acute basal ganglia ischemic stroke (BGIS). *Methods.* In the present study, thirty-four patients with acute BGIS and forty-four healthy controls were examined by resting-state functional magnetic resonance imaging (rs-fMRI) from May 2019 to December 2020. Two amplitude methods including amplitude of low-frequency fluctuations (ALFF) and fractional ALFF (fALFF) calculated in three frequency bands (conventional frequency band: 0.01-0.08 Hz; slow-5 frequency band: 0.01-0.027 Hz; and slow-4 frequency band: 0.027-0.073 Hz) were conducted to evaluate the spontaneous brain activity in patients with acute BGIS and healthy controls (HCs). Gaussian Random Field Theory (GRF, voxel $p < 0.01$ and cluster $p < 0.05$) correction was applied. The correlation analyses were performed between clinical scores and altered metrics values. *Results.* Compared to HCs, patients with acute BGIS showed decreased ALFF in the right supramarginal gyrus (SMG) in the conventional and slow-4 bands, increased fALFF in the right middle frontal gyrus (MFG) in the conventional and slow-4 bands, and increased fALFF in the bilateral caudate in the slow-5 frequency band. The fALFF value of the right caudate in the slow-5 frequency band was negatively correlated with the clinical scores. *Conclusion.* In conclusion, this study showed the alterations in ALFF and fALFF in three frequency bands between patients with acute BGIS and HCs. The results reflected that the abnormal LFO amplitude might be related with different frequency bands and promoted our understanding of pathophysiological mechanism in acute BGIS.

1. Introduction

Acute stroke is a prominent cause of mortality and disability worldwide and leads to a heavy burden on individual, families, and society [1–3]. Acute ischemic stroke which is caused by a sudden interruption of blood supply resulted from to occlusion or obstruction by a thrombus or embolus accounts for more than 80% of all strokes [4]. The basal ganglia region is rich in blood supply and is a common site of ischemic stroke [5]. Acute ischemic stroke occurring in the basal ganglia region is defined as acute basal ganglia ischemic stroke (BGIS). The acute BGIS has been considered to have association with motor impairments, sensory disturbance, emotional blunting, poststroke depression, and loss of

spontaneous speech [6–8]. Therefore, the exploration of the pathophysiological mechanism of acute BGIS is vital and could provide potential help for the rehabilitation therapy in the patients with acute BGIS.

Resting-state functional magnetic resonance imaging (rs-fMRI) was first proposed by Biswal et al. to explore brain activity in 1995 [9]. As a noninvasive method to study brain physiological activity, it has been widely used in neuropsychiatric diseases [10–12]. Previous studies have found the disrupted functional connectivity (FC) in acute BGIS patients which characterized the function of whole-brain network [13, 14]. However, the local variation in brain function of acute BGIS patients remains to be explored. At present, various methods, such as amplitude of low frequency fluctuation (ALFF) and fractional ALFF (fALFF), can be used to analyze the changes of brain function [9, 15, 16]. As a promising method, the ALFF is proposed to examine the blood oxygen level-dependent (BOLD) signal fluctuations and to measure the local brain activity of diseases [15–17]. Based on ALFF, Zou et al. proposed the fALFF which is the ratio of the power spectrum of low frequency to that of the entire frequency range [16]. Unlike ALFF, which indicates the strength and intensity of the low-frequency oscillations (LFOs), fALFF reflects the relative contribution of specific LFOs to the whole detectable frequency range [18]. Evidence shows that fALFF can inhibit the nonspecific signal components in fMRI, making the detection of spontaneous brain activities more sensitive and specific [16], while ALFF often has higher reliability than fALFF in the test-retest reliability of amplitude measures [18]. Hence, the combination of these two methods mentioned above can reflect a more complete picture of spontaneous neural activity of the brain. Also, these two methods have been widely used in rs-fMRI studies of neurocognitive diseases [11, 19, 20].

Most studies using the two methods focused on the LFOs which is known as conventional frequency band ranging from 0.01 to 0.08 Hz. The human brain is capable of executing complex functions which are supported by a multitude of oscillatory waves [18]. Based on natural logarithmic linear theory of neural oscillations, the neural oscillations of the human brain can be divided into different frequency bands, and the neural oscillations of different frequency bands show different brain functions [21]. The conventional frequency band is related to the spontaneous neural activities and has the physiological meaning [19]. However, a recent study has found that the results obtained from conventional frequency band only are lack of frequency characteristics [22]. Zuo et al. [18] found that the conventional frequency band of 0.01-0.08 Hz could be divided into two subfrequency bands: slow-4 frequency band of 0.027-0.073 Hz and slow-5 frequency band of 0.01-0.027 Hz. Slow-4 band (0.027-0.073 Hz) mainly reflects the alteration of gray matter signals, while slow-5 band (0.01-0.027 Hz) could reflect the alteration of ventromedial prefrontal cortices [18]. LFOs at different frequency bands show different properties and physiological functions [18, 21, 23]. Meanwhile, the spontaneous LFOs of the subcortical stroke are thought to contain frequency-dependent rs-fMRI patterns, which may serve as potential neuroimaging markers of the neural substrates associated with hand function outcomes following stroke [24]. However, the characteristics of different frequency bands to the spontaneous brain activity in patients with acute BGIS remain unclear. The mechanism of low frequency oscillation in BGIS in specific frequency band needs to be further explored.

In the present study, ALFF and fALFF were used to demonstrate the frequency-specific alteration of the local spontaneous brain activity of acute BGIS patients. The correlations between LFOs in significant brain regions and clinical scores were explored in the patient group.

2. Materials and Methods

2.1. Participants. From May 2019 to December 2020, 43 acute BGIS patients who had neurologic symptoms and have been judged by clinical neurologists were consecutively recruited from Department of Neurology, the First Affiliated Hospital of Guangxi Medical University. The inclusion criteria for all patients are as follows: (1) first onset acute BGIS diagnosed by a consensus of a clinical neurologist and a radiologist; (2) age between 30 and 75 years; (3) illness duration of stroke less than 10 days; (4) right-handedness before stroke; (5) the National Institutes of Health Stroke Scale (NIHSS) scores ranging from 0 to 16. The exclusion criteria of this study included the following: (1) inability to perform clinical scale examination, such as severe aphasia, auditory, and/or visual disorder; (2) other neurological disorders that would affect the experiment, such as hemorrhage, multiple infarcts, leukoaraiosis, migraine, epilepsy, or psychiatric diseases; (3) any contraindications for MRI, including pregnancy and metal implants; and (4) excessive head motion during rs-fMRI scanning. This protocol was approved by the Ethics Committee of the First Affiliated Hospital of Guangxi Medical University. All participants signed a written informed consent before the study.

In this study, forty-seven age-matched healthy controls (HCs) with no physical diseases or history of psychiatric or neurologic disorders who were recruited from local community were also recruited through advertising at the same time.

Nine patients were excluded from the final analysis due to poor image quality ($n = 1$), excessive head motion ($n = 2$), missing data ($n = 1$), and incomplete scanning of cerebellum ($n = 5$), leaving 34 acute BGIS patients in the final analysis. Three HCs were excluded from the final analysis due to poor image quality ($n = 1$), excessive head motion ($n = 1$), and incomplete scanning of cerebellum ($n = 1$), leaving 44 HCs in the final analysis.

2.2. Clinical Scale Tests. Stroke severity and neurological deficits were assessed using the NIHSS. And motor function was assessed by the Fugl-Meyer Assessment (FMA) scale.

2.3. MRI Data Acquisition. For each participant, a total of 186 time points (6 minutes and 12 seconds) were collected on a 3.0 T MR scanner (SIEMENS MAGNETOM Prisma), which is equipped with a 64-channel phased array head coil

at 3.0 T MRI center, in the First Affiliated Hospital of Guangxi Medical University. During the data acquisition, participants were instructed to keep awake, relax with their eyes closed, and remain motionless as much as possible.

The rs-fMRI was acquired using an echoplanar imaging (EPI) sequence with the following parameters: repetition time (TR) = 2000 ms, echo time (TE) = 35 ms, flip angle (FA) = 90°, field of view (FOV) = 240 × 240 mm^2, voxel size = 2.6 × 2.6 × 3 mm^3, matrix = 64 × 64, gap = 0 mm, and slice number = 40. This session lasted for 6 minutes and 12 seconds.

The anatomical 3D-MPRAG T1-weighted images (T1WI) were recorded by magnetization prepared rapid gradient echo: TR = 2300 ms, TE = 2.98 ms, reverse time = 900 ms, FOV = 256 × 256 mm^2, voxel size = 1 × 1 × 1 mm^3, matrix = 256 × 256, gap = 0 mm, and slice number = 176. This session lasted for 5 minutes and 21 seconds.

2.4. RS-fMRI Data Preprocessing. All algorithms were implemented in Matlab R2018a (https://uk.mathworks.com/products/matlab). RS-fMRI data preprocessing and statistical analyses were carried out using RESTplus V1.24 (http://www.restfmri.net), and SPM12 (http://www.fil.ion.ucl.ac.uk/spm/software/spm12/); multiple comparison corrections were performed using the Data Processing & Analysis for Brain Imaging (DPABI) V5.1 (http://rfmri.org/dpabi). The preprocessing steps included the following: (1) removing the first 10 time points to make the longitudinal magnetization achieve steady-state and to let the participants get used to the scanning environment; (2) slice timing correction; (3) head motion correction. We excluded the participants whose head motion exceeded 3 mm or 3°. Hence, two patients and one HC were excluded; (4) the functional images were spatially normalized to the Montreal Neurological Institute (MNI) space via the deformation fields derived from new segmentation of structural images (resampling voxel size = 3 mm × 3 mm × 3 mm); (5) spatial smoothing with a Gaussian kernel of 4 mm full-width at half-maximum (FWHM); (6) removing the linear trend of the time series; (7) regressing out nuisance variables, including the Friston-24 head motion parameters [25], polynomial trend, white matter signals, and cerebrospinal flow signals.

2.5. ALFF Calculation. The ALFF is a rs-fMRI metric that calculates the amplitude of each voxel in the local brain region in conventional frequency band of 0.01-0.08 Hz and reflects the extent of local spontaneous neuronal activity in the resting state [15, 26]. For ALFF calculations, the time series of each voxel was transformed to frequency domain by fast Fourier transform (FFT) and the power spectrum was then obtained. The square root was calculated at each frequency of the power spectrum, and the averaged square root obtained across conventional frequency band at each voxel was regarded as the ALFF value, which was further divided by the global mean ALFF of each participant. In order to study the frequency-dependent changes in BGIS patients during the acute phase, we also calculated the ALFF values of subfrequency bands including slow-4 frequency band of 0.027-0.073 Hz and slow-5 frequency band of 0.01-0.027 Hz.

2.6. fALFF Calculation. After data preprocessing, the BOLD signal was converted from time domain to frequency domain by FFT formula, and the power spectrum of BOLD signal in frequency domain was obtained. The power spectrum of BOLD signal in frequency domain was obtained by square calculation. The ratios of the power in the conventional frequency band were calculated relative to the full frequency band (0-0.25 Hz). The result mentioned above was known as fALFF. Then, fALFF divided by global mean fALFF of every individual was applied for standardization purposes. To investigate the frequency-dependent alterations in BGIS patients during the acute phase, we also calculated the fALFF of sub-frequency bands including slow-4 frequency band (0.027-0.073 Hz) and slow-5 frequency band (0.01-0.027 Hz).

2.7. Statistical Analysis. Statistical analyses were performed using SPSS version 26.0 (IBM, Armonk, NY, USA). Categorical variables are presented as *n*, and continuous variables are presented as the mean ± standard deviation (SD). Gender difference was tested with a chi-square test. A two-sample *t*-test was performed to compare the age difference between the acute BGIS patients and HCs. All tests of demographic were two-tailed, and $p < 0.05$ was considered significant.

Two sample *t*-tests were performed to compare the ALFF and fALFF maps between patients with BGIS and HCs, respectively. Frame-wise displacement (FD, Jenkinson [27]) parameters were regressed in the two-sample *t*-test to avoid the influence of head motion. The resultant T-maps were conducted with Gaussian Random Field Theory (GRF) correction for multiple comparisons with voxel $p < 0.01$, cluster $p < 0.05$.

For each metric (ALFF, fALFF) which shows acute BGIS related alterations, Pearson's correlation analysis was used to assess their associations with clinical scales (NIHSS scores and FMA scores) of patients. The correlations were considered significant at a threshold of $p < 0.05$.

3. Results

3.1. Participants' Characteristics. A total of 43 patients with acute BGIS and 47 HCs underwent the rs-fMRI scan in the present study from May 2019 to December 2020. Nine patients and three HCs were excluded according to the above exclusion criteria (Figure 1). Demographics and clinical data of the acute BGIS patients and HCs were calculated (Table 1). There were no significant differences in age ($p = 0.736$) but in gender ($p = 0.007$) between acute BGIS patients and HCs. The statistical analysis results after gender regressed out are provided in the supplementary materials (Table S1, Figure S1 and Figure S2 in the supplementary materials). The lesion map for enrolled acute basal ganglia ischemic stroke is displayed in the supplementary materials (Figure S3 in the supplementary materials).

3.2. Disrupted Local Function in BGIS in Multifrequency Bands

3.2.1. ALFF Analysis in Different Frequency Bands. Compared with HCs, the BGIS patients exhibited decreased

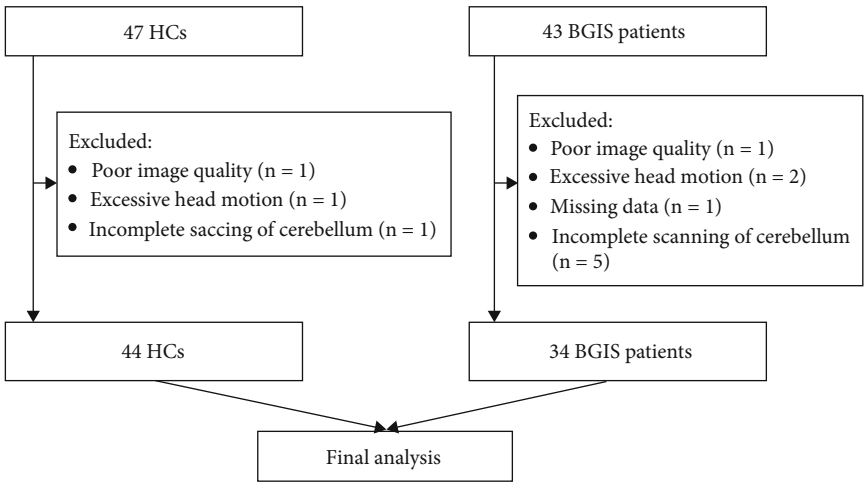

Figure 1: Flow chart. HCs: healthy controls; BGIS: basal ganglia ischemic stroke.

Table 1: Demographic and clinical characteristics of the participants.

	BGIS ($n = 34$)	HCs ($n = 44$)	p value
Age (years)	56.500 ± 10.999	55.340 ± 11.485	0.736
Gender (male/female)	25/9	19/25	0.007
Education (year)	11.500 ± 3.587		
NIHSS score	3.760 ± 2.463		
FMA score	74.910 ± 18.907		

BGIS: basal ganglia ischemic stroke; NIHSS: National Institutes of Health Stroke Scale; FMA: Fugl-Meyer Assessment.

ALFF in the right supramarginal gyrus (SMG) in conventional frequency band and slow-4 frequency band (GRF correction, voxel $p < 0.01$, cluster $p < 0.05$). No significant brain region was found between acute BGIS patients and HCs in slow-5 band (Table 2 and Figure 2).

3.2.2. fALFF Analysis in Different Frequency Bands. Compared with HCs, the BGIS patients exhibited increased fALFF in the right middle frontal gyrus (MFG) in conventional frequency band and slow-4 frequency band (GRF correction, voxel $p < 0.01$, cluster $p < 0.05$). The cluster size of the right MFG in the conventional frequency band was larger than that of slow-4 band (Table 2 and Figure 3).

Compared with HCs, the BGIS patients exhibited increased fALFF in the bilateral caudate in the slow-5 frequency band (GRF correction, voxel $p < 0.01$, cluster $p < 0.05$) (Table 2 and Figure 3).

3.3. Relationship Between Local Metrics and Clinical Scales. In the BGIS patients, increased fALFF values of the slow-5 frequency band in the right caudate were negatively correlated with FMA scores ($p = 0.035$, $r = -0.363$) (Table 3 and Figure 4). However, no significant correlations were detected between abnormal ALFF values in the conventional frequency band and slow-4 band and clinical scores (Table 3 and Figure 4).

4. Discussion

In the present study, we utilized ALFF and fALFF to investigate the sensitivity and characteristics of the LFOs of the spontaneous neural activity in the conventional frequency band (0.01-0.08 Hz), slow-5 frequency band (0.01-0.027 Hz), and slow-4 frequency band (0.027-0.073 Hz) in acute BGIS patients and further explored the relationship between metrics values and the clinical scales. Compared to the HCs, the acute BGIS patients exhibited decreased ALFF values in the right SMG in the conventional band and slow-4 band and increased fALFF in the right MFG in the conventional band and slow-4 band and bilateral caudate in the slow-5 band. In the ALFF analysis of the three frequency bands, the clusters detected in the slow-4 band were larger than those in the conventional frequency band, suggesting that the slow-4 band was more sensitive to the detection of spontaneous brain activity in the ALFF in patients with acute BGIS. However, increased fALFF in the bilateral caudate were only observed in the slow-5 band. In addition, increased fALFF values in the right caudate in the slow-5 band were negatively correlated with FMA scores. These findings indicated that frequency-dependent alterations in intrinsic activity of specific brain regions may serve as potential neuroimaging markers for the mechanism of pathophysiology in patients with acute BGIS.

ALFF was thought to reflect the degree of spontaneous neuronal activity [15]. The increased ALFF indicates the increase of neuronal excitability and metabolism, while the decreased ALFF indicates the inhibition of neuronal spontaneous activity. In the present study, the right SMG of BGIS patients showed decreased ALFF, which indicated decreased spontaneous neuronal activity in this brain region compared with HCs. The SMG was involved in verbal working memory, phonological processing/storage of speech (i.e., spoken and written language), and motor control [28–30]. A previous study showed that decreased functional connectivity (FC) between hippocampal and SMG was associated with impaired working memory function in stroke patients [31]. Similar results were also found in the previous studies

Table 2: Brain regions showing ALFF and fALFF differences between groups.

Regions (AAL)	Brodmann area	Cluster size	Peak t value	MNI coordinate X	Y	Z
ALFF						
Conventional band (0.01~ 0.08 Hz)						
SupraMarginal_R	40	111	-3.9736	36	-39	36
Slow-4 (0.027~ 0.073 Hz)						
SupraMarginal_R	40	117	-4.01	36	-39	36
fALFF						
Conventional band (0.01~ 0.08 Hz)						
Frontal_Mid_R	6	35	4.0499	42	6	60
Slow-4 (0.027~ 0.073 Hz)						
Frontal_Mid_R	6	27	3.7735	48	6	54
Slow-5 (0.01~ 0.027 Hz)						
Caudate_R	—	40	4.6062	18	6	15
Caudate_L	—	34	4.3024	-18	0	24

The clusters located in the cerebellum are not reported. AAL: automated anatomical labeling; MNI: Montreal Neurological Institute; SupraMarginal_R: right supramarginal gyrus; Frontal_Mid_R: right medial frontal gyrus; Caudate_R: right caudate; Caudate_L: left caudate; ALFF: amplitude of low frequency fluctuation; fALFF: fractional amplitude of low frequency fluctuation.

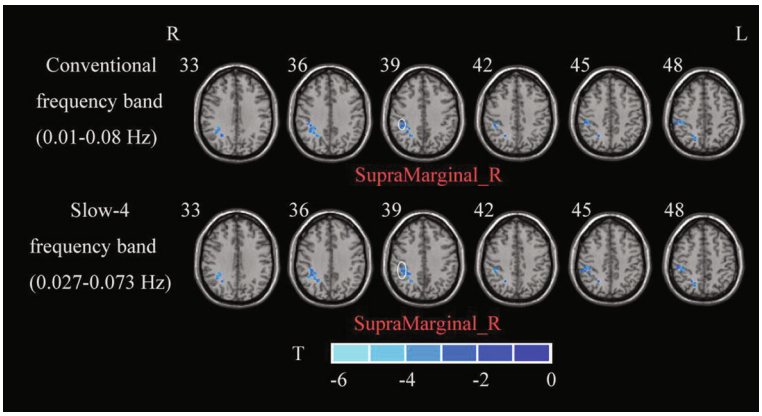

Figure 2: A two-sample t-test was performed between acute BGIS patients and HCs. R: right hemisphere; L: left hemisphere; BGIS: basal ganglia ischemic stroke; HCs: healthy controls; ALFF: amplitude of low frequency fluctuation.

focusing on the patients with acute BGIS which observed the decreased degree centrality (DC) and voxel-mirrored homotopic connectivity (VMHC) values in SMG [32]. Furthermore, aphasia is a common symptom in stroke [33]. And the brain injury in SMG has been proposed to be associated with poststroke aphasia [34]. Also, one study has revealed the association between phonological agraphia and SMG in patients with ischemic stroke [35]. In addition to the studies focusing on motor dysfunction, numerous functional neuroimaging studies showed that stroke survivors exhibited deficits of learning, memory, language processing function, and cognition [36–39]. The results of the present study supported the findings above from the perspective of neuroimaging.

fALFF reflects the ratio of power of low-frequency band to that of detectable frequency range [16]. fALFF has been described as "superior" in comparisons to ALFF due to its higher specificity in capturing gray matter signal [16, 40]. The MFG, located in Brodmann areas 9 and 10, constitutes an important part of the cognitive function [41]. In the present study, several brain regions with different fALFF values in the right MFG were identified, which echoes the finding of previous studies [42, 43]. Moreover, the fALFF value changes from increased to decreased in MFG after repetitive transcranial magnetic stimulation (rTMS) in the patient with poststroke cognitive impairment [42]. The observed increased fALFF value in the MFG in the current study further verified the importance of the MFG in acute BGIS patients and enriched the pathogenesis research of acute BGIS.

The acute BGIS patients exhibited increased fALFF value in the bilateral caudate in the present study which showed the functional compensation in the caudate. A previous study has revealed that the bilateral caudate regions are involved in the impaired connections in the early-state stroke patients [44]. In addition, the caudate is associated

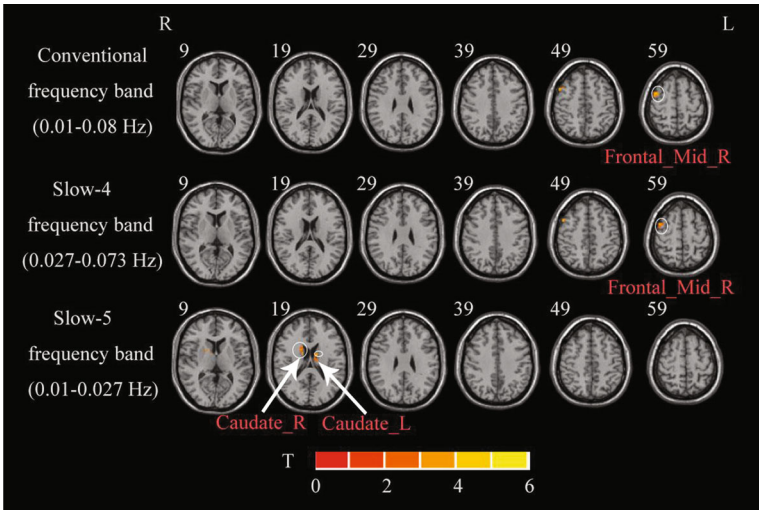

Figure 3: A two-sample t-test was performed between acute BGIS patients and HCs. R: right hemisphere; L: left hemisphere; BGIS: basal ganglia ischemic stroke; HCs: healthy controls; fALFF: fractional amplitude of low frequency fluctuation.

Table 3: The correlation results between brain regions and clinical measures.

Regions	Correlation values	
	NIHSS	FMA
ALFF		
Conventional frequency band (0.01-0.08 Hz)		
SupraMarginal_R	$r = 0.044$ $p = 0.807$	$r = -0.144$ $p = 0.415$
Slow-4 frequency band (0.027-0.073 Hz)		
SupraMarginal_R	$r = -0.010$ $p = 0.955$	$r = -0.140$ $p = 0.429$
fALFF		
Conventional frequency band (0.01-0.08 Hz)		
Frontal_Mid_R	$r = 0.187$ $p = 0.289$	$r = -0.114$ $p = 0.520$
Slow-4 frequency band (0.027-0.073 Hz)		
Frontal_Mid_R	$r = 0.070$ $p = 0.692$	$r = 0.211$ $p = 0.231$
Slow-5 frequency band (0.01-0.027 Hz)		
Caudate_R	$r = 0.338$ $p = 0.051$	$r = -0.363^*$ $p = 0.035$
Caudate_L	$r = 0.062$ $p = 0.729$	$r = -0.024$ $p = 0.891$

$^*p < 0.05$. ALFF: amplitude of low-frequency fluctuations; fALFF: fractional amplitude of low-frequency fluctuations; SupraMarginal_R: right supramarginal gyrus; Frontal_Mid_R: right medial frontal gyrus; Caudate_R: right caudate; Caudate_L: left caudate; BGIS: basal ganglia ischemic stroke; NIHSS: National Institutes of Health Stroke Scale; FMA: Fugl-Meyer Assessment scale.

with language production such as monitoring and controlling lexical and language alternatives [45]. The abnormal connections in the poststroke patients may led to poor language task performance. Meanwhile, the involvement in motor control of caudate has also been found [46]. The research of Nierhaus and colleagues has showed increased functional connectivity between the caudate nucleus and red nucleus in patients with poststroke motor disturbance [47]. Li et al. who used graph-based theoretical approach found that the nodal efficiency of acute stroke patients with unimanual motor deficits was reduced in the caudate [48]. However, correlation results in the current study showed that there was a significant negative correlation between FMA scores and fALFF value of the right caudate. The

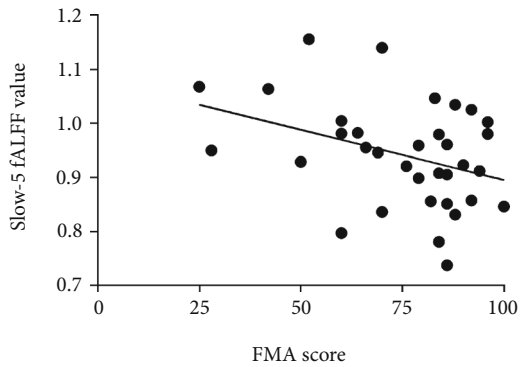

Figure 4: Abnormal cluster of the fALFF was significantly correlated with FMA score in BGIS patients in the slow-5 band ($p < 0.05$). BGIS: basal ganglia ischemic stroke; fALFF: fractional amplitude of low frequency fluctuation; FMA: Fugl-Meyer Assessment scale.

higher the spontaneous nerve activity of caudate, the more obvious the motor deficits. There is an imbalance between spontaneous activity in right caudate and clinical manifestations. It is speculated that in the process of acute BGIS, right caudate attempted to maintain motor function by increasing the spontaneous activity. However, compensation is difficult to maintain and gradually enters the stage of decompensation as the progress of pathology.

In the current study, the ALFF in the acute BGIS patients decreased in the SMG in the slow-4 frequency band but there was no significant alteration in the slow-5 frequency band. It indicated that the spontaneous activity was sensitive to specific frequency bands. The slow-4 band might be more sensitive to detect abnormal intrinsic brain activity in the SMG in patients with acute BGIS. The similar pattern was also observed in other disorders. Zhang et al. [49] revealed the sensitivity of slow-4 band in detecting the intrinsic activity in Parkinson's disease (PD). A study using ReHo method also reported that ReHo changed significantly in the slow-4 band rather than in the slow-5 band [50].

As for the results of fALFF, increased fALFF was found in conventional band and slow-4 band. However, the increased fALFF in the bilateral caudate was only detected in the slow-5 frequency band. It reflected that the results in the conventional band were mainly contributed by results in the slow-4 band, while the slow-5 band was more sensitive in detecting additional results in the patients with acute BGIS compared with slow-4 and conventional bands. The sensitivity of slow-5 has been proposed in the study about poststroke depression [51]. Here, we provided the evidence from the perspective of acute BGIS patients. Our finding suggested that the combination of two measurements (ALFF and fALFF) could maximize the reliability of the study. In addition, our discovery of frequency-dependent results has had theoretical and clinical significance. The neural oscillations are not only the basic mechanism for coordinating activities during the normal operation of the brain but also the basic mechanism for stroke recovery, which has important reference value for the formulation of early rehabilitation treatment strategies for patients with BGIS.

Considering the prevalence of motor deficits in acute BGIS patients, the relationship between the altered brain regions detected by the ALFF and fALFF and motor function is worthy of attention. A study has revealed the increased connections between bilateral supramarginal gyrus and basal ganglia [52]. The supramarginal gyrus is a major component of the somatosensory association cortex which plays an important role in motor-related functions, such as integration of motor signals and various sensory data, transmission of integration information, and high level of cognitive motor control [53]. As for the medial frontal cortex, evidence from functional near infrared spectroscopy (fNIRS) proposed the importance of medial frontal cortex in motor response inhibition [54]. Also, Achala et al. [55] found that the medial frontal cortex was associated with manual motor response control.

Our results suggested that the right caudate was significantly associated with FMA score. The caudate belonged to the neostriatum and participated in the cortico-basal ganglia-thalamo-cortical loops and is involved in motor control, depression, and cognition [56, 57]. A study explored the relationship between lesion and FMA based on voxel-based lesion-symptom mapping. The result showed that declined motor outcome (walking capacity) tended to be affected by damage of the corona radiata, external capsule, and caudate [58]. One study examined structural connectivity changes of the motor execution network following therapy intervention after a stroke based on graph theory measures. The result showed that decreased degree centrality of caudate was associated with FMA. It should be noted that our interpretation is based on functional remolding of the cortico-basal ganglia-thalamo-cortical loops. Approaches targeting neural pathway may shed light on a better characterization and therapy innovation of stroke in the early-stage onset of stroke.

Several limitations should be acknowledged in the study. First, the sample size is relatively small in the present study. Larger sample size will be needed to confirm these results. Second, our research provided the different results in slow-5 and slow-4 bands measured by ALFF and fALFF in the acute BGIS patients. Studies which help to understand the underlying physiological mechanisms of altered ALFF and fALFF in each frequency band are also needed to be explored. Third, in order to eliminate the effects resulted from many times of stroke onset, we recruit merely first-onset acute patients with BGIS. The strict inclusion criteria lead to large gender differences between patient and HC groups, which may add some degree of selection bias.

5. Conclusion

In conclusion, this study showed the alterations in ALFF and fALFF in three frequency bands between patients with acute BGIS. The results reflected that the abnormal LFO amplitude might be related with different frequency bands and promoted our understanding of pathophysiological mechanism in acute BGIS.

Data Availability

The relevant raw data supporting the conclusions of this article will be made available upon request, without undue reservation.

Ethical Approval

The study was approved by the Ethics Committee of the First Affiliated Hospital, Guangxi Medical University, and has been performed in accordance with the ethical standards laid down in the 1964 Declaration of Helsinki and its later amendments.

Consent

Written informed consent was obtained from each participant or from his/her guardian.

Conflicts of Interest

All the authors declare that they have no conflict of interests.

Authors' Contributions

Zhijian Liang, Mengting Li, and Xuemei Quan conceived and design the study; Wenmei Li, Yujie Lu, Chaoguo Meng, and Yumei Xia performed the experiments and collected materials; Xuemei Quan and Su Hu wrote the first manuscript; Su Hu analyzed the data; Huo Liang and Lulu Cheng helped coordinate the study and reviewed the manuscript. All authors read and approved the present text. Xuemei Quan and Su Hu contributed equally to this work and share the first authorship.

Acknowledgments

We thank all patients and healthy volunteers for their participations in this study. We would like to acknowledge LinLin Zhan for editing this manuscript. This work was supported by grants from the National Key R&D Program of China (No. 2018YFC1311305) and Nanning Qingxiu District Science and Technology Plan (No. 2020043).

Supplementary Materials

Table S1: brain regions showing ALFF and fALFF differences between groups. Figure S1: a two-sample *t*-test was performed between BGIS patients and HCs. Figure S2: a two-sample *t*-test was performed between BGIS patients and HCs. Figure S3: lesion map for enrolled acute basal ganglia ischemic stroke. *(Supplementary Materials)*

References

[1] M. Zhou, H. Wang, X. Zeng et al., "Mortality, morbidity, and risk factors in China and its provinces, 1990-2017: a systematic analysis for the Global Burden of Disease Study 2017," *Lancet*, vol. 394, no. 10204, pp. 1145–1158, 2019.

[2] Collaborators GDaI, "Global burden of 369 diseases and injuries in 204 countries and territories, 1990-2019: a systematic analysis for the Global Burden of Disease Study 2019," *The Lancet*, vol. 396, no. 10258, pp. 1204–1222, 2020.

[3] A. Knight-Greenfield, J. J. Q. Nario, and A. Gupta, "Causes of acute stroke: a patterned approach," *Radiologic Clinics of North America*, vol. 57, no. 6, pp. 1093–1108, 2019.

[4] R. V. Krishnamurthi, S. Barker-Collo, V. Parag et al., "Stroke incidence by major pathological type and ischemic subtypes in the Auckland Regional Community Stroke Studies: changes between 2002 and 2011," *Stroke*, vol. 49, no. 1, pp. 3–10, 2018.

[5] Y. Yamori, T. Taguchi, A. Hamada, K. Kunimasa, H. Mori, and M. Mori, "Taurine in health and diseases: consistent evidence from experimental and epidemiological studies," *Journal of Biomedical Science*, vol. 17, Supplement 1, p. S6, 2010.

[6] J. W. Mink, "The basal ganglia: focused selection and inhibition of competing motor programs," *Progress in Neurobiology*, vol. 50, no. 4, pp. 381–425, 1996.

[7] M. Radanovic and L. L. Mansur, "Aphasia in vascular lesions of the basal ganglia: a comprehensive review," *Brain and Language*, vol. 173, pp. 20–32, 2017.

[8] R. Mehanna and J. Jankovic, "Movement disorders in cerebrovascular disease," *Lancet Neurology*, vol. 12, no. 6, pp. 597–608, 2013.

[9] B. Biswal, F. Zerrin Yetkin, V. M. Haughton, and J. S. Hyde, "Functional connectivity in the motor cortex of resting human brain using echo-planar MRI," *Magnetic Resonance in Medicine*, vol. 34, no. 4, pp. 537–541, 1995.

[10] Y. Han, J. Wang, Z. Zhao et al., "Frequency-dependent changes in the amplitude of low-frequency fluctuations in amnestic mild cognitive impairment: a resting-state fMRI study," *NeuroImage*, vol. 55, no. 1, pp. 287–295, 2011.

[11] M. J. Hoptman, X. N. Zuo, P. D. Butler et al., "Amplitude of low-frequency oscillations in schizophrenia: a resting state fMRI study," *Schizophrenia Research*, vol. 117, no. 1, pp. 13–20, 2010.

[12] L. Wang, Q. Kong, K. Li et al., "Frequency-dependent changes in amplitude of low-frequency oscillations in depression: a resting-state fMRI study," *Neuroscience Letters*, vol. 614, pp. 105–111, 2016.

[13] L. Xu, L. Huang, W. Cui, and Q. Yu, "Reorganized functional connectivity of language centers as a possible compensatory mechanism for basal ganglia aphasia," *Brain Injury*, vol. 34, no. 3, pp. 430–437, 2020.

[14] Q. G. Li, C. Zhao, Y. Shan et al., "Dynamic neural network changes revealed by voxel-based functional connectivity strength in left basal ganglia ischemic stroke," *Frontiers in Neuroscience*, vol. 14, article 526645, 2020.

[15] Y. F. Zang, Y. He, C. Z. Zhu et al., "Altered baseline brain activity in children with ADHD revealed by resting- state functional MRI," *Brain & Development*, vol. 29, no. 2, pp. 83–91, 2007.

[16] Q. H. Zou, C. Z. Zhu, Y. Yang et al., "An improved approach to detection of amplitude of low-frequency fluctuation (ALFF) for resting-state fMRI: fractional ALFF," *Journal of Neuroscience Methods*, vol. 172, no. 1, pp. 137–141, 2008.

[17] D. Cordes, V. M. Haughton, K. Arfanakis et al., "Frequencies contributing to functional connectivity in the cerebral cortex in "resting-state" data," *AJNR. American Journal of Neuroradiology*, vol. 22, no. 7, pp. 1326–1333, 2001.

[18] X. N. Zuo, A. di Martino, C. Kelly et al., "The oscillating brain: complex and reliable," *NeuroImage*, vol. 49, no. 2, pp. 1432–1445, 2010.

[19] W. B. Guo, F. Liu, G. L. Xun et al., "Reversal alterations of amplitude of low-frequency fluctuations in early and late onset, first-episode, drug-naive depression," *Progress in Neuro-Psychopharmacology & Biological Psychiatry*, vol. 40, pp. 153–159, 2013.

[20] W. Cao, X. Sun, D. Dong, S. Yao, and B. Huang, "Sex differences in spontaneous brain activity in adolescents with conduct disorder," *Frontiers in Psychology*, vol. 9, p. 1598, 2018.

[21] G̈. Buzsáki and A. Draguhn, "Neuronal oscillations in cortical networks," *Science*, vol. 304, no. 5679, pp. 1926–1929, 2004.

[22] J. Yu, W. Wang, D. Peng et al., "Intrinsic low-frequency oscillation changes in multiple-frequency bands in stable patients with chronic obstructive pulmonary disease," *Brain Imaging and Behavior*, vol. 15, no. 4, pp. 1922–1933, 2021.

[23] M. Penttonen and G. Buzsáki, "Natural logarithmic relationship between brain oscillators," *Thalamus & Related Systems*, vol. 2, no. 2, pp. 145–152, 2003.

[24] Z. Zhao, C. Tang, D. Yin et al., "Frequency-specific alterations of regional homogeneity in subcortical stroke patients with different outcomes in hand function," *Human brain mapping.*, vol. 39, no. 11, pp. 4373–4384, 2018.

[25] K. J. Friston, S. Williams, R. Howard, R. S. J. Frackowiak, and R. Turner, "Movement-related effects in fMRI time-series," *Magnetic Resonance in Medicine*, vol. 35, no. 3, pp. 346–355, 1996.

[26] M. D. Fox and M. E. Raichle, "Spontaneous fluctuations in brain activity observed with functional magnetic resonance imaging," *Nature Reviews. Neuroscience*, vol. 8, no. 9, pp. 700–711, 2007.

[27] M. Jenkinson, P. Bannister, M. Brady, and S. Smith, "Improved optimization for the robust and accurate linear registration and motion correction of brain images," *NeuroImage*, vol. 17, no. 2, pp. 825–841, 2002.

[28] D. P. Roeltgen, S. Sevush, and K. M. Heilman, "Phonological agraphia: writing by the lexical-semantic route," *Neurology*, vol. 33, no. 6, pp. 755–765, 1983.

[29] E. E. Smith, J. Jonides, C. Marshuetz, and R. A. Koeppe, "Components of verbal working memory: evidence from neuroimaging," *Proceedings of the National Academy of Sciences of the United States of America*, vol. 95, no. 3, pp. 876–882, 1998.

[30] E. Ben-Shabat, T. A. Matyas, G. S. Pell, A. Brodtmann, and L. M. Carey, "The right supramarginal gyrus is important for proprioception in healthy and stroke-affected participants: a functional MRI study," *Frontiers in Neurology*, vol. 6, p. 248, 2015.

[31] J. Jung, R. Laverick, K. Nader et al., "Altered hippocampal functional connectivity patterns in patients with cognitive impairments following ischaemic stroke: a resting-state fMRI study," *Neuroimage Clin.*, vol. 32, article 102742, 2021.

[32] G. Yao, J. Li, S. Liu et al., "Alterations of functional connectivity in stroke patients with basal ganglia damage and cognitive impairment," *Frontiers in Neurology*, vol. 11, p. 980, 2020.

[33] P. M. Pedersen, H. Stig Jørgensen, H. Nakayama, H. O. Raaschou, and T. S. Olsen, "Aphasia in acute stroke: incidence, determinants, and recovery," *Annals of Neurology*, vol. 38, no. 4, pp. 659–666, 1995.

[34] S. Kiran, "What is the nature of poststroke language recovery and reorganization?," *ISRN Neurology*, vol. 2012, Article ID 786872, 2012.

[35] R. Nardone, P. De Blasi, G. Zuccoli, F. Tezzon, S. Golaszewski, and E. Trinka, "Transient beneficial effects of excitatory theta burst stimulation in a patient with phonological agraphia after left supramarginal gyrus infarction," *Brain and Language*, vol. 120, no. 3, pp. 422–426, 2012.

[36] D. A. Levine, A. T. Galecki, K. M. Langa et al., "Trajectory of cognitive decline after incident stroke," *Journal of the American Medical Association*, vol. 314, no. 1, pp. 41–51, 2015.

[37] J. W. Lo, J. D. Crawford, D. W. Desmond et al., "Profile of and risk factors for poststroke cognitive impairment in diverse ethnoregional groups," *Neurology*, vol. 93, no. 24, pp. e2257–e2271, 2019.

[38] N. D. Prins, E. J. van Dijk, T. den Heijer et al., "Cerebral small-vessel disease and decline in information processing speed, executive function and memory," *Brain*, vol. 128, no. 9, pp. 2034–2041, 2005.

[39] D. Pinter, C. Enzinger, T. Gattringer et al., "Prevalence and short-term changes of cognitive dysfunction in young ischaemic stroke patients," *European Journal of Neurology*, vol. 26, no. 5, pp. 727–732, 2019.

[40] J. A. Turner, H. Chen, D. H. Mathalon et al., "Reliability of the amplitude of low-frequency fluctuations in resting state fMRI in chronic schizophrenia," *Psychiatry Research*, vol. 201, no. 3, pp. 253–255, 2012.

[41] X. Deng, Z. Liu, Q. Kang, L. Lu, Y. Zhu, and R. Xu, "Cortical structural connectivity alterations and potential pathogenesis in mid-stage sporadic Parkinson's disease," *Frontiers in Aging Neuroscience*, vol. 13, article 650371, 2021.

[42] Y. Li, H. Luo, Q. Yu et al., "Cerebral functional manipulation of repetitive transcranial magnetic stimulation in cognitive impairment patients after stroke: an fMRI study," *Frontiers in Neurology*, vol. 11, p. 977, 2020.

[43] L. Fan, J. Hu, W. Ma, D. Wang, Q. Yao, and J. Shi, "Altered baseline activity and connectivity associated with cognitive impairment following acute cerebellar infarction: a resting-state fMRI study," *Neuroscience Letters*, vol. 692, pp. 199–203, 2019.

[44] V. A. Nair, B. M. Young, C. la et al., "Functional connectivity changes in the language network during stroke recovery," *Annals of Clinical Translational Neurology*, vol. 2, no. 2, pp. 185–195, 2015.

[45] J. Crinion, R. Turner, A. Grogan et al., "Language control in the bilingual brain," *Science*, vol. 312, no. 5779, pp. 1537–1540, 2006.

[46] A. C. Kreitzer and R. C. Malenka, "Striatal plasticity and basal ganglia circuit function," *Neuron*, vol. 60, no. 4, pp. 543–554, 2008.

[47] T. Nierhaus, Y. Chang, B. Liu et al., "Somatosensory stimulation with XNKQ acupuncture modulates functional connectivity of motor areas," *Frontiers in Neuroscience*, vol. 13, p. 147, 2019.

[48] Y. Li, Z. Yu, P. Wu, and J. Chen, "The disrupted topological properties of structural networks showed recovery in ischemic stroke patients: a longitudinal design study," *BMC Neuroscience*, vol. 22, no. 1, p. 47, 2021.

[49] J. Zhang, L. Wei, X. Hu et al., "Specific frequency band of amplitude low-frequency fluctuation predicts Parkinson's disease," *Behavioural Brain Research*, vol. 252, pp. 18–23, 2013.

[50] S. Xue, X. Wang, W. Wang, J. Liu, and J. Qiu, "Frequency-dependent alterations in regional homogeneity in major depression," *Behavioural Brain Research*, vol. 306, pp. 13–19, 2016.

[51] N. Egorova, M. Veldsman, T. Cumming, and A. Brodtmann, "Fractional amplitude of low-frequency fluctuations (fALFF) in post-stroke depression," *Neuroimage Clin.*, vol. 16, pp. 116–124, 2017.

[52] J. Ballester-Plané, R. Schmidt, O. Laporta-Hoyos et al., "Whole-brain structural connectivity in dyskinetic cerebral palsy and its association with motor and cognitive function," *Human Brain Mapping*, vol. 38, no. 9, pp. 4594–4612, 2017.

[53] L. Fogassi and G. Luppino, "Motor functions of the parietal lobe," *Current Opinion in Neurobiology*, vol. 15, no. 6, pp. 626–631, 2005.

[54] S. C. Wriessnegger, G. Bauernfeind, K. Schweitzer, S. Kober, C. Neuper, and G. R. Müller-Putz, "The interplay of prefrontal and sensorimotor cortices during inhibitory control of learned motor behavior," *Front Neuroeng.*, vol. 5, p. 17, 2012.

[55] A. H. Rodrigo, S. I. Domenico, H. Ayaz, S. Gulrajani, J. Lam, and A. C. Ruocco, "Differentiating functions of the lateral and medial prefrontal cortex in motor response inhibition," *Neuroimage*, vol. 85, pp. 423–431, 2014.

[56] G. E. Alexander and M. D. Crutcher, "Functional architecture of basal ganglia circuits: neural substrates of parallel processing," *Trends in Neurosciences*, vol. 13, no. 7, pp. 266–271, 1990.

[57] A. Parent and L. N. Hazrati, "Functional anatomy of the basal ganglia. I. The cortico-basal ganglia-thalamo- cortical loop," *Brain Research. Brain Research Reviews*, vol. 20, no. 1, pp. 91–127, 1995.

[58] S. Frenkel-Toledo, S. Ofir-Geva, L. Mansano, O. Granot, and N. Soroker, "Stroke lesion impact on lower limb function," *Frontiers in Human Neuroscience*, vol. 15, article 592975, 2021.

Hindawi
Neural Plasticity
Volume 2022, Article ID 5771634, 9 pages
https://doi.org/10.1155/2022/5771634

Research Article

Effectiveness of a Novel Contralaterally Controlled Neuromuscular Electrical Stimulation for Restoring Lower Limb Motor Performance and Activities of Daily Living in Stroke Survivors: A Randomized Controlled Trial

Ying Shen,[1] Lan Chen,[2] Li Zhang,[2] Shugang Hu,[3] Bin Su,[2] Huaide Qiu,[1] Xingjun Xu,[1] Guilan Huang,[2] Zhifei Yin,[1] Jinyu Yang,[2] Chuan Guo,[1] and Tong Wang[1]

[1]*Rehabilitation Medicine Center, The First Affiliated Hospital of Nanjing Medical University, Nanjing, China*
[2]*Rehabilitation Department, The Affiliated Wuxi Mental Health Center of Nanjing Medical University, Wuxi, China*
[3]*Rehabilitation Department, The Affiliated Jiangning Hospital of Nanjing Medical University, Nanjing, China*

Correspondence should be addressed to Jinyu Yang; yangjinyu2423@163.com, Chuan Guo; guochuanrehab@126.com, and Tong Wang; wangtong60621@163.com

Received 13 September 2021; Revised 11 November 2021; Accepted 20 December 2021; Published 11 January 2022

Academic Editor: Xi-Ze Jia

Background. Contralaterally controlled neuromuscular electrical stimulation (CCNMES) is a novel electrical stimulation treatment for stroke; however, reports on the efficacy of CCNMES on lower extremity function after stroke are scarce. *Objective*. To compare the effects of CCNMES versus NMES on lower extremity function and activities of daily living (ADL) in subacute stroke patients. *Methods*. Forty-four patients with a history of subacute stroke were randomly assigned to a CCNMES group and a NMES group ($n = 22$ per group). Twenty-one patients in each group completed the study per protocol, with one subject lost in follow-up in each group. The CCNMES group received CCNMES to the tibialis anterior (TA) and the peroneus longus and brevis muscles to induce ankle dorsiflexion motion, whereas the NMES group received NMES. The stimulus current was a biphasic waveform with a pulse duration of 200 μs and a frequency of 60 Hz. Patients in both groups underwent five 15 min sessions of electrical stimulation per week for three weeks. Indicators of motor function and ADL were measured pre- and posttreatment, including the Fugl–Meyer assessment of the lower extremity (FMA-LE) and modified Barthel index (MBI). Surface electromyography (sEMG) assessments included average electromyography (aEMG), integrated electromyography (iEMG), and root mean square (RMS) of the paretic TA muscle. *Results*. Values for the FMA-LE, MBI, aEMG, iEMG, and RMS of the affected TA muscle were significantly increased in both groups after treatment ($p < 0.01$). Patients in the CCNMES group showed significant improvements in all the measurements compared with the NMES group after treatment. Within-group differences in all post- and pretreatment indicators were significantly greater in the CCNMES group than in the NMES group ($p < 0.05$). *Conclusion*. CCNMES improved motor function and ADL ability to a greater extent than the conventional NMES in subacute stroke patients.

1. Introduction

Stroke is one of the most frequently occurring diseases in the world, leading to permanent disability and a decline in quality of life, resulting in a heavy burden of illness [1]. There are more than 2 million new cases in China each year, 70-80% of which are unable to live independently because of disability [2]. Most stroke patients have impaired walking ability and can only walk at home, and the restoration of mobility is often one of the primary goals of rehabilitation [3].

Neuromuscular electrical stimulation (NMES) is an effective therapeutic method for facilitating the recovery of

motor function in paralyzed lower limbs of stroke survivors [4]. During NMES, a low-frequency pulse current is applied over the motor nerves or muscles to mimic exercise therapy via smooth tetanic muscle contractions [5, 6]. NMES can help maintain joint range of motion (ROM), strengthen muscle, and promote motor relearning. NMES can be utilized to modulate neural activity to either restore contraction of the tibialis anterior (TA) and peroneus longus and brevis muscles or prevent an abnormal triceps surae reaction due to causes such as spasticity. NMES of the peroneal nerve provokes ankle dorsiflexion. Indeed, NMES of the peroneal nerve can be used not only to correct drop-foot but also to modulate long-term neuromuscular system function, thereby promoting the rehabilitation of lower limb function after stroke [7]. However, a major weakness of NMES is that patients cannot initiate active movement as NMES is a completely passive treatment. To better promote functional gain, NMES should be combined with subjective efforts; however, this is difficult to achieve, especially in patients with acute or severe motor dysfunction.

Contralaterally controlled neuromuscular electrical stimulation (CCNMES), an innovative NMES method, was recently used to restore ankle dorsiflexion in patients with chronic stroke [8]. A few groups have begun to investigate the impact of CCNMES on ankle dorsiflexion in hemiplegic stroke patients [9]. In one study, Knutson and colleagues used a sensor attached to patient's sock that was worn on the nonparetic foot to measure the angle of ankle activity, as well as two surface electrodes positioned, one positioned over the peroneal nerve and the other over the TA muscle, to activate ankle dorsiflexion motion. The current stimulus intensity was directly proportional to the degree of active ankle dorsiflexion of the unaffected side [8]. It was also reported that both CCNMES and NMES plus walking training could improve lower limb motor function in patients with chronic stroke [10]. CCNMES uses the joint angles or electromyographic (EMG) signal from the nonparetic side for a predefined movement to control the intensity of the electrical stimulation delivered to the paretic side to induce a similar movement [11, 12]. The major differences between CCNMES and NMES are as follows: (i) the range of motion and speed of affected limb movement are in the control of patients themselves; (ii) bilateral symmetrical joint movement [10, 12]. However, the clinical benefit of using CCNMES to restore hemiplegic lower limb function remains unclear.

Here, we applied the CCNMES that uses an electromyographic EMG signal instead of an angle sensor attached to patient's sock to trigger the stimulator. The intensity of the electrical stimulation delivered to the peroneal nerve and TA muscle was inducted by the electromyographic value instead of the degree of volitional dorsiflexion. The objective of this study was to investigate whether the application of this innovative CCNMES method could restore lower limb motor function in hemiplegic patients.

2. Materials and Methods

2.1. Design. This study was a randomized controlled trial designed to compare the clinical outcomes between CCNMES and NMES on motor function recovery after stroke. Forty-four patients were randomly assigned to two groups in a 1 : 1 ratio using a simple randomization procedure.

2.2. Subjects. Participants with lower-extremity hemiplegia were recruited from Wuxi Tongren Rehabilitation Hospital from April 2021 to July 2021. The criteria for inclusion were as follows: (i) diagnosis of stroke was confirmed by computed tomography (CT) and/or magnetic resonance imaging (MRI); (ii) initial, unilateral onset or previous episodes without neurological impairment between 1 and 6 months post-stroke; (iii) aged 40 to 80 years; (iv) a grade of ankle dorsiflexion strength ≤3/5 (Lovett scale); (v) lower extremity Brunnstrom stage I–III; and (vi) the hemiplegic side with normal passive ankle movement. The criteria for exclusion were (i) progressive stroke with nonstable condition; (ii) cerebellar or brainstem stroke; (iii) unable to cooperate with assessment and treatment due to severe cognitive and communication impairment; (iv) complication with severe heart, lung, liver, kidney, or infectious disease; (v) the wearing of a cardiac pacemaker; and (vi) motor dysfunction due to other causes before the onset of stroke.

This study was approved by the Ethics Committee of the Affiliated Wuxi Mental Health Center of Nanjing Medical University (Wuxi Tongren Rehabilitation Hospital) (No.: WXMHCIRB2020LLky040). This trial was registered in the China Clinical Trial Registration Center (ChiCTR2100045143). All patients provided signed informed consent.

2.3. Electrical Stimulation Equipment. The electrical stimulator (S4, Vishee Co., Nanjing, China) delivered pulses (pulse width 200 μs, biphasic asymmetrical rectangular) at 60 Hz. The CCNMES device consisted of a stimulator and a electromyographic sensor. The electromyographic sensorn the unaffected limb is used to trigger the stimulator. One recording electrode was placed below the head of the fibula over the common peroneal nerve and another at the motor point of the unaffected TA muscle [10]; a third reference electrode was placed in the middle. For the hemiplegic side, one stimulating electrode was placed below the head of the fibula over the common peroneal nerve and another at the motor point of the TA muscle, with one reference electrode in the middle [10]. The patients were not supposed to feel pain due to the administered electrical stimulation.

For the CCNMES treatment (Figure 1), the intensity of the electrical stimulation applied to induce dorsiflexion in the hemiplegic ankle was modulated by the EMG value of the contraction of the unaffected TA muscle [10, 12]. Before treatment, the patients were asked to dorsiflex their unaffected ankle to almost 10% ROM and hold that position. The electrical equipment then recorded the EMG value of the muscle contraction obtained by the sensor attached to the recording electrodes. Simultaneously, an operator increased the stimulating current in a stepwise fashion until the current was sufficiently strong to induce dorsiflexion of up to 10% ROM in the hemiplegic ankle. The intensity of the stimulating current was also automatically recorded by the equipment. Thus, the EMG value of the muscle contraction of the affected side corresponded to the electric current

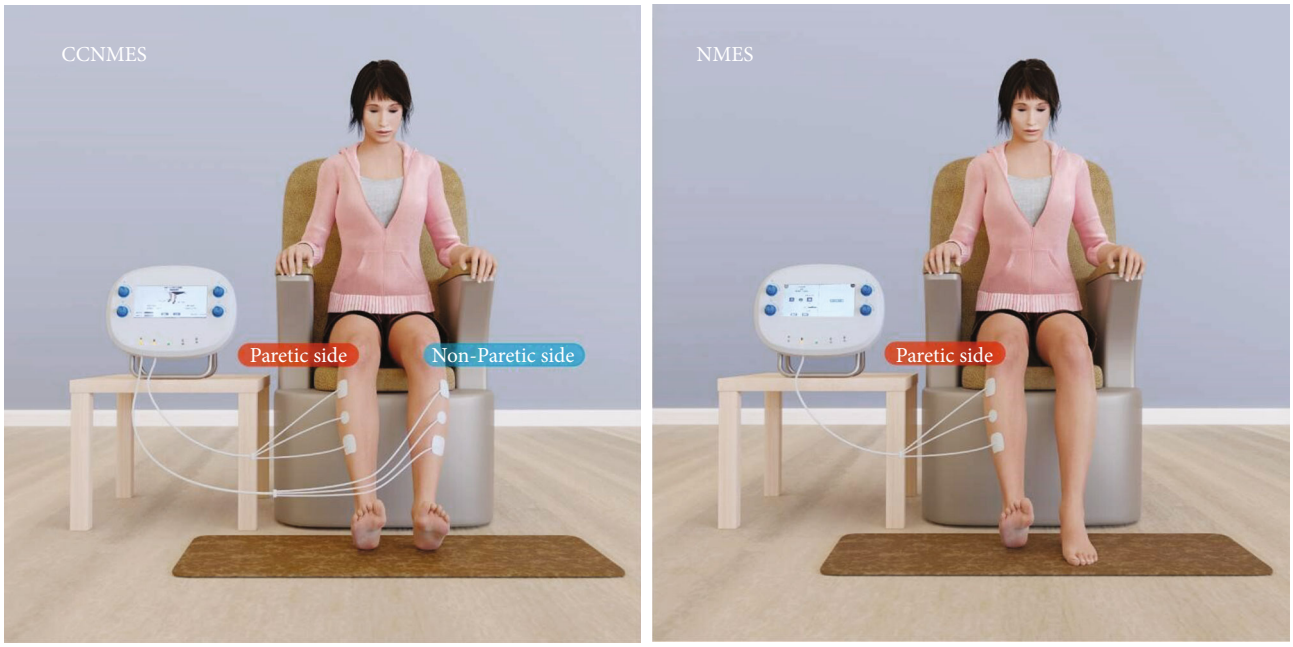

Figure 1: Graphical presentation of contralaterally controlled neuromuscular electrical stimulation (CCNMES) and neuromuscular electrical stimulation (NMES).

intensity in the contralateral unaffected muscle. The same procedure was then applied with patients dorsiflexing their nonparetic ankle to 50% and 100% ROM. Once these three steps had been completed, the current intensity of the hemiplegic side corresponding to the EMG value of the unaffected side could be calculated and recorded by the electrical stimulation equipment. Before the CCNMES treatment, the patients were taught how to use the equipment by their respective physiotherapists so they could perform the electrical stimulation by themselves. During the treatment, the patients had to try to dorsiflex both ankles after hearing the cueing tone. As the EMG value of the unaffected ankle dorsiflex was detected, the electrical instrument immediately stimulated the affected peroneal nerve and the motor point of the unaffected TA muscle using the proportional current intensity calculated by the instrument [12]. This resulted in both ankles being able to complete the same action almost simultaneously in the treatment. For the NMES treatment (Figure 1), the stimulation sites and parameters of the hemiplegic limb were the same as those for the CCNMES treatment.

2.4. Intervention. Patients in both groups underwent five 15 min sessions of electrical stimulation per week for 3 consecutive weeks. All patients received routine rehabilitation treatment. Each CCNMES pulse lasted for 15 s with 10 s breaks for a total of 36 pulses. The patients repeatedly attempted to stretch both ankles according to the sound cues until full ankle dorsiflexion was achieved for 15 s with a 10 s resting period. Each NMES pulse lasted 15 s with 10 s breaks for a total of 36 pulses.

2.5. Allocation and Assessment. Patients were assigned to the CCNMES or NMES groups at a 1 : 1 ratio using simple randomization. The randomization sequence was generated before the treatment, and the information was concealed in sequentially numbered, sealed, opaque envelopes. Patients selected an envelope after signing the informed consent form, following which the staff, who were blinded to the trials, informed the physiotherapist about the allocated intervention regimen. All the outcome measures were assessed pre- (T1) and posttreatment (T2; at the end of the 3-week treatment).

2.6. Outcome Assessment. The primary outcome measure was the Fugl–Meyer assessment of the lower extremity (FMA-LE). Secondary outcomes included the modified Barthel index (MBI) score, as well as the average electromyography (aEMG), integrated electromyography (iEMG), and root mean square (RMS) values for the affected TA muscle.

2.6.1. FMA-LE. The FMA-LE was used to assess the motor function of the lower limb [13]. The maximum score for the whole FMA-LE was 34. The higher the score, the better the motor function in the paretic lower limb.

2.6.2. MBI. The MBI score was used to evaluate the ability to perform activities of daily living (ADL). The maximum score for the whole MBI assessment was 100. The higher the score, the better the level of physical function [14].

2.6.3. sEMG. A wireless BTS-FREEEMG 300 (BTS Bioengineering, Milan, Italy) was used to collect the surface electromyography (sEMG) signals of the paretic TA muscle, which were synchronously transmitted to a BTS EMG-Analyzer (BTS Bioengineering) [15]. Patients were asked to sit comfortably in a chair with knees flexed at 90 degrees, ankles in an anatomically neutral position. Before data collection, the skin was cleaned using alcohol and shaved if needed. A

pair of silver–silver chloride electrodes (H124SG, 30 mm × 24 mm; COVIDIEN-Kendall, Waukegan, IL, USA) were placed on the belly of the TA muscle with an interelectrode distance of 2 cm while a reference electrode was placed on the affected ankle. Before the sEMG recording, patients were taught how to perform the maximum voluntary isometric contraction (MVIC) of ankle dorsiflexion until they could complete it correctly [16]. For each patient, three 3 s trails of MVIC were recorded with a 2 min rest between each trail. The sampling frequency of the sEMG signals was 1,000 Hz, and the signals were recorded for off-line analysis.

EMG signals were automatically analyzed by the BTS EMG-Analyzer with the band-pass filtered from 20 to 500 Hz. aEMG is the average of the instantaneous amplitude of the 3 s MVIC, which represents the degree of muscle activation during movement and the type and synchronization of activated motor units [17]. iEMG is defined as the total magnitude of discharge of motor units involved in muscle activities in the 3 s period and partially reflects the number of involved motor units and their discharge in that period [18]. RMS, the mean square root of the square of the amplitude of instantaneous EMG signals in a 3 s period, is determined by changes in the amplitude and reflects the recruitment of motor units [19].

2.6.4. Sample Size Calculation. The sample size was calculated using G∗Power Software (version 3.1.9.4). The effect size (f) was calculated as 1.095 based on the FMA-LE score from a group of individuals as previously reported [20]. To achieve 90% power with an alpha error of 5%, a minimum sample size of 38 patients (19 per group) was needed to detect statistical significance for a between-group difference in FMA-LE. Assuming a 10% dropout rate, the minimum number of enrolled patients was determined to be 44 (22 per group).

3. Statistical Analysis

Statistical analysis was performed using SPSS23.0 (IBM Inc., Chicago, IL, USA). Enrolled patients and drop-out cases with corresponding reasons were recorded. Clinicodemographic data were summarized using descriptive statistics. Specifically, counts and percentages were applied for categorical variables. The continuous data were checked for normality using the Shapiro-Wilk test; continuous data were presented as means with standardized deviation (SD) when data conformed to normal distribution; otherwise, median and interquartile range were applied. Paired t-tests were used for intragroup comparisons, while independent samples t-tests were used for comparisons between groups. For nonnormally distributed data or data lacking homogeneity of variance, the Wilcoxon rank-sum test (Mann–Whitney U test) was used to compare paired and between-group samples. $p < 0.05$ was considered statistically significant.

4. Results

4.1. Participants. A total of 44 stroke patients were randomly divided into a CCNMES group and a NMES group (22 patients per group) using SPSS software. One patient in the CCNMES group withdrew due to low compliance with the training protocol, while one patient in the NMES group withdrew owing to their failure to complete the sEMG evaluation. The progress of patients throughout the study is shown in the CONSORT flow diagram (Figure 2). No significant differences in baseline data were found between the two groups ($p > 0.05$) (as detailed in Table 1).

4.2. Motor Performance and ADL. As presented in Table 2, no significant differences in FMA-LE and MBI scores were observed between the two groups at baseline ($p = 0.269$ and 0.732, respectively). Within-group differences in FMA-LE scores for both the CCNMES and NMES groups were statistically significant after treatment ($p < 0.001$); a between-group comparison indicated that the improvement in the CCNMES group was significantly better than that of the NMES group (difference = 1.71, 95% CI 0.47–2.96, $p = 0.009$). Similarly, CCNMES was associated with a significantly greater improvement in the MBI score as compared with NMES (difference = 6.10, 95% CI 0.84–11.35, $p = 0.024$), while within-group improvements were observed in both groups ($p < 0.001$) (Table 2).

The forest plot (Figure 3) presenting treatment effects of CCNMES and NMES in the FMA-LE and MBI assessment also showed greater benefits for CCNMES. For the FMA-LE, the effect size was 1.710 (95% CI 0.470–2.960, $p = 0.009$) favoring CCNMES, while for MBI, the effect size was 6.100 (95% CI 0.840–11.350, $p = 0.024$), also favoring CCNMES.

4.3. sEMG. As depicted in Table 3, no significant differences in aEMG, iEMG, or RMS values were detected between the groups at baseline ($p = 0.660$, 0.575, and 0.473, respectively); however, after electrical stimulation, the above three sEMG values were significantly increased in both groups ($p < 0.001$). Additionally, a between-group comparison indicated that patients in the CCNMES group displayed significantly improvements in the assessed parameters compared with those of patients in the NMES group (for aEMG: difference = 8.22, 95% CI 1.76–14.67, $p = 0.013$; for iEMG: difference = 16.93, 95% CI 3.51–30.34, $p = 0.016$; for RMS: difference = 21.68, 95% CI 4.82–38.54, $p = 0.014$).

The increase in the aEMG value from baseline to post-treatment for the CCNMES group was higher than that for the NMES group (effect size = 2.67, 95% CI 1.760–14.670, $p = 0.013$). A similar pattern could be seen in the iEMG and RMS assessments (increases = 16.93, 95% CI 3.510–30.340, $p = 0.016$; and 21.68, 95% CI 4.82–38.54, $p = 0.014$, respectively) (Figure 3).

5. Discussion

In our study, we compared the efficacy of CCNMES versus NMES on the lower limb function and ADL in stroke survivors. Our results indicated that although FMA-LE, MBI, and sEMG values were significantly improved in both groups after treatment, patients in the CCNMES group exhibited better recovery than those in the NMES group. This

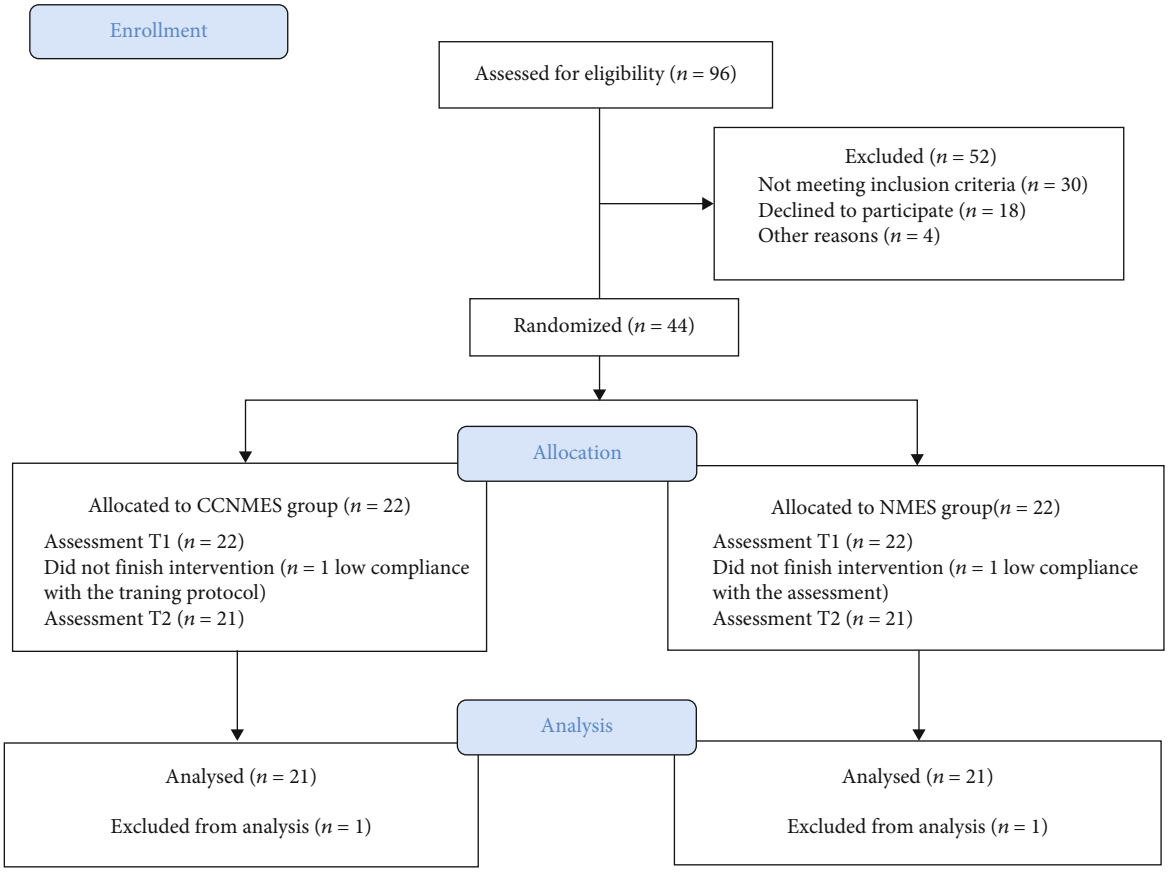

Figure 2: CONSORT flow diagram.

Table 1: Clinicodemographic data of the study cohort at baseline.

	CCNMES group ($n = 21$)	NMES group ($n = 21$)	t / χ^2	p value
Age, years, mean (SD)	62.86 (12.96)	66.09 (6.38)	-1.048	0.301
Sex, n (% male)	18 (81.82%)	15 (68.18%)	1.091	0.296
Type of stroke				
Ischaemic, n (%)	15 (68.18%)	18 (81.82%)	1.091	0.296
Haemorrhagic, n (%)	7 (31.82%)	4 (18.18%)		
Lesion site, n (%left)	12 (54.55%)	10 (45.45%)	0.364	0.546
Time since stroke onset (days), mean (SD)	84.00 (39.60)	73.45 (33.15)	0.985	0.344

CCNMES: contralaterally controlled functional electrical stimulation; NMES: neuromuscular electrical stimulation; SD: standard deviation.

suggested that CCNMES might be more effective at promoting the recovery of lower limb function in hemiplegic patients and improvements in ADL abilities. In addition, we also recorded sEMG activity in the TA muscle. Significant increases in the aEMG, iEMG, and RMS values were observed in both groups, with patients in the CCNMES group again showing the best results. NMES is effective at improving muscle fiber recruitment [21]. The sEMG data in our study support that CCNMES was better at increasing the number and synchronization of activated motor units during TA muscle contraction.

To date, relatively few studies have investigated the efficacy of CCNMES on the recovery of lower limb function after stroke. Knutson and Chae were the first to report on the feasibility of using CCNMES at the paretic ankle to improve lower limb function in patients with chronic stroke [8]. Despite the small sample size, the results of that study indicated that CCNMES may exert positive effects on the functional recovery of lower limbs in poststroke patients. In a follow-up study, the authors randomized 26 patients with chronic stroke (≥6 months) into a CCNMES and a NMES group and found that 6 weeks of CCNMES or NMES plus walking training could improve lower limb motor function; however, neither treatment was found to be superior [10]. The reason for the different result between ours and the above-mentioned study may be due to the different

Table 2: Comparison of motor performance and ADL in two groups and at before and after treatment.

	CCNMES group Mean (SD)	NMES group Mean (SD)	Z	p value	Difference between groups (95% CI)
FMA-LE					
Before treatment	8.81 (2.52)	7.95 (2.40)	−1.106	0.269	0.86 [−0.68–2.39]
After treatment	14.48 (2.96)[a]	11.90 (3.35)[a]	−2.362	0.018	2.57 [0.60–4.54]
Difference	5.67 (2.13)	3.95 (1.87)	−2.267	0.009	1.71 [0.47–2.96][b]
MBI					
Before treatment	39.43 (10.53)	37.05 (6.11)	−0.343	0.732	2.38 [−2.99–7.75]
After treatment	56.62 (11.96)[a]	48.14 (9.86)[a]	−2.222	0.026	8.48 [1.63–15.32]
Difference	17.19 (9.73)	11.10 (6.79)	−2.261	0.024	6.10 [0.84–11.35][b]

SD: standard deviation; CI: confidence interval; ADL: activities of daily living; FMA-LE: Fugl–Meyer assessment-lower extremity; MBI: modified Barthel Index. [a]$p < 0.001$, differences before and after treatment; [b]$p < 0.05$, differences between groups.

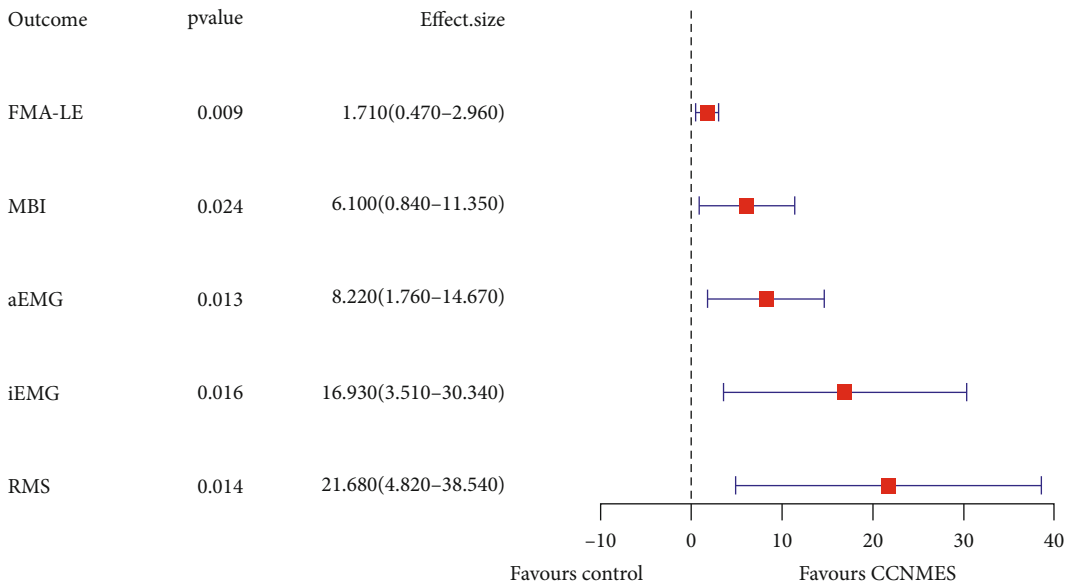

Figure 3: Forest plot presenting the treatment effects of CCNMES and NMES on the different parameters assessed. FMA-LE: Fugl–Meyer assessment-lower extremity; MBI: modified Barthel index; aEMG: average electromyography; iEMG: integrated electromyography; RMS: root mean square.

disease duration of patients. In the study of Knutson et al. [10], the mean illness duration was 2.7 years in the CCNMES group, compared with 84 days in the present study. This suggests that stroke patients with a shorter disease course tend to benefit more from CCNMES than those with a longer disease course.

NMES is considered to be a promising adjuvant therapy for the rehabilitation of the motor control deficits caused by stroke. The benefits of NMES can be interpreted in terms of some possible peripheral mechanisms, including that (i) NMES can maintain and increase joint ROM, although to achieve this, the intensity of NMES must be large enough to attain maximum range with joint activity; (ii) NMES can minimize and prevent muscle atrophy [22]; and (iii) NMES can reduce spasticity by improving motor function [18, 23]. In addition, NMES may promote motor function rehabilitation after stroke through several central mechanisms. For instance, somatosensory input, in the form of peripheral nerve stimulation through electrodes applied on the skin surface, can reportedly enhance motor performance. Sensory-level somatosensory stimulation induced by NMES was found to activate large cutaneous and proprioceptive fibers, with increased somatosensory nerve input through stimulated peripheral nerve leading to improved motor control performance [17]. The peripheral stimulation of the hemiplegic limb sends neural input to the cortex of the cerebrum which induces changes in cortical plasticity in the primary somatosensory cortex, primary motor cortex, and premotor cortex [19]. Improving cortical excitability is conducive to enhancing muscle strength [24].

In this study, patients in the CCNMES group showed better motor function and ADL recovery compared with those in the NMES group. Despite the similarities between CCNMES and NMES, the former has several potential advantages over the latter. First, CCNMES is an active physical therapy method and does not require the paralyzed

Table 3: Comparison of sEMG-related indices between the two groups and between before and after treatment.

	CCNMES group Mean (SD)	NMES group Mean (SD)	Z	p value	Difference between groups (95% CI)
aEMG (μV)					
Before treatment	18.69 (16.03)	16.93 (17.35)	−0.440	0.660	1.77 [−8.65–12.18]
After treatment	38.15 (17.55)[a]	28.16 (20.77)[a]	−1.497	0.134	9.99 [−2.02–21.99]
Difference	19.45 (11.30)	11.24 (9.31)	−2.478	0.013	8.22 [1.76–14.67][b]
iEMG (μV·s)					
Before treatment	43.04 (41.75)	35.29 (36.36)	−0.667	0.505	7.60 [−16.66–32.18]
After treatment	82.91 (43.39)[a]	58.22 (42.04)[a]	−1.824	0.068	24.69 [−1.96–51.33]
Difference	39.86 (24.68)	22.94 (17.79)	−2.402	0.016	16.93 [3.51–30.34][b]
RMS (μV)					
Before treatment	54.54 (52.03)	44.35 (45.66)	−0.717	0.473	10.19[−20.34–40.71]
After treatment	104.40 (53.58)[a]	72.53 (50.80)[a]	−2.025	0.043	31.87 [−0.70–64.43]
Difference	49.86 (30.76)	28.18 (22.71)	−2.453	0.014	21.68 [4.82–38.54][b]

SD: standard deviation; CI: confidence interval; aEMG: average electromyography; iEMG: integrated electromyography; RMS: root mean square; [a]$p < 0.001$, differences before and after treatment; [b]$p < 0.05$, differences between groups.

limbs to retain any residual motor function. In contrast, NMES, which is applied to stroke patients with acute or severe motor dysfunction, is a completely passive treatment. Passive NMES does not sufficiently fit the current theory underlying motor relearning because motor relearning requires the subjective efforts of the patient and task-oriented training [25]. During CCNMES, patients must use an active predefined movement of the nonaffected limbs to trigger the electric stimulation equipment. The intensity of the electric stimulation is directly proportional to the degree of active muscle contraction of the contralateral limb, thereby enabling the ROM and speed of the affected limb to be controlled by the patients themselves. For the hemiplegic upper extremity in stroke patients, improved motor control was reported to be easier to achieve when voluntary movements were used to trigger electric stimulation instead of conventional electric stimulation [26]. Thus, CCNMES may be better at promoting motor control ability, especially for stroke patients with subacute or severe motor dysfunction who have no or little residual motor function.

Secondly, CCNMES can potentially be used to induce synchronized presynaptic and postsynaptic activity of the affected population of anterior horn cells. It is well known that, based on this mechanism, functional electrical stimulation (FES), such as that provided by a foot-drop stimulator, can promote the recovery of motor function in hemiplegic lower limbs after stroke [18]. The key underlying the ability of electrical stimulation to induce synchronous presynaptic and postsynaptic activity lies with the simultaneous provision of electrical stimulation and patients' subjective effort [27]. Indeed, when repetitive movements controlled by the central nervous system were paired with somatosensory stimulation provided by electrical stimulation, there was a demonstrable improvement in motor function and sensory cortex activation [28]. Changes in the sensory cortex can also reflect a heightened sensitization of neurons associated with limb movement, which may behave like a long-term potentiation process [29]. The traditional and completely passive NMES would not work through this mechanism [18]. In contrast, CCNMES emphasizes intention-driven movement, thereby allowing the synchronization of motor intention and stimulated limb movement [9]. The electrical stimulation and the antidromic impulse produced by CCNMES are combined with simultaneous voluntary motor intention and efforts. This endows CCNMES with the potential for therapeutic application to artificially initiate synchronized presynaptic and postsynaptic activity in the affected anterior horn cells through activating the residual pyramidal tract.

Finally, another advantage of CCNMES over NMES is that it utilizes the "bilateral exercise" principle [12]. Bilateral exercise uses the interlimb coupling effect to take advantage of the nonaffected limb to promote motor function recovery in the affected limb [30]. To achieve this effect, both limbs of the stroke patient must be repetitively and intensively trained simultaneously [31]. A balance in interhemispheric inhibition is essential for normal voluntary movement. When a patient suffers a stroke in one hemisphere, this balance is broken, and the reduced interhemispheric inhibition from the ipsilateral to the contralateral hemisphere may result in increased inhibition from the latter to the former, thereby decreasing the excitability of the ipsilateral hemisphere [32]. Bilateral exercise poststroke may accelerate cortical neural plasticity and promote interhemispheric disinhibition, which allows better use of the spared pathways of the affected hemisphere [33]. Additionally, bilateral exercise can supplement the damaged crossed corticospinal pathways by recruiting the ipsilateral pathways from the contralesional or contralateral hemisphere [34]. Activity in the contralesional hemisphere is likely to contribute to motor function recovery after stroke *via* a small proportion (10%) of the pyramidal tract that did not decussate [35]. Cunningham et al. showed that this type of bilateral neuromuscular electrical stimulation can reduce the interhemispheric inhibition from unaffected motor cortices and maintain the ipsilesional output to the paretic limb [36].

This indicates that bilateral and unilateral electrical stimulation act through different neurophysiological mechanisms in stroke participants and that CCNMES has the potential to promote the recovery of paretic limbs through symmetric bilateral movement, which reduces inhibition between the bilateral hemispheres.

This study had several limitations. The selected patients were between 1 and 6 months poststroke, and it was uncertain whether the outcomes were affected by a natural recovery from the disease. Further studies will be needed to assess the clinical generalization of this interventional technique for stroke patients and other neurological patients with similar functional motor impairments that affect their daily activities. Another limitation of our study was the absence of a control group receiving routine rehabilitation treatment without electrical stimulation. Thus, the results observed in the NMES group could not be solely attributed to the unique effects of NMES.

6. Conclusions

CCNMES may involve a variety of rehabilitation principles that are crucial for promoting motor function recovery. The ability of CCNMES to promote neuroplastic changes is based on principles such as repetitive, active, and bilateral symmetric movement; neuromuscular electrical stimulation; and the activation of motor neurons, afferent fibers, and the primary motor cortex [37]. In our study, both the CCNMES and NMES interventions resulted in a marked amelioration of paretic lower extremity function and ADL ability; however, CCNMES showed better motor function and greater recovery in ADL abilities than the conventional NMES treatment. CCNMES represents an effective therapeutic method to accelerate the recovery of hemiplegic lower limbs and has the potential for use in stroke rehabilitation.

Data Availability

The datasets generated and analyzed during the current study are available from the corresponding author on reasonable request.

Conflicts of Interest

The authors declare that they have no competing interest.

Authors' Contributions

YS, ZY, and TW conceived and designed the study; LZ, LC, BS, and JY performed the study and collect materials; JY and HQ analyzed the results; YS, SH, and CG wrote the manuscript; TW and XX helped coordinate the study and reviewed the manuscript. All authors contributed to the article and approved the submitted version. Ying Shen, Lan Chen, Li Zhang, and Shugang Hu contributed equally to this work.

Acknowledgments

We thank all the patients for their voluntary contributions during the completion of this study. This study was funded by the Nanjing Municipal Science and Technology Bureau (no. 2019060002); the National Key R&D Program of China (nos. 2962018YFC2001600 and 2018YFC2001603); Wuxi Taihu Talent Project (no. WXTT P2020008); and Top Talent Support Program for Young and Middle-aged People of Wuxi Health Committee and Major Scientific Research Project of Wuxi Health Committee (no. Z202013).

References

[1] J. Mehrholz, M. Pohl, J. Kugler, and B. Elsner, "The improvement of walking ability following stroke," *Deutsches Ärzteblatt International*, vol. 115, pp. 639–645, 2018.

[2] S. Wu, B. Wu, M. Liu et al., "Stroke in China: advances and challenges in epidemiology, prevention, and management," *The Lancet Neurology*, vol. 18, no. 4, pp. 394–405, 2019.

[3] C. J. Winstein, J. Stein, R. Arena et al., "Guidelines for adult stroke rehabilitation and Recovery," *Stroke*, vol. 47, no. 6, pp. e98–e169, 2016.

[4] Z. Hong, M. Sui, Z. Zhuang et al., "Effectiveness of neuromuscular electrical stimulation on lower limbs of patients with hemiplegia after chronic stroke: a systematic review," *Archives of Physical Medicine and Rehabilitation*, vol. 99, no. 5, pp. 1011–1022.e1, 2018.

[5] J. S. Knutson, M. J. Fu, L. R. Sheffler, and J. Chae, "Neuromuscular electrical stimulation for motor restoration in hemiplegia," *Physical Medicine and Rehabilitation Clinics of North America*, vol. 26, no. 4, pp. 729–745, 2015.

[6] E. L. Nussbaum, P. Houghton, J. Anthony, S. Rennie, B. L. Shay, and A. M. Hoens, "Neuromuscular electrical stimulation for treatment of muscle impairment: critical review and recommendations for clinical practice," *Physiotherapy Canada*, vol. 69, no. 5, pp. 1–76, 2017.

[7] I. J. MJ, G. J. Renzenbrink, and A. C. Geurts, "Neuromuscular stimulation after stroke: from technology to clinical deployment," *Expert Review of Neurotherapeutics*, vol. 9, no. 4, pp. 541–552, 2009.

[8] J. S. Knutson and J. Chae, "A novel neuromuscular electrical stimulation treatment for recovery of ankle dorsiflexion in chronic Hemiplegia," *American Journal of Physical Medicine & Rehabilitation*, vol. 89, no. 8, pp. 672–682, 2010.

[9] J. S. Knutson, M. Y. Harley, T. Z. Hisel, N. S. Makowski, M. J. Fu, and J. Chae, "Contralaterally controlled functional electrical stimulation for stroke rehabilitation," in *2012 Annual International Conference of the IEEE Engineering in Medicine and Biology Society*, pp. 314–317, San Diego, CA, 2012.

[10] J. S. Knutson, K. Hansen, J. Nagy et al., "Contralaterally controlled neuromuscular electrical stimulation for recovery of ankle Dorsiflexion," *American Journal of Physical Medicine & Rehabilitation*, vol. 92, no. 8, pp. 656–665, 2013.

[11] J. S. Knutson, M. Y. Harley, T. Z. Hisel, and J. Chae, "Improving hand function in stroke survivors: a pilot study of contralaterally controlled functional electric stimulation in chronic hemiplegia," *Archives of Physical Medicine and Rehabilitation*, vol. 88, no. 4, pp. 513–520, 2007.

[12] Y. Shen, Z. Yin, Y. Fan et al., "Comparison of the effects of contralaterally controlled functional electrical stimulation and

neuromuscular electrical stimulation on upper extremity functions in patients with stroke," *CNS & Neurological Disorders Drug Targets*, vol. 14, no. 10, pp. 1260–1266, 2015.

[13] C. K. Balasubramanian, C.-Y. Li, M. G. Bowden, P. W. Duncan, S. A. Kautz, and C. A. Velozo, "Dimensionality and item-difficulty hierarchy of the lower extremity Fugl-Meyer assessment in individuals with subacute and chronic stroke," *Archives of Physical Medicine and Rehabilitation*, vol. 97, no. 4, pp. 582–589.e2, 2016.

[14] G. Sulter, C. Steen, and Jacques de Keyser, "Use of the Barthel index and modified Rankin scale in acute stroke trials," *Stroke*, vol. 30, no. 8, pp. 1538–1541, 1999.

[15] G. Gaudet, M. Raison, F. D. Maso, S. Achiche, and M. Begon, "Intra- and intersession reliability of surface electromyography on muscles actuating the forearm during maximum voluntary contractions," *Journal of Applied Biomechanics*, vol. 32, no. 6, pp. 558–570, 2016.

[16] A. Rainoldi, J. E. Bullock-Saxton, F. Cavarretta, and N. Hogan, "Repeatability of maximal voluntary force and of surface EMG variables during voluntary isometric contraction of quadriceps muscles in healthy subjects," *Journal of Electromyography and Kinesiology*, vol. 11, no. 6, pp. 425–438, 2001.

[17] A. B. Conforto, A. Kaelin-Lang, and L. G. Cohen, "Increase in hand muscle strength of stroke patients after somatosensory stimulation," *Annals of Neurology*, vol. 51, no. 1, pp. 122–125, 2002.

[18] D. N. Rushton, "Functional electrical stimulation and rehabilitation–an hypothesis," *Medical Engineering & Physics*, vol. 25, no. 1, pp. 75–78, 2003.

[19] C. W.-H. Wu, P. van Gelderen, T. Hanakawa, Z. Yaseen, and L. G. Cohen, "Enduring representational plasticity after somatosensory stimulation," *NeuroImage*, vol. 27, no. 4, pp. 872–884, 2005.

[20] F. Sharif, S. Ghulam, A. N. Malik, and Q. Saeed, "Effectiveness of functional electrical stimulation (FES) versus conventional electrical stimulation in gait rehabilitation of patients with stroke," *Journal of the College of Physicians and Surgeons–Pakistan*, vol. 27, pp. 703–706, 2017.

[21] D. A. Lake, "Neuromuscular electrical Stimulation," *Sports Medicine*, vol. 13, no. 5, pp. 320–336, 1992.

[22] B. M. Doucet, A. Lam, and L. Griffin, "Neuromuscular electrical stimulation for skeletal muscle function," *The Yale Journal of Biology and Medicine*, vol. 85, pp. 201–215, 2012.

[23] C. Stein, C. G. Fritsch, C. Robinson, G. Sbruzzi, and R. D. M. Plentz, "Effects of electrical stimulation in spastic muscles after Stroke," *Stroke*, vol. 46, no. 8, pp. 2197–2205, 2015.

[24] A. Klaiput and W. Kitisomprayoonkul, "Increased pinch strength in acute and subacute stroke patients after simultaneous median and ulnar sensory stimulation," *Neurorehabilitation and Neural Repair*, vol. 23, no. 4, pp. 351–356, 2009.

[25] M. R. Dimitrijevic, "Clinical practice of functional electrical stimulation: from "yesterday" to "today"," *Artificial Organs*, vol. 32, no. 8, pp. 577–580, 2008.

[26] M. K.-L. Chan, R. K.-Y. Tong, and K. Y.-K. Chung, "Bilateral upper limb training with functional electric stimulation in patients with chronic stroke," *Neurorehabilitation and Neural Repair*, vol. 23, no. 4, pp. 357–365, 2009.

[27] H.-J. Lee, K.-H. Cho, and W.-H. Lee, "The effects of body weight support treadmill training with power-assisted functional electrical stimulation on functional movement and gait in stroke patients," *American Journal of Physical Medicine & Rehabilitation*, vol. 92, no. 12, pp. 1051–1059, 2013.

[28] T. J. Kimberley, S. M. Lewis, E. J. Auerbach, L. L. Dorsey, J. M. Lojovich, and J. R. Carey, "Electrical stimulation driving functional improvements and cortical changes in subjects with stroke," *Experimental Brain Research*, vol. 154, no. 4, pp. 450–460, 2004.

[29] C. M. Bütefisch, B. C. Davis, S. P. Wise et al., "Mechanisms of use-dependent plasticity in the human motor cortex," *Proceedings of the National Academy of Sciences*, vol. 97, no. 7, pp. 3661–3665, 2000.

[30] C. I. E. Renner, C. Brendel, and H. Hummelsheim, "Bilateral arm training vs unilateral arm training for severely affected patients with stroke: exploratory single-blinded randomized controlled trial," *Archives of Physical Medicine and Rehabilitation*, vol. 101, no. 7, pp. 1120–1130, 2020.

[31] K. J. Han and J. Y. Kim, "The effects of bilateral movement training on upper limb function in chronic stroke patients," *Journal of Physical Therapy Science*, vol. 28, no. 8, pp. 2299–2302, 2016.

[32] P. Chen, P. W. H. Kwong, C. K. Y. Lai, and S. S. M. Ng, "Comparison of bilateral and unilateral upper limb training in people with stroke: a systematic review and meta-analysis," *PLoS One*, vol. 14, no. 5, article e0216357, 2019.

[33] C.-S. Hung, K.-C. Lin, W.-Y. Chang et al., "Unilateral vs bilateral hybrid approaches for upper limb rehabilitation in chronic stroke: a randomized controlled trial," *Archives of Physical Medicine and Rehabilitation*, vol. 100, no. 12, pp. 2225–2232, 2019.

[34] J. H. Cauraugh and J. J. Summers, "Neural plasticity and bilateral movements: a rehabilitation approach for chronic stroke," *Progress in Neurobiology*, vol. 75, no. 5, pp. 309–320, 2005.

[35] G. di Pino, G. Pellegrino, G. Assenza et al., "Modulation of brain plasticity in stroke: a novel model for neurorehabilitation," *Nature Reviews. Neurology*, vol. 10, no. 10, pp. 597–608, 2014.

[36] D. A. Cunningham, J. S. Knutson, V. Sankarasubramanian, K. A. Potter-Baker, A. G. Machado, and E. B. Plow, "Bilateral contralaterally controlled functional electrical stimulation reveals new insights into the interhemispheric competition model in chronic stroke," *Neurorehabilitation and Neural Repair*, vol. 33, no. 9, pp. 707–717, 2019.

[37] J. S. Knutson, T. Z. Hisel, M. Y. Harley, and J. Chae, "A novel functional electrical stimulation treatment for recovery of hand function in hemiplegia: 12-week pilot study," *Neurorehabilitation and Neural Repair*, vol. 23, no. 1, pp. 17–25, 2009.

Hindawi
Neural Plasticity
Volume 2021, Article ID 1469339, 16 pages
https://doi.org/10.1155/2021/1469339

Research Article

Distinctive Gut Microbiota Alteration Is Associated with Poststroke Functional Recovery: Results from a Prospective Cohort Study

Yini Dang,[1,2] **Xintong Zhang**,[3] **Yu Zheng**,[3] **Binbin Yu**,[3] **Dijia Pan**,[3] **Xiaomin Jiang**,[3] **Chengjie Yan**,[3] **Qiuyu Yu**,[3] **and Xiao Lu**[3]

[1]*Division of Neurological Rehabilitation, Department of Gastroenterology, The First Affiliated Hospital of Nanjing Medical University, Jiangsu, China*
[2]*Department of Gastroenterology, The First Affiliated Hospital of Nanjing Medical University, Jiangsu, China*
[3]*Department of Rehabilitation Medicine, The First Affiliated Hospital of Nanjing Medical University, Jiangsu, China*

Correspondence should be addressed to Xiao Lu; luxiao1972@163.com

Received 24 August 2021; Accepted 10 November 2021; Published 7 December 2021

Academic Editor: Xi-Ze Jia

Objectives. Functional prognosis is potentially correlated with gut microbiota alterations following the dysregulation of the gut-microbiota-brain axis after stroke. This study was designed to explore the poststroke alterations of gut microbiota and potential correlations between gut microbiota and global functions. *Methods*. A total of thirty-eight patients with stroke and thirty-five healthy demographics-matched controls were recruited. Their fecal DNAs were extracted, and the V3-V4 regions of the conserved bacterial 16S RNA were amplified and sequenced on the Illumina MiSeq platform. Microbial composition, diversity indices, and species cooccurrence were compared between groups. Random forest and receiver operating characteristic analysis were used to identify potential diagnostic biomarkers. Relationships between discriminant bacteria and poststroke functional outcomes were estimated. *Results*. Higher alpha diversity of gut microbiota was observed in poststroke patients as compared to the healthy controls ($p < 0.05$). Beta diversity showed that microbiota composition in the poststroke group was significantly different from that in the control group. Relative abundance of nine genera increased significantly in poststroke patients, while 82 genera significantly decreased ($p < 0.05$). The accuracy, specificity, and susceptibility of the optimal model consisted of the top 10 discriminant species were 93%, 100%, and 86%, respectively. Subgroup analysis showed that bacterial taxa abundant between subacute and chronic stroke patients were overall different ($p < 0.05$). The modified Rankin scale (mRS) ($r = -0.370$, $p < 0.05$), Fugl-Meyer assessment (FMA) score ($r = 0.364$, $p < 0.05$), water swallow test (WST) ($r = 0.340$, $p < 0.05$), and Barthel index (BI) ($r = 0.349$, $p < 0.05$) were significantly associated with alterations of distinctive gut microbiota. *Conclusions*. The gut microbiota in patients with stroke was significantly changed in terms of richness and composition. Significant associations were detected between alterations of distinctive gut microbiota and global functional prognosis. It would facilitate novel treatment target selection in the context of stroke while the causal relationships between distinctive gut microbiota alterations and functional variations need to be further verified with well-designed studies.

1. Introduction

Stroke has been reported to be the major global health issue with an annual incidence of 258 per 100,000 person-years worldwide [1]. Patients suffering from stroke impose a heavy medical and economic burden on both society and the family [2]. With the medical advances in interventions for stroke (e.g., intravenous thrombolysis and endovascular treatment), the survival rate has been significantly improved while the disability rate increases [3]. Although medical treatment for stroke is essential for competing with the life-threatening condition in the acute phase, sequels left by stroke (e.g., motor dysfunction, cognitive dysfunction, or swallowing dysfunction) may subsequently impact the

Table 1: Summary of demographic and clinical characteristics.

	Poststroke ($n = 38$)	Control ($n = 35$)	p value
Age in year, mean (SD)	59.18 (15.34)	59.36 (15.30)	0.902
Gender, n (%)			0.995
Male	25 (65.79)	23 (65.71)	
Female	13 (34.21)	12 (34.29)	
Height in centimeter, mean (SD)	168.53 (6.95)	167.03 (6.83)	0.375
Weight in kilogram, mean (SD)	69.21 (11.33)	66.66 (8.02)	0.274
BMI in kg/m^2, mean (SD)	24.25 (2.87)	23.95 (3.07)	0.594
SBP in mmHg, mean (SD)	127.61 (15.21)	126.00 (10.72)	0.607
DBP in mmHg, mean (SD)	79.13 (10.07)	79.94 (8.16)	0.708
Glucose in mmol/L, mean (SD)	4.52 (0.55)	4.39 (0.62)	0.373
Total cholesterol in mmol/L, mean (SD)	3.38 (1.08)	3.39 (0.70)	0.964
Triglycerides in mmol/L, mean (SD)	1.44 (0.52)	1.45 (0.50)	0.944
Occupation, n (%)			0.403
Full time or part time	19 (50.00)	15 (42.86)	
Layoffs	0 (0)	1 (2.86)	
Retired	17 (44.74)	13 (37.14)	
Self-employed	1 (2.63)	4 (11.43)	
Others	1 (2.63)	2 (5.71)	
Marriage status, n (%)			0.343
Unmarried	0 (0)	1 (2.86)	
Married	36 (94.74)	30 (85.71)	
Widowed	2 (5.26)	2 (5.71)	
Divorced	0 (0)	1 (2.86)	
Others	0 (0)	1 (2.86)	
Education, n (%)			0.201
Primary school or less	0 (0)	1 (2.86)	
Secondary school	11 (28.95)	4 (11.43)	
High school	20 (52.63)	24 (68.57)	
College/university	7 (18.42)	5 (14.28)	
Postgraduate	0 (0)	1 (2.86)	
Smoking status, n (%)			0.131
Nonsmoker	23 (60.53)	20 (57.14)	
Current smoker	13 (34.21)	8 (22.86)	
Previous smoker	2 (5.26)	7 (20.00)	
Alcohol intake, n (%)			0.438
No drinking	16 (42.11)	20 (57.14)	
Light drinking	13 (34.21)	9 (25.72)	
Heavy drinking	9 (23.68)	6 (17.14)	
Regular physical activities, n (%)			0.187
Yes	6 (15.79)	10 (42.86)	
No	32 (84.21)	25 (57.14)	

SD: standard deviation; BMI: body mass index; SBP: systolic blood pressure; DBP: diastolic blood pressure.

patients' health-related quality of life and increase the burden on families and society [4, 5]. This indicates that attention should be, to some extent, moved forward to foresee the long-term functional prognosis; therefore, early modification of corresponding interventions can be provided. According to the literature review, several factors which may impact the poststroke functional recovery have been reported including age, gender, and admission National Institutes of Health Stroke Scale (NIHSS) score [6–8]. Nonetheless, these consolidated factors revealed only the individualized properties which could ever be changed or influenced [9–11]. Upon this condition, exploring novel

Table 2: Summary of clinical characteristics in patients with subacute or chronic stroke.

	Subacute ($n = 18$)	Chronic ($n = 20$)	p value
Type of stroke, n (%)			0.018
Hemorrhage stroke	4 (22.22)	13 (65.00)	
Ischemic stroke	13 (72.22)	7 (35.00)	
Hemorrhagic transformation	1 (5.56)	0 (0)	
Duration of stroke (day), median (IQR)	27 (15)	93 (111)	<0.001
Medical history, n (%)			0.821
Ischemic stroke	1 (5.56)	0 (0)	
Hemorrhage stroke	1 (5.56)	1 (5.00)	
Subarachnoid hemorrhage	0 (0)	0 (0)	
Stroke not classified	0 (0)	0 (0)	
Hypertension	5 (27.78)	9 (45.00)	
Diabetes mellitus	3 (16.67)	2 (10.00)	
Dyslipidemia	0 (0)	0 (0)	
Atrial fibrillation	1 (5.56)	1 (5.00)	
Coronary heart disease	1 (5.56)	1 (5.00)	
Congenital heart disease	0 (0)	0 (0)	
Valvular heart disease	0 (0)	0 (0)	
Other types of heart disease	0 (0)	0 (0)	
Peripheral arterial disease	0 (0)	0 (0)	
Others	0 (0)	1 (5.00)	
Hypertension history in year, mean (SD)	11.50 (5.82)	8.33 (4.47)	0.254
Diabetes mellitus history in year, mean (SD)	7.67 (2.52)	7.50 (3.54)	0.954
Family history, n (%)			—
Stroke	0 (0)	0 (0)	
Coronary heart disease	0 (0)	0 (0)	
Hypertension	1 (5.56)	1 (5.00)	
Diabetes mellitus	0 (0)	0 (0)	
Dyslipidemia	0 (0)	0 (0)	
NIHSS score, mean (SD)	9.44 (4.66)	8.55 (5.89)	0.602
mRS, n (%)			0.846
0-2	5 (27.78)	5 (25.00)	
3-6	13 (72.22)	15 (75.00)	
BI, mean (SD)	34.44 (19.77)	45.00 (27.338)	0.149
FMA-UE score, mean (SD)	19.56 (21.38)	24.05 (17.44)	0.584
FMA-LE score, mean (SD)	16.33 (10.09)	18.84 (10.30)	0.626
WST, n (%)			0.895
Grade 1	13 (72.22)	13 (65.00)	
Grade 2	2 (11.11)	3 (25.00)	
Grade 3	1 (5.56)	1 (5.00)	
Grade 4	2 (11.11)	2 (10.00)	
Grade 5	0 (0)	1 (5.00)	

SD: standard deviation; IQR: interquartile range; NIHSS: National Institutes of Health Stroke Scale; mRS: modified Rankin scale; BI: Barthel index; FMA-UE: Fugl-Meyer assessment upper extremity scale; FMA-LE: Fugl-Meyer assessment lower extremity scale; WST: water swallow test.

functional prognosis-associated factors, which may potentially serve as treatment targets, becomes the most warranted task in front of clinicians.

Among the several newly proposed theories, investigation into the role of the "gut-microbiota-brain axis" in regulating neurological function has rapidly increased over the past decades [12, 13]. Dysregulation of the gut-microbiota-brain axis has been increasingly linked to the pathophysiology of stroke [14, 15]. Interactions across gut microbiota and poststroke functional outcomes were mainly observed in animal models [16, 17]. Nonetheless, the role of human gut microbiota is indeed somewhat different from animals

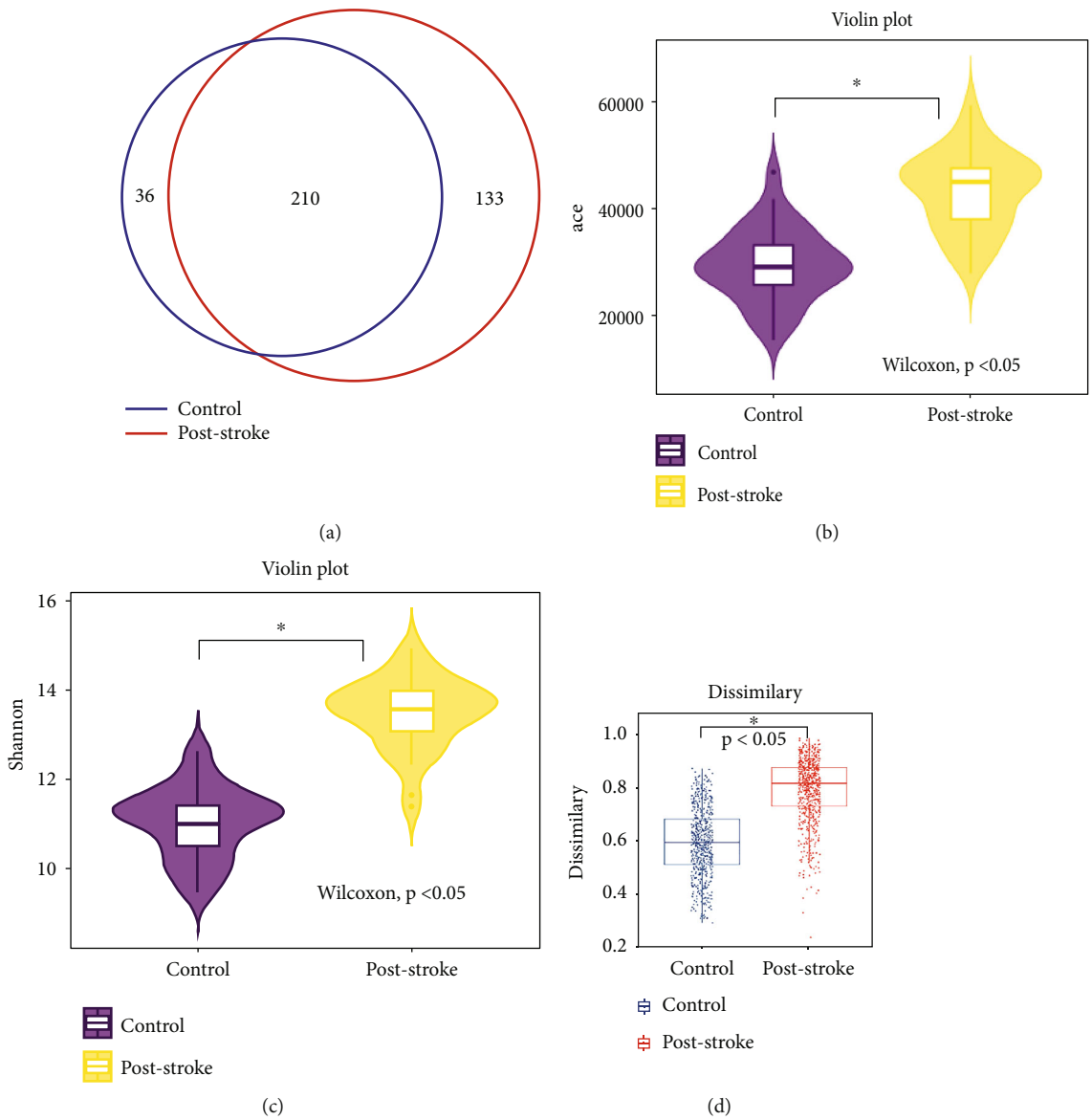

Figure 1: Continued.

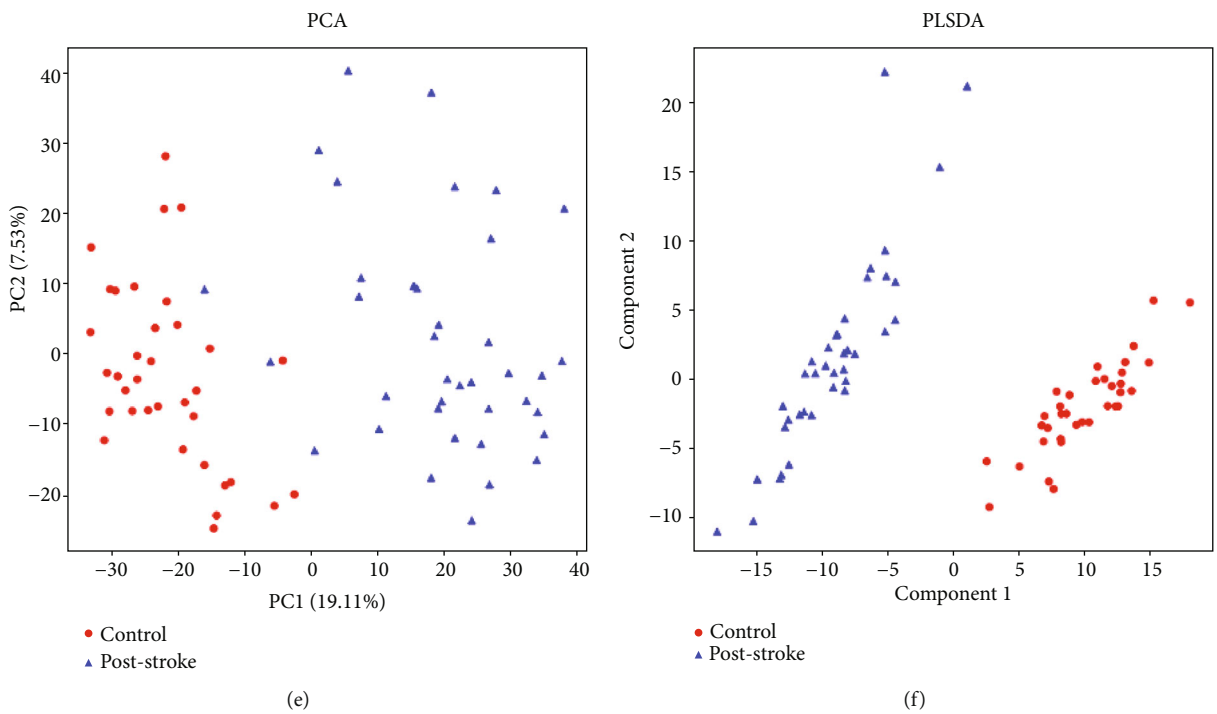

Figure 1: Diversity of gut microbiota. (a) Venn diagram of common OTUs. (b, c) Alpha diversity is estimated with the ace and Shannon index. (d–f) Beta diversity was estimated with Bray-Curtis, PCA, and PLS-DA. OTU: operational taxonomic unit; PCA: principal coordinates analysis; PLS-DA: partial least squares discrimination analysis. $^{*}p < 0.05$.

[18]. The following concerns were the limited knowledge regarding the role human gut microbiota played with neural plasticity and the following prognostic changes. A few cross-sectional studies have explored the composition of gut microbiota in patients with stroke compared with healthy demographics-matched controls. For instance, dysbiosis of short-chain fatty acid- (SCFA-) producing bacteria and SCFAs in patients with acute ischemic stroke was previously observed [19]. Alterations in trimethylamine-producing gut bacteria were proved to be associated with stroke [20]. However, these studies provided single-time point observations (e.g., data collected only at the acute phase) or enrolled only subtypes of stroke (e.g., middle cerebral artery occlusion). In addition, clinical trials remain limited in their ability to show the potential links between the gut microbiome, systematic and neural responses, and global functional changes in the context of stroke.

Based on the above concerns and rationales, we conducted this study to answer the following two clinical questions: (1) should there be any discrepancies of gut microbiota in terms of either richness or composition between poststroke patients and healthy controls and (2) should there be certain potential correlations between gut microbiota alteration and global functions including general disability, physical function, swallowing function, and activity of daily living (ADL)? With the elaboration of the above two questions, our understanding regarding the role the "gut-microbiota-brain axis" played in the development of stroke would be improved followed by promoting novel treatment target selection in the context of stroke.

2. Materials and Methods

2.1. Study Design and Patient Enrollment. The current cohort study was conducted at the First Affiliated Hospital of Nanjing Medical University from 04 July 2020 to 29 January 2021. It was approved by the Committee of Institutional Ethics (Institutional Review Board, 2018-SR-339), and all participants provided written informed consent prior to participation.

The inclusion criteria were as follows: (1) ischemic or hemorrhagic stroke confirmed with computed tomography (CT) or magnetic resonance imaging (MRI), (2) aged 18 yr or older, (3) able to verbally respond to the instructions, and (4) with stable vital signs (systolic blood pressure of 120-180 mmHg, heart rate of 50-100/min, body temperature < 37.5°C, and blood oxygen saturation > 92%) [21, 22]. Patients were excluded if (1) diagnosed with the transient ischemic attack (TIA), (2) with severe cognitive and mental dysfunctions (Montreal Cognitive Assessment < 26) [4, 23], and (3) currently enrolled in another trial or participated in a clinical trial within 6 months [24, 25]. Matched healthy controls were also enrolled according to age, nutritional status (body mass index (BMI)), and geographical area.

2.2. Functional Assessment and Sample Collection. Demographic information including age, gender, BMI, blood pressure, smoking history, alcohol intake, physical activities, stroke subtype, medical history, and family history were collected according to a face-to-face interview or from electronic medical records. Functional assessments were performed by a research assistant with validated and reliable

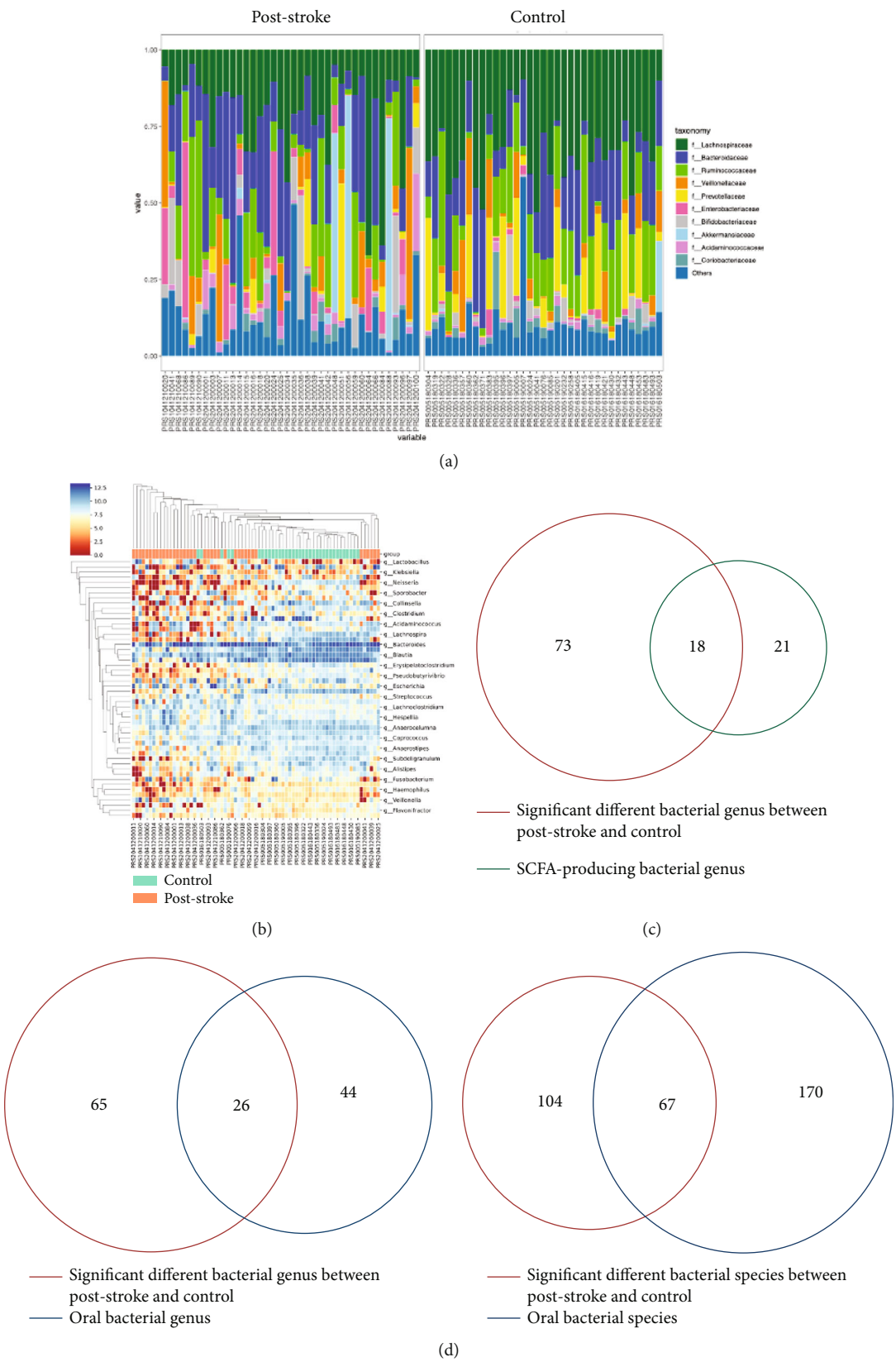

Figure 2: Alteration of gut microbiota composition. (a) Composition of gut microbiota at a family level. (b) Heatmap of gut microbiota composition at the genus level. (c) Venn diagram of the significantly different bacterial genus in poststroke and SCFA-producing bacterial genus. (d) Venn diagram of significantly different bacterial genus/species in poststroke and oral bacterial genus/species. SCFAs: short-chain fatty acids.

Table 3: Top 20 significantly increased/decreased genus in the poststroke group.

Increased genus			Decreased genus		
OTU	Average difference	Adjusted p values	OTU	Average difference	Adjusted p values
Enterococcus	3.12	0.001	Blautia	-1.35	<0.001
Lactobacillus	2.92	0.003	Erysipelatoclostridium	-2.45	<0.001
Enterobacter	2.51	0.007	Pseudobutyrivibrio	-2.47	<0.001
Helicobacter	1.36	0.001	Neisseria	-6.92	<0.001
Kluyvera	1.21	0.025	Haemophilus	-2.39	<0.001
Flavonifractor	0.99	0.004	Chryseobacterium	-1.63	<0.001
Anaeroplasma	0.76	0.024	Actinobaculum	-1.75	<0.001
Lachnoclostridium	0.76	0.018	Filifactor	-1.99	<0.001
Pectobacterium	0.60	0.039	Selenomonas	-2.04	<0.001
			Treponema	-2.05	<0.001
			Catenibacterium	-2.06	<0.001
			Lachnoanaerobaculum	-2.25	<0.001
			Caproiciproducens	-2.26	<0.001
			Lautropia	-2.28	<0.001
			Mannheimia	-2.41	<0.001
			Campylobacter	-2.60	<0.001
			Anaerostipes	-1.45	0.002
			Fusobacterium	-2.40	0.003
			Lachnospira	-2.40	0.041
			Coprococcus	-0.82	0.041

OTU: operational taxonomic unit.

scales. Specifically, stroke severity was assessed with NIHSS score; a higher score indicates greater stroke severity [26]. Modified Rankin scale (mRS) was used to measure the degree of disability and dependence in daily activities. mRS score ranges from 0 (no symptom) to 6 (death) with an unfavorable outcome scored 3-6 and a favorable outcome scored 0-2 [27, 28]. ADL was evaluated with Barthel index (BI) ranging 0-100, with a lower score indicating higher dependence [29]. Upper or lower extremity motor function was assessed with Fugl-Meyer assessment (FMA) score such that a lower score indicates worse motor function [30, 31]. Swallowing function was assessed with the water swallow test (WST); a higher grade indicates a higher risk of aspiration [32, 33]. Fecal samples were collected from both groups and immediately immersed in a solution and stored at -80°C for subsequent DNA extraction.

2.3. DNA Extraction and Illumina Sequencing. DNAs extracted from the fecal samples were used to amplify the V3-V4 region of the 16S rRNA gene targeted with primer set 341 F/806R. This action was performed to determine the gut bacterial community structure. The amplified products were further subjected to the library preparation and sequenced on the Illumina MiSeq platform according to the manufacturer instructions (Illumina technologies, USA).

2.4. Bioinformatics and Statistical Analysis. The raw fastq files obtained from the Illumina sequencing machine were quality filtered with trimmomatic, vsearch, etc. High-quality sequence was used for community structure analysis through the QIIME pipeline. Operational taxonomic unit (OTU) picking was carried out with UCLUST closed reference method, and the representative OTUs were assigned taxonomy using UCLUST classifier by using the SILVA database (Version 132) as a reference dataset.

Alpha and beta diversity indicates the gut microbial diversity of the different patients in the poststroke or control group assessed within (alpha diversity) and across (beta diversity) samples. Alpha diversity estimation was computed using the ace and Shannon indexes. Beta diversity was estimated with principal coordinates analysis (PCA), Bray-Curtis, and partial least squares discrimination analysis (PLS-DA). The Wilcoxon test was used to identify significantly differential OTUs ($p < 0.05$) for further analysis. Significant differences in the relative abundance of associated taxa between groups were further determined with linear discriminant analysis integrated with effect size (LEfSe). Random forest models (R3.4.1, randomForest 4.6-12 package) were performed to develop a predictive model. Receiver operating characteristic curve (ROC) and area under the curve (AUC) were used to evaluate the accuracy of models (R3.3.0, pROC package).

Continuous variables were presented as means and standard deviations. Categorical variables were demonstrated as numbers and percentages. Continuous nonnormal distribution variables were compared between groups with the Wilcoxon rank sum test. Fisher's exact test was used to compare intergroup differences for categorical variables. Correlations between discriminant bacterial and functional assessments were estimated with the Spearman correlation analysis.

Table 4: Top 20 increased/decreased species with the significant difference in the poststroke group.

Increased species			Decreased species		
OTU	Average difference	Adjusted p values	OTU	Average difference	Adjusted p values
Enterococcus raffinosus	1.60	0.008	Erysipelatoclostridium ramosum	-2.45	<0.001
Enterobacter ludwigii	1.71	0.012	Blautia obeum	-2.64	<0.001
Veillonella tobetsuensis	1.64	0.013	Anaerostipes butyraticus	-2.64	<0.001
Enterococcus viikkiensis	1.39	0.014	Fusicatenibacter saccharivorans	-3.01	<0.001
Lactobacillus apodemi	0.96	0.015	Gemmiger formicilis	-3.37	<0.001
Staphylococcus gallinarum	0.95	0.015	Leptotrichia goodfellowii	-2.20	<0.001
Lachnoclostridium urinimassiliense	0.68	0.015	Neisseria dentiae	-1.61	<0.001
Shigella boydii	1.18	0.015	Neisseria cinerea	-1.67	<0.001
Lactobacillus fermentum	1.88	0.017	Mannheimia granulomatis	-1.72	<0.001
Escherichia vulneris	1.28	0.019	Actinobaculum massiliense	-1.75	<0.001
Staphylococcus xylosus	1.04	0.024	Neisseria wadsworthii	-1.77	<0.001
Anaeroplasma abactoclasticum	0.75	0.024	Capnocytophaga granulosa	-1.93	<0.001
Helicobacter ganmani	0.72	0.024	Campylobacter showae	-1.93	<0.001
Megasphaera micronuciformis	1.95	0.026	Porphyromonas gingivalis	-1.96	<0.001
Enterobacter kobei	0.88	0.030	Lachnoanaerobaculum orale	-1.98	<0.001
Lactobacillus casei	1.04	0.034	Filifactor alocis	-1.99	<0.001
Lactococcus garvieae	1.05	0.039	Catenibacterium mitsuokai	-2.06	<0.001
Lactococcus formosensis	0.89	0.039	Cardiobacterium valvarum	-2.14	<0.001
Lactobacillus murinus	0.88	0.039	Campylobacter gracilis	-2.18	<0.001
Kluyvera ascorbata	0.87	0.039	Faecalibacterium prausnitzii	-1.69	0.039

OTU: operational taxonomic unit.

Differences between groups were considered significant as p values less than 0.05.

3. Results

3.1. Demographic and Clinical Characteristics. A number of 38 subjects with clinical diagnosis of poststroke patients (aged 59.18 ± 15.34; male/female 25/13) were recruited, including 18 subacute and 20 chronic patients. We followed the guideline and defined the subacute stroke as duration of stroke for less than 30 days while chronic stroke as duration of stroke for more than 30 days [34]. Meanwhile, 35 age- and sex-matched healthy individuals (aged 59.36 ± 15.30; male/female 23/12) were also enrolled. Detailed demographic and clinical characteristics of stroke patients and controls are shown in Tables 1 and 2.

3.2. Alterations of Gut Microbiota Composition in Poststroke. Venn diagram displayed 210 common OTUs between groups (Figure 1(a)). However, 133 unique OTUs were detected in the poststroke group and 36 in the control group, respectively (Figure 1(a)). Alpha diversity analysis showed that poststroke patients were characterized with higher richness and diversity than the controls (ace indexes 43335.18 ± 7270.54 *vs.* 29467.57 ± 6848.03; Shannon indexes 13.50 ± 0.78 *vs.* 11.03 ± 0.79, $p < 0.05$, Figures 1(b) and 1(c)). Results of Bray-Curtis and PCA were also demonstrated in Figures 1(d) and 1(e). In addition, PLS-DA showed that microbiota composition in the poststroke group significantly differed from that in the control group (Figure 1(f)).

At the family level, *Enterococcaceae*, *Lachnospiraceae*, *Enterobacteriaceae*, and *Helicobacteraceae* were significantly enriched while *Neisseriaceae*, *Porphyromonadaceae*, *Flavobacteriaceae*, *Weeksellaceae*, *Cardiobacteriaceae*, and *Pasteurellaceae* were markedly depleted in the poststroke group (Figure 2(a)). At the genus level, the abundance of 9 genera, including *Lachnoclostridium*, *Flavonifractor*, *Lactobacillus*, *Enterococcus*, and *Enterobacter*, was significantly elevated in the poststroke group. However, the abundance of 82 genera, including *Blautia*, *Faecalibacterium*, *Roseburia*, *Fusicatenibacter*, and *Prevotella*, was found to be significantly decreased in the poststroke group (Figure 2(b) and Table 3). Among these significantly differentiated genera, 18 genera (e.g., *Blautia*, *Fusicatenibacter*, *Ruminococcus*, *Romboutsia*, *Prevotella*, and *Roseburia*) were SCFA-producing bacteria (Figure 2(c)). According to the bacteria from the Human Oral Microbiome (HOM, Version 13) database, oral colonizers (including 26 genus and 67 species) presented significantly differentiated abundance in the poststroke group (Figure 2(d)). As compared to the controls, an abundance of 25 species elevated while 146 decreased in the poststroke group (Table 4).

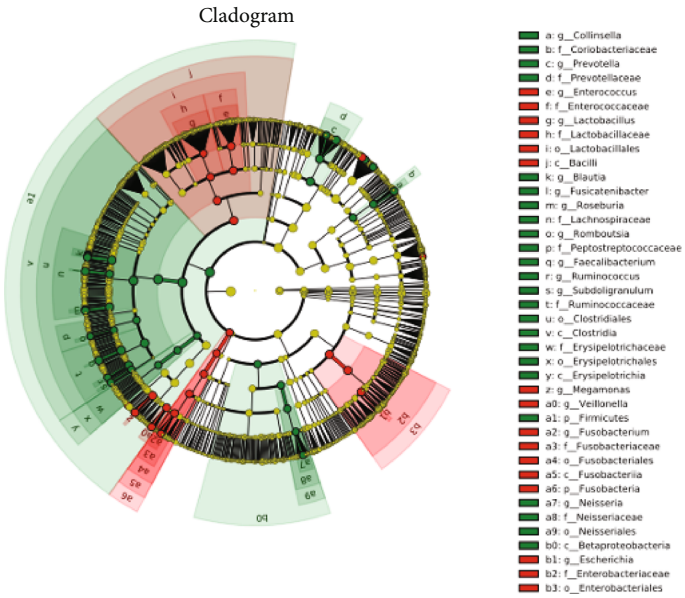

(a)

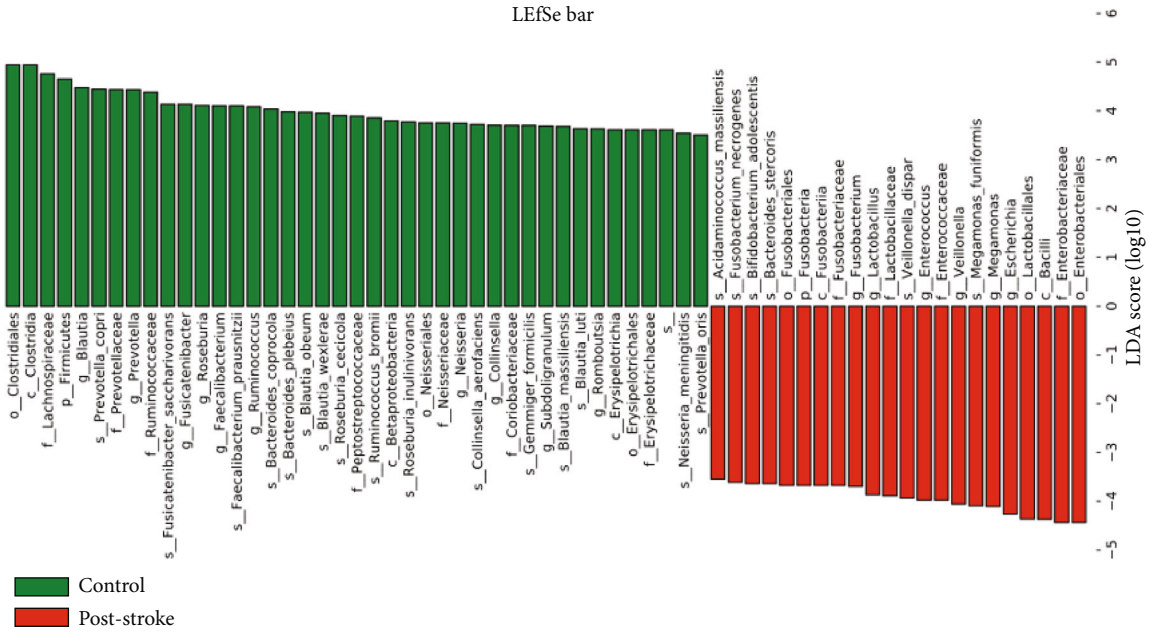

(b)

Figure 3: Continued.

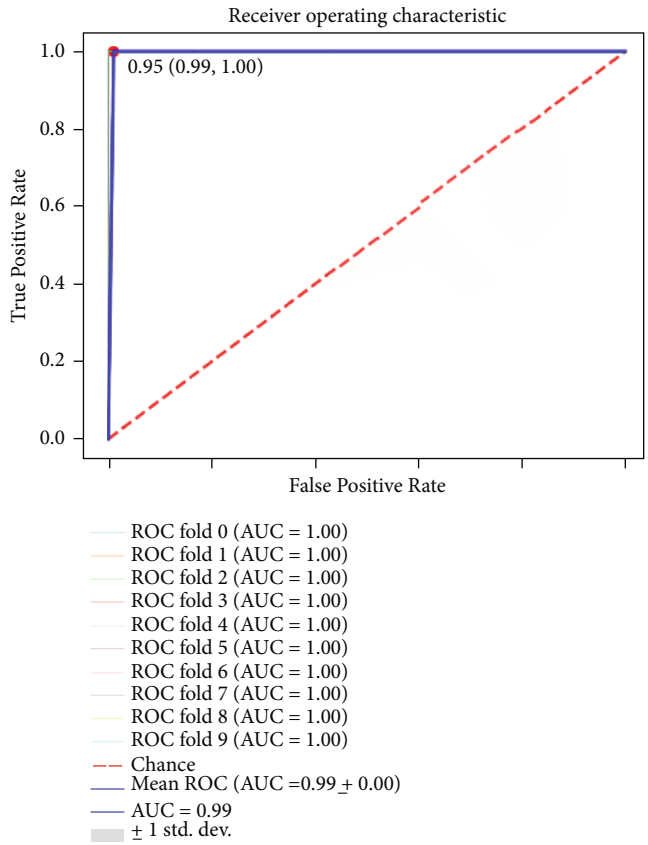

(c)

	Top features
1	k__Bacteria; p__Proteobacteria; c__Gammaproteobacteria; o__Pasteurellales; f__Pasteurellaceae; g__Aggregatibacter; s__Aggregatibacter_segnis
2	k__Bacteria; p__Proteobacteria; c__Betaproteobacteria; o__Neisseriales; f__Neisseriaceae; g__Neisseria; s__Neisseria_mucosa
3	k__Bacteria; p__Proteobacteria; c__Betaproteobacteria; o__Neisseriales; f__Neisseriaceae; g__Neisseria; s__Neisseria_meningitidis
4	k__Bacteria; p__Proteobacteria; c__Betaproteobacteria; o__Neisseriales; f__Neisseriaceae; g__Neisseria; s__Neisseria_flava
5	k__Bacteria; p__Actinobacteria; c__Actinobacteria; o__Corynebacteriales; f__Corynebacteriaceae; g__Corynebacterium; s__Corynebacterium_matruchotii
6	k__Bacteria; p__Bacteroidetes; c__Bacteroidia; o__Bacteroidales; f__Porphyromonadaceae; g__Porphyromonas; s__Porphyromonas_catoniae
7	k__Bacteria; p__Bacteroidetes; c__Bacteroidia; o__Bacteroidales; f__Prevotellaceae; g__Prevotella; s__Prevotella_intermedia
8	k__Bacteria; p__Fusobacteria; c__Fusobacteriia; o__Fusobacteriales; f__Fusobacteriaceae; g__Leptotrichia; s__Leptotrichia_shahii
9	k__Bacteria; p__Proteobacteria; c__Betaproteobacteria; o__Neisseriales; f__Neisseriaceae; g__Neisseria; s__Neisseria_elongata
10	k__Bacteria; p__Fusobacteria; c__Fusobacteriia; o__Fusobacteriales; f__Fusobacteriaceae; g__Fusobacterium; s__Fusobacterium_periodonticum

(d)

Figure 3: Identification of microbiota-based biomarkers for stroke. (a) Cladograms generated from LEfSe. (b) LDA scores for the differentially abundant bacterial taxa (LDA score > 3.5). Red bars indicate taxa enriched in the poststroke group; green bars indicate taxa enriched in the control group. (c) ROC analysis for random forest model. (d) List of 10 discriminant bacterial taxa based on random forest model. LDA: linear discriminant analysis; ROC: receiver operating characteristic curve; AUC: area under the curve.

3.3. Gut Microbiota-Based Prediction of Poststroke Functional Recovery. The linear discriminant analysis (LDA) and distribution diagram analysis (LDA score > 3.5) showed alteration of the microbiota with higher genus *Fusobacterium*, *Lactobacillus*, *Enterococcus*, *Veillonella*, *Megamonas*, and *Escherichia* levels in the poststroke group (Figures 3(a) and 3(b)). However, genus *Blautia*, *Prevotella*, *Fusicatenibacter*, *Roseburia*, *Faecalibacterium*, *Ruminococcus*, and *Neisseria* levels were significantly enriched in the control group (Figures 3(a) and 3(b)).

To explore potential biomarkers for the prediction of poststroke functional variation, a random forest model was

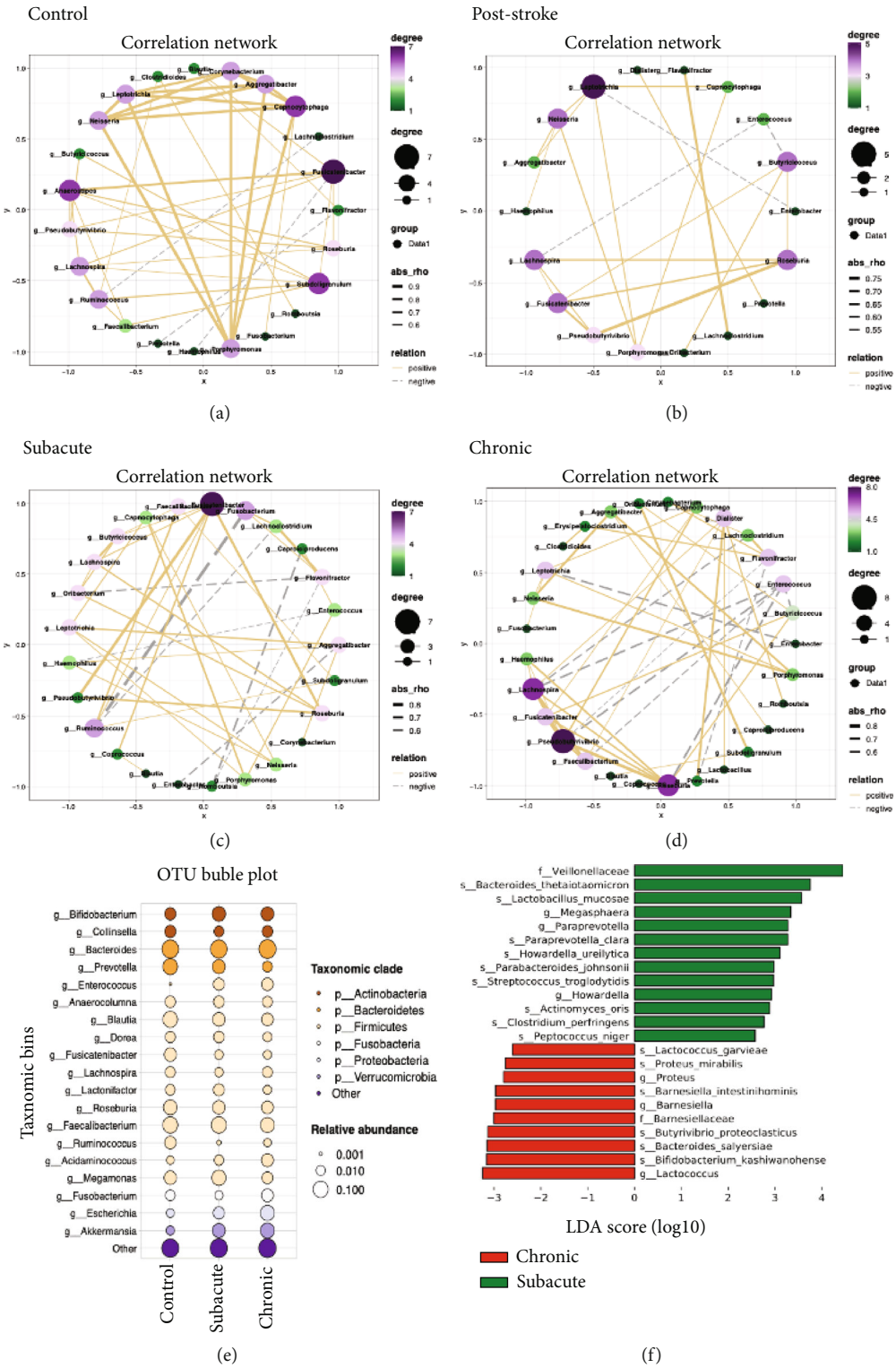

Figure 4: Continued.

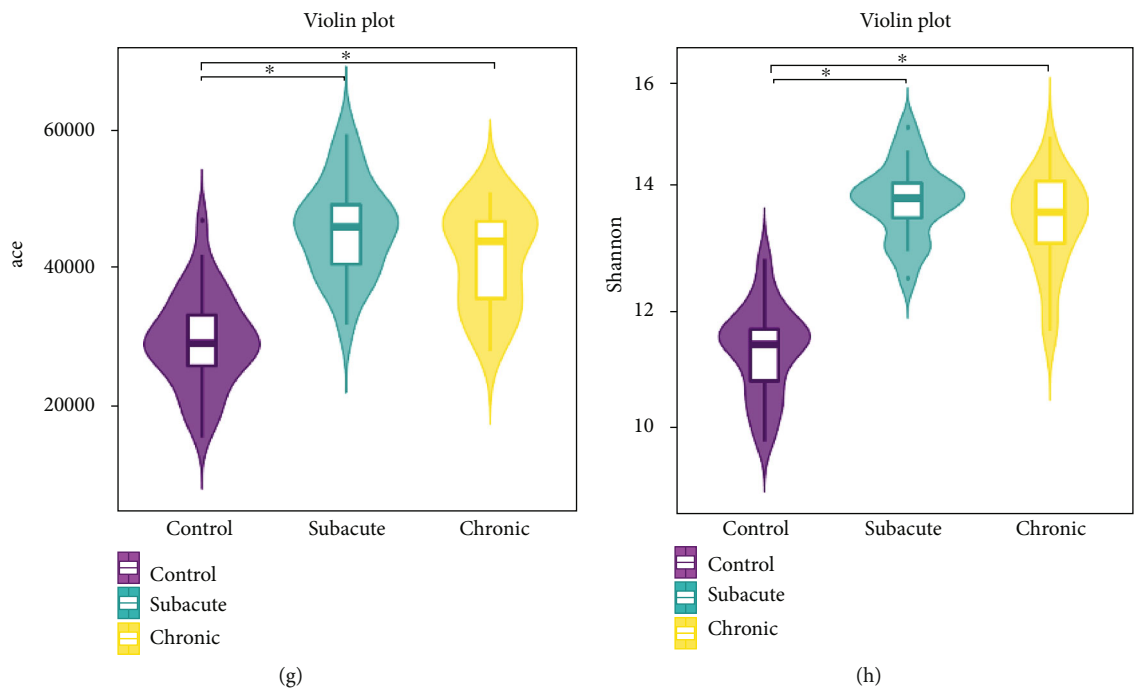

Figure 4: Subgroup analysis of gut microbiota in stroke. (a) Correlation network in the control group. (b) Correlation network in the poststroke group. (c) Correlation network in the subacute patients. (d) Correlation network in chronic patients. (e) OTU bubble plot indicated differences in genus level between subgroup of poststroke patients and control group. (f) LDA scores for differentiated bacterial taxa are abundant between the subacute and chronic patients (LDA score > 2.5). Red bars indicate taxa enriched in the chronic group; green bars indicate taxa in the subacute group. (g, h) Alpha diversity is estimated with the ace and Shannon index. OTU: operational taxonomic unit; LDA: linear discriminant analysis. $^{*}p < 0.05$.

constructed based on the differentiated species (relative abundance > 0). Tenfold cross-validation analysis showed the AUCs of 95% (Figure 3(c)). As per the above analysis, the accuracy, specificity, and susceptibility of the optimal model consisted of the top 10 species (Figure 3(d)) were 93%, 100%, and 86%, respectively.

3.4. Disease Duration-Dependent Variation of Gut Microbiota. Genera cooccurrence networks between groups based on the Pearson correlation analysis are demonstrated in Figures 4(a) and 4(b). Positive correlations were demonstrated between *Aggregatibacter* and *Neisseria*, *Porphyromonas*, *Corynebacterium* and between *Capnocytophaga* and *Leptotrichia*, *Porphyromonas*, *Neisseria* (rho ranged 0.87-0.97, $p < 0.05$) in the control group, while between *Pseudobutyrivibrio* and *Roseburia*, *Flavonifractor* and *Lachnoclostridium*, and *Fusicatenibacter* and *Pseudobutyrivibrio* (rho ranged 0.66-0.76, $p < 0.05$) in the poststroke group. The subacute patients showed positive correlations between *Fusicatenibacter* and *Pseudobutyrivibrio*, *Flavonifractor* and *Lachnoclostridium*, *Fusicatenibacter* and *Roseburia*, and *Pseudobutyrivibrio* and *Roseburia* (rho ranged 0.67-0.80, $p < 0.05$) (Figure 4(c)). In the chronic subgroup, we observed that *Pseudobutyrivibrio* and *Roseburia*, *Aggregatibacter* and *Neisseria*, *Aggregatibacter* and *Porphyromonas*, *Capnocytophaga* and *Leptotrichia*, *Capnocytophaga* and *Pseudobutyrivibrio* (rho ranged 0.53-0.81, $p < 0.05$) were positively correlated (Figure 4(d)).

In addition, the bubble plots and LEfSe (LDA score > 2.5) showed significantly increased/decreased bacterial taxa abundant in both subacute and chronic stroke patients (Figures 4(e) and 4(f)). Genus (e.g., *Megasphaera*, *Paraprevotella*, and *Howardella*) and species (e.g., *Bacteroides thetaiotaomicron*, *Lactobacillus mucosae*, and *Parabacteroides johnsonii*) were significantly enriched in subacute patients, while *Lactococcus*, *Barnesiella*, *Bifidobacterium kashiwanohense*, *Bacteroides salyersiae*, and *Lactococcus garvieae* were significantly enriched in the chronic subgroup. According to the alpha diversity analysis, no significant differences were detected between the subacute and chronic groups (Figures 4(g) and 4(h)).

3.5. Correlation between Differentiated Bacterial Genus with Poststroke Functional Variation. Several bacterial taxa (e.g., *Barnesiella*, *Blautia*, *Coprococcus*, *Enterococcus*, and *Lactococcus*) demonstrated significantly differentiated abundance in the poststroke group. Significant positive correlations were observed between variations of *Prevotella* and FMA-UE ($r = 0.328$, $p < 0.05$), *Enterococcus* and FMA-LE ($r = 0.364$, $p < 0.05$), *Lactococcus* and WST ($r = 0.340$, $p < 0.05$), and *Prevotella* and BI ($r = 0.349$, $p < 0.05$), respectively (Figure 5). Significant negative correlations, between variations of *Butyricicoccus* and FMA-LE ($r = -0.333$, $p < 0.05$) and *Enterococcus* and mRS ($r = -0.370$, $p < 0.05$), were also detected (Figure 5).

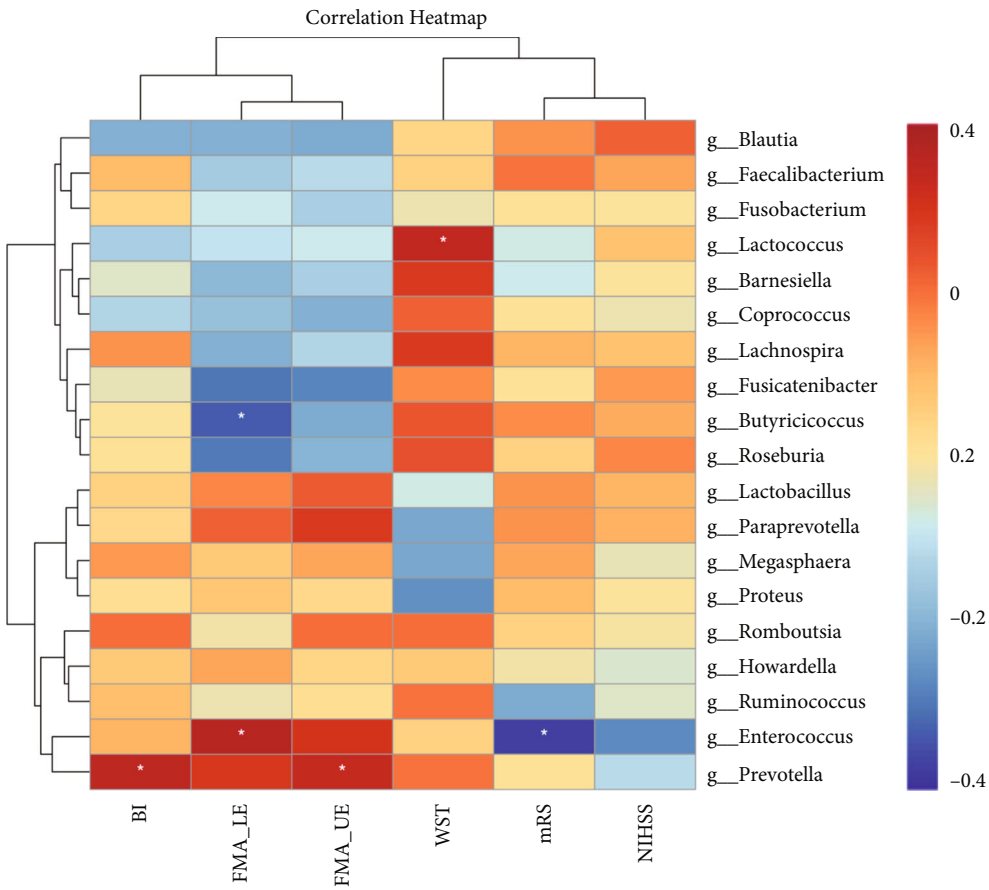

Figure 5: Correlations between differentiated bacterial genus and variations of functional status. BI: Barthel index; FMA-LE: Fugl-Meyer assessment lower extremity scale; FMA-UE: Fugl-Meyer assessment upper extremity scale; WST: water swallow test; mRS: modified Rankin scale; NIHSS: National Institutes of Health Stroke Scale. $^{*}p < 0.05$.

4. Discussion

In the current study, we firstly observed the higher alpha diversity and beta diversity of gut microbiota in poststroke patients as compared to those in the healthy controls, indicating the poststroke community richness and composition of gut microbiota differed from healthy controls. Afterward, a panel of microbiota was identified as biomarkers (e.g., *Aggregatibacter segnis* and *Neisseria mucosa*) to distinguish disease status. Furthermore, sensitivity analysis was performed to explore the gut microbiota alteration according to the length of stroke from onset (e.g., subacute and chronic) [34]. Significantly variated gut microbiota composition was observed along with the progress of stroke. Finally, we also demonstrated that general disability level, motor function either for upper limb or lower limb, swallowing function, and ADL were significantly associated with alterations of distinctive gut microbiota. Taken together, our results further provided evidence to support the point of view that gut microbiota varies following stroke. The hypothesized linkage between gut microbiota alterations and functional prognosis was preliminary observed while the causal relationships underlying these observations need to be further verified with well-designed animal and clinical studies.

Upon the great complexity of gut microbiota and huge heterogeneity of individual properties, studies into the role of gut microbiota on stroke were started with animal experiments to avoid the interference of confounding factors on outcome observation. By using two distinct mouse models of stroke, the overgrowth of microbiota (e.g., *Firmicutes*, *Bacteroidetes*, and *Actinobacteria*) was previously identified as biomarkers of poststroke microbiota dysbiosis, indicating that microbiota dysbiosis could serve as instruments to guide diagnosis and prognosis prediction of stroke [35, 36]. Due to the discrepancy of gut microbiota between humans and animals, several studies on humans were initiated to better understand the poststroke gut microbiota alterations. For instance, a novel parameter termed as Stroke Dysbiosis Index (SDI) was proposed to discriminate stroke patients from healthy controls with AUCs ranging 74.9%-84.3% [37]. This is the first compound biomarker proposed to account for the poststroke gut microbiota alterations. However, the accuracy of the discriminative ability was not as high as in the current study. Here, we used the random forest model with which a panel of 10 significantly variated gut microbiota was detected with AUCs ranging 93%-95%. The accuracy of the discriminative ability was further improved with our model, and it provided reliable results for the following analysis.

The poststroke gut microbiota alterations can be explained by several proposed theories. For instance, central stress responses induced reduction of gastrointestinal motility that may lead to bacterial overgrowth [38]. The autonomic nervous system has also been implicated in mediating the effects of stroke on dysbiosis [39]. Specifically, poststroke stress responses may lead to imbalanced activities of the autonomic nervous system which in turn increase intestinal permeability via releasing corticotropin and glucocorticoid hormones and consequently lead to gut bacterial translocation [40, 41]. In addition, mouse model transplanted with poststroke fecal microbiota showed higher expression of the inflammatory T cells Th1 and Th17 indicating that systemic metabolic, immunologic, and inflammatory responses may play roles in the poststroke gut microbiota alterations [35, 42]. To elaborate on the underlying mechanisms of the above responses, our results preliminarily demonstrated a decreased abundance of SCFA-producing bacteria (e.g., *Blautia*, *Fusicatenibacter*, and *Ruminococcus*) in patients with stroke. Liu and colleagues also found that a deficiency of SCFA-producing bacteria was significantly associated with poststroke cognitive impairment [43]. Transplantation of fecal microbiota rich in SCFAs was found to be effective in the improvement of stroke [44]. This protective effect was related to the enhancement of gut barrier integrity and attenuating systemic inflammation, which may improve function of the blood-brain barrier, decrease cerebral edema, and attenuate brain injury [45]. This further verified the role of SCFAs in the development and prognosis of stroke; it may serve as a novel treatment target for stroke. With the clarification of specific mechanisms in animal steps, this flow also indicated that it needs to be moved forward to clinical circumstances for better facilitating the application of achievements from human trials.

In addition, poststroke variation of specific bacteria may have subsequent influences on regional organ responses. According to our results, an increased abundance of opportunistic pathogens was observed in patients with stroke. The potential role of opportunistic pathogens, such as *Enterobacteriaceae*, was reported to be associated with intestinal epithelial dysfunction [46]. Overgrowth of the *Enterobacteriaceae* may lead to inflammation exacerbation or exogenous pathogen invasion while internal homeostasis was disrupted [47]. These biological communications between the human body and gut microbiota may highlight the novel targets of stroke management. We also observed decreased potential probiotics. Based on the literature review, probiotics or a combination of probiotics and prebiotics could alter the composition of the gut microbiome followed by neuroinflammatory changes and cytokine releases. On the other hand, probiotics was demonstrated to increase brain-derived neurotrophic factor (BDNF) and inhibit apoptosis [48]. Taken together, the specific bacteria may influence the prognosis of stroke. Identification of this distinctive gut microbiota may contribute to the development of innovative treatment targets.

Although we observed the above promising variations of gut microbiota followed by the explanation of the potential internal mechanisms of subsequent consequences, the next question is that "should there be certain potential correlations between gut microbiota alterations and global functions" based on the newly discovered variations of gut microbiota across healthy and stroke status. The abundance of *Christensenellaceae* and *Ruminococcaceae* has been reported to be positively correlated with NIHSS score and mRS while *Enterobacter* was negatively correlated [49]. Our results preliminarily demonstrated that global functions, including general disability level, motor function, swallowing function, and ADL, were significantly associated with alterations of distinctive gut microbiota. There has been published a number of studies on exploring the relationship between microbiome and prognosis after stroke. Li et al. reported a negative correlation of *Enterobacter* with mRS score at one month [49]. Similar results have been also observed in our study. Apart from that, *Prevotella* was found to be correlated with motor function and ADL. The potential explanation would be that *Prevotella* was considered to be associated with mucosal inflammation, which may impact poststroke functional recovery due to the immune response [50, 51]. However, the next challenge in front of us is to answer the question "whether the alterations of distinctive gut microbiota are the causes or consequences of poststroke neural plasticity." This would further improve our understanding of the role the "gut-microbiota-brain axis" played in the development of stroke and facilitate the treatment target selection.

The current study has several strengths and limitations. Firstly, we applied the random forest model to estimate the distinctive gut microbiota across stroke patients and healthy controls. This action further improved the accuracy of discriminative ability in detecting distinctive gut microbiota as compared to the previous studies. Nonetheless, the results should be further verified and validated in larger samples so that several subgroup analyses in terms of microbiota discrepancy could be performed. In addition, the current study preliminarily reported the potential correlations between gut microbiota alterations and global functions while the underlying mechanisms and the causal relationships between the gut microbiota, systematic and neural responses, and global functional changes need to be further investigated to build up the whole picture of the role the "gut-microbiota-brain axis" played in the context of stroke.

5. Conclusion

To sum up, poststroke gut microbiota was significantly modified as compared to healthy controls. The main characteristics of the stroke-induced shift in composition were the decreased abundance of SCFA-producing bacteria and the increased abundance of opportunistic pathogens. Significant associations were detected between alterations of distinctive gut microbiota and poststroke functional prognosis. A better understanding of the precise interactions between gut microbiota, systematic and neural responses, and global functional changes may be helpful in the identification of novel therapeutic targets to improve poststroke functional recovery.

Data Availability

The data used to support the findings of this study are available from the corresponding author upon request.

Conflicts of Interest

The authors declare that there is no conflict of interest regarding the publication of this article.

Authors' Contributions

Yini Dang, Xintong Zhang, and Yu Zheng contributed equally to this work.

Acknowledgments

Dr. Xiangyu Wang is appreciated for his assistance in sample and data collection. We also thank other medical and research staff from the Department of Rehabilitation Medicine in the First Affiliated Hospital of Nanjing Medical University. This work was supported by the National Natural Science Foundation of China (grant numbers 81772441, 81902288, 82000529, and 82072546), the Natural Science Foundation of Jiangsu Province (grant number SBK2020042595), and the Nanjing Municipal Science and Technology Bureau (grant number 2019060002).

References

[1] G. J. Hankey, "Stroke," *The Lancet*, vol. 389, no. 10069, pp. 641–654, 2017.

[2] E. E. Mihai, L. Dumitru, I. V. Mihai, and M. Berteanu, "Long-term efficacy of extracorporeal shock wave therapy on lower limb post-stroke spasticity: a systematic review and meta-analysis of randomized controlled trials," *Journal of Clinical Medicine*, vol. 10, no. 1, p. 86, 2021.

[3] M. Zhou, H. Wang, X. Zeng et al., "Mortality, morbidity, and risk factors in China and its provinces, 1990-2017: a systematic analysis for the Global Burden of Disease Study 2017," *The Lancet*, vol. 394, no. 10204, pp. 1145–1158, 2019.

[4] A. Viktorisson, E. M. Andersson, E. Lundström, and K. S. Sunnerhagen, "Levels of physical activity before and after stroke in relation to early cognitive function," *Scientific Reports*, vol. 11, no. 1, p. 9078, 2021.

[5] A. Gouveia, M. Seegobin, T. S. Kannangara et al., "The aPKC-CBP pathway regulates post-stroke neurovascular remodeling and functional recovery," *Stem Cell Reports*, vol. 9, no. 6, pp. 1735–1744, 2017.

[6] R. C. Nogueira, E. Bor-Seng-Shu, N. P. Saeed, M. J. Teixeira, R. B. Panerai, and T. G. Robinson, "Meta-analysis of vascular imaging features to predict outcome following intravenous rtPA for acute ischemic stroke," *Frontiers in Neurology*, vol. 7, p. 77, 2016.

[7] J. L. Clua-Espuny, S. Abilleira, L. Queralt-Tomas et al., "Long-term survival after stroke according to reperfusion therapy, cardiovascular therapy and gender," *Cardiology Research*, vol. 10, no. 2, pp. 89–97, 2019.

[8] K. W. Nam, C. K. Kim, S. Yu et al., "Elevated troponin levels are associated with early neurological worsening in ischemic stroke with atrial fibrillation," *Scientific Reports*, vol. 10, no. 1, 2020.

[9] B. Jiang, H. Sun, X. Ru et al., "Prevalence, incidence, prognosis, early stroke risk, and stroke-related prognostic factors of definite or probable transient ischemic attacks in China, 2013," *Frontiers in Neurology*, vol. 8, p. 309, 2017.

[10] B. Jiang, D. Sun, H. Sun et al., "Annual rates of and factors influencing inpatient and outpatient transient ischaemic attacks in Chinese population: a nationally representative cross-sectional survey," *BMJ Open*, vol. 10, no. 3, 2020.

[11] K. Z. Alawneh, M. al Qawasmeh, L. A. Raffee et al., "A snapshot of ischemic stroke risk factors, sub-types, and its epidemiology: cohort study," *Annals of Medicine and Surgery*, vol. 59, no. 59, pp. 101–105, 2020.

[12] S. Hu, A. Li, T. Huang et al., "Gut microbiota changes in patients with bipolar depression," *Advanced science*, vol. 6, no. 14, 2019.

[13] A. Sarkar, S. M. Lehto, S. Harty, T. G. Dinan, J. F. Cryan, and P. W. J. Burnet, "Psychobiotics and the manipulation of bacteria-gut-brain signals," *Trends in Neurosciences*, vol. 39, no. 11, pp. 763–781, 2016.

[14] V. Osadchiy, C. R. Martin, and E. A. Mayer, "The gut-brain axis and the microbiome: mechanisms and clinical implications," *Clinical Gastroenterology and Hepatology*, vol. 17, no. 2, pp. 322–332, 2019.

[15] L. H. Morais, "The gut microbiota-brain axis in behaviour and brain disorders," *Nature Reviews Microbiology*, vol. 19, no. 4, pp. 241–255, 2021.

[16] W. Jiang, L. Gong, F. Liu, Y. Ren, and J. Mu, "Alteration of gut microbiome and correlated lipid metabolism in post-stroke depression," *Frontiers in Cellular and Infection Microbiology*, vol. 11, 2021.

[17] J. W. Nelson, S. C. Phillips, B. P. Ganesh, J. F. Petrosino, D. J. Durgan, and R. M. Bryan, "The gut microbiome contributes to blood-brain barrier disruption in spontaneously hypertensive stroke prone rats," *FASEB Journal*, vol. 35, no. 2, 2021.

[18] D. Ndeh, A. Baslé, H. Strahl et al., "Metabolism of multiple glycosaminoglycans by *Bacteroides thetaiotaomicron* is orchestrated by a versatile core genetic locus," *Nature Communications*, vol. 11, no. 1, p. 646, 2020.

[19] C. Tan, Q. Wu, H. Wang et al., "Dysbiosis of gut microbiota and short-chain fatty acids in acute ischemic stroke and the subsequent risk for poor functional outcomes," *JPEN Journal of Parenteral and Enteral Nutrition*, vol. 45, no. 3, pp. 518–529, 2021.

[20] B. W. Haak, W. F. Westendorp, T. S. R. van Engelen et al., "Disruptions of anaerobic gut bacteria are associated with stroke and post-stroke infection: a prospective case-control study," *Translational Stroke Research*, vol. 12, no. 4, pp. 581–592, 2021.

[21] S. Hatano, "Experience from a multicentre stroke register: a preliminary report," *Bulletin of the World Health Organization*, vol. 54, no. 5, pp. 541–553, 1976.

[22] Y. Tong, Z. Cheng, G. B. Rajah et al., "High intensity physical rehabilitation later than 24 h post stroke is beneficial in patients: a pilot randomized controlled trial (RCT) study in mild to moderate ischemic stroke," *Frontiers in Neurology*, vol. 10, p. 113, 2019.

[23] L. Burton and S. F. Tyson, "Screening for cognitive impairment after stroke: a systematic review of psychometric properties and clinical utility," *Journal of Rehabilitation Medicine*, vol. 47, no. 3, pp. 193–203, 2015.

[24] A. F. Abdul Aziz, M. F. Ali, M. F. Yusof, Z. Che' Man, S. Sulong, and S. M. Aljunid, "Profile and outcome of post stroke patients managed at selected public primary care health centres in Peninsular Malaysia: a retrospective observational study," *Scientific Reports*, vol. 8, no. 1, 2018.

[25] A. P. Yelnik, V. Quintaine, C. Andriantsifanetra et al., "AMOBES (active mobility very early after stroke): a randomized controlled trial," *Stroke*, vol. 48, no. 2, pp. 400–405, 2017.

[26] M. Reinholdsson, A. Palstam, and K. S. Sunnerhagen, "Pre-stroke physical activity could influence acute stroke severity (part of PAPSIGOT)," *Neurology*, vol. 91, no. 16, pp. e1461–e1467, 2018.

[27] R. M. Zellweger, S. Yacoub, Y. F. Z. Chan et al., "Disentangling etiologies of CNS infections in Singapore using multiple correspondence analysis and random forest," *Scientific Reports*, vol. 10, no. 1, p. 18219, 2020.

[28] J. P. Appleton, L. J. Woodhouse, A. Adami et al., "Imaging markers of small vessel disease and brain frailty, and outcomes in acute stroke," *Neurology*, vol. 94, no. 5, pp. e439–e452, 2020.

[29] A. Sia, W. W. S. Tam, A. Fogel, E. H. Kua, K. Khoo, and R. C. M. Ho, "Nature-based activities improve the well-being of older adults," *Scientific Reports*, vol. 10, no. 1, p. 18178, 2020.

[30] D. J. Lin, A. M. Cloutier, K. S. Erler et al., "Corticospinal tract injury estimated from acute stroke imaging predicts upper extremity motor recovery after stroke," *Stroke*, vol. 50, no. 12, pp. 3569–3577, 2019.

[31] K. Dong, S. Meng, Z. Guo et al., "The effects of transcranial direct current stimulation on balance and gait in stroke patients: a systematic review and meta-analysis," *Frontiers in Neurology*, vol. 12, 2021.

[32] D. G. Smithard, P. A. O'Neill, C. Park et al., "Can bedside assessment reliably exclude aspiration following acute stroke?," *Age and Ageing*, vol. 27, no. 2, pp. 99–106, 1998.

[33] M. Toscano, E. Cecconi, E. Capiluppi et al., "Neuroanatomical, clinical and cognitive correlates of post-stroke dysphagia," *European Neurology*, vol. 74, no. 3-4, pp. 171–177, 2015.

[34] B. K. Kang, D. G. Na, J. W. Ryoo, H. S. Byun, H. G. Roh, and Y. S. Pyeun, "Diffusion-weighted MR imaging of intracerebral hemorrhage," *Korean Journal of Radiology*, vol. 2, no. 4, pp. 183–191, 2001.

[35] V. Singh, S. Roth, G. Llovera et al., "Microbiota dysbiosis controls the neuroinflammatory response after stroke," *The Journal of Neuroscience*, vol. 36, no. 28, pp. 7428–7440, 2016.

[36] J. Yin, S. X. Liao, Y. He et al., "Dysbiosis of gut microbiota with reduced trimethylamine-N-oxide level in patients with large-artery atherosclerotic stroke or transient ischemic attack," *Journal of the American Heart Association*, vol. 4, no. 11, 2015.

[37] G. H. Xia, C. You, X. X. Gao et al., "Stroke dysbiosis index (SDI) in gut microbiome are associated with brain injury and prognosis of stroke," *Frontiers in Neurology*, vol. 10, p. 397, 2019.

[38] B. Y. Q. Tan, P. R. Paliwal, and V. K. Sharma, "Gut microbiota and stroke," *Annals of Indian Academy of Neurology*, vol. 23, no. 2, pp. 155–158, 2020.

[39] D. Battaglini, P. M. Pimentel-Coelho, C. Robba et al., "Gut microbiota in acute ischemic stroke: from pathophysiology to therapeutic implications," *Frontiers in Neurology*, vol. 11, p. 598, 2020.

[40] J. R. Caso, O. Hurtado, M. P. Pereira et al., "Colonic bacterial translocation as a possible factor in stress-worsening experimental stroke outcome," *American Journal of Physiology Regulatory, Integrative and Comparative Physiology*, vol. 296, no. 4, pp. R979–R985, 2009.

[41] A. Houlden, M. Goldrick, D. Brough et al., "Brain injury induces specific changes in the caecal microbiota of mice via altered autonomic activity and mucoprotein production," *Brain, Behavior, and Immunity*, vol. 57, pp. 10–20, 2016.

[42] A. K. Arya and B. Hu, "Brain-gut axis after stroke," *Brain Circulation*, vol. 4, no. 4, pp. 165–173, 2018.

[43] Y. Liu, C. Kong, L. Gong et al., "The association of post-stroke cognitive impairment and gut microbiota and its corresponding metabolites," *Journal of Alzheimer's Disease: JAD*, vol. 73, no. 4, pp. 1455–1466, 2020.

[44] R. Chen, Y. Xu, P. Wu et al., "Transplantation of fecal microbiota rich in short chain fatty acids and butyric acid treat cerebral ischemic stroke by regulating gut microbiota," *Pharmacological Research*, vol. 148, 2019.

[45] H. Wang, W. Song, Q. Wu et al., "Fecal transplantation from db/db mice treated with sodium butyrate attenuates ischemic stroke injury," *Microbiology Spectrum*, vol. 9, no. 2, 2021.

[46] Y. Litvak, M. X. Byndloss, R. M. Tsolis, and A. J. Bäumler, "Dysbiotic _Proteobacteria_ expansion: a microbial signature of epithelial dysfunction," *Current Opinion in Microbiology*, vol. 39, pp. 1–6, 2017.

[47] N. R. Shin, T. W. Whon, and J. W. Bae, "_Proteobacteria_ : microbial signature of dysbiosis in gut microbiota," *Trends in Biotechnology*, vol. 33, no. 9, pp. 496–503, 2015.

[48] M. Koszewicz, J. Jaroch, A. Brzecka et al., "Dysbiosis is one of the risk factor for stroke and cognitive impairment and potential target for treatment," *Pharmacological Research*, vol. 164, 2021.

[49] N. Li, X. Wang, C. Sun et al., "Change of intestinal microbiota in cerebral ischemic stroke patients," *BMC Microbiology*, vol. 19, no. 1, p. 191, 2019.

[50] J. M. Larsen, "The immune response to Prevotella bacteria in chronic inflammatory disease," *Immunology*, vol. 151, no. 4, pp. 363–374, 2017.

[51] R. R. Jenq, Y. Taur, S. M. Devlin et al., "Intestinal _Blautia_ is associated with reduced death from graft-versus-host disease," *Biology of Blood and Marrow Transplantation*, vol. 21, no. 8, pp. 1373–1383, 2015.

Hindawi
Neural Plasticity
Volume 2021, Article ID 6144304, 12 pages
https://doi.org/10.1155/2021/6144304

Research Article

A New Classification System for Postinterventional Cerebral Hyperdensity: The Influence on Hemorrhagic Transformation and Clinical Prognosis in Acute Stroke

Yuan Shao, Yuyun Xu, Yumei Li, Xuehua Wen, and Xiaodong He

Department of Radiology, Zhejiang Provincial People's Hospital, Affiliated People's Hospital, Hangzhou Medical College, Hangzhou, Zhejiang, China

Correspondence should be addressed to Xiaodong He; 15888815645@163.com

Received 27 July 2021; Revised 29 October 2021; Accepted 5 November 2021; Published 23 November 2021

Academic Editor: Xi-Ze Jia

Background. Postinterventional cerebral hyperdensity (PCHD) is commonly seen in acute ischemic patients after mechanical thrombectomy. We propose a new classification of PCHD to investigate its correlation with hemorrhagic transformation (HT). The clinical prognosis of PCHD was further studied. *Methods*. Data from 189 acute stroke patients were analyzed retrospectively. According to the European Cooperative Acute Stroke Study criteria (ECASS), HT was classified as hemorrhagic infarction (HI-1 and HI-2) and parenchymal hematoma (pH-1 and pH-2). Referring to the classification of HT, PCHD was classified as PCHD-1, PCHD-2, PCHD-3, and PCHD-4. The prognosis included early neurological deterioration (END) and the modified Rankin Scale (mRS) score at 3 months. *Results*. The incidence of HT was 14.8% (12/81) in the no-PCHD group and 77.8% (84/108) in the PCHD group. PCHD was highly correlated with HT ($r = 0.751$, $p < 0.01$). After stepwise regression analysis, PCHD and the National Institutes of Health Stroke Scale (NIHSS) score at admission were found to be independent factors for END ($p < 0.001$, $p = 0.015$, respectively). The area of curves (AUC) of PCHD, the NIHSS at admission, and the combined model were 0.810, 0.667, and 0.832, respectively. The optimal diagnostic cutoff of PCHD for END was PCHD > 2. PCHD, the NIHSS score at admission, and good vascular recanalization (VR) were independently associated with 3-month mRS (all $p < 0.05$). The AUC of PCHD, the NIHSS at admission, good VR, and the combined model were 0.779, 0.733, 0.565, and 0.867, respectively. And the best cutoff of PCHD for the mRS was PCHD > 1. *Conclusion*. The relationship of PCHD and HT suggested PCHD was an early risk indicator for HT. The occurrence of PCHD-3 and PCHD-4 was a strong predictor for END. PCHD-1 is considered to be relatively benign in relation to the 3-month mRS.

1. Introduction

Postinterventional cerebral hyperdensity (PCHD) is fairly commonly seen in patients with acute ischemic stroke following intra-arterial treatment [1–3]. Recently, with advances in technology, intravascular stents have been widely used for acute stroke patients; however, there have been few studies on patients with PCHD after mechanical thrombectomy. Previous small-sample studies revealed that PCHD was a strong predictor for final infarction size [4, 5] but was not a risk factor for symptomatic hemorrhage or poor prognosis [5, 6]. This low predictive efficiency may be due to the analysis of only the occurrence of PCHD, rather than the classification of PCHD. Later, Xu et al. found that "metallic hyperdensities" with a CT density of over 90 HU and a larger volume with a bulging contour could predict the occurrence of parenchymal hemorrhage at 24 h [7]. However, there were no further investigations into the effect on clinical prognosis in that study. The classification standard of CT values was formulated in clinical trials evaluating arterial thrombolysis [3], and a later study of intra-arterial revascularization suggested that a CT value of >90 poorly predicted hemorrhagic transformation (HT) with low sensitivity (23%) [8]. There were no further studies of PCHD on clinical prognosis in people with mechanical thrombectomy.

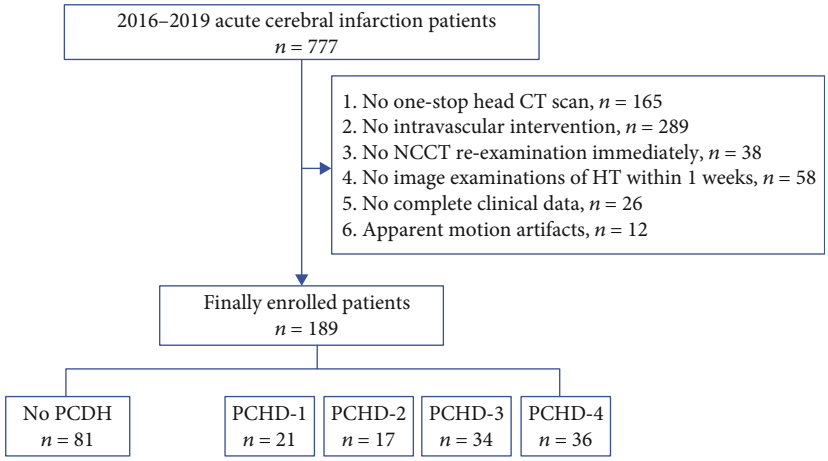

Figure 1: The flowchart of participant recruitment.

According to the European Cooperative Acute Stroke Study (ECASS) criteria, HT was further divided into four levels [9]. Different types of HT after stroke require corresponding targeted treatment and are closely related to prognosis [10, 11]. However, the correlation between various degrees of HT and PHCD was not clear. Thus, we proposed a new classification of PCHD, which divides PCHD into four levels according to the definition of HT, to provide a more direct and pragmatic early reference sign. The influence and the optimal diagnostic threshold of PCHD subtypes on clinical prognosis were further analyzed.

The aim of our study was to predict HT and clinical prognosis by evaluating the new classification system for PCHD and to provide a theoretical and experimental basis for the formulation of a treatment plan after intra-arterial intervention.

2. Materials and Methods

2.1. Subjects. The study was approved by the local Ethics Committee, and the requirement for informed consent of every patient was waived.

The data of 777 patients with acute cerebral infarction from 2016 to 2019 were retrospectively analyzed in the PACS. Among these patients, 189 patients treated with intravascular intervention were enrolled in this study. A flowchart of participant recruitment is shown in Figure 1. According to whether a hyperdensity was found on noncontrast CT scans (NCCT) after intravascular intervention, the patients were divided into a no-PCHD group ($n = 81$) and a PCHD group ($n = 108$). Referring to the new PCHD classification standard, the PCHD group was further divided into PCHD-1, PCHD-2, PCHD-3, and PCHD-4.

The inclusion criteria were as follows: (1) age ≥ 18 years; (2) a clinical diagnosis of acute ischemic stroke at admission; (3) preoperative one-stop head CT scan performed; (4) intravascular intervention performed within the time window; (5) NCCT scan performed immediately after intravascular intervention to observe PCHD; (6) CT reexaminations or SWI examinations performed within 48 h-1 w to observe HT; and (7) availability of complete clinical and imaging data. The exclusion criteria were as follows: (1) vascular malformation; (2) intracranial hemorrhage, infection, or space-occupying lesions; (3) serious heart, lung, or kidney diseases; and (4) obvious motion artifacts.

2.2. Clinical Data Acquisition. The following basic clinical characteristics were collected: (1) demographic data, including sex and age; (2) past medical history, history of smoking, hypertension, diabetes, atrial fibrillation, and anticoagulant use; (3) National Institutes of Health Stroke Scale (NIHSS) score at admission; and (4) hematological test data, including total cholesterol (TC), high-density lipoprotein (HDL), low-density lipoprotein (LDL), activated partial thromboplastin time (APTT), and prothrombin time (PT).

Early neurological deterioration (END) was indicated when the NIHSS score increased ≥4 points within 72 h of onset [12].

The mRS score at 3 months: 0-2 scores indicated a good prognosis (no symptoms or mild disability); 3-6 scores indicated a poor prognosis (moderate to severe disability or death) [13, 14].

2.3. Image Data Acquisition. Intravascular intervention: for patients without contraindications of venous thrombolysis, mechanical thrombolysis was administered after venous thrombolysis. The time window for anterior circulation strokes was up to 8 h after symptom onset, and that for posterior circulation strokes was 24 h. The time window could be extended appropriately according to ischemic core/penumbra mismatch. The femoral artery was selected for puncture, and the thrombus was removed using a Solitaire stent (Medtronic). Digital subtraction angiography (Allura Xper Fd20 by Philips, Netherlands) was used during mechanical thrombectomy. The sequence included the anterior and lateral positions of each artery. The exposure was automatically adjusted with a delay of 0.5 s, and images of the arterial, parenchymal, and venous phases were collected at a rate of 6 frames per second. Successful recanalization was defined as grade 2b-3 of the modified

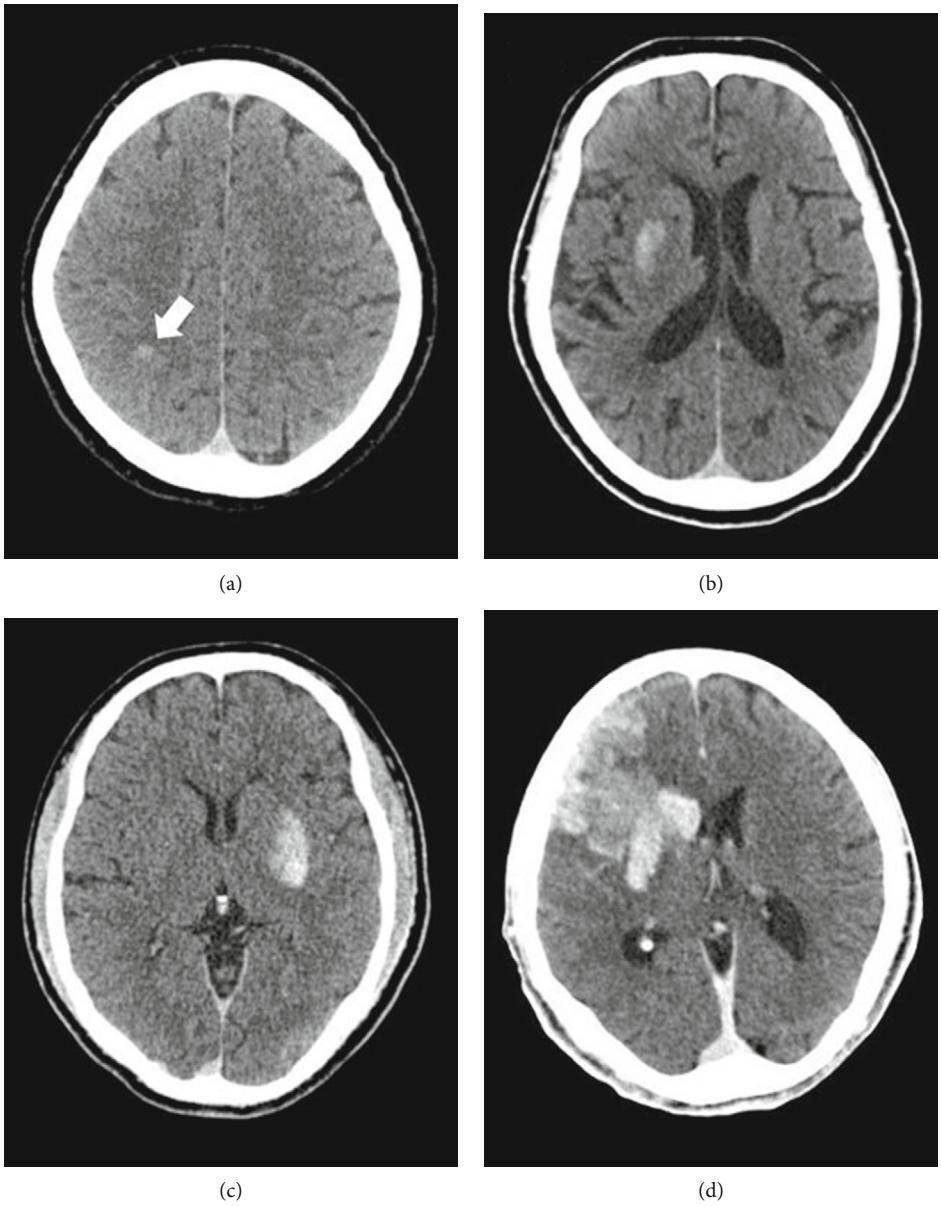

Figure 2: Continued.

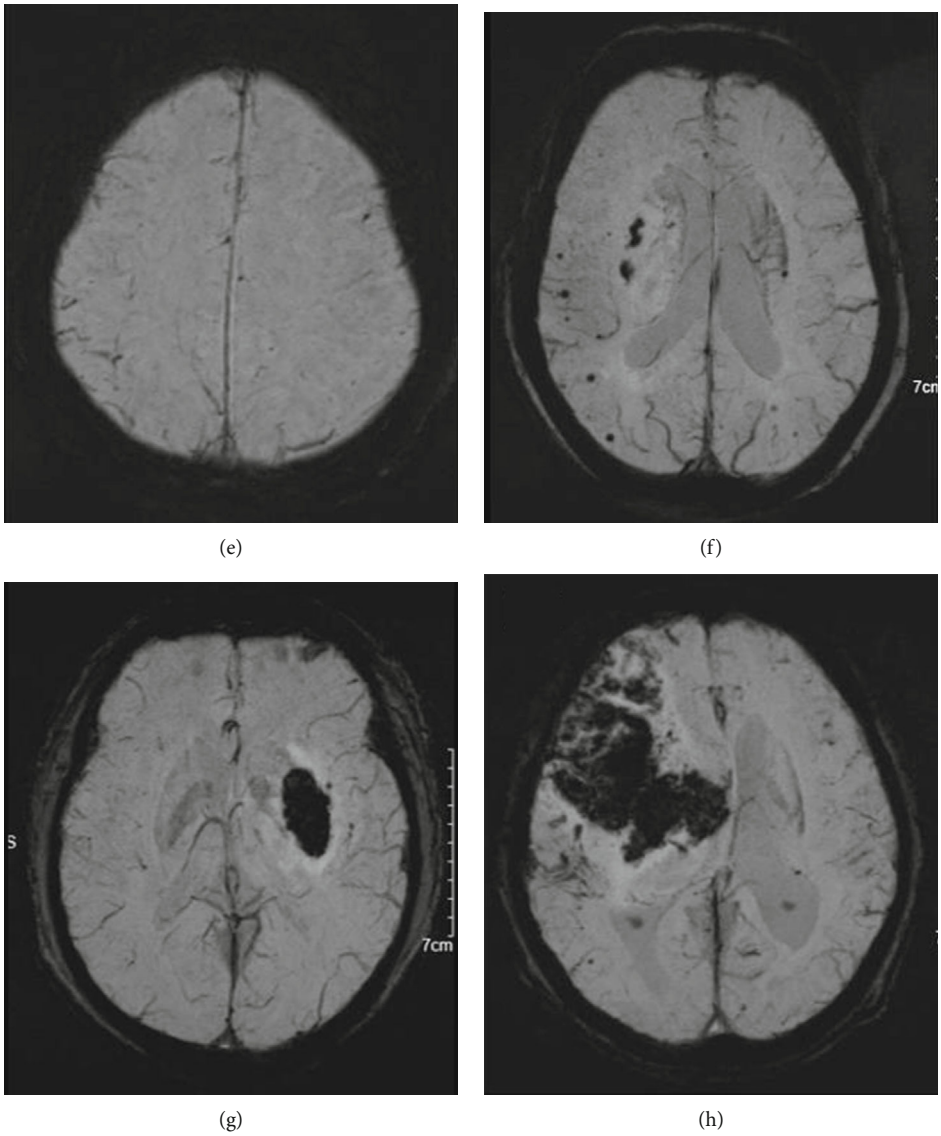

(e) (f) (g) (h)

Figure 2: The upper row of images (a–d) show the four types of PCHD, and the lower row of images (e–h) show the prognosis of TH in the corresponding four patients. PCHD-1 showing small area of hyperdensity (the white arrow) without space-occupying effects (a), no TH in follow-up SWI image (e). PCHD-2 showing more confluent hyperdensity at the right basal ganglia without space-occupying effects (b), HI-1 was observed during follow-up (f). PCHD-3 showing hyperdensity at the right basal ganglia accompany the ipsilateral narrow sulci (c), pH-1 was observed during follow-up (g). PCHD-4 showing hyperdensity with a significant space-occupying effect (d), pH-2 was observed during follow-up (h).

Thrombolysis in Cerebral Infarction (mTICI) scoring criteria.

Axial NCCT reexamination scan: the SIEMENS Definition AS 128 CT scanner was used. The routine head scan protocol: the tube voltage = 120 kV, the reference current = 400 mA, the actual current can be adjusted by using the combined applications reduce exposure dose 4 dimensions (CARE dose 4D) technology, acquisition matrix = 512 × 512, rebuild field of view (FOV) = 300 mm × 300 mm, layer thickness = 1 mm, and interslice gap = 0. The emergency head scan protocol: the tube voltage = 120 kV, the reference current = 400 mA, the actual current can be adjusted by using the CARE dose 4D technology, acquisition matrix = 512 × 512, rebuild FOV = 300 mm × 300 mm, and pitch = 0.9 mm.

SWI: TR = Minimum, TE = 24.3 ms, FOV = 200 × 200 mm, slice thickness = 1.6 mm, and interslice gap = 0.

HT was defined as a hyperdensity that persisted or was extended on CT reexamination within 1 week or on a susceptibility-weighted imaging sequence (SWI) that showed a low signal in the infarct range. HT was classified according to the ECASS definition. HI means hemorrhagic infarction, and pH means parenchymal hemorrhage.

(i) HI-1: small confluent petechiae without a space-occupying effect or nonsolid

Table 1: Basic characteristics of the no-PCHD and PCHD groups.

	No-PCHD group ($n = 81$)	PCHD group ($n = 108$)	p
Age	70.19 ± 12.74	70.27 ± 12.18	0.964
Sex (male; %)	43; 53.1%	61; 56.5%	0.642
History of smoking	15; 18.5%	21; 19.4%	0.873
History of hypertension	56; 69.1%	88; 81.5%	0.049
History of atrial fibrillation	32; 39.5%	56; 51.9%	0.092
History of diabetes	11; 13.6%	22; 20.4%	0.224
History of anticoagulant use	11; 13.6%	24; 22.2%	0.130
TC	3.86 ± 0.97	3.82 ± 0.94	0.774
HDL	1.06 ± 0.24	1.07 ± 0.26	0.668
LDL	2.32 ± 0.78	2.20 ± 0.77	0.295
APTT	27.41 ± 5.48	32.76 ± 24.52	0.030
PT	13.17 ± 3.39	13.35 ± 4.01	0.744
NIHSS score at admission	19.27 ± 9.61	22.86 ± 7.82	0.007
ASPECT score (<6 scores)	17; 21.0%	56; 51.9%	<0.001
Location of occlusion			0.900
ICA isolated or in tandem with MCA	11; 13.6%	15; 13.9%	
MCA isolated	56; 69.1%	77; 71.3%	
Posterior circulation	14; 17.3%	16; 14.8%	

TC: total cholesterol; HDL: high-density lipoprotein; LDL: low-density lipoprotein; APTT: activated partial thromboplastin time; PT: prothrombin time; ICA: internal carotid artery; MCA: middle cerebral artery.

(ii) HI-2: more confluent petechiae without a space-occupying effect or nonsolid

(iii) pH-1: less than 30% of the infarcted area has a mild mass effect

(iv) pH-2: greater than 30% of the infarcted area has a significant space-occupying effect

PCHD was defined by visually distinctive parenchymal hyperdense areas diagnosed within 24 h after intravascular intervention, with a diameter of at least 0.1 cm^2 and an increased density of at least 5 HU (HUmax) compared to the unaffected contralateral area. The example diagram of PCHD is shown in Figure 2.

(i) PCHD-1: small area of hyperdensity without space-occupying effects

(ii) PCHD-2: more confluent hyperdensity without space-occupying effects

(iii) PCHD-3: less than 30% of the infarcted area has a mild mass effect

(iv) PCHD-4: greater than 30% of the infarcted area has a significant space-occupying effect

Imaging indexes (the Alberta Stroke Program Early CT (ASPECT) score and the classification of PCHD and HT) were evaluated by two neuroradiologists (Dr. Shao, who has 3 years of experience, and Dr. He, who has 13 years of experience). The two doctors first evaluate independently and finally reach a consensus through discussion where there is disagreement.

2.4. Statistical Analysis. Statistical analysis was performed with SPSS 20.0 (IBM, Chicago, IL, United States). Comparisons of the basic clinical characteristics were conducted with a t-test, the chi-square test, or the Mann–Whitney U test, depending on the circumstances. The Crosstabs test and ANOVA were used for the four subtypes of PCHD. The intraclass correlation coefficient was calculated to evaluate the consistency between the two observers. The Spearman rank correlation test was used to analyze the correlation between PCHD and HT, and $r > 0.75$ was considered to be a good correlation. Univariate logistic regression analysis was used to explore the relationship between dependent variables and independent variables. A forest plot was established to show the relationship. Then, through multivariate logistic regression analysis, the independent factors that were associated with END and mRS were further identified. Finally, a receiver-operating characteristic (ROC) curve was constructed. The area of curves (AUC) was used to evaluate the diagnostic efficacy of the independent risk factors for END and mRS at 3 months. Cutoff value was used to identify the threshold that predicts clinical outcomes. Statistical significance was set at $p \leq 0.05$.

3. Results

3.1. Demographic and Clinical Characteristics. A total of 189 patients were included in this study, with 81 (42.9%)

Table 2: Demographic and clinical characteristics of the four subtypes of PCHD.

	PCHD-1 ($n = 21$)	PCHD-2 ($n = 17$)	PCHD-3 ($n = 34$)	PCHD-4 ($n = 36$)	p
Age	68.90 ± 15.16	70.29 ± 9.71	71.39 ± 13.71	70.27 ± 12.18	0.900
Sex (male; %)	8; 38.1%	10; 58.8%	22; 64.7%	21; 58.3%	0.271
Smoking	3; 14.3%	3; 17.6%	6; 17.6%	9; 25.0%	0.763[f]
Hypertension	17; 81.0%	15; 88.2%	27; 79.4%	29; 80.6%	0.875[f]
Atrial fibrillation	11; 52.4%	8; 47.1%	19; 55.9%	18; 50.0%	0.934
Diabetes	2; 9.5%	1; 5.9%	10; 29.4%	9; 25.0%	0.082[f]
Anticoagulant use	5; 23.8%	5; 29.4%	11; 32.4%	3; 8.3%	0.063[f]
TC	3.77 ± 0.87	3.77 ± 1.39	3.80 ± 0.72	3.89 ± 0.95	0.956
HDL	1.11 ± 0.17	1.02 ± 0.27	1.05 ± 0.25	1.09 ± 0.30	0.633
LDL	2.15 ± 0.75	2.25 ± 1.10	2.11 ± 0.52	2.28 ± 0.82	0.802
APTT	27.83 ± 4.65	34.65 ± 31.43	37.34 ± 37.03	30.42 ± 6.24	0.487
PT	13.10 ± 1.66	11.95 ± 3.20	13.59 ± 4.27	13.94 ± 4.94	0.390
Time of onset (h)	3.65 ± 2.47	4.64 ± 3.20	4.10 ± 1.61	4.18 ± 2.45	0.647
NIHSS at admission	24.05 ± 7.72	20.71 ± 5.44	21.47 ± 9.44	24.50 ± 6.90	0.219
ASPECT score	5; 23.8%	8; 47.1%	24; 70.6%	19; 52.8%	0.009
OP (AC; %)	16; 76.2%	17; 100.0%	28; 82.4%	31; 86.1%	0.077[f]
CT value (HU)	65.38 ± 35.68	61.88 ± 27.56	83.56 ± 47.21	148.53 ± 156.52	0.002*
Subarachnoid HD	4; 19.0%	1; 5.9%	5; 14.7%	4; 11.1%	0.628[f]
Intraventricular HD	0; 0.0%	0; 0.0%	1; 2.9%	8; 22.2%	0.002[f]
Operation time (h)	5.38 ± 2.47	5.89 ± 2.60	5.19 ± 1.70	5.70 ± 2.78	0.726
VR (good, %)	19; 90.5%	15; 88.2%	30; 88.2%	28; 77.8%	0.510[f]
Bridging treatment	6; 28.6%	9; 52.9%	15; 44.1%	14; 38.9%	0.467
HT	11; 52.4.0%	9; 52.9%	31; 91.2%	33; 91.7%	<0.001[f]
END	5; 23.8%	5; 29.4%	14; 41.2%	26; 72.2%	0.001
3-month mRS	12; 57.1%	12; 70.6%	31; 91.2%	35; 97.2%	<0.001[f]

TC: total cholesterol; HDL: high-density lipoprotein; LDL: low-density lipoprotein; APTT: activated partial thromboplastin time; PT: prothrombin time; OP: occluded position; AC: anterior circulation; HD: hyperdensity; VR: vascular recanalization; HT: hemorrhagic transformation; END: early neurological deterioration; f: Fisher's exact test; *: the CT value of the high-density PCHD-4 group was higher than that of the PCHD-1 and PCHD-2 groups, but no difference was found between these three subgroups and the PCHD-3 group.

patients in the no-PCHD group and 108 (57.1%) patients in the PCHD group. The incidence of HT in our study was 50.8% (96/189), HI = 31.2% (59/189), and pH = 19.6% (37/189).

As shown in Table 1, there were significant differences in the history of hypertension, APTT, the NIHSS score at admission, and the ASPECT score between the no-PCHD group and the PCHD group ($p < 0.05$). There was no significant difference in the location of occluded artery between the two groups ($p > 0.05$).

As shown in Table 2, there were significant differences in the ASPECT score among the four PCHD subgroups ($p = 0.009$). The CT value of the high-density PCHD-4 group was higher than that of the PCHD-1 and PCHD-2 groups ($p = 0.002$), but no difference was found between these three subgroups and the PCHD-3 group. Patients in the PCHD-1/2 group lacked intraventricular hyperdensity, which was significantly different from that in PCHD-3/4 group ($p = 0.002$). Moreover, there were significant differences in clinical prognosis among the four groups (HT, END, and mRS, all $p < 0.05$).

The two observers performed radiographic evaluations with a high degree of consistency. The intraclass correlation coefficients of the ASPECT score, PCHD and HT were 0.950, 0.986, and 0.978, respectively, all $p < 0.01$.

3.2. The Correlation between PCHD and HT. The incidence of HT was 14.8% (12/81) in the no-PCHD group and 77.8% (84/108) in the PCHD group. As shown in Figure 3, in the no-PCHD group, 69 of the patients did not present HT and 12 of the patients presented HI-1; however, no patients presented HI-2, pH-1, and pH-2. All patients with subsequent pH-2 were in the PCHD-3 and PCHD-4 subgroup in the early stage (PCHD − 3 = 86.67%, PCHD − 4 = 13.33%). The Spearman rank correlation analysis showed that there was a good correlation between PCHD and HT ($r = 0.751$, $p < 0.01$).

3.3. Predicting Early Neurological Deterioration (END). The image and clinical data of END- and END+ group were shown in Table s1. The univariate analysis revealed there were significant differences in the NIHSS score, the

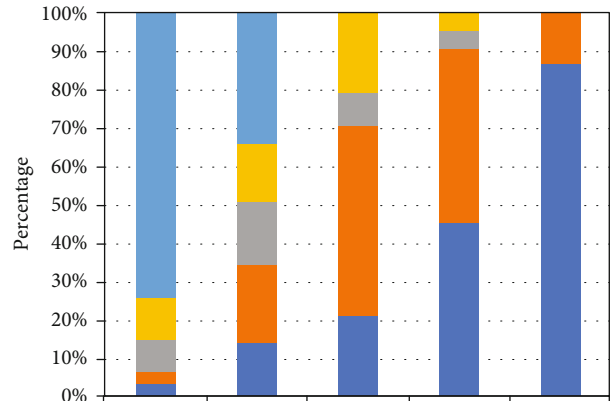

	No HT ($n = 93$)	HI-1 ($n = 35$)	HI-2 ($n = 24$)	PH-1 ($n = 22$)	PH-2 ($n = 15$)
No PCHD ($n = 81$)	69	12	0	0	0
PCHD-1 ($n = 21$)	10	5	5	1	0
PCHD-2 ($n = 17$)	8	6	2	1	0
PCHD-3 ($n = 34$)	3	7	12	10	2
PCHD-4 ($n = 36$)	3	5	5	10	13

Figure 3: The correlation between the classifications of PCHD and HT.

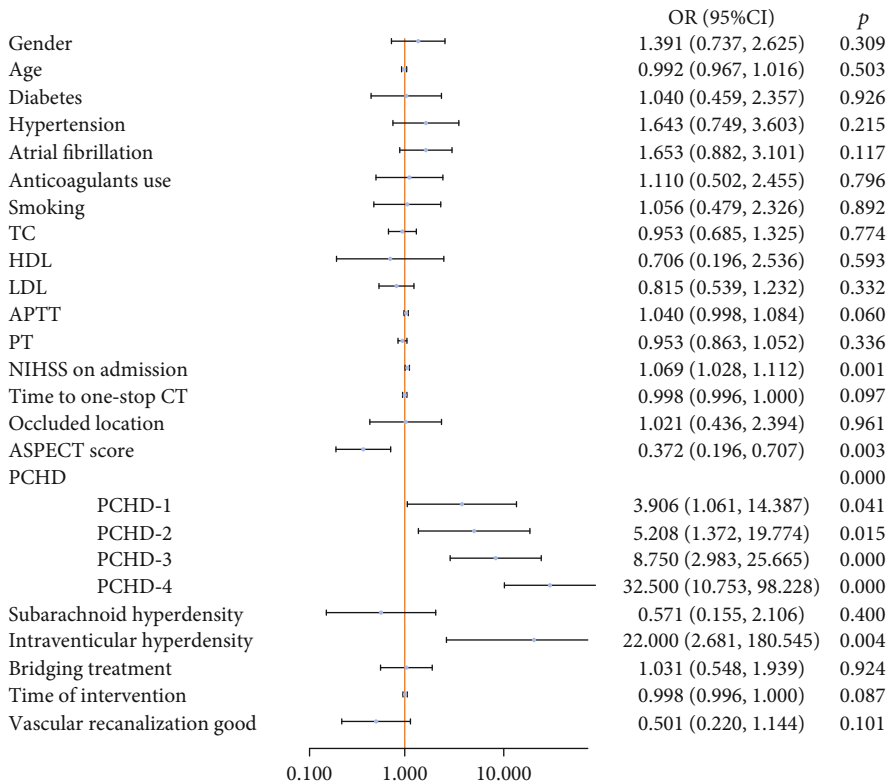

Figure 4: Univariate predictors of END.

ASPECT score, PCHD classification, and interventricular hyperdensity between the two groups ($p < 0.05$, illustrated Figure 4). After the multivariate regression analysis, the NIHSS score at admission and PCHD were independent factors for END ($p = 0.015$, $p < 0.001$, respectively), as in Table 3. Figure 5 showed that AUC of PCHD was 0.810, and the optimal diagnostic cutoff value was PCHD > 2. The AUC of the NIHSS score at admission was 0.667. The AUC of the combined model was 0.832.

3.4. Predicting the mRS Score at 3 Months. The image and clinical data of mRS- and mRS+ group were shown in

Table 3: Stepwise logistic regression analysis predicting END.

	Univariate logistic regression		Multivariate logistic regression	
	OR (95% CI)	p	OR (95% CI)	p
Sex	1.391 (0.737, 2.625)	0.309		
Age	0.992 (0.967, 1.016)	0.503		
Diabetes	1.040 (0.459, 2.357)	0.926		
Hypertension	1.643 (0.749, 3.603)	0.215		
Atrial fibrillation	1.653 (0.882, 3.101)	0.117		
Anticoagulant use	1.110 (0.502, 2.455)	0.796		
Smoking	1.056 (0.479, 2.326)	0.892		
TC	0.953 (0.685, 1.325)	0.774		
HDL	0.706 (0.196, 2.536)	0.593		
LDL	0.815 (0.539, 1.232)	0.332		
APTT	1.040 (0.998, 1.084)	0.060		
PT	0.953 (0.863, 1.052)	0.336		
NIHSS at admission	1.069 (1.028, 1.112)	0.001	1.061 (1.011, 1.113)	0.015
Time to one-stop CT	0.998 (0.996, 1.000)	0.097		
Occluded location	1.021 (0.436, 2.394)	0.961		
ASPECT score	0.372 (0.196, 0.707)	0.003	/	/
PCHD		<0.001		<0.001
PCHD-1	3.906 (1.061, 14.387)	0.041	3.197 (0.847, 12.070)	0.086
PCHD-2	5.208 (1.372, 19.774)	0.015	5.362 (1.386, 20.746)	0.015
PCHD-3	8.750 (2.983, 25.665)	<0.001	8.581 (2.853, 25.804)	<0.001
PCHD-4	32.500 (10.753, 98.228)	<0.001	28.240 (9.206, 86.626)	<0.001
Subarachnoid HD	0.571 (0.155, 2.106)	0.400		
Intraventricular HD	22.000 (2.681, 180.545)	0.004	/	/
Bridging treatment	1.031 (0.548, 1.939)	0.924		
Time of intervention	0.998 (0.996, 1.000)	0.087		
VR (good)	0.501 (0.220, 1.144)	0.101		

TC: total cholesterol; HDL: high-density lipoprotein; LDL: low-density lipoprotein; APTT: activated partial thromboplastin time; PT: prothrombin time; HD: hyperdensity; VR: vascular recanalization.

Table s2. Univariate analysis revealed that the NIHSS score at admission, the ASPECT score, PCHD classification, and good vascular recanalization were associated with the 3-month mRS (all $p < 0.05$), as shown in Figure 6. The multivariate analysis revealed that the NIHSS score, PCHD, and good vascular recanalization were independently associated with the mRS score at 3 months (all $p < 0.05$). Good vascular recanalization was a protective factor (OR = 0.256, 0.070-0.933), but the predictive efficiency was lower (AUC = 0.565), as in Table 4. Figure 7 showed that AUC of PCHD was 0.779, and the optimal diagnostic cutoff value was PCHD > 1. The AUC of the NIHSS score at admission, good vascular recanalization, and the combined model were 0.733, 0.565, and 0.867, respectively.

4. Discussion

This study shows that there was a good correlation between the new classification system for PCHD and HT. The patients with PCHD-3 and PCHD-4 were more likely to have early neurological deterioration. The 3-month mRS was poorer in patients with PCHD classified as PCHD-2, PCHD-3, and PCHD-4, but PCHD-1 was considered to be relatively benign.

In our study, the incidence of PCHD after intra-arterial reperfusion therapy was 57.1%, which was consistent with the incidence of PCHD reported by others (32.9% to 84.2%) [1–3, 15]. The incidence of HT in our study was 50.8% (HI = 31.2%; pH = 19.6%). The incidence of pH was higher than that in several published multicenter randomized clinical trials, ranging from 3.6% to 11% [16–20]. However, our rate was determined from real-world data after mechanical thrombectomy. The lack of strict control over the time window, which was extended according to ischemic core/penumbra mismatch, may be one of the reasons for this discrepancy. Another reason may be the use of SWI to detect HT, which may result in a visual overestimation of hematoma size due to susceptibility effects [21].

This study is the first to classify PCHD according to the ECASS definition in an attempt to develop a simpler and more intuitive method to predict different types of HT.

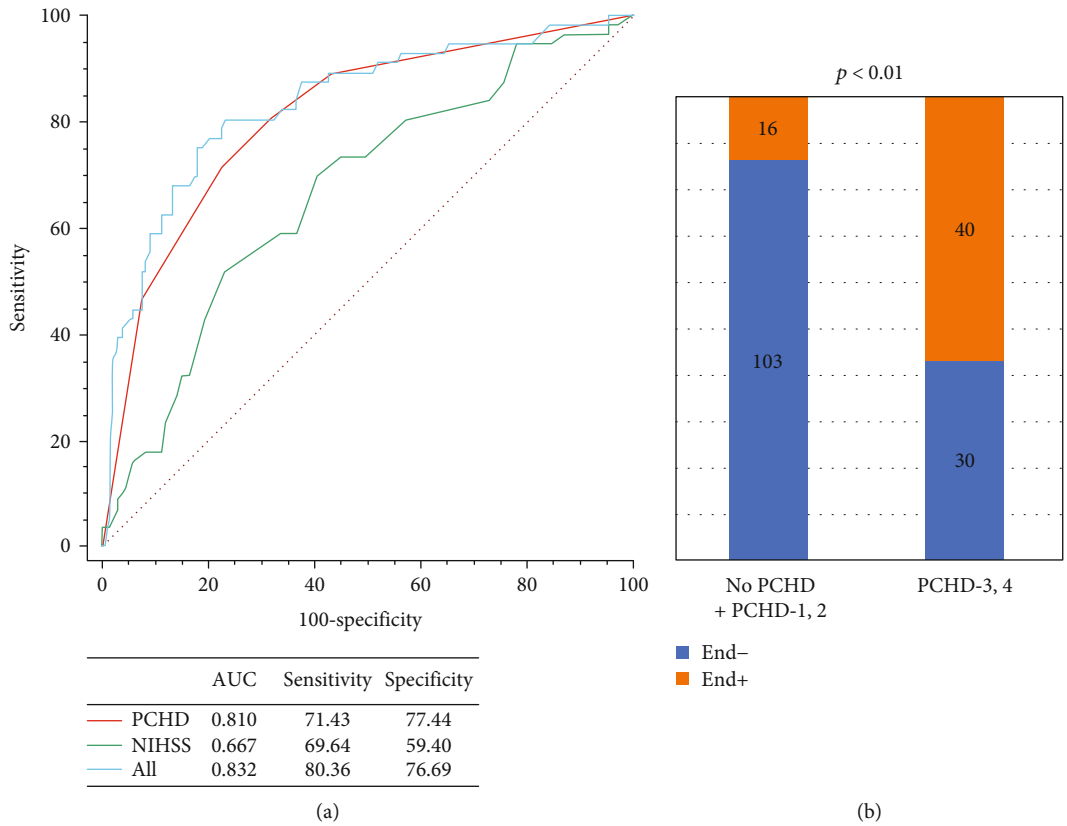

Figure 5: Evaluation of the accuracy of END. (a) ROC curves for the NIHSS score at admission and PCHD in predicting END. (b) The probability of END in the high-risk group was significantly higher than that in the low-risk group, and the optimal diagnostic cutoff value was PCHD > 2.

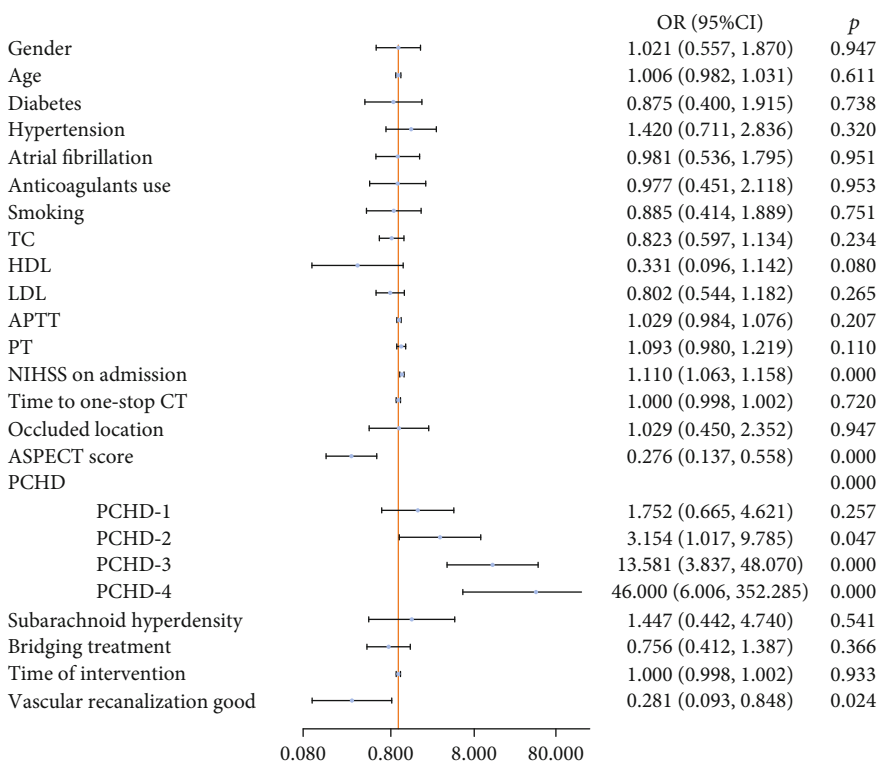

Figure 6: Univariate predictors of the mRS score at 3 months.

Table 4: Stepwise logistic regression analysis predicting mRS score at 3 months.

	Univariate logistic regression		Multivariate logistic regression	
	OR (95% CI)	*p*	OR (95% CI)	*p*
Sex	1.021 (0.557, 1.870)	0.947		
Age	1.006 (0.982, 1.031)	0.611		
Diabetes	0.875 (0.400, 1.915)	0.738		
Hypertension	1.420 (0.711, 2.836)	0.320		
Atrial fibrillation	0.981 (0.536, 1.795)	0.951		
Anticoagulant use	0.977 (0.451, 2.118)	0.953		
Smoking	0.885 (0.414, 1.889)	0.751		
TC	0.823 (0.597, 1.134)	0.234		
HDL	0.331 (0.096, 1.142)	0.080		
LDL	0.802 (0.544, 1.182)	0.265		
APTT	1.029 (0.984, 1.076)	0.207		
PT	1.093 (0.980, 1.219)	0.110		
NIHSS at admission	1.110 (1.063, 1.158)	<0.001	1.108 (1.054, 1.165)	<0.001
Time to one-stop CT	1.000 (0.998, 1.002)	0.720		
Occlusion location	1.029 (0.450, 2.352)	0.947		
ASPECT score	0.276 (0.137, 0.558)	<0.001	/	/
PCHD		<0.001		<0.001
PCHD-1	1.752 (0.665, 4.621)	0.257	1.272 (0.438, 3.695)	0.658
PCHD-2	3.154 (1.017, 9.785)	0.047	3.250 (0.988, 10.688)	0.052
PCHD-3	13.581 (3.837, 48.070)	<0.001	18.778 (4.801, 73.450)	<0.001
PCHD-4	46.000 (6.006, 352.285)	<0.001	36.294 (4.593, 286.822)	0.001
Subarachnoid HD	1.447 (0.442, 4.740)	0.541		
Bridging treatment	0.756 (0.412, 1.387)	0.366		
Time of intervention	1.000 (0.998, 1.002)	0.933		
VR (good)	0.281 (0.093, 0.848)	0.024	0.245 (0.066, 0.908)	0.035

TC: total cholesterol; HDL: high-density lipoprotein; LDL: low-density lipoprotein; APTT: activated partial thromboplastin time; PT: prothrombin time; HD: hyperdensity; VR: vascular recanalization.

Our results showed that there was a good correlation between the subtypes of PCHD and HT. Therefore, we propose that both of these occurrences have a similar pathological basis, resulting from microvascular damage and increased permeability of the BBB. A scholar proposed that when the BBB loss is small, the main extravasation content is contrast agent, which will be absorbed during follow-up. Larger red blood cells also leak out when BBB breakdown is evident. A large number of red blood cells in the brain parenchyma can cause a significant mass effect, resulting in poor clinical prognosis [15, 22, 23]. The treatment and clinical prognosis of different types of HT vary, and this study provides a theoretical basis for selecting the appropriate subsequent treatment through the early evaluation of PCHD. In this study, we also found that the CT values in the PCHD-3 group were not well differentiated from those in the other three groups, which may explain the low predictive ability of CT values for HT [8].

Previous studies have shown that the presence of hyperdensity in patients with arterial thrombolysis has no significant effect on the clinical prognosis [5, 6]. There were no further studies of PCHD on clinical prognosis in patients with mechanical thrombectomy. In our study, hyperdensity was classified into more detailed grades, and our results suggested that there were different cutoff points for early or long-term clinical prognosis. The finding of space-occupying, intervention-related PCHD 3 and PCHD-4 was associated with a high likelihood of END. This suggests that in patients with large-vessel infarction, the accumulation of mass effects may lead to further deterioration of neurological function [23].

PCHD and the NIHSS score at admission were independent risk factors for mRS at 3 months, while good vascular recanalization was a protective factor. Our results suggested that PCHD-2, PCHD-3, and PCHD-4 had a negative impact on the long-term functional outcome compared with PCHD-1. Our finding was similar to that of a previous study [11], which demonstrated the influence of hemorrhagic transformation on long-term prognosis after thrombolysis, confirming the greater clinical relevance of the new classification system for PCHD and HT.

4.1. Limitations. This study was a single-center retrospective analysis. HT was diagnosed by two imaging methods, follow-up CT or SWI. Although both diagnostic methods have been used in other studies, some bias may still be present [24, 25].

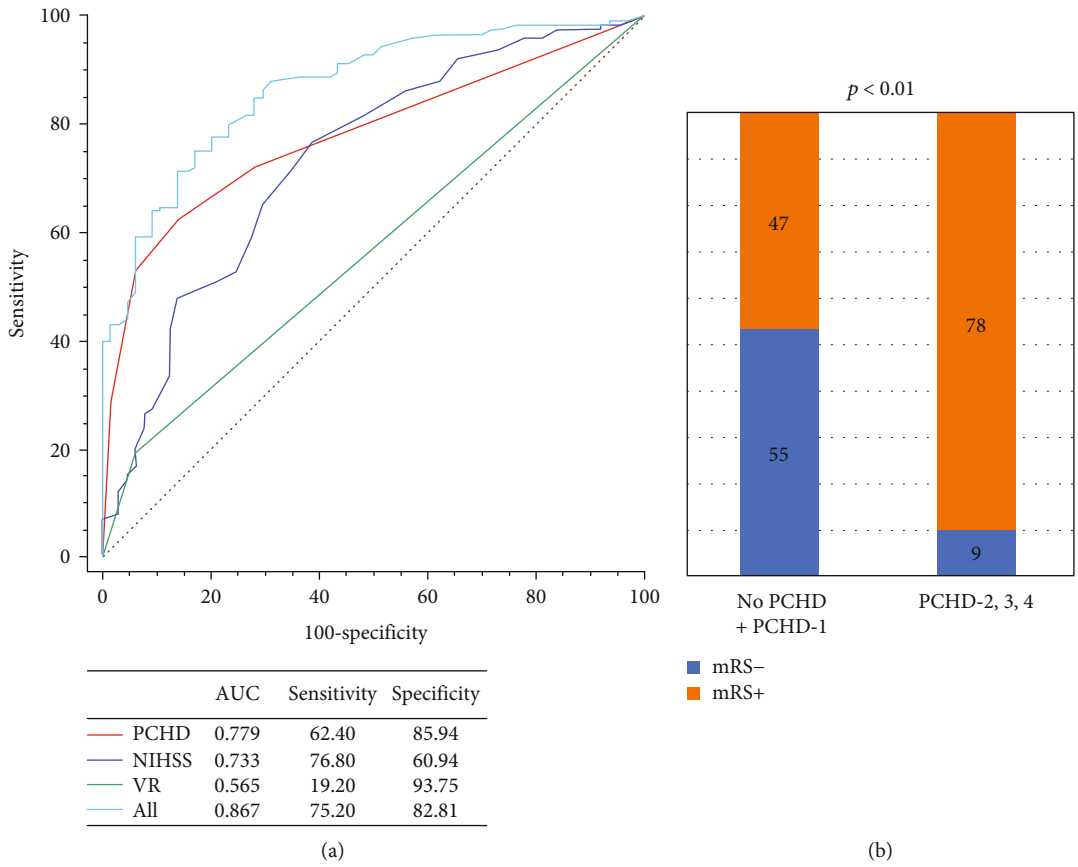

Figure 7: Evaluation of the accuracy of the mRS score at 3 months. (a) ROC curves for good vascular recanalization (VR), the NIHSS score at admission, and PCHD in predicting the mRS+ (≥3 score) at 3 months. (b) The probability of the mRS+ at 3 months in the high-risk group was significantly higher than that in the low-risk group, and the optimal diagnostic cutoff value was PCHD > 1.

5. Conclusions

There was a good correlation between HT and PCHD after intravascular intervention in ischemic stroke patients. PCHD was an independent factor for END and the mRS score at 3 months with different cutoff points. The new classification system for PCHD was suggested to have some clinical significance for predicting both the subtypes of HT and clinical prognosis.

Data Availability

Data can be accessed by inquiring the corresponding author.

Conflicts of Interest

The authors declare that the research was conducted in the absence of any commercial or financial relationships that could be construed as a potential conflict of interest.

Acknowledgments

We would like to acknowledge Professor Xiangyang Gong for his guidance during this research. The work was supported by the Natural Science Foundation of Zhejiang Province Health Department (grant no. 2021KY067).

Supplementary Materials

The following supplementary materials are available for this paper: image and clinical data of END- and END+ group (Table s1), and image and clinical data of mRS- and mRS+ group (Table s2). *(Supplementary Materials)*

References

[1] S. Nakano, T. Iseda, H. Kawano, T. Yoneyama, T. Ikeda, and S. Wakisaka, "Parenchymal hyperdensity on computed tomography after intra-arterial reperfusion therapy for acute middle cerebral artery Occlusion," *Stroke*, vol. 32, no. 9, pp. 2042–2048, 2001.

[2] W. Yoon, J. J. Seo, J. K. Kim, K. H. Cho, J. G. Park, and H. K. Kang, "Contrast enhancement and contrast extravasation on computed tomography after intra-arterial thrombolysis in patients with acute ischemic stroke," *Stroke*, vol. 35, no. 4, pp. 876–881, 2004.

[3] Y. M. Jang, D. H. Lee, H. S. Kim et al., "The fate of high-density lesions on the non-contrast CT obtained immediately after intra-arterial thrombolysis in ischemic stroke patients," *Korean Journal of Radiology*, vol. 7, no. 4, pp. 221–228, 2006.

[4] F. B. Cabral, L. H. Castro-Afonso, G. S. Nakiri et al., "Hyper-attenuating brain lesions on CT after ischemic stroke and thrombectomy are associated with final brain infarction,"

Interventional Neuroradiology, vol. 23, no. 6, pp. 594–600, 2017.

[5] G. Parrilla, B. García-Villalba, M. Espinosa de Rueda et al., "Hemorrhage/contrast staining areas after mechanical intra-arterial thrombectomy in acute ischemic stroke: imaging findings and clinical significance," *American Journal of Neuroradiology*, vol. 33, no. 9, pp. 1791–1796, 2012.

[6] H. An, W. Zhao, J. Wang et al., "Contrast staining may be associated with intracerebral hemorrhage but not functional outcome in acute ischemic stroke patients treated with endovascular thrombectomy," *Aging and Disease*, vol. 10, no. 4, pp. 784–792, 2019.

[7] C. Xu, Y. Zhou, R. Zhang et al., "Metallic hyperdensity sign on noncontrast CT immediately after mechanical thrombectomy predicts parenchymal hemorrhage in patients with acute large-artery occlusion," *American Journal of Neuroradiology*, vol. 40, no. 4, pp. 661–667, 2019.

[8] J.-T. Kim, S.-H. Heo, B.-H. Cho et al., "Hyperdensity on noncontrast CT immediately after intra-arterial revascularization," *Journal of Neurology*, vol. 259, no. 5, pp. 936–943, 2012.

[9] P. Trouillas and R. von Kummer, "Classification and pathogenesis of cerebral hemorrhages after thrombolysis in ischemic stroke," *Stroke*, vol. 37, no. 2, pp. 556–561, 2006.

[10] R. G. Nogueira, R. Gupta, T. G. Jovin et al., "Predictors and clinical relevance of hemorrhagic transformation after endovascular therapy for anterior circulation large vessel occlusion strokes: a multicenter retrospective analysis of 1122 patients," *Journal of Neurointerventional Surgery*, vol. 7, no. 1, pp. 16–21, 2015.

[11] I. Dzialowski, J. H. Pexman, P. A. Barber, A. M. Demchuk, A. M. Buchan, and M. D. Hill, "Asymptomatic hemorrhage after thrombolysis may not be Benign," *Stroke*, vol. 38, no. 1, pp. 75–79, 2007.

[12] X. Hou, W. Chen, H. Xu, Z. Zhu, Y. Xu, and H. Chen, "The rate of early neurological deterioration occurring after thrombolytic therapy: a meta-analysis," *Brain and Behavior*, vol. 9, no. 2, article e01210, 2019.

[13] A. Ganesh, R. Luengo-Fernandez, R. M. Wharton, and P. M. Rothwell, "Ordinal vs dichotomous analyses of modified Rankin scale, 5-year outcome, and cost of stroke," *Neurology*, vol. 91, no. 21, pp. e1951–e1960, 2018.

[14] L. Wei, Y. Zhu, J. Deng et al., "Visualization of thrombus enhancement on thin-slab maximum intensity projection of CT angiography: an imaging sign for predicting stroke source and thrombus compositions," *Radiology*, vol. 298, no. 2, pp. 374–381, 2021.

[15] N. Lummel, G. Schulte-Altedorneburg, C. Bernau et al., "Hyperattenuated intracerebral lesions after mechanical recanalization in acute stroke," *AJNR. American Journal of Neuroradiology*, vol. 35, no. 2, pp. 345–351, 2014.

[16] P. S. S. Berkhemer, D. B. Fransen, D. Beumer et al., "A randomized trial of intraarterial treatment for acute ischemic stroke," *The New England Journal of Medicine*, vol. 372, no. 1, pp. 11–20, 2015.

[17] B. C. V. Campbell, P. J. Mitchell, T. J. Kleinig et al., "Endovascular therapy for ischemic stroke with perfusion-imaging selection," *The New England Journal of Medicine*, vol. 372, no. 11, pp. 1009–1018, 2015.

[18] M. Goyal, A. M. Demchuk, B. K. Menon et al., "Randomized assessment of rapid endovascular treatment of ischemic stroke," *The New England Journal of Medicine*, vol. 372, no. 11, pp. 1019–1030, 2015.

[19] T. G. Jovin, A. Chamorro, E. Cobo et al., "Thrombectomy within 8 hours after symptom onset in ischemic stroke," *The New England Journal of Medicine*, vol. 372, no. 24, pp. 2296–2306, 2015.

[20] J. L. Saver, M. Goyal, A. Bonafe et al., "Stent-retriever thrombectomy after intravenous t-PA vs. t-PA alone in stroke," *The New England Journal of Medicine*, vol. 372, no. 24, pp. 2285–2295, 2015.

[21] R. E. Burgess, S. Warach, T. J. Schaewe et al., "Development and validation of a simple conversion model for comparison of intracerebral hemorrhage volumes measured on CT and gradient recalled echo MRI," *Stroke*, vol. 39, no. 7, pp. 2017–2020, 2008.

[22] T. Tomsick, "Hyperattenuated intracerebral lesions after mechanical recanalization in acute stroke: contrast and compare," *American Journal of Neuroradiology*, vol. 35, no. 2, pp. 352-353, 2014.

[23] G. C. Jickling, D. Liu, B. Stamova et al., "Hemorrhagic transformation after ischemic stroke in animals and humans," *Journal of Cerebral Blood Flow and Metabolism*, vol. 34, no. 2, pp. 185–199, 2014.

[24] S. Payabvash, M. H. Qureshi, S. M. Khan et al., "Differentiating intraparenchymal hemorrhage from contrast extravasation on post-procedural noncontrast CT scan in acute ischemic stroke patients undergoing endovascular treatment," *Neuroradiology*, vol. 56, no. 9, pp. 737–744, 2014.

[25] S. Payabvash, A. A. Khan, M. H. Qureshi, O. Saeed, M. F. K. Suri, and A. I. Qureshi, "Detection of intraparenchymal hemorrhage after endovascular therapy in patients with acute ischemic stroke using immediate postprocedural flat-panel computed tomography scan," *Journal of Neuroimaging*, vol. 26, no. 2, pp. 213–218, 2016.

Hindawi
Neural Plasticity
Volume 2021, Article ID 3536234, 11 pages
https://doi.org/10.1155/2021/3536234

Research Article

Structural and Functional Deficits in Patients with Poststroke Dementia: A Multimodal MRI Study

Huaying Cai,[1] **Zhiyong Zhao**,[2] **Linhui Ni**,[1] **Guocan Han**,[3] **Xingyue Hu**,[1] **Dan Wu**,[2] **Xianjun Ding**,[4] **and Jin Wang**[1]

[1]*Department of Neurology, Neuroscience Center, Sir Run Run Shaw Hospital, Zhejiang University, Hangzhou, China*
[2]*Key Laboratory for Biomedical Engineering of Ministry of Education, Department of Biomedical Engineering, College of Biomedical Engineering & Instrument Science, Zhejiang University, Hangzhou, China*
[3]*Department of Radiology, Sir Run Run Shaw Hospital, Zhejiang University, Hangzhou, China*
[4]*Department of Orthopaedic Surgery, Sir Run Run Shaw Hospital, Zhejiang University, Hangzhou, China*

Correspondence should be addressed to Jin Wang; wangjinjoy@zju.edu.cn

Received 29 June 2021; Revised 25 September 2021; Accepted 12 October 2021; Published 3 November 2021

Academic Editor: Yating Lv

Although many neuroimaging studies have reported structural and functional abnormalities in the brains of patients with cognitive impairments following stroke, little is known about the pattern of such brain reorganization in poststroke dementia (PSD). The present study was aimed at investigating alterations in spontaneous brain activity and gray matter volume (GMV) in PSD patients. We collected T1-weighted and resting-state functional magnetic resonance imaging data from 20 PSD patients, 24 poststroke nondementia (PSND) patients, and 21 well-matched normal controls (NCs). We compared the differences among the groups in GMV and the fractional amplitude of low-frequency fluctuations (fALFF). Then, we evaluated the relationship between these brain measures and cognitive assessments and explored the possible distinguisher for PSD by receiver operating characteristic (ROC) curve analysis. PSD patients showed smaller GMV in the right superior temporal gyrus and lower fALFF values in the right inferior frontal gyrus than both PSND patients and NCs, but such differences were not observed between PSND patients and NCs. Moreover, GMV in the left medial prefrontal cortex showed a significant positive correlation with the Mini-Cog assessment in PSD patients, and GMV in the left CPL displayed the highest area under the ROC curve among all the features for classifying PSD versus PSND patients. Our findings suggest that PSD patients show dementia-specific structural and functional alteration patterns, which may help elucidate the pathophysiological mechanisms underlying PSD.

1. Introduction

Poststroke dementia (PSD), irrespective of the presumed cause, is a clinical entity that encompasses all types of dementia following a stroke and characterized as cognitive decline [1]. Previous studies have reported the prevalence of poststroke dementia (PSD) ranging from 13% to 27% [2–4], and this variation may be related to many factors, including race [5, 6], educational level [7], economic level [4], lifestyle [8], and aging population [3]. Moreover, PSD may have potential influences on various aspects of daily living activities, especially stroke recurrence [9] and functional outcome [10], and has become a significant public health burden [11]. Although previous neuroimaging studies based on structural or functional MRI have attempted to explore PSD-related patterns in brain reorganization [12–14, 42], few studies used multimodal MRI to explore the neural mechanisms underlying PSD.

In the neuroimaging field, functional magnetic resonance imaging (fMRI) has been widely used to investigate the pathogenesis of neurological diseases [15–17]. Compared with task-based fMRI, resting-state fMRI (rs-fMRI) shows the advantage of application in stroke studies since it does not require specific tasks [18, 19]. rs-fMRI mainly examines the low-frequency (0.01-0.08 Hz) fluctuations in

blood oxygenation level-dependent (BOLD) fMRI signals at rest [20, 21]. As a valid method to detect local spontaneous neuronal activity [22], the amplitude of low-frequency fluctuations (ALFF) has been used to study various cognitive and neuropsychiatric disorders, including mild cognitive impairment [23] and schizophrenia [24]. However, compared with ALFF, the fractional amplitude of low-frequency fluctuations (fALFF) could be robust against nonspecific signal components [25], allows the analysis of frequency-specific activity [26], and improves the sensitivity and specificity in detecting regional spontaneous brain activity [27]. Using this method, previous stroke studies found that compared to normal controls (NCs), patients with acute cerebellar infarction showed increased fALFF values in the right frontal lobe, left hippocampus, and right cingulate gyrus and decreased fALFF values in the cerebellum posterior lobe (CPL) [18]; stroke patients with depression symptoms have higher fALFF values in the left dorsolateral prefrontal cortex and the right precentral gyrus compared to nondepressed patients [26]. Moreover, depressive symptom scores in stroke patients were positively correlated with fALFF values in the left insula, superior temporal lobe, thalamus, cerebellum, and right caudate [28]. These findings suggest that fALFF could be used to explore neuronal functional alterations in patients after stroke. However, this method has never been used to detect changes in spontaneous neural activity in PSD patients.

In addition, gray matter volume (GMV), quantitatively calculated by voxel-based morphometry (VBM) [29] analysis of T1-weighted images, has become an ideal morphological measurement to explore structural alterations in poststroke patients [30, 31]. For example, Stebbins et al. found that patients with cognitive impairments after stroke showed significant GMV reductions in the thalamus, cingulate gyrus, and frontal, temporal, parietal, and occipital lobes compared with patients without cognitive impairments [32]. Ahn et al. observed significantly lower GMV in the bilateral cerebellum in chronic stroke patients with cognitive impairments than in NCs [33]. In addition, Yang and colleagues reported that compared with NCs, patients with poststroke aphasia showed increased GMV in the right superior temporal gyrus, right inferior parietal lobule, and left middle occipital gyrus and decreased GMV in the right caudate gyrus and bilateral thalami [34]. These results indicated that patients with different poststroke cognitive dysfunctions show different GMV alteration patterns. However, the GMV alterations in PSD patients remain unclear, and the utility of structural neuroimaging studies with MRI has not been fully explored.

The current study was aimed at exploring the potential structural and functional changes using fALFF and GMV methods in patients with PSD. Based on previous findings of alterations in fALFF and GMV in patients with different poststroke dysfunctions [18, 26, 32], we hypothesized that disease-specific patterns of fALFF and GMV changes would be discovered in patients with PSD. Furthermore, based on the report that clinical symptoms were correlated with neural alterations in stroke patients [23], we also hypothesized that the fALFF/GMV alterations in patients with PSD would be related to their cognitive functions.

2. Materials and Methods

2.1. Participants. Fifty-nine poststroke patients (PSD/PSND: $N = 25/34$) and twenty-five NCs were recruited at Sir Run Run Shaw Hospital from September 2017 to October 2019. The Institutional Review Board provided ethical approval of this study at the local hospital. All participants provided informed consent. The inclusion criteria for the patients were as follows: (1) age > 18 years, (2) complement of neuropsychological tests at the acute phase and the third month after stroke, (3) eligibility for a scan between 1 and 6 months after stroke onset, (4) first-episode stroke, and (5) definitive acute ischemic stroke based on DWI of the head. The exclusion criteria for all participants were as follows: (1) any neuropsychiatric comorbidity such as depression (total score ≥ 8 on the17-item Hamilton Depression Rating Scale), anxiety (total score ≥ 7 on the Hamilton Anxiety Rating Scale), epilepsy, brain tumor, brain trauma, and drug or alcohol abuse; (2) any clinically significant or unstable medical disorder; (3) any contraindication for MRI; (4) prestroke dementia (-Informant Questionnaire on Cognitive Decline in the Elderly (IQCODE) score > 3:31); and (5) aphasia before or after the stroke. A total of 19 subjects were excluded because of the excessive head motion (>2 mm/degree) (4 PSD patients, 7 PSND patients, and 4 NCs) and lesion volume (>10 ml) (1 PSD and 3 PSND patients). Finally, based on matching age and education among the three groups, 21 NCs, 20 PSD, and 24 PSND patients were included in the final analysis in the present study.

2.2. Clinical Assessments. The National Institutes of Health Stroke Scale (NIHSS) and modified Rankin Scale (mRS) scores were recorded upon patient consent. According to the poststroke cognitive impairment assessment guideline by the Chinese Stroke Centre Alliance, the IQCODE was used to evaluate the prestroke cognitive status of each patient [35], and both the Mini-Mental State Examination (MMSE) [36] and Mini-Cog [37] assessments were used to evaluate the cognitive performance of each patient both at the acute stage and at the third month poststroke. We controlled for vascular risk factors, such as blood pressure, blood lipids, blood sugar, and smoking, for each patient after stroke via antihypertensive drugs, glucose-lowering drugs, and lipid-lowering drugs. All patients underwent standardized treatment based on the "Guideline for Early Management of Adults with Ischemic Stroke" [38] and were followed up in the outpatient clinic with the same clinician. All normal controls underwent cognitive assessment (both the MMSE and Mini-Cog) before the MRI scan. Two neurologists (HY C and LH N) who were blinded to the MRI data recorded the clinical data and performed the cognitive examinations.

PSD was diagnosed by two neurologists with 15 years of experience and 4 years of experience according to the 2019 Chinese Vascular Cognitive Impairment Guideline, which defines PSD as a status in which cognitive impairment lasts for three months after a stroke [39]. We therefore determined the diagnosis at three months after stroke onset, which is also consistent with the international consensus [40] (within 6 months). PSD was identified if the patient satisfied one of the following two criteria: (1) MMSE scores

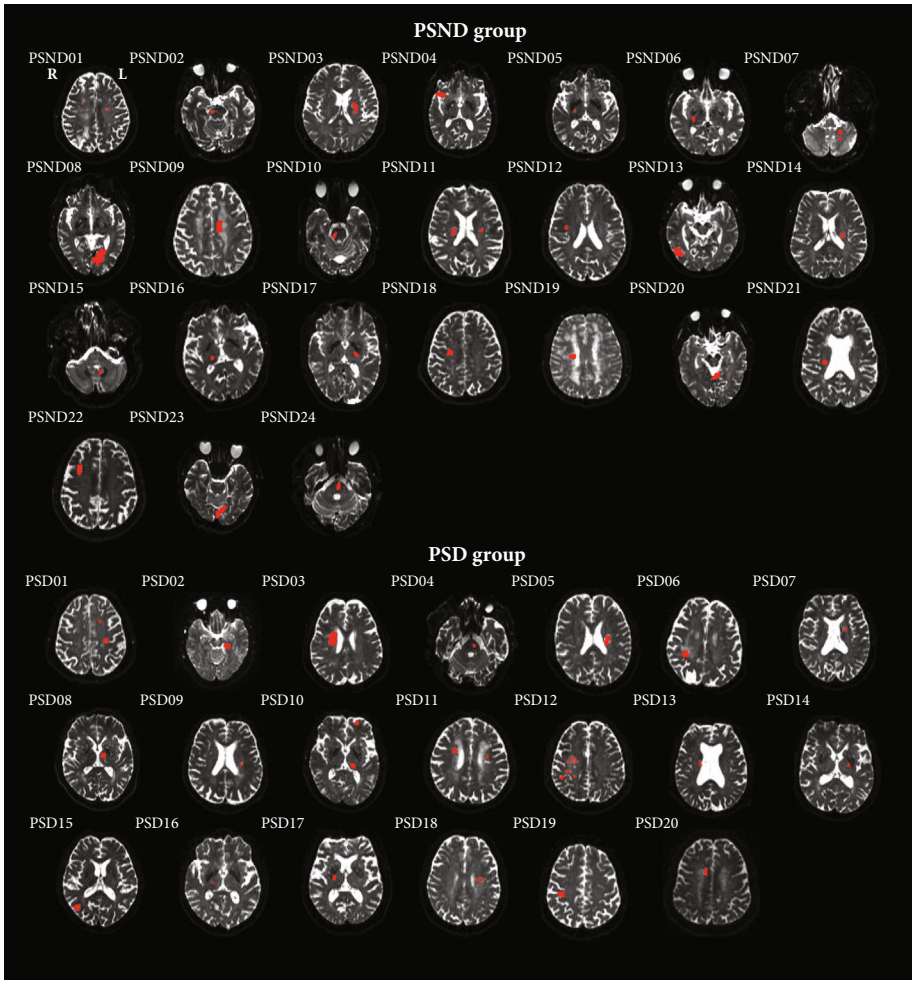

Figure 1: Lesion display for each patient in the PSD and PSND groups. The red region represents an individual lesion.

below a certain cutoff value depending on the education level: (i) MMSE < 24 for patients with education higher than junior middle school, (ii) MMSE ≤ 19 for patients with primary school education, or (iii) MMSE ≤ 17 for patients with illiteracy, and (2) an adjusted Mini-Cog score of <3. Finally, poststroke patients were divided into two subgroups (PSD and PSND).

2.3. MRI Data Acquisition. Multimodal MRI scans, including resting-state fMRI and T1- and diffusion-weighted images, were performed for each patient approximately three months after stroke. All data were acquired on a Siemens 3 T MAGNETOM Skyra MRI scanner (Siemens Healthcare, Erlangen, Germany) with a 20-channel head coil. The sequences and parameters were identical to those in our previous study [41].

2.4. Lesion Analysis. We manually drew lesion regions slice by slice on the nondiffusion-weighted image (b0) using MRIcro software (http://www.mricro.com) (Figure 1), and lesion masks were confirmed by two neurologists (HY C and LH N). Then, we determined the location and number of lesions and calculated the lesion volume for each patient.

2.5. FMRI Data Processing. We preprocessed the resting-state fMRI data using the *Advanced* DPARSF (http://www.restfmri.net) and SPM12 (http://www.fil.ion.ucl.ac.uk/spm) toolkits. The first 5 functional volumes were discarded, and the remaining 115 volumes underwent slice timing and head motion corrections. Then, white matter, cerebrospinal fluid, and the Friston 24-parameter model of head motion were regressed out as nuisance variables. Next, the data were spatially normalized to an EPI template in the MNI space. Finally, we conducted the fALFF analysis. Specifically, a ratio of the low-frequency amplitude within 0.01-0.1 Hz from fast Fourier transformation to the power spectrum of the entire frequency range was computed at each voxel to obtain fALFF values [25]. The fALFF maps were normalized by subtracting the mean value for the entire brain and then dividing by the whole-brain standard deviation. The maps were further smoothed by a Gaussian kernel at a full width half maximum (FWHM) of 6 mm [42, 43].

2.6. VBM Analysis. We performed the VBM analysis with SPM12. We first registered the T1 images to the Montreal Neurological Institute (MNI) template and then segmented the whole-brain structural data into white matter, gray

Table 1: Demographic and clinical information of all participants.

	NCs ($n = 21$)	PSND ($n = 24$)	PSD ($n = 20$)	$F/t/\chi^2$	p value
Age[†], mean (SD)	60.71 (10.36)	61.67 (7.21)	66.95 (9.04)	2.94	0.06
Male[‡], n (%)	9 (43)	20 (83)	11 (55)	8.27	0.02*
Handiness	R	R	R	N/A	N/A
ICV (L)[†], mean (SD)	1.46 (0.14)	1.41 (0.31)	1.30 (0.26)	8.35	0.02*
FD[†], mean (SD)	0.09 (0.07)	0.11 (0.07)	0.08 (0.05)	5.16	0.08
Education level[‡], n (%)				19.36	0.01*
None	0	4 (17)	7 (35)		
Primary	14 (67)	6 (25)	5(25)		
Junior high school	5 (24)	8 (33)	5 (25)		
Senior high school	2 (9)	5 (21)	3 (15)		
Superior	0	1 (4)	0		
Duration of illness (day)[†], mean (SD)	N/A	99.04 (62.14)	104.55 (69.69)	-0.28	0.78
NIHSS[1†], mean (SD)	N/A	1.79 (2.36)	1.55 (2.21)	0.35	0.73
NIHSS[2†], mean (SD)	N/A	0.17 (0.38)	0.25 (0.44)	-0.67	0.51
mRS[1‡], n (%)				3.03	0.39
0-1-2-4	N/A	15 (63)-7 (29)-0-2 (8)	14 (70)-5 (25)-1 (5)-0		
mRS[2‡], n (%)				0.11	0.74
0-1	N/A	19 (79)-5 (21)	15 (75)-5 (25)		
MMSE[1†], mean (SD)	25.88 (3.04)	26.88 (2.91)	20.30 (4.50)	20.77	<0.001***
MMSE[2†], mean(SD)	25.88 (3.04)	27.17 (2.32)	20.45 (4.38)	24.19	<0.001***
Mini-Cog[1‡], n (%)				79.46	<0.001***
0-1-2-3-4-5-6-7	0-0-0-0-1 (5)-5 (24)-3 (14)-12 (57)	0-0-3 (13)-12 (50)-0-9 (37)-0-0	2 (10)-0-7 (35)-9 (45)-2 (10)-0-0-0		
Mini-Cog[1‡], n (%)				65.34	<0.001***
0-1-2-3-4-5-6-7	0-0-0-0-1 (5)-5 (24)-3 (14)-12 (57)	0-0-2 (8)-8 (33)-1 (5)-13 (54)-0-0	3 (15)-1 (5)-4 (20)-7 (35)-1 (5)-4 (20)-0-0		

[1]Acute phase; [2]third month; [†]one-way ANOVA analysis/two-sample t-test; [‡]chi-square test. Age, ICV, duration of illness, and MMSE are shown as mean (standard deviation); other data (n (%)) are number of participants (percentage). *, **, and *** represent $p < 0.05$, $p < 0.01$, and $p < 0.001$, respectively. NCs: normal controls; PSND: poststroke nondemented; PSD: poststroke demented; ICV: intracranial volume; FD: framewise displacement; NIHSS: National Institutes of Health Stroke Scale; mRS: modified Rankin Scale; MMSE: Mini-Mental State Examination.

Table 2: Lesion information of all patients.

Lesion	PSND ($n = 24$)	PSD ($n = 20$)	t/χ^2	p value
Location of stroke[‡]			0.45	0.80
Left	11	11		
Right	11	8		
Bilateral	2	1		
Lesion volume (ml)[†], mean (SD)	1.28 (1.32)	0.96 (1.12)	0.87	0.39
Lesion number[‡]				
1-2-3	17 : 7 : 0	16 : 3 : 1	2.29	0.32

[†]Two-sample t-test; [‡]chi-square test. PSND: poststroke nondemented; PSD: poststroke demented; SD: standard deviation.

matter, and cerebrospinal fluid. We conducted bias correction to remove intensity nonuniformities. Segmented images of the gray matter were preserved to assess the number of volume changes based on spatial registration, and the modulated images of the gray matter could reflect the tissue volumes for using VBM analysis. Finally, we smoothed the

Table 3: The information of stroke lesions in patients.

Patient ID	Hemisphere	Location	Number	Volume (ml)
PSND_01	Bilateral	White matter	2	0.65
PSND_02	Right	White matter, cerebellum	1	0.35
PSND_03	Left	White matter, caudate	1	2.73
PSND_04	Right	White matter	1	1.19
PSND_05	Right	White matter	1	0.36
PSND_06	Right	White matter	1	2.23
PSND_07	Left	Cerebellum	2	0.47
PSND_08	Left	Occipital lobe	1	3.22
PSND_09	Left	White matter, cingulate gyrus	2	0.52
PSND_10	Right	White matter	1	1.06
PSND_11	Bilateral	White matter	2	1.65
PSND_12	Right	Insula	1	0.21
PSND_13	Left	Occipital, temporal lobes	2	2.06
PSND_14	Left	White matter	2	0.83
PSND_15	Left	Cerebellum	1	0.12
PSND_16	Right	Thalamus	1	0.65
PSND_17	Left	Thalamus	1	0.26
PSND_18	Right	White matter	1	0.96
PSND_19	Right	White matter	1	1.90
PSND_20	Left	Cerebellum	1	0.44
PSND_21	Right	White matter	1	1.86
PSND_22	Right	White matter, frontal lobe	2	0.57
PSND_23	Left	Occipital lobe	1	6.02
PSND_24	Left	White matter	1	0.47
PSD_01	Left	White matter, frontal lobe	3	0.42
PSD_02	Left	White matter	1	0.24
PSD_03	Right	White matter, putamen, thalamus, insula	1	4.79
PSD_04	Left	White matter	1	0.28
PSD_05	Left	White matter, caudate	1	1.84
PSD_06	Left	White matter	1	0.59
PSD_07	Right	White matter	1	1.28
PSD_08	Left	White matter, putamen	2	2.27
PSD_09	Left	Thalamus	1	0.84
PSD_10	Left	White matter	1	0.35
PSD_11	Left	White matter, frontal lobe	2	0.81
PSD_12	Bilateral	White matter, putamen	2	1.43
PSD_13	Right	White matter, parietal/frontal lobe	1	2.03
PSD_14	Right	White matter	1	0.23
PSD_15	Left	Thalamus	1	0.15
PSD_16	Right	Temporal lobe	1	0.32
PSD_17	Right	Thalamus	1	0.03
PSD_18	Right	White matter, putamen	1	0.40
PSD_19	Left	White matter	1	0.34
PSD_20	Right	White matter	1	0.48

normalized gray matter images using an 8 mm FWHM Gaussian filter [42, 43].

2.7. Statistical Analysis. We first performed one-way ANCOVA to compare fALFF and GMV maps among the three groups within a gray matter mask with age, sex, education, head motion, intracranial volume (ICV) and volume, location, and number of lesions as the covariates. A two-tailed Gaussian random field correction with a voxel-level $p < 0.01$ and a cluster-level $p < 0.05$ was used to control false

discoveries due to multiple comparisons. Then, for the regions showing a significant group-level main effect, post hoc t-tests were performed to detect the pairwise differences in fALFF and GMV (Bonferroni corrected, $p < 0.05$). Next, to examine the relationships between the fALFF/GMV values in the regions with between-group differences and cognitive functions (MMSE or Mini-Cog scores) and between fALFF and GMV values, partial correlation analyses were separately performed in each patient group while controlling for age, sex, education, head motion, ICV and volume, location, and number of lesions. Finally, we used the fALFF/GMV in the regions showing significant differences between groups as the feature to perform receiver operating characteristic (ROC) curve analysis to discriminate PSD from PSND patients.

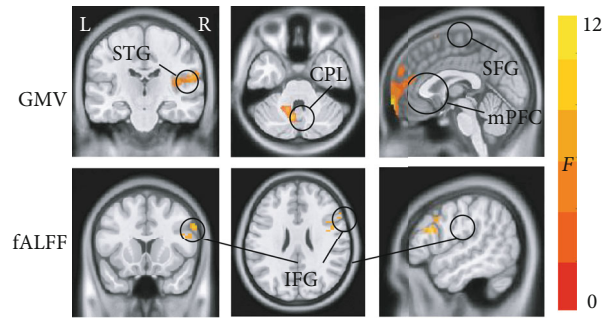

Figure 2: The regions showing significant differences in GMV/fALFF values among the PSND, PSD, and NC groups. GMV: gray matter volume; fALFF: fractional amplitude of low-frequency fluctuation; STG: superior temporal gyrus; CPL: cerebellum posterior lobe; SFG: superior frontal gyrus; mPFC: medial prefrontal cortex; IFG: inferior frontal gyrus; L: left; R: right. Color bar represents F values.

3. Results

The three groups did not have significant differences in age, handedness, head motion, or intracranial volume (Table 1). Additionally, the duration of illness and stroke severity were matched between the two patient groups. Notably, sex and education showed significant differences between NCs and the patient groups but not between PSD and PSND (sex: $p = 0.053$; education: $p = 0.60$). Cognition scores (MMSE and Mini-Cog) in the PSD patients were significantly lower than those in the PSND group (Table 1). In addition, the two patient subgroups did not have significant differences in the volume, location, or number of stroke lesions (Table 2). None of the patients showed hemorrhagic transformation after stroke. The number of patients with cortical/subcortical lesions was 4/20 in the PSND group and 4/16 in the PSD group (Table 3).

ANCOVA found that GMV showed significant differences between the three groups in the left CPL, left medial prefrontal cortex (mPFC), superior frontal gyrus (SFG), and right superior temporal gyrus (STG); significant differences in fALFF values were observed in the right inferior frontal gyrus (IFG) (Figure 2 and Table 4). Post hoc analysis showed that both PSND and PSD patients had smaller GMV than NCs in the left medial prefrontal cortex (mPFC) and SFG; the left CPL displayed larger GMV in the PSND group compared with the NC and PSD groups. Importantly, we found dementia-specific changes in which the PSD group showed decreased GMV in the right STG and decreased fALFF in the right IFG compared with PSND and NC groups, but such differences were not found between PSND and NC groups (Figure 3).

Moreover, we found significant positive correlations between GMV in the left mPFC and Mini-Cog scores at the third month in the PSD group ($p = 0.04$, $r = 0.56$) and between GMV in the right STG and MMSE scores at the third month in the PSND group ($p = 0.03$, $r = 0.52$) (Figure 4), although they did not pass the Bonferroni correction of $p < 0.05$. In addition, ROC analysis showed that GMV in the left CPL and right STG and fALFF values in the right IFG significantly discriminated the PSD patients from the PSND patients (Figure 5 and Table 5). Specifically, the AUC in left CPL, left mPFC, left SFG, right STG, and right IFG were 0.804, 0.531, 0.502, 0.783, and 0.717, respectively. Also, the performance was improved (AUC = 0.898, $p < 0.001$) after combining the three brain regions with high AUC values5.

4. Discussion

The present study evaluated alterations in GMV and fALFF in patients with PSD, and the results supported our hypotheses that (1) PSD patients showed dementia-specific decreases in GMV in the right STG and fALFF in the right IFG; (2) GMV in the left mPFC in the PSD group was significantly positively correlated with Mini-Cog scores at the third month, and such a relationship was also found between GMV in the right STG in the PSND group and MMSE scores at the third month; and (3) fALFF values in the right IFG and GMV in the left CPL and right STG may be used to discriminate PSD patients from PSND patients. These findings provide a new insight into the neurophysiological mechanisms underlying PSD, which may motivate the development of a theoretical basis for clinical diagnosis.

4.1. PSD-Related Structural Alterations. As two core components of the prefrontal cortex, the medial gyrus and superior frontal gyrus have been linked to a variety of cognitive functional domains, especially in memory [44] and cognitive control [45]. Compared with NCs, Bhalsing et al. found GMV loss in the right mPFC in essential tremor patients with cognitive impairments [46]; Yang et al. reported significantly reduced GMV in the left SFG in silent cerebral infarction patients with cognitive impairment [47]; Li et al. observed a GMV reduction in the SFG in subcortical vascular dementia patients [48]. Moreover, Stebbins and colleagues reported decreased GMV in the bilateral mPFC and SFG in stroke patients with impaired cognitive performance compared with those without cognitive impairment [32]. These studies collectively demonstrated decreased GMV in the SFG and mPFC in patients with cognitive dysfunction, and the present study provided supporting evidence that PSD patients displayed GMV reductions in these two regions compared with NCs. Additionally, previous neuroimaging studies revealed GMV atrophy in the mPFC and SFG areas in transient ischemic attack patients [49], poststroke pain patients [50], and poststroke

Table 4: Brain regions showing significant differences in GMV and fALFF values among the PSND, PSD, and NC groups.

Region	Hemisphere	MNI coordinate			Cluster size	*F* value
		X	*Y*	*Z*		
GMV						
Cerebellum posterior lobe	Left	-12	-64.5	-36	417	20.85
Medial prefrontal cortex	Left	-3	70.5	-9	711	24.57
Superior frontal gyrus	Left	-22.5	28.5	60	511	16.01
Superior temporal gyrus	Right	60	-24	21	633	14.91
fALFF						
Inferior frontal gyrus	Right	45	3	48	138	11.16

GMV: gray matter volume; fALFF: fractional amplitude of low-frequency fluctuation; NC: normal control; PSND: poststroke nondemented; PSD: poststroke demented.

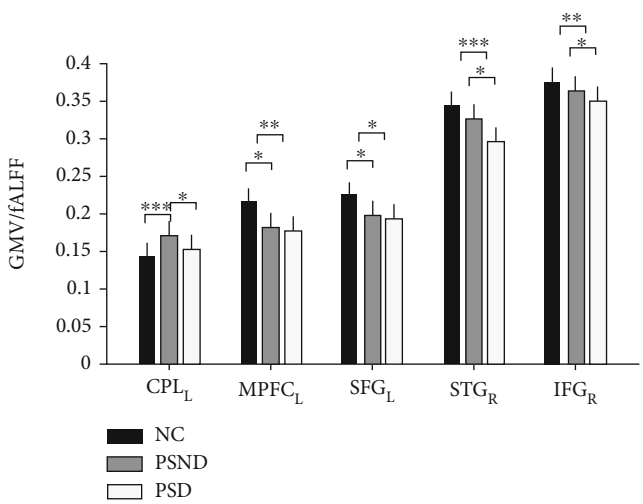

Figure 3: The differences in GMV and fALFF values among the PSND, PSD, and NC groups. GMV: gray matter volume; fALFF: fractional amplitude of low-frequency fluctuation; CPL_L: left cerebellum posterior lobe; mPFC_L: left medial prefrontal cortex; SFG_L: left superior frontal gyrus; STG_R: right superior temporal gyrus; IFG_R: right inferior frontal gyrus. ∗, ∗∗, and ∗∗∗ represent $p < 0.05$, $p < 0.01$, and $p < 0.001$, respectively.

dysphagia patients [51]. Notably, the stroke patients in these studies did not have cognitive dysfunction, implying that GMV decreases in these two regions may be related to impairments in attentional and executive control in stroke patients [52, 53]. Consistently, the present study also found that PSND patients had a smaller GMV than NCs in the left mPFC and SFG. Hence, we speculate that reduced GMV in the left mPFC and SFG are correlated with both stroke and dementia, which may help to further understand the neural mechanisms underlying PSD.

Furthermore, the cerebellum not only is involved in motor function [54, 55] but also acts as a general modulator due to the presence of cerebellar activations in higher cognitive functions [56]. Previous studies have found significant reductions in GMV in the right cerebellar region in patients with subcortical vascular dementia [57] and in left cerebellar subfields in remitted major depression patients with persistent cognitive deficits [58]. Similar results were also observed in poststroke patients [33, 59]. However, one study revealed that patients with left hemisphere subcortical stroke showed increased GMV in the ipsilesional cerebellum VI [60]. These findings suggest that the decreased GMV in the cerebellum-related region in PSD compared with PSND in the present study may be associated with both cognitive dysfunction and stroke. Moreover, the increased GMV in the cerebellum in PSND patients compared with NCs may represent motor compensation after stroke [61].

4.2. Dementia-Specific Structural and Functional Alterations. The superior temporal gyrus is considered a key structure involved in cognitive processing [62, 63]. Previous neuroimaging studies have explored structural alterations in the STG in patients with dementia or cognitive impairments. For instance, one study based on VBM analysis showed that Parkinson's disease patients with dementia had a significant decrease in GMV in the bilateral STG compared to those without dementia [64]. Using a similar method, another study revealed that compared with NCs, patients with subcortical vascular mild cognitive impairment exhibited atrophy in the bilateral STG [48]. These findings suggest that the STG might be a potential neural biomarker in cognitive impairment diseases. Consistent with previous studies, the present study found that the right STG displayed a smaller GMV in PSD patients than in PSND patients and NCs, but such a difference was not observed between PSND patients and NCs, which implied that the structural reduction in the right STG was more likely to be specific to dementia rather than stroke. Moreover, studies have demonstrated that functional alterations in the inferior frontal gyrus (IFG), which is also considered to be related to cognition [65], have been reported in several previous neuroimaging studies. For example, Zhong et al. reported decreased ALFF in the left opercular part of the IFG in patients with cognitive control impairment compared with NCs [66]. Han et al. and Li et al. both observed that compared with NCs, patients with mild cognitive impairment had decreased ALFF values in the left IFG [67, 68]. Agreeing with these studies, the present study demonstrated decreased fALFF values in the right IFG in the PSD patients compared with the PSND patients and NCs, whereas the PSND patients did not show significant GMV changes in this region compared with the NCs. This suggests that the functional alterations in the right IFG could be a related biomarker of

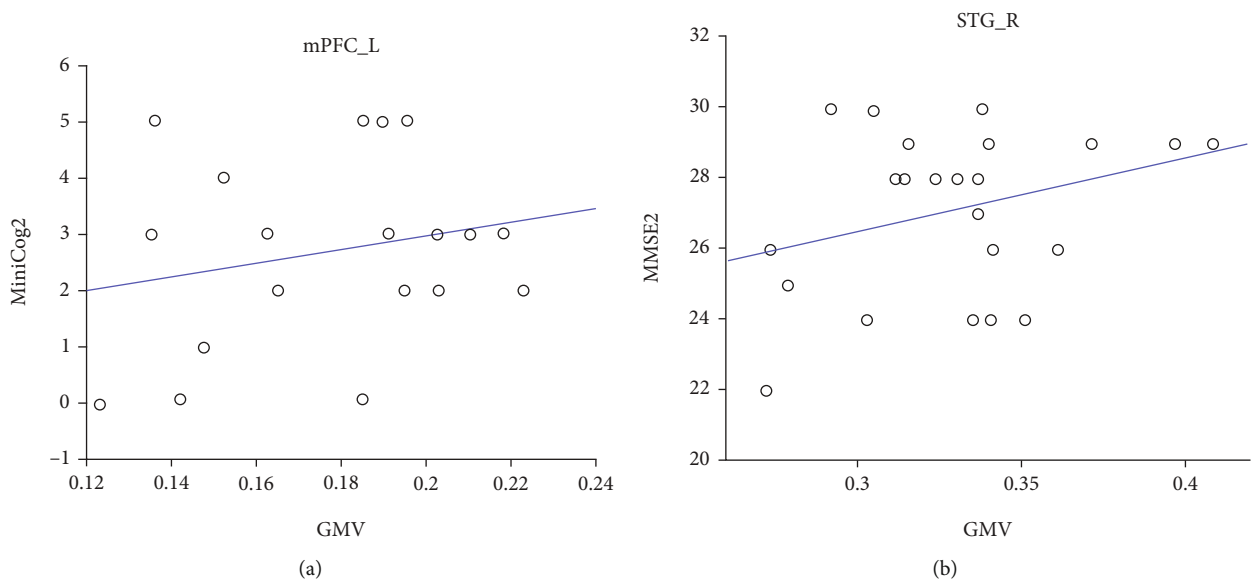

Figure 4: Correlations between clinical cognitive assessments and GMV in the mPFC_L (a) and STG_R (b) in different groups. GMV: gray matter volume; miniCog2: Mini-Cog assessment at the third month; MMSE2: Mini-Mental State Examination assessment at the third month; mPFC_L: left medial prefrontal cortex; STG_R: right superior temporal gyrus.

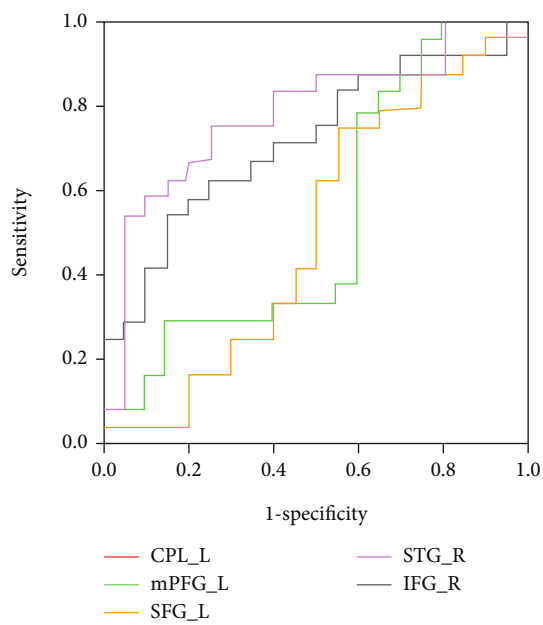

Figure 5: The receiver operating characteristic (ROC) curves for using GMV/fALFF values for the classification of PSND versus PSD patients. Specifically, the AUC in the left cerebellum posterior lobe, left medial prefrontal cortex, left superior frontal gyrus, right superior temporal gyrus, and right inferior frontal gyrus are 0.804, 0.531, 0.502, 0.783, and 0.717, respectively. AUC: area under the curve; fALFF: fractional amplitude of low-frequency fluctuation; CPL_L: left cerebellum posterior lobe; mPFC_L: left medial prefrontal cortex; SFG_L: left superior frontal gyrus; STG_R: right superior temporal gyrus; IFG_R: right inferior frontal gyrus.

Table 5: Results of ROC curve analysis for classification of PSD and PSND patients.

Variables	AUC	SE	*p* value	CI
CPL_L	0.804	0.066	0.001	0.675-0.933
mPFC_L	0.531	0.093	0.724	0.350-0.713
SFG_L	0.502	0.092	0.981	0.322-0.682
STG_R	0.783	0.071	0.001	0.644-0.923
IFG_R	0.717	0.077	0.014	0.565-0.868

AUC: area under the curve; SE: standard error; CI: confidence interval; CPL_L: left cerebellum posterior lobe; mPFC_L: left medial prefrontal cortex; SFG_L: left superior frontal gyrus; STG_R: right superior temporal gyrus; IFG_R: right inferior frontal gyrus.

dementia in PSD patients. Inspired by all the findings, we speculate that exploring the specific structural and functional alterations in the right STG and IFG might facilitate a deeper understanding of the pathological mechanisms underlying PSD.

4.3. Clinical Implications of the Structural Alterations. Several studies have focused on the relationships between structural alterations in the mPFC/STG and cognitive function. For example, Bhalsing et al. demonstrated a positive correlation between GMV in the right mPFC and visual memory in patients with cognitive impairments [39]. Vidoni and colleagues reported that poor performance on cognitive measures was associated with lower GMV in the mPFC in subjects with early-stage AD [69]. Tong et al. found a significant positive correlation between cognitive maturity and GMV in the STG in young normal participants with relatively low cognitive maturity [70]. In addition, Ren et al. showed significant positive correlations between gray matter

density in the left STG and accuracy of object working memory in healthy college students [71]. Similarly, the present study found significant positive correlations between GMV in the left mPFC and Mini-Cog scores at the third month in the PSD group and between GMV in the right STG and MMSE scores at the third month in the PSND group. Hence, we speculate that GMV reductions in the left mPFC and right STG may serve as a biomarker to predict cognitive function in poststroke patients. Meanwhile, using ROC analysis, the present study indicated that GMV in the left CPL has the best performance to discriminate PSD patients from PSND patients among all features. Consistently, previous studies found that structural alterations in cerebellar regions could distinguish dementia with Lewy bodies and Alzheimer's disease (AD) [72] and could discriminate AD patients from non-AD patients [73]. Therefore, decreased GMV in the CPL may be a prospective indicator to identify dementia among patients after stroke.

4.4. Limitations. Several limitations in the present study should be noted. First, the sample size was relatively small, and a larger sample size would be necessary to confirm our findings. Second, the stroke patients recruited in the present study included cortical and subcortical lesions in the bilateral hemispheres. Although we controlled for the lesions in the statistical analysis, they may still have had a certain impact on the results. In the future, we need to explore the alterations in GMV and fALFF values in PSD patients with unilateral lesions. Third, the current study was cross-sectional; therefore, we were unable to capture dynamic abnormalities in brain structure and function in PSD patients. A longitudinal study in the future may be effective in resolving this problem.

5. Conclusion

In summary, the present study was the first to use multimodal MRI data to detect alterations in GMV and fALFF in patients with PSD and found that PSD patients showed dementia-related GMV reductions in the left CPL and right STG and a decrease in fALFF in the right IFG. Moreover, GMV in the left mPFC showed a significant positive correlation with Mini-Cog scores in PSD patients, and GMV in the left CPL could effectively distinguish PSD from PSND patients. Taken together, these findings could provide new evidence to understand the neurophysiological mechanisms underlying PSD, which may promote the development of a theoretical basis for clinical diagnosis.

Data Availability

The data that support the findings of this study are available from the corresponding author upon request.

Conflicts of Interest

The authors declare that there are no conflicts of interest regarding the publication of this article.

Acknowledgments

We thank all the participants and their families for their virtuous support. This work was supported by grants from the Natural Science Foundation of China (81400926 and 82001907), Natural Science Foundation of Zhejiang Province of China (LY19H090027 and LY16H060002), Medical and Health Research Project of Zhejiang Province of China (2018RC045), and China Postdoctoral Science Foundation (2020M671726).

References

[1] R. N. Kalaria, R. Akinyemi, and M. Ihara, "Stroke injury, cognitive impairment and vascular dementia," *Biochimica et Biophysica Acta*, vol. 1862, no. 5, pp. 915–925, 2016.

[2] V. C. Mok, A. Wong, W. W. Lam et al., "Cognitive impairment and functional outcome after stroke associated with small vessel disease," *Journal of Neurology, Neurosurgery, and Psychiatry*, vol. 75, no. 4, pp. 560–566, 2004.

[3] W. K. Tang, S. S. M. Chan, H. F. K. Chiu et al., "Frequency and determinants of poststroke dementia in Chinese," *Stroke*, vol. 35, no. 4, pp. 930–935, 2004.

[4] D. H. Zhou, J. Y. J. Wang, J. Li, J. Deng, C. Gao, and M. Chen, "Study on frequency and predictors of dementia after ischemic stroke: the Chongqing stroke study," *Journal of Neurology*, vol. 251, no. 4, pp. 421–427, 2004.

[5] D. W. Desmond, J. T. Moroney, M. C. Paik et al., "Frequency and clinical determinants of dementia after ischemic stroke," *Neurology*, vol. 54, no. 5, pp. 1124–1131, 2000.

[6] L. N. Koenig, L. M. McCue, E. Grant et al., "Lack of association between acute stroke, post-stroke dementia, race, and β-amyloid status," *NeuroImage: Clinical*, vol. 29, p. 102553, 2021.

[7] T. Pohjasvaara, R. Mäntylä, O. Salonen et al., "How complex interactions of ischemic brain infarcts, white matter lesions, and atrophy relate to poststroke dementia," *Archives of Neurology*, vol. 57, no. 9, pp. 1295–1300, 2000.

[8] Y. Teuschl, K. Matz, and M. Brainin, "Prevention of post-stroke cognitive decline: a review focusing on lifestyle interventions," *European Journal of Neurology*, vol. 20, no. 1, pp. 35–49, 2013.

[9] The PICASSO investigators, H. S. Kwon, D. Lee et al., "Post-stroke cognitive impairment as an independent predictor of ischemic stroke recurrence: PICASSO sub-study," *Journal of Neurology*, vol. 267, no. 3, pp. 688–693, 2020.

[10] V. Foster, A. E. Oakley, J. Y. Slade et al., "Pyramidal neurons of the prefrontal cortex in post-stroke, vascular and other ageing-related dementias," *Brain*, vol. 137, no. 9, pp. 2509–2521, 2014.

[11] G.-C. Hu and Y.-M. Chen, "Post-stroke dementia: epidemiology, mechanisms and management," *International Journal of Gerontology*, vol. 11, no. 4, pp. 210–214, 2017.

[12] J. S. Lim, N. Kim, M. U. Jang et al., "Cortical hubs and subcortical cholinergic pathways as neural substrates of poststroke dementia," *Stroke*, vol. 45, no. 4, pp. 1069–1076, 2014.

[13] J. Yang, A. Wong, Z. Wang et al., "Risk factors for incident dementia after stroke and transient ischemic attack," *Alzheimers Dement*, vol. 11, no. 1, pp. 16–23, 2015.

[14] Z. Zhao, H. Cai, W. Zheng et al., "Atrophic pattern of hippocampal subfields in post-stroke demented patient," *Journal of Alzheimer's Disease*, vol. 80, no. 3, pp. 1299–1309, 2021.

[15] P. Zhang, J. Wang, Q. Xu, Z. Song, J. Dai, and J. Wang, "Altered functional connectivity in post-ischemic stroke depression: A resting- state functional magnetic resonance imaging study," *European Journal of Radiology*, vol. 100, pp. 156–165, 2018.

[16] Y. S. Min, J. W. Park, E. Park et al., "Interhemispheric functional connectivity in the primary motor cortex assessed by resting-state functional magnetic resonance imaging aids long-term recovery prediction among subacute stroke patients with severe hand weakness," *Journal of Clinical Medicine*, vol. 9, no. 4, p. 975, 2020.

[17] C. Li, M. Dong, F. Y. Womer et al., "Transdiagnostic time-varying dysconnectivity across major psychiatric disorders," *Human Brain Mapping*, vol. 42, no. 4, pp. 1182–1196, 2021.

[18] L. Fan, J. Hu, W. Ma, D. Wang, Q. Yao, and J. Shi, "Altered baseline activity and connectivity associated with cognitive impairment following acute cerebellar infarction: a resting-state fMRI study," *Neuroscience Letters*, vol. 692, pp. 199–203, 2019.

[19] Z. Zhao, J. Wu, M. Fan et al., "Altered intra- and inter-network functional coupling of resting-state networks associated with motor dysfunction in stroke," *Human Brain Mapping*, vol. 39, no. 8, pp. 3388–3397, 2018.

[20] Z. Zhao, C. Tang, D. Yin et al., "Frequency-specific alterations of regional homogeneity in subcortical stroke patients with different outcomes in hand function," *Human Brain Mapping*, vol. 39, no. 11, pp. 4373–4384, 2018.

[21] D. Yin, Y. Luo, F. Song et al., "Functional reorganization associated with outcome in hand function after stroke revealed by regional homogeneity," *Neuroradiology*, vol. 55, no. 6, pp. 761–770, 2013.

[22] Y. F. Zang, Y. He, C. Z. Zhu et al., "Altered baseline brain activity in children with ADHD revealed by resting- state functional MRI," *Brain and Development*, vol. 29, no. 2, pp. 83–91, 2007.

[23] J. Tao, J. Liu, X. Chen et al., "Mind-body exercise improves cognitive function and modulates the function and structure of the hippocampus and anterior cingulate cortex in patients with mild cognitive impairment," *NeuroImage: Clinical*, vol. 23, p. 101834, 2019.

[24] P. Wang, J. Yang, Z. Yin et al., "Amplitude of low-frequency fluctuation (ALFF) may be associated with cognitive impairment in schizophrenia: a correlation study," *BMC Psychiatry*, vol. 19, no. 1, p. 30, 2019.

[25] Q. H. Zou, C. Z. Zhu, Y. Yang et al., "An improved approach to detection of amplitude of low-frequency fluctuation (ALFF) for resting-state fMRI: fractional ALFF," *Journal of Neuroscience Methods*, vol. 172, no. 1, pp. 137–141, 2008.

[26] N. Egorova, M. Veldsman, T. Cumming, and A. Brodtmann, "Fractional amplitude of low-frequency fluctuations (fALFF) in post-stroke depression," *NeuroImage: Clinical*, vol. 16, pp. 116–124, 2017.

[27] X. F. du, J. Liu, Q. F. Hua, and Y. J. Wu, "Relapsing-remitting multiple sclerosis is associated with regional brain activity deficits in motor- and cognitive-related brain areas," *Frontiers in Neurology*, vol. 10, p. 1136, 2019.

[28] P. Goodin, G. Lamp, R. Vidyasagar et al., "Correlated resting-state functional MRI activity of frontostriatal, thalamic, temporal, and cerebellar brain regions differentiates stroke survivors with high compared to low depressive symptom scores," *Neural Plasticity*, vol. 2019, 2019.

[29] J. Ashburner and K. J. Friston, "Voxel-based morphometry–the methods," *NeuroImage*, vol. 11, no. 6, pp. 805–821, 2000.

[30] Q. Diao, J. Liu, C. Wang et al., "Gray matter volume changes in chronic subcortical stroke: a cross-sectional study," *NeuroImage: Clinical*, vol. 14, pp. 679–684, 2017.

[31] Y. Wei, C. Wang, J. Liu et al., "Progressive gray matter atrophy and abnormal structural covariance network in ischemic pontine stroke," *Neuroscience*, vol. 448, pp. 255–265, 2020.

[32] G. T. Stebbins, D. L. Nyenhuis, C. Wang et al., "Gray matter atrophy in patients with ischemic stroke with cognitive impairment," *Stroke*, vol. 39, no. 3, pp. 785–793, 2008.

[33] D. Ahn, S. Kyeong, H. Kang, and D. H. Kim, "Bihemispheric changes associated with cognition in patients with chronic brainstem stroke," *Neuroreport*, vol. 30, no. 18, pp. 1278–1283, 2019.

[34] M. Yang, P. Yang, Y. S. Fan et al., "Altered structure and intrinsic functional connectivity in post-stroke aphasia," *Brain Topography*, vol. 31, no. 2, pp. 300–310, 2018.

[35] A. F. Jorm, R. Scott, J. S. Cullen, and A. J. MacKinnon, "Performance of the Informant Questionnaire on Cognitive Decline in the Elderly (IQCODE) as a screening test for dementia," *Psychological Medicine*, vol. 21, no. 3, pp. 785–790, 1991.

[36] Z. Wang and M. Zhang, *The Application of the Chinese Version of Mini-Mental State Examination (MMSE)*, Shanghai Psychiatry, 1989.

[37] S. Borson, J. Scanlan, M. Brush, P. Vitaliano, and A. Dokmak, "The mini-cog: a cognitive 'vital signs' measure for dementia screening in multi-lingual elderly," *International Journal of Geriatric Psychiatry*, vol. 15, no. 11, pp. 1021–1027, 2000.

[38] S. Rezaei, K. Asgari Mobarake, A. Saberi, P. Keshavarz, and E. K. Leili, "Brain-derived neurotrophic factor (BDNF) Val66-Met polymorphism and post-stroke dementia: a hospital-based study from northern Iran," *Neurological Sciences*, vol. 37, no. 6, pp. 935–942, 2016.

[39] A. CMD, "A guideline for the diagnosis and treatment of Chinese vascular cognitive impairment in 2019," *Chinese Medical Journal*, vol. 99, no. 35, pp. 2737–2744, 2019.

[40] O. A. Skrobot, J. O'Brien, S. Black et al., "The vascular impairment of cognition classification consensus study," *Alzheimers Dement*, vol. 13, no. 6, pp. 624–633, 2017.

[41] Z. Zhao, H. Cai, M. Huang et al., "Altered functional connectivity of hippocampal subfields in poststroke dementia," *Journal of Magnetic Resonance Imaging*, vol. 54, no. 4, pp. 1337–1348, 2021.

[42] Z. Gao, X. Guo, C. Liu, Y. Mo, and J. Wang, "Right inferior frontal gyrus: an integrative hub in tonal bilinguals," *Human Brain Mapping*, vol. 41, no. 8, pp. 2152–2159, 2020.

[43] P. Liu, G. Li, A. Zhang et al., "Brain structural and functional alterations in MDD patient with gastrointestinal symptoms: a resting-state MRI study," *Journal of Affective Disorders*, vol. 273, pp. 95–105, 2020.

[44] R. Lopes, C. Bournonville, and G. Kuchcinski, "Author Response: Prediction of long-term cognitive Function after minor Stroke using functional connectivity," *Neurology*, vol. 97, no. 14, p. e703, 2021.

[45] S. L. Brownsett, J. E. Warren, F. Geranmayeh, Z. Woodhead, R. Leech, and R. J. S. Wise, "Cognitive control and its impact on recovery from aphasic stroke," *Brain*, vol. 137, no. 1, pp. 242–254, 2014.

[46] K. S. Bhalsing, N. Upadhyay, K. J. Kumar et al., "Association between cortical volume loss and cognitive impairments in

essential tremor," *European Journal of Neurology*, vol. 21, no. 6, pp. 874–883, 2014.

[47] T. Yang, L. Zhang, M. Xiang et al., "Cognitive impairment and gray matter volume abnormalities in silent cerebral infarction," *Neuroreport*, vol. 26, no. 15, pp. 890–895, 2015.

[48] M. Li, Y. Meng, M. Wang et al., "Cerebral gray matter volume reduction in subcortical vascular mild cognitive impairment patients and subcortical vascular dementia patients, and its relation with cognitive deficits," *Brain and Behavior: A Cognitive Neuroscience Perspective*, vol. 7, no. 8, article e00745, 2017.

[49] R. Li et al., "Alterations in the gray matter volume in transient ischemic attack: a voxel-based morphometry study," *Neurological Research*, vol. 37, no. 1, pp. 43–49, 2015.

[50] T. Krause, S. Asseyer, B. Taskin et al., "The cortical signature of central poststroke pain: gray matter decreases in somatosensory, insular, and prefrontal cortices," *Cerebral Cortex*, vol. 26, no. 1, pp. 80–88, 2016.

[51] J. Wilmskoetter, L. Bonilha, B. Martin-Harris, J. J. Elm, J. Horn, and H. S. Bonilha, "Factors influencing oral intake improvement and feeding tube dependency in patients with poststroke dysphagia," *Journal of Stroke and Cerebrovascular Diseases*, vol. 28, no. 6, pp. 1421–1430, 2019.

[52] R. Schumacher, A. D. Halai, and M. A. Lambon Ralph, "Assessing and mapping language, attention and executive multidimensional deficits in stroke aphasia," *Brain*, vol. 142, no. 10, pp. 3202–3216, 2019.

[53] T. Hanakawa, M. A. Dimyan, and M. Hallett, "Motor planning, imagery, and execution in the distributed motor network: a time-course study with functional MRI," *Cerebral Cortex*, vol. 18, no. 12, pp. 2775–2788, 2008.

[54] M. Tanaka, J. Kunimatsu, T. W. Suzuki et al., "Roles of the cerebellum in motor preparation and prediction of timing," *Neuroscience*, vol. 462, pp. 220–234, 2021.

[55] M. J. Wagner, T. H. Kim, J. Kadmon et al., "Shared cortex-cerebellum dynamics in the execution and learning of a motor task," *Cell*, vol. 177, no. 3, pp. 669–682.e24, 2019.

[56] J. D. Schmahmann, "The cerebellum and cognition," *Neuroscience Letters*, vol. 688, pp. 62–75, 2019.

[57] C. Liu, C. Li, L. Gui et al., "The pattern of brain gray matter impairments in patients with subcortical vascular dementia," *Journal of the Neurological Sciences*, vol. 341, no. 1-2, pp. 110–118, 2014.

[58] M. S. Depping, M. M. Schmitgen, C. Bach et al., "Abnormal cerebellar volume in patients with remitted major depression with persistent cognitive deficits," *Cerebellum*, vol. 19, no. 6, pp. 762–770, 2020.

[59] L. Jiang, J. Liu, C. Wang et al., "Structural alterations in chronic capsular versus pontine stroke," *Radiology*, vol. 285, no. 1, pp. 214–222, 2017.

[60] F. Fan, C. Zhu, H. Chen et al., "Dynamic brain structural changes after left hemisphere subcortical stroke," *Human Brain Mapping*, vol. 34, no. 8, pp. 1872–1881, 2013.

[61] F. E. Buma, J. van Kordelaar, M. Raemaekers, E. E. H. van Wegen, N. F. Ramsey, and G. Kwakkel, "Brain activation is related to smoothness of upper limb movements after stroke," *Experimental Brain Research*, vol. 234, no. 7, pp. 2077–2089, 2016.

[62] H. Marrero, S. N. Yagual, E. García-Marco et al., "Enhancing memory for relationship actions by transcranial direct current stimulation of the superior temporal sulcus," *Brain Sciences*, vol. 10, no. 8, p. 497, 2020.

[63] L. Riecke, J. C. Peters, G. Valente, V. G. Kemper, E. Formisano, and B. Sorger, "Frequency-selective attention in auditory scenes recruits frequency representations throughout human superior temporal cortex," *Cerebral Cortex*, vol. 27, no. 5, pp. 3002–3014, 2017.

[64] S. H. Lee, S. S. Kim, W. S. Tae, S. Y. Lee, K. U. Lee, and J. Jhoo, "Brain volumetry in Parkinson's disease with and without dementia: where are the differences?," *Acta Radiologica*, vol. 54, no. 5, pp. 581–586, 2013.

[65] A. Hampshire, S. R. Chamberlain, M. M. Monti, J. Duncan, and A. M. Owen, "The role of the right inferior frontal gyrus: inhibition and attentional control," *NeuroImage*, vol. 50, no. 3, pp. 1313–1319, 2010.

[66] W. J. Zhong, Z. M. Zhou, J. N. Zhao, W. Wu, and D. J. Guo, "Abnormal spontaneous brain activity in minimal hepatic encephalopathy: resting-state fMRI study," *Diagnostic and Interventional Radiology*, vol. 22, no. 2, pp. 196–200, 2016.

[67] Y. Han, J. Wang, Z. Zhao et al., "Frequency-dependent changes in the amplitude of low-frequency fluctuations in amnestic mild cognitive impairment: a resting-state fMRI study," *NeuroImage*, vol. 55, no. 1, pp. 287–295, 2011.

[68] Y. Li, B. Jing, H. Liu et al., "Frequency-dependent changes in the amplitude of low-frequency fluctuations in mild cognitive impairment with mild depression," *Journal of Alzheimer's Disease*, vol. 58, no. 4, pp. 1175–1187, 2017.

[69] E. D. Vidoni, R. A. Honea, and J. M. Burns, "Neural correlates of impaired functional independence in early Alzheimer's disease," *Journal of Alzheimer's Disease*, vol. 19, no. 2, pp. 517–527, 2010.

[70] D. Tong, P. Lu, W. Li et al., "Critical thinking and regional gray matter volume interact to predict representation connection in scientific problem solving," *Experimental Brain Research*, vol. 237, no. 8, pp. 2035–2044, 2019.

[71] Z. Ren, Y. Zhang, H. He, Q. Feng, T. Bi, and J. Qiu, "The different brain mechanisms of object and spatial working memory: voxel-based morphometry and resting-state functional connectivity," *Frontiers in Human Neuroscience*, vol. 13, p. 248, 2019.

[72] T. Nakatsuka, E. Imabayashi, H. Matsuda, R. Sakakibara, T. Inaoka, and H. Terada, "Discrimination of dementia with Lewy bodies from Alzheimer's disease using voxel-based morphometry of white matter by statistical parametric mapping 8 plus diffeomorphic anatomic registration through exponentiated Lie algebra," *Neuroradiology*, vol. 55, no. 5, pp. 559–566, 2013.

[73] K. Persson, G. Selbæk, A. Brækhus, M. Beyer, M. Barca, and K. Engedal, "Fully automated structural MRI of the brain in clinical dementia workup," *Acta Radiologica*, vol. 58, no. 6, pp. 740–747, 2017.

Hindawi
Neural Plasticity
Volume 2021, Article ID 7031178, 9 pages
https://doi.org/10.1155/2021/7031178

Research Article

Longitudinal Changes of Sensorimotor Resting-State Functional Connectivity Differentiate between Patients with Thalamic Infarction and Pontine Infarction

Peipei Wang,[1,2] Zhenxiang Zang,[1,2] Miao Zhang,[1,2] Yanxiang Cao,[1,2] Zhilian Zhao,[1,2] Yi Shan,[1,2] Qingfeng Ma,[3] and Jie Lu[1,2]

[1]*Department of Radiology and Nuclear Medicine, Xuanwu Hospital, Capital Medical University, Beijing, China*
[2]*Beijing Key Laboratory of Magnetic Resonance Imaging and Brain Informatics, Beijing, China*
[3]*Department of Neurology, Xuanwu Hospital, Capital Medical University, Beijing, China*

Correspondence should be addressed to Jie Lu; imaginglu@hotmail.com

Received 6 July 2021; Revised 13 August 2021; Accepted 14 September 2021; Published 8 October 2021

Academic Editor: Yating Lv

Purpose. We investigated the disparate influence of lesion location on functional damage and reorganization of the sensorimotor brain network in patients with thalamic infarction and pontine infarction. *Methods*. Fourteen patients with unilateral infarction of the thalamus and 14 patients with unilateral infarction of the pons underwent longitudinal fMRI measurements and motor functional assessment five times during a 6-month period (<7 days, at 2 weeks, 1 month, 3 months, and 6 months after stroke onset). Twenty-five age- and sex-matched controls underwent MRI examination across five consecutive time points in 6 months. Functional images from patients with left hemisphere lesions were first flipped from the left to the right side. The voxel-wise connectivity analyses between the reference time course of each ROI (the contralateral dorsal lateral putamen (dl-putamen), pons, ventral anterior (VA), and ventral lateral (VL) nuclei of the thalamus) and the time course of each voxel in the sensorimotor area were performed for all five measurements. One-way ANOVA was used to identify between-group differences in functional connectivity (FC) at baseline stage (<7 days after stroke onset), with infarction volume included as a nuisance variable. The family-wise error (FWE) method was used to account for multiple comparison issues using SPM software. Post hoc repeated-measure ANOVA was applied to examine longitudinal FC reorganization. *Results*. At baseline stage, significant differences were detected between the contralateral VA and ipsilateral postcentral gyrus (cl_VA-ip_postcentral), contralateral VL and ipsilateral precentral gyrus (cl_VL-ip_precentral). Repeated measures ANOVA revealed that the FC change of cl_VA-ip_postcentral differ significantly among the three groups over time. The significant changes of FC between cl_VA and ip_postcentral at different time points in the thalamic infarction group showed that compared with 7 days after stroke onset, there was significantly increased FC of cl_VA-ip_postcentral at 1 month, 3 months, and 6 months after stroke onset. *Conclusions*. The different patterns of sensorimotor functional damage and reorganization in patients with pontine infarction and thalamic infarction may provide insights into the neural mechanisms underlying functional recovery after stroke.

1. Introduction

Motor function impairment, as well as rehabilitation, depends highly on infarction locations in patients with stroke [1, 2]. A previous structural neuroimaging study revealed that patients with basal ganglia infarction displayed structural impairment in the ipsilesional sensorimotor cortex, whereas patients with pontine stroke mainly displayed cerebellar damage as well as structural restructuring in the precuneus [3], indicating that different types of brain damage and reorganization might be caused by location-specific lesions in patients with stroke [4]. However, the neural mechanisms underlying brain functional connectivity changes caused by distinct stroke locations remain poorly understood.

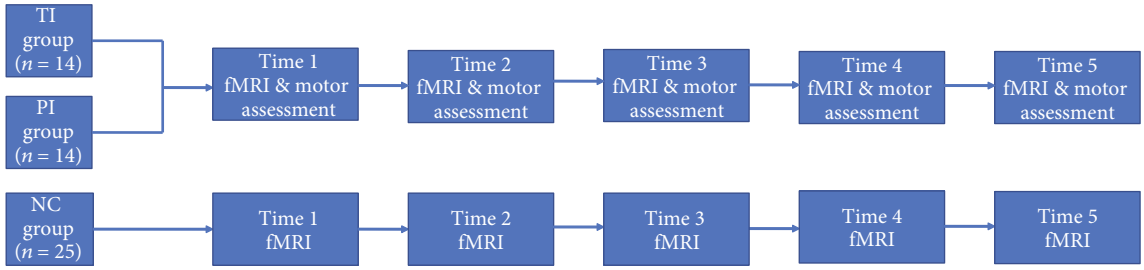

Figure 1: Study protocol. TI: thalamic infarction, PI: pontine infarction: NC: normal control, fMRI: functional magnetic resonance imaging, Time 1: within 7 days after stroke onset, Time 2: 2 weeks after stroke onset, Time 3: 1 month after stroke onset, Time 4: 3 months after stroke onset, Time 5: 6 months after stroke onset.

Based on the anatomical site of cerebral infarction, patients can be subdivided into supratentorial and infratentorial cerebral infarctions. Most supratentorial infarction-associated functional magnetic resonance imaging (fMRI) studies have focused on stroke patients with lesions in the basal ganglia or corona radiata [5, 6], yet overlooked thalamic infarctions. The thalamus has been the focus of investigation in neuroscience, as nearly all incoming information to the cortex is routed through this brain area [7]. Pontine regions are common sites of infratentorial cerebral infarction [8] and involve the motor pathway. Through the ventral anterior (VA) and ventral lateral nuclei (VL) of the thalamus, information processing in the basal ganglia (putamen and caudate) returns to the cerebral cortex, and minor output from the basal ganglia descends to the brain stem in the cortico-basal ganglia loop [9]. Thalamic and pontine infarctions may affect sensorimotor function differently.

Previous evidence suggests that thalamic and pontine infarction could cause impairment of functional connections in brain regions outside of the lesion [10, 11]. However, it is not clear whether patients with thalamic infarction and patients with pontine infarction display different characteristics of functional connectivity involving the sensorimotor brain areas. Thus, we retrospectively analyzed a longitudinal dataset in which we collected data for patients with stroke with thalamic lesions, pontine lesions, and healthy controls. We hypothesized that thalamic infarction and pontine infarction patients experience different patterns of sensorimotor functional damage and reorganization.

2. Methods

2.1. Participants. Twenty-eight right-handed stroke patients with different degrees of neurological dysfunction were recruited from inpatient services at Xuanwu Hospital of Capital Medical University (Beijing, China). All participants provided written informed consent prior to assessment. The inclusion criteria were as follows: (1) first-ever ischemic stroke (within 7 days of symptom onset), (2) unilateral lesions involving pons or thalamus were confirmed by diffusion-weighted imaging (DWI), and (3) age 18 to 75 years old. Exclusion criteria were as follows: (1) unclear onset time, (2) lesions outside the pons or thalamus, (3) recurrence of infarction or secondary hemorrhage during follow-up, and (4) deafness and/or blindness, or aphasia that might prevent completion of the study. Fourteen patients with unilateral infarction of the thalamus (TI group) and 14 patients with unilateral infarction of the pons (PI group) were enrolled in the current study. Twenty-five age-and sex-matched healthy control participants were included as the normal control group (NC group).

2.2. Study Protocol. The current study protocol was planned as a 6-month longitudinal design, during which patients with stroke underwent assessment using the Fugl-Meyer (FM) scale and magnetic resonance imaging (MRI). Those data were collected five times after infarction occurred, during the first week after symptom onset (<7 days), 2 weeks, 1 month, 3 months, and 6 months after stroke onset. We then acquired MRI data on day 0 (baseline), 2 weeks, 1 month, 3 months, and 6 months for the normal controls (Figure 1).

2.3. Image Acquisition. All participants (patients with stroke and healthy volunteers) were invited to participate in 5 imaging sessions. MRI data were acquired using a 3T MR scanner equipped with a 12-channel coil (TimTrio, Siemens AG, Erlangen, Germany). Full brain structural images were collected using a sagittal 3D-magnetization-prepared rapid acquisition gradient echo (3D-MPRAGE) T1-weighted sequence with the following parameters: TR/TE = 1600/2.15 msec, flip angle = 9°, FOV = 256 mm × 256 mm, matrix size = 256 × 256, and voxel size = $1 \times 1 \times 1\ \text{mm}^3$. Resting-state functional MRI (fMRI) data were obtained using a gradient-echo echo-planar imaging sequence with the following parameters: TR/TE = 3000/30 msec, flip angle = 90°, voxel size = $3 \times 3 \times 3\ \text{mm}^3$, matrix size = 64 × 64, gap = 0 mm, number of slices = 43, and 124 time points. During fMRI scanning, all participants were instructed to remain motionless, stay awake, and keep their eyes open. Axial fast spin-echo T2-weighted, fluid attenuation inversion-recovery, and DWI examinations were also performed.

2.3.1. Behavioral Assessment. The degree of motor deficit was assessed independently by two neurologists on the same day as the MRI data acquisition. The two scores were averaged to provide an estimate. Thirty-three tasks in the FM scale were used to evaluate patients' motor function, limb coordination, and active joint function of the upper limbs [12, 13]. Each score was given on a scale of 0 to 2, according to the patient's response to the specific task (0 = patient was unable to

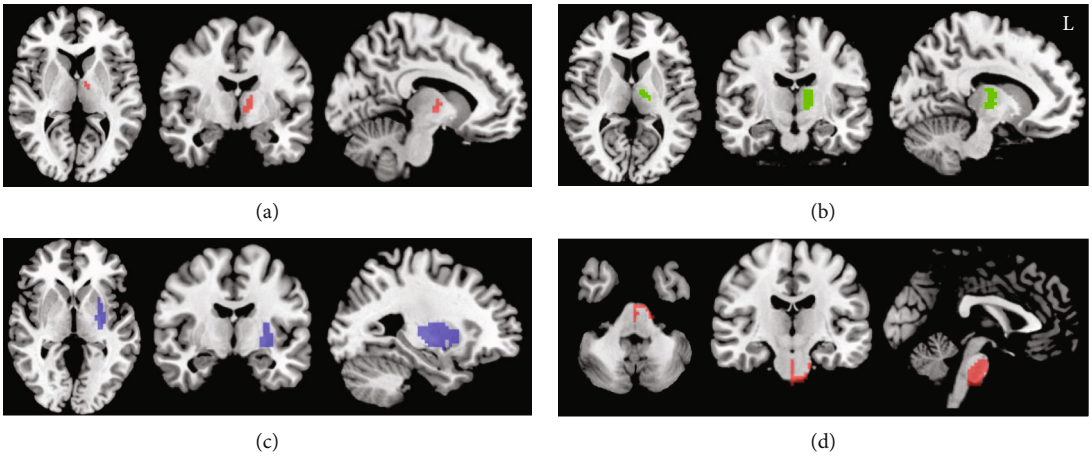

Figure 2: The four ROIs in the contralesional VA nuclei of thalamus (a), contralesional VL nuclei of thalamus (b), contralesional dorsal lateral putamen (c), and pons (d). L: left.

perform the task, 1 = patient could partially perform the task, and 2 = patient could accomplish the task), thus, the maximum possible total score was 66. All scores of the total 33 tasks were summed and normalized to a score between 0 and 100 as the following formula:

$$\text{The normalized FM score} = \frac{\text{the sum of the 33 scores}}{66} \times 100\%. \quad (1)$$

2.4. Normalized Infarction Volume Measurement. Measurement of infarction lesion volumes of PI and TI was performed manually using MRIcron software (version 1.40), including the following steps: (1) infarction volume measurement: two experienced physicians individually measured the infarction size using DWI images for patients during the subacute stage and fluid-attenuated inversion recovery (FLAIR) images during the chronic stage. The scores measured by the two physicians were then averaged. (2) Normalized infarction volume measurement: the infarction volume of patients was normalized to reduce the individual differences in brain volume. The median sagittal plane area was measured in the 3D-MPRAGE image [14], which is highly correlated with the volume of the brain (correlation coefficient = 0.98) [15]. The following formula was used to standardize the infarction volume of the TI and PI groups:

$$\text{normalized cerebral infarction volume} = \frac{\text{infarciton volume} \times \text{average area of the median sagital plane}}{\text{area of median sagittal plane of stroke patients}}. \quad (2)$$

2.5. Resting-State fMRI Data Preprocessing. Resting-state fMRI data were preprocessed using data processing and analysis of brain imaging (DPABI) software [16] and SPM12 toolbox (http://www.fil.ion.ucl.ac.uk/spm/software/spm12). The following steps were performed: (1) discard the first 10 EPI volumes, (2) slice timing correction, (3) head motion correction, (4) spatial normalization to MNI space using an EPI template with a voxel size of 3 mm × 3 mm × 3 mm by DARTEL, (5) data were smoothed using a Gaussian kernel of 6 mm full width at half maximum (FWHM), (6) linear regression was performed to remove the effects of the white matter and cerebrospinal fluid by 99% mask, (7) band-pass filtering between 0.01-0.1 Hz, and (8) preventing focal infarct tissue from affecting the algorithm, the imaging data from the stroke patients with lesions in the left hemisphere were flipped from left to right along the median sagittal line. The right hemisphere was defined the ipsilesional side, and the left hemisphere was defined as the contralesional side in all patients with stroke.

2.6. Regions of Interest (ROIs) Definition and Functional Connectivity Calculations. Subcortical areas, such as the basal ganglia (putamen), thalamus, cerebellum, and brainstem nuclei, are important components of the motor network [17]. They have direct or indirect structural connections with the sensorimotor cortex. According to previous, cross-sectional studies, FC changes between the brain regions of the putamen, thalamus, and sensorimotor brain areas were associated with patients with stroke [11, 18]. We defined the dorsal lateral putamen (dl-putamen) [19] and VA and VL nuclei of the thalamus [20] as seed ROIs. Meanwhile, the pons [21] was also defined as another ROI to examine whether the ROI adjacent to the lesion would affect the FC in the PI group. All ROIs are shown in Figure 2. After flipping the infarction lesion from left to right along the midline for patients with left hemispheric lesions, the left side corresponded to the contralesional hemisphere. Therefore, ROIs were extracted from the healthy hemisphere in patients with stroke.

The voxel-wise functional connectivity analyses between the reference time course of each ROI (the dl-putamen, VA, and VL nuclei of the thalamus and pons) and the time course of each voxel in the brain areas were performed to generate seed-based FC maps at baseline stage, 2weeks, 1 month, 3 months, and 6 months after stroke. Pearson's correlation coefficients between the average time series of the ROIs and sensorimotor brain areas were computed to obtain seed-based FC maps. For group analyses, the correlation

Table 1: Demographic and clinical information of all participants.

Characteristics	NC ($n = 25$)	PI ($n = 14$)	TI ($n = 14$)	p value
Age (years)	51.57 ± 10.82	58.00 ± 6.73	51.57 ± 10.82	0.103[a]
Sex (F/M)	10/15	4/10	5/9	0.719[b]
Handedness (L/R)	1/24	0/14	0/14	0.341[b]
Lesion side (L/R)	——	5/9	11/3	——
Normalized lesion volume (ml)	——			$F_{PI} = 4.77$; $p = 0.002^*$ $F_{TI} = 7.16$; $p \leq 0.001^*$
Time 1		12.72 ± 7.34	0.78 ± 0.55	
Time 2		9.68 ± 6.74	0.49 ± 0.38	
Time 3		6.05 ± 4.55	0.34 ± 0.28	
Time 4		5.43 ± 3.66	0.22 ± 0.18	
Time 5		5.43 ± 4.53	0.18 ± 0.17	
FM-upper (0-100)				$F_{PI} = 8.92$; $p \leq 0.001^*$ $F_{TI} = 4.94$; $p = 0.002^*$
Time 1		48.92 ± 33.82	86.15 ± 16.69	
Time 2		67.21 ± 28.78	91.88 ± 9.07	
Time 3		82.58 ± 18.93	96.6 ± 5.11	
Time 4		88.74 ± 13.38	97.95 ± 3.24	
Time 5		93.45 ± 0.09	99.03 ± 1.94	

Data are presented as mean ± SD. [a]One-way analysis of covariance (ANCOVA), [b]Chi-square test. Abbreviations: NC: normal control, PI: pontine infarction, TI: thalamic infarction, F: female, M: male, L: left, R: right, Time 1, Time 2, Time 3, and Time 4, and Time 5 different time subgroups from 1 week to 6 months after stroke, SD: standard deviation, $^*p < 0.05$.

coefficients were transformed to z values using Fisher's z -transformation to improve the normality of the correlation coefficient.

2.7. Statistical Analyses

2.7.1. Demographic and Clinical Data Analyses. Statistical analyses of demographic and clinical data were conducted using SPSS 17.0. The statistical significance threshold was set at $p < 0.05$. A Chi-square test was used to identify differences in sex and handedness among the PI, TI, and NC groups. For clinical variables, the differences in age, normalized infarction volume, and FM scores were analyzed by one-way ANOVA in the PI and TI groups.

2.7.2. Functional MRI Analyses. The infarction volume was the largest within 7 days of the onset of ischemic stroke compared to the follow-up time points. Therefore, we considered that larger infarct volumes would indicate more significant effects of infarct volume on FC in patients with stroke. The FC in patients with stroke (PI and TI groups) differed the most from normal controls at baseline stage. One-way ANOVA controlling for infarction volume of patients with stroke (the infarction volume of normal controls was defined as 0) was used to identify group differences of FC among PI, TI, and NC groups at baseline stage. The peak voxel of the corresponding sensorimotor area (i.e., precentral and postcentral gyrus) of automated the anatomical labeling (AAL) [22] mask was used for small volume correction (SVC). The SVC is a family wise error multiple correction method provided by SPM, which has been widely used in neuroimaging studies [23]. Then, sphere ROIs with a 5 mm radius located at the peak voxel were built for post hoc analysis. The mean FC values from the sphere ROIs were extracted for further analyses.

Next, a post hoc "5 (time) ×3 (group)" repeated-measure ANOVA model was established to explore the differences in longitudinal FC changes among the three groups. The changes in FC in different brain regions among the three groups over a long-term follow-up of 6 months were examined for interaction effects of "time" by "group." The significance threshold was set at $p < 0.05$.

3. Results

3.1. Demographic and Clinical Parameters. Detailed demographic and clinical findings for the PI, TI, and NC groups are provided in Table 1. No significant differences were observed among the PI, TI, and NC groups in terms of age ($p = 0.103$, one-way ANOVA), sex ($p = 0.719$, chi-square test), or handedness ($p = 0.341$, chi-square test). The normalized infarction volume decreased significantly during

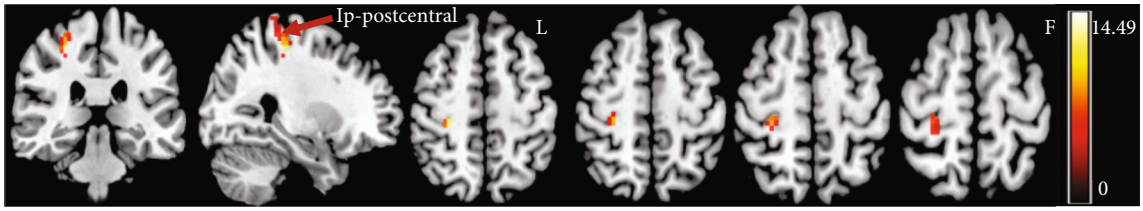

Figure 3: One-way ANOVA revealed a significant difference in FC between the contralateral VA and ipsilateral postcentral gyrus (cl_VA-ip_postcentral) among three groups at baseline stage. L: left, Ip: ipsilateral postcentral gyrus, $p_{\text{uncorrected}} < 0.001$.

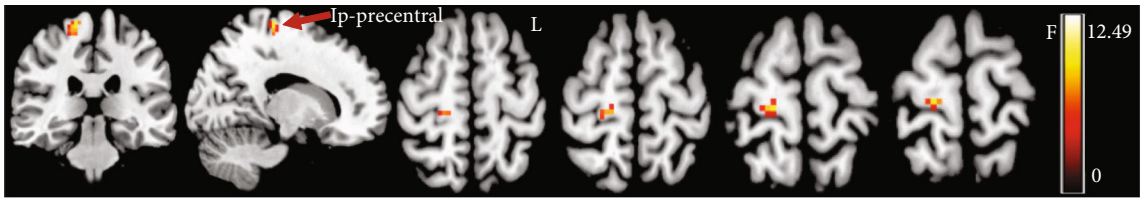

Figure 4: One-way ANOVA displayed a significant difference in FC between the contralateral VL and ipsilateral precentral gyrus (cl_VL-ip_precentral) among three groups at baseline stage. L: left, Ip: ipsilateral postcentral gyrus; $p_{\text{uncorrected}} < 0.001$.

the observation period in the PI ($F_{(4,65)} = 4.77$, $p = 0.002$) and TI groups ($F_{(4,65)} = 7.16$; $p \leq 0.001$). Longitudinal FM examination revealed significant improvement over time in the PI ($F_{(4,65)} = 8.92$, $p \leq 0.001$) and TI groups ($F_{(4,65)} = 4.94$, $p = 0.002$).

3.2. Comparison of Seed-Based FC among PI, TI, and NC Groups within 7 Days after Stroke. At baseline stage (within 7 days after stroke), one-way ANOVA analysis of FC between seed-based (the contralesional side of VA, VL, pon, and putamen) and whole-brain regions indicated a significant difference in FC between the contralateral VA and ipsilateral postcentral gyrus (cl_VA-ip_postcentral) (peak $F_{(2,49)} = 14.49$, $p_{\text{FWE}} = 0.043$, MNI: 27, -30, 54) among the three groups (Figure 3). The sensorimotor-related brain regions with significant differences in functional connectivity were also observed in the ipsilateral precentral gyrus with contralateral VL (cl_VL-ip_precentral) (peak $F_{(2,49)} = 12.49$, $p_{\text{FWE}} = 0.037$, MNI: 15, -27, 69) among the three groups (Figure 4). However, with the contralateral pon (cl_pon) and contralateral putamen (cl_putamen) as the seed-ROI, one-way ANOVA analysis of the FC indicated no significant differences in sensorimotor-related brain regions among the three groups. Post hoc comparisons of the baseline stage in the three groups showed significant difference of cl_VA-ip_postcentral FC between TI and both normal control ($t = 5.057$, $p < 0.001$) and PI groups ($t = 3.024$, $p = 0.006$). However, there was no significant difference in FC of cl_VA-ip_postcentral between normal control and PI groups ($t = 1.592$, $p = 0.12$). Meanwhile, the post hoc comparisons of the baseline stage among the three groups showed significant difference of cl_VL-ip_precentral FC between PI and both normal control ($t = 5.08$, $p < 0.001$) and TI groups ($t = 5.01$, $p < 0.001$). However, there was no significant difference in FC of cl_VL-ip_precentral between normal control and TI groups ($t = 1.592$, $p = 0.12$).

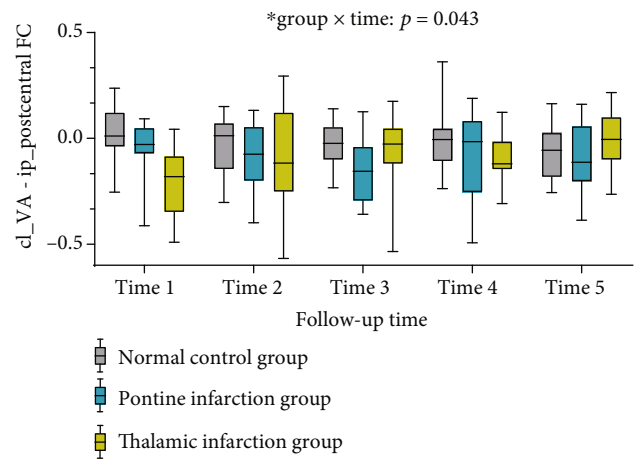

Figure 5: Longitudinal cl_VA-ip_postcentral FC changes among three groups.

3.3. Longitudinal FC Analysis among the TI, PI, and NC Groups. We further explored longitudinal FC changes during the follow-up period in the TI, PI, and NC groups by extracting FC values in cl_VA-ip_postcentral, cl_VL-ip_precentral, cl_pon-ip_postcentral, cl_pon-ip_precentral, cl_putamen-ip_postcentral, and cl_putamen-ip_precentral. No significant differences in "time" main effect were detected for cl_VA-ip_postcentral (repeated measures ANOVA: $F_{(4,200)} = 0.220$, $p = 0.927$). The "group" main effect of cl_VA-ip_postcentral differed significantly among the three groups ($F_{(2,50)} = 7.193$, $p = 0.002$). There was a significant "group×time" interaction effect of cl_VA-ip_postcentral (repeated measures ANOVA: $F_{(8,200)} = 2.702$, $p = 0.008$, Figure 5). Moreover, there was no significant difference in "time" (repeated-measure ANOVA: $p = 0.282$) or "group" (repeated-measure ANOVA: $p = 0.314$) main effect of cl_VL-ip_precentral, cl_pon-ip_postcentral, cl_pon-ip_precentral, cl_putamen-ip_postcentral, and cl_putamen-ip_precentral. The interaction effect of FC changes of cl_VL-ip_

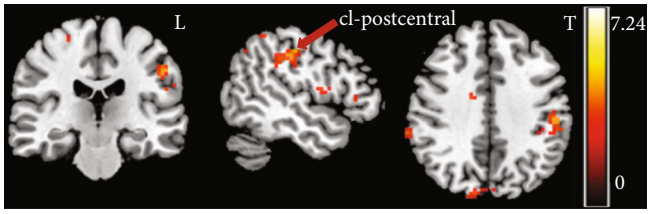

Figure 6: T test of FC between the contralateral postcentral gyrus with contralateral VA (cl_VA-cl_ postcentral) between PI1 and PI2 at baseline stage (within 7 days after stroke). L: left, $p_{\text{uncorrected}} < 0.005$.

precentral, cl_pon-ip_postcentral, cl_pon-ip_precentral, cl_putamen-ip_postcentral, and cl_putamen-ip_precentral did not differ significantly among the three groups over time ($p > 0.504$).

Results of the plot of the study indicated that the interaction effect results were mainly detected one month ago; hence, we considered one month as the cut-off point and divided the follow-up time of the study into two stages. A "time×group" repeated-measure ANOVA indicated a significant interaction effect of cl_VA-ip_postcentral that varied significantly among three groups at one month after stroke, $F_{(4,100)} = 2.980$, $p = 0.023$. However, the "time×group" repeated-measure ANOVA failed to detect a significant interaction effect among the three groups from 1 month to 6 months after stroke, $F_{(4,100)} = 1.523$, $p = 0.201$.

Repeated measurement analysis was used to detect changes in FC within each group, and the results showed the FC value of cl_VA-ip_postcentral with no significant difference between the PI and NC groups. However, the FC value of cl_VA-ip_postcentral was significantly different in the TI group. Compared with 7 days after stroke onset, there was a significant increase in FC of cl_VA-ip_postcentral at 1 month ($T_{(13)} = 2.550$, $p = 0.024$), 3 months ($T_{(13)} = 2.859$, $p = 0.013$), and 6 months ($T_{(13)} = 3.178$, $p = 0.007$) after stroke onset in the TI group, and the difference in FC in cl_VA-ip_postcentral between two time points in the TI group became increasingly greater with the prolongation of time. Compared with 7 days after stroke onset, there was no significant increase in FC of cl_VA-ip_postcentral in the TI group at 2 weeks after stroke onset ($p = 0.115$).

3.4. Heterogeneity in PI Group. The large differences in infarction lesion volume may have resulted in greater heterogeneity in the functional connectivity of patients in PI group (the range of infarction volume is 2.44 ml~ 23.2 ml); therefore, we suspected that heterogeneity of infarction lesion volume may have affected FC changes in the PI group. To confirm our hypothesis, the pontine infarction group was further divided into two subgroups according to the infarction volume at baseline. Patients with infarction volume < 10 ml were assigned to the PI1 group (7 patients) and the rest (>10 ml) were assigned to the PI2 group (7 patients). A t-test of FC between seed-based (the contralateral VA and VL) and whole-brain regions between the PI1 and PI2 groups indicated significant differences in FC of cl_VA-cl_ postcentral (peak $T = 4.8$, $p_{\text{uncorrected}} < 0.001$, Figure 6), and cl_VL-ip_postcentral (peak $T = 4.5$, $p_{\text{uncorrected}} < 0.001$, Figure 7). There was a significant difference in the brain area of the sensorimotor cortex between the PI1 and PI2 groups. Therefore, the greater heterogeneity of infarct volume in patients with pontine infarction resulted in no differences in FC among the PI, TI, and NC groups.

3.5. Correlation Analysis in the TI Group. The brain region of the cl_VA-ip_postcentral functional connectivity at baseline was not significantly correlated with motor improvement, as measured by the FM scale at 6 months after onset ($r = 0.104$, $p = 0.724$). Pearson correlation analyses indicated that the FC changes (FC changes = $FC_{\text{Time5}} - FC_{\text{Time1}}$) of cl_VA-ip_postcentral_postcentral were not correlated with the changes in the FM scale (FM changes = $FM_{\text{Time5}} - FM_{\text{Time1}}$) in the TI group ($r = -0.179$, $p = 0.540$). The correlation between infarct volume and FM was also analyzed in the TI group. No significant correlation was observed between infarction volume at baseline stage and FM at 6 months after stroke onset ($r = -0.366$, $p = 0.198$). Infarction volume changes (infarction volume changes = infarction volum e_{Time5} − infarction $\text{volume}_{\text{Time1}}$) did not correlate with the changes in the FM scale (FM changes = $FM_{\text{Time5}} - FM_{\text{Time1}}$) in the TI group ($r = -0.305$, $p = 0.289$).

4. Discussion

In the current study, we investigated the longitudinal changes in resting-state FC between patients with TI, patients with PI, and healthy participants during a 6-month, poststroke follow-up period. At the baseline stage, our results demonstrated significant differences in FC between the contralateral VA and ipsilateral postcentral gyrus, contralateral VL, and ipsilateral precentral gyrus among the three groups. However, further analysis of longitudinal FC changes revealed a significant difference in FC between cl_VA and ip_postcentral during the follow-up period among the three groups. The TI group displayed significantly decreased FC in cl_VA-ip_postcentral at the baseline stage compared with the PI and NC groups and then significantly increased FC at 1, 3, and 6 months after stroke onset.

Resting-state functional connectivity can reflect interactions between two remote regions. In a previous resting-state study, decreased connectivity between the bilateral M1 was demonstrated in patients with stroke with right hemispheric subcortical infarcts within 6 months after stroke onset [24]. In the current study, FC of the ipsilateral postcentral to contralateral VA was significantly decreased between the TI and PI and NC groups within 7 days after stroke. Recently, Golestani et al. [6] detected a decrease in resting-state functional connectivity between the ipsilesional sensorimotor cortex and subcortical regions, namely, the bilateral caudate and thalamus in patients with chronic stroke, and these changes could be detected within hours poststroke. Our results suggest that the infarct lesion disrupted the anatomical connections between two remote regions, which may further result in reduced functional

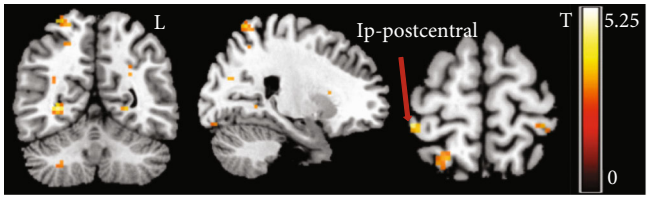

Figure 7: T test of FC between the ipsilateral postcentral gyrus with contralateral VL (cl_VL-ip_postcentral) between PI1 and PI2 at baseline stage (within 7 days after stroke). L: left, $p_{\text{uncorrected}} < 0.005$.

connectivity between the ipsilesional sensorimotor cortex and contralesional normal brain in patients with stroke.

The ventral anterior and ventral lateral nuclei of the thalamus are generally referred to as the "motor thalamus." The VA and VL of the thalamus serve as relay stations for incoming information from external sources to the sensorimotor cortex [25]. Previous research indicates had showed abnormal fiber integrity [26], decreased ReHo [27], and decreased FC [11] in brain regions related to sensorimotor motor circuits in patients with TI. He et al. reported decreased FC in the ipsilesional posterior central gyrus in patients with TI presenting with somatosensory deficits, which is related to somatosensory dysfunction in patients with TI [11]. Lower thalamo-postcentral connectivity may represent decreased sensorimotor integration [28]. In the current study, we demonstrated decreased FC between the ipsilateral postcentral and contralateral VA in the TI group at the baseline stage, which is highly consistent with previous findings. The reduced FC implies the breakdown of the harmonious interaction between the ipsilateral sensorimotor and contralateral thalamus after thalamic stroke.

Another interesting finding of the current study is a gradual increase in FC between cl_VA and ip_postcentral was observed from 2 weeks to 6 months after stroke onset. Compared with within the 7th day after stroke onset, the change in FC between the cl_VA and ip_postcentral increased significantly at 1, 3, and 6 months after stroke onset in patients with thalamic infarction. A previous study investigated a similar trend of FC changes, which decreased at the acute stage of stroke and then gradually increased thereafter [29]. More severe symptoms were associated with decreased functional connectivity, and recovery of behavioral function was associated with increased functional connectivity [30, 31]. We considered that the reorganization of FC between cl_VA and ip_postcentral contributed to the recovery of sensorimotor function in our participants. In patients with sufficient integrity of the ipsilesional sensorimotor cortex and its corticospinal tract, motor recovery may occur rapidly after stroke and is mediated by the reacquisition of normal dominance by the ipsilesional sensorimotor cortex. FC between the ipsilesional sensorimotor areas and bilateral thalamus in patients with TI, which demonstrates that there are changes in functional connectivity associated with recovery, is increased in patients with TI presenting with somatosensory deficits [11]. The increased FC in the sensorimotor network or ipsilesional motor cortex may be related to gradual disappearance of diaschisis [32] or axonal sprouting [33] to establish new connections, and motor recovery is related to the normalization of its reinstatement [11, 34, 35].

However, we did not detect a significant correlation between functional connectivity in the cl_VA-ip_postcentral and FM scales in the TI group. Patients with TI with mild motor deficits and a small sample size in this study have caused this result. Another probable cause was that we evaluated patients' motor function of the upper limbs (i.e., reflex activity and flexor synergy). Nevertheless, the postcentral gyrus is also involved in sensory processing, and the decreased activation in the postcentral cortex is indicative of attenuated sensory processing [28, 36]. Although we did not observe a significant correlation between the infarct volume at onset and FM scores at 6 months in the TI group, the relatively strong correlation coefficient may indicate that a significant correlation between the infarct volume and FM scores may be detectable with a larger sample of the TI group.

In our study, there were no significant differences in FC changes between ROIs and the sensorimotor cortex in patients with PI. Wei et al. [29] explored longitudinal FC alterations during the follow-up period in patients with the left pontine infarction (LPI) and right pontine infarction (RPI) groups, using brain regions with altered cerebral blood flow (CBF) in longitudinal analysis as seed-ROIs. In the RPI group, there were no brain regions with significant longitudinal differences among the four time points. As our patients with pontine infarction had both left and right lesions, we investigated the intrapontine group differences in functional connectivity induced by infarction lesion size. We observed significant differences in functional connectivity between cl_VA and cl_ postcentral as well as between cl_VL and ip_postcentral. We considered that the heterogeneity within the pontine group might be associated with nonsignificant results during intergroup comparisons.

5. Conclusions

In this study, we analyzed the FC changes in sensorimotor brain areas in patients with PI versus those with TI during follow-up of 6 months. The main findings were that FC significantly decreased between cl_VA and ip_postcentral in patients with TI at baseline as compared with the PI and NC groups, and the TI group exhibited gradual increases in FC between cl_VA and ip_postcentral thereafter. Therefore, FC increase between cl_VA and ip_postcentral suggests that the sensorimotor brain area may be responsible for the recovery of motor function in patients with thalamic stroke. Additionally, we did not detect any significant differences in FC changes between ROIs and the sensorimotor cortex in patients with PI. Heterogeneity within the pontine group may be associated with nonsignificant results during the intergroup comparisons.

5.1. Limitations. There are a few limitations to consider. One of the weaknesses of our pilot study was the lack of data regarding assessment of other functions, for example,

sensory and cognitive function. Future studies should address the sensory and cognitive function changes in patients with thalamic infarction and pontine infarction. Second, a limited number of cases due to the rarity of isolated unilateral thalamic strokes and isolated unilateral pontine strokes may have prevented us from providing conclusive evidence for FC changes in patients with thalamic infarction and pontine infarction. We expect to expand the sample size in our future work to further elucidate our findings.

Data Availability

Datasets analyzed during the current study are available from the corresponding author on reasonable request.

Conflicts of Interest

The authors have no conflict of interest to declare.

Authors' Contributions

Peipei Wang did the volunteer recruitment, experimental design, data collection, statistics, and manuscript preparation. Zhenxiang Zang did the data analysis and statistics. Miao Zhang/Yanxiang Cao/ZhiLian Zhao/Yi Shan did the patient recruitment and data collection. Qingfeng Ma did the patient recruitment and clinical data collection. Jie Lu did the conception, funding, study design, supervision, and manuscript preparation.

Acknowledgments

We acknowledge the support from the Beijing Municipal Administration of Hospitals' Ascent Plan (code: DFL20180802).

References

[1] P. Sommer, A. Posekany, W. Serles et al., "Is functional outcome different in posterior and anterior circulation stroke?," *Stroke*, vol. 49, no. 11, pp. 2728–2732, 2018.

[2] J. T. Kim, M. S. Park, K. H. Choi et al., "Clinical outcomes of posterior versus anterior circulation infarction with low national institutes of health stroke scale scores," *Stroke*, vol. 48, no. 1, pp. 55–62, 2017.

[3] L. Jiang, J. Liu, C. Wang et al., "Structural alterations in chronic capsular versus pontine stroke," *Radiology*, vol. 285, no. 1, pp. 214–222, 2017.

[4] C. Wang, P. Miao, J. Liu et al., "Cerebral blood flow features in chronic subcortical stroke: Lesion location- dependent study," *Brain Research*, vol. 1706, pp. 177–183, 2019.

[5] L. Wang, C. Yu, H. Chen et al., "Dynamic functional reorganization of the motor execution network after stroke," *Brain*, vol. 133, no. 4, pp. 1224–1238, 2010.

[6] A. M. Golestani, S. Tymchuk, A. Demchuk, B. G. Goodyear, and VISION-2 Study Group, "Longitudinal evaluation of resting-state fmri after acute stroke with hemiparesis," *Neurorehabilitation and Neural Repair*, vol. 27, no. 2, pp. 153–163, 2013.

[7] T. E. J. Behrens, H. Johansen-Berg, M. W. Woolrich et al., "Non-invasive mapping of connections between human thalamus and cortex using diffusion imaging," *Nature neuroscience*, vol. 6, no. 7, pp. 750–757, 2003.

[8] C. Bassetti, J. Bogousslavsky, A. Barth, and F. Regli, "Isolated infarcts of the pons," *Neurology*, vol. 46, no. 1, pp. 165–175, 1996.

[9] C. O. Oluigbo, A. Salma, and A. R. Rezai, "Deep brain stimulation for neurological disorders," *IEEE reviews in biomedical engineering*, vol. 5, pp. 88–99, 2012.

[10] Y. Wang, C. Wang, P. Miao et al., "An imbalance between functional segregation and integration in patients with pontine stroke: a dynamic functional network connectivity study," *NeuroImage: Clinical*, vol. 28, article 102507, 2020.

[11] M. He, J. Song, T. Luo et al., "Alteration of resting-state functional connectivity in the sensorimotor network in patients with thalamic infarction," *Clinical Neuroradiology*, vol. 31, no. 3, pp. 721–728, 2021.

[12] D. J. Gladstone, C. J. Danells, and S. E. Black, "The fugl-meyer assessment of motor recovery after stroke: a critical review of its measurement properties," *Neurorehabilitation and neural repair*, vol. 16, no. 3, pp. 232–240, 2002.

[13] A. R. Fugl-Meyer, L. Jääskö, I. Leyman, S. Olsson, and S. Steglind, "The post-stroke hemiplegic patient. 1. A method for evaluation of physical performance," *Scandinavian journal of rehabilitation medicine*, vol. 7, no. 1, pp. 13–31, 1975.

[14] R. N. Nandigam, Y. W. Chen, M. E. Gurol, J. Rosand, S. M. Greenberg, and E. E. Smith, "Validation of intracranial area as a surrogate measure of intracranial volume when using clinical mri," *Journal of Neuroimaging*, vol. 17, no. 1, pp. 74–77, 2007.

[15] M. E. Gurol, M. C. Irizarry, E. E. Smith et al., "Plasma β -amyloid and white matter lesions in ad, mci, and cerebral amyloid angiopathy," *Neurology*, vol. 66, no. 1, pp. 23–29, 2006.

[16] C. G. Yan, X. D. Wang, X. N. Zuo, and Y. F. Zang, "Dpabi: data processing & analysis for (resting-state) brain imaging," *Neuroinformatics*, vol. 14, no. 3, pp. 339–351, 2016.

[17] F. A. Middleton and P. L. Strick, "Basal ganglia and cerebellar loops: motor and cognitive circuits," *Brain Research Reviews*, vol. 31, no. 2–3, pp. 236–250, 2000.

[18] S. R. Almeida, J. Vicentini, L. Bonilha, B. M. de Campos, R. F. Casseb, and L. L. Min, "Brain connectivity and functional recovery in patients with ischemic stroke," *Journal of Neuroimaging*, vol. 27, no. 1, pp. 65–70, 2017.

[19] L. Fan, H. Li, J. Zhuo et al., "The human brainnetome atlas: a new brain atlas based on connectional architecture," *Cerebral Cortex*, vol. 26, no. 8, pp. 3508–3526, 2016.

[20] J. Ashburner, "A fast diffeomorphic image registration algorithm," *NeuroImage*, vol. 38, no. 1, pp. 95–113, 2007.

[21] M. D. Rosenberg, E. S. Finn, D. Scheinost et al., "A neuromarker of sustained attention from whole-brain functional connectivity," *Nature Neuroscience*, vol. 19, no. 1, pp. 165–171, 2016.

[22] N. Tzourio-Mazoyer, B. Landeau, D. Papathanassiou et al., "Automated anatomical labeling of activations in spm using a macroscopic anatomical parcellation of the mni mri single-subject brain," *NeuroImage*, vol. 15, no. 1, pp. 273–289, 2002.

[23] J. Chen, Z. Zang, U. Braun et al., "Association of a reproducible epigenetic risk profile for schizophrenia with brain

methylation and function," *JAMA Psychiatry*, vol. 77, no. 6, pp. 628–636, 2020.

[24] Y. Zhang, K.-S. Li, Y.-Z. Ning et al., "Altered structural and functional connectivity between the bilateral primary motor cortex in unilateral subcortical stroke," *Medicine*, vol. 95, no. 31, article e4534, 2016.

[25] K. Doya, "Complementary roles of basal ganglia and cerebellum in learning and motor control," *Current opinion in neurobiology*, vol. 10, no. 6, pp. 732–739, 2000.

[26] L. Chen, T. Luo, K. Wang et al., "Effects of thalamic infarction on the structural and functional connectivity of the ipsilesional primary somatosensory cortex," *European Radiology*, vol. 29, no. 9, pp. 4904–4913, 2019.

[27] L. Chen, C. Li, J. Zhai et al., "Altered resting-state signals in patients with acute stroke in or under the thalamus," *Neuroscience Bulletin*, vol. 32, no. 6, pp. 585–590, 2016.

[28] B. A. Van Der Kolk, "Clinical implications of neuroscience research in ptsd," *Annals of the New York Academy of Sciences*, vol. 1071, no. 1, pp. 277–293, 2006.

[29] Y. Wei, L. Wu, Y. Wang et al., "Disrupted regional cerebral blood flow and functional connectivity in pontine infarction: a longitudinal mri study," *Frontiers in aging neuroscience*, vol. 12, article 577899, 2020.

[30] J. Puig, G. Blasco, A. Alberich-Bayarri et al., "Resting-state functional connectivity magnetic resonance imaging and outcome after acute stroke," *Stroke*, vol. 49, no. 10, pp. 2353–2360, 2018.

[31] B. J. He, A. Z. Snyder, J. L. Vincent, A. Epstein, G. L. Shulman, and M. Corbetta, "Breakdown of functional connectivity in frontoparietal networks underlies behavioral deficits in spatial neglect," *Neuron*, vol. 53, no. 6, pp. 905–918, 2007.

[32] J. J. S. R. Andrews, "Transhemispheric diaschisis. A review and comment," *Stroke*, vol. 22, no. 7, pp. 943–949, 1991.

[33] S. T. Carmichael, "Cellular and molecular mechanisms of neural repair after stroke: making waves," *Annals of Neurology*, vol. 59, no. 5, pp. 735–742, 2006.

[34] A. R. Carter, S. V. Astafiev, C. E. Lang et al., "Resting interhemispheric functional magnetic resonance imaging connectivity predicts performance after stroke," *Annals of Neurology*, vol. 67, no. 3, pp. 365–375, 2010.

[35] L. J. B. S. Small, "Cerebellar hemispheric activation ipsilateral to the paretic hand correlates with functional recovery after stroke," *Brain*, vol. 125, no. 7, pp. 1544–1557, 2002.

[36] S. Jeon, Y. J. Lee, I. Park et al., "Resting state functional connectivity of the thalamus in North Korean refugees with and without posttraumatic stress disorder," *Scientific reports*, vol. 10, no. 1, p. 3194, 2020.

Hindawi
Neural Plasticity
Volume 2021, Article ID 4894881, 11 pages
https://doi.org/10.1155/2021/4894881

Research Article

Electroacupuncture Promotes the Survival of the Grafted Human MGE Neural Progenitors in Rats with Cerebral Ischemia by Promoting Angiogenesis and Inhibiting Inflammation

Juan Li,[1] **Luting Chen**,[2] **Danping Li**,[1] **Min Lu**,[1] **Xiaolin Huang**,[1] **Xiaohua Han**,[1] **and Hong Chen**[1]

[1]*Department of Rehabilitation Medicine, Tongji Hospital, Tongji Medical College, Huazhong University of Science and Technology, Wuhan, Hubei, China*
[2]*Department of Rehabilitation Medicine, General Hospital of the Yangtze River Shipping, Wuhan, Hubei, China*

Correspondence should be addressed to Xiaohua Han; hanxiao1470@hust.edu.cn and Hong Chen; chenhong1129@hust.edu.cn

Juan Li and Luting Chen contributed equally to this work.

Received 10 May 2021; Revised 11 July 2021; Accepted 6 September 2021; Published 7 October 2021

Academic Editor: Xi-Ze Jia

Stem cells have the potential as a regenerative therapy for cerebral ischemia by improving functional outcomes. However, cell transplantation has some limitations, including a low rate of the grafted cell survival. There is still a major challenge of promoting the harmonious symbiosis between grafted cells and the host. Acupuncture can effectively improve the functional outcome after cerebral ischemia. The present study evaluated the therapeutic effects and explored the mechanism of combined medial ganglionic eminence (MGE) neural progenitors differentiated from human embryonic stem cells (hESCs) with electroacupuncture (EA) in a bilateral common carotid artery occlusion (2VO) rat model. The results showed that EA could promote the survival of the grafted MGE neural progenitors differentiated from hESCs and alleviate learning and memory impairment in rats with cerebral ischemia. This may have partially resulted from inhibited expression of TNF-α and IL-1β and increased vascular endothelial growth factor (VEGF) expression and blood vessel density in the hippocampus. Our findings indicated that EA could promote the survival of the grafted MGE neural progenitors and enhance transplantation therapy's efficacy by promoting angiogenesis and inhibiting inflammation.

1. Introduction

Ischemic cerebrovascular disease is a leading cause of mortality and disability worldwide after heart disease and cancer, lacking effective therapeutic methods [1]. In addition to causing hemiplegia, aphasia, swallowing disorders, etc., cerebral ischemia can also lead to a selective and delayed pyramidal neuronal death in the hippocampus and impair cognition function [2, 3]. Rapid vascular recanalization is a relatively effective therapy. However, some patients cannot get timely access to effective treatment because the window for vascular recanalization is very short [4] and often results in intracranial hemorrhage [5]. Some drugs proven effective in animals could not reach desired therapeutic benefit in the clinic [6, 7]. Therefore, further investigation on effective treatments and interventions against cerebral ischemia is urgently needed.

Recently, different kinds of stem cells have been transplanted to treat central nervous system diseases, such as stroke [8], spinal cord injury [9, 10], and Alzheimer's disease (AD) [11]. MGE (medial ganglionic eminence) is a structure of the ventral forebrain during embryonic development. A study found that in the absence of NKX2.1 (the main marker of MGE), cholinergic septohippocampal projection neurons and large subsets of basal forebrain cholinergic neurons fail to develop, causing severe deficiencies in learning and memory [12]. MGE neural progenitors can be used as a cell source to treat learning and memory impairment. Cell therapy can supply a sufficient number of cells for

transplantation, but there is a major challenge in promoting the harmonious symbiosis between grafted cells and the host. After a cerebral ischemic injury, most grafted cells die as a result of malignant changes in the ischemic focus and the surrounding microenvironment; for example, inflammation or immune response, trophic factor withdrawal, oxidative stress, excitotoxicity, hypoxia, and apoptosis [13–16]. Hence, to a certain extent, the unfriendly microenvironment restricts the effect of cell transplantation therapy. Therefore, improving microenvironment and promoting the survival of MGE neural progenitors may be one of the strategies to enhance the transplantation effect and improve the cognitive impairment after cerebral ischemia.

Electroacupuncture (EA) delivers electrical stimulation to acupuncture points through acupuncture needles. Several studies have shown that EA can effectively improve neural function recovery after cerebral ischemia. The potential mechanisms include prevention of inflammatory and oxidant stress [17], suppression of apoptosis [18], and promotion of angiogenesis [19]. Additionally, a systematic review and meta-analysis indicated that its mechanism positively correlates with endogenous neurogenesis, in which EA therapy can promote the migration and differentiation of neural stem cells (NSCs) [20]. Studies have confirmed the vital role of electroacupuncture in treating central nervous system diseases combined with stem cell transplantation [21, 22]. Therefore, EA could improve the host's brain's microenvironment with cerebral ischemia and promote the survival of grafted MGE neural progenitors to improve the cognitive impairment. This article will focus on promoting angiogenesis and inhibiting inflammation after cerebral ischemia to verify the above hypothesis.

2. Materials and Methods

2.1. Human Embryonic Stem Cell (hESC) Culture and Neuronal Differentiation. The hESCs (hM3Dq-KORD, Passages 25-50; WiCell Research Institute) were cultured on a feeder layer of irradiated mouse embryonic fibroblasts (MEFs) using hESC medium, which included DMEM/F12 (Hyclone, C11330500BT), 20% knockout serum replacer (Gibco, 10828028), 1x GlutaMAX™ Supplement (Gibco, 35050061), 1x MEM Nonessential Amino Acid Solution Supplement (Gibco, 11140050), 0.1 mM β-mercaptoethanol (Sigma-Aldrich, M3148), and 8 ng/mL basic fibroblast growth factor (PeproTech, 10018B). The cells were expanded every six days.

MGE neural progenitors were differentiated by the dual SMAD inhibition differentiation protocol with MEFs as feeder layer, as described previously [23]. Briefly, the hESCs were cultured in neural differentiation medium, including 50% DMEM/F12 (Gibco, 11330032), 50% Neurobasal (Gibco, 21103049), 1x MEM Nonessential Amino Acid Solution Supplement, 1x N2 (Gibco, 17502048), 2 μM SB431542 (Selleck, S1067), 2 μM DMH1 (Selleck, S7146), and 2 μM XAV939 (Stemgent, 040046) for seven days. The stem cells were differentiated into neuroepithelia in this process. Then, for ventralization, 0.5 μM SAG (Sigma-Aldrich, 566660), a sonic hedgehog activator, was added at days 8-14 and the cells differentiated into NKX2.1 and Foxg1 coexpressing MGE neural progenitors. On day 14, the cells were digested and expanded as free-floating neural spheres for six days. On day 21, the neural spheres could be dissociated for transplantation or *in vitro* analysis. For *in vitro* analysis, the progenitor cells were spread onto polyornithine/laminin-coated coverslips with neurobasal medium with BDNF (10 ng/mL; PeproTech), GDNF (10 ng/mL; PeproTech), IGF1 (10 ng/mL; PeproTech), and cAMP (1 μM, Sigma-Aldrich) (Figure 1).

2.2. Animals and Bilateral Common Carotid Artery Occlusion (2VO) Model. SPF-grade adult male Sprague-Dawley (SD) rats, weighing 250–280 g, were purchased from the Center of Experimental Animals, Tongji Medical College, Huazhong University of Science and Technology, Wuhan, China. All the procedures were approved by the Animal Care and Use Committee of the Tongji Medical College, Huazhong University of Science and Technology, Wuhan, China. SD rats were housed at $25 \pm 2^{\circ}$C under a 12 h light/dark cycle with food and water ad libitum. The bilateral common carotid artery occlusion (2VO) model was generated as described previously [24]. Animals were divided randomly into five groups: (1) sham operation group (sham), (2) 2VO group (2VO), (3) 2VO combined with culture medium transplantation group (2VO+Vehicle), (4) 2VO combined with MGE neural progenitor transplantation group (2VO+Cell), and (5) 2VO combined with MGE neural progenitor transplantation and EA group (2VO+Cell+EA).

2.3. Electroacupuncture Therapy. The rats in the 2VO+Cell +EA group received EA treatment. The location of the "Baihui" (GV20) and "Dazhui" (GV14) acupoints was described previously [24] (Figure 2(a)). Acupuncture needles (0.3 mm diameter) were horizontally inserted at a depth of 10 mm into the GV20 and perpendicularly at 5 mm into GV14. Then, the electrical stimulation was delivered using a G6805-II electroacupuncture therapeutic apparatus (Shanghai Medical Electronic Apparatus Co., China), with a continuous current at 2 Hz for 20 min daily. The stimulation intensity was set according to the visible light facial muscle twitching. The entire treatment period was seven days starting from the first day after 2VO to the cell transplantation day (Figure 2(b)).

2.4. Cell Transplantation. Cell transplantation was performed seven days after 2VO as described previously [25]. In brief, MGE neural progenitors were dissociated with Accutase and prepared at approximately 1×10^5 cells/μL in the medium. The rats were anesthetized and fixed on the stereotaxic device. Next, the skull was exposed, and a small hole was drilled on per hemisphere. A total of 2.5 μL cell suspension was transplanted into per side of hippocampus site (coordinates: anterior-posterior (AP) = −4.0 mm, medial-lateral (ML) = ±3.0 mm, and dorsal-ventral (DV) = −3 mm; 0 reference point for AP and ML at bregma, 0 reference point for DV at skull surface at the target site), according

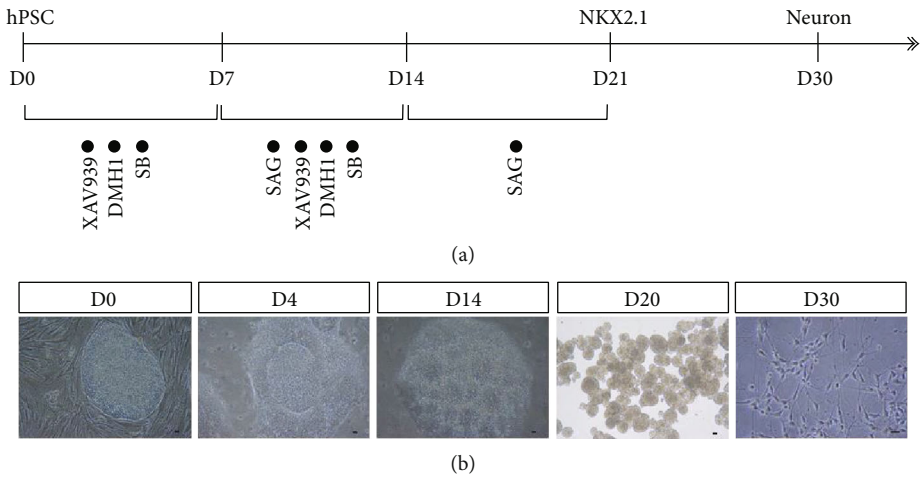

Figure 1: Differentiation of hESCs into MGE neural progenitors *in vitro*. (a) Flowchart of differentiation induced by the dual SMAD inhibition differentiation method. (b) Cell morphology at different stages of differentiation. Scale bars = 50 μm.

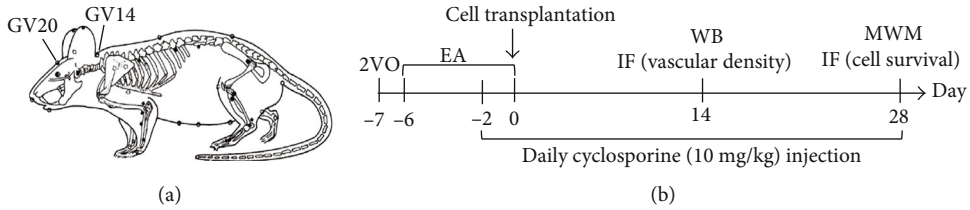

Figure 2: (a) Schematic diagram of GV20 and GV14 acupoints in the rat. (b) Flowchart of the experimental design.

to the stereotaxic coordinates given in the rat atlas of Paxinos and Watson [26]. The injection time was continuous 5 min, and the needle was left for 5 min before removal to prevent cells from overflowing the needle track. All rats were injected subcutaneously with 10 mg/kg cyclosporine A, two days before transplantation and subsequently daily.

2.5. Laser Doppler Flowmetry. The cortical cerebral blood flow (CBF) was assessed using a laser Doppler flowmetry (MoorVMS, England). Rats were anesthetized and placed in a stereotactic apparatus. A burr hole (3 mm in diameter) was made through a midline scalp incision, with an electric drill on the right frontoparietal region (anterior-posterior (AP) = −1.0 mm, medial-lateral (ML) = −5.0 mm) to set a placement device for a contact probe. The CBF was quantified before and after the ligation of the common carotid arteries. Calculated perfusion was expressed as a percentage ratio of postischemic to the preischemic brain to account for variables.

2.6. Tissue Processing. Rats were deeply anesthetized with 10% chloral hydrate (3 mL/kg) and perfused with 4% paraformaldehyde (PFA). The brains were quickly dissected out and soaked in 4% PFA for at least 12 h. The rat brain tissues were subjected to gradient dehydration in 20% and 30% sucrose sequentially. The brain specimens containing transplantation sites (from 3.0 to 5.0 mm behind the bregma) were embedded in optimal cutting temperature compound and cut into 30 μm coronal tissue sections with a frozen tissue slicer. The tissue sections were collected further in tissue cryopreservation fluid for immunohistochemical analysis.

2.7. Immunofluorescence Staining. Immunofluorescence staining was performed *in vitro* on coverslip cultures or frozen brain tissue sections as previously described [27]. Briefly, cells were fixed in 4% PFA for 20 min (frozen tissue sections did not require this step), washed with phosphate-buffered saline (PBS), and then blocked by QuickBlock™ Blocking Buffer for Immunol Staining (Beyotime, P0260) for 30 min at room temperature. The primary antibodies were added and incubated overnight at 4°C. Primary antibodies included mouse anti-Nestin (Millipore, MAB5326, 1 : 1000), rabbit anti-PAX6 (BioLegend, 901301, 1 : 1000), goat anti-SOX1 (R&D Systems, AF3369, 1 : 1000), rat anti-HOXB4 (DSHB, RRID: AB-2119288, 1 : 100), rabbit anti-Foxg1 (Abcam, Ab18259, 1 : 500), mouse anti-NKX2.1 (Millipore, MAB5460, 1 : 500), rabbit anti-GABA (Sigma-Aldrich, A2052, 1 : 1000), goat anti-CHAT (Millipore, AB144P, 1 : 300), mouse anti-neuronal class III β-tubulin (Tuj1; BioLegend, 801201, 1 : 2000), mouse anti-microtubule-associated protein-2 (Map2; Sigma-Aldrich, M1406, 1 : 1000), mouse anti-human nuclei (HuNu; Millipore, MAB1281, 1 : 500), goat anti-mCherry (Biorbyt, RRID: AB-2687829), and rabbit anti-NeuN (Millipore, ABN78, 1 : 1000). The corresponding fluorescent-conjugated secondary antibodies were applied for 1 h, and the nuclei were stained with DAPI (Boster, AR1177).

2.8. Vascular Density Analysis. Vascular density in the hippocampus was evaluated with immunofluorescence staining on the 14th day after grafting. Coronal brain sections (30 μm) on every six sections were used for vascular density analysis. The stained vasculature was observed within the hippocampus using an Olympus FV1000 confocal microscope (Olympus, Japan, ×10 objective). A lectin-positive vessel separated from adjacent vessels was counted as one vessel. The number of these vessels was added to the number of vascular branch points (number of vessel bifurcations) to obtain the total number of vessels, as described previously [28]. Five fields for each section, randomly distributed, were imaged for statistical analysis, with at least three independent replication tests. An investigator blinded to the group manually quantified vascular density, and the data were expressed as the number of stained vessels per 0.36 mm^2 under ×10 objective.

2.9. Microscopical Analysis and Cellular Quantification. As described previously [25], all nuclei of grafted cells were identified in the presence of the human-specific nuclear marker (HuNu) immunostaining. $HuNu^+/DAPI^+$ double-labeled cell counting was performed on every six sections on the 28th day after grafting [29], and images were captured using an Olympus FV1000 confocal microscope (Olympus, Japan, ×40 objective). The numbers of $HuNu^+/DAPI^+$ double-labeled cells were counted on the images by an investigator blinded to the group using ImageJ software (NIH, Bethesda, Maryland, USA), and the data were expressed as the number of positive cells per area under ×40 objective. Five areas were randomly selected for each section, with at least three independent replication tests.

2.10. Western Blot Analysis. Under deep anesthesia, hippocampus brain tissue, including the grafting area, was immediately dissected on ice. After centrifugation at 12,000 rpm for 15 min, total protein was isolated by homogenization, and the supernatant was collected. The protein concentrations were estimated by BCA assay. The total protein was separated using sodium dodecyl sulfate-polyacrylamide gel electrophoresis (SDS-PAGE). After electrophoresis, it was transferred onto polyvinylidene difluoride (PVDF) membranes, blocked in milk, and incubated at 4°C overnight with primary antibodies: rabbit anti-VEGF (Affinity, AF5131, 1 : 1000), rabbit anti-TNF-α (CST, 8184S, 1 : 1000), and rabbit anti-IL-1β (CST, 12703S, 1 : 1000), followed by incubation with appropriate horseradish peroxidase-conjugated secondary antibodies. Blots were detected using the ECL Western Blotting Substrate, and the intensity of the protein band was quantified using Gel-Pro Analyzer 4.0 software (Media Cybernetics, USA).

2.11. Morris Water Maze Task. Morris water maze (MWM) task was used to evaluate hippocampus-dependent spatial learning and memory. Briefly, a circular water tank (150 cm in diameter and 50 cm in deep) was filled with water (23 ± 2°C) to a depth of 21 cm. A circular submerged platform (15 cm in diameter and 20 cm in height) was placed underwater and in the target quadrant center. Several visual cues were displayed on the wall of the test room. In the place navigation phase, rats were subjected to four trials per day for four consecutive days. Each trial lasted either until the rat found the platform or for 60 s. The starting point was changed for every trial. The rats were allowed to rest on the platform for 20 s after each trial. On the 5th day, the platform was removed for a 60 s spatial probe trial to test rats' spatial memory. The latency to find the submerged platform, the dwell time in the target quadrant, and the swimming paths were recorded automatically using a computer-based image analyzer MWM tracking system MT-200 (Chengdu Technology & Market Co., Ltd., Chengdu, Sichuan Province, China).

2.12. Statistical Analysis. SPSS 22.0 software (IBM Corporation, Somers, New York, USA) was used for statistical analysis. To assess the normal distribution of data, the Shapiro-Wilk test was employed ($P > 0.05$). Data were analyzed for multiple comparisons by one-way analysis of variance (ANOVA) followed by Tukey's multiple comparison tests among different groups. When comparing two groups at two time points (CBF values), two-way analysis of variance (ANOVA) was implemented. When comparing two groups at the same time point, Student's t-test was implemented. All data were expressed as mean ± standard error of the mean (SEM). P value < 0.05 was considered statistically significant.

3. Results

3.1. Human MGE Neural Progenitors Were Efficiently Generated from hESCs In Vitro. During the culture process, small molecules SB431542, DMH1, XAV939, and SAG were applied to promote hESC differentiation into neural progenitor cells. Morphologically, neural tube structures appeared on the 4th day of differentiation, and several rosettes, the typical structure of the neuroepithelium, appeared on the 14th day. After being expanded as free-floating neural spheres, MGE neural progenitors were obtained on the 21st day. The cells were then adherently cultured at this stage, and neurons were obtained after ten days (Figure 1(b)).

In the presence of several small-molecule inhibitors, neuroepithelium marker PAX6 and NSC marker Nestin began to appear on the 4th day (Figure 3(a)). On the 10th day, another marker of the neuroepithelium, SOX1, was observed (Figure 3(b)). Additionally, the forebrain marker, FOXG1, but no spinal cord marker, HOXB4, was observed (Figure 3(c)). Meanwhile, the cells colabeling MGE marker NKX2.1 and FOXG1 appeared on the 14th day (Figure 3(d)) and reached a peak on the 21st day. MGE neural progenitors eventually differentiated into GABAergic and cholinergic neurons on the 49th day *in vitro* (Figures 3(e) and 3(f)).

3.2. The 2VO Model Showed a Decrease in Cerebral Blood Flow (CBF). The pre- and postoperative blood flow was monitored in rats of the sham and 2VO groups with laser Doppler. Before the operation, the mean baseline CBF values in the sham and 2VO groups were 171.9 ± 6.07 (PU) and

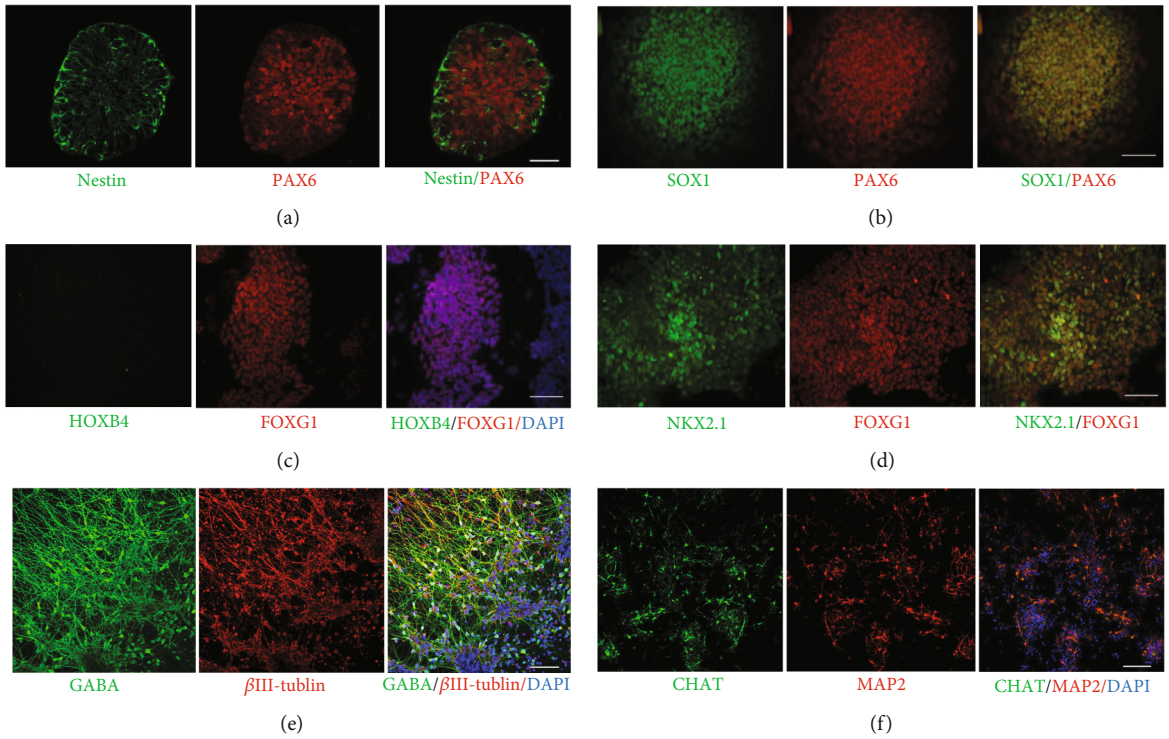

Figure 3: Generation of neural progenitors for transplantation and the neural markers of MGE neural progenitors during the process of differentiation. (a) Representative images were immunoreactive for neuroepithelium marker PAX6 and NSC marker Nestin on day 4. (b) Coimmunostaining SOX1 and PAX6 at day 10. (c) Differentiated hESCs expressed forebrain marker, FOXG1, but no spinal cord marker, HOXB4. (d) Coexpressing MGE neural progenitor marker NKX2.1 and FOXG1 on day 14. By 49 days in culture, neurons were positive for (e) GABA and (f) CHAT. Scale bars = 50 μm.

173.4 ± 5.26 (PU), respectively, with no significant difference. The CBF value in the 2VO group decreased to 54.9 ± 6.45 (PU), reaching the lowest within 5 min after the operation, and then maintained a low blood flow state, which indicated that 2VO rats suffered from persistent cerebral hypoperfusion (Figure 4).

3.3. EA Inhibited Inflammation of the Hippocampus in Rats of the 2VO+Cell Group. Earlier studies suggested that postischemic inflammation plays a vital role in various stages of cerebral ischemic injury. Activated microglia leads to inflammasome-mediated interleukin- (IL-) 1β release, as well as tumor necrosis factor (TNF) production, which feedbacks into the inflammatory cascade by inducing cytokine and chemokine production in endothelial cells and astrocytes [30]. The inflammation leads to the deterioration of the local microenvironment, which is toxic to the host neural cells and is not conducive to the survival of exogenous grafted cells. It was reported that chronic cerebral hypoperfusion-induced cognitive impairment is associated highly with inflammation [31]. Therefore, proinflammatory cytokines were detected by Western blot analysis in this study to evaluate whether EA can inhibit inflammation, promote grafted cell survival, and alleviate cognition impairment. 2VO-induced inflammatory response in rats' hippocampus was demonstrated by the increased immunoreactivity of TNF-α and IL-1β compared to the sham group ($P < 0.001$). In the 2VO+Cell+EA group, immunoreactivity of TNF-α and IL-1β in the hippocampus decreased significantly compared with that of the 2VO+Cell group ($P = 0.008$ and $P = 0.029$), indicating that EA inhibited inflammation response of the hippocampus in rats of the 2VO+Cell group (Figure 5).

3.4. EA Promoted Angiogenesis of the Hippocampus in Rats of the 2VO+Cell Group. The key regulator of vascular development and homeostasis is the vascular endothelial growth factor (VEGF) [32]. In our study, Western blot analysis revealed a significant difference in VEGF protein expression in the hippocampus among the five groups. Two-vessel occlusion induced elevated VEGF protein expression in the hippocampus. Rats in the 2VO+Cell and 2VO+Cell+EA groups showed increased VEGF expression compared with the 2VO group at day 14 after transplantation. Compared with the 2VO+Cell group, VEGF protein expression was significantly higher in the 2VO+Cell+EA group rats ($P < 0.001$). Additionally, the vascular density of the cell grafting area in the hippocampus was detected by immunofluorescence staining. Vascular density in the 2VO+Cell +EA group rats (52.25 ± 6.50) was significantly higher than that in the 2VO+Cell group (32.75 ± 3.25) on day 14 after cell grafting ($P = 0.017$) (Figure 6). The above results indicated that EA promoted angiogenesis of the hippocampus in 2VO+Cell rats.

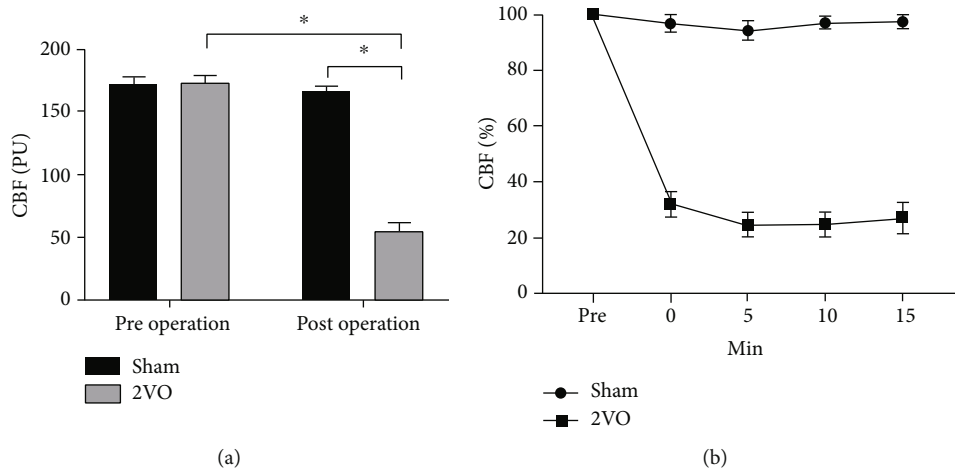

Figure 4: Laser Doppler monitoring of CBF in rats of the sham and 2VO groups. (a) Preoperative and postoperative blood flow values of the sham and 2VO group analysis of variance (two-way ANOVA, $F = 275.036$, $P < 0.001$). (b) The ratio of postischemic to preischemic CBF changes within 0–15 min before and after surgery. Values are mean ± SEM ($N = 5$ rats/per group). $^{*}P < 0.05$.

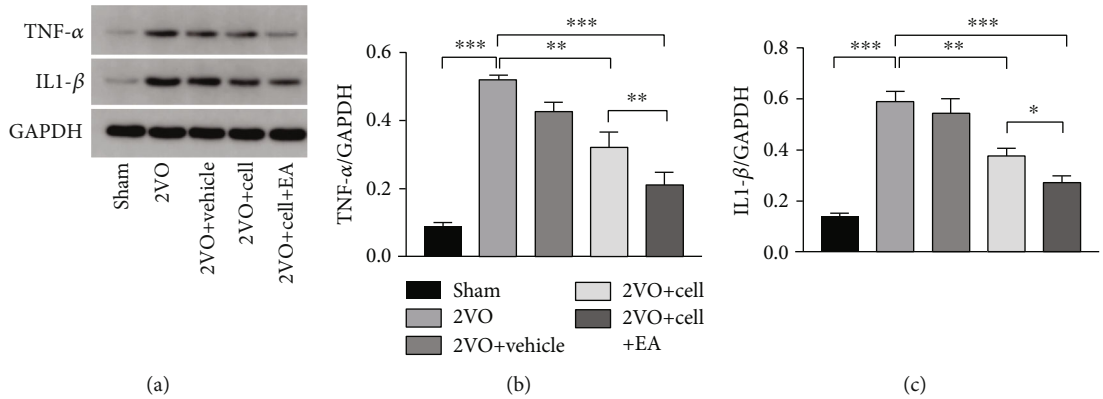

Figure 5: Effects of MGE neural progenitors and EA treatment on the expression of TNF-α and IL-1β in the hippocampus were evaluated by Western blot 14 days after grafting. (a) Gel electrophoresis of TNF-α and IL-1β. (b, c) Densitometric analysis of TNF-α (one-way ANOVA, $F = 91.711$, $P < 0.001$) and IL-1β (one-way ANOVA, $F = 57.059$, $P < 0.001$). Values are mean ± SEM ($N = 5$ rats/per group). $^{*}P < 0.05$, $^{**}P < 0.01$, and $^{***}P < 0.001$.

3.5. EA Promoted the Survival of the Grafted MGE Neural Progenitors in the Hippocampus. To better trace the grafted cells, hESCs modified by mCherry at AAVS1 site were used to differentiate into MGE neural progenitors for transplantation. Four weeks after transplantation, a large number of cells comarked with HuNu and mCherry were observed at the grafting area, indicating that grafted MGE neural progenitors differentiated from hESCs still survived in rats (Figure 7(a)). Some grafted MGE neural progenitors differentiated into neurons, weakly expressing NeuN (Figure 7(b)). Further analysis revealed that much more $HuNu^{+}$ cells survived in the 2VO +Cell+EA group (1151 ± 260) than in the 2VO+Cell group (540 ± 123) in the grafting area ($P = 0.021$), indicating that EA promoted the survival of the grafted MGE neural progenitors in the hippocampus (Figures 7(c) and 7(d)).

3.6. MGE Neural Progenitor Transplantation Alleviated Learning and Memory Impairment in 2VO Rats and EA Enhanced Transplantation Therapy's Efficacy. Four weeks after transplantation, the MWM task was used to assess the learning and memory ability of rats in each group, including spatial learning (Figure 8(a), A–E) and spatial memory test (Figure 8(a), F–J). After four days of spatial learning training, the escape latencies of rats in the 2VO group (47.2 ± 4.5 s) and the 2VO+Vehicle group (46.4 ± 5.4 s) were significantly longer than those in the sham group (23.7 ± 1.9 s) ($P < 0.001$). Compared with rats in the 2VO group, rats in the 2VO+Cell group showed a reduction in the escape latency (36.5 ± 9.5 s, $P < 0.05$) (Figure 8(b)) and showed increased time spent in the target quadrant (14.2 ± 3.9 s, $P = 0.036$) (Figure 8(c)), while the frequency of crossing in the platform was not different (1.4 ± 0.55, $P = 0.759$) (Figure 8(d)). Compared with the 2VO+Cell group, the escape latency of rats in the 2VO +Cell+EA group was shortened without significant difference (32.0 ± 2.2 s, $P = 0.786$) (Figure 8(b)). However, rats in the 2VO+Cell+EA group showed increased time spent in the target quadrant (21.6 ± 3.5 s, $P = 0.019$) and increased

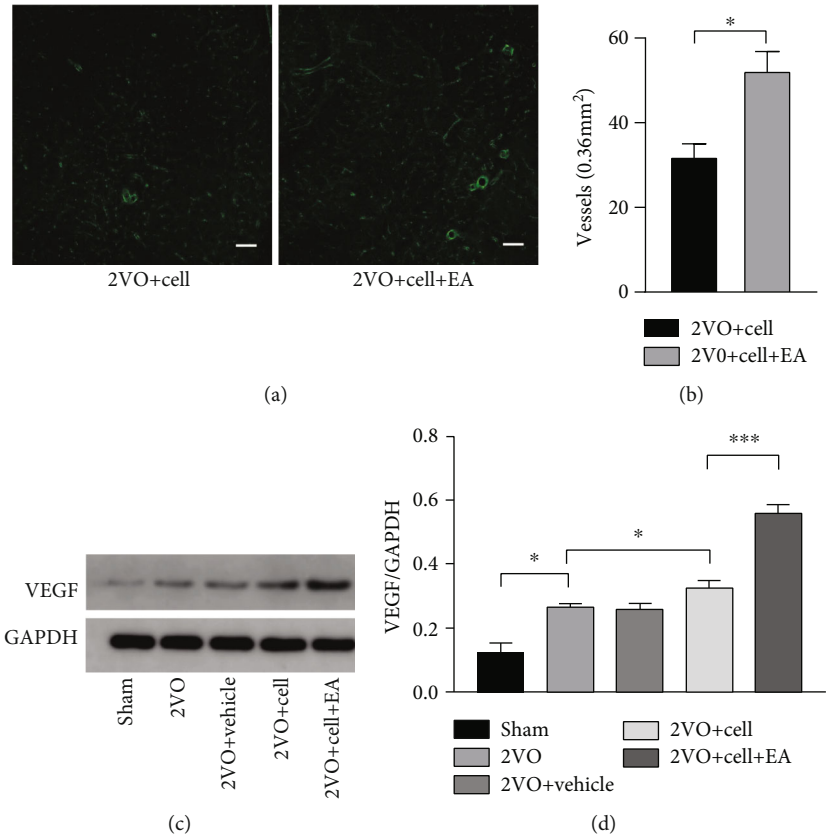

Figure 6: EA facilitates hippocampal angiogenesis in 2VO+Cell rats. (a) Immunofluorescence staining of blood vessels (green) in the hippocampus on the 14th day after grafting. Scale bar = 100 μm. (b) Quantification of vascular density in the 2VO+Cell and 2VO+Cell +EA groups. (c) Representative Western blots of VEGF on the 14th day after grafting. (d) The densitometric analysis of VEGF level detected from the hippocampus in each group (one-way ANOVA, $F = 13.574$, $P < 0.001$). Values are mean ± SEM ($N = 5$ rats/per group). $^{*}P < 0.05$ and $^{***}P < 0.001$.

frequency of crossing the platform (2.8 ± 0.83, $P = 0.047$) compared with the 2VO+Cell group (Figures 8(c) and 8(d)). There were no significant differences between rats in the 2VO and 2VO+Vehicle groups in escape latency, time spent in the target quadrant, and the frequency of crossing the platform. The above results of the MWM task indicated that MGE neural progenitor transplantation alleviated learning and memory impairment in 2VO rats, and EA enhanced transplantation therapy's efficacy.

4. Discussion

Some neurological diseases are closely related to different types of neuronal damage, reduction, and death. For example, cognitive dysfunction in cerebral ischemia is related to cholinergic neuron loss in the hippocampus [33, 34]. Recently, with the development of differentiation technology, human pluripotent stem cells, including human embryonic stem cells (hESC) and human-induced pluripotent stem cells (hiPSC), can be induced to differentiate into specific neurons and glial cells *in vitro*, which provide a good source for cell transplantation therapy for these neurological diseases [35].

MGE (medial ganglionic eminence) is a structure of the ventral forebrain during embryonic development, having the main marker, NKX2.1. NKX2.1 is very important for the development of embryonic septal neuroepithelium and cholinergic neurons in the basal forebrain and the hippocampal cholinergic projection system. A study found that in the absence of NKX2.1, cholinergic septohippocampal projection neurons and large subsets of basal forebrain cholinergic neurons fail to develop, causing alterations in the hippocampal theta rhythms and severe deficiencies in learning and memory [12]. MGE neural progenitors are mainly differentiated into GABAergic neurons and cholinergic neurons *in vitro*, used as a cell source to treat learning and memory impairment. In this study, human embryonic stem cells were used to differentiate into MGE neural progenitors by combining induction using different small molecules for subsequent cell transplantation treatment. In the in vitro cell differentiation stage, a large number of NKX2.1-positive cells were observed on the 21st day. After another 28 days, the differentiated cells expressed GABA and CHAT, suggesting that the MGE neural progenitors obtained according to our differentiation protocol can further differentiate into GABAergic and cholinergic neurons *in vitro*. It thus lays the foundation for MGE neural progenitors grafting to improve the cognitive impairment caused by cerebral hypoperfusion in rats.

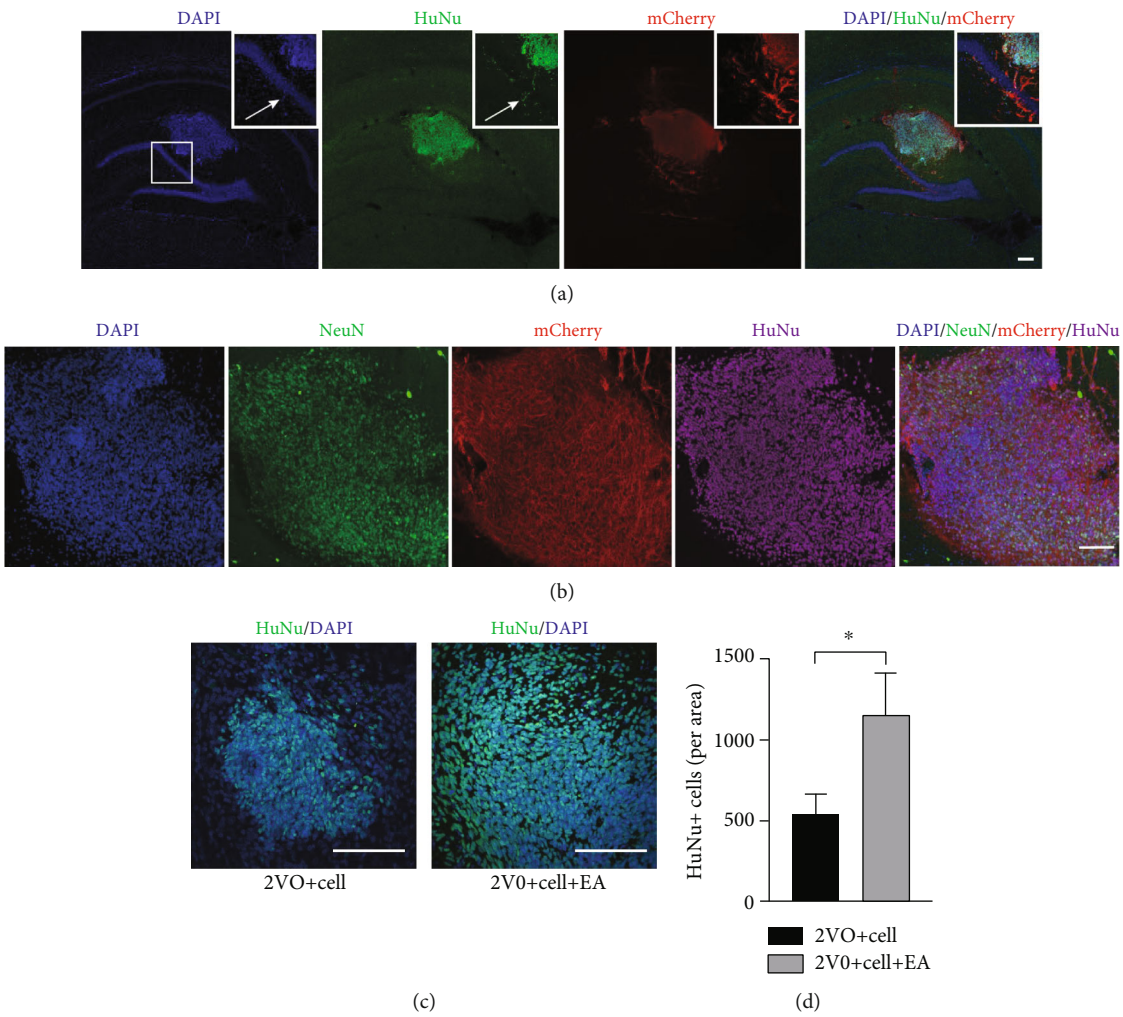

Figure 7: Effect of EA treatment on the survival of the grafted MGE neural progenitors in the hippocampus. (a) Fluorescence photomicrographs of $HuNu^+/mCherry^+$-positive cells from the 2VO+Cell+EA group. Scale bar = 200 μm. (b) Some $HuNu^+/mCherry^+$-positive cells from the 2VO+Cell+EA group weakly expressed NeuN. Scale bar = 100 μm. (c) Fluorescence photomicrographs of $HuNu^+$-positive cells from the 2VO+Cell and 2VO+Cell+EA groups. Scale bar = 100 μm. (d) Quantification of $HuNu^+$-positive cells in the 2VO +Cell and 2VO+Cell+EA groups. Values are mean ± SEM ($N = 5$ rats/per group). $^*P < 0.05$.

Neural stem cell transplantation can replace lost neurons and improve functional deficits because it has the inherent ability to differentiate into various cell phenotypes. Therefore, currently, cell transplantation has growing potential. However, there is still a long way to go, and some obstacles must be overcome before cell transplantation therapy can be actively used in the clinic. One of the major problems with cell transplantation is the low survival rate of grafted cells (5–20%). Most cell death occurs during the first few days after transplantation as a result of inflammation or immune response, trophic factor withdrawal, oxidative stress, excitotoxicity, hypoxia, and apoptosis [13–16]. Thus, for successful transplantation, improving the ischemic and hypoxic state of the hippocampus and inhibiting the inflammation in the grafted area, thereby improving the survival environment of grafted cells, may be an important strategy to improve the survival rate of grafted cells.

As an important treatment of Traditional Chinese Medicine, EA delivers electrical stimulation to acupoints through acupuncture needles. It has been recommended as a complementary therapy in stroke rehabilitation in Asian and Western countries. An increasing number of studies have shown that acupuncture can effectively improve the functional recovery of neurons after cerebral ischemia [36, 37]. The potential mechanisms include preventing inflammatory and oxidant stress, suppressing apoptosis, promoting angiogenesis, and endogenous neural regeneration. Since EA can promote angiogenesis and anti-inflammatory, it was combined with cell transplantation to study the survival of grafted cells in this study. Our findings showed that the 2VO model increased the expression of inflammatory factors, TNF-α and IL-1β, in the hippocampus, and the hypoperfusion produced by 2VO induced a slight increase in VEGF protein, consistent with the results of other studies [17, 28]. Compared with the 2VO+Cell group, EA inhibited TNF-α and IL-1β expression and increased the expression of VEGF protein and blood vessel density in the hippocampus of the 2VO+Cell+EA group. In the grafting area, several

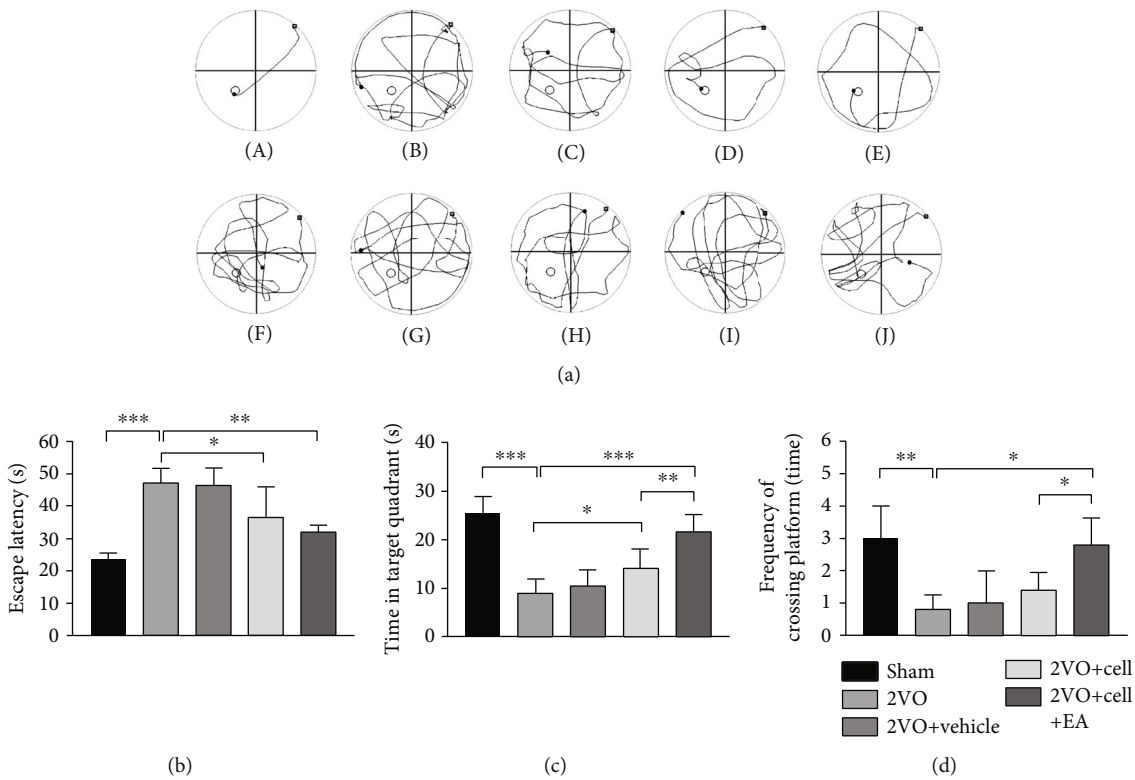

Figure 8: Comparison of the effects on spatial learning and memory test in rats from different groups. (a) (A–E) The swimming track of different groups of rats in spatial learning training; (F–J) the swimming track of different groups of rats in the spatial memory test. (A) and (F) from the sham group; (B) and (G) from the 2VO group; (C) and (H) from the 2VO+Vehicle group; (D) and (I) from the 2VO +Cell group; (E) and (J) from the 2VO+Cell+EA group. (b) Comparison of the average escape latencies of five groups in four days of spatial learning training (one-way ANOVA, $F = 12.354$, $P < 0.001$). (c) Comparison of the swimming time in target quadrant of five groups in the spatial memory test (one-way ANOVA, $F = 22.159$, $P < 0.001$). (d) Comparison of the frequency of crossing in the platform of five groups in the spatial memory test (one-way ANOVA, $F = 8.281$, $P < 0.01$). Values are mean ± SEM ($N = 5$ rats/per group). $^{*}P < 0.05$, $^{**}P < 0.01$, and $^{***}P < 0.001$.

surviving cells coexpressing HuNu (for analysis of the survival of grafted cells, all nuclei of grafted cells were identified based on HuNu immunostaining) and mCherry were observed. These cells also expressed NeuN (fluorescence intensity was not as strong as the host cells), suggesting that they were gradually differentiating toward mature neurons. More $HuNu^{+}$ cells were detected in the 2VO+Cell+EA group compared with the 2VO+Cell group through cell count analysis. Considering the above research results, we speculated that the higher survival of grafted cells in the 2VO+Cell+EA group was related to the EA effect on suppressing inflammatory and promoting angiogenesis.

As already established, the hippocampus plays a critical role in cognitive function [38]. As the basic structure or constitution, neurons of the hippocampus serve its local circuitry and process information. Since the loss of hippocampal neurons would induce cognitive deficits [39], cerebral ischemia could lead to selective and delayed pyramidal neuronal death in the hippocampal CA 1 area [40]. Thus, replenishing lost hippocampal neurons after ischemia may become an important treatment strategy to reduce cognitive damage. In the MWM task, compared with the rats in the 2VO group, the rats in the 2VO+Cell group showed a reduction in the escape latency and increased time spent in the target quadrant, indicating that learning and memory impairment in 2VO rats was alleviated. We speculated that the improved cognitive function was related to the replacement of partial dead hippocampal neurons by MGE neural progenitor transplantation. Compared with the 2VO+Cell group, the rats in the 2VO+Cell+EA group showed increased time spent in the target quadrant, and the frequency of crossing the platform was increased. This indicated that the ability of rats to learn and memorize in the 2VO+Cell+EA group was improved more significantly. Considering that more $HuNu^{+}$-positive cells were observed in the 2VO+Cell+EA group in cellular quantification analysis, we speculated that EA facilitated the cell grafting effect on learning and memory impairment by promoting the grafted cells' survival in the hippocampus.

In summary, our study demonstrated that EA could promote the survival of the grafted MGE neural progenitors differentiated from human embryonic pluripotent stem cells and alleviated learning and memory impairment in rats with cerebral ischemia, which partially resulted from inhibited inflammation response and increased angiogenesis. This observation indicates that the combination of MGE neural progenitors with EA might be a promising approach to treat cognitive deficits after cerebral infarct. However, further

studies and long-term observations are required to explore whether the grafted cells can differentiate into cholinergic and GABAergic neurons after maturation, their interaction and integration with host cells, and the formation of synaptic circuits to alleviate neural function deficits.

Data Availability

The data used to support the findings of this study are available from the corresponding author upon reasonable request.

Conflicts of Interest

The authors have declared no conflict of interest.

Authors' Contributions

Xiaohua Han and Hong Chen conceived and designed the project. Juan Li, Luting Chen, and Danping Li carried out the experiment. Min Lu and Xiaolin Huang analyzed the data. Juan Li, Luting Chen, and Xiaohua Han drafted the manuscript. All authors read and approved the final manuscript. Juan Li and Luting Chen contributed equally to this work.

Acknowledgments

This study was supported by the National Natural Science Foundation of China (Grant No. 81774404). Thanks are due to Professor Su-chun Zhang from Singapore Duke-NUS for kindly providing the H9 human embryonic stem cell line and the chemically modified H9-mCherry human embryonic stem cell line.

References

[1] D. Mozaffarian, E. J. Benjamin, A. S. Go et al., "Heart disease and stroke statistics-2016 update: a report from the American Heart Association," *Circulation*, vol. 133, no. 4, pp. e38–e360, 2016.

[2] A. Kiryk, R. Pluta, I. Figiel et al., "Transient brain ischemia due to cardiac arrest causes irreversible long- lasting cognitive injury," *Behavioural Brain Research*, vol. 219, no. 1, pp. 1–7, 2011.

[3] M. Gulinello, D. Lebesgue, T. Jover-Mengual, R. S. Zukin, and A. M. Etgen, "Acute and chronic estradiol treatments reduce memory deficits induced by transient global ischemia in female rats," *Hormones and Behavior*, vol. 49, no. 2, pp. 246–260, 2006.

[4] J. Emberson, K. R. Lees, P. Lyden et al., "Effect of treatment delay, age, and stroke severity on the effects of intravenous thrombolysis with alteplase for acute ischaemic stroke: a meta-analysis of individual patient data from randomised trials," *Lancet*, vol. 384, no. 9958, pp. 1929–1935, 2014.

[5] W. J. Powers, A. A. Rabinstein, T. Ackerson et al., "2018 guidelines for the early management of patients with acute ischemic stroke: a guideline for healthcare professionals from the American Heart Association/American Stroke Association," *Stroke*, vol. 49, no. 3, pp. e46–e110, 2018.

[6] D. L. Rimmele and G. Thomalla, "Wake-up stroke: clinical characteristics, imaging findings, and treatment option â€ an update," *Frontiers in Neurology*, vol. 5, no. 35, 2014.

[7] C. Xie, X. Gao, Y. Luo, Y. Pang, and M. Li, "Electroacupuncture modulates stromal cell-derived factor-1α expression and mobilization of bone marrow endothelial progenitor cells in focal cerebral ischemia/reperfusion model rats," *Brain Research*, vol. 1648, no. Part A, pp. 119–126, 2016.

[8] S. Palma-Tortosa, D. Tornero, M. G. Hansen et al., "Activity in grafted human iPS cell-derived cortical neurons integrated in stroke-injured rat brain regulates motor behavior," *Proceedings of the National Academy of Sciences of the United States of America*, vol. 117, no. 16, pp. 9094–9100, 2020.

[9] E. Curtis, J. R. Martin, B. Gabel et al., "A first-in-human, phase I study of neural stem cell transplantation for chronic spinal cord injury," *Cell Stem Cell*, vol. 22, no. 6, pp. 941–950.e6, 2018.

[10] S. Gao, X. Guo, S. Zhao et al., "Differentiation of human adipose-derived stem cells into neuron/motoneuron- like cells for cell replacement therapy of spinal cord injury," *Cell Death & Disease*, vol. 10, no. 8, p. 597, 2019.

[11] L. Zhao, C. Zhou, L. Li et al., "Acupuncture improves cerebral microenvironment in mice with Alzheimer's disease treated with hippocampal neural stem cells," *Molecular Neurobiology*, vol. 54, no. 7, pp. 5120–5130, 2017.

[12] L. Magno, C. Barry, C. Schmidt-Hieber, P. Theodotou, M. Häusser, and N. Kessaris, "NKX2-1 is required in the embryonic septum for cholinergic system development, learning, and memory," *Cell Reports*, vol. 20, no. 7, pp. 1572–1584, 2017.

[13] M. Emgård, U. Hallin, J. Karlsson, B. A. Bahr, P. Brundin, and K. Blomgren, "Both apoptosis and necrosis occur early after intracerebral grafting of ventral mesencephalic tissue: a role for protease activation," *Journal of Neurochemistry*, vol. 86, no. 5, pp. 1223–1232, 2003.

[14] C. E. Sortwell, M. R. Pitzer, and T. J. Collier, "Time course of apoptotic cell death within mesencephalic cell suspension grafts: implications for improving grafted dopamine neuron survival," *Experimental Neurology*, vol. 165, no. 2, pp. 268–277, 2000.

[15] M. Uemura, M. M. Refaat, M. Shinoyama et al., "Matrigel supports survival and neuronal differentiation of grafted embryonic stem cell-derived neural precursor cells," *Journal of Neuroscience Research*, vol. 88, no. 3, pp. 542–551, 2010.

[16] W. M. Zawada, D. J. Zastrow, E. D. Clarkson, F. S. Adams, K. P. Bell, and C. R. Freed, "Growth factors improve immediate survival of embryonic dopamine neurons after transplantation into rats," *Brain Research*, vol. 786, no. 1-2, pp. 96–103, 1998.

[17] M.-h. Shen, C.-b. Zhang, J.-h. Zhang, and P.-f. Li, "Electroacupuncture attenuates cerebral ischemia and reperfusion injury in middle cerebral artery occlusion of rat via modulation of apoptosis, inflammation, oxidative stress, and excitotoxicity," *Evidence-Based Complementary and Alternative Medicine*, vol. 2016, Article ID 9438650, 2016.

[18] X. Han, X. Zhao, and M. Lu, "Electroacupuncture ameliorates learning and memory via activation of the CREB signaling pathway in the hippocampus to attenuate apoptosis after cerebral hypoperfusion," *Evidence-based complementary and alternative medicine*, vol. 2013, Article ID 156489, 2013.

[19] S. J. Wang, N. Omori, G. Jin et al., "Functional improvement by electro-acupuncture after transient middle cerebral artery

occlusion in rats," *Neurological Research*, vol. 25, no. 5, pp. 516–521, 2003.

[20] L. Lu, X. G. Zhang, and L. L. Zhong, "Acupuncture for neurogenesis in experimental ischemic stroke: a systematic review and meta-analysis," *Scientific Reports*, vol. 6, 2016.

[21] H. Jin, Y.-T. Zhang, Y. Yang et al., "Electroacupuncture facilitates the integration of neural stem cell-derived neural network with transected rat spinal cord," *Stem Cell Reports*, vol. 12, no. 2, pp. 274–289, 2019.

[22] Y. R. Kim, S. M. Ahn, M. E. Pak et al., "Potential benefits of mesenchymal stem cells and electroacupuncture on the trophic factors associated with neurogenesis in mice with ischemic stroke," *Scientific Reports*, vol. 8, no. 1, 2018.

[23] S. M. Chambers, C. A. Fasano, E. P. Papapetrou, M. Tomishima, M. Sadelain, and L. Studer, "Highly efficient neural conversion of human ES and iPS cells by dual inhibition of SMAD signaling," *Nature Biotechnology*, vol. 27, no. 3, pp. 275–280, 2009.

[24] C. X. Zheng, M. Lu, and Y. B. Guo, "Electroacupuncture ameliorates learning and memory and improves synaptic plasticity via activation of the PKA/CREB signaling pathway in cerebral hypoperfusion," *Evidence-Based Complementary and Alternative Medicine*, vol. 2016, Article ID 7893710, 2016.

[25] J.-J. Peng, R. Sha, M.-X. Li et al., "Repetitive transcranial magnetic stimulation promotes functional recovery and differentiation of human neural stem cells in rats after ischemic stroke," *Experimental Neurology*, vol. 313, pp. 1–9, 2019.

[26] G. Paxinos and C. Watson, *The Rat Brain in Stereotaxic Coordinates*, Academic Press, New York, 2008.

[27] Y. Liu, J. P. Weick, H. Liu et al., "Medial ganglionic eminence-like cells derived from human embryonic stem cells correct learning and memory deficits," *Nature Biotechnology*, vol. 31, no. 5, pp. 440–447, 2013.

[28] J. Wang, X. Fu, C. Jiang et al., "Bone marrow mononuclear cell transplantation promotes therapeutic angiogenesis via upregulation of the VEGF-VEGFR2 signaling pathway in a rat model of vascular dementia," *Behavioural Brain Research*, vol. 265, no. 2014, pp. 171–180, 2014.

[29] D. Yang, Z. J. Zhang, and M. Oldenburg, "Human embryonic stem cell-derived dopaminergic neurons reverse functional deficit in parkinsonian rats," *Stem Cells (Dayton, Ohio)*, vol. 26, no. 1, pp. 55–63, 2008.

[30] J. Anrather and C. Iade, "Inflammation and stroke: an overview," *Neurotherapeutics*, vol. 13, no. 4, pp. 661–670, 2016.

[31] J. Miyanohara, M. Kakae, K. Nagayasu et al., "TRPM2 channel aggravates CNS inflammation and cognitive impairment via activation of microglia in chronic cerebral hypoperfusion," *The Journal of Neuroscience*, vol. 38, no. 14, pp. 3520–3533, 2018.

[32] A. S. Chung and N. Ferrara, "Developmental and pathological angiogenesis," *Annual Review of Cell and Developmental Biology*, vol. 27, no. 1, pp. 563–584, 2011.

[33] E.-h. Chung, K. Iwasaki, K. Mishima, N. Egashira, and M. Fujiwara, "Repeated cerebral ischemia induced hippocampal cell death and impairments of spatial cognition in the rat," *Life Sciences*, vol. 72, no. 4-5, pp. 609–619, 2002.

[34] H. J. Park, H. S. Shim, K. S. Kim, and I. Shim, "The protective effect of black ginseng against transient focal ischemia-induced neuronal damage in rats," *The Korean Journal of Physiology & Pharmacology*, vol. 15, no. 6, pp. 333–338, 2011.

[35] Y. Tao and S. C. Zhang, "Neural subtype specification from human pluripotent stem cells," *Cell Stem Cell*, vol. 19, no. 5, pp. 573–586, 2016.

[36] X. Han, H. Jin, K. Li et al., "Acupuncture modulates disrupted whole-brain network after ischemic stroke: evidence based on graph theory analysis," *Neural Plasticity*, vol. 2020, Article ID 8838498, 10 pages, 2020.

[37] H. Liu, L. Chen, G. Zhang et al., "Scalp acupuncture enhances the functional connectivity of visual and cognitive-motor function network of patients with acute ischemic stroke," *Evidence-Based Complementary and Alternative Medicine*, vol. 2020, Article ID 8836794, 11 pages, 2020.

[38] R. A. Epstein, E. Z. Patai, J. B. Julian, and H. J. Spiers, "The cognitive map in humans: spatial navigation and beyond," *Nature Neuroscience*, vol. 20, no. 11, pp. 1504–1513, 2017.

[39] G. Li, H. Cheng, X. Zhang et al., "Hippocampal neuron loss is correlated with cognitive deficits in SAMP8 mice," *Neurological Sciences*, vol. 34, no. 6, pp. 963–969, 2013.

[40] L. Kamali Dolatabadi, M. Emamghoreishi, M. R. Namavar, and H. Badeli Sarkala, "Curcumin effects on memory impairment and restoration of irregular neuronal distribution in the hippocampal CA1 region after global cerebral ischemia in male rats," *Basic and Clinical Neuroscience*, vol. 10, no. 5, pp. 527–539, 2019.

Hindawi
Neural Plasticity
Volume 2021, Article ID 5664647, 8 pages
https://doi.org/10.1155/2021/5664647

Research Article

Intrahemispheric EEG: A New Perspective for Quantitative EEG Assessment in Poststroke Individuals

Rodrigo Brito,[1,2] **Adriana Baltar**,[1,2] **Marina Berenguer-Rocha**,[1] **Lívia Shirahige**,[1,2] **Sérgio Rocha**,[1] **André Fonseca**,[3] **Daniele Piscitelli**,[4,5] **and Kátia Monte-Silva**[1,2]

[1]*Applied Neuroscience Laboratory, Department of Physical Therapy, Universidade Federal de Pernambuco, Recife, Pernambuco, Brazil*
[2]*NAPeN Network (Núcleo de Assistência e Pesquisa em Neuromodulação), Brazil*
[3]*Center of Mathematics, Computation and Cognition, Universidade Federal do ABC, Sao Paulo, Brazil*
[4]*School of Medicine and Surgery, University of Milano Bicocca, Milano, Italy*
[5]*School of Physical and Occupational Therapy, McGill University, Montreal, Canada*

Correspondence should be addressed to Daniele Piscitelli; daniele.piscitelli@unimib.it

Received 27 May 2021; Revised 18 August 2021; Accepted 6 September 2021; Published 22 September 2021

Academic Editor: Xi-Ze Jia

The ratio between slower and faster frequencies of brain activity may change after stroke. However, few studies have used quantitative electroencephalography (qEEG) index of ratios between slower and faster frequencies such as the delta/alpha ratio (DAR) and the power ratio index (PRI; delta + theta/alpha + beta) for investigating the difference between the affected and unaffected hemisphere poststroke. Here, we proposed a new perspective for analyzing DAR and PRI within each hemisphere and investigated the motor impairment-related interhemispheric frequency oscillations. Forty-seven poststroke subjects and twelve healthy controls were included in the study. Severity of upper limb motor impairment was classified according to the Fugl–Meyer assessment in mild/moderate ($n = 25$) and severe ($n = 22$). The qEEG indexes (PRI and DAR) were computed for each hemisphere (intrahemispheric index) and for both hemispheres (cerebral index). Considering the cerebral index (DAR and PRI), our results showed a slowing in brain activity in poststroke patients when compared to healthy controls. Only the intrahemispheric PRI index was able to find significant interhemispheric differences of frequency oscillations. Despite being unable to detect interhemispheric differences, the DAR index seems to be more sensitive to detect motor impairment-related frequency oscillations. The intrahemispheric PRI index may provide insights into therapeutic approaches for interhemispheric asymmetry after stroke.

1. Introduction

Stroke is one of the leading causes of adult disability worldwide [1]. Following a stroke, an imbalance in the interhemispheric cortical interaction may be established [2]. The ability to perform skilled limb movements requires a dynamic interaction between the hemispheres. Maladaptive functioning of this interhemispheric interaction and consequently changes in hemisphere neural activity after stroke are thought to be factors underlying motor impairments and the poorest motor recovery in these patients [3–5].

The abnormal interhemispheric interaction after a brain injury has been mainly investigated by functional magnetic resonance imaging (fMRI), positron emission tomography (PET), and transcranial magnetic stimulation (TMS) [5, 6]. The quantitative electroencephalography (qEEG) may also be a reliable instrument for detecting alterations of interhemispheric interaction poststroke. The presence of low-frequency oscillations (delta and theta rhythm) in the EEG signal is linked to the decline in neuronal integrity [7, 8], whereas the presence of fast-frequency oscillations (alpha, beta, and gamma rhythm) after stroke is associated with the motor recovery and functional outcome following stroke [7, 9]. Thus, the qEEG index of ratio between slower and faster frequencies such as the delta/alpha ratio (DAR) [10], the power ratio index (PRI; delta + theta/alpha + beta) [11, 12],

and the theta/beta ratio (TBR) [13, 14] has been largely employed in stroke studies [10, 13, 15–19].

However, to the best of our knowledge, few studies have used PRI and DAR indexes for investigating the difference between affected and unaffected hemisphere in poststroke subjects. In a recent study, Fanciullacci et al. (2017) did not find any significant interhemispheric difference for DAR in subacute poststroke individuals with cortical-subcortical and subcortical lesions. Moreover, Fanciullacci et al. [18] did not consider motor impairment severity, while recent findings using TMS suggested that cortical activity changes within both hemispheres are strongly associated with motor impairments [20].

Our matched controlled study proposed a new perspective for the analysis of these qEEG indexes within each hemisphere. We hypothesized that ratios between slower and faster frequencies in each hemisphere would be more appropriate to study neural activity changes for considering the interhemispheric differences after stroke. Moreover, we expected that such interhemispheric differences of DAR and PRI after stroke might critically depend on motor impairments.

2. Methods

2.1. Participants. Forty-seven poststroke patients were recruited from local rehabilitation clinics. These patients had mild/moderate (25; 52% males; mean age: 59.6) and severe (22; 45.5% males; mean age: 58.2) motor impairment based on the upper limb section of the Fugl–Meyer assessment [21]. It included patients with upper limb hemiparesis resulting from ischemic or hemorrhagic stroke (>3 months) aged from 18 to 75 years old. We excluded patients with cognitive impairment (<18 in the mini mental state examination (MMSE)) or with any psychiatric disorder. As a control study, self-reported healthy volunteers aged and sex-matched with the patients were also included in the study. This study was reviewed and approved by the local human ethical committee. All patients and healthy controls signed the informed consent before participating in the study. Clinical sociodemographic characteristics were collected. Handedness was self-reported.

2.2. Motor Impairment Severity. The upper limb section of the Fugl–Meyer assessment (UL-FMA) with a maximum score of 66 [21] was applied to evaluate the level of motor impairment. Poststroke patients were classified: with mild/-moderate (>19 ± 2 points in UL-FMA) and with severe motor impairment (<19 ± 2 points) according to the classification described by Woodbury et al. [22].

2.3. EEG Data Acquisition and Processing. EEG was recorded for 60 seconds in an isolated room with volunteers with eyes opened and seated in a comfortable armchair, as recommended by the American Clinical Neurophysiology Society Guideline [23, 24]. EEG was recorded using a digital EEG equipment (Neuron-Spectrum/Neurosoft, Russia) with nine Ag/AgCl scalp electrodes placed at F3, C3, P3, Fz, Cz, Pz, F4, C4, and P4 and the reference electrodes at A1 and A2 according to the international 10/20 system at a sampling frequency of 500 Hz. The electrode impedances were kept well below 15 kΩ. The signal was filtered with a bandpass (0.5–100 Hz) and a notch filter of 60 Hz.

Offline signal processing was performed by the toolbox EEGLab in the MATLAB® R2014a for Windows. EEG data file was segmented into 30 data points. The artifact analysis was performed in the continuous data by the independent component analysis (ICA) with the RUNICA algorithm. The ICA may be used to remove artifacts embedded in the data (muscle, eye blinks, or eye movement) without removing the affected data position. Following the identification of the artifacts, the rejection was performed by the Multiple Artifact Rejection Algorithm (MARA), considering a cutoff of 50% [25]. Then, the spectral power density (PSD) was computed for each electrode using the Welch estimator, through an approximation of the edge over the Hanning window [26]. The absolute power was calculated for delta (δ) (0.5 to ≤4 Hz), theta (θ) (>4 to ≤8 Hz), alpha (α) (>8 to ≤13 Hz), beta (β) (>13 to ≤30 Hz), and gamma (γ) (<30 *a* ≤ 45 Hz) [27]. Moreover, the relative band power was calculated by dividing each band's absolute band power with the total power in 0.5-45 Hz. The relative power at each electrode was averaged to obtain global relative power and this global relative power was used to calculate power ratio index (PRI), delta to alpha ratio (DAR), and theta to beta ratio (TBR). PRI was calculated as $\mathrm{PRI} = (r\delta + r\theta)/(r\alpha + r\beta)$ [11]. DAR was calculated as $\mathrm{DAR} = r\delta/r\alpha$ [10]. TBR was calculated as $\mathrm{TBR} = r\theta/r\beta$ [13].

The qEEG index (PRI and DAR) was computed for each hemisphere (intrahemispheric index) and for both hemispheres (cerebral index). The intrahemispheric index was defined as the mean of the global relative power over electrodes within each hemisphere (left side: F3, C3, and P3; right side: F4, C4, and P4). The cerebral index was defined as the mean of the global relative power over all nine electrodes (F3, C3, P3, Fz, Cz, Pz, F4, C4, and P4).

2.4. Data Analysis. Kolmogorov-Smirnov was performed to assess the data normality. First, the independent sample *t* -test was used to compare the cerebral index between poststroke patients and healthy volunteers. One-way ANOVA repeated measure analysis for each population separately (poststroke and healthy volunteers) was performed for the intragroup comparison among each intrahemispheric index and cerebral index. For poststroke patients, a two-way ANOVA repeated measure with intrahemispheric/cerebral index (affected hemispheric index, unaffected hemispheric index, and cerebral index) as within factor and motor impairment (mild/moderate and severe) as between factors was performed. When necessary, post hoc analysis was performed using *t*-test. For multiple comparisons, Bonferroni's correction was applied. Mauchly's sphericity was checked, and Greenhouse-Geisser correction was performed when necessary. For all analysis, the observed power of statistical (η^2) analysis was calculated; also, the *t*-test Cohen's D (d) was reported. Statistical analysis was performed using SPSS (Statistical Package for the Social Sciences) software 20.0 for Windows, adopting a significance level (p) of 0.05.

3. Results

Fifty-six poststroke patients and fourteen healthy volunteers were assessed. Nine poststroke patients and two healthy volunteers had the data missing for EEG acquisition errors. Thus, forty-seven poststroke and twelve healthy volunteers had the data analyzed. Figure 1 shows the flowchart of the volunteers in the study. Table 1 depicts the demographic and clinical characteristics of the participants.

3.1. Power Ratio Index. Considering the cerebral index, the independent sample t-test revealed a slowing in brain activity in poststroke patients when compared to healthy volunteers (poststroke: 2.71 ± 0.51; healthy: 2.09 ± 0.71; $d = 1.00$; $t = 3.41$; $p = 0.001$).

The one-way ANOVA showed a significant effect of intrahemispheric/cerebral index for the poststroke patients ($F_{(1.06,48.6)} = 10.74$; $p = 0.02$; $\eta^2 = 0.91$), but not for healthy volunteers ($F_{(1.01,12.1)} = 0.38$; $p = 0.57$; $\eta^2 = 0.09$). The post hoc analysis revealed an increased intrahemispheric PRI index in the affected hemisphere when compared to the unaffected intrahemispheric (affected hemisphere: 2.75 ± 0.54; unaffected hemisphere: 2.63 ± 0.47; $d = 0.23$; $t = -3.26$; $p = 0.002$) and cerebral index (cerebral index: 2.71 ± 0.51; $d = 0.07$; $t = 2.20$; $p = 0.03$). A decreased intrahemispheric PRI index in the unaffected hemisphere was found when compared to cerebral index (unaffected hemisphere: 2.62 ± 0.47; cerebral index: 2.71 ± 0.51; $d = 0.18$; $t = -3.91$; $p < 0.001$).

The two-way ANOVA showed a significant main effect for intrahemispheric/cerebral index ($F_{(1.06,47.8)} = 12.65$; $p = 0.001$; $\eta^2 = 0.95$) and for interaction between the two main factors ($F_{(1.06,47.8)} = 5.14$; $p = 0.026$; $\eta^2 = 0.62$), but not for motor impairment factor ($F_{(1,45)} = 2.72$; $p = 0.11$; $\eta^2 = 0.36$). In contrast to healthy controls (non-domH: 2.08 ± 0.70; domH: 2.11 ± 0.67; $d = 0.04$; $t = 0.64$; $p = 0.54$) and poststroke patients with mild/moderate motor impairment (mild/moderate-affected hemisphere: 2.60 ± 0.41; mild/moderate-unaffected hemisphere: 2.56 ± 0.41; $d = 0.09$; $t = -1.62$; $p = 0.12$), the post hoc analysis revealed a significant difference between intrahemispheric PRI index of the affected and nonaffected hemisphere in the patients with severe motor impairment (severe-affected hemisphere: 2.91 ± 0.62; severe-unaffected hemisphere: 2.70 ± 0.51; $d = 0.36$; $t = -3.00$; $p = 0.007$). All intrahemispheric PRI index differed to the cerebral index, except for the affected hemisphere of poststroke patients with mild/moderate motor impairment (mild/moderate cerebral index: 2.60 ± 0.41; severe cerebral index: 2.83 ± 0.59; $d = 0.45$; $t = -3.91$; $p < 0.001$). Table 2 shows the intrahemispheric and cerebral power ratio index (PRI) in poststroke patients with upper limb mild/moderate and severe motor impairment and healthy subjects.

3.2. Delta to Alpha Ratio. Similar to cerebral PRI index, the independent sample t-test revealed a statistical slowing in brain activity, as revealed by increased DAR index, in poststroke patients when compared to healthy controls (poststroke: 2.20 ± 0.36; healthy: 1.79 ± 0.50; $d = 0.94$; $t = 3.28$; $p = 0.02$). Table 3 shows the DAR in poststroke and healthy individuals.

The one-way ANOVA showed no significant effect of intrahemispheric/cerebral index for the poststroke patients ($F_{(1.69,77.9)} = 0.22$; $p = 0.80$; $\eta^2 = 0.08$) and for healthy controls ($F_{(1.07,11.8)} = 0.19$; $p = 0.83$; $\eta^2 = 0.08$).

The two-way ANOVA showed a significant effect only for motor impairment factor ($F_{(1,45)} = 13.11$; $p = 0.01$; $\eta^2 = 0.94$). The post hoc test revealed increased DAR index for poststroke patients with severe motor impairment when compared to the mild/moderate motor impairment for intrahemispheric index (mild/moderate-affected hemisphere: 2.06 ± 0.29; severe-affected hemisphere: 2.41 ± 0.26; $d = 1.27$; $t = -4.30$; $p < 0.001$; mild/moderate-unaffected hemisphere: 2.05 ± 0.32; severe-unaffected hemisphere: 2.36 ± 0.42; $d = 0.83$; $t = -2.90$; $p = 0.006$) and for cerebral index (mild/moderate: 2.07 ± 0.31; severe: 2.35 ± 0.36; $d = 0.83$; $t = -2.87$; $p = 0.006$).

3.3. Theta to Beta Ratio. Even as PRI and DAR, the independent sample t-test revealed an increased TBR index meaning a statistical slowing in brain activity in poststroke patients when compared to healthy controls (poststroke: 5.07 ± 2.18; healthy: 2.09 ± 0.71; $d = 1.83$; $t = 7.85$; $p < 0.01$). Table 4 shows the TBR in poststroke and healthy controls.

Similar to the PRI index, the one-way ANOVA showed a statistical difference for intrahemispheric/cerebral index for the poststroke patients ($F_{(1.04,47.99)} = 5.60$; $p = 0.02$; $\eta^2 = 0.65$) and no differences for healthy volunteers ($F_{(1.09,12.08)} = 0.38$; $p = 0.56$; $\eta^2 = 0.09$). The post hoc analysis showed an increased intrahemispheric TBR index in the affected hemisphere when compared to the unaffected intrahemispheric (affected hemisphere: 5.39 ± 2.44; unaffected hemisphere: 4.85 ± 2.09; $d = 0.23$; $t = -2.38$; $p = 0.02$) and cerebral index (cerebral index: 5.07 ± 2.18; $d = 0.13$; $t = 2.51$; $p = 0.01$). In addition, a decreased intrahemispheric TBR index in the unaffected hemisphere was found when compared to cerebral index ($d = 0.10$; $t = -2.04$; $p = 0.04$).

According to the motor impairment analysis, the two-way ANOVA showed a significant main effect for intrahemispheric/cerebral index ($F_{(1.04,47.07)} = 6.32$; $p = 0.01$; $\eta^2 = 0.70$). However, no interaction was revealed between the two main factors ($F_{(1.04,47.07)} = 2.80$; $p = 0.09$; $\eta^2 = 0.38$) and for motor impairment factor ($F_{(1,45)} = 3.48$; $p = 0.06$; $\eta^2 = 0.44$). In addition, the post hoc analysis revealed a significant difference between intrahemispheric TBR index only for the severe motor impairment poststroke patients in the affected and unaffected hemisphere (severe-affected hemisphere: 6.21 ± 2.70; severe-unaffected hemisphere: 5.27 ± 2.37; $d = 0.37$; $t = -2.35$; $p = 0.02$), affected hemisphere and cerebral index (severe cerebral index: 5.66 ± 2.49; $d = 0.21$; $t = 2.33$; $p = 0.03$), and unaffected hemisphere and cerebral index ($d = 0.16$; $t = -2.17$; $p = 0.04$).

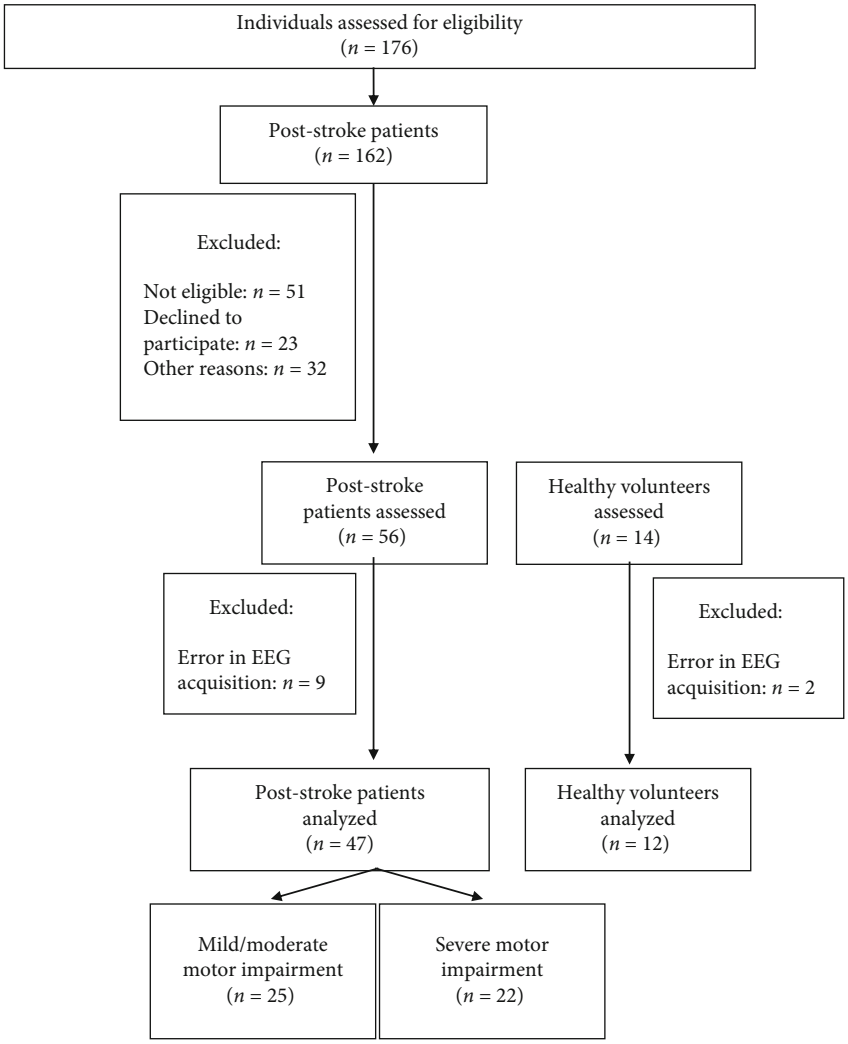

Figure 1: Flowchart of the study.

Table 1: Demographic and clinical characteristics of participants.

	Poststroke patients		Healthy volunteers
	Mild/moderate motor impairment ($n = 25$)	Severe motor impairment ($n = 22$)	($n = 12$)
Age, mean ± SD (years)	59.6 ± 8.4	58.2 ± 10.0	53.3 ± 6.3
Gender (%)			
Male	52%	45.5%	50%
Handedness (%)			
Right	88%	95.5%	91.7%
UL-FMA, mean ± SD (score)	38.7 ± 12.5	12.2 ± 4.0	—
Hemiparesis (%)			
Left	60%	63.6%	—
Time since stroke, mean ± SD (months)	38.3 ± 32.7	54.9 ± 40.4	—

SD: standard deviation; UL-FMA: upper limb Fugl–Meyer assessment.

4. Discussion

As expected, we found a slowing brain electrical activity of poststroke patients. The presence of low-frequency oscillations (delta and theta) has been associated with brain injuries, as in our poststroke patients [28, 29].

A previous study has investigated the PSD in acute poststroke, showing a higher delta power in poststroke patients

Table 2: Intrahemispheric and cerebral power ratio index (PRI) in poststroke patients with upper limb mild/moderate and severe motor impairment and healthy subjects.

	Intrahemispheric index		Cerebral index	Within-group differences		
	Affected/non-domH	Unaffected/domH		Affected/non-domH vs. unaffected/domH	Affected/non-domH vs. cerebral index	Affected/domH vs. cerebral index
Healthy	2.08 ± 0.70	2.11 ± 0.67	2.10 ± 0.71	—	—	—
Poststroke patients	2.75 ± 0.54	2.63 ± 0.47	2.71 ± 0.51	$t = -3.26$; $p = 0.002$	$t = 2.20$; $p = 0.03$	$t = -3.91$; $p < 0.001$
Mild/moderate	2.60 ± 0.41	2.56 ± 0.41	2.60 ± 0.41	—	—	—
Severe	2.91 ± 0.62	2.70 ± 0.53	2.83 ± 0.59	$t = -3.00$; $p = 0.007$	—	—

non-domH: nondominant hemisphere; domH: dominant hemisphere. Data are mean ± SD. Significant post hoc test values for within-group differences are shown.

Table 3: Intrahemispheric and cerebral delta to alpha ratio (DAR) in poststroke patients with upper limb mild/moderate and severe motor impairment and healthy subjects.

	Intrahemispheric index		Cerebral index
	Affected/non-domH	Unaffected/domH	
Healthy	1.77 ± 0.49	1.79 ± 0.48	1.79 ± 0.50
Poststroke patients	2.22 ± 0.32	2.20 ± 0.40	2.20 ± 0.36
Mild/moderate	2.06 ± 0.29	2.05 ± 0.32	2.07 ± 0.31
Severe	2.41 ± 0.26	2.36 ± 0.42	2.35 ± 0.36

non-domH: nondominant hemisphere; domH: dominant hemisphere. Data are mean ± SD.

when compared to healthy volunteers [10, 30] and in the affected hemisphere of subcortical poststroke patients [18]. The delta oscillations originate in neurons in the thalamus and in deep cortical layers, which may reflect hyperpolarization and inhibition of cortical neurons, resulting in a decrease in neural activity [31]. In addition, it is expected in the poststroke patients, a suppression of high frequency alpha and beta band rhythms [32], since the presence of these rhythms is functionally related to the sensorimotor system, which is activated through motor preparation or execution [33].

In our study, we found an increased intrahemispheric PRI and TBR index in the affected hemisphere when compared to unaffected intrahemispheric and cerebral index and a decreased intrahemispheric PRI and TBR index in the unaffected hemisphere when compared to cerebral index. An increase in these indexes in a specific brain hemisphere supports our hypothesis that the qEEG index for the poststroke patients should be assessed to separate the affected and unaffected hemispheres. PRI seems to be a sensitive index to detect interhemispheric changes in cortical activity.

These findings were in line with previous studies that measure poststroke cerebral and interhemispheric activity by fMRI or TMS [34, 35]. The interhemispheric activity has been used as a surrogate outcome and prognostic factor to predict and monitor stroke progression [15, 34]. In this way, this imbalance could represent the worst prognosis as suggested by Min et al. (2019), which demonstrated slow PSD in the affected hemisphere, while the unaffected hemisphere has a higher PSD.

In contrast to the PRI and TBR indexes, the DAR analysis did not show a difference between the affected and unaffected hemispheres (intrahemispheric DAR index) or in comparison to the cerebral DAR index. Theta band is a potential predictive biomarker for cognitive impairment in patients with cerebral infarcts [36]. The TBR index is also a biomarker of brain processes involved in executive control processes [36], that is, the theta contribution can bring more and valuable information about the poststroke patient. The beta contribution in PRI measure is expected to be increased to determine a better motor recovery outcome (smaller PRI). Indeed, the increase of fast qEEG waves, especially beta rhythm, had been associated with motor recovery in poststroke [7, 9].

Another interesting result is related to the severity of motor impairment. The DAR seems to be a more sensitive index to assessing the severity of the motor impairment in poststroke patients than the PRI index. This trend could be seen for the affected and unaffected hemispheres of the interhemispheric index, as well as for the cerebral index. At the same time, the PRI had detected the difference only at the affected hemisphere. This finding supports the current literature that shows an association between DAR and clinical outcomes [29, 37]. The presence of alpha oscillation indicates neuronal survival [38] and indirectly reflects a decreased DAR. Some studies have demonstrated that the extension of area affected by the infarct is related to motor severity and recovery [39].

Some studies have claimed that an imbalance between interhemispheric connections is related to the severity of the sensorimotor impairment and to the motor recovery post cerebral infarct [2, 6, 20, 37].

Understanding the behavior of the affected and unaffected hemisphere and the severity of motor impairment of the poststroke patients can allow some interventions targeting the individual need, as through neurofeedback by brain-computer interface [14, 19, 40]. With the present study results, we would to suggest a neurofeedback aiming the increase of beta rhythm and decrease of delta for the reduction of the hemispheric PRI in the affected hemisphere.

The main limitation of this study was the limited number of channels in EEG acquisition. We used nine channels

Table 4: Intrahemispheric and cerebral theta to beta ratio (TBR) in poststroke patients with upper limb mild/moderate and severe motor impairment and healthy subjects.

	Intrahemispheric index		Cerebral index	Within-group differences		
	Affected/ non-domH	Unaffected/ domH		Affected/non-domH vs. unaffected/domH	Affected/non-domH vs. cerebral index	Affected/domH vs. cerebral index
Healthy	2.08 ± 0.70	2.11 ± 0.67	2.09 ± 0.71	—	—	—
Poststroke patients	5.39 ± 2.44	4.85 ± 2.09	5.07 ± 2.18	$t = -2.38$; $p = 0.02$	$t = 2.51$; $p = 0.01$	$t = -2.04$; $p = 0.04$
Mild/ moderate	4.67 ± 1.90	4.49 ± 1.78	4.54 ± 1.74	—	—	—
Severe	6.21 ± 2.7	5.27 ± 2.37	5.66 ± 2.49	$t = -2.35$; $p = 0.02$	$t = 2.33$; $p = 0.03$	$t = -2.17$; $p = 0.04$

non-domH: nondominant hemisphere; domH: dominant hemisphere. Data are mean ± SD. Significant post hoc test values for within-group differences are shown.

that were distributed to capture the cerebral activity of the right and left hemispheres. The extension and lesion location of the affected hemisphere were not controlled. Indeed, evidence suggests that EEG response can vary in patients with stroke depending on lesion [41].

5. Conclusion

The intrahemispheric PRI and TBR indexes are able to find significant interhemispheric differences of frequency oscillations. Despite being unable to detect interhemispheric differences, the DAR index seems to be more sensitive to detect motor impairment-related frequency oscillations. As PRI has the four more usable EEG frequency (delta, theta, alpha, and beta), the intrahemispheric PRI index could provide insights into a precise therapeutic approach through noninvasive brain stimulation or neurofeedback for interhemispheric asymmetry after stroke. These results point out a new perspective of analysis for the cerebral activity in poststroke patients, which could be used as a biomarker of motor recovery and/or as a prognostic measure. Additionally, DAR is the more sensitive index to assessing the severity of motor impairment. This information added to the analysis of each hemisphere's spectral power could guide some interventions as neurofeedback or noninvasive brain stimulations.

Data Availability

The data that support the findings of this study are available from the corresponding author (DP) upon reasonable request.

Conflicts of Interest

The authors report no conflicts of interest.

Acknowledgments

This study was financed in part by the Coordenação de Aperfeiçoamento de Pessoal de Nível Superior–Brasil (CAPES)–Finance Code 001. KMS is supported by CNPq, Grant No. 308291/2015-8.

References

[1] WHO, *WHO | The Atlas of Heart Disease and Stroke*, WHO, 2010.

[2] D. A. Nowak, C. Grefkes, M. Ameli, and G. R. Fink, "Interhemispheric competition after stroke: brain stimulation to enhance recovery of function of the affected hand," *Neurorehabilitation and Neural Repair*, vol. 23, no. 7, pp. 641–656, 2009.

[3] Y. S. Min, J. W. Park, K. E. Jang et al., "Power spectral density analysis of long-term motor recovery in patients with subacute stroke," *Neurorehabilitation and Neural Repair*, vol. 33, no. 1, pp. 38–46, 2019.

[4] M. P. A. van Meer, K. van der Marel, K. Wang et al., "Recovery of sensorimotor function after experimental stroke correlates with restoration of resting-state interhemispheric functional connectivity," *Journal of Neuroscience*, vol. 30, no. 11, pp. 3964–3972, 2010.

[5] N. Murase, J. Duque, R. Mazzocchio, and L. G. Cohen, "Influence of interhemispheric interactions on motor function in chronic stroke," *Annals of Neurology*, vol. 55, no. 3, pp. 400–409, 2004.

[6] C. Grefkes and G. R. Fink, "Connectivity-based approaches in stroke and recovery of function," *The Lancet Neurology*, vol. 13, no. 2, pp. 206–216, 2014.

[7] A. Thibaut, M. Simis, L. R. Battistella et al., "Using brain oscillations and corticospinal excitability to understand and predict post-stroke motor function," *Frontiers in Neurology*, vol. 8, pp. 1–8, 2017.

[8] B. Kim and C. Winstein, "Can neurological biomarkers of brain impairment be used to predict poststroke motor recovery? A systematic review," *Neurorehabilitation and Neural Repair*, vol. 31, no. 1, pp. 3–24, 2017.

[9] F. Pichiorri, M. Petti, S. Caschera, L. Astolfi, F. Cincotti, and D. Mattia, "An EEG index of sensorimotor interhemispheric coupling after unilateral stroke: clinical and neurophysiological study," *European Journal of Neuroscience*, vol. 47, no. 2, pp. 158–163, 2018.

[10] S. Finnigan, A. Wong, and S. Read, "Defining abnormal slow EEG activity in acute ischaemic stroke: Delta/alpha ratio as an optimal QEEG index," *Clinical Neurophysiology*, vol. 127, no. 2, pp. 1452–1459, 2016.

[11] K. Nagata, K. Tagawa, S. Hiroi, F. Shishido, and K. Uemura, "Electroencephalographic correlates of blood flow and oxygen metabolism provided by positron emission tomography in

patients with cerebral infarction," *Electroencephalography and Clinical Neurophysiology*, vol. 72, no. 1, pp. 16–30, 1989.

[12] K. Nagata, C. E. Gross, G. W. Kindt, M. J. Geier, and G. R. Adey, "Topographic electroencephalographic study with power ratio index mapping in patients with malignant brain tumors," *Neurosurgery*, vol. 17, no. 4, pp. 613–619, 1985.

[13] R. Mane, E. Chew, K. S. Phua, K. K. Ang, A. P. Vinod, and C. Guan, "Quantitative EEG as biomarkers for the monitoring of post-stroke motor recovery in BCI and tDCS rehabilitation," in *Proceedings of the Annual International Conference of the IEEE Engineering in Medicine and Biology Society, EMBS*, vol. 2018, pp. 3610–3613, Honolulu, HI, USA, 2018.

[14] R. Mane, E. Chew, K. S. Phua et al., "Prognostic and monitory EEG-biomarkers for BCI upper-limb stroke rehabilitation," *IEEE transactions on neural systems and rehabilitation engineering*, vol. 27, no. 8, pp. 1654–1664, 2019.

[15] C. Bentes, A. R. Peralta, P. Viana et al., "Quantitative EEG and functional outcome following acute ischemic stroke," *Clinical Neurophysiology*, vol. 129, no. 8, pp. 1680–1687, 2018.

[16] J. Leon-Carrion, J. F. Martin-Rodriguez, J. Damas-Lopez, J. M. B. y Martin, and M. R. Dominguez-Morales, "Delta-alpha ratio correlates with level of recovery after neurorehabilitation in patients with acquired brain injury," *Clinical Neurophysiology*, vol. 120, no. 6, pp. 1039–1045, 2009.

[17] M. Saes, C. G. M. Meskers, A. Daffertshofer, J. C. de Munck, G. Kwakkel, and E. E. H. van Wegen, "How does upper extremity Fugl-Meyer motor score relate to resting-state EEG in chronic stroke? A power spectral density analysis," *Clinical Neurophysiology*, vol. 130, no. 5, pp. 856–862, 2019.

[18] C. Fanciullacci, F. Bertolucci, G. Lamola et al., "Delta power is higher and more symmetrical in ischemic stroke patients with cortical involvement," *Frontiers in Human Neuroscience*, vol. 11, pp. 1–10, 2017.

[19] P. Trujillo, A. Mastropietro, A. Scano et al., "Quantitative EEG for predicting upper limb motor recovery in chronic stroke robot-assisted rehabilitation," *IEEE Transactions on Neural Systems and Rehabilitation Engineering*, vol. 27, no. 5, pp. 1058–1067, 2017.

[20] J. Veldema, K. Bösl, and D. A. Nowak, "Cortico-spinal excitability and hand motor recovery in stroke: a longitudinal study," *Journal of Neurology*, vol. 265, no. 5, pp. 1071–1078, 2018.

[21] E. J. Woytowicz, J. C. Rietschel, R. N. Goodman et al., "Determining levels of upper extremity movement impairment by applying a cluster analysis to the Fugl-Meyer assessment of the upper extremity in chronic stroke," *Archives of Physical Medicine and Rehabilitation*, vol. 98, no. 3, pp. 456–462, 2017.

[22] M. L. Woodbury, C. A. Velozo, L. G. Richards, P. W. Duncan, S. Studenski, and S.-M. Lai, "Longitudinal stability of the Fugl-Meyer assessment of the upper extremity," *Archives of Physical Medicine and Rehabilitation*, vol. 89, no. 8, pp. 1563–1569, 2008.

[23] J. J. Halford, D. Sabau, F. W. Drislane, T. N. Tsuchida, and S. R. Sinha, "American Clinical Neurophysiology Society guideline 4: recording clinical EEG on digital media," *Journal of Clinical Neurophysiology*, vol. 33, no. 4, pp. 317–319, 2016.

[24] S. R. Sinha, L. Sullivan, D. Sabau et al., "American Clinical Neurophysiology Society guideline 1: minimum technical requirements for performing clinical electroencephalography," *Journal of Clinical Neurophysiology*, vol. 33, no. 4, pp. 303–307, 2016.

[25] I. Winkler, S. Brandl, F. Horn, E. Waldburger, C. Allefeld, and M. Tangermann, "Robust artifactual independent component classification for BCI practitioners," *Journal of Neural Engineering*, vol. 11, no. 3, article 035013, 2014.

[26] Z. Li, L. Zhang, F. Zhang, R. Gu, W. Peng, and L. Hu, "Demystifying signal processing techniques to extract resting-state EEG features for psychologists," *Brain Science Advances*, vol. 6, no. 3, pp. 189–209, 2020.

[27] A. J. Casson, M. Abdulaal, M. Dulabh, S. Kohli, S. Krachunov, and E. Trimble, "Electroencephalogram," in *Seamless Healthcare Monitoring*, pp. 45–81, Springer International Publishing, Cham, 2018.

[28] W. J. Freeman and R. Q. Quiroga, "Imaging brain function with EEG: advanced temporal and spatial analysis of electroencephalographic signals," *Imaging Brain Function With EEG: Advanced Temporal and Spatial Analysis of Electroencephalographic Signals*, vol. 9781461449, pp. 1–248, 2013.

[29] S. Finnigan and M. J. A. M. van Putten, "EEG in ischaemic stroke: quantitative EEG can uniquely inform (sub-)acute prognoses and clinical management," *Clinical Neurophysiology*, vol. 124, no. 1, pp. 10–19, 2013.

[30] R. Poryazova, R. Huber, R. Khatami et al., "Topographic sleep EEG changes in the acute and chronic stage of hemispheric stroke," *Journal of Sleep Research*, vol. 24, no. 1, pp. 54–65, 2015.

[31] E. R. John and L. S. Prichep, "The relevance of QEEG to the evaluation of behavioral disorders and pharmacological interventions," *Clinical EEG and Neuroscience*, vol. 37, no. 2, pp. 135–143, 2006.

[32] W. J. Freeman and R. Q. Quiroga, "Frequency analysis," in *Imaging Brain Function With EEG*, pp. 21–36, Springer New York, New York, NY, 2013.

[33] G. Pfurtscheller and C. Neuper, "Motor imagery activates primary sensorimotor area in humans," *Neuroscience Letters*, vol. 239, no. 2–3, pp. 65–68, 1997.

[34] P. Wu, F. Zeng, Y. Li et al., "Changes of resting cerebral activities in subacute ischemic stroke patients," *Neural Regeneration Research*, vol. 10, no. 5, pp. 760–765, 2015.

[35] M. Simis, V. di Lazzaro, A. Kirton et al., "Étude transversale multicentrique de mesures neurophysiologiques du cortex moteur lese ou non lese dans l'AVC," *Neurophysiologie Clinique*, vol. 46, no. 1, pp. 53–61, 2016.

[36] D. van Son, F. M. De Blasio, J. S. Fogarty, A. Angelidis, R. J. Barry, and P. Putman, "Frontal EEG theta/beta ratio during mind wandering episodes," *Biological Psychology*, vol. 140, pp. 19–27, 2019.

[37] S. P. Finnigan, M. Walsh, S. E. Rose, and J. B. Chalk, "Quantitative EEG indices of sub-acute ischaemic stroke correlate with clinical outcomes," *Clinical Neurophysiology*, vol. 118, no. 11, pp. 2525–2532, 2007.

[38] A. Alawieh, J. Zhao, and W. Feng, "Factors affecting post-stroke motor recovery: implications on neurotherapy after brain injury," *Behavioural Brain Research*, vol. 340, pp. 94–101, 2018.

[39] F. Bertolucci, C. Chisari, and F. Fregni, "The potential dual role of transcallosal inhibition in post-stroke motor recovery," *Restorative Neurology and Neuroscience*, vol. 36, no. 1, pp. 83–97, 2018.

[40] S. E. Kober, D. Schweiger, J. L. Reichert, C. Neuper, and G. Wood, "Upper alpha based neurofeedback training in chronic stroke: brain plasticity processes and cognitive effects," *Applied Psychophysiology Biofeedback*, vol. 42, no. 1, pp. 69–83, 2017.

[41] W. Park, G. H. Kwon, Y. H. Kim, J. H. Lee, and L. Kim, "EEG response varies with lesion location in patients with chronic stroke," *Journal of Neuro Engineering and Rehabilitation*, vol. 13, no. 1, pp. 1–10, 2016.

Hindawi
Neural Plasticity
Volume 2021, Article ID 9733926, 8 pages
https://doi.org/10.1155/2021/9733926

Research Article

The Frequency and Associated Factors of Asymmetrical Prominent Veins: A Predictor of Unfavorable Outcomes in Patients with Acute Ischemic Stroke

Yue Wang,[1] Jingjing Xiao,[2,3] Li Zhao,[4] Shaoshi Wang,[2,3] Mingming Wang,[3,5] Yu Luo,[3,5] Huazheng Liang,[3] and Lingjing Jin[1,6]

[1]*Department of Neurological Rehabilitation, Shanghai YangZhi Rehabilitation Hospital (Shanghai Sunshine Rehabilitation Center), School of Medicine, Tongji University, Shanghai 201619, China*
[2]*Department of Neurology, Shanghai Fourth People's Hospital, School of Medicine, Tongji University, Shanghai, China*
[3]*Translational Research Institute of Brain and Brain-Like Intelligence Affiliated to Tongji University School of Medicine, Shanghai, China*
[4]*Administration Department of Nosocomial Infection Affiliated to Zhongshan Hospital of Dalian University, China*
[5]*Department of Radiology, Shanghai Fourth People's Hospital, School of Medicine, Tongji University, Shanghai, China*
[6]*Neurotoxin Research Center of Key Laboratory of Spine and Spinal Cord Injury Repair and Regeneration of Ministry of Education, Tongji University School of Medicine, 389 Xincun Road, 200065 Shanghai, China*

Correspondence should be addressed to Yu Luo; duolan@hotmail.com, Huazheng Liang; huazheng_liang@tongji.edu.cn, and Lingjing Jin; lingjingjin@163.com

Received 25 April 2021; Revised 13 August 2021; Accepted 16 August 2021; Published 17 September 2021

Academic Editor: Xi-Ze Jia

Objectives. The present study is aimed at investigating the frequency and associated factors of asymmetrical prominent veins (APV) in patients with acute ischemic stroke (AIS). *Methods*. Consecutive patients with AIS admitted to the Comprehensive Stroke Center of Shanghai Fourth People's Hospital between January 2013 and December 2017 were enrolled. MRI including diffusion-weighted imaging (DWI), perfusion-weighted imaging (PWI), and susceptibility-weighted imaging (SWI) was performed within 12 hours of symptom onset. The volume of asymmetrical prominent veins (APV) was evaluated using the Signal Processing In nuclear magnetic resonance software (SPIN, Detroit, Michigan, USA). Multivariate analysis was used to assess relationships between APV findings and medical history, clinical variables as well as cardio-metabolic indices. *Results*. Seventy-six patients met the inclusion criteria. The frequency of APV ≥ 10 mL was 46.05% (35/76). Multivariate analyses showed that proximal artery stenosis or occlusion (≥50%) ($P < 0.001$, adjusted odds ratio (OR) = 660.0, 95%CI = 57.28-7604.88) and history of atrial fibrillation ($P < 0.001$, adjusted OR = 10.48, 95%CI = 1.78-61.68) were independent factors associated with high APV (≥10 mL). *Conclusion*. Our findings suggest that the frequency of APV ≥ 10 mL is high in patients with AIS within 12 hours of symptom onset. History of atrial fibrillation and severe proximal artery stenosis or occlusion are strong predictors of high APV as calculated by SPIN on the SWI map.

1. Introduction

Susceptibility-weighted imaging (SWI) has been increasingly used to observe asymmetrical prominent veins (APV) in the cerebral cortex and deep brain structures in patients with acute ischemic stroke (AIS) [1–6]. It is generally believed that APV includes asymmetrical prominent cortical veins (APCV) and asymmetrical deep medullary veins (ADMV) [7]. The presence of ADMV is related to APCV on SWI [7].

Subsequent studies have shown that APV is associated with the prognosis of AIS patients. A recent study on 43 patients with AIS demonstrated that APV was an independent prognostic factor for clinical outcome at 3 months [5]. Another study on 61 patients treated with recombinant

tissue plasminogen activator reported that multiple hypointense vessels on SWI could predict early neurological deterioration [1]. A recent study on 145 patients with AIS showed that APV might be a useful predictor for poor outcome at 3 months [2].

APV was typically defined as (1) the diameter of veins in the ischemic hemisphere was larger than that of the contralateral side and/or (2) the length and the number of veins in the ischemic hemisphere were increased compared to the contralateral hemisphere [1, 5, 8–10]. The presence of APV has been proposed to be related to increased deoxyhemoglobin which is closely related to the reduction of oxygen saturation and increase of oxygen extraction fraction [11–13].

It has been hypothesized that the ischemic area with APV represents the penumbra in ischemic stroke [11, 14, 15]. Recent studies have also shown that the APV is correlated with hypoperfusion [5, 16, 17]. A recent study on AIS patients with severe intracranial arterial stenosis or occlusion reported a 55% (60/109) prevalence of APV on SWI, which suggested that vascular stenosis or occlusion might be related to APV [3]. In clinical practice, we have noted that APV often occurs in patients with larger infarction [5]. Additionally, patients' clinical symptoms might be related to the APV volume. However, there are few studies on the frequency and associated factors of APV in AIS patients. Therefore, the present study is aimed at assessing the frequency and associated factors in AIS patients.

2. Materials and Methods

2.1. Design, Setting, and Participants. This retrospective study was carried out in the Stroke Center of Shanghai Fourth People's Hospital between 1st January 2013 and 31st December 2017. The Institutional Review Board of Shanghai Fourth People's Hospital approved the present study. Written informed consent was obtained from all subjects. The inclusion criteria were (1) >18 years old; (2) patients presented with ischemic stroke and diagnosed by two certified stroke neurologists using Chinese guidelines for diagnosis and treatment of acute ischemic stroke 2018; and (3) MRI scans included diffusion-weighted imaging (DWI), perfusion-weighted imaging (PWI), and SWI within 12 hours after symptom onset. The exclusion criteria were (1) imaging data were unavailable or clinical data were incomplete and (2) being pregnant or lactating. Multimodality MRI examination was completed at the same time as intravenous thrombolysis before initiating intravascular thrombectomy. A total of 76 patients (56 males and 20 females) were included in the present study.

Demographic information including age and vascular risk factors such as hypertension, diabetes mellitus, atrial fibrillation (AF), smoking, and drinking histories were recorded. Neurologic impairment on admission was assessed using the National Institute of Health Stroke Scale (NIHSS). Neurological deterioration (ND) on day 14 was evaluated as poor outcome. The definition of ND in our study refers to neurological deterioration with an increase in the NIHSS score ≥ 2 points on day 14 after admission [18]. The NIHSS and outcome were assessed by two experienced stroke neurologists who were blind to the imaging results.

2.2. MR Imaging Protocol. Multimodal MRI was performed on a 1.5 T scanner (MAGNETOM Avanto, Siemens Healthcare, Germany) using a standard 8-channel head coil. The scan protocol included T1-weighted images (T1WI), T2-weighted images (T2WI), fluid-attenuated inversion recovery (FLAIR), DWI, SWI, time-of-flight MR angiography (TOF-MRA), and PWI. Imaging parameters were listed below. DWI: TR = 3600 ms, TE = 102 ms, b value = 0 and 1000 s/mm^2, acquisition matrix = 192 × 192, FOV = 230 mm, section thickness = 5.5 mm, section gap = 1 mm, and duration = 70 s. PWI = TR/TE = 1590/32 ms, acquisition matrix = 128 × 128, dynamic scans = 50, FOV = 230 mm, section thickness = 5 mm, section gap = 1.5 mm, and duration = 84 s. Gadopentetate dimeglumine contrast agent (Shanghai Pharmaceutical Corporation, Shanghai, China) was intravenously injected (0.2 mmol/kg body weight) at a flow rate of 4 mL/s after flushing with 30 mL saline. SWI = 3D multiecho T2 ∗ −weighted gradient − echo sequence, TR/TE/flip angle = 49 ms/40 ms/15°, FOV = 230 mm, acquisition matrix = 221 × 320, section thickness = 1.6 mm, and duration = 351 s. TOF − MRA = TR/TE/flip angle = 25 ms/7 ms/25°, acquisition matrix = 241 × 256, section thickness = 0.7 mm, 1 slab, and duration = 189 s. The entire duration of the MR imaging protocol was 16 min. Both SWI and TOF-MRA were performed precontrast.

2.3. Radiologic Assessment. Original diffusion and perfusion imaging was postprocessed with an automated Rapid Processing of Perfusion and Diffusion (RAPID) software (Ischemaview USA, Version 4.9). The infarct lesion was measured by using the volume of the infarct core on ADC (ADC < 0.62×10^3 mm^2/s) and DWI (bright sign) maps. Meanwhile, DWI volume corresponds to ADC < 0.62×10^3 mm^2/s. The hypoperfused lesion (the volume of PWI) was defined as the volume of time-to-maximum of the residue function (Tmax) delay > 6 s [19]. By using the arterial input function of the contralateral middle cerebral artery, the Tmax graphs were generated by deconvolving of the tissue concentration-time curve.

The MRA was independently rated by 2 experienced neuroradiologists. Artifactual lesion areas were visually identified by an experienced stroke neurologist (Y.W.) and a neuroradiologist (Y.L.).

2.4. Definition of the APV. The processing included the following steps: firstly, the Susceptibility Mapping and phase Artifacts Removal Toolbox (SMART; Detroit, MI, USA) software was used to reconstruct the SWI mapping (SWIM) and maximum intensity projections (MIPs, slice thickness = 7 mm) [20]. Secondly, the Signal Processing In nuclear magnetic resonance (SPIN; Detroit, Michigan, USA) software was used to analyze and measure the APV volume on SWIM [8]. Thirdly, a threshold of the mean susceptibility value plus two times the standard deviation of the veins from the contralateral hemisphere was applied to remove the background brain tissue [8]. Fourthly, the final volume of APV of each participant was calculated using the Cavalieri

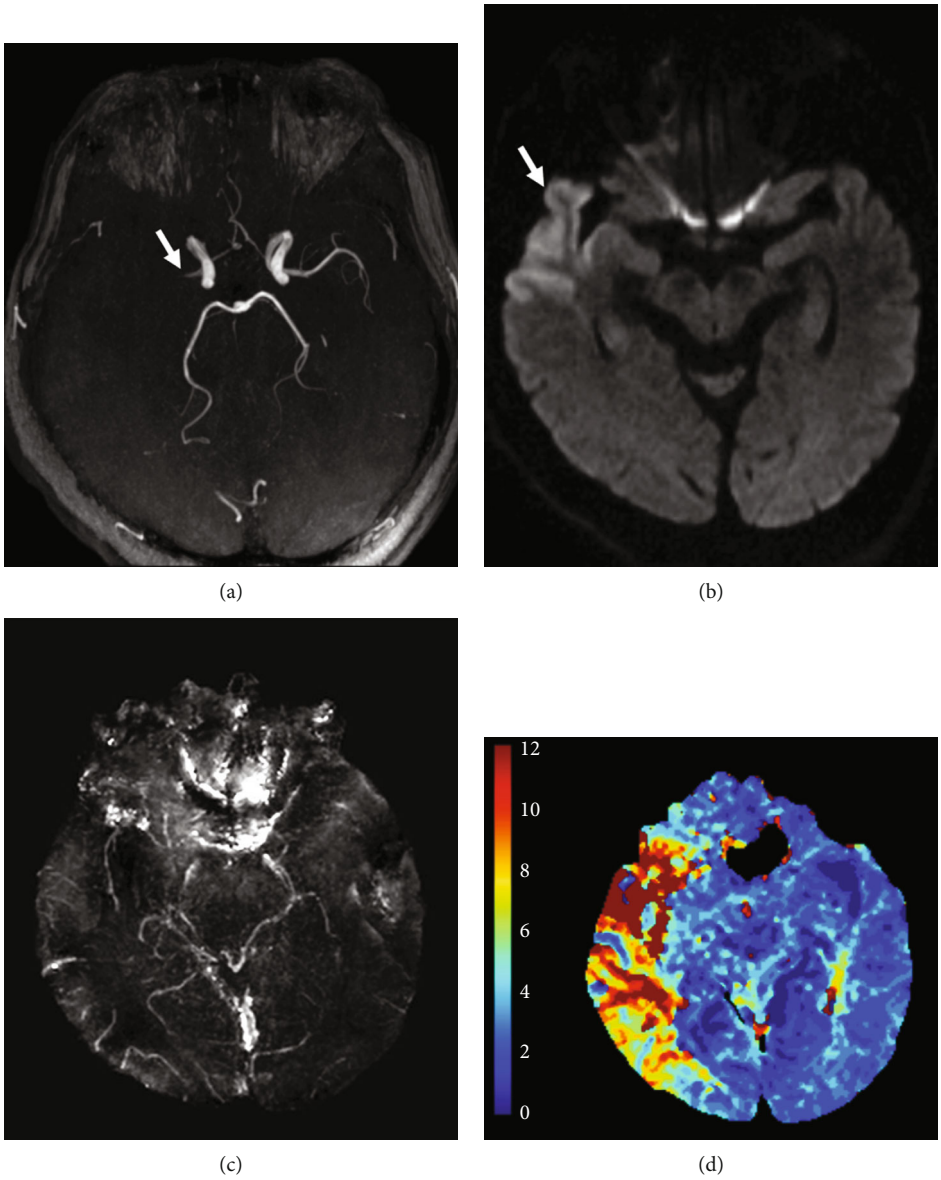

Figure 1: Examples of asymmetrical prominent veins on SWIM with corresponding DWI and time to maximum (Tmax) maps. (a) MR angiography showed occlusion of the right middle cerebral artery. (b) DWI showed a few small acute infarction lesions. (c) SWIM showed the APV region (yellow), which extended beyond the infarct core. The white arrow pointed to the thrombus. (d) Tmax > 6 s map (red and yellow).

method with the slice thickness and gap [8, 20] (see the Supplementary materials for details (available here)). Figure 1 showed an example of MRA, DWI, APV, and PWI.

All assessments were independently performed by two neuroradiologists (with 7 years and 10 years of MRI experience, respectively) who were blind to clinical data and other MR results. If their results were consistent, the final volume of APV for each participant was recorded as the mean of two individual values. If results from these two neuroradiologists were inconsistent, a third expert would be invited to work on this until a consensus was reached. The volume value of patients with negative APV was marked as 0 mL. Based on clinical research results, a threshold of 10 mL for APV was optimal to distinguish the high (≥10 mL) risk group from the low (<10 mL) risk group [21–26].

3. Statistical Analysis

Continuous variables were expressed as mean ± SD or median and interquartile range; categorical variables were presented as percentages. Interrater reliability of APV was assessed by using intraclass correlation coefficient (ICC) statistics. Clinical and imaging variables between low and high APV groups were analyzed by using t-test or Mann–Whitney U-test for continuous variables and Pearson chi-square test or Fisher's exact test for categorical variables. All participants were divided into two groups with regard to the volume of APV (APV < 10 mL as normal and APV ≥ 10 mL as abnormal). Univariate and multivariate binary logistic regression models were used to screen independent contributing factors to APV. Specific variables (age, sex, NIHSS, and

DWI) were preselected for entry into the model. Other possible variables were selected for entry into the model if $P \leq 0.05$ in the univariate analysis. Relationships between probably associated variables were examined by calculating Spearman correlation coefficients for continuous data or Kendall's tau-*b* for categorical data. Independent risk factors of APV were analyzed using multivariate logistic regression analysis. All association data were expressed as OR with corresponding 95% confidence intervals (CI) and *P* values. Statistical significance was defined as $P < 0.05$ (two sided). All data were analyzed using SPSS (version 20.0) for Windows (SPSS Inc., Chicago, IL, USA).

4. Results

A total of 159 patients were screened for AIS within 12 h after onset at the Stroke Center of Shanghai Fourth People's Hospital Affiliated to Tongji University School of Medicine, between January 2013 and December 2017. Seventy-six patients met the inclusion criteria. Eighty-three patients were excluded; among them, 43 had lesions not in the territory of MCA, 7 patients had bilateral lesions or more, 5 completed SWI over 12 h after symptom onset, 11 had inadequate information, and 17 had other issues (Figure 2).

4.1. Patient Characteristics. A total of 76 subjects, including 56 males and 20 females, were included in the study. The mean age of patients was 70.07 ± 1.37 years in the range of 37 to 94. The median time between SWI and symptom onset was 3.5 h (interquartile range (IQR): 2–7 h).

The median (IQR) NIHSS on admission was 6 (2–12). The median (IQR) DWI volume was 2 mL (1–20) (Table 1).

Table 1 presented the sociodemographic characteristics and clinical risk factors associated with different APV volumes. There was significant difference in history of AF ($P < 0.001$), admission NIHSS ($P = 0.001$), DWI volumes ($P < 0.01$), PWI volumes ($P < 0.001$), and stenosis (50%) ($P < 0.001$) between patients with low (APV < 10 mL) and high APV volumes (APV ≥ 10 mL). Patients with high APV tended to have poorer outcome than those with low APV 14 days later ($P = 0.031$).

4.2. Interrater Agreement for Evaluation of Prominent APV. Interrater agreement for the evaluation of APV volume was excellent (ICC = 0.995). High APV (APV ≥ 10 mL) was seen in 35/76 (46.05%) patients (mean: 116 mL; range: 35-271 mL).

4.3. Factors Associated with High APV. In univariate binary logistic regression analysis, history of AF ($P < 0.001$, OR = 16.89, 95%CI = 4.37 – 65.32), baseline NIHSS score ($P < 0.001$, OR = 1.14, 95%CI = 1.05 – 1.23), time to imaging (h) ($P < 0.001$, OR = 0.81, 95%CI = 0.70 – 0.94), DWI volume (mL) ($P < 0.01$, OR = 0.81, 95%CI = 1.10 – 1.17), and symptomatic stenosis (50%) ($P < 0.001$, OR = 660.0, 95 %CI = 57.28 – 7604.88) were significantly associated with high APV after ischemic stroke (Table 2). There was a positive correlation between history of AF and stenosis (50%) ($r = 0.62$, $P < 0.001$) and baseline NIHSS and DWI volume ($r = 0.55$, $P < 0.001$) in all patients.

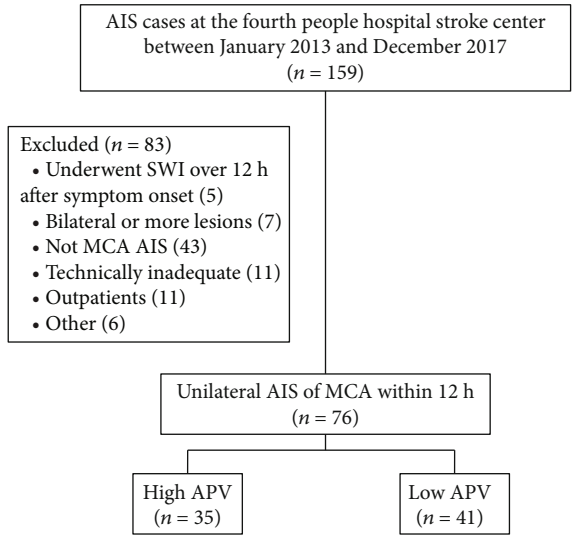

Figure 2: Flow chart of patient recruitment. AIS: acute ischemic stroke; SWI: susceptibility weighted imaging; MCA: middle cerebral artery; APV: asymmetrical prominent cortical veins.

Multivariate logistic regression modeling was performed for independent predictors with $P < 0.05$ in the univariate analysis and without significant correlation. In the multivariate logistic regression analysis, history of atrial fibrillation was significantly associated with high APV (OR: 10.48; 95% CI: 1.78-61.68) after adjusting for history of AF, baseline NIHSS, and time to imaging (h) (model 1). According to the MR imaging data, stenosis (50%) was significantly associated with high APV (OR: 660.0; 95% CI: 57.28-7604.88) after adjusting for time to imaging (h), DWI volume, and stenosis (50%) (model 2) (Table 2).

4.4. Correlation between Hypoperfusion and APV. Time to maximum (Tmax) maps were automatically produced using the RAPID software. Volumes of hypoperfusion based on different Tmax map thresholds (Tmax > 4 s, Tmax > 6 s, Tmax > 8 s, and Tmax > 10 s) were calculated. The volume of Tmax > 6 s is the most commonly used one representing ischemic penumbra [27–29]. There was a significant positive correlation between APV and Tmax > 6 s ($r = 0.865$, $P < 0.001$) and between APV and Tmax > 8 s ($r = 0.845$, $P < 0.001$) (Table 3 and Figure 3).

5. Discussion

To our best knowledge, this is the first study to report both the frequency and associated risk factors of asymmetrical prominent veins in AIS patients within 12 hours after symptom onset. The frequency of high APV (volume ≥ 10 mL) was 46.05% (35/76). Furthermore, we found that history of AF and DWI volume were independent factors associated with high APV.

5.1. The Frequency of MR Perfusion Abnormality. Our study showed a 46.05% (95% CI: 35.31-57.17%) frequency of high asymmetrical prominent veins (APV ≥ 10 mL) in AIS

Table 1: Clinical and imaging characteristics of AIS patients with low or high APV.

Characteristics	Total ($n = 76$)	Low 0-10 ($n = 41$)	High ≥10 ($n = 35$)	P value
Age (yr)	70.04 ± 1.37	67.85 ± 12.71	72.6 ± 10.58	0.087
Sex, male	56 (73.7)	28 (68.3)	28 (80.0)	0.251
Medical history				
Hypertension	56 (73.7)	33 (80.5)	23 (65.71)	0.149
Diabetes mellitus	26 (34.2)	17 (41.5)	9 (25.71)	0.152
Atrial fibrillation	23 (30.3)	3 (7.3)	20 (57.14)	0.000
Prior TIA or stroke	12 (15.8)	7 (17.1)	5 (14.29)	0.740
Smoking	27 (35.5)	17 (41.5)	10 (28.57)	0.244
Drinking	14 (18.4)	8 (19.5)	6 (17.14)	0.791
Ghb (g/L)	135.72 ± 2.01	138.34 ± 15.46	132.66 ± 19.45	0.162
FBG (mmol/L)	6.05 (5.03-7.95)	6.0 (4.9-7.7)	6.1 (5.1-8.1)	0.528
LDL (mmol/L)	2.71 (2.03-3.43)	2.05 (2.85-3.53)	2.64 (2.01-3.29)	0.418
Baseline NIHSS score	6 (2-12)	5 (2-9)	10 (10-25)	0.001
Time to imaging (h)	3.5 (2-7)	5 (2.25-10)	3 (1-5)	0.005
DWI volume (mL)	2 (1-20)	1 (1-3.5)	20 (1-33)	0.002
PWI volume (mL)	10.5 (0-96.25)	0 (0-1.5)	137 (49-154)	0.001
Stenosis (50%)	34 (44.7)	1 (2.4)	33 (94.29)	0.000
Poor outcome	27 (35.5)	10 (24.4)	17 (48.6)	0.031

Table cells express results in mean ± SD for normally distributed continuous variables, n (%) for dichotomous variables, and median (interquartile range) for ordinal variables and nonnormally distributed continuous variables, respectively. The DWI volume of the infarct core has been acquired on ADC maps (ADC $< 0.62 \times 10^3$ mm^2/s) and the volume of PWI on Tmax > 6 s maps.

Table 2: Factors associated with high volume of asymmetrical prominent veins.

Variable	Univariate analysis Crude OR (95% CI)	P value	Model 1 Adjusted OR (95% CI)	P value	Model 2 Adjusted OR (95% CI)	P value
Atrial fibrillation	16.89 (4.37-65.32)	0.000	10.48 (1.78-61.68)	0.009		
Baseline NIHSS score	1.14 (1.05-1.23)	0.001	1.03 (0.92-1.16)	1.033		
Time to imaging (h)	0.81 (0.70-0.94)	0.005	0.84 (0.71-0.99)	0.038	0.79 (0.53-1.18)	0.247
DWI volume (mL)	1.10 (1.04-1.17)	0.002			1.06 (0.96-1.18)	0.271
Stenosis (50%)	660.0 (57.28-7604.88)	0.000			432.14 (30.93-6038.35)	0.000

Model 1: based on clinical inquiry and physical examination. Adjusted for history of atrial fibrillation, baseline NIHSS, and time to imaging (h). Model 2: based on relevant MR imaging data. Adjusted for time to imaging (h), DWI volume, and stenosis (50%).

patients within 12 hours. This is higher than that of a previous report which showed a prevalence of 24.14% (35/145)[2], but lower than that of the other two studies whose prevalence was 55.05% (60/109) [3] and 60.78% (31/51)[4], respectively. There are a few possible reasons for this difference. First, the variability of results in these studies is related to the inconsistent definition of asymmetrical prominent veins. In this study, APV included asymmetric deep medullary veins (ADMV) and asymmetric prominent cortical veins (APCV). In other studies, the prominent asymmetric veins predominantly include APCV. Second, the present study calculated quantitative volumes of APV using a semiautomatic software, while other studies categorized APV using manual evaluation. In two recent studies, APCV was defined as a regional prominence of low-intensity vessels with increased vessel number and/or diameter on the ipsilateral side than on the contralateral hemisphere [2, 3]. Meanwhile, APCV was divided into two categories (positive and negative) [3] and four grades (0, normal appearance of cortical veins; 1, slight; 2, moderate; and 3, distinct) [2], respectively. Third, the asymmetrical prominent veins of the subjects were related to the time of onset and the time of SWI completion. In this study, SWI scan was completed within 12 hours after stroke onset for all AIS patients. The median interval between SWI completion and symptom onset was 3.5 (interquartile range (IQR): 2–7) hours. In a recent study, brain MRI was performed within 72 hours after ischemic stroke onset with a median time of 22 (range: 8–58) hours[2]. In another study, SWI was performed within 3 days after stroke onset with a mean over 30 (34.4 ± 27.36 in APCV positive group; 39.80 ± 28.87 in APCV negative group) hours [4].

5.2. Risk Factors Associated with APV. The initial observation by Xia et al. [8] in 2014 of asymmetrically prominent

Table 3: Correlation between Tmax and APV.

Tmax	APV	
	r	P value
Tmax > 4 s	0.785	$P < 0.001$
Tmax > 6 s	0.864	$P < 0.001$
Tmax > 8 s	0.845	$P < 0.001$
Tmax > 10 s	0.801	$P < 0.001$

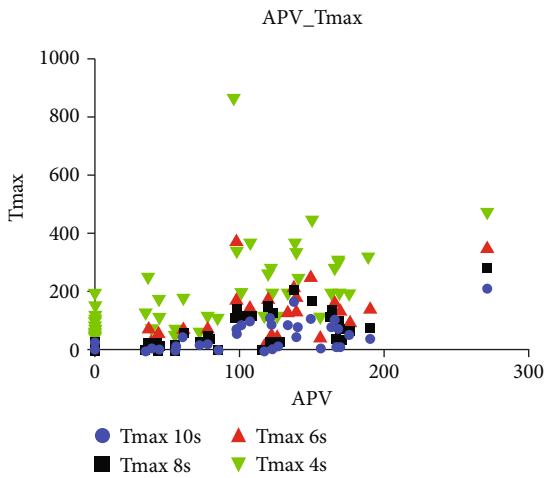

Figure 3: Correlation between Tmax and APV.

cortical veins in the ipsilateral hemisphere of AIS participants was quantified by comparing with contralateral changes in oxygen extraction fraction (OEF) [30]. Subsequent studies have shown a strong relationship between the presence of APV and early prognosis in patients with acute stroke [1–3, 5]. SWI is very sensitive for the detection of susceptibility differences [30]. After AIS, the venous blood volume increases as a result of vasodilation due to increase in oxygen extraction [31] and in the venous deoxyhemoglobin concentration [12, 13]. APV may appear on SWI due to differences in the concentrations of deoxyhemoglobin between cerebral veins and the surrounding parenchyma caused by cerebral vascular occlusion.

There are a number of possible clinical risk factors for APV in patients with AIS. Our first hypothesis, based on results of previous studies, was that clinical manifestations and vascular risk factors were associated with APV in patients with AIS [1, 4, 7]. Of the 76 stroke subjects included in this study, 30.3% had a history of AF, which is similar to a previous report in China which showed a prevalence of 20.2% (305/1511) among patients with ischemic stroke and TIA [32]. Among 35 patients with APV ≥ 10 mL after acute stroke onset, 57.14% had a history of AF. The high APV group completed the SWI examination about 2 hours earlier than the low APV group. According to results of model 1 in multifactor analysis, history of AF (OR: 10.48; 95% CI: 1.78-61.68; $P < 0.001$) and time to imaging (h) (OR: 0.81; 95% CI: 0.74-0.99; $P = 0.038$) were independent risk factors of high APV with ischemic stroke. In the present study, the baseline NIHSS was not associated with high APV. However, there was a strong positive correlation between baseline NIHSS and DWI volume ($r = 0.55$, $P < 0.001$) in patients with AIS. Therefore, these findings suggest that the earlier the examination was completed, the more likely the AIS patients with a history of AF were to have high APV within 12 hours of onset.

Our second hypothesis was that MR imaging was associated with high APV in AIS patients. Among 76 stroke patients included in this study, 44.7% had proximal artery stenosis or occlusion (≥50%), which is similar to that of a previous study [1, 5]. In the present study, 33 of 35 patients with APV ≥ 10 mL after acute stroke onset had proximal artery stenosis or occlusion (≥50%). These findings support that proximal artery stenosis or occlusion (≥50%) was an independent risk factor of high APV in AIS patients (OR: 660.0; 95% CI: 57.28-7604.88; $P < 0.001$) as shown in model 2 using the multiple logistic regression analysis. In this study, it was found that the DWI volume was not an independent risk factor of high APV using the same method.

The present study showed a strong relationship between the presence of proximal artery stenosis or occlusion (≥50%) and asymmetrical prominent veins in AIS patients within 12 hours. Causes of acute proximal artery stenosis or occlusion were listed below. First, embolization can cause stenosis of large blood vessels in patients with atrial fibrillation [33]. Second, rupture of large atherosclerotic plaques leads to insufficient blood supply to the distal end due to thrombosis after exposing highly thrombogenic, red cell-rich necrotic core material [34]. Third, thrombi formed on lesions (plaque erosion) without rupture render pathological intimal thickening or fibroatheromas [34]. Vascular stenosis or blockage results in decrease in SPO_2 in both arteries and veins in the ischemic area [4] and increase in OEF [30], which consequently increased paramagnetic substances (deoxyhemoglobin) in blood vessels. As a result, the appearance of APV was observed on SWI [20, 30]. Our research showed that there was a significant positive correlation between low perfusion (Tmax > 6 s, $r = 0.865$, $P < 0.001$; Tmax > 8 s, $r = 0.845$, $P < 0.001$) and APV, which is consistent with findings of a recent study [26].

The current study has a couple of limitations. First, it is a crosssectional study with a relatively small sample size ($n = 76$). Therefore, it cannot demonstrate direct causality between risk factors and APV in AIS patients. Second, the present study lacks follow-up results. It is unknown whether APV observed in our study progressed or disappeared after initial imaging. Therefore, findings of this study should be considered preliminary and be further verified in the future.

6. Conclusions

In conclusion, history of atrial fibrillation and proximal artery stenosis or occlusion (≥50%) are strong predictors of asymmetrical prominent veins observed on SWI maps of AIS patients within 12 hours of symptom onset.

Data Availability

Data produced for this manuscript are available from the corresponding author upon reasonable request.

Conflicts of Interest

The authors declare that there is no conflict of interests.

Authors' Contributions

YW, HL, and YL contributed to design and conceptualization of the study, data collection, analysis, interpretation of the data, and drafting the manuscript. YL and LJ contributed to data collection and revision of the manuscript. JX, LZ, SW and MW contributed to data collection and interpretation. Yue Wang, Jingjing Xiao, and Li Zhao contributed equally to this manuscript.

Acknowledgments

We thank all participants and their families, as well as technicians in the Radiology Department. This work was supported by the Natural Scientific Foundation of China (grant number 81971590) and Science and Technology Innovation Action Plan of Shanghai Science and Technology Commission (19441908000).

Supplementary Materials

Supplementary file 1: supplementary table 1 showing MR imaging parameters. Supplementary file 2: APV volume measurement. *(Supplementary Materials)*

References

[1] Y. L. Liu, H. P. Yin, D. H. Qiu et al., "Multiple hypointense vessels on susceptibility-weighted imaging predict early neurological deterioration in acute ischaemic stroke patients with severe intracranial large artery stenosis or occlusion receiving intravenous thrombolysis," *Stroke and Vascular Neurology*, vol. 5, no. 4, pp. 361–367, 2020.

[2] Y. L. Liu, W. M. Xiao, J. K. Lu et al., "Asymmetrical cortical vessel sign predicts prognosis after acute ischemic stroke," *Brain and Behavior: A Cognitive Neuroscience Perspective*, vol. 10, no. 7, article e01657, 2020.

[3] W. Li, W. M. Xiao, G. P. Luo et al., "Asymmetrical cortical vein sign predicts early neurological deterioration in acute ischemic stroke patients with severe intracranial arterial stenosis or occlusion," *BMC Neurology*, vol. 20, no. 1, p. 331, 2020.

[4] Y. Luo, Z. Gong, Y. Zhou et al., "Increased susceptibility of asymmetrically prominent cortical veins correlates with misery perfusion in patients with occlusion of the middle cerebral artery," *European Radiology*, vol. 27, no. 6, pp. 2381–2390, 2017.

[5] X. Yu, L. Yuan, A. Jackson et al., "Prominence of medullary veins on susceptibility-weighted images provides prognostic information in patients with subacute stroke," *AJNR. American Journal of Neuroradiology*, vol. 37, no. 3, pp. 423–429, 2016.

[6] E. M. Haacke, Y. Xu, Y. C. Cheng, and J. R. Reichenbach, "Susceptibility weighted imaging (SWI)," *Magnetic Resonance in Medicine*, vol. 52, no. 3, pp. 612–618, 2004.

[7] Z. Xu, Y. Duan, B. Yang, X. Huang, Y. Pei, and X. Li, "Asymmetric deep medullary veins in patients with occlusion of a large cerebral artery: association with cortical veins, leptomeningeal collaterals, and prognosis," *Frontiers in Neurology*, vol. 10, p. 1292, 2019.

[8] S. Xia, D. Utriainen, J. Tang et al., "Decreased oxygen saturation in asymmetrically prominent cortical veins in patients with cerebral ischemic stroke," *Magnetic Resonance Imaging*, vol. 32, no. 10, pp. 1272–1276, 2014.

[9] H. W. Kao, F. Y. Tsai, and A. N. Hasso, "Predicting stroke evolution: comparison of susceptibility-weighted MR imaging with MR perfusion," *European Radiology*, vol. 22, no. 7, pp. 1397–1403, 2012.

[10] E. M. Haacke, S. Mittal, Z. Wu, J. Neelavalli, and Y. C. Cheng, "Susceptibility-weighted imaging: technical aspects and clinical applications, part 1," *AJNR. American Journal of Neuroradiology*, vol. 30, no. 1, pp. 19–30, 2009.

[11] P. Huang, C. H. Chen, W. C. Lin, R. T. Lin, G. T. Khor, and C. K. Liu, "Clinical applications of susceptibility weighted imaging in patients with major stroke," *Journal of Neurology*, vol. 259, no. 7, pp. 1426–1432, 2012.

[12] C. Kesavadas, K. Santhosh, and B. Thomas, "Susceptibility weighted imaging in cerebral hypoperfusion-can we predict increased oxygen extraction fraction?," *Neuroradiology*, vol. 52, no. 11, pp. 1047–1054, 2010.

[13] H. Tamura, J. Hatazawa, H. Toyoshima, E. Shimosegawa, and T. Okudera, "Detection of deoxygenation-related signal change in acute ischemic stroke patients by t2∗-weighted magnetic resonance imaging," *Stroke*, vol. 33, no. 4, pp. 967–971, 2002.

[14] C. Kesavadas, B. Thomas, H. Pendharakar, and P. N. Sylaja, "Susceptibility weighted imaging: does it give information similar to perfusion weighted imaging in acute stroke?," *Journal of Neurology*, vol. 258, no. 5, pp. 932–934, 2011.

[15] S. Luo, L. Yang, and L. Wang, "Comparison of susceptibility-weighted and perfusion-weighted magnetic resonance imaging in the detection of penumbra in acute ischemic stroke," *Journal of Neuroradiology*, vol. 42, no. 5, pp. 255–260, 2015.

[16] M. Hermier, N. Nighoghossian, L. Derex et al., "Hypointense transcerebral veins at t2∗-weighted MRI: a marker of hemorrhagic transformation risk in patients treated with intravenous tissue plasminogen activator," *Journal of Cerebral Blood Flow and Metabolism*, vol. 23, no. 11, pp. 1362–1370, 2003.

[17] A. Seiler, N. P. Blockley, R. Deichmann et al., "The relationship between blood flow impairment and oxygen depletion in acute ischemic stroke imaged with magnetic resonance imaging," *Journal of Cerebral Blood Flow and Metabolism*, vol. 39, no. 3, pp. 454–465, 2019.

[18] J. E. Siegler and S. Martin-Schild, "Early neurological deterioration (end) after stroke: the end depends on the definition," *International Journal of Stroke*, vol. 6, no. 3, pp. 211-212, 2011.

[19] J. M. Olivot, M. Mlynash, V. N. Thijs et al., "Optimal tmax threshold for predicting penumbral tissue in acute stroke," *Stroke*, vol. 40, no. 2, pp. 469–475, 2009.

[20] E. M. Haacke, J. Tang, J. Neelavalli, and Y. C. Cheng, "Susceptibility mapping as a means to visualize veins and quantify oxygen saturation," *Journal of Magnetic Resonance Imaging*, vol. 32, no. 3, pp. 663–676, 2010.

[21] T. Ogata, S. Christensen, Y. Nagakane et al., "The effects of alteplase 3 to 6 hours after stroke in the epithet-defuse combined dataset: post hoc case-control study," *Stroke*, vol. 44, no. 1, pp. 87–93, 2013.

[22] N. Asdaghi, M. D. Hill, J. I. Coulter et al., "Perfusion MR predicts outcome in high-risk transient ischemic attack/minor stroke: a derivation-validation study," *Stroke*, vol. 44, no. 9, pp. 2486–2492, 2013.

[23] S. M. Davis, G. A. Donnan, M. W. Parsons et al., "Effects of alteplase beyond 3 h after stroke in the echoplanar imaging thrombolytic evaluation trial (epithet): a placebo-controlled randomised trial," *The Lancet Neurology*, vol. 7, no. 4, pp. 299–309, 2008.

[24] G. W. Albers, V. N. Thijs, L. Wechsler et al., "Magnetic resonance imaging profiles predict clinical response to early reperfusion: the diffusion and perfusion imaging evaluation for understanding stroke evolution (defuse) study," *Annals of Neurology*, vol. 60, no. 5, pp. 508–517, 2006.

[25] Y. Wang, H. Liang, Y. Luo et al., "History of hypertension is associated with MR hypoperfusion in Chinese inpatients with DWI-negative TIA," *Frontiers in Neurology*, vol. 10, p. 867, 2019.

[26] X. Lu, L. Meng, Y. Zhou et al., "Quantitative susceptibility-weighted imaging may be an accurate method for determining stroke hypoperfusion and hypoxia of penumbra," *European Radiology*, vol. 31, no. 8, pp. 6323–6333, 2021.

[27] V. Rao, S. Christensen, A. Yennu et al., "Ischemic core and hypoperfusion volumes correlate with infarct size 24 hours after randomization in defuse 3," *Stroke*, vol. 50, no. 3, pp. 626–631, 2019.

[28] H. Ma, B. C. V. Campbell, M. W. Parsons et al., "Thrombolysis guided by perfusion imaging up to 9 hours after onset of stroke," *The New England Journal of Medicine*, vol. 380, no. 19, pp. 1795–1803, 2019.

[29] B. C. Campbell, H. Ma, P. A. Ringleb et al., "Extending thrombolysis to 4.5-9 h and wake-up stroke using perfusion imaging: a systematic review and meta-analysis of individual patient data," *The Lancet*, vol. 394, no. 10193, pp. 139–147, 2019.

[30] S. Buch, Y. Ye, and E. M. Haacke, "Quantifying the changes in oxygen extraction fraction and cerebral activity caused by caffeine and acetazolamide," *Journal of Cerebral Blood Flow and Metabolism*, vol. 37, no. 3, pp. 825–836, 2017.

[31] C. Rosso, M. Belleville, C. Pires et al., "Clinical usefulness of the visibility of the transcerebral veins at 3t on t2∗-weighted sequence in acute stroke patients," *European Journal of Radiology*, vol. 81, no. 6, pp. 1282–1287, 2012.

[32] X. Yang, S. Li, X. Zhao et al., "Atrial fibrillation is not uncommon among patients with ischemic stroke and transient ischemic stroke in China," *BMC Neurology*, vol. 17, no. 1, p. 207, 2017.

[33] H. Kamel, P. M. Okin, M. S. Elkind, and C. Iadecola, "Atrial fibrillation and mechanisms of stroke: time for a new model," *Stroke*, vol. 47, no. 3, pp. 895–900, 2016.

[34] J. F. Bentzon, F. Otsuka, R. Virmani, and E. Falk, "Mechanisms of plaque formation and rupture," *Circulation Research*, vol. 114, no. 12, pp. 1852–1866, 2014.

Hindawi
Neural Plasticity
Volume 2021, Article ID 6718184, 9 pages
https://doi.org/10.1155/2021/6718184

Research Article

sLOX-1: A Molecule for Evaluating the Prognosis of Recurrent Ischemic Stroke

Yangmin Zheng,[1,2] **Yuyou Huang**,[1] **Lingzhi Li**,[1] **Pingping Wang**,[1] **Rongliang Wang**,[1,2] **Zhen Tao**,[1,2] **Junfen Fan**,[1,2] **Ziping Han**,[1,2] **Fangfang Li**,[1] **Haiping Zhao**,[1,2] **Fangfang Zhao**,[1] **Feng Yan**,[1,2] **Yumei Liu**,[3] **and Yumin Luo**[1,2]

[1]*Institute of Cerebrovascular Disease Research and Department of Neurology, Xuanwu Hospital of Capital Medical University, Beijing 100000, China*
[2]*Beijing Geriatric Medical Research Center and Beijing Key Laboratory of Translational Medicine for Cerebrovascular Diseases, Beijing 100000, China*
[3]*Vascular Ultrasonography Department, Xuanwu Hospital, Capital Medical University, Beijing 100000, China*

Correspondence should be addressed to Yumei Liu; yumeiliu@xwhosp.org and Yumin Luo; yumin111@ccmu.edu.cn

Received 14 April 2021; Revised 1 July 2021; Accepted 12 August 2021; Published 29 August 2021

Academic Editor: Xi-Ze Jia

Several clinical parameters and biomarkers have been proposed as prognostic markers for stroke. However, it has not been clarified whether the risk factors affecting the prognosis of patients with recurrent and first-ever stroke are similar. In this study, we aimed to explore the relationship between soluble lectin-like oxidized low-density lipoprotein receptor 1 (sLOX-1) levels and the prediction of the functional outcome in patients with recurrent and first-ever stroke. A total of 266 patients with recurrent and first-ever stroke, who underwent follow-up for 3 months, were included in this study. Plasma samples were collected within 24 h after onset. The results showed that biomarkers for the prognosis of patients with recurrent stroke were different from that of those with first-ever stroke. sLOX-1 levels were correlated with modified Rankin Scale scores of patients with recurrent stroke alone ($r = 0.3232$, $p = 0.001$). sLOX-1 levels were also associated with an increased risk of unfavorable outcomes in patients with recurrent stroke with an adjusted odds ratio of 1.489 (95% confidence interval, 1.204–1.842, $p < 0.0001$). Combining the risk factors showed greater accuracy for prognosis, yielding a sensitivity of 93.2% and a specificity of 75%, with an area under the curve of 0.916, evaluated by the receiver operating characteristic curve. These findings suggest that the diagnosis and prognosis are different between patients with recurrent stroke and those with first-ever stroke, and sLOX-1 level is an independent prognostic marker in patients with recurrent stroke.

1. Introduction

Stroke is a type of cerebrovascular disorder with high morbidity, disability, mortality, and recurrence rate. Its consequences are severe, especially after recurrence [1]. There are differences in the treatment and rehabilitation between patients with first-ever stroke and those with recurrent stroke [2]. Patients with previous stroke have a significantly increased risk of recurrence, and their severe disability and mortality rates are significantly higher [3]. However, it has not been clarified whether the risk factors of recurrent and first-ever stroke are completely similar, and there are few studies on the severity and short-term prognosis of recurrent ischemic stroke. Therefore, it is important to explore the risk factors affecting the prognosis of patients with recurrent ischemic stroke and to assess the condition and short-term prognosis of patients with recurrent stroke to improve their quality of life [4]. In addition, after screening patients with a history of stroke during clinical diagnosis and treatment, the direction of future research is to determine whether individualized treatment can be provided.

Lectin-like oxidized low-density lipoprotein receptor 1 (LOX-1), a type II integrin membrane glycoprotein receptor, is an acute-phase reactant, usually with low basal expression

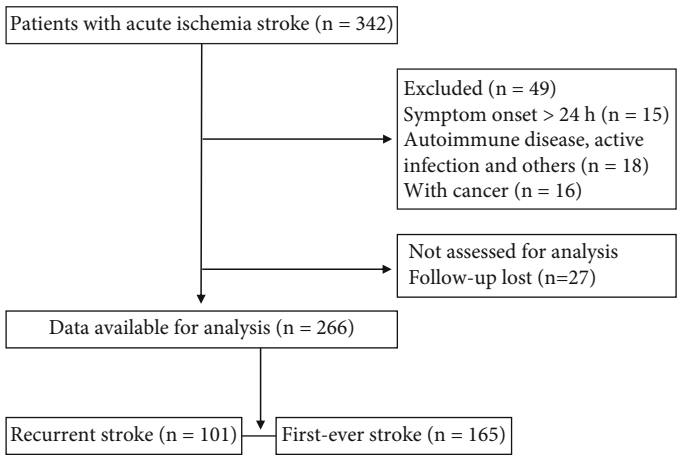

Figure 1: Study flowchart for participant selection.

levels in the cells. Its expression increases rapidly due to various prooxidation and proinflammatory cytokines [5, 6]. Therefore, it plays an important role in oxidative stress and cell damage induced by inflammatory factors. Soluble LOX-1 (sLOX-1) is a proteolytic form of LOX-1 that is released from the plasma membrane into the extracellular circulation after cell damage [7]. Clinical studies have shown that increased sLOX-1 levels might be positively correlated with intracranial artery stenosis in patients with stroke [8–12]. Furthermore, plasma sLOX-1 levels are also associated with the risk of carotid plaque inflammation and occurrence of ischemic stroke [13]. Therefore, plasma sLOX-1 levels can be used to evaluate the severity of stroke and intracranial arterial stenosis. Studies have shown that inflammatory factors enhance sLOX-1 cleavage in tumor necrosis factor- (TNF-) activated cultured endothelial cells and LOX-1 transgenic mice in vivo [14]. Meanwhile, clinical studies have shown that increased sLOX-1 levels are positively correlated with various inflammatory markers such as TNF-α [15]; it is possible to use sLOX-1 levels to predict the functional prognosis of stroke. Plasma sLOX-1 levels may be a novel potential biomarker for predicting the risk for multiple subtypes of stroke [9–11, 16–18]. Serum sLOX-1 level was higher in patients with large artery atherosclerotic (LAA) stroke and is used as a biomarker in patients with LAA ischemic stroke [16]. Serum sLOX-1, which is positively associated with hemorrhagic severity, may have the potential to be a biomarker for delayed cerebral ischemia after aneurysmal subarachnoid hemorrhage [19]. sLOX-1 levels may also be a potential biomarker for predicting the risk for acute ischemic stroke (AIS) in patients with internal carotid artery stenosis [9]. In addition, sLOX-1 can be used to predict the long-term prognosis of AIS [11]. However, the role of sLOX-1 in AIS remains unclear, especially between recurrent ischemic stroke and first-ever ischemic stroke. Therefore, this study enrolled a total of 266 patients with AIS, including 101 with recurrent ischemic stroke and 165 with first-ever ischemic stroke, to evaluate the relationship between sLOX-1 levels and the prediction of functional outcomes in patients with AIS.

2. Materials and Methods

2.1. Study Participants. This study was reviewed and approved by the Ethics Committee of the Institutional Review Board of Capital Medical University, Beijing, China and was in accordance with the Declaration of Helsinki. All patients signed an informed consent form. Two hundred and sixty-six patients with AIS (101 with recurrent ischemic stroke and 165 first-ever ischemic stroke) undergoing follow-up for 3 months at the Cerebrovascular Diseases Research Institute of Xuanwu Hospital of Capital Medical University were included in this study. Basic data were collected within 24 h after the onset of AIS. The study flowchart for participant selection is shown in Figure 1.

The inclusion criteria were as follows: (1) admission within 24 h of symptom onset, (2) AIS confirmed by brain magnetic resonance imaging (MRI) or computed tomography (CT), and (3) recurrent ischemic stroke with a clear history of ischemic stroke and more than 1 month away from onset. In addition, there should be clinical symptoms and signs of new ischemic stroke, and imaging should show new lesions. The exclusion criteria were the following: (1) autoimmune disease, (2) cerebral hemorrhage, (3) transient ischemic attack, and (4) progressive stroke or progressive deterioration of stroke.

2.2. Clinical Data. Clinical baseline data were collected after the onset of the disease (including the patient's general admission data, routine blood biochemistry, other hematological examinations, MRI/CT infarct volume, National Institutes of Health Stroke Scale (NIHSS) score, and modified Rankin Scale (mRS)). After admission, the NIHSS score was used to evaluate the degree of neurological impairment. The mRS score at 90 days follow-up was recorded by an experienced neurologist by telephone. An mRS score of 0–2 at follow-up was defined as a favorable outcome and 3–6 as an unfavorable outcome. The boundary of the patients' lesions was measured by using RadiAnt DICOM Viewer on the first brain CT or brain MRI diffusion-weighted imaging sequence after admission. Finally, the lesion area of each

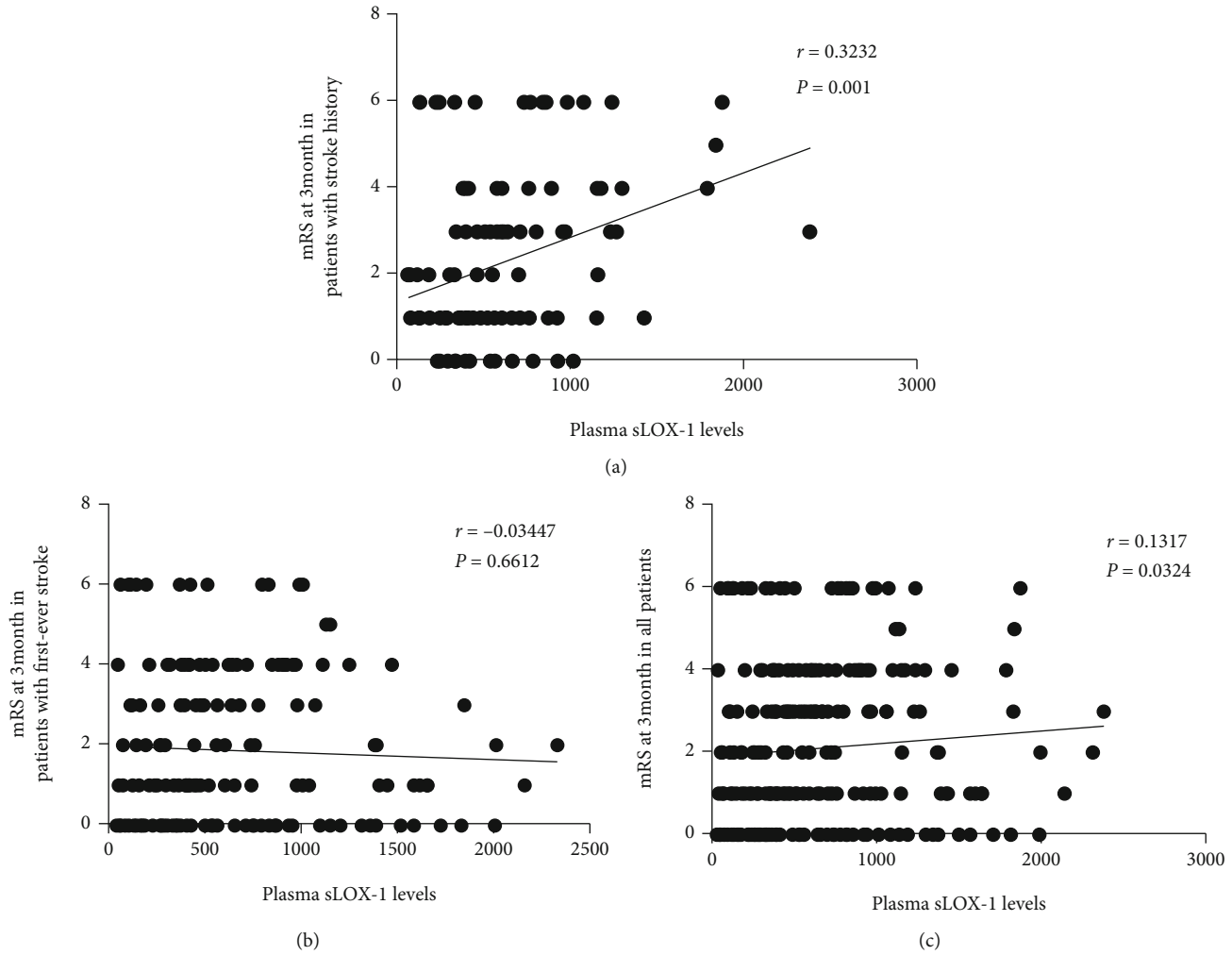

Figure 2: Correlations between sLOX-1 levels and 3-month mRS score. Correlation of 3-month mRS score with the plasma sLOX-1 level in patients with AIS with recurrent ischemic stroke (a), with first-ever stroke (b), and in all patients with AIS (c). $N = 101$ for patients with recurrent ischemic stroke, $N = 165$ for patients with first-ever ischemic stroke, and $N = 266$ for all patients with AIS. AIS: acute ischemic stroke; sLOX-1: soluble lectin-like oxidized low-density lipoprotein receptor-1; mRS: modified Rankin Scale.

layer was multiplied by a thickness of 0.5 cm to obtain the infarct volume layer by layer.

2.3. Measurement of Soluble LOX-1. Before treatment, the blood samples of patients with AIS were collected in K3 EDTA tubes. The plasma was separated and frozen at -80°C. The concentrations of sLOX-1 were determined using commercially available enzyme-linked immunosorbent assay kits according to the manufacturer's instructions (Solarbio Life Science, Beijing, China).

2.4. Statistical Analyses. All analyses were conducted using SPSS software (version 22.0; IBM Corp., Armonk, NY, USA) and Prism7 software (GraphPad Software Inc., USA). The Kolmogorov–Smirnov test was used to determine whether the data were normally distributed. Continuous variables that were normally distributed were expressed as the mean value ± standard deviation and analyzed using the independent t-test, while continuous variables that were not normally distributed were expressed as medians with interquartile ranges (25th–75th percentiles) and analyzed using the Mann–Whitney U test. Categorical variables were expressed as counts and proportions and were compared using the chi-square test. Variables with p values < 0.1, from univariate analyses and variables that were previously reported, were incorporated in the multivariate analysis. Based on the receiver operating characteristic (ROC) curve analysis, the corresponding sensitivity, specificity, and area under the curve (AUC) were calculated to evaluate the accuracy of serum sLOX-1 in predicting the prognosis of AIS. Furthermore, Prism7 software was used to draw a forest plot to show the results of the multivariate regression analysis.

3. Results and Discussion

3.1. Elevated sLOX-1 Levels Were Correlated with an Increased Risk of Adverse Outcomes in Patients with AIS with Recurrent Ischemic Stroke but Not with First-Ever Stroke. Plasma sLOX-1 levels were positively correlated with the mRS score at 3 months in patients with recurrent

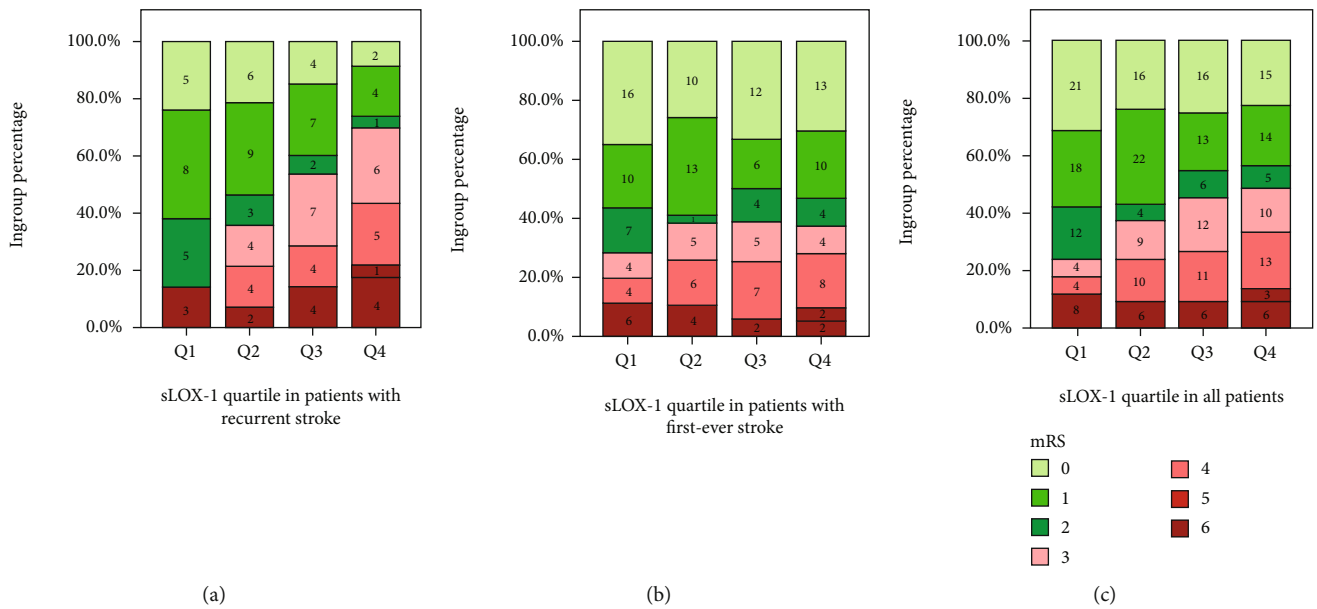

(a) (b) (c)

Figure 3: Elevated sLOX-1 levels were correlated with an increased risk of adverse outcomes in patients with recurrent stroke but not in those with first-ever stroke. The proportion of patients with favorable (mRS score = 0–2) and unfavorable outcomes (mRS score = 3–6) in patients with recurrent ischemic stroke (a), with first-ever stroke (b), and in all patients with AIS (c). Grouped according to the quartile of sLOX-1 level: Q1 represents ≤316.72 pg/mL, Q2 represents 316.72–510.52 pg/mL, Q3 represents 510.52–877.48 pg/mL, and Q4 represents ≥877.48 pg/mL. Numbers indicate the number of cases per subgroup.

ischemic stroke, as shown in Figure 2 ($r = 0.3232$, $p = 0.001$). However, no linear correlation was found between sLOX-1 levels and mRS score at 3 months in all patients with AIS or with first-ever stroke.

To further observe this correlation, we grouped sLOX-1 by quartiles. Figure 3 shows that after being grouped in quartiles of sLOX-1 level the proportion of patients in each quartile group with an unfavorable outcome in patients with AIS with recurrent ischemic stroke showed a gradient increase with increasing sLOX-1 levels. Meanwhile, no such change was observed in patients with first-ever ischemic stroke.

3.2. Baseline Characteristics of Patients Grouped by Recurrent Ischemic Stroke and First-Ever Ischemic Stroke. A total of 266 patients with AIS were enrolled in this study. These patients were grouped into having either recurrent ischemic stroke or first-ever ischemic stroke. Their baseline characteristics are shown in Table 1.

We found that patients with recurrent ischemic stroke were older than those with first-ever ischemic stroke, as shown in Figure 4(a), although there was no difference in sex composition. We also found that the neutrophil-to-lymphocyte ratio (NLR) of patients with recurrent ischemic stroke was higher than those with first-ever ischemic stroke. Furthermore, we found that lymphocyte count, total cholesterol and triglyceride levels, and low-density lipoprotein content were significantly different, and these indicators were significantly higher in patients with first-ever ischemic stroke than in those with recurrent ischemic stroke, as shown in Figures 4(c)–4(f).

We speculated that the patients with recurrent ischemic stroke received sufficient treatment and rehabilitation after the first-ever stroke, which allowed some stroke risk factors to be controlled. This may also explain why sLOX-1 levels were correlated with the mRS score at 3 months in patients with recurrent stroke but not in those with first-ever stroke. However, the stroke risk factors were not effectively controlled in patients with first-ever stroke before the occurrence of stroke, and the risk factors of stroke are relatively complex; thus, no correlation was found between sLOX-1 levels and mRS score in patients with first-ever stroke.

3.3. sLOX-1 Levels Represented an Independent Predictor for Unfavorable Outcomes in Patients with AIS with Recurrent Ischemic Stroke but Not with First-Ever Stroke. We further examined the predictive value of sLOX-1 levels for unfavorable outcomes after recurrent or first-ever stroke. Univariate analyses showed that high sLOX-1 levels were associated with an increased risk of unfavorable outcomes with recurrent ischemic stroke, as shown in Table 2 ($p < 0.0001$), but not with first-ever ischemic stroke.

However, there was no significant difference in sLOX-1 levels between patients with recurrent ischemic stroke and those with first-ever stroke (526.36 pg/mL vs. 510.51 pg/mL, $p = 0.824$). In addition, in the univariate analysis, lymphocyte and neutrophil counts and atrial fibrillation were associated with unfavorable outcomes in patients with first-ever stroke, but not in those with recurrent stroke. This suggests that the prognostic biomarkers in patients with recurrent ischemic stroke may be different from those in patients with first-ever stroke. After adjusting for age, admission NIHSS score, NLR, and other variables in the binominal multivariate logistic analysis, sLOX-1 levels remained an independent predictor of unfavorable outcomes in patients with

Table 1: Baseline characteristics in patients with first-ever and recurrent stroke.

Baseline characteristics	All ($N = 266$)	Recurrent stroke ($N = 101$)	First-ever stroke ($N = 165$)	p value
Age (year)	63.0(56.0–73.5)	68.0(58.0–78.0)	61.0 (55.0–69.0)	0.013
Male, n (%)	196.0	76.0 (75.2%)	120.0 (72.7%)	0.65
Baseline systolic BP (mmHg)	150 (140–168.3)	150 (138.5–166.5)	150.0 (140.0–170.0)	0.5
Baseline diastolic BP (mmHg)	78.0 (89.0–94.3)	80.0 (77.0–93.0)	90.0 (80.0–95.0)	0.1
Time from onset (h)	3.0 (1.5–5.1)	2.8 (1.4–4.7)	3.0 (1.7–5.9)	0.55
Baseline NIHSS score	6.0 (3.0–11.0)	7.00 (4.0–13.0)	6.0 (3.0–10.0)	0.012
Clinical parameters (median)				
Neutrophil count (10^9/L)	5.16 (3.95–6.85)	4.87 (3.90–7.49)	5.16 (3.98–6.54)	0.5
Lymphocyte count (10^9/L)	1.53 (1.13–2.21)	1.37 (0.92–1.93)	1.71 (1.24–2.35)	0.006
Neutrophil-to-lymphocyte ratio	2.97 (2.13–5.55)	3.32 (2.18–6.62)	2.85 (2.11–4.67)	0.041
Platelet count (10^9/L)	206.0 (170.5–243.5)	196.0 (161.0–224.5)	210.0(180.0–259.0)	0.055
Leukocyte count (10^9/L)	7.66 (6.27–9.25)	7.66 (5.69–9.24)	7.66 (6.4–9.17)	0.966
Triglycerides (mmol/L)	1.51 (1.0–2.62)	1.39 (0.91–1.91)	1.69 (1.08–2.8)	0.025
Total cholesterol (mmol/L)	4.73 ± 1.19	4.35 ± 1.24	4.97 ± 1.12	0.000
High-density lipoprotein (mmol/L)	1.14 (0.97–1.40)	1.15 (0.97–1.39)	1.14 (0.97–1.40)	0.739
Low-density lipoprotein (mmol/L)	2.77 (2.20–3.46)	2.50 (1.77–3.30)	2.82 (2.38–3.60)	0.001
Risk factors, n (%)				
Hypertension	179	76 (75.2%)	103 (62.4%)	0.036
Diabetes mellitus	93	39 (38.6%)	54 (32.7%)	0.37
Hyperlipemia	72	32 (31.7%)	40 (24.2%)	0.21
Coronary heart disease	52	27 (26.7%)	25 (15.2%)	0.021
Atrial fibrillation	44	23(22.8%)	21 (12.7%)	0.14
Site of infarction (%)				0.72
Total anterior circulation (TAC)	17	5 (5%)	12 (7.3%)	
Partial anterior circulation (PAC)	199	76 (75.2%)	123 (74.5%)	
Posterior circulation (POC)	38	13 (12.9%)	25 (15.2%)	
Stroke etiologic subtypes (%)				0.89
Large artery atherosclerosis	151	57 (56.4%)	94 (57%)	
Small vessel disease	72	27 (26.7%)	45(27.3%)	
Cardioembolic	13	5 (5%)	8(4.8%)	
Other or unknown cause	1	0 (0%)	1(0.6%)	
Biomarkers (ng/mL), median				
sLOX-1 (pg/mL)	510.51 (314.53–877.60)	526.36 (339.32–826.61)	500.66 (288.44–915.42)	0.824

recurrent ischemic stroke with an adjusted odds ratio of 1.489, as shown in Figure 5 (95% confidence interval, 1.204–1.842, $p < 0.0001$).

Based on the ROC curve analysis, the optimal cutoff value of serum sLOX-1 level as an indicator for unfavorable outcome was projected to be 575.39 pg/mL, yielding a sensitivity of 68.2% and a specificity of 73.2%, with an AUC of 0.739. The ROC curves of sLOX-1 levels for the prediction of unfavorable outcomes in patients with recurrent ischemic stroke outcomes are shown in Figure 6 (yellow curve).

We further used the ROC curve to evaluate the diagnostic value of sLOX-1 levels for the prognosis of the subjects in combination with variables of the binominal multivariate logistic analysis. Compared with any of the variables of the binominal multivariate logistic analysis or sLOX-1 levels alone, the combination of sLOX-1 and the variables showed greater accuracy, yielding a sensitivity of 93.2%, positive predictive value of 93.3%, negative predictive value of 74.5%, specificity of 75%, diagnostic accuracy of 83%, and an AUC of 0.916 (Figure 6, red curve).

4. Discussion

This is the first study to show that biomarkers for prognosis are different in recurrent and first-ever strokes. Previous studies have focused on the risk factors for the occurrence and prognosis of first-ever stroke, although these studies have ignored the fact that the prognostic risk factors for recurrent ischemic stroke may be different from those for first-ever stroke. We found that elevated sLOX-1 levels were correlated with an increased risk of adverse outcomes in patients with AIS with recurrent ischemic stroke, but not in those with first-ever stroke. With this, sLOX-1 levels

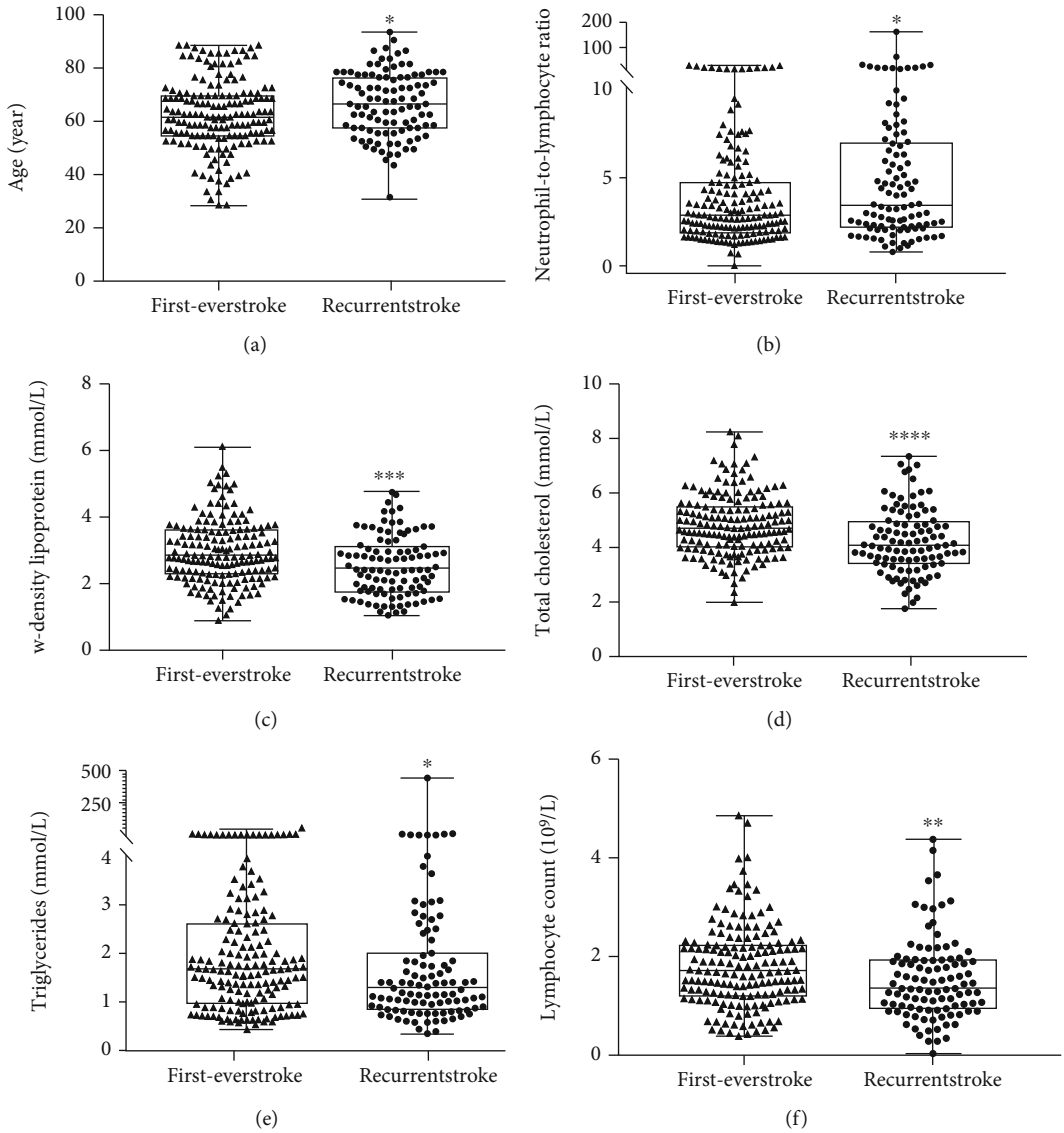

Figure 4: Significant differences were found in baseline data between patients with recurrent stroke and those with first-ever stroke. Patients with first-ever stroke were younger (a), and the neutrophil-to-lymphocyte ratio (b) was higher in patients with recurrent stroke; patients with first-ever stroke had higher low-density lipoprotein content (c), total cholesterol levels (d), total triglyceride levels (e), and lymphocyte count (f) than patients recurrent stroke. $^{*}p < 0.05$, $^{**}p < 0.005$, and $^{***}p < 0.001$.

might be used as an indicator for risk stratification and prognosis assessment of patients with recurrent ischemic stroke.

Recurrent ischemic stroke occurs in relation to the first-ever stroke. Brain tissue ischemia and hypoxia cause irreversible damage to some nerve functions. Under the combined action of multiple risk factors, recurrent stroke causes the brain tissue to suffer from hypoperfusion and oxidative stress again, further aggravating the nerve injury [20]. However, it has not been clarified whether the risk factors for recurrent and first-ever stroke are completely similar, and there are few studies on the severity and short-term prognosis of recurrent ischemic stroke. LOX-1 is involved in endothelial cell dysfunction, monocyte proliferation, adhesion and migration, platelet activation, and other inflammatory responses [21]. The sLOX-1 levels can effectively reflect the expression of LOX-1 in the organism [22]. Therefore, it is of great importance to study the role of sLOX-1 in cardiovascular and cerebrovascular diseases. Here, we found that sLOX-1 concentrations were positively correlated with the mRS score at 3 months in patients with recurrent ischemic stroke, and the poor prognosis proportion of the top quartile of the sLOX-1 index was higher than that of the low-level groups. Several known stroke risk factors, such as total cholesterol levels, triglycerides, and low-density lipoprotein content, are lower in patients with recurrent stroke than in patients with first-ever stroke. Therefore, we speculated that many patients had other underlying diseases, for which they did not receive treatment, before AIS occurred, and subsequent changes in the blood sample indexes affected the assessment for the real cause of stroke. Patients with a history of stroke were found to have other diseases, such as hyperlipidemia, at the first stroke attack and were then managed with

Table 2: Univariate logistic regression analyses for favorable outcome in patients with first-ever and recurrent stroke.

Univariable logistic regression				
	Recurrent stroke (N = 101)		First-ever stroke (N = 165)	
	OR (95% CI)	p value	OR (95% CI)	p value
Age (year)	1.064(1.024–1.105)	0.002	1.028(1.002–1.054)	0.035
Male, n (%)	1.24 (0.5–3.076)	0.642	1.705(0.844–3.444)	0.137
Baseline systolic BP (mmHg)	0.992(0.976–1.009)	0.387	0.999(0.986–1.012)	0.854
Baseline diastolic BP (mmHg)	1.001(0.972–1.032)	0.934	0.994(0.974–1.015)	0.598
Time from onset (h)	1.102(0.966–1.258)	0.15	1.056(0.981–1.136)	0.147
Baseline NIHSS score	1.201(1.105–1.306)	0.000	1.299(1.192–1.415)	0.000
Clinical parameters (median)				
Neutrophil count (10^9/L)	1.087(0.954–1.239)	0.212	1.2 (1.058–1.362)	0.005
Lymphocyte count (10^9/L)	0.726(0.438–1.202)	0.213	0.417(0.258–0.674)	0.000
Neutrophil-to-lymphocyte ratio	1.084(1.000–1.175)	0.05	1.3 (1.142–1.48)	0.000
Platelet count (10^9/L)	0.994(0.986–1.003)	0.176	0.998 (0.993–1.003)	0.425
Leukocyte count (10^9/L)	1.065(0.931–1.217)	0.36	1.104 (0.99–1.232)	0.076
Triglycerides (mmol/L)	0.966(0.807–1.156)	0.702	1.032(0.959-1.11)	0.404
Total cholesterol (mmol/L)	0.873(0.62-1.231)	0.439	0.968(0.729–1.286)	0.824
High-density lipoprotein (mmol/L)	1.042(0.278–3.901)	0.951	2.05(0.833–5.044)	0.118
Low-density lipoprotein (mmol/L)	0.983(0.633–1.528)	0.939	1.005 (0.722–1.4)	0.975
Risk factors, n (%)				
Hypertension	0.806(0.325–1.999)	0.642	1.312(0.669–2.576)	0.429
Diabetes mellitus	1.48(0.656–3.339)	0.345	1.874(0.954–3.68)	0.068
Hyperlipemia	0.556(0.233–1.327)	0.186	0.551 (0.246–1.23)	0.146
Coronary heart disease	1.544(0.636–3.749)	0.338	1.866 (0.789–4.412)	0.155
Atrial fibrillation	1.533(0.584–4.029)	0.386	2.773(1.131–6.802)	0.026
Site of infarction (%)	1.398(0.690–2.831)	0.353	0.749(0.418–1.343)	0.333
Total anterior circulation (TAC)				
Partial anterior circulation (PAC)				
Posterior circulation (POC)				
Stroke etiologic subtypes (%)	0.541 (0.2–1.468)	0.228	0.831 (0.416–1.66)	0.6
Large artery atherosclerosis				
Small vessel disease				
Cardioembolic				
Other or unknown cause				
Biomarkers (ng/mL), median				
sLOX-1 (per 100 pg/mL increase)	1.284 (1.123–1.470)	0.000	0.983 (0.919–1.05)	0.608

the corresponding treatment. Thus, molecular changes, due to the treatment and control of other basic diseases, in the plasma samples of patients with a history of stroke may be more able to reflect the direct factors of stroke recurrence.

Current studies on sLOX-1 and other molecules as potential prognostic markers do not consider the patient's history of stroke (or not mentioned) [9–11, 17] or may have already excluded patients with a history of stroke upon enrollment [12, 16, 19]. Therefore, information on the incidence of stroke-related molecules or markers may be missing. Since recurrent ischemic stroke occurs relative to the initial ischemic stroke, it is speculated that both have similar risk factors. To identify the risk factors affecting the prognosis of recurrent ischemic stroke, univariate and multivariate logic analyses were conducted on the established risk factors of initial ischemic stroke in patients with recurrent ischemic stroke and found that age, NIHSS scores, and sLOX-1 levels could affect the prognosis. However, in our study, the sLOX-1 level was not a marker of prognosis in patients with first-ever stroke, which is different from previous findings. We speculated that this might be due to the different receiving times of the plasma samples. The plasma samples of the patients in our study were collected within 24 h of the onset of stroke, while those in other studies were different; some were collected within 72 h [11] and others within 6 days of onset [16]. It may also be that the subtypes of stroke were different among the enrolled patients. Our enrolled patients were diagnosed with AIS as confirmed by brain MRI or CT,

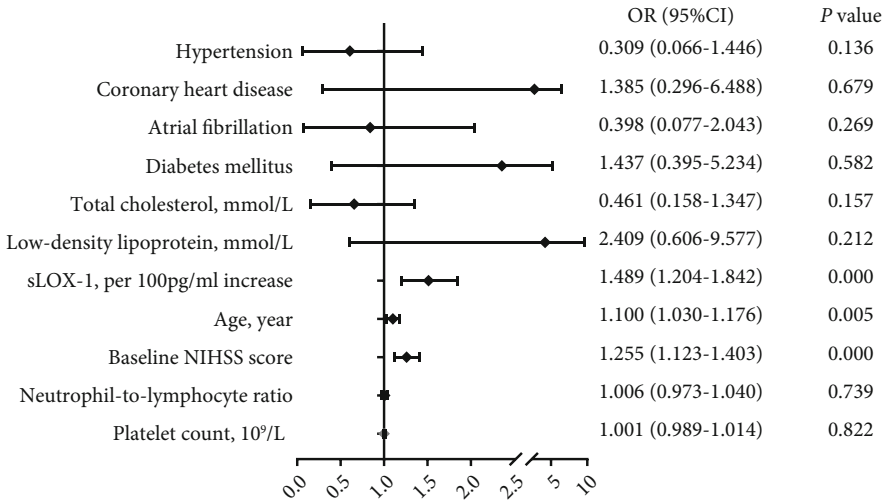

Figure 5: Forest plot shows the risk of the primary outcome after AIS. After adjusting for age, admission NIHSS score, neutrophil-to-lymphocyte ratio, diabetes mellitus, atrial fibrillation, coronary heart disease, hypertension, platelet count, low-density lipoprotein, and total cholesterol, binominal multivariate logistic analysis showed that sLOX-1 level was an independent predictor for unfavorable outcome in patients with recurrent ischemic stroke.

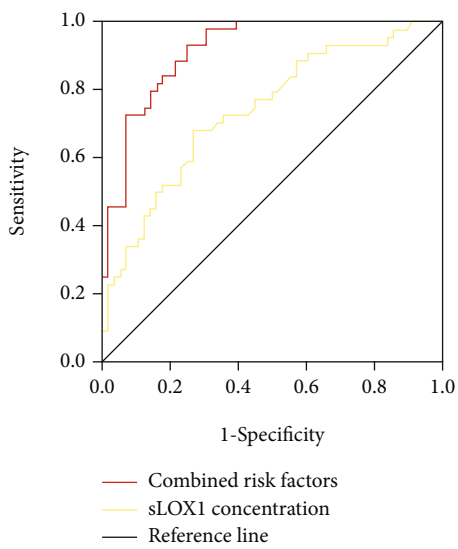

Figure 6: ROC curve analysis on predictive values of age, baseline NIHSS score, sLOX-1 concentration, time from onset, neutrophil count, and combined risk factors. The optimal cutoff value was 575.39 pg/mL, with a sensitivity of 93.2% and a specificity of 75% (AUC: 0.916, 95% confidence interval: 0.863–0.968, $p < 0.0001$).

while in the other studies, the enrolled patients had undergone percutaneous coronary intervention [17]. This study has some limitations that require consideration. First, the sample size of the enrolled patients in our study was small, and further studies are needed to validate our findings with a larger sample size. Second, information on the current medications of the enrolled patients was insufficient, because of which further research is needed to clarify other comorbidities and the medications of the enrolled patients. Third, we were unable to monitor the long-term prognosis of the patients. Further studies on this matter are recommended.

5. Conclusion

In summary, we provide the first evidence that the diagnosis and prognosis differ between patients with recurrent ischemic stroke and those with initial ischemic stroke. Plasma sLOX-1 levels are an independent prognostic marker in patients with recurrent AIS. Therefore, based on the history of stroke and strength of predictive factors, early and targeted intervention and secondary prevention should be conducted for patients with recurrent AIS. These measures are important in the prevention and treatment of recurrent ischemic stroke.

Data Availability

The original data of this study are available from the corresponding authors upon reasonable request.

Conflicts of Interest

There are no conflicts among the authors.

Acknowledgments

This study was supported by the National Natural Science Foundation of China (Nos. 82001390, 81971222, and 81801299) and Capital Funds for Health Improvement and Research (2020-2-1032).

References

[1] W. Wang, B. Jiang, H. Sun et al., "Prevalence, incidence, and mortality of stroke in China: results from a nationwide population-based survey of 480 687 adults," *Circulation*, vol. 135, no. 8, pp. 759–771, 2017.

[2] C. Wu, D. Wu, J. Chen, C. Li, and X. Ji, "Why not intravenous thrombolysis in patients with recurrent stroke within 3 months?," *Aging and Disease*, vol. 9, no. 2, pp. 309–316, 2018.

[3] G. J. Hankey, "Secondary stroke prevention," *Lancet Neurology*, vol. 13, no. 2, pp. 178–194, 2014.

[4] R. Oza, K. Rundell, and M. Garcellano, "Recurrent ischemic stroke: strategies for prevention," *American family physician*, vol. 96, no. 7, pp. 436–440, 2017.

[5] T. Sawamura, Y. Fujita, S. Horiuchi, and A. Kakino, "LOX-1 in ischemic stroke," *Journal of atherosclerosis and thrombosis.*, vol. 24, no. 6, pp. 566–568, 2017.

[6] S. Singh and A. S. Gautam, "Upregulated LOX-1 receptor: key player of the pathogenesis of atherosclerosis," *Current atherosclerosis reports.*, vol. 21, no. 10, p. 38, 2019.

[7] T. Murase, N. Kume, H. Kataoka et al., "Identification of soluble forms of lectin-like oxidized LDL receptor-1," *Arteriosclerosis, thrombosis, and vascular biology.*, vol. 20, no. 3, pp. 715–720, 2000.

[8] T. Otsuki, S. Maeda, J. Mukai, M. Ohki, M. Nakanishi, and T. Yoshikawa, "Association between plasma sLOX-1 concentration and arterial stiffness in middle-aged and older individuals," *Journal of clinical biochemistry and nutrition.*, vol. 57, no. 2, pp. 151–155, 2015.

[9] P. Chaiyawatthanananthn, K. Suwanprasert, and S. Muengtaweepongsa, "Differentiation of serum sLOX-1 and NO levels in acute ischemic stroke patients with internal carotid artery stenosis and those without internal carotid artery stenosis," *Journal of the Medical Association of Thailand = Chotmaihet thangphaet*, vol. 99, Supplement 4, 2016.

[10] C. Yokota, T. Sawamura, M. Watanabe et al., "High levels of soluble lectin-like oxidized low-density lipoprotein receptor-1 in acute stroke: an age- and sex-matched cross-sectional study," *Journal of atherosclerosis and thrombosis.*, vol. 23, no. 10, pp. 1222–1226, 2016.

[11] X. M. Li, P. P. Jin, J. Xue et al., "Role of sLOX-1 in intracranial artery stenosis and in predicting long-term prognosis of acute ischemic stroke," *Brain and Behavior: A Cognitive Neuroscience Perspective*, vol. 8, no. 1, article e00879, 2018.

[12] T. Skarpengland, M. Skjelland, X. Y. Kong et al., "Increased levels of lectin-like oxidized low-density lipoprotein receptor-1 in ischemic stroke and transient ischemic attack," *Journal of the American Heart Association*, vol. 12, 2018.

[13] H. Markstad, A. Edsfeldt, I. Yao Mattison et al., "High levels of soluble lectinlike oxidized low-density lipoprotein receptor-1 are associated with carotid plaque inflammation and increased risk of ischemic stroke," *Journal of the American Heart Association.*, vol. 8, no. 4, article e009874, 2019.

[14] H. Mitsuoka, N. Kume, K. Hayashida et al., "Interleukin 18 stimulates release of soluble lectin-like oxidized LDL receptor-1 (sLOX-1)," *Atherosclerosis*, vol. 202, no. 1, pp. 176–182, 2009.

[15] V. Lubrano, S. Del Turco, G. Nicolini, P. Di Cecco, and G. Basta, "Circulating levels of lectin-like oxidized low-density lipoprotein receptor-1 are associated with inflammatory markers," *Lipids*, vol. 43, no. 10, pp. 945–950, 2008.

[16] W. Huang, Q. Li, X. Chen et al., "Soluble lectin-like oxidized low-density lipoprotein receptor-1 as a novel biomarker for large-artery atherosclerotic stroke," *The International Journal of Neuroscience*, vol. 127, no. 10, pp. 881–886, 2017.

[17] Z.-w. Zhao, Y.-w. Xu, S.-m. Li et al., "Baseline serum sLOX-1 concentrations are associated with 2-year major adverse cardiovascular and cerebrovascular events in patients after percutaneous coronary intervention," *Disease markers*, vol. 2019, Article ID 4925767, 2019.

[18] Q. Lin, H.-J. Ba, J.-X. Dai et al., "Serum soluble lectin-like oxidized low-density lipoprotein receptor-1 concentrations and prognosis of aneurysmal subarachnoid hemorrhage," *Clinica chimica acta; international journal of clinical chemistry*, vol. 500, pp. 54–58, 2020.

[19] Q. Lin, H.-. J. Ba, J.-. X. Dai et al., "Serum soluble lectin-like oxidized low-density lipoprotein receptor-1 as a biomarker of delayed cerebral ischemia after aneurysmal subarachnoid hemorrhage," *Brain and Behavior: A Cognitive Neuroscience Perspective*, vol. 10, no. 2, p. e01517, 2020.

[20] X. Ling, S. M. Yan, B. Shen, and X. Yang, "A modified Essen Stroke Risk Score for predicting recurrent ischemic stroke at one year," *Neurological Research*, vol. 40, no. 3, pp. 204–210, 2018.

[21] P. Jin and S. Cong, "LOX-1 and atherosclerotic-related diseases," *Clinica chimica acta; international journal of clinical chemistry*, vol. 491, pp. 24–29, 2019.

[22] X. Guo, Y. Xiang, H. Yang, L. Yu, X. Peng, and R. Guo, "Association of the LOX-1 rs 1050283 polymorphism with risk for atherosclerotic cerebral infarction and its effect on sLOX-1 and LOX-1 expression in a Chinese population," *Journal of atherosclerosis and thrombosis.*, vol. 24, no. 6, pp. 572–582, 2017.

Hindawi
Neural Plasticity
Volume 2021, Article ID 2662585, 14 pages
https://doi.org/10.1155/2021/2662585

Review Article

Neuroplasticity of Acupuncture for Stroke: An Evidence-Based Review of MRI

Jinhuan Zhang,[1] Chunjian Lu,[1] Xiaoxiong Wu,[1] Dehui Nie,[1] and Haibo Yu[1,2]

[1]*The Fourth Clinical Medical College of Guangzhou University of Chinese Medicine, Shenzhen 518033, China*
[2]*Shenzhen Traditional Chinese Medicine Hospital, Shenzhen 518033, China*

Correspondence should be addressed to Haibo Yu; 13603066098@163.com

Received 23 May 2021; Revised 6 July 2021; Accepted 2 August 2021; Published 20 August 2021

Academic Editor: Yating Lv

Acupuncture is widely recognized as a potentially effective treatment for stroke rehabilitation. Researchers in this area are actively investigating its therapeutic mechanisms. Magnetic resonance imaging (MRI), as a noninvasive, high anatomical resolution technique, has been employed to investigate neuroplasticity on acupuncture in stroke patients from a system level. However, there is no review on the mechanism of acupuncture treatment for stroke based on MRI. Therefore, we aim to summarize the current evidence about this aspect and provide useful information for future research. After searching PubMed, Web of Science, and Embase databases, 24 human and five animal studies were identified. This review focuses on the evidence on the possible mechanisms underlying mechanisms of acupuncture therapy in treating stroke by regulating brain plasticity. We found that acupuncture reorganizes not only motor-related network, including primary motor cortex (M1), premotor cortex, supplementary motor area (SMA), frontoparietal network (LFPN and RFPN), and sensorimotor network (SMN), as well as default mode network (aDMN and pDMN), but also language-related brain areas including inferior frontal gyrus frontal, temporal, parietal, and occipital lobes, as well as cognition-related brain regions. In addition, acupuncture therapy can modulate the function and structural plasticity of post-stroke, which may be linked to the mechanism effect of acupuncture.

1. Introduction

Stroke is a common disease that affects one in four people during their lifetime [1], globally, and it continues to be a leading cause of death and long-term disability worldwide, imposing a significant financial burden on healthcare systems and families [2, 3]. Although stroke incidence and prevalence have declined worldwide, however, a recent national epidemiological survey [4, 5] indicated that China has an estimated 11 million prevalent cases of stroke, 2.4 million new cases of stroke, and 1.1 million stroke-related deaths. Hemiparesis and aphasia are two of the prominent impairments caused by a stroke that affect activities of daily living activities and quality of life [6–8]. More than 80% of post-stroke patients experience upper or lower limb hemiplegia, severely disturbing their daily activities [9]. Some studies have found that almost 20%-40% of all stroke survivors have chronic aphasic symptoms [10, 11]. It is well known that returning to work and social activities is the key priority for stroke survivors. Therefore, it is critical to understand stroke pathogenesis and explore its appropriate treatment.

Previous studies [12, 13] have demonstrated that post-stroke patients have structural and connectivity changes in their brains. Luckily, the brain's plasticity, a broad term for the proof the human brain to adapt to environmental pressure, experiences, and challenges including brain damage [14, 15], enables stroke rehabilitation. Although many patients experience some degree of spontaneous recovery, that is, a time-determined amount of improvement in physical function and activity [16], it is often incomplete and the recovery rates of neurological function vary. Therefore, external stimulus interventions are still needed. However, despite extensive research efforts on multiple treatment modalities, no single rehabilitation intervention has been demonstrated to be definitively beneficial for recovery [17]. Even the most commonly used repetitive transcranial

magnetic stimulation (rTMS) and transcranial direct current stimulation (tDCS) were not recommended for routine stroke treatment in two Cochrane reviews [18, 19]. Due to a lack of effective therapy, researchers considered alternative approaches that improve stroke recovery. As a relatively inexpensive and safe treatment, acupuncture has been widely employed to improve motor, sensation, and some neurological functions of stroke for thousands of years. Furthermore, several clinical [20–22] research and systematic reviews [17, 23, 24] revealed that acupuncture, as a promising intervention, could improve motor and language function and daily living activities. Numerous studies [25–27] have suggested that plasticity and reorganization contribute to the recovery.

However, the current understanding of neuroplasticity after stroke is primarily based on invasive methods, such as histology and immunohistochemistry, which do not allow for dynamic assessment of functional recovery and tissue remodeling [28]. In contrast, magnetic resonance imaging (MRI) can noninvasively monitor dynamic change after stroke and in vivo. Structural magnetic resonance imaging (sMRI) technique can provide a high anatomical resolution [29], whereas functional magnetic resonance imaging (fMRI) can reveal real-time brain activity by indirect measurement of regional blood flow [30]. Combined with sMRI and fMRI, the central nervous effect of acupuncture for stroke could be fully elucidated from an anatomical and functional perspective. Moreover, emerging clinical studies have demonstrated that acupuncture could reorganize motor-related networks and increase functional connectivity between premotor cortex (PM)/adjacent supplementary motor area (SMA) and supramarginal gyrus (SMG) [31–33]. In addition, acupuncture therapy has various properties, such as the choice of acupoints, whether deqi or not, which may be the influencing factors of acupuncture on the plasticity of stroke patients.

Nevertheless, the underlying neuroplasticity mechanisms on acupuncture for stroke have received little attention to date. Therefore, the review will mainly focus on the evidence to elucidate the possible mechanisms of acupuncture therapy in treating stroke through regulating brain plasticity based on MRI to better select and stratify patients for future appropriate treatment strategies that promote poststroke recovery. We firstly describe research characteristics of acupuncture for stroke based on MRI. Then, we discuss the neuroplasticity mechanism of acupuncture and its properties on stroke. Furthermore, we also review the limitations and prospects to be explored in the future.

2. Materials and Methods

We conducted a literature search for MRI studies on acupuncture for stroke published in PubMed, Web of Science, and Embase from inception to April 9, 2021. Database searches were conducted using the following keywords: (acupuncture OR electroacupuncture OR moxibustion) AND (stroke OR cerebral ischemia OR ischemic cerebrovascular disease OR hemiparesis or hemiplegia OR post-stroke) AND (MRI OR magnetic resonance imaging OR functional MRI and structural MRI OR BOLD OR ReHo OR ALFF OR fALFF OR white matter OR voxel-based analysis OR VBM OR voxel-based morphometry OR Freesurfer OR surface-based morphometry OR cortical thickness OR surface area OR cortical volume OR gray matter volume OR gray matter density OR DTI). Studies were eligible if they met the following inclusion criteria: (1) randomized controlled trials (RCTs) and nonrandomized studies (i.e., observational studies, case-control studies, and cohort studies); (2) patients met established diagnostic criteria of stroke; (3) subjects in the study at least underwent MRI of the brain on one occasion: under the acupuncture state or before and after acupuncture treatment. We excluded studies that met the following criteria: (1) protocol, case reports, or case series. (2) Other interventions that do not belong to traditional acupuncture, such as transcutaneous electrical nerve stimulation and transcutaneous vagus nerve stimulation. (3) Comorbid severe mental illness or neurological illness.

All identified studies were imported into EndNote; duplicate studies were removed first, and then after scanning titles and abstracts and reading the full text, eligible studies were decided whether they should be included in the review.

Two authors extracted the following data: publishing year, author, number of participants, type of ischemic stroke, intervention/control groups, needling details, types of acupuncture, acupuncture points, data analysis, and experimental design. Any inconsistencies were discussed and resolved with the third author until an agreement is reached. Twenty-four human studies and five animal studies were finally included (Figure 1).

In this review, 24 stroke patient studies were included that use MRI to investigate the mechanism of acupuncture for stroke. The results indicated that acupuncture could modulate brain plasticity in motor-related and language-related networks of stroke patients. For acupuncture modality, 20 studies applied manual acupuncture (MA), and two studies used electroacupuncture (EA). Stroke types were found to be related to ischemic stroke. The publication years ranged from 2006 to 2020, indicating that research on this aspect has gradually become a research hotspot over the last 15 years. The sample size of the study ranged from 7 to 43 (mean 24). The study design mainly has several kinds: before vs. after acupuncture, acupuncture vs. sham acupuncture (SA), acupuncture vs. waiting group, patients vs. healthy controls (HC), and acupuncture plus drugs/conventional therapy vs. drugs/conventional therapy. In addition, except for five studies [34–38] with resting-state (RS) and long-term effects, all other studies investigated task-stating and instant effects. The detailed characters of included studies are listed in Table 1. In addition, five animal experiments also were included. The years of publication ranged from 2011 to 2021, and the study design mainly includes middle cerebral artery occlusion (MCAO) vs. MCAO plus EA group vs. sham operation group and EA vs. non-EA group. The detailed characters of the included studies are listed in Table 2.

3. Modulation of Brain Plasticity in Stroke

Stroke alters the landscape of the brain and impairs the function of various systems and structures [59]. One of the most striking features of the brain is its ability to adapt to external

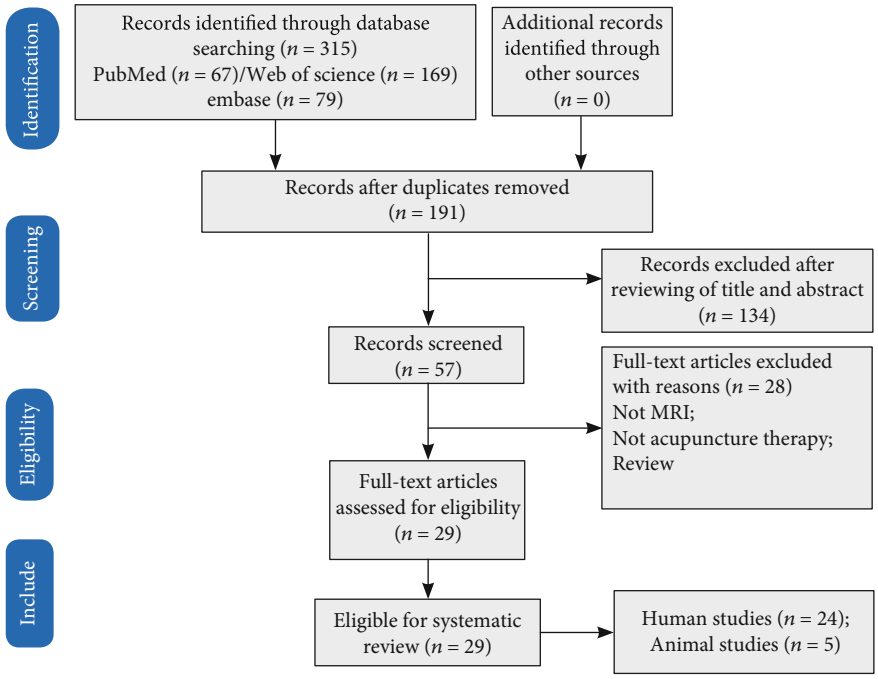

Figure 1: PRISMA flow diagram. Note: PRISMA: preferred reporting items for systematic reviews and meta-analyses.

and internal stimuli. Indeed, several decades ago, Hebb [60] puts forward a theoretical framework that described the phenomenon of brain adaptation to the environment based on experience and development. The theories of neuroplasticity showed that thinking and learning change both the brain's physical structure and functional organization. Basic mechanisms that are involved in plasticity include neurogenesis, programmed cell death, and activity-dependent synaptic plasticity [61]. As the research progresses, neural plasticity is a general term that refers to functional and structural changes that occur in the brain during development, interaction with the environment, aging, learning, and in response to trauma [62, 63]. Adult brain plasticity following stroke is due to numerous diffuse and redundant connections in the central nervous system and the ability to form new structural and functional circuits through remappings between related cortical regions [64]. MRI has the advantage of providing repeated whole-brain measurements, making it ideal for longitudinal studies of network-level brain plasticity [62].

Brain plasticity occurs at many levels from molecules to cortical reorganization [27]. Advances in MRI technology have allowed system-level monitoring of brain structure and function in vivo. Functional plasticity can be detected through changes in the strength of functional interactions between brain regions, whereas structural changes can be identified in vivo indirectly and nonspecifically via sMRI measures [62].

Pathologically, damage to regions of the motor-related cerebral cortex, such as primary motor area (M1), premotor area (PMA), supplementary motor area (SMA), somatosensory area (S1), prefrontal cortex (PFC), and posterior parietal cortex (PPC) [65], results in hemiplegia. In contrast, damage to regions of the left perisylvian network, including inferior frontal gyrus (IFG), middle frontal gyrus (MFG), angular gyrus (AG), supramarginal gyrus (SMG), superior temporal gyrus (STG), middle temporal gyrus (MTG), inferior temporal gyrus (ITG), and supplementary motor area (SMA), leads to aphasia. Fortunately, a large body of research evidence indicates that the brain recovers rapidly and reorganizes its structure and function following a stroke. In other words, specific linguistic impairments caused by stroke showed substantial recovery in the first few months following a stroke [66], and hemispheric interactions have complex effects on the recovery of brain function after stroke [67, 68].

As research on poststroke recovery increases, one meta-analysis [69] of motor-related neural activity after stroke included 36 studies and demonstrated that consistently activated regions include contralesional primary motor cortex (M1), bilateral ventral premotor cortex, and supplementary motor area (SMA) compared with healthy controls (HC). Interestingly, this is consistent with another meta-analysis [9], which investigated the modulation of interhemispheric activation balance (IHAB) in stroke patients with motor recovery and demonstrated that IHAB is upregulated in sensorimotor cortex(SMC) and premotor cortex (PMC), but not significantly changed in SMA and cerebellum (CB). In addition, several studies also investigated the underlying mechanism of language processing in aphasia and found that early stroke patients showed significantly decreased functional connectivity (FC) in the language network [70]. Rs-fMRI studies also revealed a significant correlation between disrupted functional connectivity and the severity of post-stroke language impairment [71].

4. Brain Plasticity in Stroke with Acupuncture

Brain plasticity provides a critical theoretical basis for central nervous system therapy [72]. In this review, 24 human and

Table 1: Characteristics of the 24 included stroke patients studies.

N	Author (year)	Journal	Stroke information				MRI information	Acupuncture information			Data analysis	Experimental design
			Subjects	Affected side	Type of stroke, lesions (N)	Interval since stroke	Scanner	Intervention	Comparison	Acupoints		
1	Li et al. 2006 [39]	Journal of magnetic resonance imaging	12 stroke	The left side somatosensory deficits	IS, right hemispheric striatocapsular infarction	More than 6 months	1.5 T	MA	Stroke vs. HC	LI4 and LI11	SPM	Block/R(45 s)-S(45 s), 3 times
2	Schaechter et al. 2007 [34]	The journal of alternative and complementary medicine	7 stroke	NA	IS (5), HS (2), 5 left, and 2 right	4.6 ± 3.2 years	3 T	MA, SA (Streitberger needle, noninvasive control)	4 VA vs. 3 SA	N	GLM	RS/twice weekly for 10 weeks.
3	Li and Yang 2010 [40]	Complementary therapies in medicine	7 aphasia stroke/14 HC	The right side of the body	IS (6), HS (1); the occlusion of the middle cerebral artery, left hemisphere	More than 6 months	1.5 T	EA	Stroke vs. HC	SJ8	SPM	Block/R(45 s)-S(45 s), 3 times
4	Huang et al. 2011 [41]	NRR	12 stroke	The left hemiataxia and sensory disturbance	IS, right hemisphere	6.08 ± 6.40 months	3 T	MA, SA (nonacupuncture points in close proximity to acupuncture points)	6 VA vs. 6 SA	SJ5	ReHo	Block/S(30 s)-R(30sn), 6 times
5	Shen et al. 2012 [37]	ECAM	20 stroke	Basal ganglia, and completely or partially covered the internal capsules	IS	10.70 ± 11.13 hours	1.5 T	MA	10 acupuncture plus conventional treatments vs. 10 only conventional treatments	Du23, Du 20, EX-HN3, PC 6, and Sp 6	FA and ADC	RS/30 min, once a day, for 2 weeks
6	Cho et al. 2013 [42]	Chinese journal of integrative medicine	11 stroke/10 HC	The left side of the body	IS, right hemisphere	2-6 months	3 T	MA	Stroke vs. HC	LI11 and ST36	SPM	Block/R(30 s)-S(30 s), 3 times
7	Huang et al. 2013 [43]	Acupuncture in medicine	10 stroke	The right hemiplegia	IS, left hemispheric	1-12 months	3 T	MA	Before vs. after	SJ5	GLM	Tactile control (6 min)-R(5 min)-block/S(30 s)-R(30 s), 6 times
8	Chen et al. 2013 [44]	NRR	10 stroke/6 HC	The right hemiataxia	IS, left basal ganglia	5.30 ± 3.71 months	3 T	MA	Stroke vs. HC	SJ5	FC	Block/R(30s)-S(30s), 6 times
9	Bai et al. 2014 [31]	ECAM	9 stroke/8 HC	The left side of the body	IS, right hemispheric striatocapsular	2-12 weeks	3 T	MA	Before vs. after	GB34	FC	NRER/R(1 min)-S(1 min)-R(8 min)

Table 1: Continued.

N	Author (year)	Journal	Stroke information				MRI information	Acupuncture information			Data analysis	Experimental design
			Subjects	Affected side	Type of stroke, lesions (N)	Interval since stroke	Scanner	Intervention	Comparison	Acupoints		
10	Chen et al. 2014 [45]	PLoS one	24 stroke	The right hemiplegia	IS, left basal ganglia	1 month-1 year	3 T	MA, SA (tactile control, a noninvasive control)	12 VA vs. 12 SA	SJ5	FC	Block/rested for 5 min-SA(6 min 30 s)-R(6 min 2 s)-VA(6 min 30 s).
11	Qi et al. 2014 [46]	NRR	16 stroke	The right hemiataxia	IS, primarily in the left hemisphere	4.63 ± 3.85 months/4.63 ± 4.41 months	3 T	MA, SA (nonacupuncture points in close proximity to acupuncture points)	8 VA vs. 8 SA	SJ5	SPM	Block/R(30 s)-S(30 s), total 6 min 6 s
12	Xie et al. 2014 [32]	ECAM	9 stroke/8 HC	The left side of the body	IS, unilateral right-sided striatocapsular lesions	53.6 ± 41.6 days	3 T	MA	Stroke vs. HC	GB34	GLM and GCA	NRER/R(1 min)-S(1 min)-R(8 min)
13	Zhang et al. 2014 [47]	ECAM	8 stroke/10 HC	The left side of the body	IS, right hemispheric corona radiate, internal capsule, or basal ganglia infarction	2–12 weeks	3 T	MA	Stroke vs. HC	GB34	SPM	NRER/R(1 min)-S(1 min)-R(8 min)
14	Li et al. 2015 [48]	NRR	12 stroke	The right hemiataxia	IS, left basal ganglia	1 month-12 months	3 T	MA	Before vs. after	SJ5	SPM	Block/(30 s)-S(30 s), 6 times
15	Gao et al. 2015 [49]	Experimental and therapeutic medicine	10 stroke/10 HC	NA	IS, right subcortical	At least 6 months	3 T	MA	Stroke vs. HC	ST36	GLM	Block/(30 s)-S(30 s), 6 times
16	Chang et al. 2017 [50]	Wiener klinische Wochenschrift	43 poststroke motor aphasia	NA	Cerebral hemorrhage or cerebral infarction	14 days to 2 years	3 T	EA	22 EA vs. 21 WT	HT5, GB39	GLM	Block/R(30 s)-S(30 s), total 6 min 6 s
17	Fu et al. 2017 [51]	Medicine	19 stroke/17 HC	The left hemiplegia	IS, internal capsule, and neighboring regions in the right hemisphere	2 weeks to 6 months	3 T	MA	Before vs. after	GB34	ICA	RS/R(8 min 10 s)-needing in (1 min)-S(1 min)-R(8 min 10 s)
18	Ning et al. 2017 [52]	Frontiers in human neuroscience	18 stroke/20 HC	The left motor hemiparesis	First-ever IS, right subcortical stroke	Within 6 months after the onset	3 T	MA	Before vs. after	GB34	GLM, FC	NRER/R(1 min)-S(1 min)-R(8 min)

Table 1: Continued.

N	Author (year)	Journal	Stroke information				MRI information	Acupuncture information			Data analysis	Experimental design
			Subjects	Affected side	Type of stroke, lesions (N)	Interval since stroke	Scanner	Intervention	Comparison	Acupoints		
19	Li et al. 2017 [35]	Neural plasticity	17 stroke/14 HC	The right side of the body	IS, left basal ganglia, caudate nucleus, centrum semiovale, and lenticular nucleus	At least three weeks	3 T	MA	8 MA + drug vs. 9 drug	DU20, GB20, bilateral GB-39, LI-11, LI-4, ST-36, SP-6	FC	RS/two hours a day for 5 days a week, one week a course, continuous four courses
20	Wu et al. 2017 [38]	Journal of traditional Chinese medicine	21 stroke	NA	IS	Less than six months	3 T	MA	11 MA plus CT vs. 10 CT	DU20, GB20, LI11, LI4, GB34, ST36, SP6, and GB39	ReHo	RS/30 min, 2 times/week for 5 weeks
21	Wu et al. 2018 [36]	ECAM	21 stroke	NA	IS	Less than six months	3 T	MA	11 MA plus CT vs. 10 CT	DU20, GB20, LI11, LI4, GB34, ST36, SP6, and GB39	VBM	RS/30 min, 2 times/week for 5 weeks
22	Han et al. 2019 [33]	ECAM	22 stroke/22 HC	The left side of the body	IS, right-hemispheric subcortical infarct	41.68 ± 25.02 days	3 T	MA	Stroke vs. HC	GB34	FC	NRER/R(8 min 10 sec)-S(1 min)-R(8 min 10 sec)
23	Chen et al. 2020 [53]	Chinese journal of integrative medicine	10 stroke	The left side of the body	IS, the vascular occlusion in the right basal ganglia	1 month-3 years	3 T	MA	Before vs. after	LI11 and ST36	ReHo	RS/R(5 min)-S(15 min)-R(5 min)
24	Han et al. 2020 [54]	Neural plasticity	26 stroke/21HC	The left side of the body	IS, right hemispheric subcortical infarct	41.04 ± 29.71 days	3 T	MA	Stroke vs. HC	GB34	Graph theoretical network	RS/R(8 min 10 s)-S(60 s)-R(8 min 10 s)

Note: ADC: apparent diffusion coefficient; BOLD: blood oxygen level-dependent; CT: conventional treatments; EA: electroacupuncture; ECAM: Evidence-Based Complementary and Alternative Medicine; FA: fractional anisotropy; FC: functional connectivity; GCA: granger causality analysis; GLM: general liner model; HC: health controls; HS: hemorrhagic stroke; IS: ischemic stroke; MA: manual acupuncture; *N*: number; NA: not applicable; NRER: nonrepeated event-related; RS: resting state; NRR: Neural Regeneration Research; ReHo: regional homogeneity; TBSS: tract-based spatial statistics; R: rest; s: seconds; SA: sham acupuncture; S: stimulation; VA: verum acupuncture; min: minutes; VBM: voxel-based morphometry; WT: waiting list; ICA: independent component analysis; Y: yes. A.

Table 2: Characteristics of the five included animal studies.

Study (years)	Journal	Stroke information			MRI information	Groups	Acupuncture information		Data analysis
		Main symptoms	Species	The affected side	Magnet strength (T)		Treatment group	Acupoints	
Zhang et al. 2011 [55]	Brain injury	Middle cerebral artery occlusion (MCAO) model	SD rats, after 24 hours of the surgery	Left side	NA	(1) MCAO, $n = 6$ (2) MCAO + EA, $n = 6$	EA, 30 minutes	DU20	DWI
Wu et al. 2012 [56]	Acupuncture in medicine	Transient middle cerebral artery occlusion (tMCAO)	SD rats, after 30 minutes of the surgery	Left side	1.5-T	(1) SC, $n = 12$ (2) tMCAO, $n = 12$ (3) tMCAO + EA, $n = 12$	MA, 30 minutes for 28 days	DU20, DU14, LI10, and ST36	ADC value and the FA
Liang et al. 2017 [57]	Journal of stroke and cerebrovascular diseases	Motor impairments/middle cerebral artery occlusion (MCAO)	SD rats, after 24 hours of the surgery	Left side	7.0 T	(1) SC, $n = 12$ (2) MCAO, $n = 9$ (3)MCAO + EA, $n = 9$	EA, 30 minutes per day for 7 consecutive days	ST36 and LI11	ReHo
Wen et al. 2018 [58]	Journal of stroke and cerebrovascular diseases	Middle cerebral artery occlusion induced cognitive deficit (MICD)	SD rats, after 24 hours of the surgery	Left side	7.0 T	(1) SC, $n = 12$ (2) MICD, $n = 12$ (3) MICD + EA, $n = 12$	EA, 30 minutes per day for 14 consecutive days	DU20 and DU24	ALFF
Li et al. 2021 [81]	Acupuncture in medicine	Motor impairments/middle cerebral artery occlusion (MCAO)	SD rats, after 24 hours of the surgery	Left side	7.0 T	(1) SC, $n = 12$ (2) MCAO, $n = 9$ (3) MCAO + EA, $n = 9$	EA, 30 minutes per day for 14 consecutive days	LI11 and ST36	FC, left motor cortex as the seed region

Note: ALFF: amplitude of low-frequency fluctuations; DWI: diffusion-weighted imaging; SC: sham-operated control; SD: Sprague-Dawley rats.

five experimental studies investigated the neuroplasticity mechanism of acupuncture in treating poststroke motor impairment, motor aphasia, and cognitive impairment from different analytical methods, study, and experimental designs based on MRI. We summarized the findings based on analytic methods and different rehabilitation aspects.

4.1. Stroke Patients' Studies. FC provides one method based on a system-level approach to quantify the functional integration of various brain regions by correlating brain activity to detect neural interactions between regions, which are quite compelling [73]. Moreover, FC analyses can provide experience-dependent plasticity at the macro level of large-scale functional networks, which are foundational to remediation interventions that maximize function recovery [74]. FC of the three studies used M1 as the region of seed interest, and the results revealed that acupuncture increased FC between left primary motor cortex (M1) and right M1, premotor cortex, supplementary motor area (SMA), thalamus, and cerebellum.

The Granger causality analysis is used to analyze the flow of information between time series, which has been widely used in the field of neuroscience [75]. A study [32] used the multivariate Granger causal analysis method and found that acupuncture induced a concentrated and bidirectional enhancement in effective connectivity between cerebellum and primary sensorimotor cortex in stroke patients. In addition, acupuncture probably integrated the effective connectivity internetwork by modulating multiple networks and transferring information between left frontoparietal network (LFPN) and sensorimotor network (SMN) by default mode network (aDMN and pDMN) as the relay station [51].

Graph theoretical analysis provides an uncomplicated but powerful mathematical framework to describe topological properties of brain networks, such as modularity, efficiency, and hubs [76, 77]. A study [54] using this method found that acupuncture could modulate the disrupted patterns of the whole-brain network following stroke, elucidating the possible mechanisms underlying the functional reorganization of poststroke brain networks following acupuncture intervention from a large-scale perspective.

Regional homogeneity (ReHo) is used to evaluate signal synchronization by calculating the time-series similarity in BOLD signals within local brain regions [78]. Acupuncture was found to increase ReHo values in the right precentral gyrus and superior frontal gyrus while decreasing them in the right superior parietal lobule, left fusiform gyrus, and left supplementary motor area.

Apart from that, voxel-based-morphometry (VBM) and diffusion tensor imaging (DTI) are popular structural MRI technique to investigate regional differences in brain volume and microstructural integrity [79, 80]. According to some studies [36, 37], acupuncture could lead to pronounced structural reorganization in frontal areas and network of DMN areas and increase fractional anisotropy (FA) values.

In addition, the plasticity function of acupuncture on stroke is manifested not only in motor function but also in language. Acupuncture was found to activate language-related brain areas, including frontal, temporal, parietal, and occipital lobes, as well as insula, precuneus, and other wide range of brain function areas.

In order to determine the efficacy of acupuncture, the design of comparison mainly has three kinds: stroke vs. HC, VA vs. SA, and VA plus drug vs. drug. Results demonstrated that VA compared with SA, VA plus drug compared with drug, and acupuncture in patients compared with that in HC all have the characteristics of remodeling the brain structure and function of stroke patients.

4.2. Animal Studies. Each of the five animal studies investigated the mechanism of acupuncture for stroke; among them, four studies focus on poststroke motor impairments, while the fourth examines poststroke cognitive impairment.

Wen et al. [58] investigated the effect of EA for middle cerebral artery occlusion induced cognitive deficit (MICD) group and found that brain infarction volume was reduced and ALFF was decreased in auditory cortex, cingulate gyrus, lateral nucleus group of dorsal thalamus, and hippocampus after 14 days of treatment.

One study [55] using DWI (diffusion-weighted imaging) indicated that the mechanism by which EA can treat acute stroke may be by reducing cerebral edema. While Wu et al. [56] found that acupuncture improved motor function, brain microscopy using DTI technique.

A recent study [81] showed that EA could decrease the infarct volumes of MCAO rats, improve mNSS scores, and enhance FC between the left motor cortex and left cerebellum posterior lobe, right motor cortex, left striatum, and bilateral sensory cortex.

ReHo also was used to investigate the regional neural activity alterations of stroke, and the results showed that EA could increase ReHo in auditory and motor cortex, lateral nucleus group of dorsal thalamus, hippocampus, and others [57].

Briefly, the above studies demonstrated that acupuncture promotes stroke-related neural plasticity from structural and functional aspects. The rehabilitation mechanism of acupuncture on stroke patients may be linked to the remodeling of motor and cognitive brain regions such as motor cortex, bilateral striatum, and sensory cortex hippocampus.

4.3. Factors Associated with the Brain Plasticity of Acupuncture. In this review, the influencing factors of acupuncture on stroke plasticity based on MRI include the type of SA, deqi, different acupoints, and different pathological states.

Compared to SA, four studies [34, 37, 41, 45, 46] demonstrated that VA produces a greater maximum activation change in the motor-related area, improves blood flow to ischemic areas, and promotes stroke recovery. However, one study [46] discovered significant impact variations between VA and SA at TE5, but little difference between verum acupoint and nonacupoint, implying that different SA types also have distinct brain responses.

Eight studies [32, 33, 39, 40, 42, 44, 47, 49, 54] have compared the differences in brain plasticity between stroke patients and HC and found that the modulation effect of acupuncture on stroke patients was more specific and more

obvious than that of HC in brain regions associated with disease.

In terms of the choice of acupoints, the most commonly used acupuncture points are mainly in the limbs, and the most frequently used acupoints are GB34 and SJ5.

One study [48] investigated the central mechanism of deqi of acupuncture in the treatment of ischemic stroke and found that compared with the non-deqi group, the deqi group produced marked activation of the right anterior lobe of the cerebellum and right limbic lobe.

5. Discussion

In this review, we included 24 human studies and 5 animal studies and found that that acupuncture reorganizes not only motor-related network, M1, SMA, sensorimotor network (SMN), FA, aDMN, and pDMN but also language-related brain areas include inferior frontal gyrus frontal, temporal, parietal and occipital lobes as well as cognition-related brain regions. In addition, the plasticity of acupuncture is influenced by deqi, acupoints, and physiological state.

5.1. Brain Plasticity of Acupuncture. Stroke causes not only local structural changes in the injured brain regions but also damage to neuronal networks, impairing sensation, movement, or cognition [64, 82]. Under physiological conditions, both hemispheres inhibit each other, and after a stroke, this balance of interaction/inhibition may be upset due to damage to one side of the brain. Moreover, recent studies [83, 84] have demonstrated that interhemispheric imbalance is closely related to the motor function of the affected hand in chronic stroke patients. Thus, several studies [31, 42, 43, 46] have indicated that acupuncture could inhibit contralesional brain activity while activating the ipsilesional motor cortex. Huang et al. [43] indicated that acupuncture results in lateralization in unilateral stroke patients. This lateralization may represent an enhancement of the compensatory process through acupuncture that redistributes function to the intact cortex, especially the unaffected hemisphere. In addition, studies [44, 52] also showed that acupuncture could stimulate bilateral regions, modulate whole-brain network, and enhance functional connectivity. This indicated that acupuncture could not only specifically regulate the bilateral dynamic balance of the brain but also modulate the whole brain network and functional connections as a whole.

The pathogenesis of stroke is complex, the time since stroke, lesion size, location, and other biological factors (such as age and sex) all contribute to the differences between individuals. Therefore, in clinical practice, individualized treatment is based on TCM syndrome differentiation theory, the theory of constitution, and characteristics of patient, season, and locality. However, among the included studies, the reason the current study did not apply individualized therapy is that it requires big data to explore the impact of patients, doctors, and acupuncture on efficacy. In the future, the use of artificial intelligence coupled with continuous monitoring should enable greater individualization and improve outcomes. Importantly, although different acupoints were used across studies, they all could remodel brain areas associated with stroke lesions. For instance, several studies [31, 33, 51, 52] have demonstrated that acupuncture could enhance FC of between bilateral M1s, between the cerebellum and primary sensorimotor cortex, which indicated that acupuncture has not only specific but also common effects on the disease.

Additionally, as described above, although acupuncture therapy can modulate the function and structural plasticity of poststroke in this review. Indeed, structural plasticity has been explored in only one study for the following reasons: on the one hand, the study did not detect structural changes in stroke patients; on the other hand, there was a change in structural plasticity following acupuncture, but the small changes were difficult to identify due to lacking of subdivision of brain regions.

5.2. Factors Associated with the Brain Plasticity of Acupuncture. This review found that different SA types also have distinct brain responses. The overlapping dermatomes between nonacupoints and verum acupoints may explain this phenomenon, as the segmental structure of the body and its interconnected reflex system offers neurophysiological effects [85]. Therefore, the selection of proper SA is critical in determining the efficacy of acupuncture.

When it comes to acupoint selection, the most frequently used acupoints are GB34 and SJ5. GB34 is located on the lateral aspect of the posterior knee, which is the most often used acupoints to generally improve symptoms in motor impairment patients. GB34 belongs to the sea point of gallbladder meridian of foot Shaoyang. SJ5 is found in the dorsal wrist lines on two inches between the ulna and radius. SJ5, belonging to Sanjiao Meridian of Hand Shaoyang, is one of "Ba-mai Jiao-hui point." The two acupoints have been widely used to alleviate symptoms in motor impairment patients. Although the two acupoints were located in the upper and lower extremities, the activated brain regions included bilateral brain, such as somatosensory cortex and primary sensorimotor. This indicated that various acupoints treat the same disease in a convergent manner.

For decades, it was believed that the deqi of acupuncture is associated with its clinical efficacy. Using fMRI techniques in acupuncture research, several studies [86, 87] have found that acupuncture with deqi can stimulate significant brain activity compared to acupuncture without deqi. In this review, although the deqi group exhibited significant activation of the right anterior lobe of the cerebellum and right limbic lobe (BA30), larger sample sizes are still required for further validation.

Regarding different states and based on TCM theory, this review found that acupuncture showed specific modulations of a motor-related network in stroke patients relative to HC. This phenomenon is in line with the TCM theory that acupuncture can regulate the disorder of the body in dual-direction regulation. This indicated that acupuncture in patients mainly regulate the brain regions associated with the disease, while acupuncture in HC mainly activated brain areas directly associated with the main treatment effects.

In the aspect of different states, based on TCM theory, acupuncture can regulate the disorder of the body in dual-

direction regulation. Acupuncture exhibits distinct regulatory effects on the body under physiological and pathological conditions. This indicated that acupuncture showed specific modulations of a motor-related network in stroke patients relative to HC.

In summary, the brain plasticity of acupuncture on stroke is influenced by many factors, such as deqi, acupoints, pathological state, and SA type. As a result, it is important to continue exploring the most effective strategies for treating stroke with acupuncture in the future.

5.3. Prospects for Brain Plasticity of Acupuncture. Numerous clinical and experimental researches revealed that the brain was plastic and could be remodeled by the environment and experience [88, 89]. Currently, the National Institutes of Health in the United States has recently adopted acupuncture as a treatment for poststroke rehabilitation, demonstrating that acupuncture is widely accepted for such therapy [90]. From a systematic level, this study found that the effective mechanism is that acupuncture can reorganize the brain structure and functional connections in stroke patients.

Indeed, acupuncture's function to reshape the brain is not limited to stroke, as a recent review [91] of brain plasticity in animals revealed that acupuncture could modulate the plasticity of various central nervous systems, such as depression, neuropathic pain, Alzheimer's disease, and cerebral vascular disorders. More research in humans still requires further verification.

In addition, this review stated that acupuncture's plasticity on stroke was affected by several factors, such as deqi, acupoints, pathological state, and type of sham needle. Exploring the impact of these influencing factors on the efficacy and constructing a pathway connecting "acupoint-brain" is also critical for future individualized therapy. Moreover, predicting the efficacy of individual patients receiving acupuncture treatment for stroke to achieve precision treatment impact is a problem that requires future research. The recent integration of machine learning (ML) and neuroimaging techniques provides a promising approach to understanding how acupuncture facilitates neuroplasticity at the individual level. This approach enables us to investigate not only the effect of acupuncture influencing factors on brain plasticity prediction but also the impact of specific brain plasticity on acupuncture efficacy prediction.

Interestingly, a recent review [92] examined the neuroplasticity of acupuncture using machine learning and neuroimaging techniques and found that brain functional plasticity is affected by different acupoints and acupuncture manipulations and that specific structural and functional neuroplasticity characteristics at baseline could accurately predict the improvement of symptoms after acupuncture treatment. This review summarizes two commonly used methods for predicting the efficacy of acupuncture. One method is to adopt the classification algorithms to predict patients' responses to acupuncture treatment. The other method is to construct the regression models to predict the continuous improvement in symptoms after acupuncture treatment. Currently, this is the mainly used medication for pain and functional dyspepsia. Since research in this field remains in its infancy and faces many challenges, many efforts remain to be done in the future.

Apart from that, although several reviews [93, 94] have been published on acupuncture on stroke in animals at the molecular level, there have been a few animal studies on MRI-based acupuncture in stroke treatment. One possible reason is that the MRI mechanism is easy to manipulate in humans, unlike studies at the cellular and molecular levels. The other reason is that experimental stroke models do not fit perfectly into clinical situations, influencing the extrapolation of results. However, animal research also exhibits several advantages, including low costs, small variations, controllable factors, and high reproducibility. As a result, additional experimental studies may be required to elucidate the mechanism of influencing acupuncture factors on stroke.

5.4. Limitations. Although this review comprehensively summarizes the evidence from extensive MRI-based literature on acupuncture for stroke, several limitations remain. First, the main criticism is of this review is that study design, experimental design, and analytic methods may influence the extrapolation of conclusions, which also makes it difficult to do a meta-analysis. More relatively consistent designs and methods are required to conduct a quantitative meta-analysis determining the brain region of plasticity on acupuncture for stroke in order to provide comprehensive evidence. Because systematic reviews and meta-analyses are important tools for summarizing specific topics that inform evidence-based practice in healthcare, guidelines, and policies in a comprehensive, meaningful manner [95]. Another drawback is the absence of SA as a control group, making it difficult to draw reliable conclusions and confirm acupuncture specificity. Third, the limited number of articles and small sample sizes limit the stability and reliability of this review; a large sample size and additional research are required. In addition, we include only peer-reviewed studies conducted in English, which could introduce some selection bias. Finally, since many studies did not perform correlation analyses between brain imaging and behavioral characteristics before and after treatment, it is difficult to clarify that changes in brain imaging are objective evidence of improvement in symptoms. Accordingly, future researchers should pay much attention to this research area. Therefore, to overcome the previously mentioned limitations, extensive research efforts need to be conducted in the future.

5.5. Conclusions. In summary, the cumulative evidences demonstrated that acupuncture could modulate neural plasticity of stroke, activating not only motor-related brain but also language-related and cognitive-related brain regions. Consequently, acupuncture therapy can enhance clinical recovery following a stroke. However, additional research is necessary to validate the results due to the scarcity of data.

Data Availability

Our data are from the published literature.

Conflicts of Interest

The authors declare no competing financial interest.

Authors' Contributions

Z.J.H and L.C.J designed the whole study, analyzed the data, and wrote the manuscript. W.X.X and N.D.H searched and selected the studies. Z.J.H participated in the interpretation of data. Y.H.B offered good suggestions. All authors read and approved the final manuscript. Jinhuan Zhang and Chunjian Lu contributed equally to this work.

Acknowledgments

This work was supported by the National Key R&D Program of China (2019YFC1712200), International standards research on clinical research and service of Acupuncture-Moxibustion (2019YFC1712205), and Shenzhen's Sanming Project (SZSM201612001).

References

[1] GBD 2016 Lifetime Risk of Stroke Collaborators, V. L. Feigin, G. Nguyen et al., "Global, regional, and country-specific lifetime risks of stroke, 1990 and 2016," *The New England Journal of Medicine*, vol. 379, no. 25, pp. 2429–2437, 2018.

[2] "Global, regional, and national burden of stroke, 1990-2016: a systematic analysis for the Global Burden of Disease Study 2016," *Lancet Neurology*, vol. 18, no. 5, pp. 439–458, 2019.

[3] C. M. Stinear, C. E. Lang, S. Zeiler, and W. D. Byblow, "Advances and challenges in stroke rehabilitation," *Lancet Neurology*, vol. 19, no. 4, pp. 348–360, 2020.

[4] S. Wu, B. Wu, M. Liu et al., "Stroke in China: advances and challenges in epidemiology, prevention, and management," *Lancet Neurology*, vol. 18, no. 4, pp. 394–405, 2019.

[5] W. Wang, B. Jiang, H. Sun et al., "Prevalence, incidence, and mortality of stroke in China: results from a nationwide population-based survey of 480 687 adults," *Circulation*, vol. 135, no. 8, pp. 759–771, 2017.

[6] P. P. Urban, T. Wolf, M. Uebele et al., "Occurence and clinical predictors of spasticity after ischemic stroke," *Stroke*, vol. 41, no. 9, pp. 2016–2020, 2010.

[7] E. Moulton, S. Magno, R. Valabregue et al., "Acute diffusivity biomarkers for prediction of motor and language outcome in mild-to-severe stroke patients," *Stroke*, vol. 50, no. 8, pp. 2050–2056, 2019.

[8] R. Sebastian, K. Tsapkini, and D. C. Tippett, "Transcranial direct current stimulation in post stroke aphasia and primary progressive aphasia: current knowledge and future clinical applications," *NeuroRehabilitation*, vol. 39, no. 1, pp. 141–152, 2016.

[9] Q. Tang, G. Li, T. Liu et al., "Modulation of interhemispheric activation balance in motor-related areas of stroke patients with motor recovery: systematic review and meta-analysis of fMRI studies," *Neuroscience & Biobehavioral Reviews*, vol. 57, pp. 392–400, 2015.

[10] P. M. Pedersen, H. Stig Jørgensen, H. Nakayama, H. O. Raaschou, and T. S. Olsen, "Aphasia in acute stroke: incidence, determinants, and recovery," *Annals of Neurology*, vol. 38, no. 4, pp. 659–666, 1995.

[11] B. C. Stark and E. A. Warburton, "Improved language in chronic aphasia after self-delivered iPad speech therapy," *Neuropsychological Rehabilitation*, vol. 28, no. 5, pp. 818–831, 2018.

[12] J. C. Griffis, N. V. Metcalf, M. Corbetta, and G. L. Shulman, "Structural disconnections explain brain network dysfunction after stroke," *Cell Reports*, vol. 28, no. 10, pp. 2527–2540.e9, 2019.

[13] J. H. Lee, S. Kyeong, H. Kang, and D. H. Kim, "Structural and functional connectivity correlates with motor impairment in chronic supratentorial stroke: a multimodal magnetic resonance imaging study," *Neuroreport*, vol. 30, no. 7, pp. 526–531, 2019.

[14] B. B. Johansson, "Brain plasticity and stroke rehabilitation. The Willis lecture," *Stroke*, vol. 31, no. 1, pp. 223–230, 2000.

[15] A. Pascual-Leone, A. Amedi, F. Fregni, and L. B. Merabet, "The plastic human brain cortex," *Annual Review of Neuroscience*, vol. 28, no. 1, pp. 377–401, 2005.

[16] G. Kwakkel, B. J. Kollen, J. van der Grond, and A. J. Prevo, "Probability of regaining dexterity in the flaccid upper limb: impact of severity of paresis and time since onset in acute stroke," *Stroke*, vol. 34, no. 9, pp. 2181–2186, 2003.

[17] A. Yang, H. M. Wu, J. L. Tang et al., "Acupuncture for stroke rehabilitation," *Cochrane Database of Systematic Reviews*, vol. -D4131, 2016.

[18] Z. Hao, D. Wang, Y. Zeng, M. Liu, and Cochrane Stroke Group, "Repetitive transcranial magnetic stimulation for improving function after stroke," *Cochrane Database of Systematic Reviews*, vol. D8862, 2013.

[19] B. Elsner, G. Kwakkel, J. Kugler, and J. Mehrholz, "Transcranial direct current stimulation (tDCS) for improving capacity in activities and arm function after stroke: a network meta-analysis of randomised controlled trials," *Journal of Neuroengineering and Rehabilitation*, vol. 14, no. 1, p. 95, 2017.

[20] P. Wu, E. Mills, D. Moher, and D. Seely, "Acupuncture in poststroke rehabilitation: a systematic review and meta-analysis of randomized trials," *Stroke*, vol. 41, no. 4, pp. e171–e179, 2010.

[21] A. A. Rabinstein and L. M. Shulman, "Acupuncture in clinical neurology," *The Neurologist*, vol. 9, no. 3, pp. 137–148, 2003.

[22] Y. Sun, S. A. Xue, and Z. Zuo, "Acupuncture therapy on apoplectic aphasia rehabilitation," *Journal of Traditional Chinese Medicine*, vol. 32, no. 3, pp. 314–321, 2012.

[23] L. Yang, J. Y. Tan, H. Ma et al., "Warm-needle moxibustion for spasticity after stroke: a systematic review of randomized controlled trials," *International Journal of Nursing Studies*, vol. 82, pp. 129–138, 2018.

[24] B. Zhang, Y. Han, X. Huang et al., "Acupuncture is effective in improving functional communication in post-stroke aphasia," *Wiener Klinische Wochenschrift*, vol. 131, no. 9-10, pp. 221–232, 2019.

[25] C. Cirillo, N. Brihmat, E. Castel-Lacanal et al., "Post-stroke remodeling processes in animal models and humans," *Journal of Cerebral Blood Flow and Metabolism*, vol. 40, no. 1, pp. 3–22, 2020.

[26] S. R. Zeiler, "Should we care about early post-stroke rehabilitation? Not yet, but soon," *Current Neurology and Neuroscience Reports*, vol. 19, no. 3, 2019.

[27] B. B. Johansson, "Current trends in stroke rehabilitation. A review with focus on brain plasticity," *Acta Neurologica Scandinavica*, vol. 123, no. 3, pp. 147–159, 2011.

[28] M. C. Diamond, D. Krech, and M. R. Rosenzweig, "The effects of an enriched environment on the histology of the rat cerebral cortex," *The Journal of Comparative Neurology*, vol. 123, pp. 111–120, 1964.

[29] S. M. Erhart, A. S. Young, S. R. Marder, and J. Mintz, "Clinical utility of magnetic resonance imaging radiographs for suspected organic syndromes in adult psychiatry," *The Journal of Clinical Psychiatry*, vol. 66, no. 8, pp. 968–973, 2005.

[30] G. H. Glover, "Overview of functional magnetic resonance imaging," *Neurosurgery Clinics of North America*, vol. 22, no. 2, pp. 133–139, 2011.

[31] L. Bai, Y. Tao, D. Wang et al., "Acupuncture induces time-dependent remodelling brain network on the stable somatosensory first-ever stroke patients: combining diffusion tensor and functional MR imaging," *Evidence-based Complementary and Alternative Medicine*, vol. 2014, Article ID 740480, 7 pages, 2014.

[32] Z. Xie, F. Cui, Y. Zou, and L. Bai, "Acupuncture enhances effective connectivity between cerebellum and primary sensorimotor cortex in patients with stable recovery stroke," *Evidence-Based Complementary and Alternative Medicine*, vol. 2014, Article ID 603909, 9 pages, 2014.

[33] X. Han, L. Bai, C. Sun et al., "Acupuncture enhances communication between cortices with damaged white matters in post-stroke motor impairment," *Evidence-Based Complementary and Alternative Medicine*, vol. 2019, Article ID 4245753, 11 pages, 2019.

[34] J. D. Schaechter, B. D. Connell, W. B. Stason et al., "Correlated change in upper limb function and motor cortex activation after verum and sham acupuncture in patients with chronic stroke," *The Journal of Alternative and Complementary Medicine*, vol. 13, no. 5, pp. 527–532, 2007.

[35] Y. Li, Y. Wang, C. Liao, W. Huang, and P. Wu, "Longitudinal Brain Functional Connectivity Changes of the Cortical Motor-Related Network in Subcortical Stroke Patients with Acupuncture Treatment," *Neural Plasticity*, vol. 2017, Article ID 5816263, 9 pages, 2017.

[36] P. Wu, Y. Zhou, C. Liao et al., "Structural changes induced by acupuncture in the recovering brain after ischemic stroke," *Evidence-Based Complementary and Alternative Medicine*, vol. 2018, Article ID 5179689, 8 pages, 2018.

[37] Y. Shen, M. Li, R. Wei, and M. Lou, "Effect of acupuncture therapy for postponing Wallerian degeneration of cerebral infarction as shown by diffusion tensor imaging," *The Journal of Alternative and Complementary Medicine*, vol. 18, no. 12, pp. 1154–1160, 2012.

[38] P. Wu, F. Zeng, C. Yin et al., "Effect of acupuncture plus conventional treatment on brain activity in ischemic stroke patients: a regional homogeneity analysis," *Journal of Traditional Chinese Medicine*, vol. 37, no. 5, pp. 650–658, 2017.

[39] G. Li, C. R. Jack, and E. S. Yang, "An fMRI study of somatosensory-implicated acupuncture points in stable somatosensory stroke patients," *Journal of Magnetic Resonance Imaging*, vol. 24, no. 5, pp. 1018–1024, 2006.

[40] G. Li and E. S. Yang, "An fMRI study of acupuncture-induced brain activation of aphasia stroke patients," *Complementary Therapies in Medicine*, vol. 19, pp. S49–S59, 2011.

[41] Y. Huang, H. Xiao, J. Chen et al., "Needling at the Waiguan (SJ5) in healthy limbs deactivated functional brain areas in ischemic stroke patients a functional magnetic resonance imaging study," *Neural Regeneration Research*, vol. 6, pp. 2829–2833, 2011.

[42] S. Cho, M. Kim, J. J. Sun et al., "A comparison of brain activity between healthy subjects and stroke patients on fMRI by acupuncture stimulation," *Chinese Journal of Integrative Medicine*, vol. 19, no. 4, pp. 269–276, 2013.

[43] Y. Huang, J. Chen, X. Lai et al., "Lateralisation of cerebral response to active acupuncture in patients with unilateral ischaemic stroke: an fmri study," *Acupuncture in Medicine*, vol. 31, no. 3, pp. 290–296, 2013.

[44] J. Chen, Y. Huang, X. Lai et al., "Acupuncture at Waiguan (TE5) influences activation/deactivation of functional brain areas in ischemic stroke patients and healthy people: a functional MRI study," *Neural Regeneration Research*, vol. 8, no. 3, pp. 226–232, 2013.

[45] J. Chen, J. Wang, Y. Huang et al., "Modulatory effect of acupuncture at Waiguan (TE5) on the functional connectivity of the central nervous system of patients with ischemic stroke in the left basal ganglia," *PLoS One*, vol. 9, no. 6, article e96777, 2014.

[46] J. Qi, J. Chen, Y. Huang et al., "Acupuncture at Waiguan (SJ5) and sham points influences activation of functional brain areas of ischemic stroke patients: a functional magnetic resonance imaging study," *Neural Regeneration Research*, vol. 9, no. 3, pp. 293–300, 2014.

[47] Y. Zhang, K. Li, Y. Ren et al., "Acupuncture modulates the functional connectivity of the default mode network in stroke patients," *Evidence-Based Complementary and Alternative Medicine*, vol. 2014, Article ID 765413, 7 pages, 2014.

[48] M. K. Li, Y. J. Li, G. F. Zhang et al., "Acupuncture for ischemic stroke: cerebellar activation may be a central mechanism following Deqi," *Neural Regeneration Research*, vol. 10, no. 12, pp. 1997–2003, 2015.

[49] Y. GAO, Z. LIN, J. TAO et al., "Evidence of timing effects on acupuncture: a functional magnetic resonance imaging study," *Experimental and Therapeutic Medicine*, vol. 9, no. 1, pp. 59–64, 2015.

[50] J. Chang, H. Zhang, Z. Tan, J. Xiao, S. Li, and Y. Gao, "Effect of electroacupuncture in patients with post-stroke motor aphasia," *Wiener Klinische Wochenschrift*, vol. 129, no. 3-4, pp. 102–109, 2017.

[51] C. Fu, K. Li, Y. Ning et al., "Altered effective connectivity of resting state networks by acupuncture stimulation in stroke patients with left hemiplegia," *Medicine*, vol. 96, no. 47, article e8897, 2017.

[52] Y. Ning, K. Li, C. Fu et al., "Enhanced functional connectivity between the bilateral primary motor cortices after acupuncture at Yanglingquan (GB34) in right-hemispheric subcortical stroke patients: a resting-state fMRI study," *Frontiers in Human Neuroscience*, vol. 11, 2017.

[53] S. Chen, D. Cai, J. Chen, H. Yang, and L. Liu, "Altered brain regional homogeneity following contralateral acupuncture at Quchi (LI 11) and Zusanli (ST 36) in ischemic stroke patients with left hemiplegia: an fMRI study," *Chinese Journal of Integrative Medicine*, vol. 26, no. 1, pp. 20–25, 2020.

[54] X. Han, H. Jin, K. Li et al., "Acupuncture modulates disrupted whole-brain network after ischemic stroke: evidence based on graph theory analysis," *Neural Plasticity*, vol. 2020, Article ID 8838498, 10 pages, 2020.

[55] F. Zhang, Y. Wu, and J. Jia, "Electro-acupuncture can alleviate the cerebral oedema of rat after ischemia," *Brain Injury*, vol. 25, no. 9, pp. 895–900, 2011.

[56] Z. Wu, J. Hu, F. du, X. Zhou, Q. Xiang, and F. Miao, "Long-term changes of diffusion tensor imaging and behavioural status after acupuncture treatment in rats with transient focal cerebral ischaemia," *Acupuncture in Medicine*, vol. 30, no. 4, pp. 331–338, 2012.

[57] S. Liang, Y. Lin, B. Lin et al., "Resting-state functional magnetic resonance imaging analysis of brain functional activity in rats with ischemic stroke treated by electro- acupuncture," *Journal of Stroke and Cerebrovascular Diseases*, vol. 26, no. 9, pp. 1953–1959, 2017.

[58] T. Wen, X. Zhang, S. Liang et al., "Electroacupuncture Ameliorates Cognitive Impairment and Spontaneous Low- Frequency Brain Activity in Rats with Ischemic Stroke," *Journal of Stroke and Cerebrovascular Diseases*, vol. 27, no. 10, pp. 2596–2605, 2018.

[59] J. M. Cassidy and S. C. Cramer, "Spontaneous and therapeutic-induced mechanisms of functional recovery after stroke," *Translational Stroke Research*, vol. 8, no. 1, pp. 33–46, 2017.

[60] D. Hebb, *The Organization of Behavior: A Neuropsychological Theory*, John Wiley & Sons, New York, 1949.

[61] A. Galvan, "Neural plasticity of development and learning," *Human Brain Mapping*, vol. 31, no. 6, pp. 879–890, 2010.

[62] C. Sampaio-Baptista, Z. B. Sanders, and H. Johansen-Berg, "Structural plasticity in adulthood with motor learning and stroke rehabilitation," *Annual Review of Neuroscience*, vol. 41, no. 1, pp. 25–40, 2018.

[63] L. Carey, A. Walsh, A. Adikari et al., "Finding the intersection of neuroplasticity, stroke recovery, and learning: scope and contributions to stroke rehabilitation," *Neural Plasticity*, vol. 2019, Article ID 5232374, 15 pages, 2019.

[64] T. H. Murphy and D. Corbett, "Plasticity during stroke recovery: from synapse to behaviour," *Nature Reviews. Neuroscience*, vol. 10, no. 12, pp. 861–872, 2009.

[65] M. F. Bear, B. W. Connors, and M. A. Paradiso, *Neuroscience: Exploring the Brain*, Lippincott Williams & Wilkins Publishers, 3rd edition, 2007.

[66] S. Kiran, "What is the nature of poststroke language recovery and reorganization?," *ISRN Neurology*, vol. 2012, Article ID 786872, 13 pages, 2012.

[67] C. Grefkes and G. R. Fink, "Connectivity-based approaches in stroke and recovery of function," *Lancet Neurology*, vol. 13, no. 2, pp. 206–216, 2014.

[68] G. Silasi and T. H. Murphy, "Stroke and the connectome: how connectivity guides therapeutic intervention," *Neuron*, vol. 83, no. 6, pp. 1354–1368, 2014.

[69] A. K. Rehme, S. B. Eickhoff, C. Rottschy, G. R. Fink, and C. Grefkes, "Activation likelihood estimation meta-analysis of motor-related neural activity after stroke," *NeuroImage*, vol. 59, no. 3, pp. 2771–2782, 2012.

[70] V. A. Nair, B. M. Young, C. la et al., "Functional connectivity changes in the language network during stroke recovery," *Annals of Clinical Translational Neurology*, vol. 2, no. 2, pp. 185–195, 2015.

[71] D. Zhu, J. Chang, S. Freeman et al., "Changes of functional connectivity in the left frontoparietal network following aphasic stroke," *Frontiers in Behavioral Neuroscience*, vol. 8, p. 167, 2014.

[72] J. B. Green, "Brain reorganization after stroke," *Topics in Stroke Rehabilitation*, vol. 10, no. 3, pp. 1–20, 2003.

[73] J. O. Maximo, E. J. Cadena, and R. K. Kana, "The implications of brain connectivity in the neuropsychology of autism," *Neuropsychology Review*, vol. 24, no. 1, pp. 16–31, 2014.

[74] C. Kelly and F. X. Castellanos, "Strengthening connections: functional connectivity and brain plasticity," *Neuropsychology Review*, vol. 24, no. 1, pp. 63–76, 2014.

[75] P. A. Stokes and P. L. Purdon, "A study of problems encountered in Granger causality analysis from a neuroscience perspective," *Proceedings of the National Academy of Sciences of the United States of America*, vol. 114, no. 34, pp. E7063–E7072, 2017.

[76] E. Bullmore and O. Sporns, "Complex brain networks: graph theoretical analysis of structural and functional systems," *Nature Reviews. Neuroscience*, vol. 10, no. 3, pp. 186–198, 2009.

[77] D. S. Bassett and E. T. Bullmore, "Human brain networks in health and disease," *Current Opinion in Neurology*, vol. 22, no. 4, pp. 340–347, 2009.

[78] Y. Zang, T. Jiang, Y. Lu, Y. He, and L. Tian, "Regional homogeneity approach to fMRI data analysis," *NeuroImage*, vol. 22, no. 1, pp. 394–400, 2004.

[79] C. D. Good, I. S. Johnsrude, J. Ashburner, R. N. A. Henson, K. J. Friston, and R. S. J. Frackowiak, "A voxel-based morphometric study of ageing in 465 normal adult human brains," *NeuroImage*, vol. 14, no. 1, pp. 21–36, 2001.

[80] Y. Zhang and M. A. Burock, "Diffusion tensor imaging in Parkinson's disease and Parkinsonian syndrome: a systematic review," *Frontiers in Neurology*, vol. 11, p. 531993, 2020.

[81] Z. Li, M. Yang, Y. Lin et al., "Electroacupuncture promotes motor function and functional connectivity in rats with ischemic stroke: an animal resting-state functional magnetic resonance imaging study," *Acupuncture in Medicine*, vol. 39, no. 2, pp. 146–155, 2021.

[82] S. Liang, X. Jiang, Q. Zhang et al., "Abnormal metabolic connectivity in rats at the acute stage of ischemic stroke," *Neuroscience Bulletin*, vol. 34, no. 5, pp. 715–724, 2018.

[83] D. A. Nowak, C. Grefkes, M. Ameli, and G. R. Fink, "Interhemispheric competition after stroke: brain stimulation to enhance recovery of function of the affected hand," *Neurorehabilitation and Neural Repair*, vol. 23, no. 7, pp. 641–656, 2009.

[84] U. Takechi, K. Matsunaga, R. Nakanishi et al., "Longitudinal changes of motor cortical excitability and transcallosal inhibition after subcortical stroke," *Clinical Neurophysiology*, vol. 125, no. 10, pp. 2055–2069, 2014.

[85] T. Ots, A. Kandirian, I. Szilagyi, S. M. DiGiacomo, and A. Sandner-Kiesling, "The selection of dermatomes for sham (placebo) acupuncture points is relevant for the outcome of acupuncture studies: a systematic review of sham (placebo)-controlled randomized acupuncture trials," *Acupuncture in Medicine*, vol. 38, no. 4, pp. 211–226, 2020.

[86] A. U. Asghar, G. Green, M. F. Lythgoe, G. Lewith, and H. MacPherson, "Acupuncture needling sensation: The neural correlates of _deqi_ using fMRI," *Brain Research*, vol. 1315, pp. 111–118, 2010.

[87] K. K. Hui, O. Marina, J. Liu, B. R. Rosen, and K. K. Kwong, "Acupuncture, the limbic system, and the anticorrelated networks of the brain," *Autonomic Neuroscience*, vol. 157, no. 1-2, pp. 81–90, 2010.

[88] L. Mandolesi, F. Gelfo, L. Serra et al., "Environmental factors promoting neural plasticity: insights from animal and human studies," *Neural Plasticity*, vol. 2017, Article ID 7219461, 10 pages, 2017.

[89] C. H. Zhang, Z. Z. Ma, B. B. Huo et al., "Diffusional plasticity induced by electroacupuncture intervention in rat model of

peripheral nerve injury," *Journal of Clinical Neuroscience*, vol. 69, pp. 250–256, 2019.

[90] NIH Consensus Conference, "Acupuncture," *JAMA*, vol. 280, pp. 1518–1524, 1998.

[91] L. Y. Xiao, X. R. Wang, Y. Yang et al., "Applications of acupuncture therapy in modulating plasticity of central nervous system," *Neuromodulation*, vol. 21, no. 8, pp. 762–776, 2018.

[92] T. Yin, P. Ma, Z. Tian et al., "Machine learning in neuroimaging: a new approach to understand acupuncture for neuroplasticity," *Neural Plasticity*, vol. 2020, Article ID 8871712, 14 pages, 2020.

[93] L. M. Chavez, S. S. Huang, I. MacDonald, J. G. Lin, Y. C. Lee, and Y. H. Chen, "Mechanisms of acupuncture therapy in ischemic stroke rehabilitation: a literature review of basic studies," *International Journal of Molecular Sciences*, vol. 18, no. 11, p. 2270, 2017.

[94] B. Q. Cao, F. Tan, J. Zhan, and P. H. Lai, "Mechanism underlying treatment of ischemic stroke using acupuncture: transmission and regulation," *Neural Regeneration Research*, vol. 16, no. 5, pp. 944–954, 2021.

[95] T. Muka, M. Glisic, J. Milic et al., "A 24-step guide on how to design, conduct, and successfully publish a systematic review and meta-analysis in medical research," *European Journal of Epidemiology*, vol. 35, no. 1, pp. 49–60, 2020.

Hindawi
Neural Plasticity
Volume 2021, Article ID 3045990, 7 pages
https://doi.org/10.1155/2021/3045990

Research Article

Muscle Fiber Diameter and Density Alterations after Stroke Examined by Single-Fiber EMG

Chengjun Huang,[1] Bo Yao,[2] Xiaoyan Li,[3,4] Sheng Li,[5] and Ping Zhou[6]

[1]*Guangdong Work Injury Rehabilitation Center, Guangzhou, China*
[2]*Institute of Biomedical Engineering, Chinese Academy of Medical Sciences & Peking Union Medical College, Beijing, China*
[3]*Department of Bioengineering, University of Maryland, College Park, MA, USA*
[4]*Department of Neurology, Medical College of Wisconsin, Milwaukee, WI, USA*
[5]*Department of Physical Medicine and Rehabilitation, University of Texas Health Science Center at Houston, Houston, TX, USA*
[6]*University of Health and Rehabilitation Sciences, Qingdao, China*

Correspondence should be addressed to Ping Zhou; dr.ping.zhou@outlook.com

Received 14 May 2021; Revised 1 July 2021; Accepted 30 July 2021; Published 15 August 2021

Academic Editor: Xiaozheng Liu

This study presents single-fiber electromyography (EMG) analysis for assessment of paretic muscle changes after stroke. Single-fiber action potentials (SFAPs) were recorded from the first dorsal interosseous (FDI) muscle bilaterally in 12 individuals with hemiparetic stroke. The SFAP parameters, including the negative peak duration and the peak-peak amplitude, were measured and further used to estimate muscle fiber diameter through a model based on the quadratic function. The SFAP parameters, fiber density, and muscle fiber diameter derived from the model were compared between the paretic and contralateral muscles. The results show that SFAPs recorded from the paretic muscle had significantly smaller negative peak duration than that from the contralateral muscle. As a result, the derived muscle fiber diameter of the paretic muscle was significantly smaller than that of the contralateral muscle. The fiber density of the paretic muscle was significantly higher than that of the contralateral muscle. These results provide further evidence of remodeled motor units after stroke and suggest that paretic muscle weakness can be due to both complex central and peripheral neuromuscular alterations.

1. Introduction

Stroke is one of the leading causes of death and long-term disability worldwide, which could cause significant structural and metabolic changes in skeletal muscles of the affected limb [1–3]. Electromyography (EMG) studies have been reported to examine paretic muscle changes after stroke, focusing on different levels (muscle fiber, motor unit, muscle, and muscle group) of examination [4]. Among various EMG techniques, single-fiber EMG relies on a special needle electrode with a very tiny recording surface (25 μm in diameter) which allows identification of single-fiber action potentials (SFAPs) [5]. Two parameters are often used for single-fiber EMG processing: fiber density and jitter. Fiber density is defined as the average number of muscle fibers in the recording area (within ~300 μm from the electrode) belonging to one motor unit, which reflects the local organization of muscle fibers within the motor unit. Jitter is the variation in the time interval between the two action potentials of the same motor unit, which provides an indication of the stability of neuromuscular transmission. Both fiber density and jitter are sensitive measures of denervation and reinnervation processes associated with disease or injury.

Single-fiber EMG has been used to examine paretic muscle changes after stroke [6–9]. For example, an increase in fiber density of the abductor digiti minimi muscle was found in the paretic side compared with the contralateral or control group. Fiber density increased at early stage following stroke and thereafter remained stable, indicating that reinnervation already took place in the acute phase of stroke [8]. In another

single-fiber EMG study [7], by measuring neuromuscular jitter, it was reported that mean jitters of the extensor digitorum communis and anterior tibial muscles were significantly larger in paretic side than that in normal controls, indicating dysfunction of neuromuscular transmission and an ongoing muscle fiber reinnervation process in the paretic muscle. A recent single-fiber EMG study with the first dorsal interosseous (FDI) muscle of chronic stroke patients indicated little change in jitter although the fiber density was significantly higher in the paretic muscle than that in the contralateral muscle [9].

In addition to fiber density and jitter, the shape of SFAPs also contains valuable information which has not been a focus of analysis in previous single-fiber EMG studies. Larger fibers tend to produce SFAPs with larger peak-peak amplitude and shorter negative peak duration. Based on the SFAP model [10, 11], a simulation study was performed by Zalewska et al., to describe the relationships between SFAP parameters and muscle fiber characteristics [12], from which fiber diameter can be derived from the analysis of SFAP's negative peak duration and peak-peak amplitude. The model was further validated using single-fiber EMG recordings acquired from the frontalis muscle of a healthy subject [13].

In this study, we set to explore central and peripheral neuromuscular alterations after stroke by comparing paretic and contralateral muscles of a group of chronic stroke subjects using single-fiber EMG. It was hypothesized that both central and peripheral neuromuscular changes, including transsynaptic spinal motor neuron degeneration and muscle fiber atrophy, would occur after stroke, which can be captured by single-fiber EMG analysis. More specifically, fiber density was used to assess motor unit loss and compensatory muscle fiber reinnervation. We expected to observe significantly increased fiber density in paretic muscles compared with contralateral muscles, providing evidence of spinal motor neuron degeneration after stroke. Meanwhile, muscle fiber diameter was estimated based on SFAP parameters [12]. We expected to observe significantly reduced fiber diameter in paretic muscles compared with contralateral muscles, providing evidence of muscle atrophy after stroke at the level of individual muscle fibers.

2. Methods

2.1. Participants. Twelve hemiparetic stroke survivors aged from 45–79 years (5 male, 7 female, age 61 ± 10 years) volunteered to participate in the study. Stroke participants were required to have hemiplegia secondary to an ischemic or hemorrhagic stroke with an onset for more than 6 months and have ability to follow the instructions of the experimenter and move their index finger. In this study, the duration from stroke onset to data collection varied from 1 to 15 years (6.6 ± 4.8 years). Seven subjects had paretic arm in the right side and 5 in the left side. The paretic arm was the dominant arm (before stroke) for 6 of the 12 subjects. The experiment protocol was approved by the Committee for the Protection of Human Subjects at the University of Texas Health Science Center at Houston (UTHealth) and TIRR Memorial Hermann Hospital (Houston, United States). All subjects gave written informed consent before experiment. Maximal pinch and grip forces were measured bilaterally for each stroke subject before EMG data collection.

2.2. Experiment Protocols. Subjects sat in a chair with their tested forearm pronated and placed on a height-adjustable table. Prior to electrode placement, the participant's skin above the FDI muscle was scrubbed with alcohol pads to reduce the skin-electrode impedance. A surface reference electrode was placed over the ulna styloid. A Natus UltraPro S100 electromyographic system was used for the study. Single-fiber EMG signals were obtained with a single-fiber EMG electrode (0.45 mm 26 G × 40 mm, Natus Inc.). The single-fiber EMG signals were filtered with a bandwidth of 500–10,000 Hz. The sampling frequency is 48,000 Hz.

To measure fiber density, the electrode was inserted into the FDI muscle and slowly advanced. Subjects were instructed to perform slight FDI voluntary contraction by abducting their index finger to push a 5 kg weight on the table at the horizontal direction. The electrode was optimally positioned to maximize the SFAP amplitude. After optimization, the number of associated single-fiber EMG signals time-locked to the triggering potential (a brief rise time < 300 μs, amplitude > 200 μV) was determined. After each recording, sufficient rest was provided for the subjects to avoid muscle fatigue. The electrode was then advanced to another new position in the FDI muscle, and the process of counting potentials was repeated. For each subject, 20 different recording positions (different depths at different skin insertions) in the midbelly of the FDI muscle were examined. The mean number of potentials counted in all recording sites was calculated as the fiber density.

2.3. Fiber Diameter Estimation Model. The detailed information about the model has been described in previous studies [12, 13]. Briefly, the peak-peak amplitude and the negative peak duration of SFAPs are used to determine the fiber diameter. As shown in Figure 1, the peak-peak amplitude is measured from maximum positive to maximum negative peaks. The time difference between the two zero-crossings, which are following the initial downward and subsequent upward peaks, respectively, is the negative peak duration.

The negative peak duration is approximated by a biquadratic polynomial as the following equations:

$$\text{Duration} = F(\log_{10}(a), \text{Diameter}), \tag{1}$$

where a is the peak-peak amplitude of the SFAP and F is expressed as a quadratic function:

$$F(x, y) = e_1 + y * (e_2 + y * e_3), \tag{2}$$

where

$$e_j = c_{j,1} + x * \left(c_{j,2} + x * c_{j,3}\right), \quad j = 1, 2, 3, \tag{3}$$

where y is the estimated or simulated fiber diameter and x is $\log_{10}(a)$. In order to calculate these coefficients, several

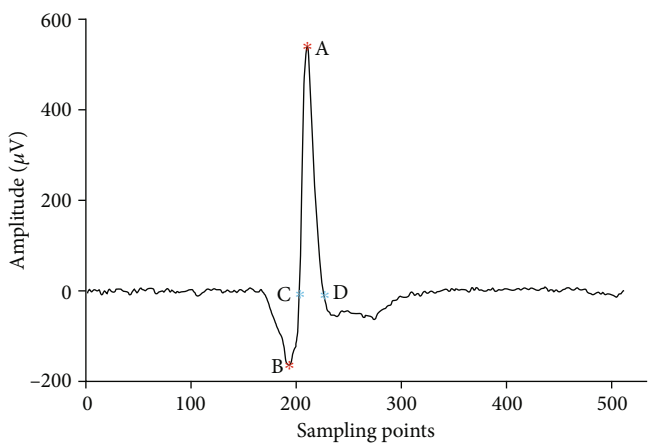

Figure 1: Definition of the SFAP parameters. The peak-peak amplitude is measured from the maximum positive and negative peaks (A to B). The time difference two between zero-crossings (C and D) is the negative peak duration.

Table 1: The values of the coefficients c in Equation (3).

$c_{1,1}$	9.5100×10^{-1}
$c_{1,2}$	-2.2321×10^{-1}
$c_{1,3}$	2.0358×10^{-1}
$c_{2,1}$	-7.3845×10^{-3}
$c_{2,2}$	3.4212×10^{-4}
$c_{2,3}$	-1.6564×10^{-3}
$c_{3,1}$	2.5574×10^{-5}
$c_{3,2}$	-3.3074×10^{-6}
$c_{3,3}$	6.4493×10^{-6}

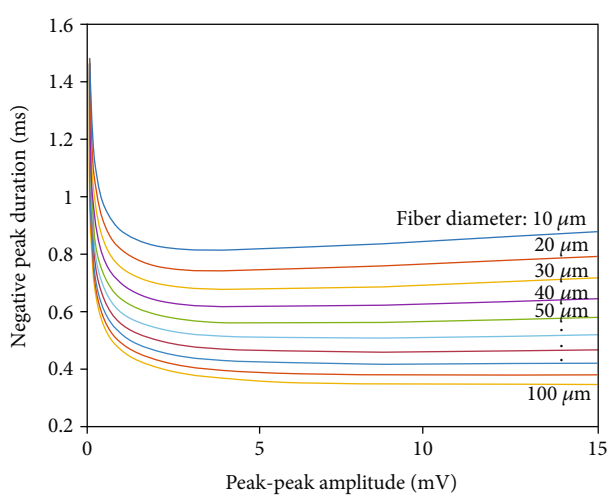

Figure 2: The quadratic relation between the peak-peak amplitude and the negative peak duration under different values of fiber diameters.

hundreds of SFAPs were simulated based on the line source model described by Nandedkar and Stalberg [14]. The coefficients e_j are determined by fitting Equations (1) and (2) to the peak-to-peak amplitudes and negative peak durations of the simulated signals. The coefficients given in Table 1 were taken from reference [12]. Based on Equation (1), the dependencies between peak-peak amplitude and negative peak duration under different values of diameter fibers are plotted in Figure 2. The simulated SFAPs of smaller diameters have longer negative peak durations and lower peak-peak amplitudes. The fiber diameters of each subject were estimated using the quadratic model with the data of negative peak durations and amplitudes of the SFAPs recorded in the fiber density session.

2.4. Statistical Analysis. Data are presented as mean ± standard deviation (SD). Statistical analysis was performed using SPSS (SPSS, Inc., 2007, Chicago, IL, United States). The Shapiro-Wilk test was used to test for possible deviations from normality. As the fiber density was normally distributed, Student's paired t-test was used to investigate side-to-side differences for the fiber density. Cohen's d was used as the effect size. Wilcoxon Rank Sum test was used to assess the side-to-side differences for the peak-peak amplitude, negative peaks duration, and fiber diameter, which did not pass the normality test. The effect size was the statistics z value divided by square root of observation number. Differences were considered significant when $p < 0.05$.

3. Results

For all subjects, the maximum pinch and grip forces (kg) of the paretic side were less than half of the contralateral side. Bilateral recordings of fiber density were successfully completed in all stroke subjects. Fiber density in the paretic muscle was larger than the contralateral muscle in 10 of the 12 subjects. The mean fiber density of the paretic side was significantly higher than the contralateral side (paretic: 1.5 ± 0.2, contralateral: 1.3 ± 0.1, $p < 0.01$, 95%confidence interval = (0.07, 0.37), size effect = 1.22).

In Figure 3, the calculated fiber diameters of the paretic and contralateral FDI muscles are plotted along with the counterlines in Figure 2. Figure 4 shows the mean SFAP amplitudes, negative peak durations, and estimated fiber diameters of the paretic and contralateral muscles of each stroke subject. The mean SFAP negative peak duration of the paretic muscle was significantly larger than the contralateral muscle (paretic: 0.70 ± 0.14 ms, contralateral: 0.65 ± 0.14 ms, $p < 0.05$, 95% confidence interval = (0.02, 0.10), size effect = 0.2). The mean SFAP peak-peak amplitude was lower in the paretic side compared with the contralateral side, but the difference was not statistically significant (paretic: 1.2 ± 0.8 mV, contralateral: 1.6 ± 1.7 mV, $p = 0.4$). The estimated mean fiber diameter was significantly smaller in the paretic muscle than the contralateral muscle (paretic: 45.3 ± 26.7 μm, contralateral: 53.8 ± 26.8 μm, $p < 0.05$, 95%confidence interval = (−18.49,−2.84), size effect = 0.2).

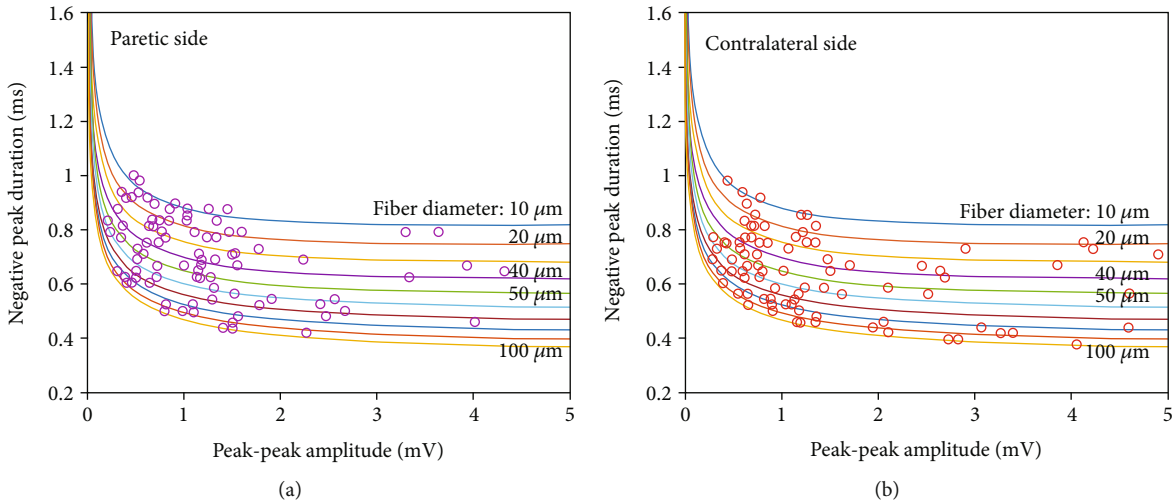

Figure 3: The estimated fiber diameters from paretic and contralateral FDI muscles.

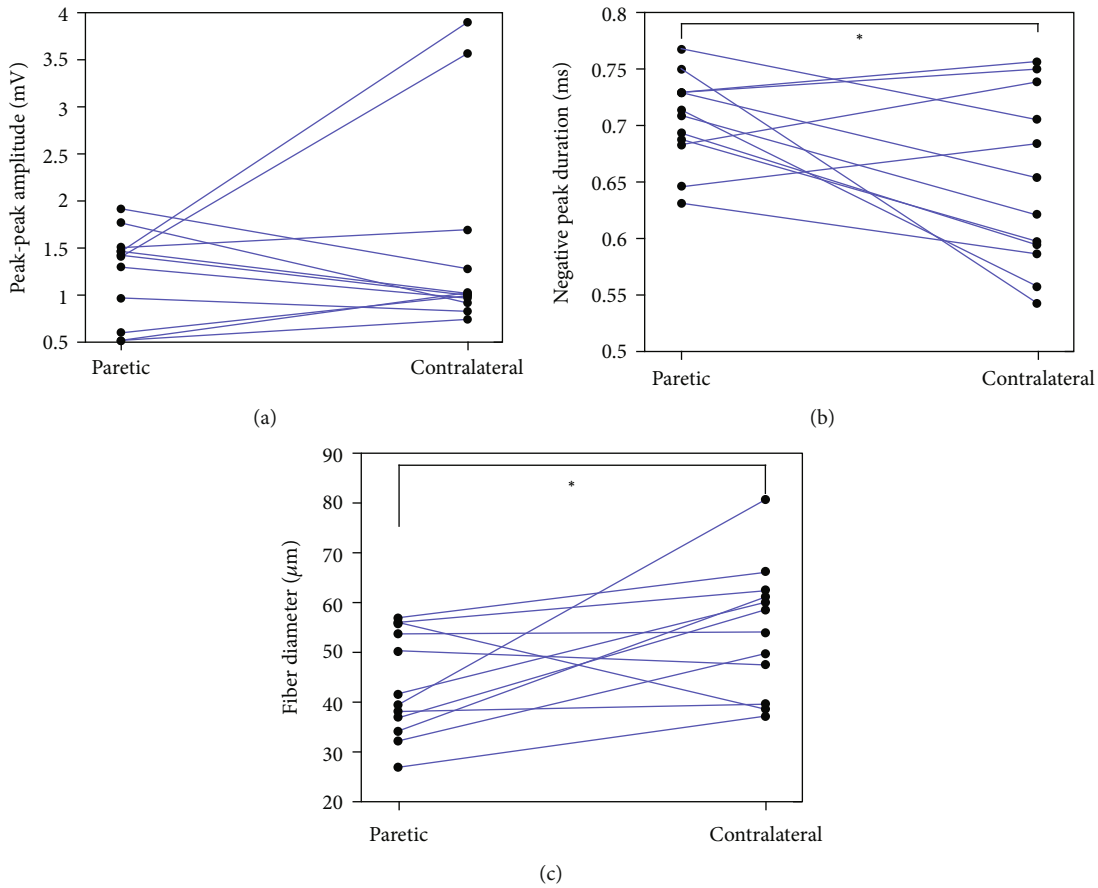

Figure 4: A comparison of (a) SFAP amplitude, (b) SFAP negative peak duration, and (c) estimated fiber diameter between paretic and contralateral muscles of the tested stroke subjects.

4. Discussion

To assess paretic muscle changes after stroke, different EMG techniques have been applied, e.g., single-fiber EMG, concentric needle EMG, fine wire EMG, macro-EMG, conventional surface EMG, and high-density surface EMG, which can perform different levels of examination from individual muscle fiber to muscle group. The objective of the current study was to assess motor unit alteration and remodeling after stroke by single fiber EMG, focusing not only on fiber density but also on muscle fiber diameter estimated from SFAP parameters.

Muscle fiber diameter provides essential information of a muscle which can be affected by various factors, such as exercise, nutrition, or disease. Increased variability of muscle fiber diameter has been reported in neuromuscular disorders [15]. Reduction in muscle fiber diameters is often associated with myopathies [16]. Muscle biopsy studies indicated decreased muscle fiber diameter for affected muscles after stroke [17, 18]. As the conduction velocity and muscle fiber diameter is positively correlated, changes in muscle fiber diameter can be indirectly assessed by measuring the conduction velocity of propagating action potentials [19–22]. Increased variability in muscle fiber diameter may lead to complex action potential waveforms, broad range of action potential amplitude distribution, and altered global surface EMG parameters [23–27].

In this study, fiber diameters were estimated from the peak-peak amplitude and the negative peak duration of SFAP based on the biquadratic polynomial model [12]. A linear relation between the propagation velocity and the fiber diameter was observed in both healthy individuals and neuromuscular disorder patients [14, 20]. For larger diameter, the time for the potential to pass the electrode is reduced, which results in the shorter negative peak duration. Conversely longer negative peak durations would be associated with smaller fiber diameters. The peak-peak amplitude can also be affected by the fiber diameter. Meanwhile, the distance of the fiber from the electrode plays an important role in determining SFAP amplitude [14]. The peak-peak amplitude will become lower when the electrode is moved further from the muscle fiber. Hence, compared with the peak-peak amplitude, negative peak duration may more accurately characterize the fiber diameter. For the tested stroke subjects, it was found that in the paretic side, the mean negative peak durations were significantly larger than the contralateral side. The peak-peak amplitudes were also smaller for the paretic muscle although not significantly compared with the contralateral muscle. The results indicated that the fiber diameter of the paretic side estimated through the model was significantly smaller than that of the contralateral side. This provides evidence of muscle atrophy at the level of individual muscle fibers. Experimentally, muscle atrophy is often seen in stroke patients due to abnormal neural innervation or long-time muscle inactivity [27].

Fiber density reflects the grouping of muscle fibers of a motor unit within its territory. Reference values of fiber density for a range of muscles were documented in previous literature [28, 29]. For FDI muscle of healthy subjects, one study reported the fiber density should be less than 1.7 [30], which could be significantly increased for patients with motor neuron disease [31–33]. In the current study with stroke subjects, the mean fiber density of the FDI muscle was relatively low compared with previous reports in motor neuron diseases. Consistent with findings from the previous studies of abductor digiti minimi and extensor digitorum communis muscles following stroke [6, 8], fiber density of the FDI muscle was found to be significantly higher in the paretic side than the contralateral side of the tested stroke subjects, suggesting that the paretic muscle had higher focal distribution of the muscle fibers in the motor unit than the contralateral muscle. Previous electrophysiological studies primarily based on motor unit number estimation have reported transsynaptic spinal motor neuron degeneration following stroke, starting as early as initial weeks to months following stroke [24, 34–37]. The degenerated muscle fibers are likely reinnervated by collateral sprouting from intact motor neuron axons, resulting in higher focal distribution of the muscle fibers. Muscle fiber reinnervation may also result in enlarged motor unit territory [38]. Using single-fiber EMG, we examined focal distribution of the muscle fibers in the motor unit. However, information about motor unit territory change was not provided in the current study, which can be further explored using macro-EMG or high density surface EMG techniques [38, 39].

In previous motor unit action potential (MUAP) quantitative analysis of stroke subjects using concentric needle electrodes, it was reported that MUAP parameters (such as amplitude, duration, and complexity) in the paretic muscle were not significantly different between the paretic and contralateral muscles [9, 40]. By recording both single-fiber EMG and concentric needle EMG, it was found that fiber density measures may be more sensitive than MUAP parameters in reflecting changes in the number of muscle fibers innervated by each motor unit, as decreases in muscle fiber diameter will reduce MUAP amplitude, masking increases in amplitude due to increases in the number of innervated muscle fibers. As a result, there might be no significant difference in MUAP parameters between the paretic and contralateral sides although more outliers may be observed from paretic muscles [9, 40].

The FDI is selected as the target muscle, as it is easily accessible for clinical EMG testing and assessment of motor unit properties [41, 42]. Although the maximum voluntary contraction of the FDI muscle was not directly measured in this study, it is likely the paretic FDI muscle had significant weakness given that the maximal pinch and grip strength of the paretic hand was less than half of the contralateral side. Our results indicate that the weakness of the paretic muscle is partly due to muscle atrophy because of reduced fiber diameter or loss of motor units, while muscle fiber reinnervation (as indicated by increased fiber density) can prevent more severe muscle atrophy or weakness that would otherwise occur from motor unit loss. There are other factors that will also contribute to paretic muscle weakness which are not addressed in this study, such as motor unit inactivation or reduced firing rates despite maximum effort as a result of reduced central activation of the muscle poststroke [43–49].

In summary, single-fiber EMG is a useful method to study paretic muscle changes after stroke. A novel feature of the study is a combined examination of both fiber density and fiber diameter to assess the characteristics of voluntarily recruited motor units in chronic stroke subjects. Derivation of muscle fiber diameter from SFAP parameters can provide complementary information to the routine single-fiber EMG analysis. A significant decrease in fiber diameter and a significant increase in fiber density were found in the paretic FDI muscle compared with the contralateral muscle. These findings provide evidence of motor unit remodeling and neuromuscular alterations after stroke.

Data Availability

All the datasets are available from the corresponding author (PZ) on request.

Conflicts of Interest

The authors declare that they have no competing interests.

Authors' Contributions

Chengjun Huang and Bo Yao are co-first authors. Affiliation 1 and affiliation 2 are co-first affiliations.

Acknowledgments

This study was supported in part by the Shandong Provincial Natural Science Foundation under grant ZR2020KF012 and in part by the Guangzhou Science and Technology Program under grant 201704030039.

References

[1] R. Dattola, P. Girlanda, G. Vita et al., "Muscle rearrangement in patients with hemiparesis after stroke: an electrophysiological and morphological study," *European Neurology*, vol. 33, no. 2, pp. 109–114, 2004.

[2] C. E. Hafer-Macko, A. S. Ryan, F. M. Ivey, and R. F. Macko, "Skeletal muscle changes after hemiparetic stroke and potential beneficial effects of exercise intervention strategies," *The Journal of Rehabilitation Research and Development*, vol. 45, no. 2, pp. 261–272, 2008.

[3] J. M. Sions, C. M. Tyrell, B. A. Knarr, A. Jancosko, and S. A. Binder-Macleod, "Age- and stroke-related skeletal muscle Changes," *Journal of Geriatric Physical Therapy*, vol. 35, no. 3, pp. 155–161, 2012.

[4] P. Zhou, C. Klein, X. Zhang, X. Li, and S. Li, "Electromyography (EMG) examination on motor unit alterations after stroke," in *in Intelligent Biomechatronics in Neurorehabilitation*, pp. 51–64, Elsevier, 2020.

[5] D. B. Sanders, K. Arimura, L. Y. Cui et al., "Guidelines for single fiber EMG," *Clinical Neurophysiology*, vol. 130, no. 8, pp. 1417–1439, 2019.

[6] A. C. Martinez, F. Del Campo, M. R. Mingo, and M. C. P. Conde, "Altered motor unit architecture in hemiparetic patients. A single fibre EMG study," *Journal of Neurology, Neurosurgery & Psychiatry*, vol. 45, no. 8, 1982.

[7] C.-W. Chang, "Evident trans-synaptic degeneration of motor neurons after stroke: a study of neuromuscular jitter by axonal microstimulation," *Electroencephalography and Clinical Neurophysiology/Electromyography and Motor Control*, vol. 109, no. 3, pp. 199–202, 1998.

[8] M. Lukács, L. Vécsei, and S. Beniczky, "Changes in muscle fiber density following a stroke," *Clinical Neurophysiology*, vol. 120, no. 8, pp. 1539–1542, 2009.

[9] B. Yao, C. S. Klein, H. Hu, S. Li, and P. Zhou, "Motor unit properties of the first dorsal interosseous in chronic stroke subjects: concentric needle and single fiber EMG analysis," *Frontiers in Physiology*, vol. 9, 2018.

[10] M. Nielsen, T. Graven-Nielsen, and D. Farina, "Effect of innervation-zone distribution on estimates of average muscle-fiber conduction velocity," *Muscle & Nerve*, vol. 37, no. 1, pp. 68–78, 2008.

[11] S. D. Nandedkar, E. V. Stalberg, and D. B. Sanders, "Simulation techniques in electromyography," *IEEE Transactions on Biomedical Engineering*, vol. BME-32, no. 10, pp. 775–785, 1985.

[12] E. Zalewska, S. D. Nandedkar, and I. Hausmanowa-Petrusewicz, "A method for determination of muscle fiber diameter using single fiber potential (SFP) analysis," *Medical & Biological Engineering & Computing*, vol. 50, no. 12, pp. 1309–1314, 2012.

[13] E. Zalewska, "Deduire le diametre des fibres musculaires a partir de l'enregistrement de potentiels de fibres unitaires," *Neurophysiologie Clinique*, vol. 47, no. 5–6, pp. 413–417, 2017.

[14] S. D. Nandedkar and E. Stalberg, "Simulation of single muscle fibre action potentials," *Medical & Biological Engineering & Computing*, vol. 21, no. 2, pp. 158–165, 1983.

[15] T. E. Bertorini, E. Stalberg, C. P. Yuson, and W. K. Engel, "Single-fiber electromyography in neuromuscular disorders: correlation of muscle histochemistry, single-fiber electromyography, and clinical findings," *Muscle & Nerve*, vol. 17, no. 3, pp. 345–353, 1994.

[16] A. Fuglsang-Frederiksen, "The role of different EMG methods in evaluating myopathy," *Clinical Neurophysiology*, vol. 117, no. 6, pp. 1173–1189, 2006.

[17] V. Dubowitz, C. A. Sewry, and A. Oldfors, *Muscle Biopsy: A Practical Approach: Expert Consult*, Goteborg, Sweden Elsevier Heal. Sci, 2013.

[18] R. P. Segura and V. Sahgal, "Hemiplegic atrophy: electrophysiological and morphological studies," *Muscle & Nerve*, vol. 4, no. 3, pp. 246–248, 1981.

[19] W. Troni, R. Cantello, and I. Rainero, "Conduction velocity along human muscle fibers in situ," *Neurology*, vol. 33, no. 11, pp. 1453–1459, 1983.

[20] P. J. Blijham, H. J. Ter Laak, H. J. Schelhaas, B. G. M. Van Engelen, D. F. Stegeman, and M. J. Zwarts, "Relation between muscle fiber conduction velocity and fiber size in neuromuscular disorders," *Journal of Applied Physiology*, vol. 100, no. 6, pp. 1837–1841, 2006.

[21] B. Yao, X. Zhang, S. Li et al., "Analysis of linear electrode array EMG for assessment of hemiparetic biceps brachii muscles," *Frontiers in Human Neuroscience*, vol. 9, 2015.

[22] M. O. Conrad, D. Qiu, G. Hoffmann, P. Zhou, and D. G. Kamper, "Analysis of muscle fiber conduction velocity during finger flexion and extension after stroke," *Topics in Stroke Rehabilitation*, vol. 24, no. 4, pp. 262–268, 2017.

[23] E. Stålberg, S. D. Nandedkar, D. B. Sanders, and B. Falck, "Quantitative motor unit potential analysis," *Journal of Clinical Neurophysiology*, vol. 13, no. 5, pp. 401–422, 1996.

[24] X. Li, M. Fisher, W. Z. Rymer, and P. Zhou, "Application of the F-response for estimating motor unit number and amplitude distribution in hand muscles of stroke survivors," *IEEE Transactions on Neural Systems and Rehabilitation Engineering*, vol. 24, no. 6, pp. 674–681, 2016.

[25] X. Li, H. Shin, P. Zhou, X. Niu, J. Liu, and W. Z. Rymer, "Power spectral analysis of surface electromyography (EMG) at matched contraction levels of the first dorsal interosseous muscle in stroke survivors," *Clinical Neurophysiology*, vol. 125, no. 5, pp. 988–994, 2014.

[26] M. Lukács, "Electrophysiological signs of changes in motor units after ischaemic stroke," *Clinical Neurophysiology*, vol. 116, no. 7, pp. 1566–1570, 2005.

[27] L. V. Thompson, "Skeletal muscle adaptations with age, inactivity, and therapeutic exercise," *Journal of Orthopaedic & Sports Physical Therapy*, vol. 32, no. 2, pp. 44–57, 2002.

[28] J. M. Gilchrist, "Ad hoc committee of the AAEM special interest group on SFEMG. Single fiber EMG reference values: a collaborative effort," *Muscle & Nerve*, vol. 15, pp. 151–161, 1992.

[29] M. B. Bromberg and D. M. Scott, "Single fiber EMG reference values: reformatted in tabular form," *Muscle & Nerve*, vol. 17, no. 7, pp. 820-821, 1994.

[30] M. S. Schwartz and M. Swash, "Pattern of involvement in the cervical segments in the early stage of motor neurone disease: a single fibre EMG study," *Acta Neurologica Scandinavica*, vol. 65, no. 5, pp. 424–431, 1982.

[31] M. Swash and M. S. Schwartz, "A longitudinal study of changes in motor units in motor neuron disease," *Journal of the Neurological Sciences*, vol. 56, no. 2–3, pp. 185–197, 1982.

[32] M. Swash, "Vulnerability of lower brachial myotomes in motor neurone disease: a clinical and single fibre EMG study," *Journal of the Neurological Sciences*, vol. 47, no. 1, pp. 59–68, 1980.

[33] M. Gantayat, M. Swash, and M. S. Schwartz, "Fiber density in acute and chronic inflammatory demyelinating polyneuropathy," *Muscle & Nerve*, vol. 15, no. 2, pp. 168–171, 1992.

[34] X. Li, Y.-C. Wang, N. L. Suresh, W. Z. Rymer, and P. Zhou, "Motor unit number reductions in paretic muscles of stroke survivors," *IEEE Transactions on Information Technology in Biomedicine*, vol. 15, no. 4, pp. 505–512, 2011.

[35] X. Li, J. Liu, S. Li, Y.-C. Wang, and P. Zhou, "Examination of hand muscle activation and motor unit indices derived from surface EMG in chronic stroke," *IEEE Transactions on Biomedical Engineering*, vol. 61, no. 12, pp. 2891–2898, 2014.

[36] Y. Hara, Y. Masakado, and N. Chino, "The physiological functional loss of single thenar motor units in the stroke patients: when does it occur? Does it progress?," *Clinical Neurophysiology*, vol. 115, no. 1, pp. 97–103, 2004.

[37] K. Arasaki, O. Igarashi, Y. Ichikawa et al., "Reduction in the motor unit number estimate (MUNE) after cerebral infarction," *Journal of the Neurological Sciences*, vol. 250, no. 1–2, pp. 27–32, 2006.

[38] T. M. Vieira, T. Lemos, L. A. S. Oliveira et al., "Postural muscle unit plasticity in stroke survivors: altered distribution of gastrocnemius' action potentials," *Frontiers in Neurology*, vol. 10, 2019.

[39] M. Lukács, L. Vécsei, and S. Beniczky, "Fiber density of the motor units recruited at high and low force output," *Muscle & Nerve*, vol. 40, no. 1, pp. 112–114, 2009.

[40] I. Kouzi, E. Trachani, E. Anagnostou et al., "Motor unit number estimation and quantitative needle electromyography in stroke patients," *Journal of Electromyography and Kinesiology*, vol. 24, no. 6, pp. 910–916, 2014.

[41] X. Li, A. Suresh, P. Zhou, and W. Z. Rymer, "Alterations in the peak amplitude distribution of the surface electromyogram poststroke," *IEEE Transactions on Biomedical Engineering*, vol. 60, no. 3, pp. 845–852, 2013.

[42] J. L. Young and R. F. Mayer, "Physiological alterations of motor units in hemiplegia," *Journal of the Neurological Sciences*, vol. 54, no. 3, pp. 401–412, 1982.

[43] P. Zhou, X. Li, and W. Zev Rymer, "EMG-force relations during isometric contractions of the first dorsal interosseous muscle after stroke," *Topics in Stroke Rehabilitation*, vol. 20, no. 6, pp. 537–543, 2013.

[44] J. J. Gemperline, S. Allen, D. Walk, and W. Z. Rymer, "Characteristics of motor unit discharge in subjects with hemiparesis," *Muscle & Nerve*, vol. 18, no. 10, pp. 1101–1114, 1995.

[45] L.-W. Chou, J. A. Palmer, S. Binder-Macleod, and C. A. Knight, "Motor unit rate coding is severely impaired during forceful and fast muscular contractions in individuals post stroke," *Journal of Neurophysiology*, vol. 109, no. 12, pp. 2947–2954, 2013.

[46] P. A. McNulty, G. Lin, and C. G. Doust, "Single motor unit firing rate after stroke is higher on the less-affected side during stable low-level voluntary contractions," *Frontiers in Human Neuroscience*, vol. 8, 2014.

[47] X. Hu, A. K. Suresh, W. Z. Rymer, and N. L. Suresh, "Altered motor unit discharge patterns in paretic muscles of stroke survivors assessed using surface electromyography," *Journal of Neural Engineering*, vol. 13, no. 4, p. 046025, 2016.

[48] X. Li, A. Holobar, M. Gazzoni, R. Merletti, W. Z. Rymer, and P. Zhou, "Examination of poststroke alteration in motor unit firing behavior using high-density surface EMG decomposition," *IEEE Transactions on Biomedical Engineering*, vol. 62, no. 5, pp. 1242–1252, 2015.

[49] S. Li, J. Liu, M. Bhadane, P. Zhou, and W. Z. Rymer, "Activation deficit correlates with weakness in chronic stroke: evidence from evoked and voluntary EMG recordings," *Clinical Neurophysiology*, vol. 125, no. 12, pp. 2413–2417, 2014.